FINAL REPORT

(June 1, 1968 to May 31, 1971)

to

National Aeronautics and Space Administration

Office of Scientific and Technical Information (Code U.S.)

Washington, D. C. 20546

NASA GRANT: NO. NGR 17-001-034

TITLE OF PROJECT:

OPTIMIZATION OF LIFE SUPPORT SYSTEMS AND THEIR SYSTEMS RELIABILITY

INVESTIGATORS:

L. T. Fan (Principal Investigator)

C. L. Hwang

L. E. Erickson

INSTITUTE FOR SYSTEMS DESIGN AND OPTIMIZATION

Kansas State University - Manhattan

FINAL REPORT

(June 1, 1968 to May 31, 1971)

to

National Aeronautics and Space Administration

Office of Scientific and Technical Information (Code U.S.)

Washington, D. C. 20546

NASA GRANT: NO. NGR 17-001-034

TITLE OF PROJECT

OPTIMIZATION OF LIFE SUPPORT SYSTEMS AND THEIR SYSTEMS RELIABILITY

INVESTIGATORS

Dr. L. T. Fan, Professor and Head (Principal Investigator)
Department of Chemical Engineering
Director, Institute for Systems Design and Optimization

Dr. C. L. Hwang, Associate Professor
Department of Industrial Engineering

Dr. L. [illegible] Erickson, Associate Professor
Department of Chemical Engineering

Institute for Systems Design and Optimization
and
Engineering Experiment Station
Kansas State University
of Agriculture and Applied Science
Manhattan, Kansas 66502

August 15, 1971

TABLE OF CONTENTS

PREFACE

This is the final report of the research project "Optimization of Life Support Systems and Their Systems Reliability (NASA Grant No. NGR 17-001-034)". The project was initiated on June 1, 1968 and terminated on May 31, 1971.

Since a majority of significant results from the project have been published, no attempt is made to give an exhaustive account of the project. Instead, a brief summary is provided here and readers are referred to copies of papers and reports which are appended for details.

SUMMARY

The identification, analysis, and optimization of life support systems and subsystems have been investigated. For each system or subsystem that has been considered, the procedure involves the establishment of a set of system equations (or mathematical model) based on theory and experimental evidences; the analysis and simulation of the model; the optimization of the operation, control, and reliability; analysis of sensitivity of the system based on the model; and, if possible, experimental verification of the theoretical and computational results.

The work so far has evolved into several distinct activities and the results of these activities have been published extensively. The research activities include:

(a) modeling of air flow in a confined space - a study in age distribution,

(b) review of several different gas-liquid contactors utilizing centrifugal force,

(c) review of carbon dioxide reduction contactors in space vehicles and other enclosed structures,

(d) application of modern optimal control theory to environmental control of confined spaces,

(e) optimal control of class of nonlinear diffusional distributed parameter systems,

(f) optimization of system reliability of life support systems and sub-systems,

(g) modeling, simulation and optimal control of the human thermal system,

(h) analysis and optimization of the water-vapor electrolysis cell.

These works are summarized and presented in this final report.

Publication List for NASA Grant No. NGR-17-001-034

OPTIMIZATION OF LIFE SUPPORT SYSTEMS AND

THEIR SYSTEMS RELIABILITY

(June 1, 1968 - May 31, 1971)

(a) Modeling of Air Flow in a Confined Space

*1. "Air Flow Models in a Confined Space--A study in Age Distribution," by M. S. K. Chen, L. T. Fan, C. L. Hwang, and E. S. Lee, International Journal of Building Science, vol. 4, pp. 133-144 (1969).

(b) Review of Several Different Gas-Liquid Contactors Utilizing Centrifugal Force

*1. "Several Different Gas-Liquid Contactors Utilizing Centrifugal Force," by T. Takahashi and L. T. Fan, Report No. 10, Institute for Systems Design and Optimization, Kansas State University, Manhattan, Kansas (1968).

(c) Review of Carbon Dioxide Reduction Contactors in Space Vehicles and Other Enclosed Structures

*1. "Carbon Dioxide Reduction Contactors in Space Vehicles and Other Enclosed Structures," by T. Takahashi, and L. T. Fan, Report No. 11, Institute for Systems Design and Optimization, Kansas State University, Manhattan, Kansas (1968).

(d) Application of Modern Optimal Control Theory to Environmental Control of Confined Spaces

*1. "Applications of Modern Optimal Control Theory to Environmental Control of Confined Spaces and Life Support Systems," Part 1. Modeling and Simulation," by L. T. Fan, Y. S. Hwang, and C. L. Hwang, International Journal of Building Science, voi. 5, pp. 57-71 (1970).

*2. "Application of Modern Optimal Control Theory to Environmental Control of Confined Spaces and Life Support Systems, Part 2--Basic Computational Algorithm of Pontryagin's Maximum Principle and its Applications," by L. T. Fan, Y. S. Hwang, and C. L. Hwang, Building Science, vol. 5, pp. 81-94 (1970).

*3. "Application of Modern Optimal Control Theory to Environmental Control of Confined Spaces and Life Support Systems, Part 3. Optimal Control of Systems in which State Variables Have Equality Constraints at the Final Process Time," by L. T. Fan, Y. S. Hwang and C. L. Hwang, Building Scinece, vol. 5, pp. 125-136 (1970).

*A copy of this paper or report is attached.

*4. "Application of Modern Optimal Control Theory to Environmental Control of Confined Spaces and Life Support Systems, Part 4. Control of Systems with Inequality Constraints Imposed on State Variables," by L. T. Fan, Y. S. Hwang and C. L. Hwang, Building Science, vol. 5, pp. 137-147 (1971).

*5. "Application of Modern Optimal Control Theory to Environmental Control of Confined Spaces and Life Support Systems, Part 5. Optimality and sensitivity Analysis," by L. T. Fan, Y. S. Hwang and C. L. Hwang, Building Science, vol. 5, pp. 149-152 (1971).

*6. "Application of Modern Optimal Control Theory to Environmental Control of Confined Spaces," by L. T. Fan, Y. S. Hwang, and C. L. Hwang, proceedings of the Air Force Office of Scientific Research/ Lockheed Missiles and Space Company Symposium, "Thermodynamic and Thermophysics of Space Flight," March 23-25, 1970, Palo Alto, Calif. pp. 175-189.

7. "Optimal Environmental Control of Confined Spaces of Life Support Systems with Impulse Heat Disturbance," by C. L. Hwang, L. T. Fan, and M. S. Bhandiwad, submitted for publication, (1970).

8. "Simultaneous Control of Temperature and Humidity in a Confined Space, Part I. Mathematical Modeling of the Dynamic Behavior of Temperature and Humidity in a Confined Space", by E. Nakanishi, N. C. Pereira, L. T. Fan, and C. L. Hwang, paper submitted for publication (1971).

9. "Simultaneous Control of Temperature and Humidity in a Confined Space, Part 2. Feedback Control Synthesis via Classical Control Theory", by E. Nakanishi, N. C. Pereira, L. T. Fan and C. L. Hwang, paper submitted for publication (1971).

10. "Simultaneous Control of Temperature and Humidity in a Confined Space, Part 3. Feedback Control Synthesis via Optimal Control Theory", by N. C. Pereira, E. Nakanishi, L. T. Fan, and C. L. Hwang, paper submitted for publication (1971).

(e) Optimal Control of Class of Nonlinear Distributed Parameter Systems

*1. "Optimal Startup Control of a Jacketed Tubular Reactor," by D. R. Hahn, L. T. Fan, and C. L. Hwang, 11th Joint Automatic Control Conference of the American Automatic Control Council, Paper No. 19-A, pp. 451-461 (1970).

*2. "Control of a Class of Nonlinear Distributed Parameter Systems via Direct Search on the performance Index," by D. R. Hahn, L. T. Fan, and C. L. Hwang, presented at IFAC Kyoto Symposium on Systems Engineering Approach to Computer Control, Kyoto, Japan, August 11-14, 1970, Paper No. 11.4, pp. 170-176.

*3 "Feedforward-Feedback Control of Distributed Parameter Systems," by D. R. Hahn, L. T. Fan, and C. L. Hwang, International Journal of Control vol. 13, pp. 363-382.

*4 "Optimal Wall Temperature Control of a Heat Exchanger," by H. S. Huang, L. T. Fan and C. L. Hwang, Report No. 15, Institute for Systems Design and Optimization, Kansas State University, Manhattan, Kansas (1969).

*5. "Terminal Control of Linear Distributed Parameter System by Linear Programming," by H. S. Huang, L. T. Fan and C. L. Hwang, Report No. 17, Institute for Systems Design and Optimization, Kansas State University, Manhattan, Kansas (1969).

6. "Optimal Startup Control of a Jacketed Tubular Reactor," by D. R. Hahn, L. T. Fan and C. L. Hwang, AIChE Journal (1971, in press).

7. "Optimal Set-Point Change Control of a Tubular Heat Exchanger," by D. R. Hahn, L. T. Fan, and C. L. Hwang, Journal of Institute of Chinese Chemical Engineers (1971, in press).

8. "Optimal Wall Temperature of a Steady State Axial Dispersion Tubular Reactor with a Reversible Reaction," By D. R. Hahn, L. T. Fan and C. L. Hwang, British Chemical Engineer (1971, in Press).

(f) Optimization of Systems Reliability

1. "Optimization by Integer Programming of Constrained Reliability Problems with Several Modes of Failure," by F. A. Tillman, IEEE Transactions on RELIABILITY, R-18, 47-53 (1969). (A69-37069)

2. "Optimal Reliability of Complex System," by F. A. Tillman, C. L. Hwang, L. T. Fan and K. C. Lai, Transaction of IEEE on Reliability, vol. R-19, pp. 95-100 (1970). (A71-26161)

3. "Optimization of System Reliability of Life Support Systems by an Integer Programming," by C. L. Hwang, L. T. Fan, S. Kumar, and F. A. Tillman, AIIE Trans. (1971, in press)

4. "Optimization of Systems Reliability by the Sequential Unconstrained Minimization Technique," by C. L. Hwang, K. C. Lai, F. A. Tillman, and L. T. Fan, submitted for publication, (1970).

(g) Modeling, Simulation and Optimal Control of the Human Thermal System

1. "A Review on Mathematical Models of the Human Thermal System," by L. T. Fan, F. T. Hsu and C. L. Hwang, IEEE Trans. on Bio-Medical Engineering, vol. BME-18, pp. 218-234 (1971). (A71-29400)

*2. "Steady-State Simulation of the Human Thermal System," by L. T. Fan, F. T. Hsu, and C. L. Hwang, presented at 23rd ACEMB--Washington Hilton Hotel, Washington, D.C., Nov. 15-19, 1970, Paper No. 6.24.

*3. "Unsteady-State Simulation of the Human Thermal System," by F. T. Hsu, L. T. Fan and C. L. Hwang, presented at 23rd ACEMB--Washington Hilton Hotel, Washington, D.C., Nov. 15-19, 1970, Paper No. 6.25.

*4. "Steady-State Simulations of the Human Thermal System," by F. T. Hsu, L. T. Fan, and C. L. Hwang, Report No. 23, Institute for Systems Design and Optimization, Kansas State University, Manhattan, Kansas (1970).

5. "An Integrated Human Thermal System and Its Unsteady-State Simulation," by F. T. Hsu, C. L. Hwang, S. A. Konz and L. T. Fan, International J. of Bio-Medical Engineering (1971, in press).

6. "Steady-State Optimization of an Integrated Human Thermal System", by F. T. Hsu, C. L. Hwang, and L. T. Fan, submitted for publication (1971).

(h) Analysis and Optimization of the Water-Vapor Electrolysis Cell

1. "Weight Optimization of a Water-Vapor Electrolysis Cell", by B. C. Pande, L. T. Fan, L. E. Erickson and C. L. Hwang, (under preparation, 1971).

2. "Modeling of the Absorption Chamber of a Water-Vapor Electrolysis Cell," by L. T. Fan, L. E. Erickson, B. C. Pande, L. E. Stamets, and C. L. Hwang (under preparation, 1971).

3. Ionic Transport in Water-Vapor Electrolysis Cell", by L. E. Erickson, B. C. Pande, L. T. Fan, and C. L. Hwang (under preparation, 1971).

(i) Graduate Students' Thesis and Report

M.S. Thesis and Report

1. "Optimization of Preventative Sampling and Stratified Sampling," by T. Janakiraman, M. S. Report (1970).

2. "Optimization of System Reliability of Life Support Systems Using an Integer Programming," by S. Kumar, M. S. Report (1970).

3. "Identification and Optimization of Management and Environmental Systems," by T. W. Choa, M. S. Thesis (1969).

4. "Application of Modern Optimal Control Theory to Environmental Control of Confined Spaces and Life Support Systems," by Y. S. Hwang, M. S. Thesis (1970).

5. "Optimization of Complex Systems Reliability in Life Support Systems by Sequential Unconstrained Minimization Technique," by K. C. Lai, M. S. Report (1970).

6. "Application of Modern Control Theory to the Environmental Control of Confined Spaces," by M. A. Bhandiwad, M. S. Report (1970).

7. "Application of the Maximum Principle to the Optimal Control of Life Support Systems, by G. Nadimuthu, M.S. Report (1971).

8. "Optimal Control of Integrated Human Thermal System by Response Surface Methodology", by H. N. Ozarkar, M.S. Report (1971).

9. "Analysis and Optimization of the Water-Vapor Electrolysis Cell," by B. C. Pande, M. S. Thesis (1971).

Ph.D. Thesis

1. "Modeling, Simulation, and Optimal Control of the Human Thermal System," by F. T. Hsu, Ph.D. Thesis (1971).

(a) 1

Build. Sci. Vol. 4, pp. 133–144. Pergamon Press 1969. Printed in Great Britain

SfB	Ab8
UDC	697.92

Air Flow Models in a Confined Space A Study in Age Distribution

MICHAEL S. K. CHEN*
L. T. FAN*
C. L. HWANG*
E. S. LEE*

It has been shown that a fairly general model for the distribution of air in a confined space can be established based on the concept of the age distribution. The use of such a model in design, data correlation, control, and scale-up problems is discussed and the experimental determination of the model is outlined. It is indicated that some of the parameters of the model can be estimated based on a simple entrainment concept. Results of simulation of the model on digital computer are presented in detail.

INTRODUCTION

A PROPER air distribution is essential in air heating, ventilating, and air-conditioning systems. Even though a system delivers the required quality and quantity of conditioned air (or oxygen) to a confined space such as a room or a space craft or an underground shelter, unsatisfactory conditions result if the air is poorly distributed and improperly circulated. The mechanism of air flow and distribution in a confined space is very complicated. Although, theoretically speaking, the Navier-Stokes equation can be used to represent air flow and distribution in such a system, it is extremely difficult, if not impossible, to solve it exactly. Thus, engineers are often compelled to seek approximate solutions based on simplified assumptions.

In this paper, the concept of age distribution will be used to study the air distribution in a confined space. This concept has been used successfully in the study of mixing in chemical reactors[4, 5]. A fairly general flow model which encompasses several specific flow models based on this concept are proposed. The use of these models in design, data correlation, control, and scale-up problems is discussed. Experimental procedures for verifying the proposed models and predicting the various parameters in the models are also discussed.

The use of the concept of age distribution in the study of mixing and flow in a confined space is especially useful for systems such as an underground shelter, a space craft, and a submarine, where the purity of air is important. Knowing the age distribution of the contaminated air, the optimum way to purify this air for undesirable components may be determined. Furthermore, the impulse response study discussed in this paper should be a useful tool for studying the dynamic behavior of air in a confined space.

* Institute for System Design and Optimization, Kansas State University, Manhattan, Kansas, U.S.A.

SPACE AIR DISTRIBUTIONS AND AGE DISTRIBUTIONS IN A ROOM

A qualitative description of various types of space air distributions is presented in reference[1]. It is based on the results of performance tests of various types of the air outlets at the University of Illinois [2, 3]. Different space air distributions for the following five groups of outlets are discussed in reference[1].

(1) Group *A*. Outlets mounted in or near the ceiling and discharging the air horizontally.

(2) Group *B*. Outlets mounted in or near the floor and discharging the air vertically in a non-spreading jet,

(3) Group *C*. Outlets mounted in or near the floor and discharging the air vertically in a vertical spreading jet,

(4) Group *D*. Outlets mounted in or near the floor and discharging the air horizontally,

(5) Group *E*. Outlets mounted in or near the ceiling and projecting the primary air vertically.

It has been noted that the space air distributions also depend on whether the discharging air is used for heating or cooling. By examining these distributions it has been shown[1] that we can roughly divide the air space into the following zones.

(1) The primary air zone. This is the part of the space from the outlet down to where air velocity becomes approximately 150 ft/min.

(2) The total air zone. This is the space comprising the air discharged from the primary air zone and the entrained air from the general room air motion zone (described below in 4). The air velocity in this zone is still high as it is influenced by the primary air, but less than 150 ft/min. The air temperature is generally within 1°F of the room temperature.

(3) The stagnant zone (or dead space). This is the space where the air velocities are usually low, 15–20 ft/min. It exchanges mass and heat with other zones mainly by natural convection,

(4) The general room air motion zone. This is the part of space in which there is a gentle drift toward the total air zone (i.e. entrainment). Air motion in this space is attributed to the recycle stream of total air.

As an example, let us take the space air distribution of Group A which is shown schematically in figure 1. The side view is shown in figure 2, where A denotes the space of volume V_A comprised of the primary air and total air zones and B denotes the

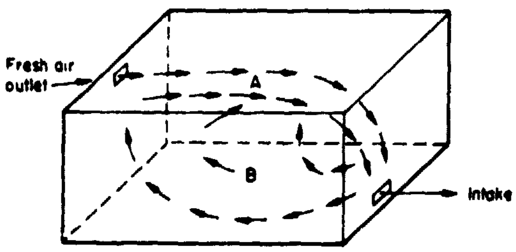

Fig. 1. Typical air flow pattern in a room.

space of volume V_B corresponding to the general room air motion zone. Below zone B is the stagnant zone. This picture can be represented by a flow model which is schematically shown in figure 3. In this flow model, v is the volumetric flow-rate of discharged fresh air and intake air under steady-state condition, βv is the recycle flow rate and V_d is the volume of the stagnant zone which exchanges mass and heat with V_B by natural convective currents. The dotted arrows between V_A and V_B indicate recirculation streams between these two zones. To simplify the discussion, these recirculation streams will be omitted and V_d will be taken as zero in the present treatment.

Each air fluid element upon entering the outlet of duct (or jet) will spend some time in the room before leaving. It is obvious that the exit time of one

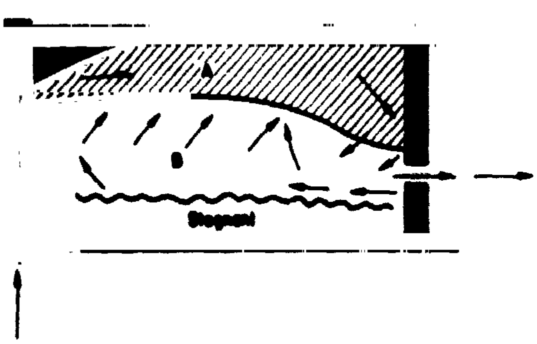

Fig. 2. Typical air flow pattern in a room—side view.

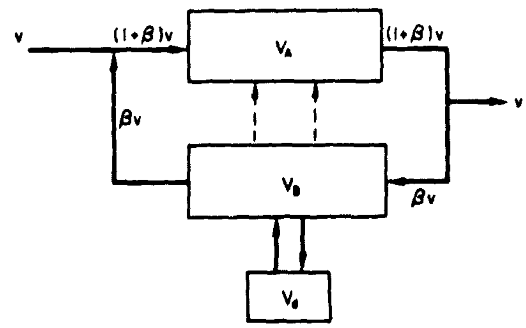

Fig. 3. The schematic diagram of a flow model.

element is different from that of another not only because of the circulation of air stream in the room but because of the internal mixing (due to the turbulence and velocity profile effect, etc.) in each zone. Therefore, there is an *exit age distribution* in the leaving air stream. This exit age distribution will be denoted by $E(t)$. $E(t)\mathrm{d}t$ represents the fraction of the fluid elements in the exit stream having spent the time between t to $t+\mathrm{d}t$ in the room, and

$$\int_0^\infty E(t)\mathrm{d}t = 1. \tag{1}$$

It should be noted that $E(t)$ is completely determined by the space air distribution and the mixing characteristics within the space. On the other hand if we know $E(t)$ from experimental measurements (e.g. by tracer techniques to be discussed later), a flow model characterizing the space air distribution can be established. Note that there may be several possible models which may give rise to the same exit age distribution $E(t)$. However, we can often choose the best by knowing the geometrical, fluid-mechanical, and other physical and chemical characteristics of the system.

Intimately related to the exit age distribution, $E(t)$, is the *internal age distribution*, $I(t)$, which accounts for the distributions of the ages (the lengths of time elapsed since the entrance into the room) of fluid air elements at any moment in the room; $I(t)\mathrm{d}t$ represents the fraction of air with internal age between t and $t+\mathrm{d}t$. We can see that

$$\int_0^\infty I(t)\mathrm{d}t = 1. \tag{2}$$

There is a unique relationship between the two age distributions $E(t)$ and $I(t)$. It has been shown that[4]

$$E(t) = -\bar{t}\,\frac{\mathrm{d}I(t)}{\mathrm{d}t} \tag{3}$$

where

$$\bar{t} = \frac{V}{v} = \text{mean holding time.} \tag{4}$$

It has also been shown[4] that the mean exit age defined by

$$\bar{t}_E = \int_0^{\infty} tE(t)\mathrm{d}t \tag{5}$$

is equal to mean holding time $\bar{t}$ for the enclosed system, i.e.

$$\bar{t} = \bar{t}_E = \frac{V}{v}. \tag{6}$$

Note that this relationship has been shown to hold only for the enclosed systems. When movement into or out of the system can take place in ways other than by bulk flow (e.g. diffusion boundary), $\bar{t} \neq \bar{t}_E$.

These two age distributions, namely, the exit age distribution and the internal age distribution, together with their derived properties such as variances and skewness have been used successfully in characterizing and designing the nonideal flow system in process industries. It is the purpose of this paper to explore their applications to the analysis and design of an air distribution in the enclosed system.

In the following sections, we shall first derive some useful representations of age distributions based on the flow models such as those shown in figures 1-3. Then the determination or prediction of the various parameters in the models will be discussed. Experiments which can be used for this prediction will also be proposed.

DERIVATION OF EXIT AGE DISTRIBUTIONS

In this section, several basic building blocks of flow models will be discussed. They will then be used to obtain age distributions proposed in figure 3.

As discussed earlier, different internal (back) mixing conditions exist in different zones of the space air. To characterize such mixing along the general flow direction, two models, namely, the dispersion model and the completely mixed tanks in series model[5], are often used. The dispersion model is characterized by a diffusion type equation which is useful mainly to represent flow closer to the ideal case of piston flow. The mixed tanks in series model is often used when flow closer to the other extreme case of completely mixed (backmix) flow (i.e. large mixing effect). The latter model appears to describe more closely the mixing in a confined space and will be used in this work.

The completely stirred tank model (CSTM)

This is shown in figure 4. It assumes that each fluid element in the system has equal probability to leave the system no matter how long it has stayed in the system. Define

$\lambda \mathrm{d}t$ = the probability of a fluid element leaving the system during the time interval $(t, t+\mathrm{d}t)$ where λ is a constant, which is independent of time t,

$P(t)$ = the probability of a fluid element to be found in the system at time t.

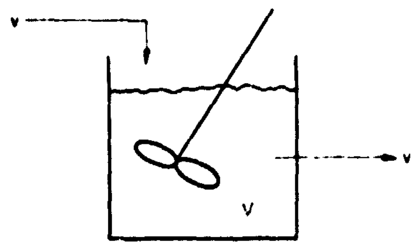

Fig. 4. A completely stirred tank model (CSTM).

Then the probability of a fluid element to be found in the system at time $t+\mathrm{d}t$ is equal to the probability of the fluid element found in the system at time t multiplied by the probability of staying in the system during the interval $(t, t+\mathrm{d}t)$, i.e.

$$P(t+\mathrm{d}t) = (1-\lambda \mathrm{d}t)P(t) \tag{7}$$

or

$$\frac{P(t+\mathrm{d}t)-P(t)}{\mathrm{d}t} = -\lambda P(t). \tag{8}$$

Equation (8) reduces to

$$\frac{\mathrm{d}P(t)}{\mathrm{d}t} = -\lambda P(t). \tag{9}$$

The initial condition is clearly

$$P(0) = 1. \tag{10}$$

The solution of equations (9) and (10) is obtained as

$$P(t) = e^{-\lambda t}. \tag{11}$$

Let T be the random variable representing the exit age of each fluid element. Then the probability of $T < t$ is equal to the probability of the fluid element has left the system at time t. This implies, from equation (11), that

$$\text{Prob}\,(T < t) = 1-e^{-\lambda t}. \tag{12}$$

This equation holds for each fluid element at the exit of the system. Since the probability of the occurrence of a certain event is interpreted as the relative frequency of the occurrence of that event, the probability of $T < t$ is simply the fraction of fluid elements at the exit with age from 0 to t. Equation (12), therefore, can be written as

$$\int_0^t E(t)\mathrm{d}t = 1-e^{-\lambda t}. \tag{13}$$

Differentiating equation (13) yields

$$E(t) = \lambda e^{-\lambda t}. \tag{14}$$

From equations (5), (6), and (14), we can show that

$$\lambda = \frac{1}{\bar{t}} = \frac{1}{\bar{t}_E} = \frac{v}{V}. \tag{15}$$

Therefore, the exit age distribution becomes

$$E(t) = \frac{1}{\bar{t}}\, e^{-t/\bar{t}}. \tag{16}$$

It can be shown through equation (3) that $I(t)$ has the same distribution as $E(t)$. $E(t)$ or $I(t)$ is plotted in figure 5. This distribution function is often called a decay function and is used in designing a ventilation system[6].

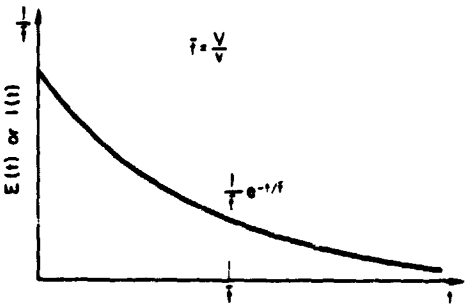

Fig. 5. Age distributions of a CSTM.

The Laplace transform of equation (1) gives the first order transfer function.

$$E(s) = \frac{1}{\bar{t}s+1}, \tag{17}$$

which has been used as the transfer function in connection with the automatic control of room temperature[7], where the time constant is simply the mean holding time $\bar{t}$. In actual space air distribution such as the one shown in figure 1, the transfer function is not of the first order and the major time constant would be quite different from $\bar{t}$.

The n-CSTM in series model

In case the mixing is less complete than the one CSTM, we can use the n-CSTM in series model with the fixed total volume to characterize the system as shown in figure 6. Volumes may be different or simply equal from tank to tank depending on how the mode of mixing changes along the flow. For simplicity we assume that the volumes of tanks are equal in this work. Then the number of tanks used represents the degree of mixing in the flow system.

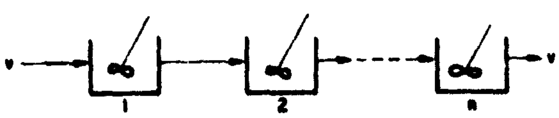

Fig. 6. The n-CSTM in series model.

To obtain the exit age distribution for this model, let us define the random time T_i, $i = 1, 2, \ldots, n$ be the exit age of each fluid element at tank i, $i = 1, 2, \ldots, n$. Each of this exit random time through each tank is independently and identically distributed as given by equation (16), i.e.,

$$E_i(t) = \frac{1}{\bar{t}_i}\, e^{-t/\bar{t}_i}, \qquad i = 1, 2, \ldots, n \tag{18}$$

where

$$\bar{t}_i = \frac{\bar{t}}{n}, \qquad i = 1, 2, \ldots, n. \tag{19}$$

Combining equations (18) and (19) gives

$$E_i(t) = \frac{n}{\bar{t}}\, e^{-nt/\bar{t}}, \qquad i = 1, 2, \ldots, n. \tag{20}$$

The overall exit age distribution can be derived as follows;

the total exit random time T is

$$T = T_1 + T_2 + \ldots + T_n. \tag{21}$$

The characteristic function of T_i and that of T are defined respectively as

$$\psi_{T_i}(u) = \int_{-\infty}^{\infty} e^{iut} E_i(t)\,dt = E[e^{iuT_i}] \tag{22}$$

and

$$\psi_T(u) = \int_{-\infty}^{\infty} e^{iut} E(t)\,dt = E[e^{iuT}]$$

where the second E in each equation above is the expectation operator.

From equations (20) and (22), it can be shown that[8]

$$\psi_{T_i}(u) = [1 - iu(\bar{t}/n)]^{-1}, \qquad i = 1, 2, \ldots, n \tag{23}$$

and

$$\begin{aligned}\psi_T(u) &= E[e^{iuT}] \\ &= E[e^{iu(T_1+T_2+\ldots+T_n)}] \\ &= E[e^{iuT_1}]\,E[e^{iuT_2}]\ldots E[e^{iuT_n}] \\ &= \psi_{T_1}(u)\,\psi_{T_2}(u)\ldots\psi_{T_n}(u)\end{aligned}$$

since the expectation of the product of mutually independent variables, $e^{iuT_1}, e^{iuT_2}, e^{iuT_3}, \ldots, e^{iuT_n}$, is equal to the product of their expectations,

$$E[e^{iuT_1}], E[e^{iuT_2}] \ldots, E[e^{iuT_n}]$$

or

$$\psi_T(u) = [\psi_{T_i}(u)]^n. \tag{24}$$

Subtituting equation (23) into equation (24) yields

$$\psi_T(u) = [1 - iu(\bar{t}/n)]^{-n}. \tag{25}$$

The density function of $\psi_T(u)$ is well known[8] and is given by

$$E(t) = \left(\frac{n}{\bar{t}}\right) e^{-nt/\bar{t}} \frac{(nt/\bar{t})^{n-1}}{(n-1)!}. \qquad (26)$$

This is the desired exit age distribution of the n-CSTM in series model. It is more convenient to express it in dimensionless form by noting that

$$1 = \int_0^{\infty} E(t)\mathrm{d}t = \int_0^{\infty} \bar{t}E(t/\bar{t})\,\mathrm{d}(t/\bar{t}) = \int_0^{\infty} \bar{t}E(t/\bar{t})\mathrm{d}\theta$$

$$= \int_0^{\infty} E(\theta)\mathrm{d}\theta$$

where

$$E(\theta) = \bar{t}E(t) = n^n e^{-n\theta} \frac{\theta^{n-1}}{(n-1)!}. \qquad (27)$$

Equation (27) is plotted for various values of n in figure 7. For $n = 1$, equation (26) reduces to equation (16) of the one CSTM model. As we can see from figure 7, as n increases, the peak increases

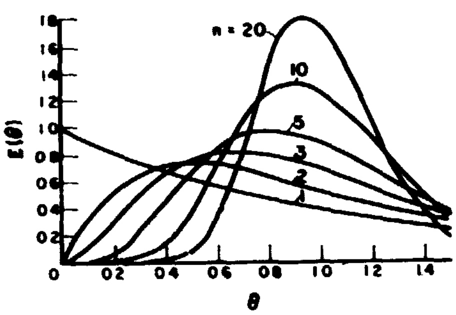

Fig. 7. Dimensionless exit age distribution of the n-CSTM in series model.

and this peak shifts to the right asymtotically to $\theta = 1$. This can be shown by differentiating equation (26) and then setting the results equal to zero. This gives

$$\theta_{\max} = \frac{n-1}{n} \qquad (28)$$

or

$$t_{\max} = \left(\frac{n-1}{n}\right)\bar{t}. \qquad (29)$$

The above information is useful in evaluating the values of the parameters and will be discussed later. It can be shown that[5]

$$\text{mean: } \bar{\theta} = 1 \qquad (30)$$

$$\text{variance: } \sigma^2 = \frac{1}{n}. \qquad (31)$$

Equation (31) indicates the significance of parameter n in characterizing the degree of mixing for the system. If we substitute s for $(-iu)$ in equation (25), we obtain the transfer function for the n-CSTM system

$$E(s) = \frac{1}{[(\bar{t}/n)s + 1]^n}. \qquad (32)$$

Now, if we make use of this model to characterize the mixing both in zone A and zone B in the space air distribution described in the preceding section (see figures 1, 2, and 3), we can obtain the age distribution for the whole system. Let T be the random exit age of each fluid element of the system. Then

$$T = T_1 + T_2 + \ldots + T_{2M+1} \qquad (33)$$

where M is a random number representing the recycle passes with probability density function pq^m. When $M = m$, and $m = 1, 2, \ldots, q$ is the probability of recycle for each pass and is equal to $\beta v/(1+\beta)v = \beta/(1+\beta)$; while p is the probability of leaving and is equal to $1 - q = 1/(1+\beta)$. pq^m is the probability of each fluid element having m recycles before leaving the system so that T_i, $i = 1, 3, 5, \ldots, 2M+1$ is the time each element has to spend through zone A and T_i, $i = 2, 4, \ldots, 2M$ is the time through zone B. By using the method of the characteristic function[8], we obtain

$$\begin{aligned}
\psi_T(u) &= E\{e^{iu(T_1+T_2+\ldots+T_{2M+1})}\} \\
&= E_M\{E[e^{iu(T_1+T_2+\ldots+T_{2M+1})} \mid M]\}^* \\
&= E_M\{(E[e^{iuT_A}])^{M+1}(E[e^{iuT_B}])^M\} \\
&= E_M\left\{\left(1 - iu\frac{\bar{t}_A}{n_A}\right)^{-(M+1)n_A}\left(1 - iu\frac{\bar{t}_B}{n_B}\right)^{-Mn_B}\right\} \\
&= \sum_{m=0}^{\infty}\left(1 - iu\frac{\bar{t}_A}{n_A}\right)^{-n_A(m+1)}\left(1 - iu\frac{\bar{t}_B}{n_B}\right)^{-n_B m} pq^m \\
&= p\left(1 - iu\frac{\bar{t}_A}{n_A}\right)^{-n_A}\sum_{m=0}^{\infty} \\
&\qquad \left[\left(1 - iu\frac{\bar{t}_A}{n_A}\right)^{-n_A}\left(1 - iu\frac{\bar{t}_B}{n_B}\right)^{-n_B} q\right]^m \\
&= \frac{p(1 - iu[\bar{t}_A/n_A])^{-n_A}}{1 - (1 - iu[\bar{t}_A/n_A])(1 - iu[\bar{t}_B/n_B])^{-n_B}}
\end{aligned}$$

or

$$\psi_T(u) = \frac{(1 - iu[\bar{t}_A/n_A])^{-n_A}}{(1+\beta) - \beta(1 - iu[\bar{t}_A/n_A])^{-n_A}(1 - iu[\bar{t}_B/n_B])^{-n_B}} \qquad (34)$$

where

$$\bar{t}_A = \frac{V_A}{(1+\beta)v}, \quad \bar{t}_B = \frac{V_B}{\beta v},$$

* $E[\,.\mid M]$ denotes the conditional expectation of $\exp[iu(T_1 + T_2 + \ldots + T_{2M+1})]$ given that M equals to any positive integers. $E_M\{.\}$ denotes the expectation of random variable M.

and n_A and n_B are the values of the parameters of the models representing zones A and B respectively. The transfer function of it can be obtained by substituting s for $(-iu)$ in equation (34).

$$E(s) = \frac{(1+s[\bar{t}_A/n_A])^{-n_A}}{(1+\beta)-\beta(1+s[\bar{t}_A/n_A])^{-n_A}(1+s[\bar{t}_B/n_B])^{-n_B}}. \tag{35}$$

The inverse transform or exit age distribution of equation (35) in general has no analytic expression, but we can often simulate it on an analog or a digital computer if we know the values of parameters β, n_A, n_B, $\bar{t}_A$ and $\bar{t}_B$. A typical exit age distribution $E(t)$ for the proposed flow model is shown in figure 8.

SIMULATION

It is often more convenient to write equation (35) in the dimensionless form

$$E(s') = \frac{(1+s'[\theta_A/n_A])^{-n_A}}{(1+\beta)-\beta(1+s'[\theta_A/n_A])^{-n_A}(1+s'[\theta_B/n_B])^{-n_B}} \tag{36}$$

where

$$s' = s\bar{t}$$
$$\theta_A = \bar{t}_A/\bar{t}$$
$$\theta_B = \bar{t}_B/\bar{t}.$$

Note that these five parameters β, n_A, n_B, θ_A and θ_B are not all independent. They must satisfy the equations

$$V = V_A + V_B$$
$$\bar{t} = \frac{V}{v}$$
$$= \frac{V_A}{v}+\frac{V_B}{v}$$
$$= \frac{V_A}{(1+\beta)v}(1+\beta)+\frac{V_B}{\beta v}.\beta$$
$$= (1+\beta)\bar{t}_A+\beta\bar{t}_B$$

or

$$1 = (1+\beta)\theta_A+\beta\theta_B. \tag{37}$$

Besides, since β, θ_A and θ_B are non-negative quantities, the following two natural constraints exist.

$$0 \leq (1+\beta)\theta_A \leq 1 \tag{38}$$

$$0 \leq \beta\theta_B \leq 1. \tag{39}$$

In the simulation of equation (36), the constraint as given by equations (37), (38), and (39) must be taken into consideration. Several specific examples are presented below.

Case 1. $n_B = \beta = 0$

Equation (36) reduces to

$$E(s') = \left(1+s'\frac{\theta_A}{n_A}\right)^{-n_A} \tag{40}$$

and its inverse transform is equation (27) and is shown in figure 7.

Case 2. $n_A = n_B = 1$

Equation (36) reduces to

$$E(s') = \frac{1+\theta_B s'}{(1+\beta)\theta_A\theta_B s'^2+(1+\beta)(\theta_A+\theta_B)s'+1} \tag{41}$$

and the inverse can be obtained analytically as

$$E(\theta) = \frac{ca-b}{c-d}e^{-c\theta}+\frac{da-b}{d-c}e^{-d\theta} \tag{42}$$

where

$$a = \frac{1}{(1+\beta)\theta_A}$$

$$b = \frac{1}{(1+\beta)\theta_A\theta_B}$$

$$c = \frac{(\theta_A+\theta_B)+\sqrt{\{(\theta_A+\theta_B)^2-4\theta_A\theta_B/(1+\beta)\}}}{2\theta_A\theta_B}$$

$$d = \frac{(\theta_A+\theta_B)-\sqrt{\{(\theta_A+\theta_B)^2-4\theta_A\theta_B/(1+\beta)\}}}{2\theta_A\theta_B}.$$

Figures 9 and 10 show the simulated results for case 2 with β and θ_A as parameters.

Case 3. $n_A = 2, n_B = 1$.

The inverse transform for this case can also be obtained analytically. The expression can be found in any Laplace transform table. Figures 11 and 12 show dimensionless aged distributions for $\beta = 0{\cdot}1$ and 1 with θ_A as the parameter. It should be observed from these curves that peaks exist and shift

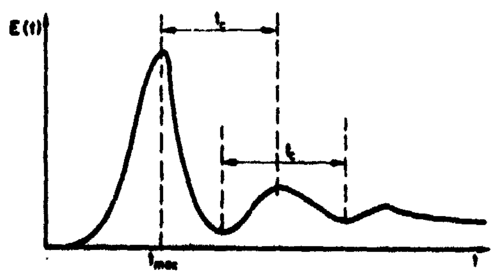

Fig. 8. Exit age distribution of the proposed model.

away from the ordinate as θ_A increases. These indicate quite different characteristics from the preceding two cases where all curves exhibit a similar exponential type of decay as θ increases.

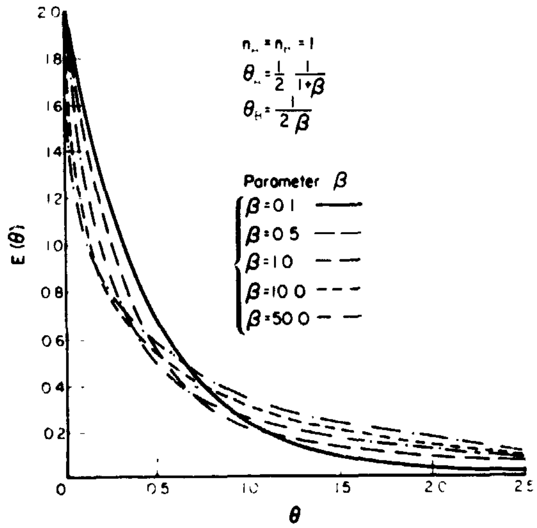

Fig. 9. Dimensionless exit age distribution for $n_A = n_B = 1$, $\theta_A = 1/2(1+\beta)$, $\theta_B = 1/2\beta$ with β as parameter.

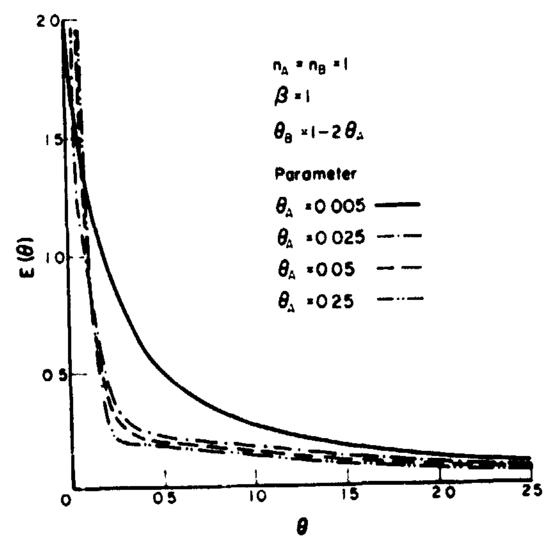

Fig. 10. Dimensionless exit age distribution for $n_A = n_B = 1$, $\beta = 1$, $\theta_B = 1-2\theta_A$ with θ_A as the parameter.

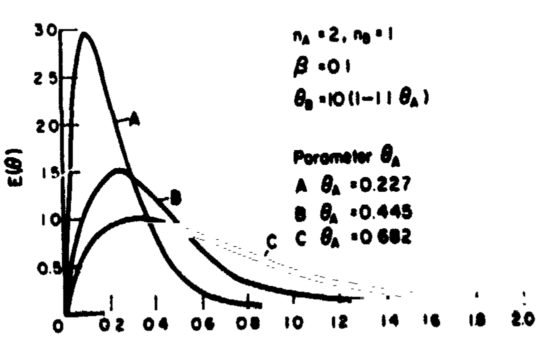

Fig. 11. Dimensionless exit age distribution for $n_A = 2$, $n_B = 1$, $\beta = 0.1$, $\theta_B = 10(1-1.1\theta_A)$ with θ_A as the parameter.

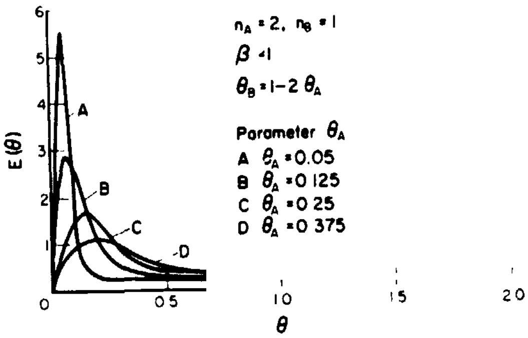

Fig. 12. Dimensionless exit age distribution for $n_A = 2$, $n_B = 1$, $\beta = 1$, $\theta_B = 1-2\theta_A$ with θ_A as the parameter.

Case 4. $n_A = n_B = 2$.

Figure 13 shows the age distribution with β as parameter. It can be seen that as β increases, the peak not only shifts toward the origin, but the second peak starts to take shape. It can be shown that such a phenomenon of the existence of two peaks in the age distribution can occur only when both n_A and n_B are greater than 2.

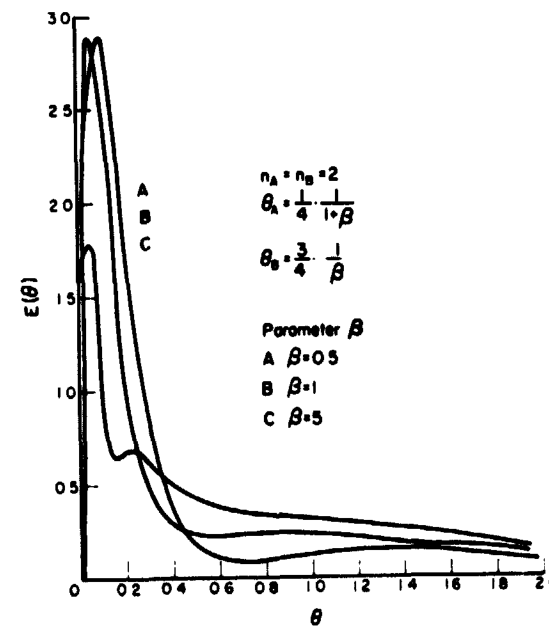

Fig. 13. Dimensionless exit age distribution for $n_A = n_B = 2$, $\theta = \frac{1}{4}[1/(1+\beta)]$, $\theta_B = \frac{3}{4}(1/\beta)$ with β as parameter.

If n_A and n_B go beyond 2, it will be extremely difficult to obtain analytically the inverse transform of equation (36).

A numerical solution with the aid of a digital computer to simulate the flow model for $(n_A + n_B)$ up to 36 will be discussed. Equation (36) can be reduced to the form

$$E(s') = \frac{A^{n_A}}{1+\beta}\,\frac{(B+s')^{n_B}}{(A+s')^{n_A}(B+s')^{n_B}-\beta A^{n_A}B^{n_B}}$$

$$= \frac{A^{n_A}}{1+\beta}\,\frac{(B+s')^{n_B}}{H(s')} \qquad (43)$$

where $$A=\frac{n_A}{\theta_A}$$

$$B=\frac{n_B}{\theta_B}.$$

Since the denominator $H(s')$ is a polynomial of s' with order (n_A+n_B), $H(s')$ can be represented by

$$H(s') = (s'-r_1)(s'-r_2)\ldots(s'-r_{n_A+n_B}) \quad (44)$$

where $r_1, r_2, \ldots, r_{n_A+n_B}$ are its roots (complex in general). If these roots are all separated, the inverse transform of each root will be

$$y_i(\theta) = \frac{A^{n_A}}{1+\beta}\,\frac{(B+r_i)^{n_B}}{\underset{j\neq i}{\pi}\,(r_i-r_j)}\,e^{r_i\theta},$$

$$i = 1, 2, \ldots, (n_A+n_B). \quad (45)$$

Furthermore, for a complex root r_i, $y_i(\theta)$ can be written as

$$y_i(\theta) = \frac{A^{n_A}}{1+\beta}\,\frac{(B+r_i)^{n_B}}{\underset{j\neq i}{\pi}\,(r_i-r_j)}\,e^{RR_i\theta}$$

$$(\cos RI_i\theta + j\sin RI_i\theta) \quad (46)$$

where RR_i and RI_i are the real part and the imaginary part of the complex root r_i respectively.

The exist age distribution is then

$$E(\theta) = y(\theta) = \sum_{i=1}^{n_A+n_B} y_i(\theta). \quad (47)$$

A computer flow chart for simulating the proposed flow model is shown in figures 14, 15, and 16. $E(\theta)$ for the case $n_A = 10$ and $n_B = 5$, is shown in figure 17.

TRACER EXPERIMENTS, IMPULSE RESPONSE, AND THE DETERMINATION OF MODEL PARAMETERS

Tracer experiments

A small quantity of a gaseous tracer such as H_2, CO_2 or Freon-12 can be injected impulsively at the inlet stream and the exit concentration of the tracer is monitored and recorded continuously at the air exit. This impulse response corresponds to the exit age distribution. The following factors can be systematically varied and parametrically studied.

(a) Air (or gas) flow rate v through the system,
(b) Size and shape (circular or slot etc.) of the nozzle or air jet,
(c) Relative position of air discharge and intake of the system,
(d) Internal pressure and temperature at various positions inside the system,
(e) Volume and dimensions of the system.

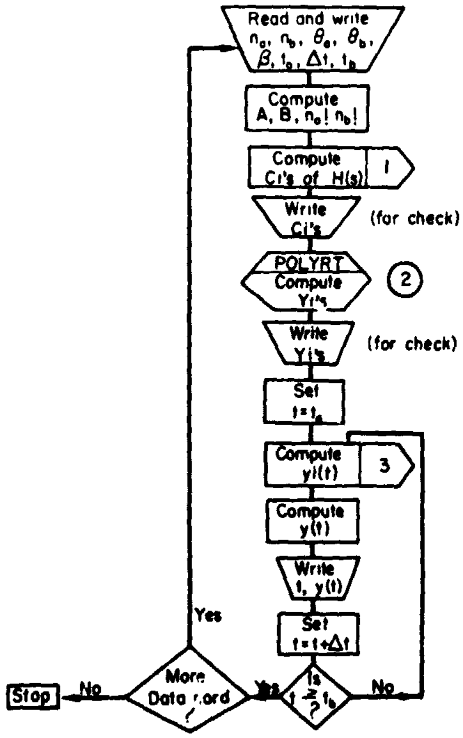

② POLYRT is an IBM's subroutine for calculating the complex and real roots of a real polynomial

Fig. 14. Computer flowchart of obtaining exit age distribution $E(\theta)$.

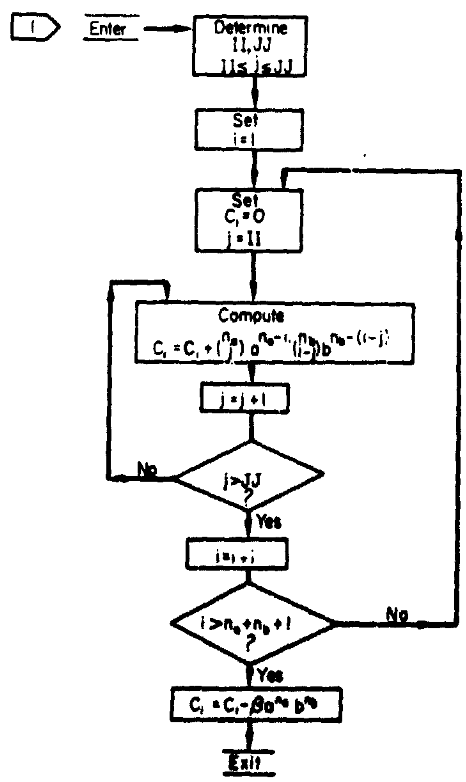

Fig. 15. Computer flowchart of computing the coefficients in the polynomial $H(S')$.

At the initial stage of the investigation each parameter should be observed independently by changing only one parameter at a time. However, effects of interactions among the various parameters on the exit age distribution must then be studied to find the scale-up factors.

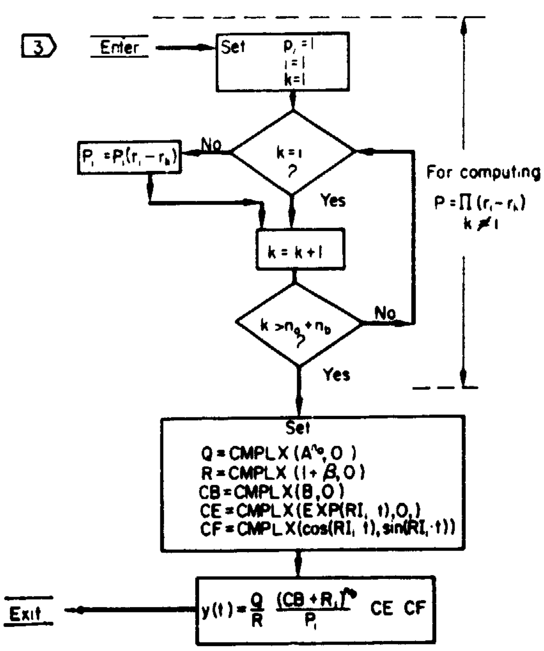

Fig. 16. Computer flowchart of computing the inverse transform of each complex root.

Determination of model parameters from response curves

There are five apparent parameters of the model described by equation (35) in the preceding section; the recycle constant β, the mean residence times $\bar{t}$ and $\bar{t}_B$, and the mixing indices n_A and n_B. These parameters can be determined from tracer responses to impulse inputs such as the one shown in figure 8. It is seen that the time t_c between two peaks or two valleys would be the mean recirculation time of each fluid element such that

$$t_c = \frac{\text{total volume}}{\text{internal flow rate}} = \frac{V}{\beta v}. \tag{48}$$

Note that the internal flow rate through zone A is $(1+\beta)v$ which is different from the internal flow rate through zone B, βv. Since β is in general much greater than 1, the overall internal flow rate is taken βv for simplicity.

It was found[9] that in a cylindrical vessel having jet nozzles at the inlet and outlet respectively and filled with water, when the response curves were plotted in the dimensionless form, $E(\theta)$ vs. θ (or $t/\bar{t}$), they were remarkably similar to each other with various flow rates for a given nozzle size. These results indicate that for a given nozzle diameter, a flow pattern is established, which is essentially independent of flow rates. Hence it also implies that within the experimental range, the

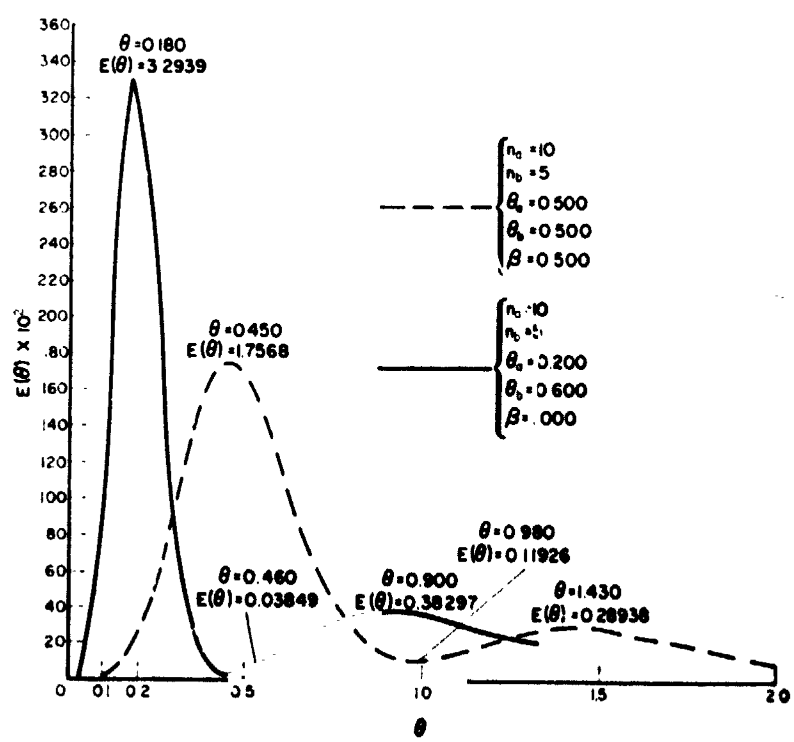

Fig. 17. Dimensionless exit age distribution for $n_A = 10$, $n_B = 5$.

c

dimensionless circulation time $\theta_c = t_c/\bar{t}$ is independent of flow rate and is only a function of nozzle size. It would be very important to see if the same property holds for the air flow system. We can test this by plotting t_c vs. $1/v$ for various nozzle diameters as shown in figure 18. If it turns out to be

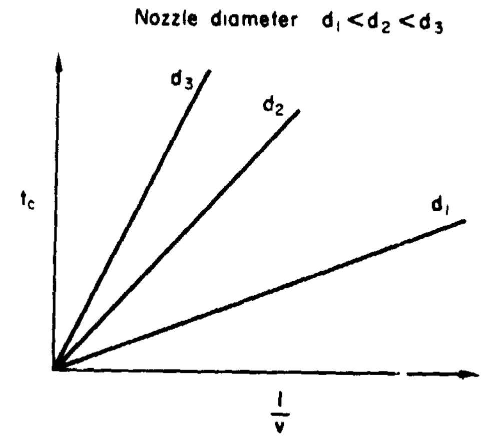

Fig. 18. Circulation time versus inverse of flow rate for various nozzle size.

a straight line for a given nozzle size, then $\theta_c = t_c/\bar{t}$ is independent of flow rate v. It follows from equation (36) that

$$\theta_c = \frac{t_c}{\bar{t}} = \frac{1}{\beta}. \qquad (49)$$

Equation (37) is essentially saying that the recycle constant β can be found from the dimensionless circulation time θ_c, and is a function of the nozzle size only. This then establishes the method for the determination of the first parameter β, the recycle constant.

On the other hand, a good prediction of the recycle constant β is possible on the basis of a simple entrainment concept. It has been assumed that the recirculation flow in the room is entirely promoted by entrainment in the inlet jet.

Equations for the entrainment of circular jets and of jets from long slots have been mathematically presented in ref.[1]. They are

$$\beta = \frac{\beta v}{v} = \frac{\text{entrained flow}}{\text{initial flow}} = \frac{2}{K'} \frac{X}{\sqrt{A_0}} \quad \text{(circular jets)} \qquad (50)$$

$$\beta = \frac{\beta v}{v} = \frac{\text{entrained flow}}{\text{initial flow}} = \sqrt{\left(\frac{2}{K'}\right)}\sqrt{\left(\frac{X}{H_0}\right)} \quad \text{(long slots)} \qquad (51)$$

where

X = distance from face of outlet,

A_0 = effective area of the stream at discharge from an open end duct or at a contracted section.

H_0 = width of slot,

K' = proportional constant, approximately 7.

For a given vessel the entrainment distance can roughly be assumed constant. Equations (38) and (39) require that β is inversely proportional to the nozzle size. Experimental values of $1/\beta$, found from the dimensionless circulation time can be plotted against nozzle diameter d as shown in figure 19.

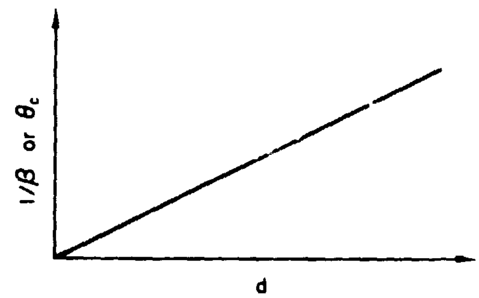

Fig. 19. Influence of nozzle diameter on recycle constant.

A circular jet has been assumed. If it turns out to be a straight line, it will justify partially the use of the proposed model. Also from the slope of the line, one can estimate the actual distance the fluid elements travel.

Once we have determined the recycle constant β, the other four parameters can be determined as follows.

The height and the time t_{max} of the first peak in the response curve are completely determined by the flow condition through zone A. Equation (29) can be written in the dimensionless form as

$$\theta_{max} = \left(\frac{n_A - 1}{n_A}\right)\bar{\theta}_A \qquad (52)$$

where

$$\theta_{max} = \frac{t_{max}}{\bar{t}}, \quad \bar{\theta}_A = \frac{\bar{t}_A}{\bar{t}}.$$

Equation (26) can also be written in a dimensionless form for zone A as

$$E_A(\theta) = \bar{t}\,E_A(t) = \frac{n_A}{\bar{\theta}_A} \frac{\left(\frac{n_A \theta}{\bar{\theta}_A}\right)^{n_A - 1}}{(n_A - 1)!} e^{-(n_A\theta/\bar{t}_A)} \qquad (53)$$

For a given θ_{max} and height of the first peak we can determine $\bar{\theta}_A$ and n_A uniquely by a trial-and-error procedure.

Having established $\bar{\theta}_A$, $\bar{\theta}_B$ is readily found since

$$\theta_c = \bar{\theta}_A + \bar{\theta}_B. \tag{54}$$

Note that $\bar{\theta}_B$ is uniquely determined from θ_c and $\bar{\theta}_A$, and θ_c is determined from equation (49). We may reduce the number of parameters from five to four.

The last parameter n_B can be found by trial-and-error until the simulated response of equation (35) matches the experimental one.

DISCUSSION

A flow model with four parameters is proposed to describe a typical space air distribution in a room. It is indicated that the exit age distribution $E(t)$ or $E(\theta)$ can be determined by using a impulse tracer experiment and various parameters of the model, in turn, can be determined from $E(t)$. It is also shown that the model can be partially justified on the basis of a simple entrainment theory of air jets.

This model is believed to be useful because the model parameters are closely related to physical quantities of the system. The recycle constant β is the reciprocal of the dimensionless circulation time θ_c. The mean residence times $\bar{\theta}_A$ and $\bar{\theta}_B$ of zone A and zone B respectively account for the mean time each fluid element must spend in zone A and zone B of the system. The mixing indices n_A and n_B are useful in understanding the mixing characteristics in both zones. These informations are directly helpful in the design, data correlation, and scale-up of the system represented by the model.

For the ventilation problem in a room equation (35) is a more realistic model than the decay function[6]. The same equation with some modification (with enthalpy balance including heat source and the location of temperature measuring element) can be used in the closed loop automatic control system of room temperature.

The model proposed in this paper is only one of the many applications of flow models based on the concept of age distributions. The same approach can be intelligently employed for the study of other types of space air distributions.

Acknowledgements—This work was supported in part by the Air Force Office of Scientific Research, Office of Aerospace Research, United States Air Force, under Contract F44620-68-C-0020, (Themis Project), and by NASA Grant No. 17-001-034.

REFERENCES

1. *ASHRAE Guide and Data Book*, Space Air Distribution, Chapter 29, pp. 537–552 (1965).
2. H. E. Straub, S. F. Gilman and S. Konzo, Distribution of air within a room for year round air conditioning—Part I, *Univ. Illinois Exp. Stn. Bull.*, No. 435 (1956).
3. H. E. Straub and M. M. Chen, Distribution of air within a room for year round air conditioning—Part II, *Univ. Illinois Exp. Stn. Bull.*, No. 442 (1957).
4. P. V. Danckwerts, Continuous flow systems, *Chem. Eng Sci.*, 2 (1), 1 (1953).
5. O. Levenspiel and K. B. Bischoff, Patterns of Flow in Chemical Process Vessels, *Advances in Chemical Engineering*, Vol. 4, pp. 95–198, Academic Press, N. Y. (1963).
6. W. P. Jones, *Air conditioning engineering*, Chapter 17, pp. 460–472, Edward Arnold, Glasgow (1967).
7. R. O. Zermuehlen and H. L. Harrison, Room temperature response to a sudden heat disturbance input, *ASHRAE Trans.* 71 (1), 206–211 (1965).
8. E. Parzen, *Stochastic processes*, p. 14, Table 1.2, Holden-Day, San Francisco (1962).
9. G. T. Clegg and R Coates, A flow model for a filled cylindrical vessel, *Chem. Engng Sci.* 22, 1177 (1967).

Es ist gezeigt worden, dass ein ziemlich allgemeines Modell für die Luftverteilung in einem begrenzten Raum auf Grund der Auffassung über Altersverteilung festgelegt werden kann. Die Verwendung eines solchen Modells In Entwurfs-, Datenwechselbeziehungen-, Kontroll- und Bemessungs-problemen wird besprochen und die experimentale Festlegung eines solchen Modells wird umrissen. Es wird darauf hingewiesen, dass einige Parameter des Modells auf Grund einer einfachen Strömungsauffassung geschätzt werden können. Simulationsergebnisses des Modells aufDigitalrechnern werden in Einzelheiten dargelegt.

Il a été démontré qu'un modèle assez général de distribution d'air dans un espace restreint peut être établi sur la base du concept de la distribution d'age. L'utilisation d'un tel modèle en fonction de la conception, de la corrélation des données, du contrôle et des problèmes de la mise à l'échelle est discutés et la détermination expérimentale du modèle est tracée. Il est indiqué que certains paramètres de modèle peuvent être estimés sur la base d'une conception d'enchaînement simple. Les résultats de simulation du modèle sur un ordinateur numérique sont donnés en détail.

(b) 1

SEVERAL DIFFERENT GAS-LIQUID CONTACTORS UTILIZING CENTRIFUGAL FORCE

Report No. 10

T. Takahashi and L. T. Fan

Institute for Systems Design and Optimization

KANSAS STATE UNIVERSITY MANHATTAN

Several Different Gas-Liquid
Contactors Utilizing Centrifugal Force*

by

T. Takahashi

L. T. Fan

December 19, 1968

DEPARTMENT OF CHEMICAL ENGINEERING

KANSAS STATE UNIVERSITY

MANHATTAN, KANSAS 66502

*This work was partially supported financially by NASA (Grant 17-001-034) and AFOSR (Grant USAFOSR F44620-68-C-0020).

Various types of contactors utilizing centrifugal force (centrifugal contactors) have been used commercially especially in the chemical industry for production of petro chemicals, organics, and pharamacenticals, for refining petroleum, and for other purposes. The centrifugal contactors have been known to have characteristics of high efficiency, large gas and liquid through-put, small liquid holdup, and short contact time.

Centrifugal contactors can be classified according to methods of utilizing the centrifugal force as follows (1):

i) Tray type. In this type of contactor, kinetic energy of the gas from the lower tray is used to impart centrifugal motion to the liquid on the upper tray.

ii) Mechanically agitated type. In this type of contactor, gas or liquid in the contactor is mechanically agitated to increase interfacial area by atomizing dispersion of fluid, and to reduce resistance for mass transfer at the interface by disturbance induced in both fluid phases. The column or tank with an agitator, and the apparatus with a rotating part have been invented for this purpose.

iii) Rotating type. This type of contactor consists of multistage concentric cylinders fixed to a rotating shaft. The gas and liquid in the contactor are brought into contact cocurrently or cross currently.

Since it is difficult to give a detailed description of all types of contactors utilizing centrifugal force, emphasis will be placed on the description of the fluid dynamical and mass transfer aspects of several specific types such as the rotational current tray, the rotating concentric column, Piazza type contactor, Podobielniak contactor, and centrifugal contactor of the rotating type, investigated by the first author. These contactors are currently employed for industrial distillation, absorption, and humidification. It is expected that the centrifugal contactor of the rotating type which consists of all rotating parts will be applied in the near future to the life support of men in space crafts, air planes, submarines and civil defense shelters, and to prevention of air pollution because of its compactness and other advantages. It also appears that it can be used as a blood oxygenator.

1. Tray types

Various tray type systems in which mass transfer operations are carried out have been developed and employed industrially. In a plate column, when the gravitational force is the only force affecting phase separation, the vapor velocity and resulting liquid entrainment in the column may set the maximum allowable vapor velocity and liquid velocity. However, if the centrifugal force is used to separate the entrainment, the capacity of such a tray may be increased.

In the system constructed by Manning (2), the column wall is used as the outer cylinder of a cyclone, and the contacting of gas and liquid takes place on a small perforated tray section which receives liquid from the tray above and vapor from the tray below. The two-phase mixture is discharged tangentially into the settling zone. The liquid is forced outward against the column wall by centrifugal force and flows into the downcomer leading to the next lower tray. The vapor enters the tray above through a conduit located inwardly from the column shell. It has been reported that the through-put of this tray is larger than those of many other trays (2).

In contrast to Manning's tray, the Kittel tray (3) and the rotational current tray (4,5) are designed so that the flow of the ascending gas or vapor is directed almost horizontally across the tray surface through the openings.

The Kittel tray consists of a pair of upper and lower grids, and each one is divided into six equal basic parts. The openings in the tray are in the shape of slots inclined at an angle to the horizontal plane of the grids. Thus some of the energy associated with the gas pressure drop is utilized to give centrifugal and centripetal motion to the liquid on the tray. That is, on the upper grid this motion is towards the wall of the column and on the lower grid towards the center. Because of the absence of the overflow weir and downcomer area, the free cross-sectional area of the Kittel tray is more than that of the sieve tray. Detailed review of this tray has been reported (3).

In the following paragraphs, emphasis will be placed on the description of the performance of the rotational current tray. The structure of the tray is shown in Figure 1. The shape of holes in the tray is a half ellipse, and it has a guide inclined at an angle to the surface of the tray. As shown in the figure there are two types of the rotational current tray, the upper guide tray (U.G.T.) and the down guide tray (D.G.T.). The liquid on the tray is carried along by gas and is brought into intimate contact with the gas. For this reason, the tray has many advantages in comparison with other trays.

In Figures 2 and 3, the pressure drop of gas flow through a tray and the liquid holdup on a tray of this type are compared with some trays of the counter current type without downcomer (4). It can be concluded that the pressure drop through the D.G.T. is smaller than those through other trays. It is, therefore, expected that a larger volume of gas can be treated with this type of tray than with other trays. Furthermore, it is interesting to note that the behavior of the tray is similar to that of the Ripple tray, as shown in Figure 2. From Figure 3, it is also evident that the liquid holdup on the D.G.T. is smaller than those of other types. This is probably due to the fact that the falling of liquid through the tray is made easy by the down guide.

The residence time of liquid on the tray was measured experimentally, and the desorption experiments were carried out by using the water-oxygen-air system to determine the liquid phase resistance to the mass transfer (5). The gas absorption experiments were carried out by using the water-ammonia-air system to determine the gas phase reisitance to the mass transfer (5). The results of these experiments have indicated that the gas flow rate and the residence time of liquid on the tray control strongly the plate efficiency. The Murphree plate efficiency of this tray for gas absorption based on the liquid phase is compared with those of other types of trays as shown in Figure 4. It can be concluded that the rotational current tray can be operated at high efficiency up to large gas flow rate.

The tray type centrifugal contactors are used for gas cleaning and dust collection in air pollution control. One particular tray, the Kettel tray, has been extensively used for air pollution control in Europe.

2. Mechanically agitated types

The rotating cone column (6, 7), the rotating basket column, the rotating flat plate column, and the spinning band column (8, 9, 10) belong to this class of distillation columns, each containing a rotating agitator which disturbs both the gas and liquid phases. The small laboratory scale columns of these types perform excellently and are effective for the separation of components from a mixture with a narrow boiling temperature range, for instance, the separation of isotopes (6). The mechanism of flow of both gas and liquid in these systems is not yet well known and the prediction of the capacity in these systems can not be made accurately. Therefore, it is difficult to design a commercial tower of this type.

The rotating concentric tube distilling column (11) is similar to the rotating cone column, the rotating basket column, the rotating flat plate column, and the spinning band column. The column has the characteristics of the small liquid holdup and the low pressure drop which is similar to that of the wetted wall column, and of the high flow rate. The liquid contacts with the vapor in the narrow annular space between the stationary outer cylinder and the rotating inner cylinder. The mass transfer coefficient increases as the speed of the rotor becomes greater because the flow of vapor is disturbed by the rotation of the inner cylinder. This can be seen from the results of the investigation by Taylor (12) and Lewis (13), who studied theoretically and experimentally the mechanism of fluid flow in an annular space between the rotating double cylinder. It has been theoretically determined that the efficiency of distillation increases with the increase in the degree of turbulence in the vapor phase and with the decrease in the annular space and in the flow rate through the annular space (14). This fact has also been confirmed experimentally (15, 16, 17, 18).

Willingham and coworkers (11) carried out experiments in a column with a diameter of 9.62 cm and a height of 58.4 cm. The column was provided with a rotor with a diameter of 7.44 cm which was operated at speeds in the range of 0 ∿ 4,000 R.P.M. The feed in liquid form was maintained in the range of 600 ∿ 4,700 cm^3/hr. The pressure drop was lower than those of similar type columns described previously and it increased with the revolution speed of the rotor and with the flow rate of liquid, as shown in Figure 5.

If it is assumed that the surface of rotating cylinder is not wetted and that the rate of reflux which flows down along the inner wall of a stationary cylinder is independent of the rotation of the cylinder, the liquid holdup can be calculated by the following equation (19).

$$w = \left(\frac{3\ Q\ \mu_\ell}{\rho_\ell\ g}\right)^{1/3} \tag{1}$$

where w is the thickness of liquid film, Q is the volume flow rate per wetted perimeter, μ_ℓ and ρ_ℓ are the viscosity and density of liquid respectively, and g is the acceleration of gravity.

The values of holdup calculated from equation (1) for the rotating concentric tube distilling column are shown in Table 1. The number of theoretical plates decreases with the increase in flow rate and increases with the speed of revolution, which is illustrated in Figure 6. A high efficiency is obtained above the speed of about 2,300 R.P.M., as shown in Figure 7. The reason may be due to the fact that the vapor phase becomes highly disturbed above this critical velocity.

In a plate column, the gas bubbles are passed into a liquid holdup through the submerged openings in the tray to increase the contacting area of the gas and liquid. The amount of agitation that can be obtained in this way is limited essentially by the rate of gas flow.

The tank with an agitator is a more efficient device than the plate column for agitation of the liquid on the tray regardless of the gas throughput. The tank, therefore, may have to be used for the agitation of viscous liquids or slurries. Since the agitation also increases the residence time of the bubbles in the liquid, the tank may be an efficient device where absorption is accompanied by a chemical reaction especially a slow reaction (20).

It has also been reported that a horizontal cylinder with an agitator can be used for the absorption operation (21). The agitator consists of several discs fixed to a rotary shaft placed in the center of a horizontal cylinder. The structure of the disc is shown in Figure 8. The liquid fed near the end of the cylinder flows through the discs in the form of sprays, sheets, and droplets by centrifugal action. The gas is sent through the cylinder cocurrently or countercurrently to the liquid. According to the studies by Ganz and coworkers (22), this absorber is highly efficient, but its performance and efficiency for industrial scale operation are unknown.

These systems with agitators have been reported in detail (23, 24).

3. Rotating types

Recently centrifugal contactors consisting of all rotating parts have been developed for mass transfer operations. Many of these contactors have been described in detail (21).

The Podobielniak centrifugal rectifier used in the distillation operation belongs to this class of contactors (25). The main part of the rectifier is a rotating drum made of a spiral metal sheet. The liquid fed near the center flows in radial direction by the centrifugal action as a thin film along the metal sheet. The apparatus can be operated at a relatively large flow rate without any entrainment which decreases the distillation efficiency. It has been reported (26) that when a small apparatus with a rotating drum made of a metal strip, 1/4 inch in width, 100 feet in length, and 1/8 inch for distance between coil of spiral, is run at a speed of 1,200 R.P.M., the approximate feed rate is 12 liter/hr, the liquid holdup is 30 liter/hr, the pressure drop ranges from 10 to 20 mm Hg, and its efficiency corresponds to that of a 80 plate column.

The rotary surface vapor compression still whose main part consists of the conical disc was fabricated in 1952 by Hickman (27). This apparatus has been further developed for application to sea water distillation (27). The schematic diagram of the apparatus is shown in Figure 9. Feed water is supplied to the inside surface of the rotor and vapor is condensed on the outside surface. The industrial scale rotary surface vapor compression stills have been in operation for several years. To be able to design this system intelligently, however, the mechanism of the evaporation and condensation on a rotating heat transfer surface must be known.

The penetration theory (28) and the surface renewal theory (29) predict that the absorption rate on the renewed surface of liquid is excellent. These theories may be employed generally for the design of contactors by utilizing the centrifugal action. For example, these theories can be applied to the Piazza type centrifugal absorber. As shown in Figure 10, the absorber consists of several concentric cylinders fixed to a rotating shaft and several stationary cylinders. The liquid fed near the center flows over the periphery of a rotary cylinder by centrifugal action as sprays, sheets, and droplets, and then collides with the wall of a stationary cylinder. After the impact one part of the flow backmixes with the sprays and the other part flows down along the cylinder wall.

On the other hand, one of the authors and his coworkers (30) have designed a centrifugal contactor of the rotating type whose main part consists of multistage concentric perforated cylinders. The schematic diagram of the contactor is shown in Figure 11. The liquid fed near the center of the cylinder is spouted from a small hole drilled through the rotating cylinder wall, and gas is sent cross currently to the liquid in an annular space between the rotating cylinders.

To understand the fluid dynamic and mass transfer aspects of these rotating type contactors, investigations on the gas absorption by the short liquid jets (31) and the droplets issued from a capillary (32) in the gravitational field have been carried out. Furthermore, the fluid flow and mass transfer in the centrifugal field have also been investigated (33, 34, 35, 36, 37).

The distribution of droplets which are broken off from the liquid jet issued from a rotating cylinder and a spinning cup has been studied by Walton and Prewett (39), Adler and Marshall (40), and Hinze and Milborn (41). The photographic observation of the flow pattern of liquid jets injected from a rotating cone cup has indicated that the liquid from such a cup forms a sheet or film, at the periphery of which the liquid jets are formed and break into droplets. Furthermore, Hinze and coworkers (41) have investigated experimentally the effects of the speed of rotor, the flow rate of liquid, and the angular velocity of the cup on the flow mechanism. Figure 12 shows the distribution of the drop diameter as a function of the rotating velocity. These experimental results were obtained with a cup having a diameter of 10 cm operated at the liquid rate of 80 liter/hr. Walton and coworkers (39) have found that the drop diameter goes through the maximum value when the angular velocity is increased and that the drop diameter is given by the equation,

$$d = \frac{K}{\omega}\sqrt{\frac{\sigma}{D\,\rho_\ell}} \tag{2}$$

where d and D are the diameter of the drop and that of the cup, respectively, ω is the angular velocity, σ is the surface tension of the liquid, and K is a constant. Although equation (2) agrees with the experimental results of Hinze and coworkers (41), it does not contain the effect of the viscosity of liquid.

Dixon, Russel, and Swallow (42) have investigated the effect of the density, viscosity, and surface tension of the liquid. Furthermore, they have carried out a theoretical analysis, by assuming that the different behavior of the formation of sheets in the different liquid is due to the trajectory of the liquid flow from a feed tube to the periphery of a cup.

As a part of the fundamental studies of fluid dynamics of the centrifugal contactor of the rotating type (30), the first author defined theoretically the discharge coefficient in the centrifugal field, neglecting the effects of the physical properties of liquids but taking into account the effects of hole diameter, wall thickness, cylinder diameter, revolution speed of the cylinder, and discharge pressure of liquid (33). Eventually, the effects of viscosity and surface tension of discharged liquids were taken into account and the equations applicable to the liquids of various viscosities and surface tensions in the centrifugal field were derived (33). Other studies on the flow pattern of a round liquid jet in the centrifugal field are a study of the discharge from a rotating pipe (43), a study of the discharge from an orifice (37), and a study of the atomizing pattern of liquids spouted from a cylindrical nozzle (44).

The flow pattern of the liquid jet spouted from a rotating small hole is very complex. However, it is known that the jet travels due to the combination of the circumferential velocity and the radial velocity (37). Therefore, it is clear that these give rise to the relative velocity against the surrounding gas. As the discharge velocity of liquid is increased, it undergoes transition consecutively through the stages of drops, laminar flow, turbulent flow, and spray. Figure 13 shows the most typical forms of liquid jet spouted from a rotating small hole (38). In this figure, (a) is the dripping flow, (c) and (d) are the laminar flow, (e) is the turbulent flow, and (g) is the spray. It can be seen that these flow patterns in the centrifugal field are similar to those in the gravitational field.

According to the experimental results of Tanazawa, Kurabayashi, and Saito (43), the flow pattern of liquid jet in the gravitational field can be divided as follows:

$Je < 0.1$	dripping
$Je \simeq 0.1 \sim 10$	laminar flow
$Je \simeq 10 \sim 500$	turbulent flow
$Je > 500$	spray

where the Jet number of liquid stream, Je, is defined by

$$Je = \left(\frac{d\, w^2 \rho_g}{\sigma}\right)\left(\frac{\rho_\ell}{\rho_g}\right)^{0.45} \qquad (3)$$

and d is the diameter of hole, w is the discharge velocity of liquid, and ρ_g is the density of gas.

Furthermore, from the available experimental results (35), it can be seen that the flow pattern of the liquid jet in the centrifugal field must be defined by the Jet number based on the resultant velocity as mentioned previously.

The diameter of the liquid jet gradually becomes smaller due to the increase in the rotation of speed. Figure 14 shows the relation between the jet length and the ratio of jet and hole diameters, d_j/d, when the radius of cylinder is 2.5 cm (37). From the figure, it is obvious that the diameter of liquid jet decreases as the jet lengthens. The diameter of the jet when the discharge velocity is slow and angular velocity is high becomes remarkably small immediately after the liquid is spouted from a hole. Hereafter, the continuous length of liquid jet becomes short although the flow of jet is laminar, as shown in Figures 13(c) and (d). This phenomenon can not be found in the liquid jet spouted from a small hole in the gravitational field.

In these rotating type gas-liquid contactors, mass transfer takes place at the surface of the rotating liquid jets, sheets, droplets, and liquid film along the inside wall of the cylinder. It is important to know which one of these controls the mass transfer rate so as to design an apparatus of high efficiency and to determine the optimum condition for operation.

When a small scale Piazza absorber with two rotary cylinders as shown in Figure 10 was operated cocurrently, the following results were obtained (45). The absorption rate was independent of the interfacial area which was provided by the liquid films along the inside wall of the cylinders when the interfacial area of the sprays from the rotating cup was maintained constant. However, when the interfacial area due to the sprays was reduced to half and that du to the films was maintained constant, the absorption rate became half can be seen from the results that the spray from the rotating cup cont the overall absorption rate.

On the other hand, in the rotating type contactor (30), mass transfer between gas and liquid takes place as a result of contact between gas and a liquid jet or gas and a liquid film along the inside wall of the cylinder. In order to evaluate the rate of mass transfer from rotating liquid jets, the contact area of gas and liquid per unit volume of a continuous liquid jet spouted in an annular space from a small rotating hole has been determined theoretically and experimentally (37). Furthermore, the absorption of pure carbon dioxide by a liquid jet issuing from a rotating hole (35) and that by a flowing liquid film along the inside wall of the rotating cylinder (36) have been studied. It can be concluded from the results that the amount of mass transfer into the liquid film on the wall of the rotating cylinder is much less than that into the liquid jet issuing from a rotating hole. However, the absorption efficiency increases as the liquid depth on the inside wall decreases.

The pressure drop under the condition of the cocurrent flow of gas and liquid in the Piazza absorber is affected by both the rotating velocity and the liquid flow rate. The liquid holdup in this apparatus increases when the speed of revolution is lowered. This increase in the liquid hold-up tends to obstruct steady flow of gas and consequently increases the pressure drop steeply. This is the so-called flooding phenomenon. The point of flooding depends on the flow rate of liquid but is almost independent of the gas rate. In the countercurrent operation of this apparatus, these relations are complex.

As mentioned previously, it is desirable to make cylinders as large as possible for the purpose of increasing efficiency of absorption. For absorption the space between cylinders must be narrow. However, this tends to increase the pressure drop. To solve this problem a number of holes is often provided in the bottom of the rotating cylinder. Even with this improvement, the liquid throughput in radial direction cannot be maintained smoothly because the main part of the absorber consists of the rotary cylinders and stationary cylinders, which are overlapped. As a result, the consumption of power is enormous, flooding tends to occur and the countercurrent operation becomes difficult. To avoid these difficulties Alcock and Millington (46) designed the double rotor contactor. The experimental results (46, 47) indicate that the pressure drop for the double rotor type is 1/2 to 1/3 of that of the rotor stator type. The double rotor type is more desirable than the rotor stator type for the treatment of viscous liquid. However, the behavior of liquid flow into the contactor has not yet been investigated. In the centrifugal contactor of the rotating type (30), the pressure drop is much smaller than that of the Piazza type because the gas is sent crosscurrently to the liquid jet in an annular space between the rotating cylinders.

Rumford and Rae (47) have investigated experimentally the effects of the water rate, the gas rate, the concentration of the solute gas, and the revolution speed and structure of cylinders on the absorption rate in the Piazza absorber of the double rotor type operated cocurrently. They have employed three systems, namely, carbon dioxide-water, ammonia-water, and acetone-water. Table 2 shows the experimental results obtained at various flow rates of the liquid and gas. If the total volume of the centrifugal absorber is V ft^3, and if G_m moles of gas flow cocurrently with L_m moles of liquid, the following equation can be obtained from the material balance (47).

$$-G_m\, dy = L_m\, dx = k_\ell\, a(C_e - C_\ell)dV \qquad (4)$$

where $k_\ell a$ is the liquid phase coefficient on the volume basis, C_e is the concentration of solute in liquid stream which is in equilibrium with gas, C_ℓ is the concentration of solute in the main body of the liquid stream, and x and y are mole fraction of solute in liquid and gas, respectively. The number of liquid phase transfer unit, N_ℓ, is

$$N_\ell = V \cdot c \cdot K_\ell a/L_m \tag{5}$$

where c is the average molal density of the liquid. Then, the volume of a liquid phase transfer unit, V/N_ℓ, is

$$V/N_\ell = L_m/c \cdot k_\ell a \tag{6}$$

This is often denoted as $V.T.U._\ell$. And alternatively the volume of a gas phase transfer unit, $V.T.U._g$ or V/N_g, defined as

$$V.T.U._g \equiv V/N_g \equiv G_m/P \cdot k_g a \tag{7}$$

where P is the total pressure of the system. Then the volume of an overall liquid phase transfer unit, $V.T.U._{O\ell}$ is given by

$$V.T.U._{O\ell} = V.T.U._\ell + (L_m/G_m \cdot M)(V.T.U._g) \tag{8}$$

where M represents C/H.P., in which H is the Henry's law constant. On the other hand, the volume of an overall gas phase transfer unit, $V.T.U._{Og}$, is

$$V.T.U._{Og} = V.T.U._g + (G_m \cdot M/L_m)(V.T.U._\ell) \tag{9}$$

As mentioned previously, values of these quantities are given in Table 2.

Figure 15 shows one example of the effect of the rotating velocity on the absorption rate. This result was obtained at the gas rate of 1,100 ft^3/hr. The concentration of carbon dioxide in the inlet gas was 17% and the concentration of monoethanol amine and that of carbon dioxide in the inlet solution were 80% and 3.5% respectively. Furthermore, Alcock and Millington (46) found the optimum condition from their experimental results obtained by using a 6 cylinder unit and designed a large scale absorber in which 15 cylinders were fixed to a rotor, 12 inches in diameter, and have examined it with the monoethanol amine-carbon dioxide systems. The experimental result obtained with both equipment are compared in Table 3.

The absorption rate of pure carbon dioxide gas by a rotating round water jet was measured in an annular space between the rotating cylinder and a stationary concentric outside cylinder (35). Figure 16 shows an example of the relation between the gas-liquid contact time, θ, and the Murphree absorption efficiency, E_{ML} when the hole is 0.9 mm in diameter. θ was evaluated by the theoretical equation (35, 38). From this figure it can be seen that the plot of E_{ML} versus $\sqrt{\theta}$ leads to a straight line through an origin, and also that the pure carbon dioxide gas absorption by a water stream issuing from rotating jet holes conforms to the unsteady-state diffusion theory (28). Furthermore, the gas absorption rate by a water jet spouting from a rotating small hole was observed to be large immediately after the liquid was spouted from the hole. Therefore, for practical purposes, it is desirable to employ a multi-rotor type contactor in order to make as many jets of liquid as possible.

In addition to the experimental mass transfer study mentioned previously, mechanisms of fluid flow and the mass transport of the liquid film on the inside wall of a rotating wetted cylinder were theoretically investigated (36). The effects of various factors such as the gas and liquid velocities, the depth of liquid layer, the number of revolutions, and gas-liquid contact time etc. on the mass transfer rate were examined.

The centrifugal contactor of the rotating type (30) has been extensively developed in Japan as absorbers, humidifiers, rectifiers, etc. based on the fundamental and applicative studies by the first author and his coworkers (33, 34, 35, 36, 37, 38, 40).

Some of the special features of gas-liquid contactors utilizing the centrifugal force are discussed in this report. These contactors have come into general use only in the last ten years and there is as yet no literature that deals with design features and fundamental studies, and many problems are yet to be solved. However, it is expected that these contactors will be employed widely by several industrial fields in the near future because of the generally favorable mass transfer characteristics in the centrifugal field. Some contactors mentioned in this report allow treatment of a viscous solution, and also can be operated without flooding and at a large flow rate. Furthermore, they can be employed where pitching and rolling of the systems cannot be avoided.

Literature Cited

1. Takahashi, T., Kagaku Kikai Gijutsu (Japan), 16, 56 (1964).

2. Manning, E., U. S. Patent 2,772,748 (Dec. 4, 1956), also Ind. Eng. Chem., 56, 15 (1964).

3. Pollard, B., Trans. Instn. Chem. Engrs., (London), 35, 69 (1957).

4. Takahashi, T. and Akagi, Y., Kagaku Kogaku (Japan), 31, 600 (1967); ibid, Memoirs of the School of Eng., Okayama Univ., 2, 50 (1967).

5. Takahashi, T., and Akagi, Y., Memoirs of the School of Eng., Okayama Univ., 3, 51 (1968); Takahashi, T., Akagi, Y. and others, A paper presented at the Chem. Soc. of Japan Meeting, Okayama, 232 (1967).

6. Huffman, J. R. and Urey, H. C., Ind. Eng. Chem., 29, 531 (1937); Pergram, G. B., Urey, H. C., and Huffman, J. R., Phys. Rev., 49, 883 (1936).

7. Willingham, C. B., and others, J. Research Natl. Bur. Standards, 22, 519 (1939).

8. Lesesne, S. D., and Lochte, H. L., Ind. Eng. Chem., Anal. Ed., 10, 450 (1938).

9. Baker, R. H., Barkenbus, C. and Reswell, C. A., Ind. Eng. Chem., Anal. Ed., 12, 468, (1940).

10. Birch, S. F., Gripp, V., and Nathan, W. S., J. Soc. Chem. Ind., (London) 66, 33 (1947).

11. Willingham, C. B., Sedlak, V. A., and Rossini, F. D., Ind. Eng. Chem., 39, 706 (1947).

12. Taylor, G. I., Proc. Roy. Soc., A-151, 494 (1935), A-135, 678 (1932); Phil. Trans., A-223, 289 (1923).

13. Lewis, J. W., Proc. Roy. Soc., A-117, 388 (1928).

14. Westhaven, J. W., Ind. Eng. Chem., 34, 126 (1942).

15. Collins, F. C., and Lantz, V., Ind. Eng. Chem., 18, 673 (1946).

16. Hall, S. A., and Palkins, S., Ind. Eng. Chem., Anal. Ed., 12, 544 (1940).

17. Rose, A., Ind. Eng. Chem., 28, 1210 (1936).

18. Selker, M. L., Burke, R. E., and Lankelma, H. P., Ind. Eng. Chem., Anal. Ed., 12, 352 (1940).

19. Friedman, S. J., and Miller, C. O., Ind. Eng. Chem., 33, 885 (1941).

20. Valentin, F. H. H., "Absorption in gas-liquid dispersions," 130, E & F. N. Spon Ltd, London (1967).

21. Takamatsu, T., and Takahashi, T., Kagaku Kogaku (Japan), 22, 447 (1958), ibid., Chem. Eng. (Japan) 2, 66 (1957).

22. Ganz, S. N. et al., J. Applied Chem. (U.S.S.R.), 28, 145, 585, 831, (1955), 29, 108 (1956), 30, 553, 1311, 1604 (1957), 31, 191 (1958), 32, 969, 975, 1477, 2207 (1959).

23. Uchiyama, H., Kagaku Kogaku (Japan), 25, 561 (1961).

24. Uhl, V. W., and Gray, J. B., "Mixing" vols. 1 and 2, Academic Press, New York (1966).

25. Podobielniak, W. J., A paper presented at the Am. Chem. Soc. Meeting, New York (1935).

26. Glasbroak, A. C. and Williams, F. E., "Technique of Organic Chemistry," Vol. 4, 226 (1951).

27. OSW, U. S. Dept. of the Interior, Research and Development Progress No. 12, Nov. (1956), ibid., No. 15, March (1957), ibid., No. 43 Sept. (1960).

28. Higbie, R., Trans. Am. Inst. Chem. Engrs., 31, 365 (1935).

29. Danckwerts, P. V., Ind. Eng. Chem., 43, 1460 (1951).

30. Japan Patent 242, 131.

31. Edwards, G., Robertson, R., Rumford, F. and Thomson, J., Trans. Instn. Chem. Engrs., 32, S6 (1954).

32. Dixon, B. E., and Russel, A. A. W., J. Soc. Chem. Ind., 69, 284 (1950).

33. Takamatsu, T., Takahashi, T., and others, Kagaku Kogaku (Japan), 22, 555 (1958).

34. Ibid., Kagaku Kogaku (Japan), 22, 561 (1958).

35. Ibid., Kagaku Kogaku (Japan), 25, 594 (1961).

36. Ibid., Kagaku Kogaku (Japan), 27, 156 (1963).

37. Takahashi, T., Kagaku Kogaku (Japan), 30, 68 (1966).

38. Takahashi, T., Memoirs of the School of Eng., Okayama Univ., 1, 29 (1966).

39. Walton, W. H. and Prewett, W. C., Proc. Phys. Soc., 62, 13, 341 (1949).

40. Adler, C. R., and Marshall, W. R., Chem. Eng. Progr., 47, 515 (1951).

41. Hinze, J. O., and Milborn, H., J. Appl. Mech., 1, 145 (1950).

42. Dixon, B. E., Russel, A. A. W. and Swallow, J. E. C., Brit. J. Appl. Phys., 3, 115 (1952).

43. Tanazawa, Y., Kurabayashi, T. and Saito, Y., Trans. J. S. M. E. (Japan), 22, 279 (1956).

44. Kurabayashi, T., Trans. J. S. M. E. (Japan), 25, 1252, 1259, 1266, (1957), 26, 1536, 1543 (1960).

45. Chamber, H. H. and Wall, R. G., Trans. Inst. Chem. Engrs., 32, S96 (1954).

46. Alcock, J. F. and Millington, B. W., Trans. Inst. Chem. Engrs., 32, S155 (1954).

47. Rumford, F., and Rae, I. J., Trans. Inst. Chem. Engrs., 34, 195 (1956).

48. Schneerson, A. L. and Leibush, A. G., J. Appl. Chem. (U.S.S.R.), 19, 859 (1946).

49. Matsuda, M. and Fujioka, Y., Bulletin of Chem. Soc. of Japan 38, 869 (1965).

Table 1. Holdup

Liquid flow rate [ml/hr]	Holdup / Column height [ml/m]	Holdup / Number of theoretical Plate [ml]
1,000	12.8	0.10
1,500	14.5	0.14
2,000	15.9	0.19
2,500	17.2	0.24
3,000	18.2	0.29
3,500	19.2	0.36
4,000	20.1	0.40

Table 2.

L_m	G_m	$N_{0\ell}$	N_{0g}	$V.T.U._{0\ell}$	$V.T.U._{0g}$	
22.2	3.66	0.825	0.00352	0.04	9.4	$6\%\ CO_2$ in gas
44.4	3.66	0.825	0.00704	0.04	4.68	
66.6	3.66	0.825	0.01056	0.04	3.12	
88.8	3.66	3.850	0.01450	0.039	2.28	
111.0	3.66	0.870	0.01850	0.038	1.79	
44.4	1.83	0.56	0.0095	0.059	3.48	$9\%\ CO_2$ in gas
44.4	2.45	0.56	0.0072	0.059	4.60	
44.4	3.06	0.56	0.00575	0.059	5.75	
44.4	3.66	0.56	0.0048	0.059	6.89	

Table 3. Comparison of 6 Cylinder and 15 Cylinder Absorbers

	6 Cylinder Absorber			15 Cylinder Absorber		
Liquid flow rate [gal/hr]	$k_g a$	Absorbed CO_2 [lb / hr]	Pressure drop [in-W.C.]	$k_g a$	Absorbed CO_2 [lb/hr]	Pressure drop [in-W.C.]
20	7,700	13.1	5.5	31,000	17.6	12
30	10,500	16.9	5.5	41,000	19.6	14
40	12,700	18.3	5.5	47,300	20.5	16

Concentration of inlet liquid	**85% M.E.A. 2.5% CO_2**
Temperature of inlet liquid	**60°C**
Gas flow rate	**1,200 ft^3/hr**
CO_2 concentration of inlet gas	**16%**
Number of revolution	**2.300 R.P.M.**

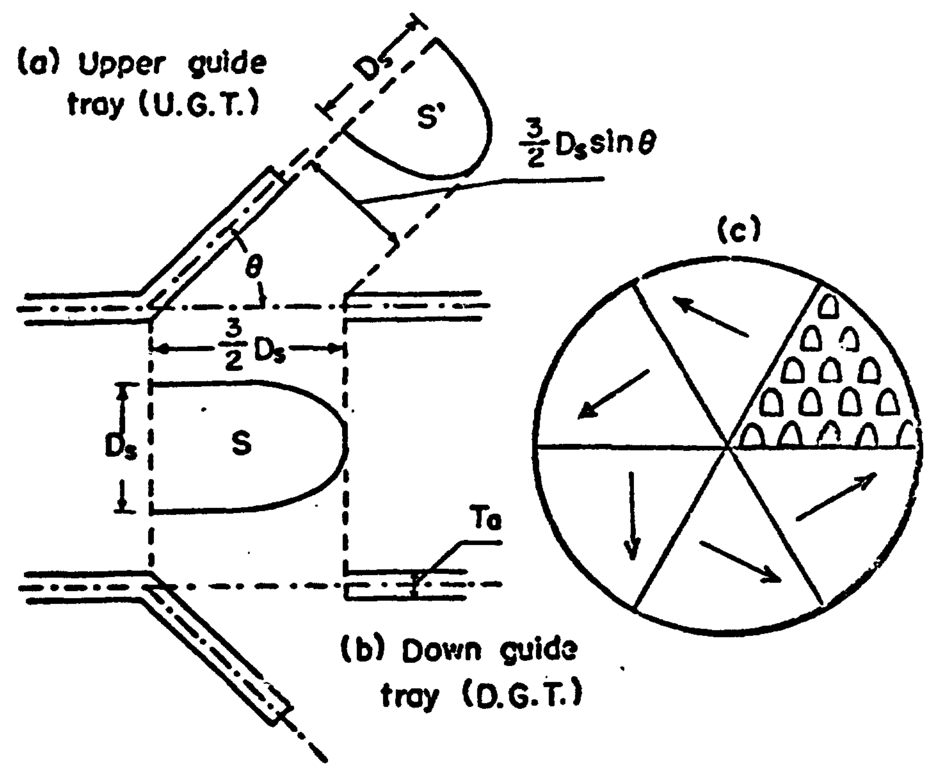

Fig. 1 Structure of rotational-current tray

	Tray	D_t	D	A_h/A_c	W
⊙	Counter-current type perforated	15	1.52	0.106	1.42
□	Kittel tray	50	0.36:0.85	0.27	1.95
	Ripple tray	69	—	—	0.57
	Ripple tray	69	—	—	1.13
○	Upper guide tray	14.6	0.72	0.172	1.77 / 2.62
△	Down guide tray	14.6	0.72	0.172	1.77 / 2.62

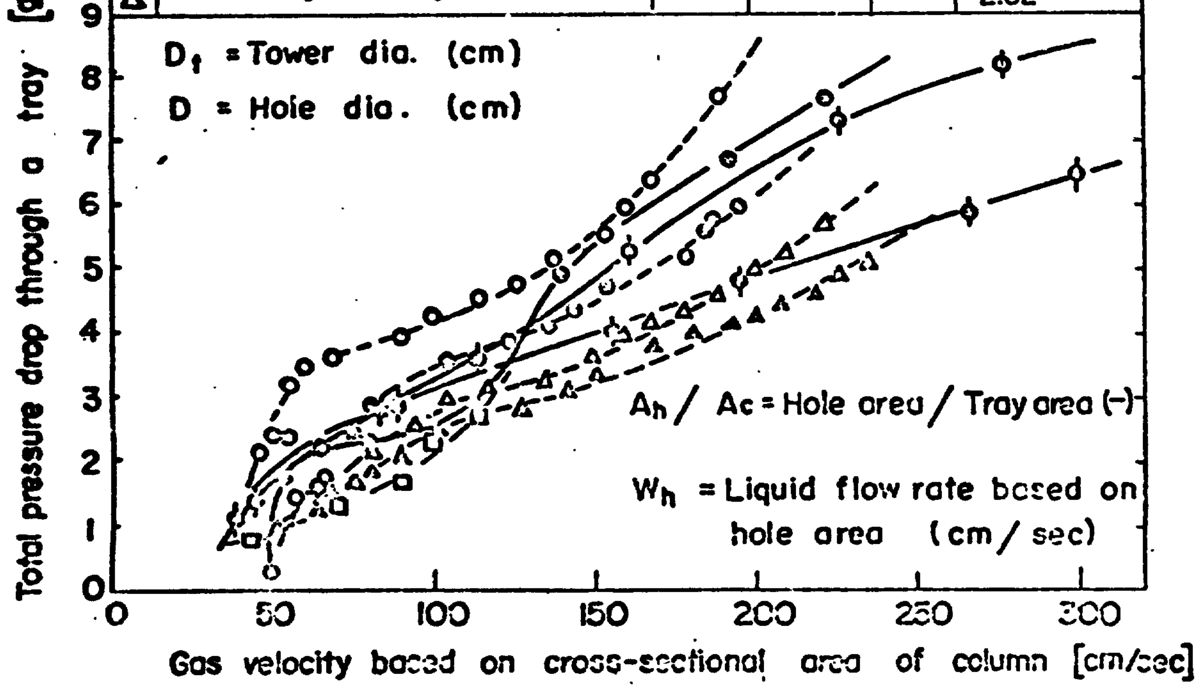

Fig.2 Comparison of total pressure drop through a tray.

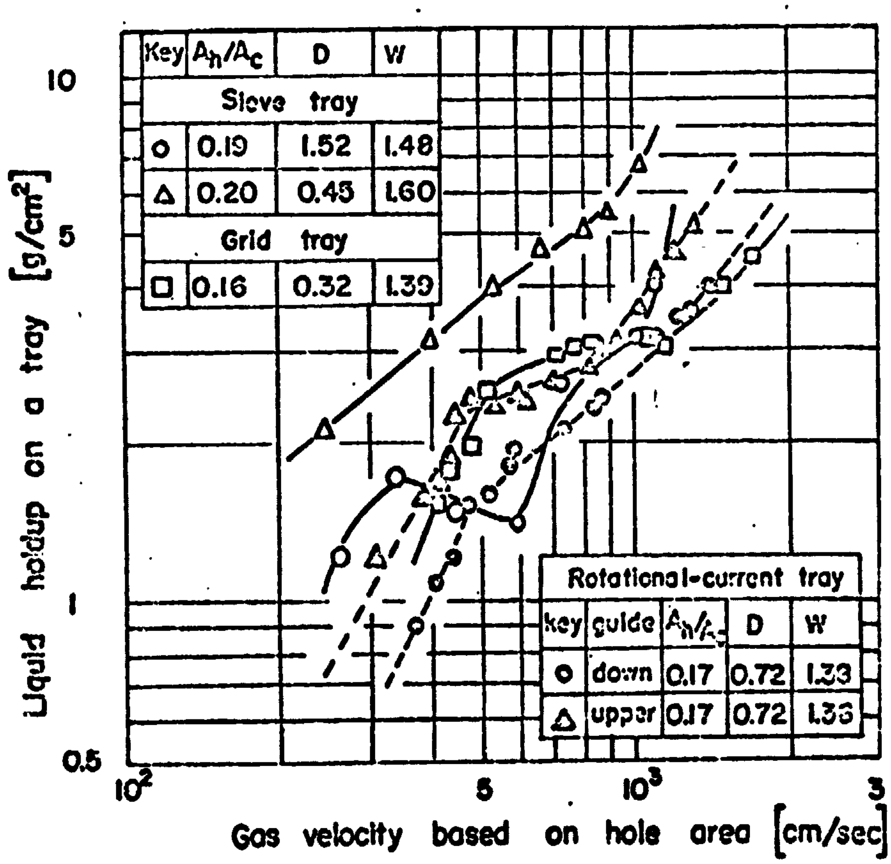

Fig. 3 Comparison of liquid holdup on various counter-current trays.

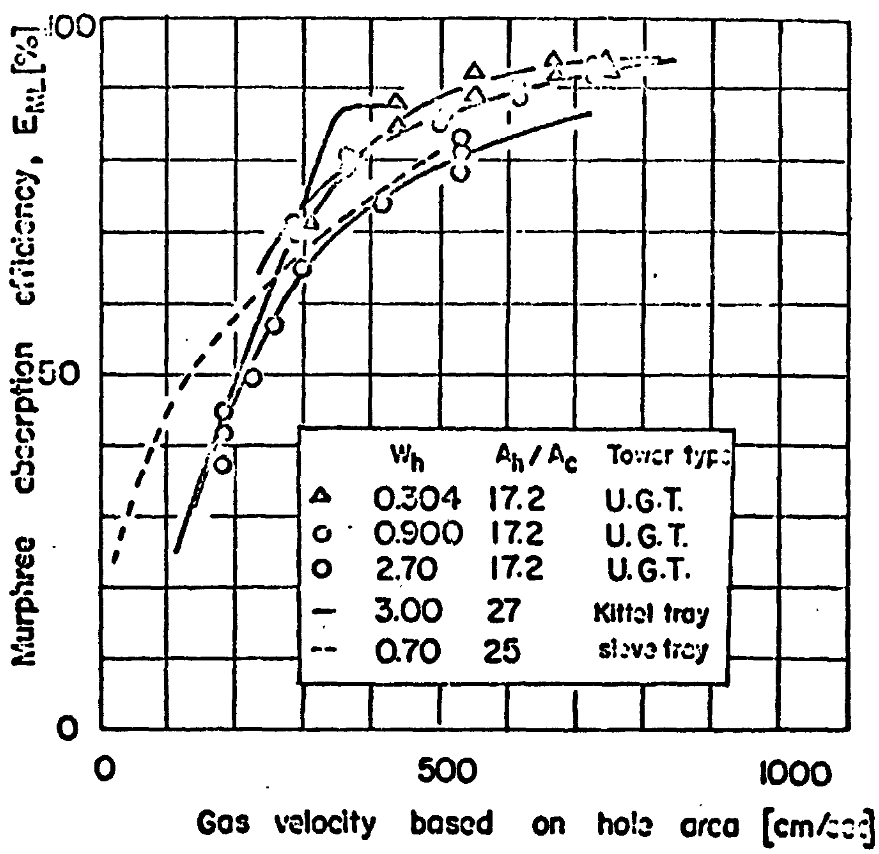

Fig. 4 Comparison of absorption efficiency based on liquid phase.

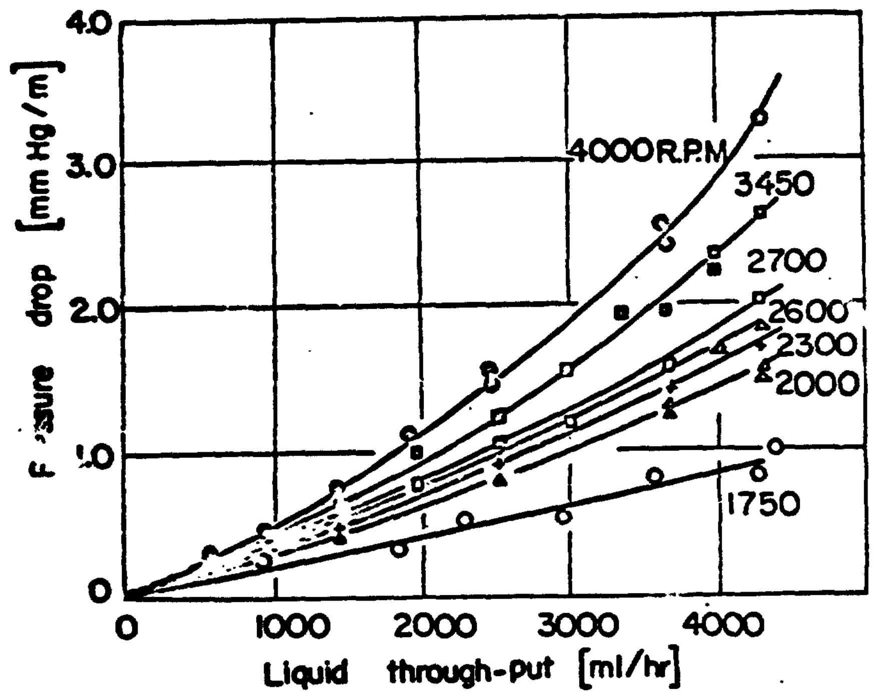

Fig. 5 Pressure drop

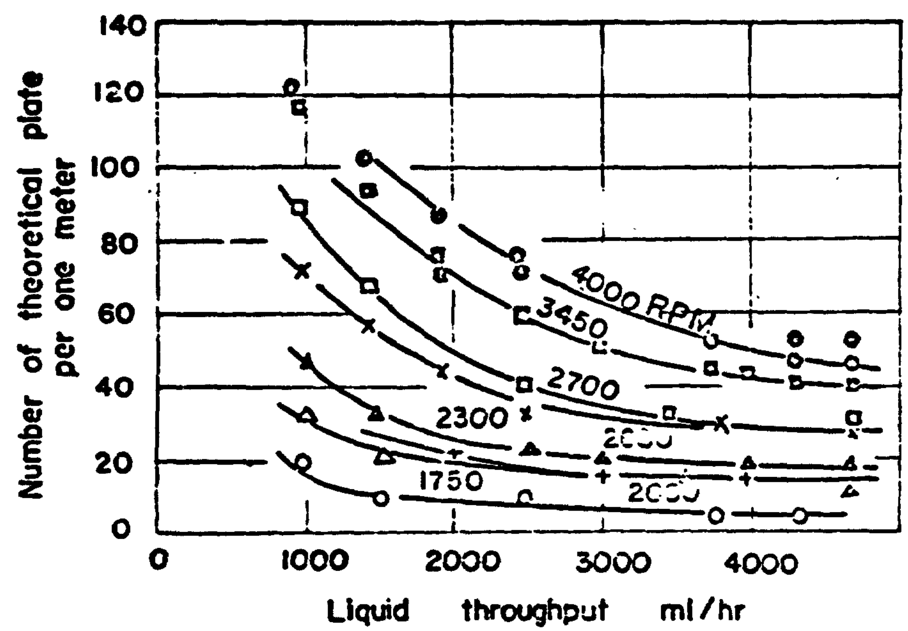

Fig.6 Number of theoretical plate

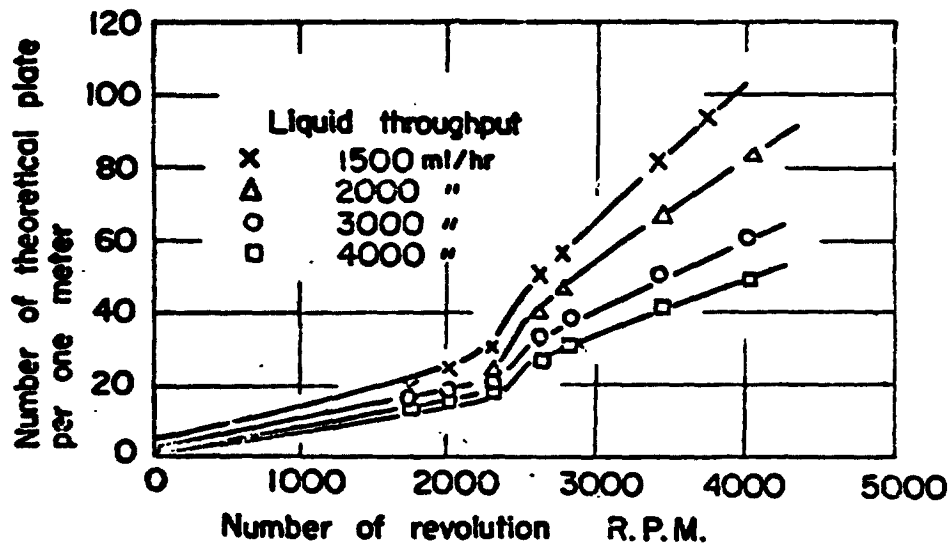

Fig. 7 Number of theoretical plate

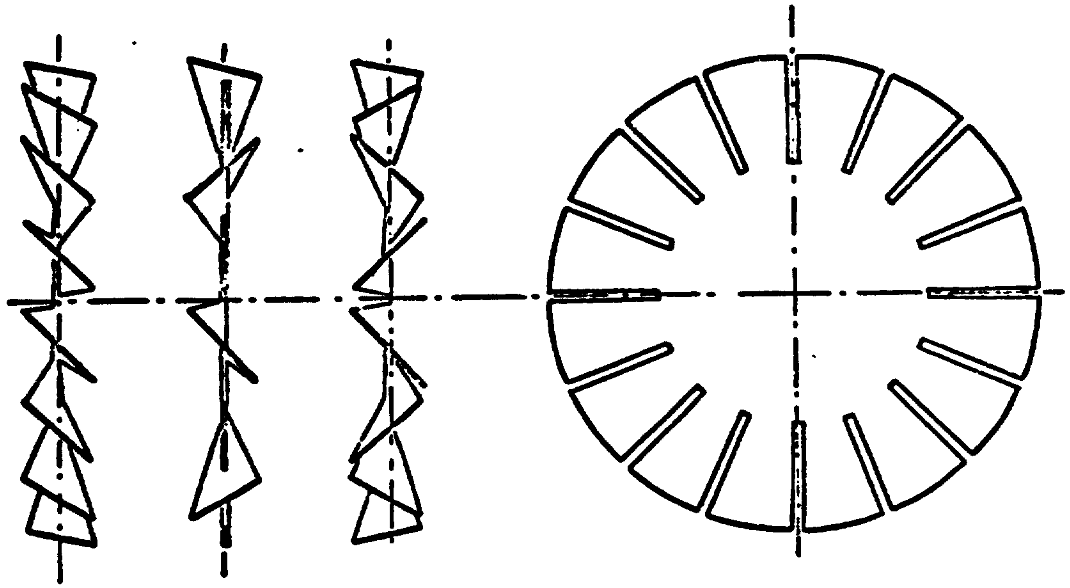

Fig. 8 Structure of impeller

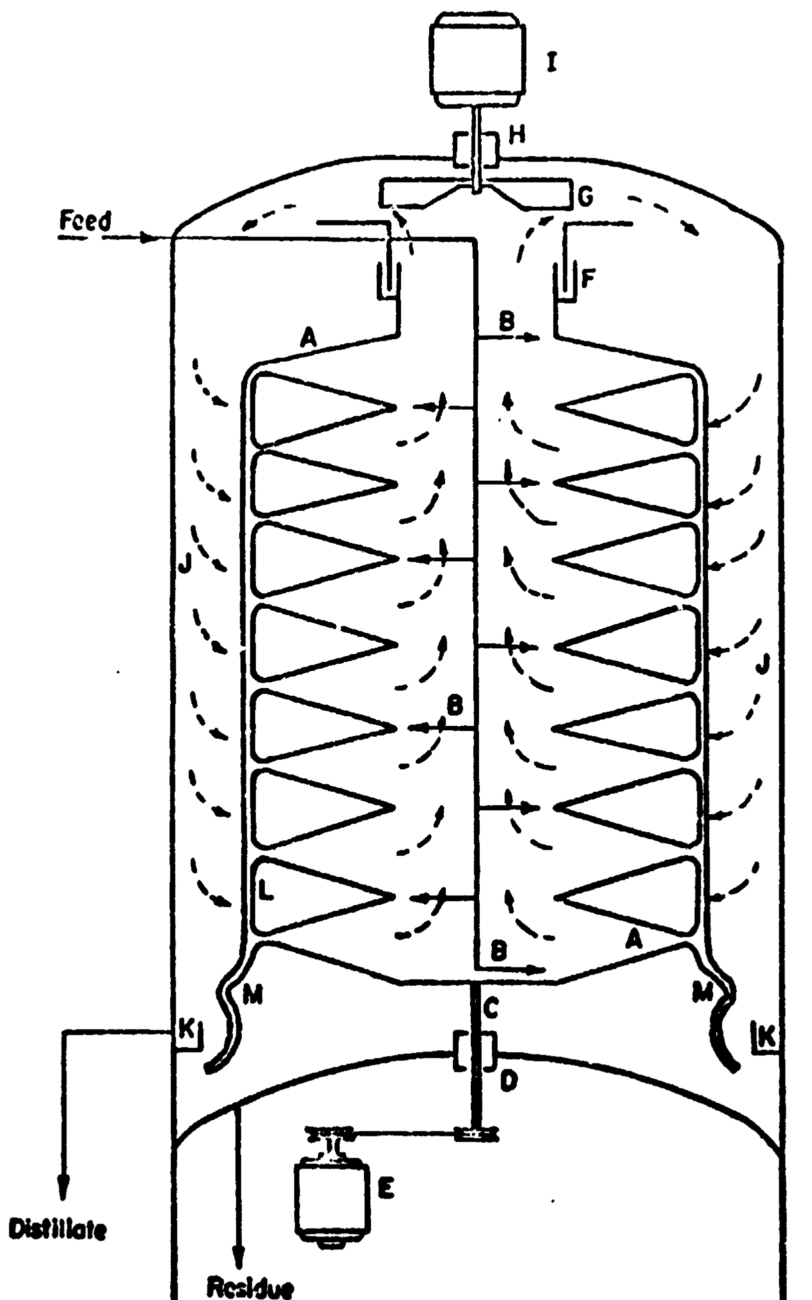

A. Rotors
B. Feed Nozzles
C. Rotor Drive Shaft
D. Rotor Shaft Seal
E. Rotor Drive Motor
F. Rotating Seal
G. Blower
H. Blower Shaft Seal
I. Blower Drive Motor
J. Outer Shell
K. Distillate Trough
L. Downspout
M. Trap

Fig. 9 Diagramatic sketch of Rotary-surface vapor-compression still.

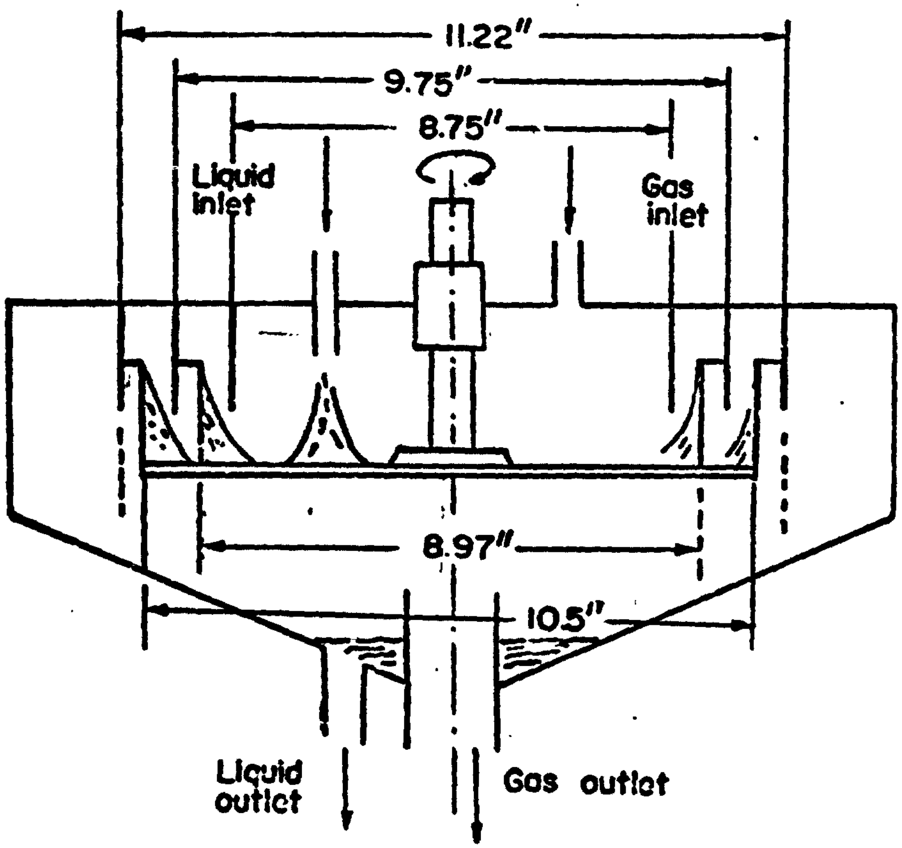

Fig. 10 Diagramatic sketch of Piazza absorber.

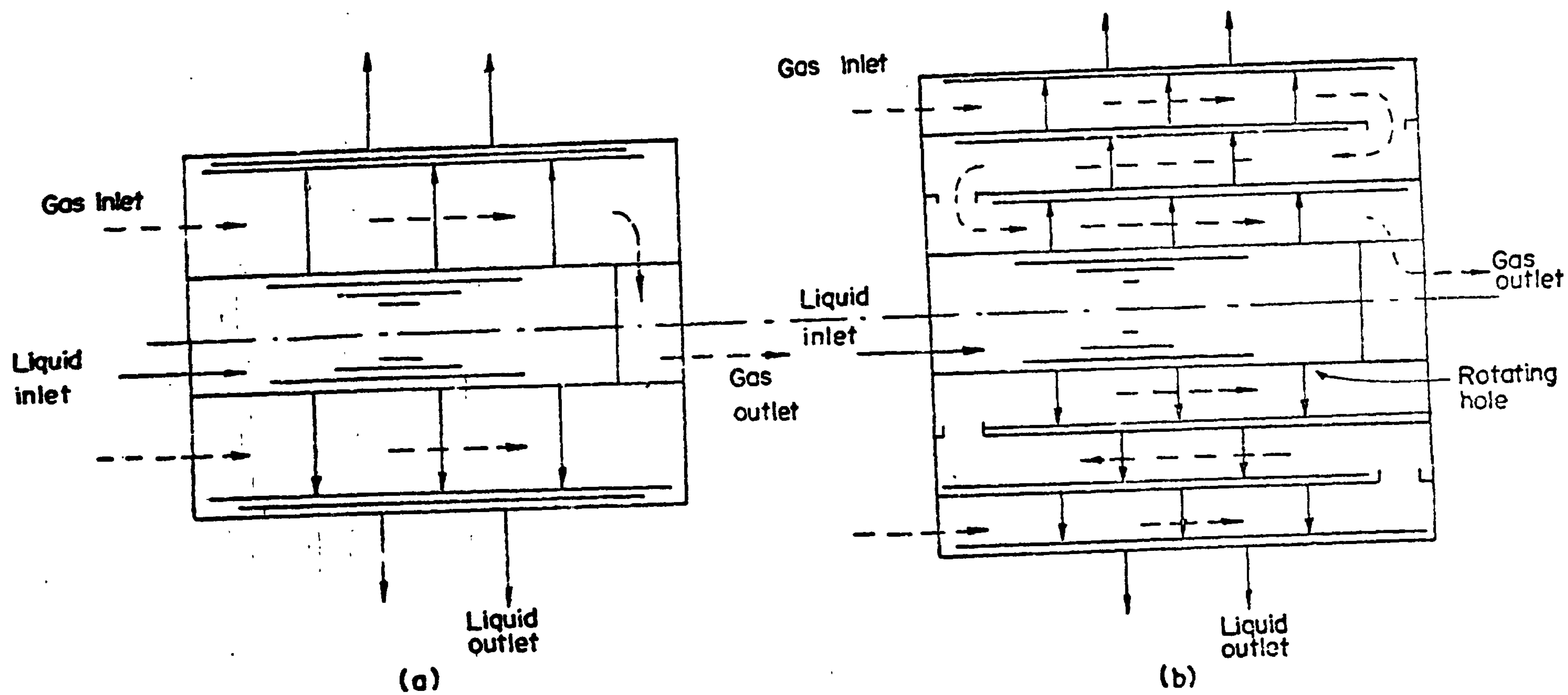

Fig. 11 Diagramatic sketch of centrifugal gas-liquid contactor.

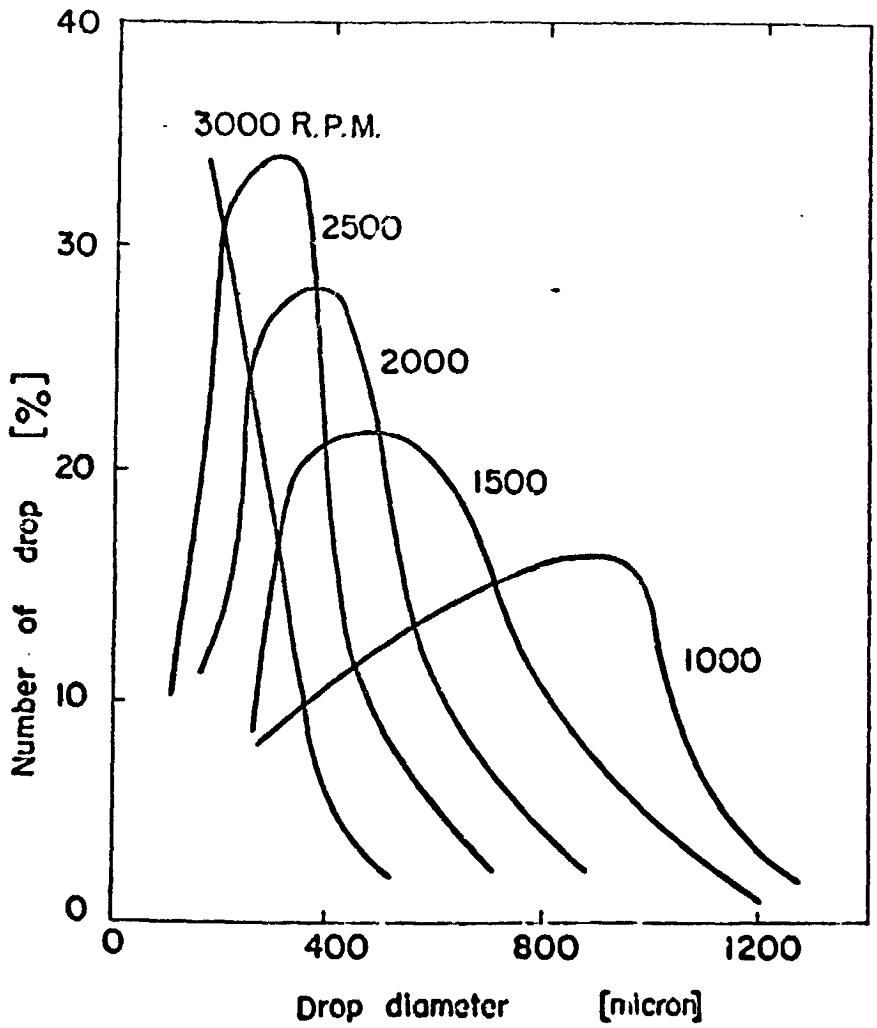

Fig. 12 Distribution of drop diameter.

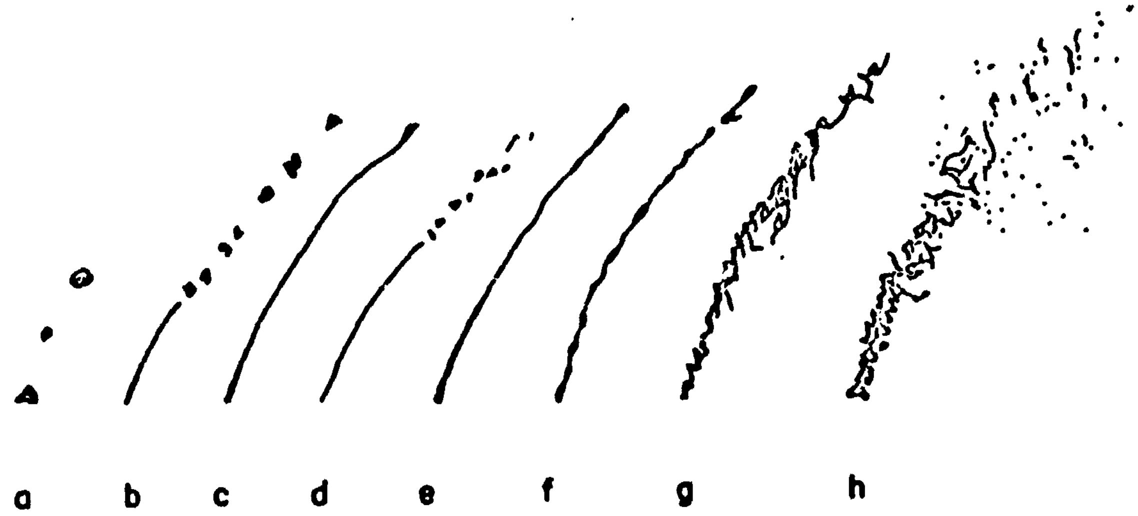

Fig. 13 Flow pattern of rotating liquid jet .

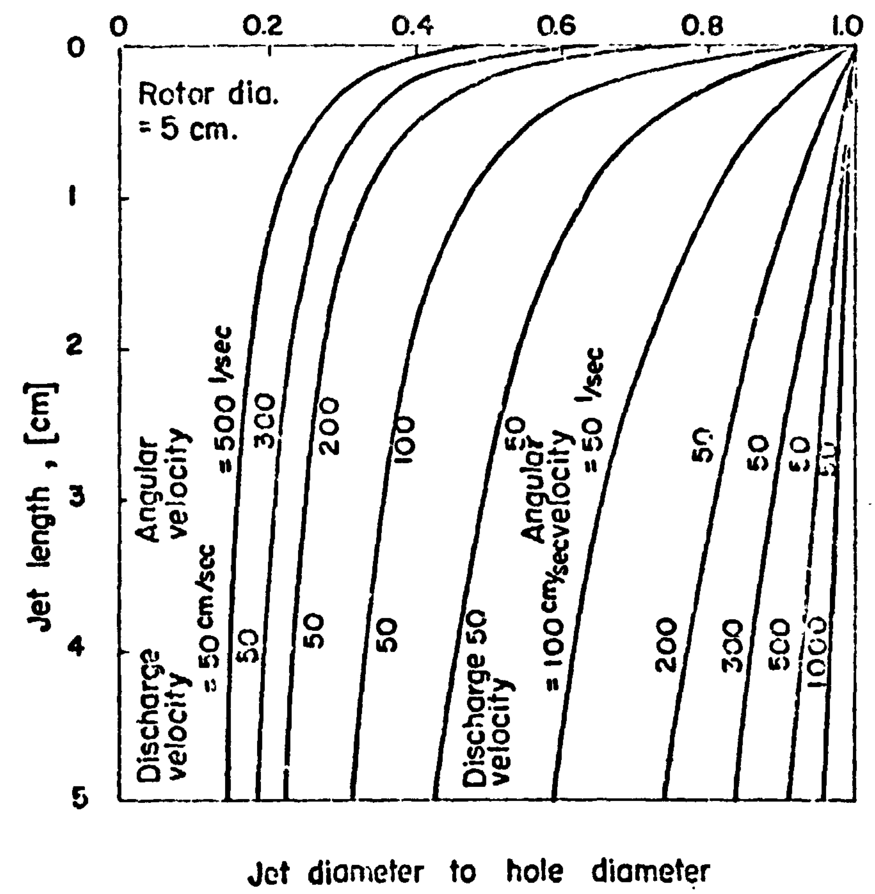

Fig. 14 Relation between jet length and diameter ratio .

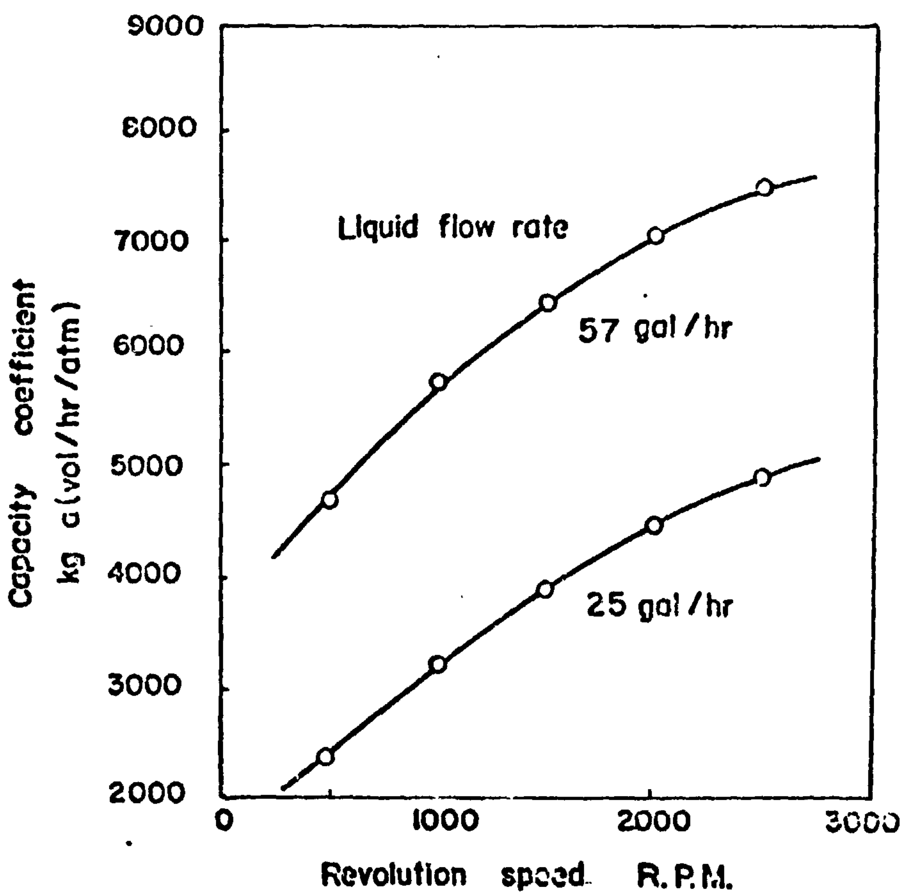

Fig. 15 Effect of revolution speed on mass transfer.

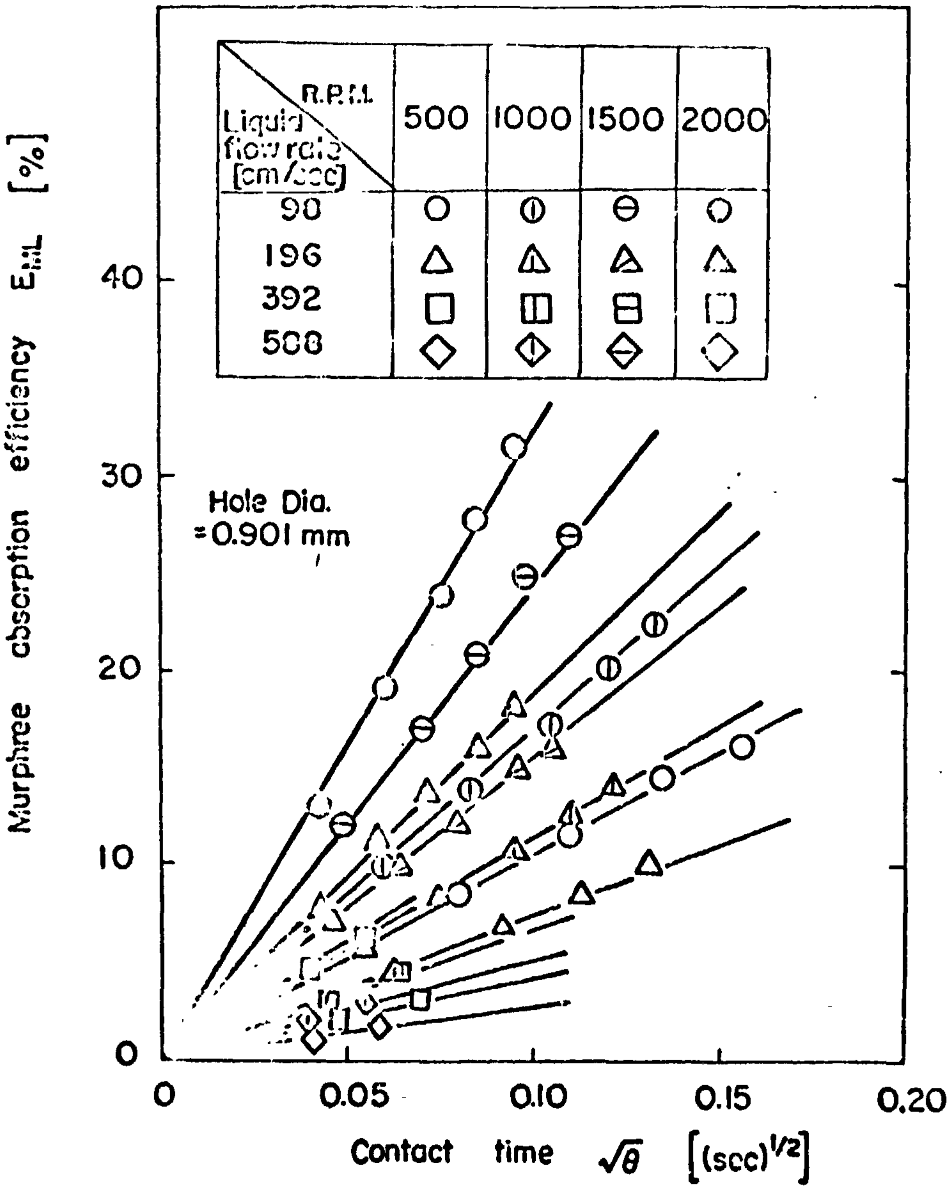

Fig. 16 Relation between contact time $\sqrt{\theta}$ and efficiency of mass transfer E_{ML}.

(c) 1

CARBON DIOXIDE REDUCTION CONTACTORS IN SPACE VEHICLES AND OTHER ENCLOSED STRUCTURES

Report No. 11

T. Takahashi, L. T. Fan

Institute for Systems Design and Optimization
KANSAS STATE UNIVERSITY MANHATTAN

Carbon Dioxide Reduction Contactors in
Space Vehicles and Other Enclosed Structures*

By

T. Takahashi

L. T. Fan

January 20, 1969

*This work was partially supported financially by NASA (Grant 17-001-034) and AFOSR (Grant USAFOSR F44620-68-C-0020).

For a man to survive in any surroundings, he has to maintain breathing, drinking, eating, and activities related to waste elimination. In solving the problem of the life support in space vehicles, the control of atmospheric temperature, humidity, carbon dioxide level, trace contaminant level, provisions for waste elimination, and the supply of oxygen, food and water must be considered. Life support systems are often categorized in terms of the extent to which the human waste products are reclaimed, that is, the degree of ecological closure. The possible degree of closure ranges from open systems which provide no waste recovery processes, to partially closed systems which provide recovery processes for water and or oxygen, and to closed systems which provide food and all other life support needs from the processing of the human wastes (1).

The removal of carbon dioxide from the enclosed space or cabin atmosphere is one of the important functions of a life support system. The concentration of carbon dioxide in normal air is usually taken as 0.03% by volume. The air exhaled by the breath of man contains approximately 4.5% of carbon dioxide. Therefore, there can be an appreciable build-up of carbon dioxide in any enclosed space.

Processes for the removal of carbon dioxide from gas mixtures have been sufficiently developed in the chemical industry. In aerospace application, however, uses of many of the techniques will be restricted severely by weight, power, and volume of the process units and other characteristics of the processes. In addition, the processes must be operated in the zero gravitational field.

Various promising methods for the removal of carbon dioxide in the cabin of space craft have been proposed. In the future, however, many other different methods will probably be proposed for different systems with different degrees of ecological closure.

The portable life support system to keep man alive and comfortable outside the space capsule is also needed. Reid and Richardson (2) reported a new process for the removal of carbon dioxide in the portable life support system. They have concluded that when ease of handling and safety are considered, when heats of vaporization are examined, and when other thermal and physical properties are evaluated, water is still the best absorbent (2). However, since the solubility of carbon dioxide in water is very low, a high water flow rate is necessary to increase the removal of metabolic carbon dioxide. For these reasons, the use of a jet momentum pump for absorption and a centrifugal contactor with turbine blades for desorption has been suggested in the process. This appears to be one of the promising methods for carbon dioxide removal in the air and space crafts.

The processes and contactors which can be operated in air and space crafts are few because they are restricted by the conditions mentioned previously. Contactors, which can be operated in the zero gravitational field and which are reviewed in this report, include the packed beds filled with adsorbent particles, venturi contactors, and centrifugal contactors. Emphasis will be placed on the description on one of the centrifugal contactors (3).

Packed Bed

The adsorption method has been developed recently because it can easily be designed for operation under the condition of weightlessness.

The typical system has two beds of molecular sieve connected in parallel. While one bed is adsorbing carbon dioxide from the exhaust cabin air, the other is being regenerated or desorbed. The desorption of the bed is usually accomplished by applying heat, vacuum or a combination of both after the bed has been isolated from the removing process (4).

Detailed reviews and studies (4, 5, 6) on the use of molecular sieve for the removal of carbon dioxide are available.

The pressure drop of gas through the bed of the adsorbing particles is generally not small. Therefore, if the duration of a space mission is prolonged or if the size of the cabin space is increased, the weight and volume of the bed and the power required to operate it may become excessive.

Venturi Contactor

Venturi contactors were originally developed for the purpose of dust and mist separation. In one mode of operation the gas to be scrubbed is passed through a tube where low pressure liquid is injected into the gas stream at the high velocity throat section of the tube. A high degree of liquid dispersion is attained when the gas velocity is high. On the other hand, the introduction of gas at the throat of the venturi, through which a liquid stream flows, results in a mixture of finely dispersed bubbles in the liquid. Both situations give rise to the effective mass transfer in the venturi contactor (7).

In general, the venturi contactor has a high capacity and an appreciably low energy requirement for a given amount of solute gas transfer. In addition, it can be directly incorporated into any process without additional equipment. Therefore, the capital cost of a venturi contactor is low compared to an absorption column. For these reasons, venturi contactors can probably be employed advantageously for the purpose of removing carbon dioxide in space crafts. However, the published studies on the mass transfer characteristics of the venturi contactor are few. One shortcoming of the venturi contactor is that the pressure drop of fluid through a venturi is generally high because the fluid throughput must be maintained at a high level.

Centrifugal Contactor

Recently centrifugal contactors consisting of all rotating parts in which mass transfer operations are carried out have been developed (8, 18). These contactors are not influenced by gravitational force and have the characteristically high gas and liquid throughput, small holdup, short contact time, and high efficiency.

Takahashi (8) has established the design method for a new centrifugal contactor (3) whose main part consists of double or multi-stage concentric perforated cylinders. The schematic diagram of the contactor is shown in Figure 1. The liquid fed near the center of the rotating cylinder via a rotating hollow shaft is spouted from many small holes drilled through the wall of the cylinder into an annular space formed by the double cylinders. The gas is sent cross-currently to the liquid jet in an annular space. Mass transfer between the gas and liquid takes place as a result of the contact between the gas and the liquid jet or the gas and the liquid film on the inside wall of the rotating wetted cylinder.

Some of the fundamental data required for designing this contactor are given in this report.

In a multi-stage centrifugal contactor of the cross-flow type, the discharge velocity of the liquid from a rotating small hole is influenced by the diameter and length of a hole, the diameter of the cylinder, the pressure of the inlet liquid, the depth of the liquid holdup in the cylinders, and the revolution speed of the rotor (12, 13). For a stable operation, the flow pattern of the liquid jet and the discharge coefficient must be considered first in the designing of this contactor.

Flow pattern of the liquid jet

As the discharge velocity increases, the flow pattern of the liquid issuing from a rotating nozzle or orifice becomes dripping flow, laminar flow, turbulent flow, and spray. This mode of flow pattern change is the same as that in the gravitational field (9, 10). Since gas flows normally to the rotating liquid jet, the behavior of the liquid jet in the contactor is influenced not only by the disturbance in the liquid but also by the friction with air. The breakup length of the laminar liquid jet increases with the discharge velocity. When the viscosity of the liquid increases, the breakup length becomes longer and the critical velocity to the spray tends to be higher at the low velocity. The effect of the surface tension on the contraction of the liquid jet may be negligible when the Weber number exceeds 4 (10). These results show that the flow pattern of the liquid depends on the Reynolds number Re_d, the Jet number Je, and the physical properties of the liquid (11, 16). The Reynolds number based on the hole diameter indicates the degree of the turbulence in the fluid. The Jet number based on the relative velocity determines the effect of the resistance of the surrounding gas.

Discharge coefficient

If the coordinate system rotating at a constant angular velocity, ω, is used, and if the Coriolis force is omitted, the Bernoulli equation for the centrifugal field is represented by

$$\frac{1}{2}(v^*)^2 - \frac{r^2\omega^2}{2} + \frac{p}{\rho} + gz = \text{const.} \qquad (1)$$

where v^* is a relative velocity of fluid with respect to the rotating coordinates.

By using the boundary conditions at I and II in Figure 2,

$$\text{B. C. 1:} \quad r = R_1, \quad p_1 = P_1, \quad v^* = 0 \tag{2}$$

$$\text{B. C. 2:} \quad r = R_2, \quad p_2 = P_2, \quad v^* = w$$

the expression for the discharge velocity w is obtained as follows:

$$w = \sqrt{2\,\frac{\Delta P}{\rho} + (R_2^2 - R_1^2)\omega^2} \tag{3}$$

where the pressure difference ΔP is given by

$$\Delta P = P_1 - P_2 \tag{4}$$

Therefore, the flow rate Q is given by the following equation in an ideal case.

$$Q = wf_2 = C_c f \sqrt{2\,\frac{\Delta P}{\rho} + (R_2{}^2 - R_1{}^2)\omega^2} \tag{5}$$

where f_2 is the cross-sectional area of jet spouted from a small hole and f is the cross-sectional area of the hole. Contraction coefficient C_c in Equation (5) is defined by the equation

$$C_c = f_2/f \tag{6}$$

In practice, however, Equation (5) does not hold because of various losses of fluid flow, and the discharge coefficient should be defined by the following equation (12).

$$Q = Cf\sqrt{2\,\frac{\Delta P}{\rho} + (R_2{}^2 - R_1{}^2)\omega^2} \quad ; \qquad C = C_c \cdot C_v \tag{7}$$

where C is the discharge coefficient in the centrifugal field and C_v is the velocity coefficient.

Solving the Navier-Stokes equation for the motion of fluid in the concentric double cylinder with the boundary conditions (see Figure 3).

$$\begin{aligned} &\text{B. C. 1;}\quad r = r_1,\quad \omega = \omega_1,\quad p = P_1 \\ &\text{B. C. 2;}\quad r = r_2,\quad \omega = \omega_2,\quad p = P_2 \end{aligned} \tag{8}$$

the following equations are obtained.

$$V_\theta(r) = \frac{1}{r_2^2 - r_1^2}\left[r(\omega_2 r_2^2 - \omega_1 r_1^2) - \frac{r_1^2 r_2^2}{r}(\omega_2 - \omega_1)\right] \tag{9}$$

$$P(r, z) = P_1(z) + \frac{\rho}{(r_2^2 - r_1^2)^2}\left[(\omega_2 r_2^2 - \omega_1 r_1^2)^2 \frac{r^2 - r_1^2}{2}\right.$$

$$\left. - 2r_1^2 r_2^2 (\omega_2 - \omega_1)(\omega_2 r_2^2 - \omega_1 r_1^2) \ln \frac{r}{r_1} - \frac{r_1^4 r_2^4}{2}(\omega_2 - \omega_1)^2\left(\frac{1}{r^2} - \frac{1}{r_1^2}\right)\right] \tag{10}$$

where z indicates the axial coordinate in the direction of gas flow. For the fluid within the rotating cylinders, the boundary conditions are

$$\begin{aligned} &\text{B. C. 1;}\quad r_1 \to 0,\quad \omega_1 = 0,\quad p = P_1 = P_s \\ &\text{B. C. 2;}\quad r = r_2 = R_1,\quad \omega_2 = \omega,\quad p = P_1 \end{aligned} \tag{11}$$

Thus, the pressure P_1 at the inner wall of the cylinder becomes (12)

$$P_1 = P_s + \frac{R_1^2\,\omega^2}{2}\rho \tag{12}$$

Consider the case in which the outer and inner cylinders rotate with the constant angular velocity ω as shown in Figure 4, and in which a heavy liquid is issued through holes because of the centrifugal pressure due to the difference in density. For this case the following equations are obtained by substituting $\omega = \omega_1 = \omega_2$ into Equations (8) and (9),

$$V_\theta(r) = r\,\omega \tag{13}$$

$$P(r, z) = P_1(z) + \frac{\rho\omega^2}{2}(r^2 - r_1^2) \tag{14}$$

Equation (13) shows that the fluid filling the horizontal cylinder rotating with a constant angular velocity ω rotates around a horizontal axis as does a solid rod (12, 13).

Assuming that the light liquid phase (or gas phase in case of a gas-liquid system) is continuous, the pressure difference between R_0 and R_1 in the heavy liquid phase (or liquid phase in case of a gas-liquid system) is obtained from Equation (14) as

$$P_1 - P_0 = \rho_h \frac{(R_1^2 - R_0^2)}{2}\,\omega^2 \tag{15}$$

The pressure difference between R_0 and R_2 in the light liquid phase (or gas phase in case of a gas-liquid system) is also similarly obtained as

$$P_2 - P_0 = \rho_\ell \frac{(R_2^2 - R_0^2)}{2}\,\omega^2 \tag{16}$$

Substituting Equations (15) and (16) into Equation (7) the following equation is obtained.

$$Q = C.f\sqrt{\frac{(\rho_h - \rho_\ell)}{\rho_h}(R_2^2 - R_0^2)\,\omega^2} \tag{17}$$

This equation defines the discharge coefficient for the liquid-liquid system in the centrifugal field. When $\rho_h >> \rho_\ell$, Equation (17) becomes (14)

$$Q = C.f.\omega\sqrt{R_2^2 - R_0^2} \tag{18}$$

which defines the discharge coefficient for the gas-liquid system for the case in which the liquid film on the inside wall of the rotating wetted cylinder is issued through a hole.

Pressure loss

The pressure loss of the gas which flows crosscurrently to the liquid jet in an annular space can be computed from the following empirical equation (15).

$$\Delta h = 0.1 \times 10^{-6} \frac{\rho_g^{3.5}\ w^2\ v^{1.83}\ D_i^{1/3}\ N^{2/3}\ d^3}{\mu_g^{2.5}\ \rho_\ell\ D_e^{0.17}\ g} \tag{19}$$

where $D_e (= D_{i+1} - D_i)$ is the equivalent diameter. This equation indicates that the pressure loss of the centrifugal contactor is very small.

Mass transfer

In a centrifugal contactor, mass transfer between gas and liquid takes place as a result of contact between gas and liquid jets and that between gas and liquid film on the inside wall of the rotating wetted cylinder. According to the experimental results (16, 17) the extent of the mass transfer into a liquid film on the inside wall of the rotating wetted cylinder is much less than that into a liquid jet issued from rotating holes.

The liquid phase capacity coefficient for the liquid jet from a rotating hole was measured experimentally by using a pure carbon dioxide-water system (16). The result is expressed as

$$K_L a = 73\left(\frac{D_L}{\Pi\theta}\right)^{1/2} \left(\frac{1}{d^{1.20}}\right)\left(\frac{R_1 N'}{w}\right)^{\alpha} \tag{20}$$

where N' is the revolution speed of the rotor (r.p.s.), D_L is diffusivity in liquid phase, Π is the total pressure, and the power α is given by

$\alpha = 0.72$ when $d > 1.0$ mm

$$\alpha = 3.93d^{0.74} \qquad \text{when} \qquad d < 1.0 \text{ mm}$$

The contacting time between gas and liquid θ can be determined theoretically as (11)

$$\theta = \frac{R_i\sqrt{(m^2 - 1)\left(\frac{R_i\omega}{w}\right)^2 + m^2} - R_i}{w\left\{\left(\frac{R_i\omega}{w}\right)^2 + 1\right\}} \tag{21}$$

where

$$m = R_{i+1}/R_i$$

According to the experimental result of adiabatic humidification in the contactor, the gas phase capacity coefficient for the liquid jet from a rotating hole can be expressed as

$$k'_G\, a = 0.422 \times 10^{-3}\, n'(NR_{i+1})^{0.5}\, G^{0.8} \tag{22}$$

where G is the mass flow rate of air, and n' is the number of holes.

Stability conditions for operation

In the design of a centrifugal contactor, the stability condition for operation must be considered. Since the discharge pressure of the liquid from a hole in the first cylinder can be fixed arbitrarily as shown in Figure 5, we shall first analyze an arbitrary stage, say the ith stage.

Assuming that the pressure drop of gas and that of liquid in the axial direction in an annular space formed by double cylinders is negligible in comparison with the centrifugal pressure, Equation (17) gives (15, 17)

$$Q = C_i F_i\, \omega \sqrt{\beta} \sqrt{R_i^2 - (R'_i - d_{Li})^2} \tag{23}$$

where β is defined as

$$\beta = (\rho_h - \rho_\ell)/\rho_h \tag{24}$$

The thickness of cylinder t is given by $(R_i - R_i')$. Therefore, from Equation (23),

$$\frac{d_{Li} + t}{R_i} = 1 - \sqrt{1 - \left(\frac{Fr_i}{C_i\sqrt{\beta}}\right)^2} \tag{25}$$

it can be seen from the equation that the liquid depth in the cylinder d_{Li} depends on R_i and Fr_i. Fr_i is the Froude number in centrifugal field at the ith stage defined by

$$Fr_i = \frac{Q_i}{F_i\ R_i\omega} \tag{26}$$

The relation of Equation (25) is shown in Figure 6.

For the design of a multistage centrifugal contactor, the different cases where

(1) cross sectional area of holes drilled through the ith cylinder wall, F_i, is constant,

(2) total hole area to cylinder area ratio e_i is constant,

(3) liquid depth in a cylinder d_{Li} is constant,

(4) d_{Li} is given,

can be considered.

Furthermore, if the discharge coefficient C_i is constant, the liquid depth d_{Li}, the total hole area F_i, the discharge velocity of liquid w_i, and the ratio of hole area to cylinder area e_i are different from stage to stage, as shown in Table 1. They are calculated by equations given in Table 2.

The discharge pressure of the liquid from a hole in the first cylinder can be arbitrarily fixed. Then, it is desirable that the 2nd stage be selected as the starting point for the design of the complete system. For designing the

2nd stage, the total hole area F_2 must be determined by Equation (23) to establish the desirable value of the discharge velocity w_2 and of liquid depth d_{L2}. Then, according to the predetermined conditions for the design, F_i, Fr_i, d_{Li}, and w_i are determined from Table 2. Since d_{Li} 0, the necessary condition for stable operation for the ith stage is obtained from Equations (23) and (25) as

$$\sqrt{1 - \left(\frac{R_i'}{R_i}\right)^2} < \frac{Fr_i}{C_i\sqrt{\beta}} < 1 \tag{27}$$

If the value of the Froude number satisfies the condition given by Equation (27), the contactor will operate stably.

For a stable operation, it can be seen from Equation (25) that the change of the liquid depth is influenced by the discharge velocity of liquid. The revolution speed of the contactor is also an important factor. Furthermore, it is evident from Figure 6 that d_L changes less in the region of the low Froude number at constant C and R. Therefore, the stability increases as F and ω become larger. When the Froude number is too small, however, Equation (27) is not satisfied. And since the stability depends not only upon the value of d_L but also on the rate of its change, a small value of the Froude number is not desirable because d_L becomes too small.

As can be seen from the expression of the Froude number, the liquid depth in the centrifugal contactor depends on the discharge velocity of liquid and the revolution speed of the contactor. This is an important feature of the centrifugal contactor. Suppose that a contactor is designed with the condition of the liquid flow rate Q and the revolution speed N. If its operating condition is changed to another liquid flow rate Q', and another revolution speed N' at which a stable operation is possible, we obtain from analogy.

Table 1

Different cases for design of the multistage centrifugal contactor

Case	d_{Li}	F_i	w_i	e_i
1	decrease	constant	constant	decrease
2	decrease	increase	decrease	constant
3	constant	decrease	increase	decrease
4	given value	---	---	---

Table 2

Equations for design of the multistage centrifugal contactor

Case	d_{Li}	F_i/F_2	F_{ri}/F_{r2}
1	Eq. (25)	1	R_2/R_i
2	Eq. (25)	R_i/R_2	$(R_2/R_i)^2$
3	$d_{Li} = d_{L2} = d_L$	$\frac{C_2}{C_i}\sqrt{\frac{2 - d_L/R_2}{2R_i/R_2 - d_L/R_2}}$	$1/(F_i/F_2)(R_i/R_2)$ at constant C_i
4	d_{Li} is given	$\frac{C_2}{C_i}\sqrt{\frac{R_2^2 - (R_2' - d_{L2})^2}{R_i^2 - (R_i' - d_{Li})^2}}$	$1/(F_i/F_2)(R_i/R_2)$

$$Fr = Fr'$$

or

$$\frac{Q}{N} = \frac{Q'}{N'} \tag{28}$$

In this case, d_L does not change. However, as the discharge velocity of liquid changes from $w_i = Q/F_i$ to $w_i' = Q'/F_i$, the change of the characteristics of mass transfer cannot be avoided. This can be seen from Equation (20). The number of stages and the magnitude of space between cylinders can be determined from the operating condition for the mass transfer.

This review leads to the general conclusions that the pressure drop of gas is small, the throughput of gas and liquid is large, and the mass transfer rate is efficient in the centrifugal contactor. Furthermore, it can be easily operated in the zero gravitational field. Therefore, the centrifugal contactor may be suitable for gas-liquid contact operation in air and space crafts.

Nomenclature

C	Discharge coefficient in the centrifugal field	[-]
d	Diameter of hole	[cm]
d_L	Liquid depth in cylinder	[cm]
D	Diameter of cylinder	[cm]
D_L	Diffusivity in liquid phase	[cm^2/sec]
e	Ratio of area of hole to cylinder	[-]
f	Cross-sectional area of hole	[cm^2]
F	Total hole area of a cylinder	[cm^2]
g	Acceleration of gravity	[cm/sec^2]
G	Mass rate of air	[g dry air/sec]
Δh	Pressure loss	[cm w.c.]
k_La	Liquid phase capacity coefficient	[1/sec]
k_Ga	Gas phase capacity coefficient	[g/cm^3 sec ΔH]
n	Number of holes in axial direction of cylinder	[-]
n'	Total number of holes in a cylinder	[-]
N	Rate of revolution	[r.p.m.]
p, P	Pressure	[dyne/cm^2]
Q	Volumetric rate of liquid flow	[cm^3/sec]
r	Radial distance	[cm]
R	Radius of cylinder	[cm]
t	Thickness of cylinder wall	[cm]
v	Flow rate of gas	[cm/sec]
w	Discharge velocity of liquid	[cm/sec]
μ	Viscosity	[g/cm sec]
ρ	Density	[g/cm^3]

σ	Surface tension	[dyne/cm]
ω	Angular velocity	[rad/sec]
Je	Jet numbers = $(\frac{dw^2\rho_g}{\sigma})(\frac{\rho_\ell}{\rho_g})^{0.45}$	[-]
Re_d	Reynolds number based on hole diameter = $dw\rho/\mu$	[-]
Fr	Froude number in centrifugal field, = $w/R\omega$	[-]
We	Weber number = $dw^2\rho/\sigma$	[-]

Literature Cited

1. Barker, R. S., Nicol, S. W., Yakut, M. M., and Anderson, J. L., A paper presented at the National Aeronautics and Space Engineering Meeting, Los Angeles, Calif., Oct. (1968).

2. Reid, R. C., and Richardson, D. C., A paper presented at the Symposium on Aerospace Life Support System, 61st Annual Meeting of A.I.Ch.E., Los Angeles, Calif. Dec. (1968).

3. Japan Patent 224,131.

4. Stolk, R. D., Chem. Eng., Oct. 24, 143, (1966).

5. Major, C. J., I&EC, Process Design and Development, 4, 327 (1965).

6. Blakely, R. C., and Barker, R. S., (Douglas Missile & Space Systems Division) Douglas Report SM-43403 May (1966).

7. Perry, J. H., "Chemical Engineers' Handbook" 4th ed. 18-55, McGraw-Hill Book Company, New York (1963).

8. Takahashi, T., Kagaku Kikai Gijutsu (Japan), 16, 56 (1964).

9. Takahashi, T., Kagaku Kogaku, (Japan), 30, 68 (1966).

10. Kuzabayashi, T., Trans. J.S.M.E., (Japan) 25, 1252, 1259, 1266 (1957), 26, 1536, 1543 (1960).

11. Takahashi, T., Memoirs of the School of Eng., Okayama Univ., 1, 29 (1966).

12. Takamatsu, T., Takahashi, T., and others, Kagaku Kogaku, (Japan) 22, 555 (1958).

13. Takamatsu, T., Takahashi, T., and others, Kagaku Kogaku, (Japan) 22, 561 (1958).

14. Takamatsu, T., Takahashi, T., and K. Tanaka, A paper presented at the 27th meeting of Soc. of Chem. Eng. Tokyo, Japan, April (1962).

15. Mizushina, T., Takamatsu, T., and Takahashi, T., a paper presented at the 24th Meeting of Soc. of Chem. Eng. Kyoto, Japan, April (1959).

16. Takamatsu, T., Takahashi, T., and others, Kagaku Kogaku (Japan) 25, 595 (1961).

17. Takamatsu, T., Takahashi, T., and others, Kagaku Kogaku (Japan) 27, 156 (1963).

18. Takahashi, T., and Fan, L. T., Report No. 10, Institute for Systems Design and Optimization, Kansas State University, Manhattan (1968).

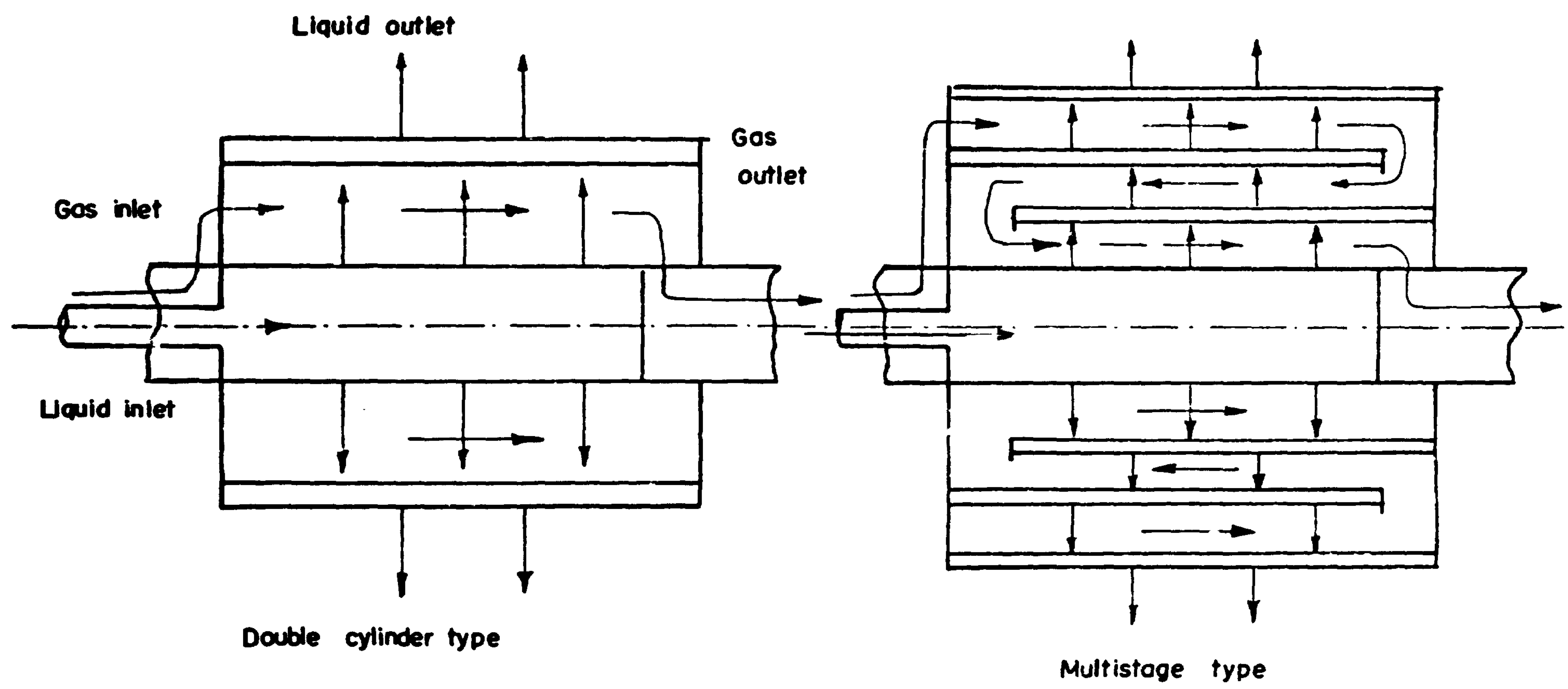

Fig. 1 Schematic diagram of the centrifugal contactor.

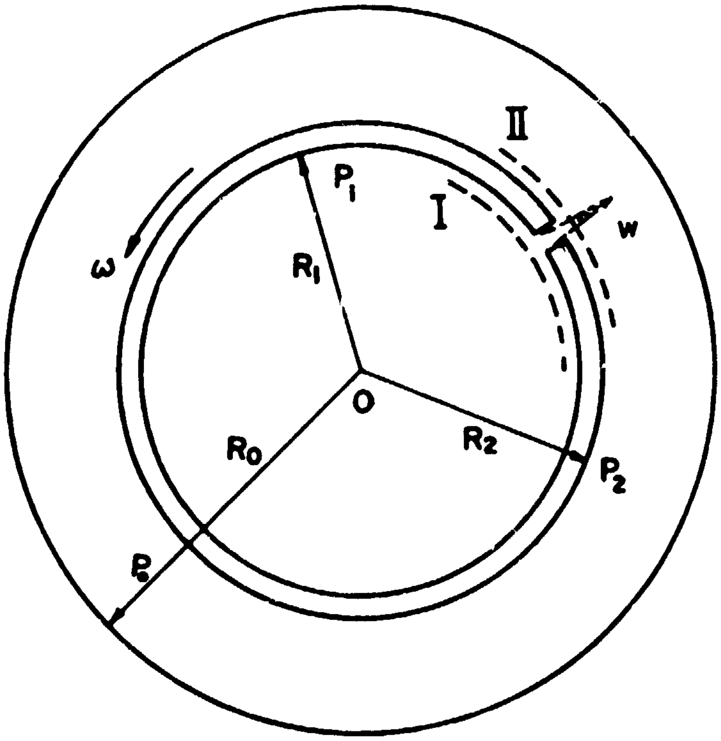

Fig. 2 Sectional diagram of rotating part .

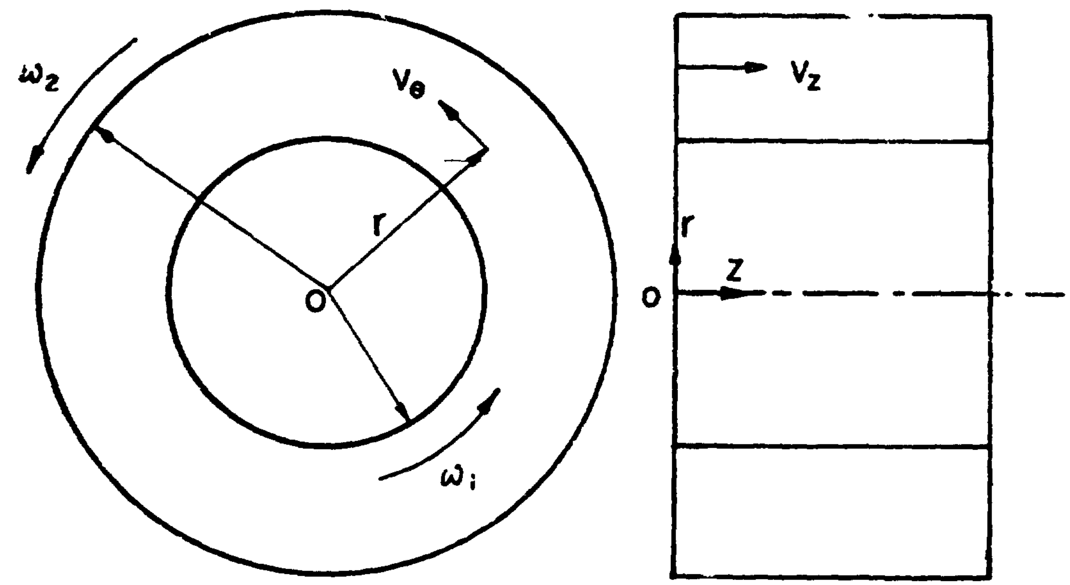

Fig. 3 Motion of fluid in concentric double cylinder.

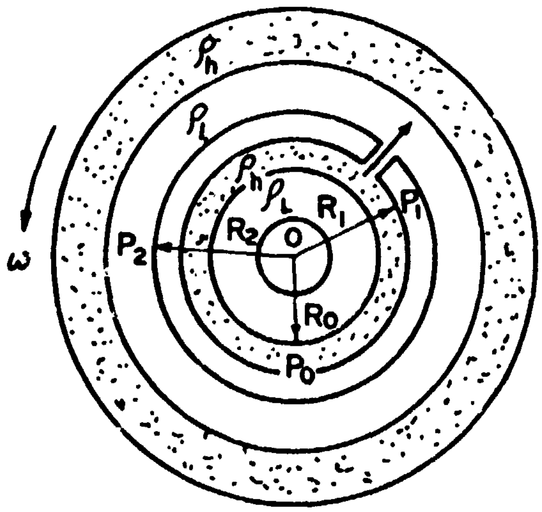

Fig. 4 Concentric double cylinder with constant angular velocity.

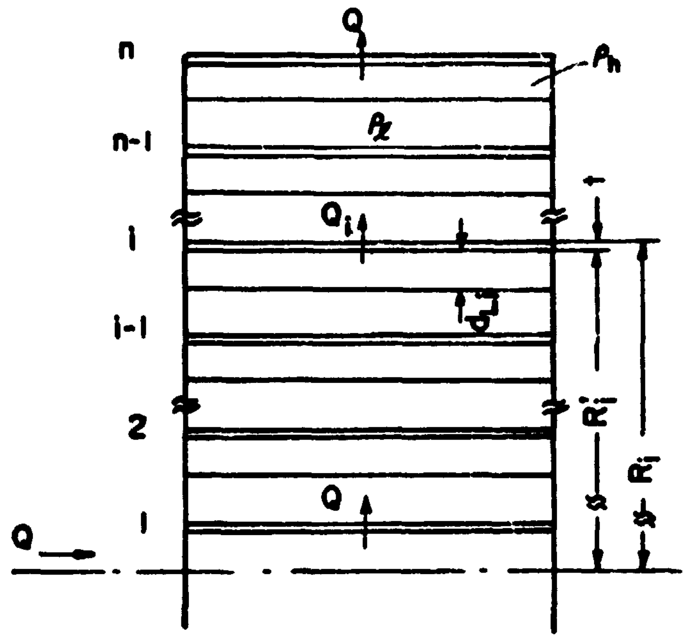

Fig. 5 Schematic diagram of the multistage centrifugal contactor.

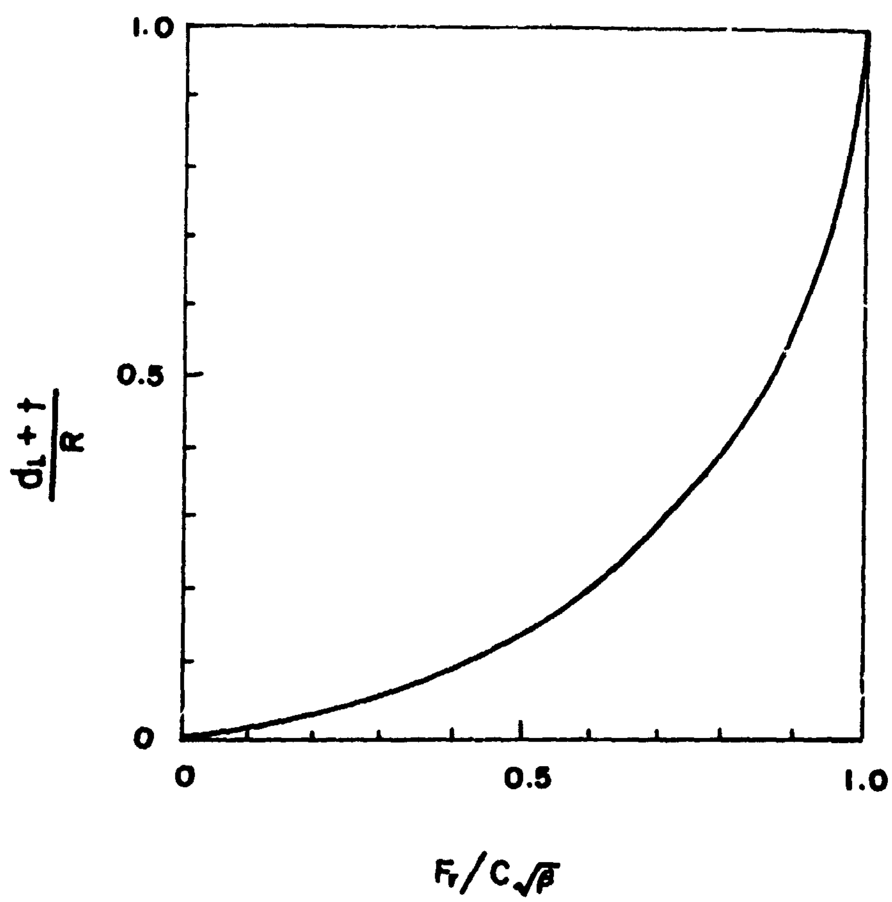

Fig. 6 Relation among liquid depth, diameter of rotor, and Froude number.

(d) 1

Build. Sci. Vol. 5, pp. 57–71. Pergamon Press 1970. Printed in Great Britain

SfB	Ab8
UDC	697

Applications of Modern Optimal Control Theory to Environmental Control of Confined Spaces and Life Support Systems*

Part 1—Modeling and Simulation

L. T. FAN†
Y. S. HWANG†
C. L. HWANG†

This paper is the first of a series of five containing the results of an original investigation of the temperature control of confined spaces such as those in any building and life support systems by means of the modern control theory. While much of the material presented in this work is original, the series has been prepared in sufficiently tutorial style that it can be used as a text for self-study by practicing air-conditioning engineers. It is hoped that this work will stimulate the applications of and research on the modern optimal control theory to the environmental control of life support systems in general, including controls of humidity, purity and noise.

Parts 2–5 will be published in the next three issues of *Building Science*.

Several mathematical models of an environmental control system which consists of a confined space or cabin, a heat exchanger, and a feedback element such as a thermostat are presented. The performance equations of the system, which represent the dynamic characteristics of the system proper and of the heat exchanger (the control element of the system) are derived. In the basic model the flow of air in the confined space is considered to be in the state of complete mixing and the disturbance is caused by an impulse heat imput. The performance equations in which the heat disturbances are of the form such as the step function and cyclic function which are different from the impulse function are also derived. Also presented are the performance equations which represent the dynamic characteristics of flow of air in a confined space or cabin characterizeu by the two completely stirred tanks-in-series (2 CST's-in-series) model.

To determine the goodness of the system model a computer simulation is carried out and the results are compared with the known characteristics of the system.

THIS series of five articles contains results of the original investigation on the control of life support systems or more specifically the temperature control of life support systems by means of the modern control theory. A life support system is a system for creating, maintaining, and controlling an environment so as to permit personnel to function efficiently. The control of temperature is probably the most important role of the life support system.

The need for providing an automatic control system to an air-conditioning system has long been recognized[1,2]. It is also a well known fact that use of the automatic control is necessary for the life support system of a space cabin or submarine or underground shelter[3,4]. It appears that analysis and synthesis of the control systems for the air-conditioning and life support systems have so far been carried out by the classical approach[1–4].

The classical approach to the analysis and synthesis of an automatic control system is essentially a trial-and-error procedure or a disturbance–response (or input–output) approach. Extensive use is made of the transform methods such as the Laplace transform (s-domain), Fourier transform (ω-domain), and z transform (discrete time-domain). Even though mathematics is extensively used, the classical approach is essentially an empirical one[5].

In recent years, an approach to the analysis and synthesis of a control system, which is distinctly different from the classical one, has been developed. This modern approach is generally called the modern (optimal) control theory [5–11]. It is based on the state–space characterization of a system.

* This work was supported by the Air Force Office of Scientific Research, Office of Aerospace Research, United States Air Force, Under Contract F 44620-68-0020 (Themis Project), and NASA Grant Under Contract NGR-17-001-034.

† Institute for systems design and optimization, Kansas State University, Manhattan, Kansas.

The state-space is the abstract space whose coordinates are the state properties of the system or the variables which define the characteristics of the system[5]. This approach involves mainly maximization or minimization of an objective function (functional) which is a function of state (plant) and control variables which are in turn functions of time and/or distance coordinate. The objective function is specified, constraints are imposed on the state and decision variables, and an optimal control policy is determined by extremizing the objective function by means of mathematical techniques such as the calculus of variations, maximum principle, and dynamic programming[5, 6]. This modern approach is entirely theoretical in the sense that no trial-and-error is involved in "adjusting the controller".

There are reasons to believe that the classical approach suffices in the analyses and syntheses of the control systems for a majority of air-conditioning and life support systems because usually the requirements are not extremely critical and specifications are not very tight. It is, therefore, justifiable that most of the control and dynamic investigations of air-conditioning and life support systems, which have appeared in the open literature, are based on the classical approach[12–20]. There is, however, a certain incentive in applying the modern approach to analysis and synthesis of automatic environmental control systems in space crafts, submarines, underground civil defense shelters and certain medical facilities. In these systems, very stringent requirements in the response time, control effort, and others are imposed. For example, the control system of a space craft must have an extremely small response time and furthermore, the amount of energy required for the control effort must be very small because of the weight limitation imposed on the space craft.

In the present work, the emphases are on the use of the maximum principle and related variational techniques[5, 7–11]. Their applications will be illustrated by means of concrete numerical examples. It is said that use of the maximum principle and the calculus of variations gives rise to a control policy of an open loop nature[5,21] which is not desirable for control of a space heating system in which room temperature variations are to be reduced and penalized[22]. In reference [22], the dynamic programming technique is employed. It will be shown, however, that the maximum principle and related techniques can be advantageously employed for the types of systems and objective functions considered in this work.

In this series of presentation, only the modeling and control of deterministic systems are considered. However, when human and physiological factors are taken into account as part of a total life support system, use of the stochastic modeling and control may be more appropriate than use of the deterministic modeling and control because the system tends to be more stochastic than deterministic.

It is hoped that this work will stimulate the applications of and research on the modern optimal control theory to the environmental control of life support systems in general, including controls of humidity, purity and noise.

The first of this series of articles on the application of the modern control theory to life support systems contains the derivation of the mathematical models of several different systems and the simulations of their behavior and characteristics. In the second of the series, the most basic form of Pontryagin's maximum principle, which together with dynamic programming constitutes the bulk of the modern control theory, is outlined and its use is fully demonstrated by means of concrete numerical examples. In Part 3 of the series, the optimal control of a system with equality state variable constraints imposed at the end of the control action is considered. The fourth of the series deals with realistic problems of controlling systems with constraints imposed on the state variable, namely the temperature in the systems. In the final part of this series, some aspects of sensitivity analysis are presented and discussed by fully exploiting the results obtained in the preceding parts.

While much of the material presented in this work is original, this series of five articles is prepared in such a manner that it can be used as a text for self-study by practicing life support systems engineers or as a text in graduate or advanced undergraduate courses concerned with life support systems or air-conditioning.

MODELING

A control system usually consists of three elements: the feedback element, the control element, and the system proper[23]. The feedback element in a life support control system or an environmental control system may be composed of a thermostat, humidistat and pressure regulator, or any combination of these, depending on the purpose of control. The control element may include a heat exchanger, humidifier, dehumidifier, blower, portable air-conditioner, or any combination of these, depending on the objective of control. For instance, both the thermostat and heat exchanger are often used to control the air temperature inside a building. The system proper may be a confined space, e.g., an underground shelter, a space vehicle, a space suit, a submarine or a building.

The system considered here is shown schematically in figure 1. The confined space may be a typical office located in a multi-story building or the cabin of a spaceship. Air or oxygen or a mixture of oxygen and nitrogen is circulated through the room or confined space via an air duct by mechanical means, e.g., a blower or fan. Control of air temperature in the system is accomplished with a duct system. The thermostat in the system adjusts the position of the control valve of the heat excnanger in order to provide the desired temperature.

The performance equations of the system, which represent the dynamic characteristics of the system and system components will be derived.

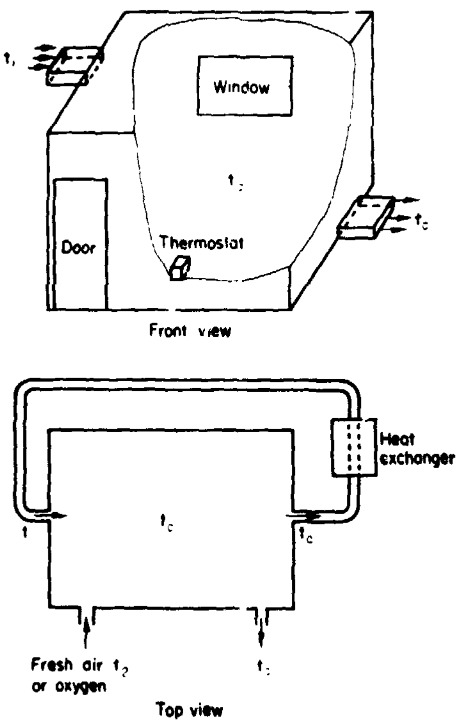

Fig. 1. Air-conditioned room.

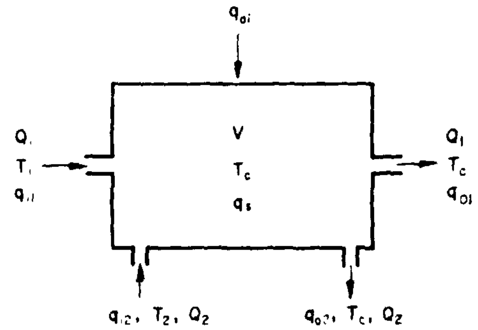

Fig. 2. Room heat flow rates.

$$[\text{heat in}] - [\text{heat out}] = [\text{heat accumulation}] \quad (1)$$

$$[\text{heat in}] = q_{i1} + q_{i2} + q_{di} \quad (2)$$

$$[\text{heat out}] = q_{01} + q_{02} \quad (3)$$

$$[\text{heat accumulation}] = q_s \quad (4)$$

where

q_{di} = heat disturbance in impulse form in kcal/s

q_{i1} = heat flow into the system proper by circulation air in kcal/s

q_{i2} = heat flow into the system proper by fresh air in kcal/s

q_{01} = heat flow out of the system proper by circulation air in kcal/s

q_{02} = heat flow out of the system proper by exhausted air in kcal/s

q_s = rate of heat stored inside the system proper in kcal/s

Whenever the unit system is needed the mks system is used in this study. Inserting equations (2), (3) and (4) into equation (1) gives

$$[q_{i1} + q_{i2} + q_{di}] - [q_{01} + q_{02}] = q_s \quad (5)$$

Based on the assumption of perfect mixing, the expressions for $q_{i1}, q_{i2}, q_{01}, q_{02}$ and q_{di} are

$$q_{i1} = Q_1 \rho C_p (t_i - t_a) = Q_1 \rho C_p T_i \quad (6)$$

$$q_{i2} = Q_2 \rho C_p (t_2 - t_a) = Q_2 \rho C_p T_2 \quad (7)$$

$$q_{01} = Q_1 \rho C_p (t_c - t_a) = Q_1 \rho C_p T_c \quad (8)$$

$$q_{02} = Q_2 \rho C_p (t_c - t_a) = Q_2 \rho C_p T_c \quad (9)$$

$$q_{di} = V_1 \rho C_p (t_d - t_a) \delta(\alpha) = V_1 \rho C_p T_d \delta(\alpha)$$

Note that here the disturbance is considered to be an impulse form. This disturbance term will appear as a forcing function which can be generally

A. The system proper

The following three main assumptions are made concerning the system proper:

(i) Room or cabin air is well mixed, or stated in another way, air temperature within the system is uniform throughout at any instant in time.

(ii) The thermal capacitance of room walls, floor, ceiling, and window is neglected, as well as that of any furniture within the system.

(iii) Heat loss through the walls and windows is negligible.

The performance equation of the system proper can be obtained by using the continuity law or heat balance. For a room, the law states that the flow of heat into the system must either be absorbed inside the room or leave the room. Referring to figure 2, we have designated as $\phi(\alpha)$ in the resulting differential equation. $\phi(\alpha)$ can be written as

$$\phi(\alpha) = M_i \delta(\alpha)$$

where

$$M_i = V_1 \rho C_p T_d$$

Also note that $\delta(\alpha)$ has a unit of $\sec^{-1}$. The rate at which heat energy is stored in the system proper can be expressed as

$$q_s = V_1 \rho C_p \frac{dt_c}{d\alpha}$$

$$= V_1 \rho C_p \frac{dT_c}{d\alpha} \quad (11)$$

where

C_p = specific heat of air in kcal kg C
Q_1 = air flow rate by circulation in m^3 s
Q_2 = flow rate of fresh air in m^3 s
V_1 = room volume in m^3
t_a = reference temperature in °C (In general this can be any arbitrarily and suitably fixed temperature)
t_c = room temperature in °C
t_d = disturbance temperature in °C
t_i = temperature of the circulation air into the system proper in °C
t_2 = outside air temperature in °C
$T_c = (t_c - t_a)$ in °C
$T_i = (t_i - t_a)$ in °C
$T_2 = (t_2 - t_a)$ in °C
$T_d = (t_d - t_a)$ in °C
α = time in s
ρ = air density in kg/m^3

The insertion of equations (6) through (11) into equation (5) yields

$$V_1 \rho C_p \frac{dT_c}{d\alpha} + [Q_1 \rho C_p + Q_2 \rho C_p] T_c = Q_1 \rho C_p T_i + Q_2 \rho C_p T_2 + V_1 \rho C_p T_d \delta(\alpha)$$

Q_1, Q_2, ρ, C_p, V_1, and T_d are considered as constants here. The above equation can be simplified by dividing both sides of the equation by $(Q_1 \rho C_p + Q_2 \rho C_p) = (Q_1 + Q_2)\rho C_p$

$$\left.\begin{array}{l} \tau_1 \dfrac{dT_c}{d\alpha} + T_c = r_1 T_i + r_2 T_2 + \tau_1 T_d \delta(\alpha) \\ T_c = T_{c0-} = 0 \quad \text{at} \quad \alpha = 0^- \quad \text{(time immediately before introduction of} \\ \text{the disturbance, i.e time right before } \alpha = 0) \end{array}\right\} \quad (12)$$

(Note that in order to have this initial condition, the room temperature, t_c, before introduction of the disturbance is taken to be the reference temperature, t_a, because $T_c = t_c - t_a$.)

or in dimensionless form

$$\left.\begin{array}{l} \dfrac{dx_1}{dt} + x_1 = \dfrac{r_1 K_1 x_2}{K_4} + r_2 K_1 + K_1 \sigma \delta(t) \\ x_1 = 0 \quad \text{at} \quad t = 0^- \end{array}\right\} (12)\text{a}$$

where

$$r_1 = \frac{Q_1}{Q_1 + Q_2}$$

$$r_2 = \frac{Q_2}{Q_1 + Q_2} = (1 - r_1)$$

$$x_1 = \frac{T_c}{T_{c0}} = \frac{K_1 T_c}{T_2} = \frac{(t_c - t_a)}{(t_{c0} - t_a)}$$

$$x_2 = \frac{T_i}{T_{i0}} = \frac{K_4 T_i}{T_2} = \frac{(t_i - t_a)}{(t_{i0} - t_a)}$$

$$\sigma = \frac{T_d}{T_2} = \frac{(t_d - t_a)}{(t_2 - t_a)}$$

$t = \alpha / \tau_1$ = dimensionless time

$$K_1 = \frac{T_2}{T_{c0}} = \frac{(t_2 - t_a)}{(t_{c0} - t_a)}$$

$$K_4 = \frac{T_2}{T_{i0}} = \frac{(t_2 - t_a)}{(t_{i0} - t_a)}$$

τ_1 = time constant of the system proper in s

$$= \frac{V_1}{Q_1 + Q_2}$$

T_{c0} = room temperature at $\alpha = 0^+$
T_{c0-} = room (system proper) temperature at $\alpha = 0^-$
T_{i0} = temperature of the circulation air into the system proper at $\alpha = 0^+$

Equation (12a) is the performance equation of the system proper. This performance equation can appear in another form in which the effect of the disturbance is taken into account in the initial condition immediately after the onset of the process as shown below:

$$\frac{dx_1}{dt} + x_1 = \frac{r_1 K_1 x_2}{K_4} + r_2 K_1$$

$$x_1 = 1 \quad \text{at} \quad t = 0^+$$

This initial condition is true because $t_c = t_{c0}$ at $t = 0^+$ and therefore,

$$x_1 = \frac{(t_c - t_a)}{(t_{c0} - t_a)} = \frac{(t_{c0} - t_a)}{(t_{c0} - t_a)} = 1 \text{ at } t = 0^+.$$

Instead of the impulse form, the heat disturbance may appear in other forms, such as the step, ramp or cyclic functions. The disturbance arises from various sources, such as sun load, turning on lights, opening window or door, temperature change in the incoming air, and heat generated by the people or animals.

If the temperature of the incoming recycle air, T_i, is kept constant, changing air flow rate may also accomplish the purpose of control. The performance equation for such a case can also be derived similarly from equation (5).

Note that if $Q_2 = 0$ or $r_2 = 0$, r_1 is unity and equation (12) becomes

$$\tau_1 \frac{dT_c}{d\alpha} + T_c = T_i + T_d \tau_1 \delta(\alpha) \qquad (13)$$

This equation is applicable to underground shelters, space crafts and submarines under conditions where no fresh air enters the systems.

B. The control element

The heat exchanger which is the control element of the system under consideration can perform its control function in various ways, for example, by changing the temperature or flow rate of the heat transfer medium, or changing both. The performance equation of the control element can be obtained again by employing the continuity law or heat balance, which can be expressed in equation form as follows:

$$[\text{heat in}] - [\text{heat out}] = [\text{heat accumulation}] \qquad (14)$$

$$[\text{heat in}] = q_{mi1} + q_{mi2}$$

$$[\text{heat out}] = q_{mo1} + q_{mo2}$$

$$[\text{heat accumulation}] = q_{ms}$$

where

q_{mi1} = heat brought into the heat exchanger by circulation air in kcal/s

q_{mi2} = heat brought into the heat exchanger by cooling water in kcal/s

q_{mo1} = heat flow out of the heat exchanger circulation air in kcal/s

q_{mo2} = heat flow out of the heat exchanger cooling water in kcal/s

q_{ms} = heat stored in the heat exchanger in kcal/s

Inserting these definitions into equation (14) gives

$$(q_{mi1} + q_{mi2}) - (q_{mo1} + q_{mo2}) = q_{ms} \qquad (15)$$

By assuming perfect mixing of both air and the heat transfer medium in the heat exchanger, ignoring the heat loss through the shell and neglecting the thermal capacitance of the heat exchanger, the expressions for q_{mi1}, q_{mi2}, q_{mo1}, and q_{mo2} are as follows:

$$q_{mi1} = Q_1 \rho C_p (t_c - t_a) = Q_1 \rho C_p T_c \qquad (16)$$

$$q_{mi2} = Q_w \rho_w C_{pw} (t_{wc} - t_a) = Q_w \rho_w C_{pw} T_{wc} \qquad (17)$$

$$q_{mo1} = Q_1 \rho C_p (t_i - t_a) = Q_1 \rho C_p T_i \qquad (18)$$

$$q_{mo2} = Q_w \rho_w C_{pw} (t_{wh} - t_a) = Q_w \rho_w C_{pw} T_{wh} \qquad (19)$$

The rate at which heat energy is stored in the heat exchanger can be expressed as

$$q_{ms} = V_2 \rho C_p \frac{dt_i}{d\alpha} = V_2 \rho C_p \frac{d(t_i - t_a)}{d\alpha} = V_2 \rho C_p \frac{dT_i}{d\alpha} \qquad (20)$$

where

C_{pw} = specific heat of coolant in kcal/kg°C

Q_w = flow rate of coolant in m^3/s

t_{wc} = inlet temperature of coolant in °C

t_{wh} = outlet temperature of coolant in °C

V_2 = volume of the heat exchanger occupied by air in m^3

ρ_w = density of coolant in kg/m^3

Insertion of equations (16) through (20) into equation (15) gives

$$(Q_1 \rho C_p T_c + Q_w \rho_w C_{pw} T_{wc}) - (Q_1 \rho C_p T_i + Q_w \rho_w C_{pw} T_{wh}) = V_2 \rho C_p \frac{dT_i}{d\alpha}$$

or dividing by $Q_1 \rho C_p$,

$$\tau_2 \frac{dT_i}{d\alpha} + T_i = T_c - \frac{Q_w \rho_w C_{pw} (T_{wh} - T_{wc})}{Q_1 \rho C_p} \qquad (21)$$

where τ_2 is the mean resident time of air in (the time constant with respect to air flow of) the heat exchanger in seconds and is defined by

$$\tau_2 = V_2 / Q_1$$

Note that $Q_w \rho_w C_{pw} (T_{wh} - T_{wc})$ is the amount of heat removed from or added to the system which can be controlled by adjusting either Q_w when ρ_w, C_{pw}, and $(T_{wh} - T_{wc})$ are constant, or $(T_{wh} - T_{wc})$ when Q_w, ρ_w, and C_{pw} are kept constant, or both Q_w and $(T_{wh} - T_{wc})$ when ρ_w and C_{pw} are constant. In order to have a mathematically neat form, a hypothetical temperature T_r is defined as

$$T_r = Q_w \rho_w C_{pw} (T_{wh} - T_{wc}) / Q_1 \rho C_p$$

Inserting this definition into equation (21) yields

$$\tau_2 \frac{dT_i}{d\alpha} + T_i = T_c - T_r \tag{22}$$

or in dimensionless form

$$\frac{\tau_2}{\tau_1}\frac{dx_2}{dt} + x_2 = \frac{x_1 K_4}{K_1} - K_4(K_2\theta + K_3) \tag{22a}$$

where

$$K_2 = \frac{1}{2T_2}(T_{r\,max} - T_{r\,min})$$

$$K_3 = \frac{1}{2T_2}(T_{r\,max} + T_{r\,min})$$

$$\theta = \frac{T_r - \frac{1}{2}(T_{r\,max} + T_{r\,min})}{T_{r\,max} - \frac{1}{2}(T_{r\,max} + T_{r\,min})}$$

$= \text{control variable}$

$$\frac{T_r}{T_2} = K_2\theta + K_3$$

Equation (22) is the performance equation of the heat exchanger which is shown schematically in figure 3. Note that $\theta = +1$ when $T_r = T_{r\,max}$ and $\theta = -1$ when $T_r = T_{r\,min}$.

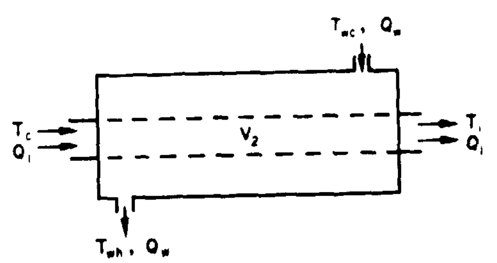

Fig. 3. Schematic diagram of the heat exchanger.

C. *The feedback element–thermostat*

Here we simply assume that the sensing element measures the room temperature instantaneously and that there is no accumulation of heat in the element, or for simplicity, it will be assumed that the sensing element is the zero order element with its time constant, τ_3, equal to zero. Reference 23 gives a detailed explanation of the response of the thermostat.

SIMULATION

With the model in hand, a simulation should be carried out extensively by means of either a digital or analog computer. The results of simulation should then be compared to the known characteristics of the system or to experimentally obtained data. The comparison enables us to determine the goodness of the model as an approximate representation of the system.

For illustration, let us consider a simple system in which the time constant of the heat exchanger is negligibly small, i.e., $\tau_2 \to 0$. For this system we have from equation (22)

$$T_i = T_c - T_r \tag{23}$$

This relation can also be obtained by simple (steady-state) heat balance around the heat exchanger. Note that T_r is positive whenever heat is removed from the system and negative when heat is added. Inserting equation (23) into equation (12) gives

$$\tau_1 \frac{dT_c}{d\alpha} + r_2 T_c = r_2 T_2 + \tau_1 T_d \delta(\alpha) - r_1 T_r$$

$$T_c = T_{c0-} = 0 \quad \text{at} \quad \alpha = 0^- \tag{24}$$

Again note that the room temperature before introduction of the disturbance is taken to be the reference temperature. As mentioned previously this set of equations can be rewritten to give

$$\tau_1 \frac{dT_c}{d\alpha} + r_2 T_c = r_2 T_2 - r_1 T_r$$

$$T_c = T_{c0} = T_d \quad \text{at} \quad \alpha = 0^+ \tag{24a}$$

Steady state Value of T_r before Disturbance, T_{r0-}

The steady state value of T_r before disturbance, T_{r0-}, can be evaluated by inserting

$$T_c = 0, T_d = 0, \quad \text{and} \quad \frac{dT_c}{d\alpha} = 0$$

into equation (24). This gives rise to

$$T_{r0-} = \frac{r_2 T_2}{r_1}, \quad r_1 \neq 0 \tag{25}$$

Note that the steady state value of T_r which is denoted by T_{r0} is zero when the outside air temperature, T_2, is zero, or when the ratio of the fresh air to the total air is zero. This solution can also be obtained by either over-all heat balance around the system or heat balances around the room and the heat exchanger.

(1) Over-all heat balance around the system (figure 4)

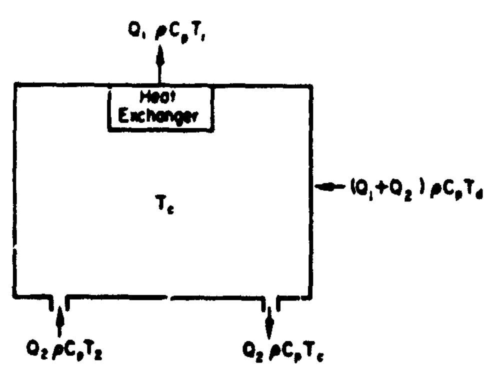

Fig. 4. Overall heat balance of the system with $\tau = 0$.

$$Q_2\rho C_p T_2-(Q_2\rho C_p T_i+Q_1\rho C_p T_r)=0$$

Therefore,

$$T_{r0^-}=\frac{Q_2T_2}{Q_1}=\frac{r_2T_2}{r_1} \tag{25a}$$

Recall that T_i equals zero.

(2) Heat balances around the room and the heat exchanger

$$(Q_1\rho C_p T_i+Q_2\rho C_p T_2)=0$$

and

$$Q_1\rho C_p T_i+Q_1\rho C_p T_r=0$$

Solving for T_{r0} from these equations, we obtain

$$T_r=T_{r0^-}=-T_i=\frac{r_2T_2}{r_1}$$

The final steady state value of T_r, T_{rf}

The final steady state value of T_r, which is denoted by T_{rf}, can be obtained by letting

$$T_c=0 \quad\text{and}\quad \frac{\mathrm{d}T_c}{\mathrm{d}\alpha}=0$$

in equation (24). Hence

$$T_{rf}=\frac{1}{r_1}\left[\tau_1T_d\delta(\alpha)+r_2T_2\right]$$

Initial value of T_c

The initial value of T_c at $t=0^+$ can be calculated by the following relation representing the heat balance between the condition before and that after the disturbance.

$$V_1\rho C_p T_{c0}=V_1\rho C_p T_d$$

or

$$T_{c0}=T_d \tag{26}$$

The desired final value of T_c is zero. Meanwhile, the lower bound of T_r, $T_{r\,\min}$, is set at 0°C. Various cases with different upper bounds of T_r, $T_{r\,\max}$, will be simulated.

The solution of T_c

Simulation of the desired model can be carried out when the form of T_r and the numerical values of the parameters are known. In case T_r is the step function, i.e., T_r remains constant after $\alpha=0$, equation (24a) can be integrated as

$$T_c(\alpha)=\exp\left(-\frac{r_2\alpha}{\tau_1}\right)\left[A_1+T_2\exp\left(\frac{r_2\alpha}{\tau_1}\right)-\frac{r_1T_r}{r_2}\exp\left(\frac{r_2\alpha}{\tau_1}\right)\right]$$

where A_1 is an integration constant. The value of A_1 can be determined by employing the initial condition at $\alpha=0^+$, that is,

$$T_c=T_{c0}\quad\text{at}\quad\alpha=0^+$$

Therefore

$$A_1=T_{c0}-T_2+\frac{r_1T_r}{r_2}$$

and

$$T_c(\alpha)\quad T_{c0}\exp\left(-\frac{r_2\alpha}{\tau_1}\right)+T_2\left[1-\exp\left(-\frac{r_2\alpha}{\tau_1}\right)\right]-\frac{r_1T_r}{r_2}\left[1-\exp\left(-\frac{r_2\alpha}{\tau_1}\right)\right],\ r_2\neq 0 \tag{27}$$

Note that we can also solve equation (24) by means of Laplace transform. Laplace transformation of equation (24) gives

$$T_c(s)=\frac{r_2T_2}{s(\tau_1s+r_2)}-\frac{r_1T_r}{s(\tau_1s+r_2)}+\frac{\tau_1T_d}{\tau_1s+r_2}$$

Inversion of the above equation gives

$$T_c(\alpha)=T_d\exp\left(-\frac{r_2\alpha}{\tau_1}\right)+T_2\left[1-\exp\left(-\frac{r_2\alpha}{\tau_1}\right)\right]-\frac{r_1T_r}{r_2}\left[1-\exp\left(-\frac{r_2\alpha}{\tau_1}\right)\right]$$

which is identical to equation (27) because $T_{c0}=T_d$ as given by equation (26). α_f can be found from equation (27) by setting $T_c=0$.

$$\alpha_f=-\frac{\tau_1}{r_2}\ln\left(\frac{r_1T_r-r_2T_2}{T_{c0}r_2-T_2r_2+r_1T_r}\right),\ r_2\neq 0 \tag{28}$$

For $r_2=0$ or equivalently $r_1=1$, equation (24) becomes

$$\frac{\mathrm{d}T_c}{\mathrm{d}\alpha}=T_d\delta(\alpha)-\frac{T_{r\,\max}}{\tau_1},\ r_2=0$$

Integrating this equation, we have

$$T_c=-\frac{T_{r\,\max}}{\tau_1}\alpha+T_{c0} \tag{27a}$$

α_f can be obtained by setting $T_c=0$ as

$$\alpha_f=\frac{T_{c0}\tau_1}{T_{r\,\max}},\ r_2=0 \tag{28a}$$

Numerical examples

It is assumed that the volume of the system proper (room or cabin), V_1, is

$$V_1=3\text{m}\times4\text{m}\times5\text{m}=60\text{m}^3$$

The flow rate of air in the system, Q, is

Q = (cross-sectional area of the system) × (air velocity in the system)
= (3m × 4m)(0·1 m/s)
= 1·2 m³/s

and flow rates of circulation air and fresh air are

$$Q_1=0{\cdot}8Q=0{\cdot}96\ \text{m}^3/\text{s}$$

$$Q_2=0{\cdot}2Q=0{\cdot}24\ \text{m}^3/\text{s}$$

The time constant of the system proper, τ_1, is

$$\tau_1 = \frac{V_1}{Q} = \frac{V_1}{Q_1+Q_2} = \frac{60}{1\cdot 2} = 50 \text{ s}$$

Other numerical values employed are

$$T_2 = 10^\circ\text{C}$$

$$T_d = 20^\circ\text{C}$$

$$T_{r\,\min} = 0^\circ\text{C}$$

$$T_{r0} = \frac{r_2 T_2}{r_1} = \frac{0\cdot 2\times 10}{0\cdot 8} = 2\cdot 5^\circ\text{C}$$

Here two examples with different heat removing (or control) capacities of the heat exchanger are considered. The first example is for the case in which the maximum load (heat removing capacity) of the heat exchanger, $T_{r\,\max}$ is set equal to 2·5°C. The second example is for the case in which the maximum load of the heat exchanger, $T_{r\,\max}$, is set to be 30°C.

Case 1: $T_{r\,\max} = 2\cdot 5^\circ\text{C}$

For this case, we have, from equations (27) and (28),

$$T_c(\alpha) = 20\exp\left(-\frac{r_2\alpha}{50}\right) + 10\left[1-\exp\left(-\frac{r_2\alpha}{50}\right)\right] - \frac{2\cdot 5 r_1}{r_2}\left[1-\exp\left(-\frac{r_2\alpha}{50}\right)\right]$$

$$\alpha_f = -\frac{50}{r_2}\ln\left[\frac{2\cdot 5r_1 - 10r_2}{2\cdot 5r_1 + 10r_2}\right]$$

if $r_2 \neq 0$, and

$$T_c(\alpha) = 20 - \alpha/20$$

$$\alpha_f = 400$$

if $r_2 = 0$.

The results of simulation are shown schematically in figure 5.

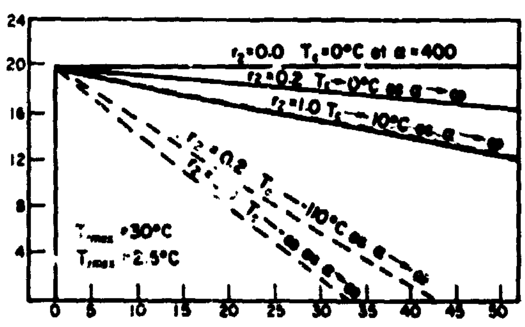

Fig. 5. Result of simulation of equation (27) with $T_2 = 10^\circ$C and $T_d = 20^\circ$C.

Case 2: $T_{r\,\max} = 30^\circ\text{C}$

For this case, we have from equations (27) and (28)

$$T_c = 20\exp\left(-\frac{r_2\alpha}{\tau_1}\right) + 10\left[1-\exp\left(-\frac{r_2\alpha}{\tau_1}\right)\right] - \frac{r_1}{r_2}\times 30\left[1-\exp\left(-\frac{r_2\alpha}{\tau_1}\right)\right]$$

$$\alpha_f = \frac{-\tau_1}{r_2}\ln\left(\frac{3r_1-r_2}{r_2+3r_1}\right) = -\frac{50}{r_2}\ln\left(\frac{3r_1-r_2}{r_2+3r_1}\right)$$

if $r_2 \neq 0$, and

$$T_c = 20 - 0\cdot 6\alpha$$

$$\alpha_f = 33\cdot 3 \text{ sec.}$$

if $r_2 = 0$. The results of simulation are shown schematically in figure 5.

Similarly, we can carry out the simulation by employing the dimensionless form of the performance equation. The performance equation in dimensionless form can be obtained by combining equations (12a) and (22a) and setting $\tau_2 = 0$ as

$$\frac{dx_1}{dt} + r_2 x_1 = r_2 K_1 + K_1\sigma\delta(t) - r_1 K_1 K_2 \theta - r_1 K_1 K_3 \tag{29}$$

Boundary conditions are

$$x_1 = 0 \quad \text{at} \quad t = 0^-$$

$$x_1 = 0 \quad \text{at} \quad t = T$$

As mentioned previously, this set of equations can also be written as

$$\frac{dx_1}{dt} + r_2 x_1 = r_2 K_1 - r_1 K_1 K_2 \theta - r_1 K_1 K_3$$

$$x_1 = 1 \quad \text{at} \quad t = 0^+ \tag{29a}$$

$$x_1 = 0 \quad \text{at} \quad t = T$$

First of all, let us assume θ is a given control action and is equal to $\theta_{\max} = 1$. Then equation (29a) can be integrated as follows:

$$x_1(t) = \exp(-r_2 t)\left[A_2 + K_1\exp(r_2 t) - \frac{r_1 K_1 K_2}{r_2}\exp(r_2 t) - \frac{r_1 K_1 K_3}{r_2}\exp(r_2 t)\right]$$

$$r_2 \neq 0$$

Application of the boundary condition, $x_1 = 1$ at $t = 0^+$, yields

$$A_2 = 1 - K_1 + \frac{r_1 K_1 K_2}{r_2} + \frac{r_1 K_1 K_3}{r_2}$$

and

$$x_1(t) = \exp(-r_2 t) + K_1[1-\exp(-r_2 t)]$$
$$-\frac{r_1 K_1 K_2}{r_2}[1-\exp(-r_2 t)] - \frac{r_1 K_1 K_3}{r_2}$$
$$[1-\exp(-r_2 t)],\ r_2 \neq 0 \tag{30}$$

Final time, T, corresponding to the end of control, can be obtained by using the condition

$$x_1 = 0 \quad \text{at} \quad t = T$$

This yields

$$T = -\frac{1}{r_2}\ln\left(\frac{r_1 K_1 K_2 + r_1 K_1 K_3 - r_2 K_1}{r_2 - r_2 K_1 + r_1 K_1 K_2 + r_1 K_1 K_3}\right),$$
$$r_2 \neq 0 \tag{31}$$

For $r_2 = 0$, equation (29) becomes

$$\frac{dx_1}{dt} = K_1 \sigma \delta(t) - K_1 K_2 - K_1 K_3$$

or in integrated form

$$x_1(t) = -K_1(K_2+K_3)t + 1, \quad r_2 = 0 \tag{30a}$$

T can be obtained by employing

$$x_1 = 0 \quad \text{at} \quad t = T$$

This gives

$$T = \frac{1}{K_1(K_2+K_3)}, \quad r_2 = 0 \tag{31a}$$

Two examples which correspond to the problems solved in dimensional form are considered here.

Case 1: $T_{r\,max} = 2{\cdot}5$°C

For this case, we have, from the definitions of K_2 and K_3 and equations (30) and (31),

$$K_2 = \frac{1}{2T_2}(T_{r\,max} - T_{r\,min}) = \frac{1}{20}(2{\cdot}5 - 0) = 0{\cdot}125$$

$$K_3 = \frac{1}{2T_2}(T_{r\,max} + T_{r\,min}) = \frac{1}{20}(2{\cdot}5 + 0) = 0{\cdot}125$$

$$x_1(t) = \exp(-r_2 t) + 0{\cdot}5[1-\exp(-r_2 t)]$$
$$-\frac{0{\cdot}125 r_1}{r_2}[1-\exp(-r_2 t)],\ r_2 \neq 0$$

$$T = -\frac{1}{r_2}\ln\left[\frac{0{\cdot}125 r_1 - 0{\cdot}5 r_2}{0{\cdot}125 r_1 + 0{\cdot}5 r_2}\right], \quad r_2 \neq 0$$

$$x_1(t) = -0{\cdot}125 t + 1, \quad r_2 = 0$$

$$T = \frac{1}{0{\cdot}125}, \qquad r_2 = 0$$

The results of simulation are shown in figure 6.

Case 2: $T_{r\,max} = 30$°C

For this case, we have

$$K_2 = \frac{1}{2T_2}(T_{r\,max} - T_{r\,min}) = \frac{1}{20}(30-0) = 1{\cdot}5$$

$$K_3 = \frac{1}{2T_2}(T_{r\,max} + T_{r\,min}) = \frac{1}{20}(30+0) = 1{\cdot}5$$

$$x_1(t) = \exp(-r_2 t) + 0{\cdot}5[1-\exp(-r_2 t)]$$
$$-1{\cdot}5\frac{r_1}{r_2}[1-\exp(-r_2 t)], \quad r_2 \neq 0$$

$$T = -\frac{1}{r_2}\ln\frac{1{\cdot}5 r_1 - 0{\cdot}5 r_2}{0{\cdot}5 r_2 + 1{\cdot}5 r_1}, \quad r_2 \neq 0$$

$$x_1(t) = -1{\cdot}5t + 1, \quad r_2 = 0$$

$$T = \frac{1}{1{\cdot}5}, \qquad r_2 = 0$$

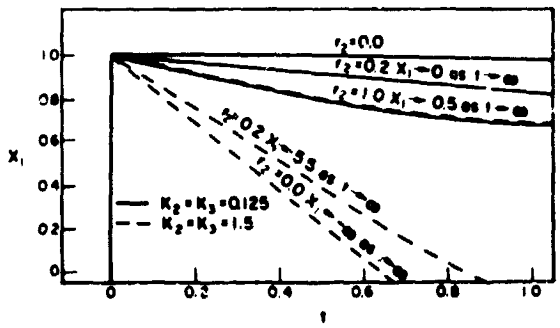

Fig. 6. Result of simulation of equation (30) with T_2 = 10°C and T_4 = 20°C.

The results of simulation are shown in figure 6 and tabulated in Table 1.

Note that the numerical examples are restricted to the cooling problems for simplicity. However,

Table 1. Simulation results for impulse heat disturbance.

		dimensional		dimensionless	
		$T_{r\,max}$ = 2·5°C	$T_{r\,max}$ = 30°C	$K_2 = K_3$ = 0·125	$K_2 = K_3$ = 1·5
r_1	r_2	t_f(sec)	t_f(sec)	T	T
1	0	400	33·3	8	0·66
0·8	0·2	∞	41·8	∞	0·84
0	1	∞	∞	∞	∞

the performance equations developed here can be applied to the case in which air is heated in the heat exchanger, i.e., T_r is negative. In other words, the performance equations can take into account both heating and cooling actions of the heat exchanger.

GENERAL SYSTEM EQUATIONS

In the preceding section, the performance equations have been derived for the cases in which the disturbance is of the form of the impulse function and air in the cabin or room is completely mixed. However, the procedure for deriving the performance equations is fairly general and can be extended to cases in which the disturbances are of the form other than the impulse function and air in the room or cabin is far from being completely mixed.

First, let us consider the case resulting from step heat disturbance while other conditions remain unchanged from those considered in the preceding section. The heat disturbance q_{ds} has the form

$$q_{ds} = (Q_1+Q_2)\rho C_p T_d U_0(\alpha) \tag{32}$$

The performance equation, for the system proper can be obtained as

$$\tau_1 \frac{dT_c}{d\alpha} + T_c = r_1 T_i + r_2 T_2 + T_d U_0(\alpha) \tag{33}$$

or in dimensionless form

$$\frac{dx_1}{dt} + x_1 = \frac{K_1 r_1 x_2}{K_4} + r_2 K_1 + K_1 \sigma U_0(t) \tag{33a}$$

Similarly, for the system with ramp heat disturbance, we have

$$q_{dr} = \frac{(Q_1+Q_2)^2}{V_1}\rho C_p T_r R(\alpha) \tag{34}$$

$$\tau_1 \frac{dT_c}{d\alpha} + T_c = r_1 T_i + r_2 T_2 + \frac{T_d R(\alpha)}{\tau_1} \tag{35}$$

and

$$\frac{dx_1}{dt} + x_1 = \frac{r_1 K_1 x_2}{K_4} + r_2 K_1 + K_1 \sigma R(t) \tag{35a}$$

In general, the dimensionless performance equation for the system element can be written as

$$\frac{dx_1}{dt} + x_1 = \frac{r_1 K_1 x_2}{K_4} + r_2 K_1 + K_1 \sigma F(t) \tag{36}$$

where $F(t)$ stands for the functional form of the heat disturbance which can be impulse function $\delta(t)$, unit step function $U(t)$, ramp function $R(t)$ [or $tU(t)$], cyclic disturbance or any other disturbance. This equation together with equation (22a) form the complete dimensionless system equations, that is,

$$\frac{dx_1}{dt} + x_1 = \frac{r_1 K_1 x_2}{K_4} + r_2 K_1 + K_1 \sigma F(t) \tag{36}$$

$$\frac{\tau_2}{\tau_1}\frac{dx_2}{dt} + x_2 = \frac{K_4 x_1}{K_1} - K_4(K_2\theta + K_3) \tag{22a}$$

It is worth noting that the initial condition for T_c is

$$T_c = T_{c0^-} = T_{c0} = 0 \quad \text{at} \quad \alpha = 0^- \text{ and } 0^+$$

and the initial condition for x_1 is

$$x_1 = \frac{T_{c0^-}}{T_{c0}} = \frac{T_{c0}}{T_{c0}} = 1 \quad \text{at} \quad t = 0^- \text{ and } 0^+$$

(Note that for the heat disturbance represented by the unit step or a higher order function, T_{c0^-}, the T_c before introduction of the disturbance is identical to T_{c0}, the T_c immediately after introduction of the disturbance. The value of T_{c0} or T_{c0} can be zero if the reference temperature t_a is taken to be t_{c0^-}, the room temperature before introduction of the disturbance as done in the case of the impulse input; however, this should be avoided because of the definition of K_1, $(t_2 - t_a)/(t_{c0} - t_a)$, which is employed in developing dimensionless forms of the systems equations. If $t_a = t_{c0}$, K_1 approaches ∞, which should be avoided). The performance equations for various types of heat disturbances are tabulated in Table 2.

Table 2. The performance equation for system element.

Type of heat disturbances	The dimensionless performance equations	Initial condition of T_c
Impulses $\delta(t)$	$\frac{dx_1}{dt} + x_1 = \frac{r_1 K_1}{K_4} x_2 + r_2 K_1 + K_1 \sigma \delta(t)$	0
	or	or
	$\frac{dx_1}{dt} + x_1 = \frac{r_1 K_1}{K_4} x_2 + r_2 K_1$	1
Step $U(t)$	$\frac{dx_1}{dt} + x_1 = \frac{r_1 K_1}{K_4} x_2 + r_2 K_1 + K_1 \sigma U_0(t)$	1
Ramp $R(t)$	$\frac{dx_1}{dt} + x_1 = \frac{r_1 K_1}{K_4} x_2 + r_2 K_1 + K_1 \sigma R(t)$	1
General $F(t)$	$\frac{dx_1}{dt} + x_1 = \frac{r_1 K_1}{K_4} x_2 + r_2 K_1 + K_1 \sigma F(t)$	1

PERFORMANCE EQUATIONS FOR TWO COMPARTMENTS MODEL

Next, let us consider the case in which air in the room or cabin is no longer in the state of complete mixing. Specifically, we shall consider the case in which flow of air in the room can be characterized by two completely stirred tanks (or pools or compartments)in-series model (2 CST's-in-series model).

The following assumptions must be added to t. .e already made for the system proper in the preceding section:

(a) The room is divided into two well mixed compartments in series. Volume of each pool is denoted by V_{11} and V_{12}, and the temperature in each pool is denoted by T_{c1} and T_{c2}.

(b) Backflow of air from the second compartment to the first compartment is negligible.

(c) Disturbances are equally distributed over the system.

(d) Fresh air comes into the first compartment at a constant flow rate, while exhaust air is released from the second compartment at a constant flow rate. The schematic diagram of the system is shown in figure 7. The performance equation for each

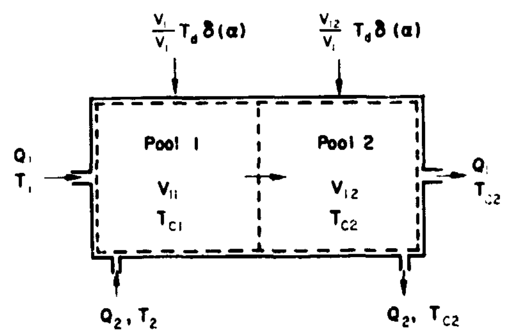

Fig. 7. Schematic expression of a room represented by the two CST's-in-series model.

pool can be obtained by using the transient heat balance around each compartment. Thus, for pool 1,

$$[\text{heat in}] - [\text{heat out}] = [\text{heat accumulation}] \tag{37}$$

or

$$[Q_1 T_i \rho C_p + Q_2 T_2 \rho C_p + \frac{V_{11}}{V_1} T_d \delta(\alpha) V_{11} \rho C_p]$$

$$-(Q_1+Q_2) T_{c1} \rho C_p = V_{11} \rho C_p \frac{dT_{c1}}{d\alpha} \tag{38}$$

Dividing this equation by $\rho C_p(Q_1+Q_2)$ yields

$$\tau_{11} \frac{dT_{c1}}{d\alpha} + T_{c1} = r_1 T_i + r_2 T_2 + \frac{\tau_{11}}{\tau_1} \tau_{11} T_d \delta(\alpha) \tag{39}$$

$$T_{c1} = 0 \quad \text{at} \quad \alpha = 0$$

or

$$\tau_{11} \frac{dT_{c1}}{d\alpha} + T_{c1} = r_1 T_i + r_2 T_2$$

$$T_{c1} = T_{c10} \quad \text{at} \quad t = 0^-$$

where τ_{11} is the time constant of pool 1 and is defined by

$$\tau_{11} = \frac{V_{11}}{Q_1+Q_2}$$

Note that

$$\frac{V_{11}}{V_1} = \frac{V_{11}/(Q_1+Q_2)}{V_1/(Q_1+Q_2)} = \frac{\tau_{11}}{\tau_1}$$

Similarly, for pool 2 we have

$$[(Q_1+Q_2) T_{c1} \rho C_p + \frac{V_{12}}{V_1} T_d \delta(\alpha) V_{12} \rho C_p]$$

$$-(Q_1+Q_2) \rho C_p T_{c2} = V_{12} \rho C_p \frac{dT_{c2}}{d\alpha} \tag{40}$$

Again dividing this equation by $\rho C_p(Q_1+Q_2)$ yields

$$\tau_{12} \frac{dT_{c2}}{d\alpha} + T_{c2} = T_{c1} + \frac{\tau_{12}}{\tau_1} \tau_{12} T_d \delta(\alpha) \tag{41}$$

$$T_{c2} = 0 \quad \text{at} \quad \alpha = 0^-$$

or

$$\tau_{12} \frac{dT_{c2}}{d\alpha} + T_{c2} = T_{c1}$$

$$T_{c2} = T_{c20} \quad \text{at} \quad \alpha = 0^+$$

where τ_{12} is the time constant of pool 2 and is defined by

$$\tau_{12} = \frac{V_{12}}{Q_1+Q_2}$$

For the heat exchanger, we have from equation (22)

$$\tau_2 \frac{dT_i}{d\alpha} + T_i = T_{c2} - T_r \tag{42}$$

Equations (39), (41) and (42) are the performance equations of the system. We may rewrite these in dimensionless form by defining

$$x_{11} = \frac{T_{c1}}{T_{c10}} = \frac{K_{11} T_{c1}}{T_2}, \quad K_{11} = \frac{T_2}{T_{1c0}}$$

$$x_{12} = \frac{T_{c2}}{T_{c20}} = \frac{K_{12} T_{c2}}{T_2}, \quad K_{12} = \frac{T_2}{T_{2c0}}$$

$$x_2 = \frac{T_i}{T_{i0}} = \frac{K_4 T_i}{T_2}$$

$$t = \frac{\alpha}{\tau_1}$$

Introducing these definitions into equations (39), (41) and (42), we have

$$\frac{dx_{11}}{dt}+r_{11}x_{11} = a_{11}x_2+a_{12}+a_{13}\delta(t) \qquad (43)$$

$$\frac{dx_{12}}{dt}+r_{12}x_{12} = a_{21}x_{11}+a_{23}\delta(t) \qquad (44)$$

$$\frac{dx_2}{dt}+rx_2 = a_{42}x_{12}-a_5\theta-a_6 \qquad (45)$$

where

$$a_{11} = r_1K_{11}r_{11}/K_4$$
$$a_{12} = r_{11}r_2K_{11}$$
$$a_{13} = T_dK_{11}/T_2r_{11}$$
$$a_{21} = r_{12}K_{12}/K_{11}$$
$$a_{23} = T_dK_{12}/T_2r_{12}$$
$$a_{42} = rK_4/K_{12}$$
$$a_5 = rK_2K_4$$
$$a_6 = rK_3K_4$$
$$r_{11} = \frac{\tau_1}{\tau_{11}}$$
$$r_{12} = \frac{\tau_1}{\tau_{12}}$$
$$r = \frac{\tau_1}{\tau_2}$$

The performance equations derived in this section can also be used for simulation either on a digital or on an analog computer by following the procedure presented in the preceding section. For any given forms of the air flow model and heat disturbance, the forms of the dimensional systems equations, which essentially represent heat balances are fixed; however, these can be transformed into a variety of dimensionless forms and the forms given here are not necessarily the most convenient ones.

CONCLUSION

Methodology and procedure used in this part can also be employed for constructing and simulating models for other systems in which mass and momentum transfer and chemical reactions are involved in addition to heat transfer. The performance equations derived in this part will be employed in the succeeding part of this series to determine the optimal control policy based on the modern optimal control theory.

NOMENCLATURE

a_5	rK_2K_4
a_6	rK_3K_4
a_{11}	$r_1K_{11}r_{11}/K_4$
a_{12}	$r_1r_2K_{11}$
a_{13}	T_dK_{11}/T_2r_{11}
a_{21}	$r_{12}K_{12}/K_{11}$
a_{23}	T_dK_{12}/T_2r_{12}
a_{42}	rK_4/K_{12}
A_1	Integration constant
A_2	Integration constant
c_p	Specific heat of air in kcal/kg°C
c_{pw}	Specific heat of coolant in kcal/kg°C
$F(t)$	Functional form of heat disturbance defined in equation (36)
K_1	$\frac{T_2}{T_{c0}}$
K_2	$\frac{1}{2T_2}(T_{r\,max}-T_{r\,min})$
K_3	$\frac{1}{2T_2}(T_{r\,max}+T_{r\,min})$
K_4	$\frac{T_2}{T_{i0}}$
K_{11}	$\frac{T_2}{T_{1c0}}$
K_{12}	$\frac{T_2}{T_{2c0}}$
M_i	$v_1\rho c_pT_d$
q_{di}	Heat disturbance rate in impulse form in kcal/.ec
q_{ds}	Heat disturbance rate in step kcal/s
q_{i1}	Heat flow into the system proper by circulation air in kcal/s
q_{i2}	Heat flow into the system proper by fresh air in kcal/s
q_{mi1}	Heat brought into the heat exchanger by circulation air in kcal/s
q_{mi2}	Heat brought into the heat exchanger by cooling water in kcal/s
q_{mo1}	Heat flow out of the heat exchanger with circulation air in kcal/s
q_{mo2}	Heat flow out of the heat exchanger by cooling water in kcal/s

q_{ms} Heat stored in the heat exchanger in kcal/s

q_{01} heat flow out of the system proper by circulation air in kcal/s

q_{02} Heat flow out of the system proper by fresh air in kcal/s

Q Q_1+Q_2, flow rate of air in the system proper in m^3/s

Q_1 Air flow rate by circulation air in m^3/s

Q_2 Flow rate of fresh air in m^3/s

Q_w Flow rate of coolant in m^3/s

r τ_1/τ_2, the ratio of time constant of system proper to that of heat exchanger

r_1 $\dfrac{Q_1}{Q_1+Q_2}$, the fraction of circulation air

r_2 $\dfrac{Q_2}{Q_1+Q_2}$, the fraction of fresh air

r_{11} $\dfrac{\tau_1}{\tau_{11}}$

r_{12} $\dfrac{\tau_2}{\tau_{12}}$

$R(t)$ Ramp heat disturbance function

t $\dfrac{\alpha}{\tau_1}$, dimensionless time

t_a Reference temperature in °C

t_c Room temperature in °C

t_d Disturbance temperature in °C

t_i Temperature of incoming circulation air in °C

t_{wc} Inlet temperature of coolant in °C

t_{wh} Outlet temperature of coolant in °C

t_2 Outside air temperature in °C

T Final time, dimensionless

T_c (t_c-t_a), room temperature in °C

$T_c(s)$ Laplace transform of $T_c(\alpha)$

T_{c0} Room temperature at $\alpha = 0^+$ in °C

T_{c1} Temperature of pool 1 in °C

T_{c10} Temperature of pool 1 at $\alpha = 0^+$ in °C

T_{c2} Temperature of pool 2 in °C

T_{c20} Temperature of pool 2 at $\alpha = 0^+$

T_d (t_d-t_a), disturbance temperature in °C

T_i (t_i-t_a), temperature of the circulation air into the system, in °C

T_{i0} Temperature of the circulation air into the system at $\alpha = 0^+$ in °C

T_r $\dfrac{Q_w\rho_w c_{pw}(T_{wh}-T_{wc})}{Q_1\rho c_p}$, hypothetical temperature

T_{rf} Final steady state value of T_r

$T_{r\,max}$ Upper bound of T_r in °C

$T_{r\,min}$ Lower bound of T_r in °C

T_{r0} Value of T_r at $\alpha = 0^-$ in °C

T_{wc} $t_{wc}-t_c$ in °C

T_{wh} $t_{wh}-t_a$ in °C

T_{11} Temperature of pool 1 in °C

T_{12} Temperature of pool 2 in °C

$U_0(t)$ Step heat disturbance function

V_1 Volume of room in m^3

V_{11} Volume of pool 1 of two completely stirred tanks in series model in m^3

V_2 Volume of heat exchanger in m^3

V_{12} Volume of pool 2 of two completely stirred tanks in series model in m^3

$x_1(t)$ $\dfrac{T_c}{T_{c0}}$, dimensionless room temperature

$x_2(t)$ $\dfrac{T_i}{T_{i0}}$, dimensionless temperature of the circulation air

x_{11} $\dfrac{T_{c1}}{T_{c10}}$, dimensionless temperature of pool 1

x_{12} $\dfrac{T_{c2}}{T_{c20}}$, dimensionless temperature of pool 2

Greek letters

α Time in sec

α_f Final time in sec

$\delta(\alpha)$ Impulse heat disturbance function, s^{-1}

ρ Air density in kg/m^3

ρ_w Density of coolant in kg/m^3

σ $\dfrac{T_d}{T_2}$, dimensionless disturbance temperature

τ_1 $\dfrac{V_1}{Q_1+Q_2}$, time constant of the system proper in s

τ_{11} $\dfrac{V_{11}}{Q_1+Q_2}$, time constant of pool 1 in s

τ_2 $\dfrac{V_2}{Q_1}$, time constant of heat exchanger in s

τ_{12} $\dfrac{V_{12}}{Q_1+Q_2}$, time constant of pool 2 in s

θ $\dfrac{T_r-\frac{1}{2}(T_{r\,max}+T_{r\,min})}{T_{r\,max}-\frac{1}{2}(T_{r\,max}+T_{r\,min})}$, control variable

$\begin{cases} +1 & \text{at } T_r = T_{r\,max} \\ -1 & \text{at } T_r = T_{r\,min} \end{cases}$

$\phi(\alpha)$ Heat disturbance function

REFERENCES

1. J. E. HAINES, *Automatic Control of Heating and Air Conditioning*, pp. v–vi, McGraw-Hill, New York (1953).
2. H. UCHIDA, *et al. Automatic Control of Air Conditioning* (in Japanese), pp. 7–44, Scientific Technology Center, Tokyo (1963).
3. P. WEBB, J. F. ANNIS, and S. J. TROUTMAN, Automatic Control of Water Cooling in Space Suits, NASA Report CR–1085, National Aeronautics and Space Administration, Washington, D.C. (1968).
4. R. L. VAUGHAN, H. M. STEPHENES, and R. S. BARKER, Generalized Environmental Control and Life Support System; Fortran Program—Vol. 1, Douglas Report SM-49403, Santa Monica, Calif. (May 1966).
5. J. C. TOU, Modern Control Theory, pp. 5–12, McGraw-Hill, New York (1964).
6. R. BELLMAN, *Some Vistas of Modern Mathematics*, pp. 1–49, University of Kentucky Lexington (1968).
7. L. S. PONTRYAGIN, V. G. BOLTYANSKII, R. V. GAMKRELIDZE, and E. F. MISHCHENKO, *The Mathematical Theory of Optimal Process*, (English translation by K. N. TRIROGOFF Interscience, New York (1962).
8. L. T. FAN, *The Continuous Maximum Principle: A Study of Complex Systems Optimization*, Wiley, New York (1966).
9. A. P. SAGE, *Optimal Systems Control*, Prentice Hall, New Jersey (1968).
10. L. LAPIDUS, and R. LUUS, *Optimal Control of Engineering Processes*, Blaisdell, Waltham, Mass. (1967).
11. C. T. LEONDES, *Modern Control Systems Theory*, McGraw-Hill, New York (1965).
12. H. L. HARRISON, W. S. HANSEN and R. E. ZELENSKI, Development of a Room Transfer Function Model for Use in the Study of Short-term Transient Response, *ASHRAE Trans.*, **74**, Part 2, 198 (1968).
13. R. O. ZERMUEHLEN, and H. L. HARRISON, Room Temperature Response to a Sudden Heat Disturbance Input, *ASHRAE, Trans.*, **71**, Part 1, 206 (1965).
14. J. R. GARTNER, H. L. HARRISON, Dynamic characteristics of water to air cross flow heat exchangers, *ASHRAE* (1965).
15. R. ALLEN, Time modulations control increases comfort, Parts I and II, *American Artisan*, July (1950).
16. H. BUCHBERG, Cooling Load from Pretabulated Impedances, *Heating, Piping and Air Conditioning*, February (1958).
17. H. BUCHBERG, Cooling Load from Thermal Network Solutions, *Heating, Piping and Air Conditioning*, October (1957).
18. W. B. DRAKE, Transfer Admittance Functions, *ASHRAE* (1959).
19. W. P. CHAPMAN, Fundamentals of Linear Control Theory, *ASHRAE J.*, **6**, 64–66 (1964).
20. K. R. SOLVANSON, Some Control Problems and Their Solutions, *ASHRAE J.*, **6**, 76–79 (1964).
21. C. W. MERRIAM III, *Optimization Theory and the Design of Feedback Control Systems*, McGraw-Hill, New York (1964).
22. A. H. ELTIMSAHY, The Optimization of Domestic Heating Systems, Ph.D. Dissertation, University of Michigan (1967).
23. D. R. COUGHANOUR, and L. B. KOPPEL, *Process Systems Analysis and Control*, McGraw-Hill, New York (1965).

Plusieurs modèles methématiques d'un système de contrôle environnant consistant d'un espace ou d'une cabine limités, d'un échangeur de chaleur et d'un élément de rétroaction tel qu'un thermostat, sont présentés. Les équations de performance du système qui représentent les caractéristiques dynamiques du système lui-même et de l'échangeur de chaleur (L'élément de contrôle du système) sont dérivés. Dans le modèle fondamental, le courant d'air dans l'espace limité est considéré être dans l'état de mélange complet et la perturbation est due à une entrée de chaleur par impulsion. Les équations de performance, dans lesquelles les perturbations de chaleur sont d'une forme telle que la fonction d'étape et la fonction cyclique qui sont différentes de la fonction d'impulsion, sont également dérivées. On présente également les équations de performance qui représentent les caractéristiques dynamiques d'un courant d'air dans un espace ou une cabine limités caractérisés par les deux modèles de vaisseaux en série complètement agités (2 CST en série).

Afin de déterminer la valeur du modèle, on utilise une simulation par ordinateur et les résultats sont comparés aux caractéristiques connues du système.

Mehrere mathematische Modelle eines Umgebungs-Kontrollsystems, das aus einem begrenzten Raum oder Kabine, einem Wärmetauscher und einem Rückwirkungselement, wie z.B. einem Thermostaten besteht, wurden dargestellt. Die Leistungsgleichungen des Systems, welche die dynamischen Eigenschaften des eigentlichen Systems und des Wärmeaustauschers (dem Kontrollelement des Systems) darstellen, werden abgeleitet. In dem grundlegenden Modell wird der Luftstrom in dem begrenzten Raum als gründlich gemischt angesehen und die Beunruhigung wird durch einen zugeführten Wärmeimpuls verursacht. Die Leistungsgleichungen, in welchen die Wärmestörungen in der Art wie die Stufenfunktion und zyklische Funktion sind, welche anders als die Impulsfunktion sind, werden ebenfalls abgeleitet. Es werden ausserdem die Leistungsgleichungen dargestellt, welche die dynamischen Eigenschaften der Luftströmung in einem begrenzten Raum oder Kabine wiedergeben, was mit dem Modell von zwei völlig aufgerührten Reihentanks (2 CST's-in-series) geschildert wird.

Eine Komputer Nachahmung wird durchgeführt, um die Güte des Systemmodells zu ermitteln, und die Ergebnisse werden mit den bekannten Eigenschaften des Systems verglichen.

Build. Sci. Vol. 5 pp. 81–94. Pergamon Press 1970. Printed in Great Britain

SfB Ab8
UDC 697

Application of Modern Optimal Control Theory to Environmental Control of Confined Spaces and Life Support Systems*

Part 2—Basic Computational Algorithm of Pontryagin's Maximum Principle and its Applications

L. T. FAN†
Y. S. HWANG†
C. L. HWANG†

The basic form of Pontryagin's maximum principle which is a keystone of the modern optimal control theory is presented. The principle is applied to the determination of optimal control policies of several life support or environmental control systems.

Three concrete examples all of which are concerned with the temperature control of a life support system consisting of an air-conditioned cabin (the system proper) subject to an impulse heat disturbance and of a heat exchanger (the control element) are considered. The first example treats the case in which the time constant of the heat exchanger is negligible. The second example considers the case in which the time constant of the heat exchanger is not ignored. In the third example the optimal policy of the system where the flow of air in the cabin can be characterized by the two completely stirred tanks-in-series (2 CST's-in-series) model is studied. In this example, the time constant of the heat exchanger is again neglected. Procedures and computational approaches employed for obtaining the optimal control policies are given in detail.

INTRODUCTION

MATHEMATICAL models of air-conditioned rooms or cabins or life support systems have been established in the preceding article[1]. In this and two of the succeeding articles, the various forms of Pontryagin's maximum principle[2–8] will be introduced and will be used to determine the optimal control policies for such systems.

Use of the maximum principle almost always gives rise to a two-point split boundary value problem, the solution of which will be further elaborated. Even though this principle leads to two-point boundary value problems which are often difficult to solve, it still provides a practical approach to process systems optimization.

Another difficulty also arises in using the maximum principle formulation as the basis for computing optimal control. The maximum principle generally provides only the necessary condition but not the sufficient condition which must be satisfied by the optimal control.

* This work was supported by the Air Force Office of Scientific Research, Office of Aerospace Research, United States Air Force, Under Contract F 44620-68-0020 (Themis Project), and NASA Grant Under Contract NGR-17-001-034.

† Institute of systems design and optimization, Kansas State University, Manhattan, Kansas.

In this particular article the most basic form of Pontryagin's maximum principle will be stated and it will then be used for determining optimal operating policies of the life support or environmental control systems which were described in Part 1 of this series[1].

STATEMENT OF ALGORITHM

Consider that the dynamic behavior of a controlled system can be represented by a set of differential equations

$$\frac{dx_i}{dt} = f_i[x_1(t), x_2(t), \ldots, x_s(t); \theta_1(t), \ldots, \theta_r(t)],$$
$$i = 1, 2, \ldots, s \qquad (1)$$
$$t_0 \leq t \leq T$$

or in vector form

$$\frac{dx}{dt} = f[x(t), \theta(t)], \quad t_0 \leq t \leq T \qquad (1a)$$

where $x(t)$ is an s-dimensional vector function representing the state of the process at time t and $\theta(t)$ is an r-dimensional vector function representing the decision at time t[2, 3]. The functions f_i, $i = 1, 2, \ldots, s$, are single valued, bounded,

PRECEDING PAGE BLANK NOT FILMED

differentiable with respect to the x's with bounded first partial derivatives, and are continuous in the θ's on a product region $x\theta$, where x and θ are closed regions in the s-dimensional x-space and r-dimensional θ-space respectively[5]. Note that we are dealing with the autonomous systems in which the right-hand side of the performance equation, equation (1), depends implicitly on time t. The non-autonomous systems are those in which the right-hand side of the performance equation, equation (1), depends explicitly on time t.

A typical optimization problem associated with such a process is to find a piecewise continuous decision vector function, $\theta(t)$ subject to the p-dimensional constraints

$$h_i[\theta(t)] \leqq 0, \quad i = 1, 2, \ldots, p \qquad (2)$$

such that the performance index

$$S = \sum_{i=1}^{s} c_i x_i(T), \quad c_i = \text{constant} \qquad (3)$$

is minimum (or maximum) when the initial conditions

$$x_i(t_0) = x_{i0}, \quad i = 1, 2, \ldots, s \qquad (4)$$

are given. The duration of control, T, is specified and the final conditions of state variables are unfixed. This type of problem is often called the free right-end problem (with fixed T). The decision vector (or a collection of control variables) so chosen is called an optimal decision vector (or optimal control variables) and is denoted by $\theta(t)$.

The procedure for solving the problem is to introduce an s-dimensional adjoint vector $z(t)$ and a Hamiltonian function $\mathscr{H}$ which satisfy the following relations

$$\mathscr{H}[x(t), \theta(t), z(t)] = \sum_{i=1}^{s} z_i(t) f_i[x(t), \theta(t)] \qquad (5)$$

$$\frac{dz}{dt} = -\frac{\partial \mathscr{H}}{\partial x_i} = -\sum_{j=1}^{s} z_j \frac{\partial f_j}{\partial x_i}, \quad i = 1, 2, \ldots, s \qquad (6)$$

$$z_i(T) = c_i, \qquad i = 1, 2, \ldots, s \qquad (7)$$

The set of equations, equations (1), (4), (6) and (7), constitutes a two-point split boundary value problem, whose solution depends on $\theta(t)$. The optimal decision vector $\theta(t)$ which makes S an extremum also makes the Hamiltonian an extremum for all t, i.e., $t_0 \leqq t \leqq T$[2,3,5,6].

A necessary condition for S to be an extremum with respect to $\theta(t)$ is

$$\frac{\partial \mathscr{H}}{\partial \theta_i} = 0, \quad i = 1, 2, \ldots, r \qquad (8)$$

if the optimal decision vector is interior to the set of admissible decision $\theta(t)$ [the set given by equation (2)]. If $\theta(t)$ is constrained, the optimal decision vector $\bar{\theta}(t)$ is determined either by solving equation (8) for $\theta(t)$ or by searching the boundary of the set. More specifically, the extremum value of Hamiltonian is maximum (or minimum) when the control variables are on the constraint boundary. Furthermore, the extremum value of the Hamiltonian is constant at every point of time under the optimal condition. It is worth noting that the final conditions of the adjoint variables, $z_i(T)$, are often given as $-c_i$ instead of c_i as shown in equation (7), in employing the maximum principle of Pontryagin. The use of such final conditions of $z_i(t)$ gives rise to the condition that the Hamiltonian is maximum when the objective function is minimized, and minimum when the objective function is maximized as stated in the original version of the maximum principle of Pontryagin[2,3,6].

If both the initial and final conditions of state variables are given, the problem is said to be a boundary value problem. The basic algorithm presented except the condition given by equation (7) is still applicable[3].

If optimization (usually minimization) of time t is involved in the objective function in a problem with an unfixed duration of control, T, the problem is then called a time optimal problem. In this case, the basic algorithm presented is still applicable with an additional condition that the extremal value of the Hamiltonian is not only a constant but also identical to zero. The simplest example of the time optimal control problem is one in which the performance index is of the form

$$S = \int_0^T dt$$

Such a problem is often called a minimum time problem.

EXAMPLES

The basic form of the maximum principle presented in the preceding section will be applied to concrete examples. Procedures and computational approaches employed will be given in detail.

Example 1—Suppose that the dynamic behavior of a life support system consisting of an air-conditioned room or cabin subject to the impulse heat disturbance and a heat exchanger with negligibly small time constant ($\tau_2 \to 0$), can be represented by the following equation[1] [equation (29a) in Part 1 of this series]:

$$\frac{dx_1}{dt} + r_2 x_1 = r_2 K_1 - r_1 K_1 K_2 \theta - r_1 K_1 K_3 \qquad (9)$$

with

$$x_1(0) = 1 \quad \text{at} \quad t = 0^+$$

$$x_1(T) = 0 \quad \text{at} \quad t = T$$

where T is the unspecified final control time. We wish to determine θ so that the response of the system can return to its desired state in a minimum period of time, that is to minimize

$$S = \int_0^T \mathrm{d}t \tag{10}$$

If an additional state variable x_2 is introduced as

$$x_2(t) = \int_0^t \mathrm{d}t,$$

it follows that

$$\frac{\mathrm{d}x_2}{\mathrm{d}t} = 1, \quad x_2(0) = 0 \tag{11}$$

The problem is thus transformed into that of minimizing $x_2(T)$.

According to equation (5), the Hamiltonian is

$$\begin{aligned}\mathscr{H}&[z(t), x(t), \theta(t)] \\ &= z_1 \frac{\mathrm{d}x_1}{\mathrm{d}t} + z_2 \frac{\mathrm{d}x_2}{\mathrm{d}t} \\ &= z_1[-r_2x_1 + r_2K_1 - r_1K_1K_2\theta - r_1K_1K_3] + z_2\end{aligned} \tag{12}$$

The components of the adjoint vector, according to equation (6), are defined by

$$\frac{\mathrm{d}z_1}{\mathrm{d}t} = -\frac{\partial\mathscr{H}}{\partial x_1} = r_2 z_1 \tag{13}$$

$$\frac{\mathrm{d}z_2}{\mathrm{d}t} = -\frac{\partial\mathscr{H}}{\partial x_2} = 0, \quad z_2(T) = 1 \tag{14}$$

Solutions of equations (13) and (14) are

$$z_1(t) = A \exp(r_2 t) \tag{15}$$

$$z_2(t) = 1, \quad 0 \leq t \leq T \tag{16}$$

where A is the integration constant to be determined later. Inserting equation (16) into equation (12) yields

$$\mathscr{H} = -r_1K_1K_2z_1\theta - r_2z_1x_1 + r_2K_1z_1 - r_1K_1K_3z_1 + 1 \tag{17}$$

Therefore the switching function $\mathscr{H}^*$, the portion of $\mathscr{H}$ which depends on θ, is

$$\mathscr{H}^* = -r_1K_1K_2z_1\theta \tag{18}$$

Recall that minimization of the Hamiltonian with respect to θ corresponds to that of the objective function. Equation (18), however, indicates that the minimization of the Hamiltonian with respect to θ is equivalent to that of the switching function. Thus, minimization of the switching function corresponds to that of the objective function. Equation (18) also indicates that for the switching function to assume the minimum value, θ must assume its minimum allowable or its maximum allowable value depending on the sign of the coefficient of θ.

$$\begin{aligned}\theta &= \theta_{max} = 1 \quad \text{if} \quad -r_1K_1K_2z_1 < 0 \\ \theta &= \theta_{min} = -1 \quad \text{if} \quad -r_1K_1K_2z_1 > 0\end{aligned} \tag{19}$$

Time optimal control policy of this type is of bang–bang type [3, 4, 6, 9].

In the case where the coefficient of θ in equation (18) vanishes, we have the possibility of singular control[10]. For singular control, the control variable takes on values which are intermediate to θ_{max} and θ_{min}; hence the name intermediate control is also used in place of the singular control[10]. Also inertialess control will be considered. An inertialess controller has the ability to shift from θ_{max} to θ_{min} instantaneously and vice versa.

The maximum principle now requires that the system equations, equations (9) and (11), be integrated simultaneously with the adjoint equation (13) so that the two-point boundary conditions

$$\begin{aligned}&x_1(0) = 1, && x_1(T) = 0 \\ &x_2(0) = 0, && x_2(T) = \text{undetermined} \\ &z_1(0) = \text{undetermined}, && z_1(T) = \text{undetermined}\end{aligned}$$

are satisfied. For this minimum time problem extremum of the Hamiltonian must vanish at every point of its response.

In order to bring the initial deviated state $x_1(0^+) = 1$ to the final desired operating state $x_1(T) = 0$, we intuitively reject the control $\theta = \theta_{min} = -1$ (which corresponds to the minimum cooling action). Equation (9) can be integrated with the conditions

$$\theta = \theta_{max} = 1 \tag{20}$$

and

$$x_1(0) = 1 \quad \text{at} \quad t = 0^+ \tag{21}$$

as

$$\begin{aligned}x_1(t) &= \exp(-r_2t) + \frac{1}{r_2}(r_2K_1 - r_1K_1K_2 \\ &\quad - r_1K_1K_3)(1 - \exp[-r_2t]) \\ &= \exp[-r_2t] + \frac{\eta}{r_2}(1 - \exp[-r_2t])\end{aligned} \tag{22}$$

where

$$\eta = r_2K_1 - r_1K_1K_2 - r_1K_1K_3 \tag{22a}$$

The integration constant A in equation (15) can be determined by using the condition that minimum H is zero for all the process time in time optimal control. At $t = 0^+$, we have from equations (15), (17), (20) and (21)

$$A = z_1(0^+) = \frac{-1}{\eta - r_2}$$

and

$$z_1(t) = \frac{-1}{\eta - r_2}\exp(r_2t) \tag{23}$$

Equation (23) implies that $z(t)$ will not change sign since $z_1(t) \to 0$ only when t approaches negative infinity, or in other words, control will not shift from θ_{max} to θ_{min} (or from θ_{min} to θ_{max}). Therefore, this problem is a particular case of bang-bang control which has the bang part only. The optimal control policy starts with $T_{r\,max}$ and then keeps operating at the upper bound of T_r until the final desired state is reached. The final control time can be obtained from equations (17) and (20) together with the final condition

$$x_1(T) = 0 \quad \text{at} \quad t = T$$

as follows

$$\mathscr{H} = z_1(T)[-r_2 x_1(T)+\eta]+1 = 0$$

or solving for $z_1(T)$

$$z_1(T) = \frac{-1}{\eta} \tag{24}$$

Also we have, from equation (23), at $t = T$

$$z_1(T) = \frac{-1}{\eta - r_2}\exp(r_2 T) \tag{25}$$

Solving for T from equations (24) and (25) gives

$$T = \frac{1}{r_2}\ln\left(\frac{\eta - r_2}{\eta}\right) \tag{26}$$

This solution may be verified by inserting it into equation (22) as

$$\begin{aligned} x_1(T) & \\ &= \exp(-r_2 T)+\frac{\eta}{r_2}\{1-\exp(r_2 T)\} \\ &= \exp\left[-r_2\frac{1}{r_2}\ln\left(\frac{\eta-r_2}{\eta}\right)\right] \\ &\quad +\frac{\eta}{r_2}\left\{1-\exp\left[-r_2\frac{1}{r_2}\ln\left(\frac{\eta-r_2}{\eta}\right)\right]\right\} \\ &= 0 \end{aligned}$$

This indicates that the Hamiltonian is kept at zero at every point of its response in this minimum time problem. For

$$r_1 = 0{\cdot}8 \quad r_2 = 0{\cdot}2$$
$$K_1 = 0{\cdot}5 \quad K_2 = 1{\cdot}5$$
$$K_3 = 1{\cdot}5 \quad \sigma = 2,$$

we have from equations (22), (23) and (26)

$$z_1(t) = \frac{1}{1{\cdot}3}\exp(0{\cdot}2t) = 0{\cdot}769\exp(0{\cdot}2t) \tag{27}$$

$$x_1(t) = 6{\cdot}5\exp(-0{\cdot}2t)-5{\cdot}5 \tag{28}$$

$$T = 0{\cdot}8353$$

and from equation (27)

$$z_1 = \frac{1}{1{\cdot}3} = 0{\cdot}769 \quad \text{at} \quad t = 0$$

$$z_1 = \frac{1}{1{\cdot}1} = 0{\cdot}909 \quad \text{at} \quad t = T$$

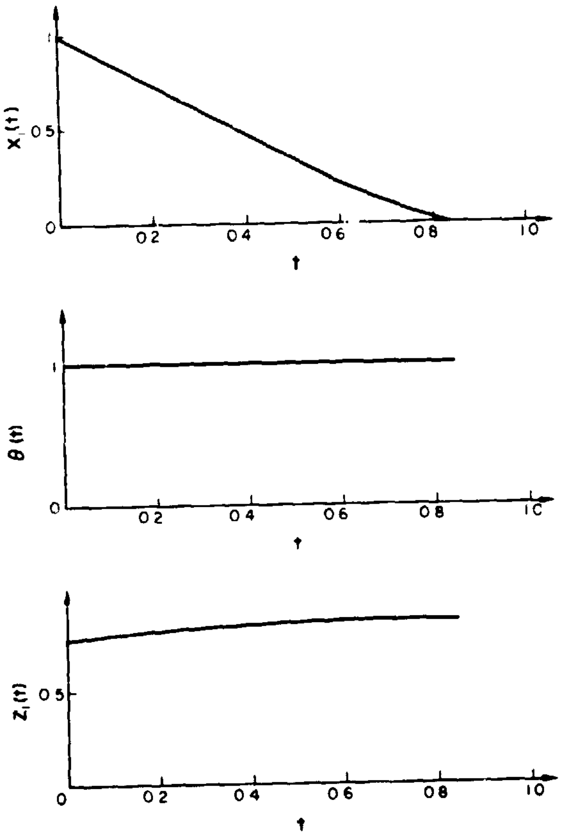

Fig. 1. Optimal control policy and system response of the one CST model $\tau_2 = 0$ [Example 1].

Equations (27) and (28) are graphically shown in figure 1. The state variable x_1 approaches asymptotically to the final state, the control variable θ remains at unity until the final state is reached, and the adjoint vector increases asymptotically. The optimal control can be verified by computing $\mathscr{H}$ at an arbitrary point, say 0·5, of the time coordinate as follows:

$$t = 0{\cdot}5$$
$$z_1(t) = \exp(-0{\cdot}1)1{\cdot}3$$
$$x_1(t) = 6.5\exp(-0{\cdot}1)-5{\cdot}5$$

and

$$\begin{aligned}\mathscr{H} &= z_1(t)[-r_2x_1+r_2K_1-r_1K_1K_2-r_1K_1K_3]+1 \\ &= \frac{\exp(0{\cdot}1)}{1{\cdot}3}\{-0{\cdot}2[6{\cdot}5\exp(-0{\cdot}1)-5{\cdot}5] \\ &\quad +0{\cdot}2\times0{\cdot}5-1{\cdot}2\}+1 \\ &= 0\end{aligned} \tag{29}$$

This computation shows that the minimum value of $\mathscr{H}$ is zero at every point of this continuous process.

Four cases with different cooling capacities of the heat exchangers are considered here. $T_{r\,\max}$ and $T_{r\,\min}$ take the following values for these four cases:

Case 1: $T_{r\,\max} = 30\ C \quad T_{r\,\min} = 0\ C$
Case 2: $T_{r\,\max} = 20\ C \quad T_{r\,\min} = 0\ C$
Case 3: $T_{r\,\max} = 10\ C \quad T_{r\,\min} = 0\ C$
Case 4: $T_{r\,\max} = 5\ C \quad T_{r\,\min} = 0\ C$

The numerical solutions for these cases are obtained from equations (22), (23) and (26), and are tabulated in Table 1.

Table 1. Optimal solutions of the one CST model together with $\tau_2 = 0$ [Example 1]

Case number	Two bounds of control variable	K_2	K_3	Final time T
1	$T_{r\,\max} = 30\ C$, $T_{r\,\min} = 0\ C$	1·50	1·50	0·8353
2	$T_{r\,\max} = 20\ C$, $T_{r\,\min} = 0\ C$	1·00	1·00	1·2566
3	$T_{r\,\max} = 10\ C$, $T_{r\,\min} = 0\ C$	0·50	0·50	2·5541
4	$T_{r\,\max} = 5\ C$, $T_{r\,\min} = 0\ C$	0·25	0·25	5·493

Example 2—Generally, responses of the heat exchanger as well as the cabin are not always instantaneous. Suppose that for the system considered in the first example, the time constant of the heat exchanger, τ_2, is not so small as to be ignored. The performance equations for such a system have been derived in the first part of this series of articles {equations (12a) and (22a) in [1]}.

$$\frac{dx_1}{dt} + x_1 = a_1 x_2 + a_2 \tag{30}$$

$$\frac{dx_2}{dt} + r x_2 = a_4 x_1 - a_5\theta - a_6 \tag{31}$$

with the initial and the final conditions

$$x_1(0^+) = 1 \quad \text{and} \quad x_2(0^+) = 1 \quad \text{at} \quad t = 0^+ \tag{32}$$

$$x_1(T) = 0 \quad \text{and} \quad x_2(T) = 1 \quad \text{at} \quad t = T \tag{32a}$$

The decision variable θ is constrained as

$$|\theta| \leqq 1$$

where

$$r = \frac{\tau_1}{\tau_2}, \quad (\tau_2 \neq 0)$$
$$a_1 = r_1 K_1 / K_4$$
$$a_2 = r_2 K_1$$
$$a_3 = K_1 \sigma$$
$$a_4 = \frac{r K_4}{K_1}$$
$$a_5 = r K_2 K_4$$
$$a_6 = r K_3 K_4$$

We wish to determine the control variable θ so that the state variables may be brought from the initial deviated state [$x_1 = 1$, $x_2 = 1$, at $t = 0^+$] to the final desired state [$x_1 = 0$, $x_2 = 1$] at $t = T$, in a minimum time. In other words

$$S = \int_0^T dt$$

is to be minimized.

If an additional state variable x_3 is introduced as

$$x_3(t) = \int_0^t dt, \tag{33}$$

it follows that

$$\frac{dx_3}{dt} = 1, \quad x_3(0^+) = 0 \tag{34}$$

and

$$x_3(T) = \int_0^T dt = S \tag{35}$$

The problem is now transformed into that of minimizing $x_3(T)$ because $x_3(T)$ and S are identical.

According to equation (5), the Hamiltonian is

$$\begin{aligned} \mathscr{H}(z, x, \theta) &= z_1 \frac{dx_1}{dt} + z_2 \frac{dx_2}{dt} + z_3 \frac{dx_3}{dt} \\ &= z_1[-x_1 + a_1 x_2 + a_2] + z_2[-r x_2 + a_4 x_1 \\ &\quad - a_5\theta - a_6] + z_3 \end{aligned} \tag{36}$$

The adjoint variables are defined by

$$\frac{dz_1}{dt} = -\frac{\partial \mathscr{H}}{\partial x_1} = z_1 - a_4 z_2 \tag{37}$$

$$\frac{dz_2}{dt} = -\frac{\partial \mathscr{H}}{\partial x_2} = r z_2 - a_1 z_1 \tag{38}$$

$$\frac{dz_3}{dt} = -\frac{\partial \mathscr{H}}{\partial x_3} = 0, \quad z_3(T) = 1 \tag{39}$$

From equation (39), the solution of z_3 is

$$z_3(t) = 1, \quad 0^+ \leqq t \leqq T \tag{40}$$

Hence, the Hamiltonian can be rewritten as

$$\begin{aligned} \mathscr{H} = z_1(-x_1 + a_1 x_2 + a_2) + z_2(-r x_2 + a_4 x_1 \\ - a_5\theta - a_6) + 1 \end{aligned} \tag{41}$$

and the switching function $\mathscr{H}^*$, the portion of $\mathscr{H}$ which depends on θ, is

$$\mathscr{H}^* = -a_5 z_2 \theta \tag{41a}$$

Inspection of $\mathscr{H}^*$ shows the basic structure of the time optimal control policy is of the bang–bang type as in the first example. The conditions for which the Hamiltonian be minimum are

$$\theta = \theta_{\max} = 1 \quad \text{if} \quad -a_5 z_2 < 0$$
$$\theta = \theta_{\min} = -1 \quad \text{if} \quad -a_5 z_2 > 0 \tag{42}$$

These conditions also imply that if the switching occurs, it will be at

$$a_5 z_2 = 0 \tag{43}$$

provided that the controller shifts from θ_{max} to θ_{min} instantaneously and inertialessly, or vice versa.

Now, the maximum principle requires that the system equations and the adjoint variables equations (30), (31), (34), (37) and (38), be integrated simultaneously in such a way that the two-point boundary conditions

$$\begin{array}{ll} x_1(0^+) = 1 & x_1(T) = 0 \\ x_2(0^+) = 1 & x_2(T) = 1 \\ x_3(0^+) = 0 & x_3(T) \text{ undetermined} \\ z_1(0^+) \text{ undetermined} & z_1(T) \text{ undetermined} \\ z_2(0^+) \text{ undetermined} & z_2(T) \text{ undetermined} \end{array}$$

be satisfied. Meanwhile, the Hamiltonian must remain at zero at every point of its response under the optimal condition.

In order to bring the initial deviated state $[x_1(0^+) = 1, x_2(0^+) = 1]$, to the final desired state $[x_1(T) = 0, x_2(T) = 1]$, we intuitively start the control from $\theta = \theta_{max} = 1$ (this corresponds to the maximum cooling action). Substituting this condition into equations (30) and (31), and eliminating x_2 give

$$\frac{d^2x_1}{dt^2} + (1+r)\frac{dx_1}{dt} + (r - a_1a_4)x_1 + (a_1a_5 + a_1a_6 - ra_2) = 0 \tag{44}$$

The solution of this equation is

$$x_1 = A_1 \exp(\lambda_1 t) + A_2 \exp(\lambda_2 t) + K, \quad 0 \leq t \leq t_s \tag{45}$$

where A_1 and A_2 are constants and their values will be determined later. λ_1 and λ_2 are roots of the characteristic equation

$$\lambda^2 + (1+r)\lambda + (r - a_1a_4) = 0$$

and K is the particular solution and its value is

$$K = \frac{ra_2 - a_1a_5 - a_1a_6}{r - a_1a_4}$$

From equation (30), the solution of x_2 is

$$x_2 = \frac{1}{a_1}[(\lambda_1+1)A_1 \exp(\lambda_1 t) + (\lambda_2+1)A_2 \exp(\lambda_2 t) + K - a_2] \tag{46}$$

The initial conditions applied to equations (45) and (46) give

$$A_1 = \frac{1}{\lambda_1 - \lambda_2}(a_1 + a_2 - \lambda_2 - 1 + K\lambda_2) \tag{47}$$

$$A_2 = 1 - A_1 - K \tag{48}$$

Suppose that the control switches from $\theta_{max} = 1$ to $\theta_{min} = -1$ at a certain time (switching time t_s). Then $x_1(t)$ and $x_2(t)$ after t_s are solved from equations (30) and (31). The results are

$$x_1(t) = D_1 \exp(\lambda_1 t) + D_2 \exp(\lambda_2 t) + K', \quad t_s \leq t \leq T \tag{49}$$

$$x_2(t) = \frac{1}{a_1}[(1+\lambda_1)D_1 \exp(\lambda_1 t) + (1+\lambda_2)D_2 \exp(\lambda_2 t) + K' - a_2] \quad t_s \leq t \leq T \tag{50}$$

where

$$K' = \frac{ra_2 + a_1a_5 - a_1a_6}{r - a_1a_4}$$

and D_1 and D_2 are constants, and their values can be determined by using the continuity of x_1 and x_2 with respect to t. We have from equations (45), (46), (49) and (50) at $t = t_s$

$$x_1(t_s) = A_1 \exp(\lambda_1 t_s) + A_2 \exp(\lambda_2 t_s) + K = D_1 \exp(\lambda_1 t_s) + D_2 \exp(\lambda_2 t_s) + K' \tag{51}$$

and

$$x_2(t_s) = \frac{1}{a_1}[(1+\lambda_1)A_1 \exp(\lambda_1 t_s) + (1+\lambda_2)A_2 \exp(\lambda_2 t_s) + K - a_2] = \frac{1}{a_1}[(1+\lambda_1)D_1 \exp(\lambda_1 t_s) + (1+\lambda_2)D_2 \exp(\lambda_2 t_s) + K' - a_2] \tag{52}$$

Solving for D_1 and D_2 in terms of A_1, A_2 and t_s from equations (51) and (52),

$$D_1 = A_1 - E_1 \exp(-\lambda_1 t_s) \tag{53}$$

and

$$D_2 = A_2 - E_2 \exp(-\lambda_2 t_s) \tag{54}$$

where

$$E_1 = \frac{\lambda_2(K' - K)}{\lambda_1 - \lambda_2}$$

$$E_2 = \frac{\lambda_1(K' - K)}{\lambda_1 - \lambda_2}$$

The value of t_s and that of T can be determined by employing the final conditions [equation (32a)] at $t = T$. Thus, equations (49) and (50) become

$$D_1 \exp(\lambda_1 T) + D_2 \exp(\lambda_2 T) + K' = 0 \tag{55}$$

$$(1+\lambda_1)D_1 \exp(\lambda_1 T) + (1+\lambda_2)D_2 \exp(\lambda_2 T) + K' - a_2 = a_1 \tag{56}$$

Subtracting equation (55) from equation (56) yields

$$\lambda_1 D_1 \exp(\lambda_1 T) + \lambda_2 D_2 \exp(\lambda_2 T) = a_1 + a_2 \tag{57}$$

Solving for $D_2 \exp(\lambda_2 T)$ from the above equation and equation (55) gives

$$D_2 \exp(\lambda_2 T) = E_4 \tag{58}$$

Subtracting equation (58) from equation (55) gives

$$D_1 \exp(\lambda_1 T) = E_3 \tag{59}$$

where

$$E_3 = \frac{a_1 + a_2 + K'\lambda_2}{\lambda_1 - \lambda_2}$$

$$E_4 = \frac{a_1 + a_2 + \lambda_1 K'}{\lambda_2 - \lambda_1}$$

We have four unknowns, D_1, D_2, t_s and T in four equations (53), (54), (58) and (59). Solving for t_s, we have

$$\left(\frac{E_3}{A_1 - E_1 \exp(-\lambda_1 t_s)}\right)^{\lambda_2} = \left(\frac{E_4}{A_2 - E_2 \exp(-\lambda_2 t_s)}\right)^{\lambda_1} \tag{60}$$

t_s can be solved from this equation by a trial and error procedure, and D_1, D_2 and T can then be obtained from equations (53), (54) and (58). The same numerical values used in Example 1 are employed for r_1, r_2, K_1, K_2, K_3 and σ. An additional constant $K_4 = -4$ appears in this and next Example. The solutions for four cases are shown in Table 2 and figures 2–4.

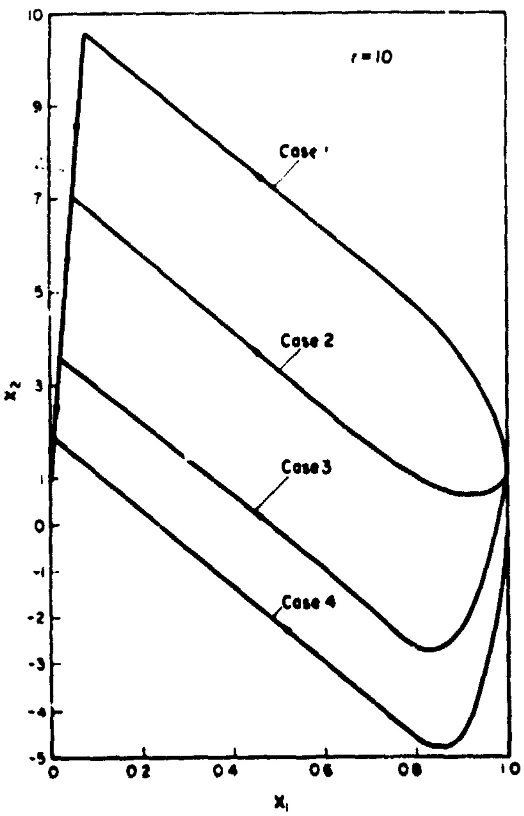

Fig. 2. Phase plane plots for different cases of the one CST model with $\tau_2 \neq 0$ and $r = 10$ [Example 2].

Figure 2 is the phase plane plot, x_2 vs. x_1, for different cases with fixed r, of 10, while figure 3 shows that of Case 1 for different values of r. Both figures show a common feature that all the trajectories of x_2 vs. x_1 show one switching point.

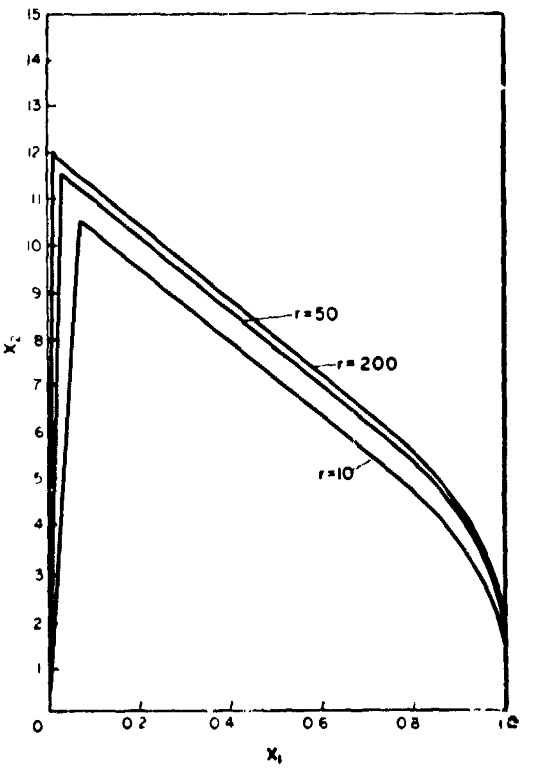

Fig. 3. Phase plane plot for Case 1 of the one CST model with $\tau_2 \neq 0$ and different values of r [Example 2].

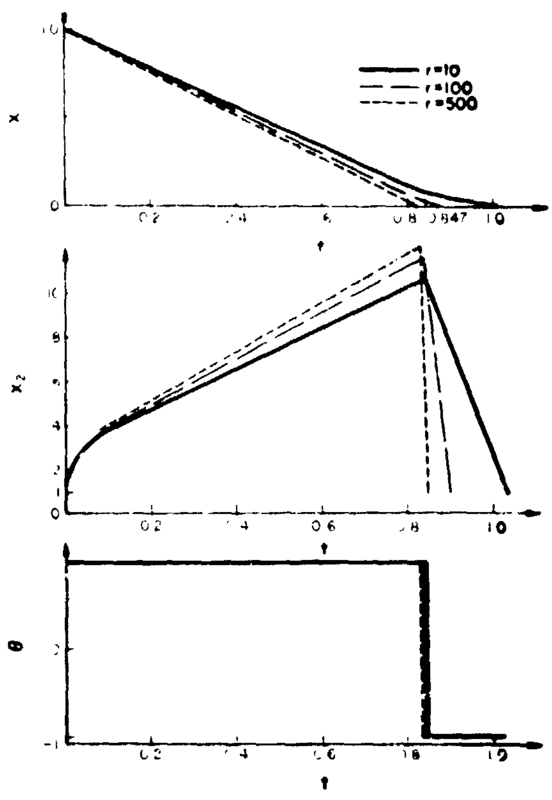

Fig. 4. Optimal control policies and system responses of Case 1 of the one CST model with $\tau_2 \neq 0$ and different values of r [Example 2].

However, the speed of response can be observed in figure 4. x_1 decreases asymptotically from $t = 0$ to $t = 0{\cdot}847$, and then approaches linearly to the final desired state. Response of x_2 concaves downward from the initial state to $t = 0{\cdot}1$, and then increases linearly to $t = 0{\cdot}847$, and finally decreases linearly to the end. This figure also shows the optimal control policy: it operates at $\theta = 1$ from $t = 0$ to $t = 0{\cdot}847$, and then switches to $\theta = -1$ and keeps operating at $\theta = -1$ until the final desired conditions are obtained. Additional results are tabulated in Table 2.

where

$$a_{42}' = K_4 K_{12}$$
$$a_5' = K_2 K_4$$
$$a_6' = K_3 K_4$$

The initial and the final conditions are

$$x_{11}(0^+) = x_{12}(0^+) = 1 \quad \text{at} \quad t = 0^+$$
$$x_{11}(T) = x_{12}(T) = 0 \quad \text{at} \quad t = T \tag{63}$$

where T is unspecified. We are to minimize

$$S = \int_0^T dt \tag{64}$$

Table 2. Optimal solutions of the one CST model together with $\tau_2 \neq 0$. [Example 2].

Case	$T_{r\,max}$	$T_{r\,min}$	K_2	K_3	r	t_s	x_{1s}	x_{2s}	T
					10	0·847	0·074	10·57	1·0770
					50	0·838	0·014	11·59	0·8875
1	30	0	1·5	1·5	100	0·837	0·008	11·80	0·8615
					200	0·836	0·004	11·92	0·8485
					500	0·835	0·002	11·97	0·8397
					10	1·266	0·048	7·10	1·4584
					50	1·256	0·012	7·80	1·2990
2	20	0	1·0	1·0	100	1·248	0·009	7·88	1·2767
					200	1·247	0·005	7·95	1·2664
					500	1·246	0·0002	7·98	1·2563
					10	2·600	0·024	3·78	2·6331
					50	2·560	0·025	3·90	2·5860
3	10	0	0·5	0·5	100	2·556	0·010	3·94	2·5654
					200	2·555	0·008	3·96	2·5598
					500	2·554	0·003	3·99	2·5545
					10	5·620	0·013	1·89	5·7103
					50	5·501	0·008	1·93	5·6211
4	5	0	0·25	0·25	100	5·498	0·005	1·98	5·5010
					200	5·494	0·001	1·985	5·4971
					500	5·493	0·0009	1·99	5·4935

A comparison of figures 1 and 4 shows that time lag of the heat exchanger is not too important.

Example 3—Suppose that a life support system consists of an air-conditioned room and a heat exchanger as in the preceding two examples. However, the flow of air in the room can be characterized by the two CST's-in-series model. The performance equations of such a system have been derived in the section entitled "General Performance Equations" in Part 1 of this series[1]. Assuming that the heat exchanger has a negligibly small time constant ($\tau_2 \to 0$), the performance equations are

$$\frac{dx_{11}}{dt} + r_{11}x_{11} = a_{11}a_{42}'x_{12} - a_{11}a_5'\theta - a_{11}a_6' + u_{12} \tag{61}$$

$$\frac{dx_{12}}{dt} + r_{12}x_{12} = a_{21}x_{11} \tag{62}$$

Introducing an additional state variable

$$x_3(t) = \int_0^t dt,$$

we have

$$\frac{dx_3}{dt} = 1, \quad x_3(0) = 0 \tag{65}$$

The problem is thus transformed into that of minimizing $x_3(T)$.

According to equation (5), the Hamiltonian is

$$\mathscr{H}(z, x, \theta) = z_{11}(-r_{11}x_{11} + a_{11}a_{42}'x_{12} - a_{11}a_5'\theta - a_{11}a_6' + a_{12}) + z_{12}(-r_{12}x_{12} + a_{21}x_{11}) + z_3 \tag{66}$$

According to the definition of the adjoint variables, we have

$$\frac{dz_{11}}{dt} = -\frac{\partial \mathscr{H}}{\partial x_{11}} = r_{11}z_{11} - a_{21}z_{12} \tag{67}$$

$$\frac{dz_{12}}{dt} = -\frac{\partial \mathscr{H}}{\partial x_{12}} = -a_{11}a_{42}'z_{11}+r_{12}z_{12} \quad (68)$$

$$\frac{dz_3}{dt} = -\frac{\partial \mathscr{H}}{\partial x_3} = 0, \quad z_3(T) = 1$$

The solution of z_3 can be obtained from this equation as

$$z_3(t) = 1, \quad 0 \leqq t \leqq T \quad (69)$$

Equation (66) can be rewritten as

$$\begin{aligned}\mathscr{H}(z,x,\theta) = {} & z_{11}(-r_{11}x_{11}+a_{11}a_{42}'x_{12} \\ & -a_{11}a_5'\theta-a_{11}a_6'+a_{12}) \\ & +z_{12}(-r_{12}x_{12}+a_{21}x_{11})+1 \end{aligned} \quad (70)$$

Therefore, the switching function $\mathscr{H}^*$ is

$$\mathscr{H}^* = -a_{11}a_5'z_{11}\theta \quad (71)$$

Inspection of $\mathscr{H}^*$ shows that the optimal controller should be of a bang–bang type. The control action for this problem, however, is constrained in such a manner that

$$|\theta| \leqq 1 \quad (72)$$

The conditions for which the Hamiltonian is to be minimum are

$$\begin{aligned}\theta = \theta_{max} = 1 \quad & \text{if} \quad -a_{11}a_5'z_{11} < 0 \\ \theta = \theta_{min} = -1 \quad & \text{if} \quad -a_{11}a_5'z_{11} > 0 \end{aligned} \quad (73)$$

In order to bring the initial deviated state, $x_{11}(0^+) = x_{12}(0^+) = 1$ at $t = 0^+$, to the final desired operating state, $x_{11}(T) = x_{12}(T) = 0$, at $t = T$, we intuitively employ the control action of $\theta = \theta_{max} = 1$ (maximum cooling action). Substituting this value of θ into equations (61) and (62) and then eliminating x_{11}, we have

$$\begin{aligned}\frac{d^2x_{12}}{dt^2} & +(r_{11}+r_{12})\frac{dx_{12}}{dt}+(r_{11}r_{12} \\ & -a_{11}a_{42}'a_{21})x_{12}+a_{11}a_5'a_{21}+a_{11}a_{21}a_6' \\ & -a_{12}a_{21} = 0 \end{aligned} \quad (74)$$

Solution of x_{12} can be written in the form

$$x_{12} = A\exp(\lambda_{11}t)+B\exp(\lambda_{12}t)+K, \quad 0 \leqq t \leqq t_s \quad (75)$$

where λ_{11} and λ_{12} are roots of the characteristic equation

$$\lambda^2+(r_{11}+r_{12})\lambda+(r_{11}r_{12}-a_{11}a_{21}a_{42}') = 0$$

and

$$K = \frac{a_{11}a_5'a_{21}+a_{11}a_{21}a_6'-a_{12}a_{21}}{a_{11}a_{42}'a_{21}-r_{11}r_{12}}$$

Inserting equation (75) and its derivative to equation (62) and solving for x_{11} yield

$$\begin{aligned}x_{11} = \frac{1}{a_{21}} & [(\lambda_{11}+r_{12})A\exp(\lambda_{11}t) \\ & +(\lambda_{12}+r_{12})B\exp(\lambda_{12}t)+r_{12}K], \\ & 0 \leqq t \leqq t_s \end{aligned} \quad (76)$$

Constants A and B in equations (75) and (76) can be determined by employing the initial condition, equation (63) and Cramer's rule as follows:

$$A = \frac{\begin{vmatrix} a_{21}-r_{12}K & r_{12}+\lambda_{12} \\ 1-K & 1 \end{vmatrix}}{\begin{vmatrix} r_{12}+\lambda_{11} & r_{12}+\lambda_{12} \\ 1 & 1 \end{vmatrix}} = \frac{a_{21}-r_{12}-\lambda_{12}+\lambda_{12}K}{\lambda_{11}-\lambda_{12}}$$

and

$$B = \frac{\begin{vmatrix} r_{12}+\lambda_{11} & a_{21}-r_{12}K \\ 1 & 1-K \end{vmatrix}}{\lambda_{11}-\lambda_{12}} = \frac{r_{12}+\lambda_{11}-\lambda_{11}K-a_{21}}{\lambda_{11}-\lambda_{12}}$$

For $\theta = -1$, $x_{11}(t)$ and $x_{12}(t)$ are solved by using equations (61) and (62).

$$\begin{aligned}x_{11}(t) = \frac{1}{a_{21}} & [(\lambda_{11}+r_{12})D_1\exp(\lambda_{11}t) \\ & +(\lambda_{12}+r_{12})D_2\exp(\lambda_{12}t)+r_{12}K'], \\ & t_s \leqq t \leqq T \end{aligned} \quad (77)$$

and

$$x_{12}(t) = D_1\exp(\lambda_{11}t)+D_2\exp(\lambda_{12}t)+K', \quad t_s \leqq t \leqq T \quad (78)$$

where

$$K' = \frac{a_{11}a_{21}a_6'-a_{11}a_5'a_{21}-a_{12}a_{21}}{a_{11}a_{21}a_{42}'-r_{11}r_{12}}$$

Constants D_1 and D_2 can be specified by noting that x_{11} and x_{12} are continuous with respect to t. We obtain from equations (76) through (78) at $t = t_s$

$$\begin{aligned}x_{12}(t_s) & = D_1\exp(\lambda_{11}t_s)+D_2\exp(\lambda_{12}t_s)+K' \\ & = A\exp(\lambda_{11}t_s)+B\exp(\lambda_{12}t_s)+K \end{aligned} \quad (79)$$

and

$$\begin{aligned}x_{11}(t_s) & \\ = \frac{1}{a_{21}} & [(\lambda_{11}+r_{12})D_1\exp(\lambda_{11}t_s) \\ & +(\lambda_{12}+r_{12})D_2\exp(\lambda_{12}t_s)+r_{12}K'] \\ = \frac{1}{a_{21}} & [(\lambda_{11}+r_{12})A\exp(\lambda_{11}t_s) \\ & +(\lambda_{12}+r_{12})B\exp(\lambda_{12}t_s)+r_{12}K] \end{aligned} \quad (80)$$

Solving for D_1 and D_2 from these equations leads to

$$D_1 = A-E_1\exp(-\lambda_{11}t_s) \quad (81)$$

$$D_2 = B-E_2\exp(-\lambda_{12}t_s) \quad (82)$$

where

$$E_1 = \frac{\lambda_{12}(K'-K)}{\lambda_{12}-\lambda_{11}}$$

$$E_2 = \frac{\lambda_{11}(K'-K)}{\lambda_{11}-\lambda_{12}}$$

We see that D_1 and D_2 are functions of t_s. The value of t_s and that of T can be obtained by using the final conditions

$$x_{11}(T) = x_{12}(T) = 0 \quad \text{at} \quad t = T$$

Equations (77) and (78) thus become

$$D_1 \exp(\lambda_{11}T)+D_2 \exp(\lambda_{12}T)+K' = 0 \qquad (83)$$

$$\frac{1}{a_{21}}[(\lambda_{11}+r_{12})D_1 \exp(\lambda_{11}T)+(\lambda_{12}+r_{12})D_2 \exp(\lambda_{12}T)+r_{12}K'] = 0 \qquad (84)$$

Eliminating T from these equations and letting

$$E_3 = \frac{\lambda_{11}K'}{\lambda_{12}-\lambda_{11}}$$

$$E_4 = \frac{K'\lambda_{12}}{\lambda_{11}-\lambda_{12}},$$

we obtain

$$\left(\frac{E_4}{A-E_1\exp(-\lambda_{11}t_s)}\right)^{\lambda_{12}} = \left(\frac{E_3}{B-E_2\exp(-\lambda_{12}t_s)}\right)^{\lambda_{11}} \qquad (85)$$

t_s can be solved from this equation by a trial and error procedure. Then D_1, D_2 and T can be calculated directly from equations (81) through (83).

The solutions of this problem are shown schematically in figures 5–7 and are tabulated in Table 3. The solutions are very similar to those of the preceding example. However, one distinct difference between the response of the dimensionless room temperature in this problem and that in the preceding one is that the dimensionless room temperature can become negative in this problem while it cannot be below zero in the preceding one.

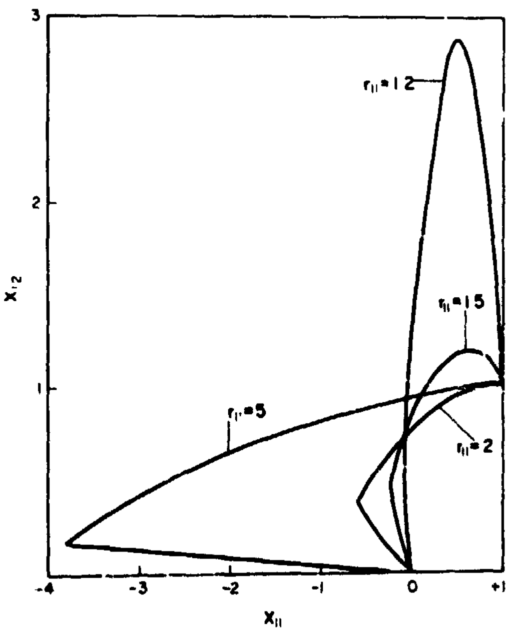

Fig. 5. Phase plane plot for Case 1 of the two CST's-in-series model with $\tau_2 = 0$ and different values of r_{11} [Example 3].

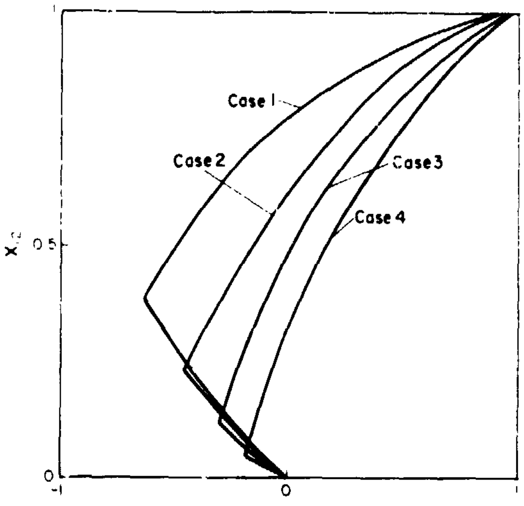

Fig. 6. Phase plane plot for different cases of the two CST's-in-series model with $\tau_2 = 0$ and $r_{11} = 2$ [Example 3].

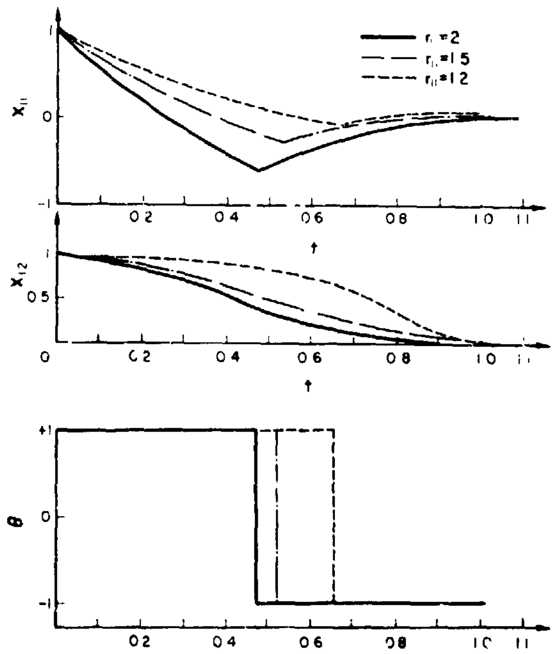

Fig. 7. Optimal control policies and system responses of Case 1 of the two CST's-in-series model with $\tau_2 = 0$ and different values of r_{11} [Example 3].

Table 3. Optimal solutions of the two CST's-in-series model with $\tau_2 = 0$ [Example 3].

Case	$T_{r\,max}$	$T_{r\,min}$	K_2	K_3	r_{11}	x_{11s}	x_{12s}	t_s	T
					1·2	−0·0760	0·7205	0·645	0·992
					1·5	−0·2298	0·4874	0·518	1·047
1	30	0	1·5	1·5	2·0	−0·6031	0·3862	0·471	1·078
					5·0	−3·8727	0·1852	0·598	1·007
					10·0	−9·4477	0·0896	0·715	0·956
					1·2	−0·0596	0·4538	0·975	1·275
					1·5	−0·1703	0·2984	0·775	1·225
2	20	0	1·0	1·0	2·0	−0·4526	0·2552	0·715	1·245
					5·0	−2·5520	0·1024	0·910	1·25
					10·0	−6·0425	0·05105	1·060	1·25
					1·2	−0·0343	0·1476	2·015	2·215
					1·5	−0·0998	0·1177	1·635	1·955
3	10	0	0·5	0·5	2·0	−0·2285	0·0882	1·500	1·860
					5·0	−1·1295	0·0353	1·875	2·115
					10·0	−2·6253	0·0171	2·180	2·310
					1·2	−0·0169	0·0192	4·520	4·625
					1·5	−0·0414	0·0223	3·780	3·940
4	5	0	0·25	0·25	2·0	−0·8831	0·0167	3·460	3·640
					5·0	−0·3865	0·0082	4·250	4·360
					10·0	−0·8734	0·0059	4·780	4·841

CONCLUSIONS

By now readers should be able to realize that the maximum principle has a certain advantage over other modern optimal control techniques. It is that it can be used to evaluate the number of switching points of the bang–bang control policy via the switching function and adjoint vectors. Three examples given in this article take advantage of this rule. Furthermore, the maximum principle can be applied not only to the system with linear performance equations but also to those with non-linear performance equations. Bellman[9] proved theoretically that the number of switching points is one less than the dimension of the problem for linear systems. However, this theory cannot be applied to non-linear systems.

It is worth noting that other forms of the objective functions can be considered. For example

$$S = \int_0^T [x_1]^2 \mathrm{d}t$$

$$S = \int_0^T [a + b_1(x_1)^2] \mathrm{d}t$$

$$S = \int_0^T [\theta]^2 \mathrm{d}t$$

$$S = \int_0^T [a + c(\theta)^2] \mathrm{d}t$$

$$= \int_0^T [a + b_1(x_1)^2 + c(\theta)^2] \mathrm{d}t$$

$$S = \int_0^T [b_1(x_1)^2 + c(\theta)^2] \mathrm{d}t$$

$$S = \int_0^T |\,\theta\,| \,\mathrm{d}t$$

The objective functions have different physical significance[3,4,6].

REFERENCES

1. L. T. Fan, Y. S. Hwang and C. L. Hwang, Applications of Modern Optimal Control Theory to Environmental Control of Confined Spaces, Part 1 Modeling and Simulation, *Build Sci*, **5**, 57 (1970).
2. L. S. Pontryagin, V. G. Boltyanskii, R. V. Gamkrelidze, and E. F. Mishchenko, *The Mathematical Theory of Optimal Processes* (English translation by K. N. Trirogoff), Interscience, New York, (1962).
3. L. T. Fan, *The Continuous Maximum Principle: A Study of Complex Systems Optimization*, Wiley, New York, (1966).
4. Y. Takahashi, The Maximum Principle and Its Applications, *ASME* paper 63-WA-333 (1963)
5. S. S. L. Chang, A Modified Maximum Principle for Optimum Control of a System with Bounded Phase Space Coordinates, *Automatica* **1**, 55 (1962).
6. A. P. Sage, Optimal System Control, Prentice Hall, New Jersey, (1968).
7. A. F. Ogunye, and W. H. Ray, Non-simple Control Policies for Reactors with Catalyst Decay, *Trans. Instn. Chem. Engrs.* **46**, T225 (1968).
8. C. M. Crowe, Optimization of Reactors with Catalyst Decay I—Single Tubular Reactor with Uniform Temperature, Presented in the A.I.Ch.E. 65th national meeting, Cleveland, Ohio, May 4–7, (1969).
9. R. Bellman, I. Glicksberg and O. Gross, On the Bang-bang Control Problems, *Quarterly Appl. Math.* **14**, 11 (1955).
10. C. D. Johnson, *Singular Solutions in Problems of Optimal Control*, (edited by C. T. Leondes), Academic Press, New York, (1965).

NOMENCLATURE

a_1	rK_1/K_4
a_2	r_2K_1
a_3	$K_1\sigma$
a_4	rK_4/K_1
a_5	rK_2K_4
a_6	rK_3K_4
a_{11}	$r_1K_{11}r_{11}/K_4$
a_{12}	$r_1r_2K_{11}$
a_{13}	T_dK_{11}/T_2r_{11}
a_{21}	$r_{12}K_{12}/K_{11}$
a_{23}	T_dK_{12}/T_2r_{12}
a_{42}	rK_4/K_{12}
a'_{42}	K_4/K_{12}
A	Integration constant
A_1	Integration constant
A_2	Integration constant
B	Integration constant
c_i	Constants defined in equation (3), $i = 1, 2, \dots, s$
c_p	Specific heat of air in kcal/kg°C
c_{pw}	Specific heat of coolant in kcal/kg°C
D_1	Constant defined in equation (53)
D_2	Constant defined in equation (54)
E_1	Constant in equation (53)
E_2	Constant in equation (54)
E_3	Constant in equation (59)
E_4	Constant in equation (58)
$h_i[(t)]$	p-dimensional constraints on decision vector function $\theta(t)$
$\mathscr{H}[x(t), \theta(t), z(t)]$	Hamiltonian function defined in equation (5)
$\mathscr{H}^*$	The portion of $\mathscr{H}$ which depends on θ
K	$\dfrac{ra_2 - a_1a_5 - a_1a_6}{r - a_1a_4}$
K'	$\dfrac{ra_2 + a_1a_5 - a_1a_6}{r - a_1a_4}$
K_1	$\dfrac{T_2}{T_{c0}}$
K_2	$\dfrac{1}{2T_2}(T_{r\,\max} - T_{r\,\min})$
K_3	$\dfrac{1}{2T_2}(T_{r\,\max} + T_{r\,\min})$
K_4	$\dfrac{T_2}{T_{i0}}$
K_{11}	$\dfrac{T_2}{T_{1c0}}$
K_{12}	$\dfrac{T_2}{T_{2c0}}$
Q	$Q_1 + Q_2$, flow rate of air in the system proper in m^3/s
Q_1	Air flow rate by circulation air in m^3/s
Q_2	Flow rate of fresh air in m^3/s
Q_w	Flow rate of coolant in m^3/s
r	$\dfrac{\tau_1}{\tau_2}$, the ratio of time constant of system proper to that of heat exchanger
r_1	$\dfrac{Q_1}{Q_1 + Q_2}$, the fraction of circulation air
r_2	$\dfrac{Q_2}{Q_1 + Q_2}$, the fraction of fresh air
r_{11}	$\dfrac{\tau_1}{\tau_{11}}$
r_{12}	$\dfrac{\tau_2}{\tau_{12}}$
S	Performance index defined in equation (3)
t	$\dfrac{\alpha}{\tau_1}$, dimensionless time
t_a	Reference temperature in °C
t_c	Room temperature in °C
t_d	Disturbance temperature in °C
t_i	Temperature of incoming circulation air in °C
t_0	Initial time
t_s	Switching time
t_{wc}	Inlet temperature of coolant in °C
t_{wh}	Outlet temperature of coolant in °C
t_2	Outside air temperature in °C
T	Final time, dimensionless
T_c	$(t_c - t_a)$, room temperature in °C

T_{c0}	Room temperature at $\alpha = 0^+$ in °C
T_{c1}	Temperature of pool 1 in °C
T_{c10}	Temperature of pool 1 at $\alpha = 0^+$ in °C
T_{c2}	Temperature of pool 2 in °C
T_{c20}	Temperature of pool 2 at $\alpha = 0^+$
T_d	$(t_d - t_a)$, disturbance temperature in °C
T_i	$(t_i - t_a)$, temperature of the circulation air into the system, in °C
T_{i0}	Temperature of the circulation air into the system at $\alpha = 0^+$ in °C
T_r	$\dfrac{Q_w \rho_w c_{pw}(T_{wh} - T_{wc})}{Q_1 \rho c_p}$, hypothetical temperature
T_{rf}	Final steady state value of T_r
$T_{r\,max}$	Upper bound of T_r in °C
$T_{r\,min}$	Lower bound of T_r in °C
T_{r0}	Value of T_r at $\alpha = 0$ in °C
T_{wc}	$t_{wc} - t_c$ in °C
T_{wh}	$t_{wh} - t_a$ in °C
T_{11}	Temperature of pool 1 in °C
T_{12}	Temperature of pool 2 in °C
$U_0(t)$	Step heat disturbance function
V_1	Volume of room in m^3
V_{11}	Volume of pool 1 of two completely stirred tanks in series model in m^3
V_2	Volume of heat exchanger in m^3
V_{12}	Volume of pool 2 of two completely stirred tanks in series model in m^3
$x(t)$	s-dimensional state vector defined in equation (1)
$x_i(t_0)$	x_{i0}, $i = 1, 2, \ldots, s$, initial value of x at $t = t_0$
$x_1(t)$	$\dfrac{T_c}{T_{c0}}$, dimensionless room temperature
$x_2(t)$	A state variable defined in equation (11)
$x_2(t)$	$\dfrac{T_i}{T_{i0}}$, dimensionless temperature of the circulation air in equation (31)
x_{11}	$\dfrac{T_{c1}}{T_{c10}}$, dimensionless temperature of pool 1
x_{12}	$\dfrac{T_{c2}}{T_{c20}}$, dimensionless temperature of pool 2
$z_i(t)$	adjoint variable defined in equation (6)

Greek letters

α	Time in s
α_f	Final time in s
$\delta(\alpha)$	Impulse heat disturbance function, s^{-1}
ρ	Air density in kg/m^3
ρ_w	Density of coolant in kg/m^3
σ	$\dfrac{T_d}{T_2}$, dimensionless disturbance temperature
τ_1	$\dfrac{V_1}{Q_1 + Q_2}$, time constant of the system proper in s
τ_{11}	$\dfrac{V_{11}}{Q_1 + Q_2}$, time constant of pool 1 in s
τ_2	$\dfrac{V_2}{Q_1}$, time constant of heat exchanger in s
τ_{12}	$\dfrac{V_{12}}{Q_1 + Q_2}$, time constant of pool 2 in s
θ	$\dfrac{T_r - \frac{1}{2}(T_{r\,max} + T_{r\,min})}{T_{r\,max} - \frac{1}{2}(T_{r\,max} + T_{r\,min})}$, control variable
θ	$\begin{cases} +1 & \text{at } T_r = T_{r\,max} \\ -1 & \text{at } T_r = T_{r\,min} \end{cases}$
$\bar{\theta}(t)$	Optimum value of $\theta(t)$
$\phi(\alpha)$	Heat disturbance function
η	Defined in equation (22a)
λ_1	Constant in equation (45)
λ_2	Constant in equation (45)
λ_{11}	Constant in equation (75)
λ_{12}	Constant in equation (75)

On présente la forme fondamentale du principe du maximum de Pontryagin qui est la clef de la théorie moderne de contrôle optimal. Le principe est appliqué à la détermination des polices de contrôle optimal de plusieurs systèmes de support de vie ou de contrôle d'entourage.

On considère trois exemples concrets dont tous se rapportent au contrôle de température d'un système de support de vie consistant d'une cabine à air conditioné (le système lui-même) soumis à une perturbation de chaleur par impulsion, et d'un échangeur de chaleur (l'élément de contrôle). Le premier exemple traite le cas dans lequel la constante de temps de l'échangeur de chaleur est négligeable. Le second exemple considère le cas où la constante de temps de l'échangeur de chaleur n'est pas ignoré. Dans le troisième exemple on étudie la police optimale du système où le courant d'air dans la cabine peut être caractérisé par les deux modèles de vaisseaux en série (2 CST en série) complètement agités. Dans cet exemple, on néglige encore la constante de temps de l'échangeur de chaleur. On donne de façon détaillée les procédés et les techniques par ordinateur employée pour obtenir les polices de contrôle optimal.

Die grundlegende Form von Pontryagin's Maximum Prinzip ist dargestellt, welches der Grundstein der modernen Optimalkontrolltheorie ist. Das Prinzip wird für die Feststellung optimaler Kontrollverfahren für verschiedene Lebensunterhaltungsoder Umgebungskontrollsysteme angewandt.

Drei konkrete Beispiele werden ins Auge gefasst, wobei alle sich mit der Temperaturkontrolle von Lebensunterhaltungssystemen befassen, die aus einer klimatisierten Kabine, (dem eigentlichen System) bestehen, die einem Wärmestörungsimpuls ausgesetzt wird, und aus einem Wärmeaustauscher, (dem Kontrollelement). Das erste Beispiel behandelt den Fall, in dem die Zeitkonstante des Wärmeaustauschers unbedeutend ist. Das zweite Beispiel behandelt den Fall, in dem die Zeitkonstante des Wärmeaustauschers nicht vernachlässigt wird. In dem dritten Beispiel wird das Optimalverfahren des Systems untersucht, in welchem die Luftströmung in der Kabine durch zwei gründlich gemischte Reihentanks (2 CST's-in-series) im Modell geschildert wird. In diesem Beispiel wird die Zeitkonstante des Wärmeaustauschers wieder vernachlässigt. Verfahren und berechenbare Betrach tungen zum Erhalten optimaler Kontrollverfahren werden mit Einzelheiten gegeben.

(d)3

Build. Sci. Vol. 5, pp. 125–136. Pergamon Press 1970. Printed in Great Britain

Applications of Modern Optimal Control Theory to Environmental Control of Confined Spaces and Life Support Systems*

Part 3—Optimal Control of Systems in which State Variables have Equality Constraints at the Final Process Time

L. T. FAN †
Y. S. HWANG †
C. L. HWANG †

The basic form of Pontryagin's maximum principle is extended to cover optimal problems with equality constraints imposed on the final state variables. The necessary conditions for optimum control policy are developed and are applied to two concrete examples.

The dynamic behavior of the life support system consisting of an air-conditioned cabin (the system proper) subject to an impulse heat disturbance and a heat exchanger (the control element) is again studied. The first example considers the optimal control policy for a system having a heat exchanger with a negligibly small time constant. The square form of the final condition of the state variable is considered as an equality constraint. The second example considers the optimal policy of a system where the flow of air in the cabin is characterized by the two completely stirred tanks-in-series (2 CST's-in-series) model. The time constant of the heat exchanger is not neglected, that is, the response of the heat exchanger is not instantaneous. The squares of the final conditions of the state variables are again considered as equality constraints.

INTRODUCTION

The basic form of Pontryagin's maximum principle, has been introduced in the preceding part[1]. Here we shall extend the basic form to cover the optimal time problem with equality constraints imposed on the final state variables.

Kopp[2,3] adjoined the equality constraints to the objective function via Lagrange multipliers and then solved the problem by a trial and error procedure. Denn and Aris[4] treated the problem by the Green's function approach. We shall first obtain the necessary conditions for optimum by adjoining the equality constraints to the objective function via Lagrange multipliers and taking a weak variation of the resulting expression[5]. The necessary conditions thus obtained will be applied to two concrete examples.

* This work was supported by the Air Force Office of Scientific Research, Office of Aerospace Research, United States Air Force, Under Contract F 44620–68–0020 (Themis Project), and NASA Grant Under Contract NGR-17-001-034.

† Institute for Systems Design and Optimization, Kansas State University, Manhattan, Kansas.

NECESSARY CONDITIONS FOR OPTIMALITY FOR TIME OPTIMAL PROBLEMS WITH EQUALITY CONSTRAINTS IMPOSED ON THE FINAL STATE VARIABLES

Again let us consider the differential equations of the following form

$$\frac{dx_i}{dt} = f_i[x_1(t), x_2(t), \ldots, x_s(t); \theta_1(t), \theta_2(t), \ldots, \theta_r(t)], \quad i = 1, 2, \ldots, s \tag{1}$$

with the initial conditions given by

$$x_i(t_0) = x_{i0}, \quad t = t_0 \tag{2}$$

Suppose that we wish to determine the control vector $\theta(t)$ so as to minimize (or maximize)

$$S = \int_{t_0}^{T} F[x(t), \theta(t)]dt \tag{3}$$

subject to the q-dimensional constraint on state variables at the unspecified terminal time, T, as shown below.

$$g_i[x(T)] = 0, \quad i = 1, 2, \ldots, q \tag{4}$$

PRECEDING PAGE BLANK NOT FILMED

where initial time t_0 is then fixed and T is the unspecified control terminal time. Here the objective function, equation (3), is different from the form used in Part 2 of this series[1]. However, we can transform equation (3) into the form used in Part 2 by introducing an additional state variable x_{s+1} such that

$$x_{s+1}(t) = \int_{t_0}^{t} F[x(t), \theta(t)]\mathrm{d}t \tag{5}$$

It follows that

$$\frac{\mathrm{d}x_{s+1}(t)}{\mathrm{d}t} = F[x(t), \theta(t)] \tag{6}$$

$$= f_{s+1}[x(t), \theta(t)]$$

$$x_{s+1}(t_0) = 0 \tag{7}$$

and hence the objective function now becomes

$$S = x_{s+1}(T) \tag{8}$$

or

$$S = \sum_{i=1}^{s+1} c_i x_i(T) \tag{9}$$

which is in the standard form used in Part 2 with

$$c_i = 0, \quad i = 1, 2, \dots, s$$
$$c_{s+1} = 1$$

Suppose that the equality constraints, $g_i[x(T)] = 0$, and the performance equations, equations (1) and (6), are adjoined to the objective function via Lagrange multipliers, v_i and z_i.

$$S' = \sum_{i=1}^{s+1} c_i x_i(T) + \sum_{i=1}^{q} v_i g_i[x(T)] + \int_{t_0}^{T} \sum_{i=1}^{s+1} z_i \left\{ f_i[x(t), \theta(t)] - \frac{\mathrm{d}x_i}{\mathrm{d}t} \right\} \mathrm{d}t \tag{10}$$

We can then define the Hamiltonian

$$\mathscr{H}[x(t), \theta(t), z(t)] = \sum_{i=1}^{s+1} z_i f_i[x(t), \theta(t)] \tag{11}$$

and substitute this relation into equation (10) to obtain

$$S' = \sum_{i=1}^{s+1} c_i x_i(T) + \sum_{i=1}^{q} v_i g_i[x(T)] + \int_{t_0}^{T} \left\{ \mathscr{H}[x(t), \theta(t), z(t)] - \sum_{i=1}^{s+1} z_i(t) \frac{\mathrm{d}x_i}{\mathrm{d}t} \right\} \mathrm{d}t \tag{12}$$

The first variation of S', $\delta S'$, which is defined as

$$\delta S' = S'[x, \theta, z, T] - S'[\bar{x}, \bar{\theta}, \bar{z}, \bar{T}]$$

may be obtained by letting

$$\begin{aligned} x_i(t) &= \bar{x}_i(t) + \delta x_i(t), \quad i = 1, 2, \dots, s+1 \\ \theta_i(t) &= \bar{\theta}_i(t) + \delta\theta_i(t), \quad i = 1, 2, \dots, r \\ T &= \bar{T} + \delta T \\ z_i(t) &= \bar{z}_i(t) + \delta z_i(t), \quad i = 1, 2, \dots, s+1, \end{aligned} \tag{13}$$

and then inserting these relations into equation (12) and carrying out the Taylor series expansion about the optimal state, $\bar{x}$, $\bar{\theta}$, $\bar{z}$, and $\bar{T}$. Retaining only the linear terms of the resulting equation and then dropping the bar notation give

$$\begin{aligned} \delta S' = \delta T \Bigg\{ & \mathscr{H}[x(T), \theta(T), z(T)] + \sum_{i=1}^{q} v_i \frac{\partial g_i}{\partial T} \\ & + \sum_{i=1}^{s+1} c_i \frac{\partial x_i}{\partial T} - \sum_{i=1}^{s+1} z_i(T) \frac{\mathrm{d}x_i(T)}{\mathrm{d}T} \Bigg\} \\ & + \sum_{i=1}^{s+1} \delta x_i(T) \left\{ \sum_{j=1}^{q} v_j \frac{\partial g_j}{\partial x_i} - z_i(T) + c_i \right\} \\ & + \int_{t_0}^{T} \left\{ \sum_{i=1}^{s+1} \delta x_i \left[\frac{\partial \mathscr{H}}{\partial x_i} + \frac{\mathrm{d}z_i}{\mathrm{d}t} \right] + \sum_{i=1}^{r} \delta\theta_i \frac{\partial \mathscr{H}}{\partial \theta_i} \right. \\ & \left. + \sum_{i=1}^{s+1} \delta z_i \left[\frac{\partial \mathscr{H}}{\partial z_i} - \frac{\mathrm{d}x_i}{\mathrm{d}t} \right] \right\} \mathrm{d}t \end{aligned} \tag{14*}$$

We must set this first variation equation at zero to obtain the necessary conditions for a minimum. The resulting equations which determine the optimal control and state vectors are as follows:

$$\mathscr{H}[x(t), \theta(t), z(t)] = \sum_{i=1}^{s+1} z_i(t) f_i[x(t), \theta(t)] \tag{15}$$

$$\frac{\partial \mathscr{H}}{\partial z_i} = + \frac{\mathrm{d}x_i}{\mathrm{d}t} = f_i[x(t), \theta(t)], \quad i = 1, 2, \dots, s+1 \tag{16}$$

$$\frac{\partial \mathscr{H}}{\partial x_i} = - \frac{\mathrm{d}z_i}{\mathrm{d}t} = \sum_{j=1}^{s+1} \frac{\partial f_j}{\partial x_i} z_j, \quad i = 1, 2, \dots, s+1 \tag{17}$$

$$\frac{\partial \mathscr{H}}{\partial \theta_i} = 0 = \sum_{j=1}^{s+1} \frac{\partial f_j}{\partial \theta_i} z_j, \quad i = 1, 2, \dots, r \tag{18}$$

These represent the $(2s+2)$ differential equations for the two-point split boundary value problems. The conditions at the initial time are given in equations (2) and (7), whereas those at the final time are

$$z_i(T) = \sum_{j=1}^{q} v_j \frac{\partial g_j}{\partial x_i(T)} + c_i, \quad i = 1, 2, 3, \dots, s+1 \tag{19}$$

and

$$\mathscr{H}[x(T), \theta(T), z(T)] + \sum_{i=1}^{q} \frac{\partial g_i}{\partial T} v_i + \sum_{i=1}^{s+1} c_i \frac{\partial x_i}{\partial T} - \sum_{i=1}^{s+1} z_i(T) \frac{\mathrm{d}x_i(T)}{\mathrm{d}T} = 0 \tag{20}$$

Equation (19) provides $(s+1)$ conditions with q Lagrange multipliers to be determined. Equation (4) provides q equations which can be used for elimination of the Lagrange multipliers, and

* Derivation of equation (14) is given in the Appendix.

equation (20) provides one additional equation which can be used for determination of the unspecified terminal time.

It is worth noting that when the constraints $g_i[x(T)] = 0$ are not imposed on the final state variables, the necessary conditions derived here reduce to those derived for the basic problems presented in the preceding article[1]. In other words, equations (19) and (20) reduce to

$$z_i(T) = c_i \tag{19a}$$

$$\mathscr{H}[x(T), \theta(T), z(T)] = 0 \tag{20a}$$

The set formed by these equations and equations (15) through (18) is identical to that formed by equations (5) through (8) in the preceding article. Equation (20a) is correct because the minimum (or maximum) value of the Hamiltonian is identical to zero at every point of time t for the time optimal problems.

The final condition, $x(T)$, which is fixed in the fixed right-end problems can be considered as the simplest case of $g_i[x(T)] = 0$.

EXAMPLES

Here the necessary conditions developed in the preceding section will be applied to the following examples.

Example 1—Let us reconsider Example 1 of the preceding article[1]. The statement of the problem remains the same. Now the square form of the final condition of the state variable can be considered as an equality constraint on the state variables at the control terminal time, i.e.,

$$g_1[x(T)] = \tfrac{1}{2}[x_1(T)]^2 = 0 \tag{21}$$

We now wish to show that at the optimal condition the two necessary conditions at the control terminal time, equations (19) and (20), are satisfied. Employing equations (19) and (20), we have

$$z_1(T) = v_1 x_1(T)\frac{\partial x_1(T)}{\partial x_1(T)} + c_1 = v_1 x_1(T) + c_1 \tag{22}$$

$$z_2(T) = \tfrac{1}{2}v_2\frac{\partial[x_1(T)]^2}{\partial x_2(T)} + c_2 = c_2 \tag{23}$$

$$\begin{aligned}
&\mathscr{H}[x(T), \theta(T), z(T)] + v_1 x_1(T)\frac{dx_1(T)}{dT} \\
&\quad + \left[c_1\frac{dx_1(T)}{dT} + c_2\frac{dx_2(T)}{dT}\right] \\
&\quad - \left[z_1(T)\frac{dx_1(T)}{dT} + z_2(T)\frac{dx_2(T)}{dT}\right] \\
&= \mathscr{H}[x(T), \theta(T), z(T)] \\
&= 0
\end{aligned} \tag{24}$$

Since

$$c_1 = 0$$

$$c_2 = 1,$$

equations (22) and (23) become

$$z_1(T) = v_1 x_1(T) \tag{22a}$$

$$z_2(T) = 1 \tag{23a}$$

Equations (24), (22a) and (23a) assure us that this type of problem can be solved by making use of the necessary conditions presented in the preceding section as well as those presented in Part 2 of this series[1].

Example 2—As mentioned in Example 2 of Part 2[1], the response of the heat exchanger as well as that of the cabin or room is not always instantaneous. In Example 3 of the preceding article, we considered the system consisting of a room or cabin with the flow of air characterized by the two CST's-in-series model and a heat exchanger whose time constant is negligibly small. Here we consider a slightly different system in which the response of the heat exchanger is not instantaneous. The performance equations are [see equations (43) through (45) in reference 6].

$$\frac{dx_{11}}{dt} + r_{11}x_{11} = a_{11}x_2 + a_{12} \tag{25}$$

$$\frac{dx_{12}}{dt} + r_{12}x_{12} = a_{21}x_{11} \tag{26}$$

$$\frac{dx_2}{dt} + rx_2 = a_{42}x_{12} - a_5\theta - a_6 \tag{27}$$

with the initial and final conditions

$$\begin{aligned}
x_{11}(0^+) = x_{12}(0^+) = x_2(0^+) = 1 \quad &\text{at} \quad t = 0^+ \\
x_{11}(T) = x_{12}(T) = 0,\ x_2(T) = 1 \quad &\text{at} \quad t = T
\end{aligned} \tag{28}$$

where T is unspecified. The control variable, θ, is constrained as

$$|\theta| \le 1 \tag{29}$$

We wish to determine a piecewise continuous control variable θ so that the response of the system can return to its desired state in a minimum period of time, that is,

$$S = \int_0^T dt \tag{30}$$

is minimized.

We shall first make use of the basic form of the maximum principle presented in Part 2 of this series to solve the problem. Let

$$x_3(t) = \int_0^t dt$$

or

$$\frac{dx_3}{dt} = 1, \quad x_3(0) = 0 \tag{31}$$

Hence we have

$$S = x_3(T)$$

$$\mathscr{H} = z_{11}[-r_{11}x_{11}+a_{11}x_2+a_{12}] + z_{12}[-r_{12}x_{12}+a_{21}x_{11}] + z_2[-rx_2+a_{42}x_{12}-a_5\theta-a_6]+z_3 \tag{32}$$

$$\frac{dz_{11}}{dt} = r_{11}z_{11}-a_{21}z_{12} \tag{33}$$

$$\frac{dz_{12}}{dt} = r_{12}z_{12}-a_{42}z_2 \tag{34}$$

$$\frac{dz_2}{dt} = rz_2-a_{11}z_{11} \tag{35}$$

$$\frac{dz_3}{dt} = 0, \quad z_3(T) = 1 \tag{36}$$

It follows from equation (36) that

$$z_3(t) = 1, \quad 0 \leqq t \leqq T \tag{37}$$

Equation (32) can then be rewritten as

$$\mathscr{H} = z_{11}[-r_{11}x_{11}+a_{11}x_2+a_{12}]+z_{12}[-r_{12}x_{12} + {}_{21}x_{11}+z_2[-rx_2+a_{42}x_{12}-a_5\theta-a_6]+1 \tag{38}$$

Therefore,

$$\mathscr{H}^* = -a_5z_2\theta \tag{39}$$

An optimal control corresponding to this case should be of the bang-bang type. Thus the conditions for optimal control (minimum $\mathscr{H}^*$) are

$$\theta = -1, \quad \text{if} \quad -a_5z_2 > 0$$

$$\theta = +1, \quad \text{if} \quad -a_5z_2 < 0$$

In order to bring the initial deviated state,

$$x_{11}(0) = x_{12}(0) = x_2(0) = 1 \quad \text{at} \quad t = 0$$

to the final desired state,

$$x_{11}(T) = x_{12}(T) = 0, x_2(T) = 1 \quad \text{at} \quad t = T,$$

we shall first apply the control $\theta = 1$. In other words, we have $\theta = 1$ in the interval $0 \leqq t \leqq t_{s1}$. Substitution of $\theta = 1$ into equations (25) through (31) and subsequent elimination of x_{11} and x_2 from the resulting expressions give rise to

$$\frac{d^3x_{12}}{dt^3}+(r+r_{11}+r_{12})\frac{d^2x_{12}}{dt^2}+(r_{11}r_{12}+rr_{11}+rr_{12})\frac{dx_{12}}{dt}+(rr_{11}r_{12}-a_{11}a_{21}a_{42})x_{12} = ra_{12}a_{21}-a_5a_{11}a_{21}-a_{11}a_{21}a_6 \tag{40}$$

The solution of x_{12} has the form

$$x_{12} = A\exp(\lambda_1t)+B\exp(\lambda_2t)+C\exp(\lambda_3t)+K, \quad 0 \leqq t \leqq t_{s1} \tag{41}$$

where A, B and C are constants and λ_1, λ_2 and λ_3 are roots of the characteristic equation

$$\lambda^3+(r+r_{11}+r_{12})\lambda^2+(r_{11}r_{12}+rr_{11}+rr_{12})\lambda+(rr_{11}r_{12}-a_{11}a_{21}a_{42}) = 0 \tag{42}$$

and K is a constant and its value equals to

$$K = \frac{ra_{12}a_{21}-a_5a_{11}a_{21}-a_{11}a_{21}a_6}{rr_{11}r_{12}-a_{11}a_{21}a_{42}} \tag{43}$$

Inserting equation (41) and its first and second derivatives to equations (25) through (27) and then solving for x_{11} and x_2 lead to

$$x_{11} = \frac{1}{a_{21}}[(\lambda_1+r_{12})A\exp(\lambda_1t)+(\lambda_2+r_{12})B\exp(\lambda_2t)+(\lambda_3+r_{12})C\exp(\lambda_3t)+r_{12}K], \quad 0 \leqq t \leqq t_{s1} \tag{44}$$

and

$$x_2 = \frac{1}{a_{11}a_{21}}\{A[\lambda_1^2+(r_{11}+r_{12})\lambda_1+r_{11}r_{12}]\exp(\lambda_1t)+B[\lambda_2^2+(r_{11}+r_{12})\lambda_2+r_{11}r_{12}]\exp(\lambda_2t)+C[\lambda_3^2+(r_{11}+r_{12})\lambda_3+r_{11}r_{12}]\exp(\lambda_3t)+r_{11}r_{12}K-a_{12}a_{21}\}, \quad 0 \leqq t \leqq t_{s1} \tag{45}$$

Let

$$\begin{aligned}
A_1 &= \lambda_1+r_{12}\\
A_2 &= \lambda_2+r_{12}\\
A_3 &= \lambda_3+r_{12}\\
A_4 &= \lambda_1^2+(r_{11}+r_{12})\lambda_1+r_{11}r_{12}\\
A_5 &= \lambda_2^2+(r_{11}+r_{12})\lambda_2+r_{11}r_{12}\\
A_6 &= \lambda_3^2+(r_{11}+r_{12})\lambda_3+r_{11}r_{12}\\
A_7 &= a_{21}-r_{12}K\\
A_8 &= 1-K\\
A_9 &= a_{11}a_{21}+a_{12}a_{21}-r_{11}r_{12}K
\end{aligned}$$

Then equations (41), (44) and (45) can be rewritten as

$$x_{11} = \frac{1}{a_{21}}[A_1A\exp(\lambda_1t)+A_2B\exp(\lambda_2t)+A_3C\exp(\lambda_3t)+r_{12}K], \quad 0 \leqq t \leqq t_{s1} \tag{46}$$

$$x_{12} = A\exp(\lambda_1t)+B\exp(\lambda_2t)+C\exp(\lambda_3t)+K, \quad 0 \leqq t \leqq t_{s1} \tag{47}$$

$$x_2 = \frac{1}{a_{11}a_{21}}[A_4A\exp(\lambda_1t)+A_5B\exp(\lambda_2t)$$

$$+A_6C\exp(\lambda_3 t)+r_{11}r_{12}K-a_{12}a_{21}],$$

$$0 \leqq t \leqq t_{s1} \tag{48}$$

Values of A, B and C can be determined by employing the initial conditions

$$x_{11}(0^+) = x_{12}(0^+) = x_2(0^+) = 1 \quad \text{at} \quad t = 0^+$$

Hence, equations (46) through (48) become

$$A_1A+A_2B+A_3C = A_7$$
$$A+B+C = A_8$$
$$A_4A+A_5B+A_6C = A_9$$

Solving for A, B and C by using Cramer's rule, we have

$$A = A_{11}/A_{10}$$
$$B = A_{12}/A_{10}$$
$$C = A_{13}/A_{10}$$

where

$$A_{10} = A_1A_6+A_2A_4+A_3A_5-A_1A_5-A_2A_6 - A_3A_4$$

$$A_{11} = A_6A_7+A_2A_9+A_3A_5A_8-A_5A_7-A_2A_6A_8 - A_3A_9$$

$$A_{12} = A_1A_6A_8+A_4A_7+A_3A_9-A_1A_9-A_6A_7 - A_3A_4A_8$$

$$A_{13} = A_1A_9+A_2A_8A_4+A_7A_5-A_1A_5A_8-A_2A_9 - A_4A_7$$

Similarly, for $t_{s1} \leqq t \leqq t_{s2}$, we have

$$\theta = -1$$

$$x_{11} = \frac{1}{a_{21}}[A_1A'\exp(\lambda_1 t)+A_2B'\exp(\lambda_2 t) + A_3C'\exp(\lambda_3 t)+r_{12}K'], \quad t_{s1} \leqq t \leqq t_{s2} \tag{49}$$

$$x_{12} = A'\exp(\lambda_1 t)+B'\exp(\lambda_2 t)+C'\exp(\lambda_3 t)+K', \quad t_{s1} \leqq t \leqq t_{s2} \tag{50}$$

and

$$x_2 = \frac{1}{a_{11}a_{21}}[A_4A'\exp(\lambda_1 t)+A_5B'\exp(\lambda_2 t) + A_6C'\exp(\lambda_3 t)+r_{11}r_{12}K'-a_{12}a_{21}], \quad t_{s1} \leqq t \leqq t_{s2} \tag{51}$$

where

$$K' = \frac{ra_{12}a_{21}+a_5a_{11}a_{21}-a_{11}a_{21}a_6}{rr_{11}r_{12}-a_{11}a_{21}a_{42}}$$

and A', B' and C' are unknown constants.

For $t_{s2} \leqq t \leqq T$, we have

$$\theta = 1$$

$$x_{11} = \frac{1}{a_{21}}[A_1A''\exp(\lambda_1 t)+A_2B''\exp(\lambda_2 t) + A_3C''\exp(\lambda_3 t)+r_{12}K], \quad t_{s2} \leqq t \leqq T \tag{52}$$

$$x_{12} = A''\exp(\lambda_1 t)+B''\exp(\lambda_2 t)+C''\exp(\lambda_3 t)+K, \quad t_{s2} \leqq t \leqq T \tag{53}$$

$$x_2 = \frac{1}{a_{11}a_{21}}[A_4A''\exp(\lambda_1 t)+A_5B''\exp(\lambda_2 t) + A_6C''\exp(\lambda_3 t)+r_{11}r_{12}K-a_{12}a_{21}], \quad t_{s2} \leqq t \leqq T \tag{54}$$

where A'', B'' and C'' are unknown constants.

We know that x_{11}, x_{12}, and x_2 are continuous functions of t. Therefore, A', B', C' and A'', B'', C'' can be determined by using the continuity of x_{11}, x_{12} and x_2 with respect to t at $t = t_{s1}$ and $t = t_{s2}$. Thus

$$x_{11}(t_{s1}) = \frac{1}{a_{21}}[A_1A\exp(\lambda_1 t_{s1})+A_2B\exp(\lambda_2 t_{s1}) + A_3C\exp(\lambda_3 t_{s1})+r_{12}K]$$
$$= \frac{1}{a_{21}}[A_1A'\exp(\lambda_1 t_{s1})+A_2B'\exp(\lambda_2 t_{s1}) + A_3C'\exp(\lambda_3 t_{s1})+r_{12}K'] \tag{55}$$

$$x_{12}(t_{s1}) = A\exp(\lambda_1 t_{s1})+B\exp(\lambda_2 t_{s1}) + C\exp(\lambda_3 t_{s1})+K$$
$$= A'\exp(\lambda_1 t_{s1})+B'\exp(\lambda_2 t_{s1}) + C'\exp(\lambda_3 t_{s1})+K' \tag{56}$$

and

$$x_2(t_{s1}) = \frac{1}{a_{11}a_{21}}[A_4A\exp(\lambda_1 t_{s1})+A_5B\exp(\lambda_2 t_{s1}) + A_6C\exp(\lambda_3 t_{s1})+r_{11}r_{12}K-a_{12}a_{21}]$$
$$= \frac{1}{a_{11}a_{21}}[A_4A'\exp(\lambda_1 t_{s1}) + A_5B'\exp(\lambda_2 t_{s1})+A_6C'\exp(\lambda_3 t_{s1}) + r_{11}r_{12}K'-a_{12}a_{21}] \tag{57}$$

Solving for A', B' and C' in terms of t_{s1} from equations (55) through (57) gives

$$A' = \frac{A_{18}}{A_{17}} \tag{58}$$

$$B' = \frac{A_{19}}{A_{17}} \tag{59}$$

$$C' = \frac{A_{20}}{A_{17}} \tag{60}$$

where

$$A_{17} = (A_1A_6+A_2A_4+A_3A_5-A_1A_5-A_2A_6$$
$$-A_3A_4)\exp(\lambda_1t_{s1})\exp(\lambda_2t_{s1})\exp(\lambda_3t_{s1})$$

$$A_{18} = (A_6A_{14}+A_2A_{16}+A_3A_5A_{15}-A_5A_{14}$$
$$-A_2A_6A_{15}-A_3A_{16})\exp(\lambda_2t_{s1})\exp(\lambda_3t_{s1})$$

$$A_{19} = (A_1A_6A_{15}+A_4A_{14}+A_3A_{16}-A_1A_{16}$$
$$-A_6A_{14}-A_3A_4A_{15})\exp(\lambda_1t_{s1})\exp(\lambda_3t_{s1})$$

$$A_{20} = (A_1A_6+A_2A_4A_{15}+A_{14}A_5-A_1A_5A_{15}$$
$$-A_2A_{16}-A_4A_{14})\exp(\lambda_1t_{s1})\exp(\lambda_2t_{s1})$$

$$A_{14} = a_{21}x_{11}(t_{s1})-r_{12}K'$$

$$A_{15} = x_{12}(t_{s1})-K'$$

$$A_{16} = a_{11}a_{21}x_2(t_{s1})+a_{12}a_{21}-r_{11}r_{12}K'$$

Similarly, A'', B'' and C'' can be determined by

$$A'' = \frac{A_{25}}{A_{24}} \tag{61}$$

$$B'' = \frac{A_{26}}{A_{24}} \tag{62}$$

$$C'' = \frac{A_{27}}{A_{24}} \tag{63}$$

where

$$A_{24} = (A_1A_6+A_2A_4+A_3A_5-A_1A_5-A_2A_6$$
$$-A_3A_4)\exp(\lambda_1t_{s2})\exp(\lambda_2t_{s2})\exp(\lambda_3t_{s2})$$

$$A_{25} = (A_6A_{21}+A_2A_{23}+A_3A_5A_{22}-A_5A_{21}$$
$$-A_2A_6A_{22}-A_3A_{23})\exp(\lambda_2t_{s2})\exp(\lambda_3t_{s2})$$

$$A_{26} = (A_1A_6A_{22}+A_4A_{21}+A_3A_{23}-A_1A_{23}$$
$$-A_6A_{21}-A_3A_4A_{22})\exp(\lambda_1t_{s2})\exp(\lambda_3t_{s2})$$

$$A_{27} = (A_1A_{23}+A_2A_4A_{22}+A_5A_{21}-A_1A_5A_{22}$$
$$-A_2A_{23}-A_4A_{21})\exp(\lambda_1t_{s2})\exp(\lambda_2t_{s2})$$

$$A_{21} = a_{21}x_{11}(t_{s2})-r_{12}K$$

$$A_{22} = x_{12}(t_{s2})-K$$

$$A_{23} = a_{11}a_{21}x_2(t_{s2})+a_{12}a_{21}-r_{11}r_{12}K$$

We can find t_{s1}, t_{s2} and T from equations (52) through (54) and the final conditions

$$x_{11}(T) = x_{12}(T) = 0,\ x_2(T) = 1,\ \text{at } t = T$$

Thus

$$A_1A''\exp(\lambda_1T)+A_2B''\exp(\lambda_2T)+A_3C''\exp(\lambda_3T)$$
$$+r_{12}K = 0 \tag{64}$$

$$A''\exp(\lambda_1T)+B''\exp(\lambda_2T)+C''\exp(\lambda_3T)+K = 0 \tag{65}$$

$$A_4A''\exp(\lambda_1T)+A_5B''\exp(\lambda_2T)+A_6C''\exp(\lambda_3T)$$
$$+r_{11}r_{12}K-a_{12}a_{21}-a_{11}a_{21} = 0 \tag{66}$$

In principle, we can solve for T, t_{s1} and t_{s2} from the above equations by a trial and error procedure. However, t_{s1} and t_{s2} appear implicitly in these equations, which increase the difficulty of solving the problem. To circumvent this difficulty, we shall continue to solve this problem by considering the square form of the final conditions of the state variables as equality constraints and by employing the additional necessary conditions developed in this article.

The equality constraints on the final state variables are

$$g_1[x(T)] = \tfrac{1}{2}[x_{11}(T)-0]^2 = \tfrac{1}{2}[x_{11}(T)]^2 = 0 \tag{67}$$

$$g_2[x(T)] = \tfrac{1}{2}[x_{12}(T)-0]^2 = \tfrac{1}{2}[x_{12}(T)]^2 = 0 \tag{68}$$

$$g_3[x(T)] = \tfrac{1}{2}[x_2(T)-1]^2 = 0 \tag{69}$$

Therefore, equations (19) and (20) for this problem are

$$z_{11}(T) = v_{11}x_{11}(T)+c_1 \tag{70}$$

$$z_{12}(T) = v_{12}x_{12}(T)+c_2 \tag{71}$$

$$z_2(T) = v_2[x_2(T)-1]+c_3 \tag{72}$$

$$z_3(T) = c_4 \tag{73}$$

$$\mathscr{H}[x(T),\theta(T),z(T)]+\left\{v_{11}x_{11}(T)\frac{dx_{11}(T)}{dT}\right.$$
$$\left.+v_{12}x_{12}(T)\frac{dx_{12}(T)}{dT}+v_2[x_2(T)-1]\frac{dx_2(T)}{dT}\right\}$$
$$+\left[c_1\frac{dx_{11}(T)}{dT}+c_2\frac{dx_{12}(T)}{dT}+c_3\frac{dx_2(T)}{dT}\right.$$
$$\left.+c_4\frac{dx_3(T)}{dT}\right]-\left[z_{11}(T)\frac{dx_{11}(T)}{dT}\right.$$
$$+z_{12}(T)\frac{dx_{12}(T)}{dT}+z_2(T)\frac{dx_2(T)}{dT}$$
$$\left.+z_3(T)\frac{dx_3(T)}{dT}\right] = 0$$

By substituting equations (70) through (73) into the above equation, it can be shown that

$$\mathscr{H}[x(T),\theta(T),z(T)] = 0 \tag{74}$$

Since the objective function, equation (30), has been transformed into the following form

$$S = c_1x_{11}(T)+c_2x_{12}(T)+c_3x_2(T)+c_4x_3(T), \tag{75}$$

$$c_1 = c_2 = c_3 = 0,\ c_4 = 1,$$

equations (70) through (73) become

$$z_{11}(T) = v_{11}x_{11}(T) \tag{76}$$

$$z_{12}(T) = r_{12}x_{12}(T) \tag{77}$$

$$z_2(T) = r_2[x_2(T)-1] \tag{78}$$

$$z_3(T) = 1 \tag{79}$$

and from equations (32) and (74), we have

$$\begin{aligned}\mathscr{H}[x(T), \theta(T), z(T)] &= 0\\ &= z_{11}(T)[-r_{11}x_{11}(T)+a_{11}x_2(T)+a_{12}]\\ &\quad +z_{12}(T)[-r_{12}x_{12}(T)+a_{21}x_{11}(T)]\\ &\quad +z_2(T)[-rx_2(T)+a_{42}x_{12}(T)-a_5\theta(T)\\ &\quad -a_6]+1\end{aligned} \tag{80}$$

Determination of the terminal control time, T, from the above equation in conjunction with the performance equations, equation for the adjoint variables, and constraints is very difficult, if not impossible. However, T may be obtained by using the gradient procedure with the penalty function approach. This penalty function can be written as

$$\begin{aligned}S'' &= [c_1x_{11}(T)+c_2x_{12}(T)+c_3x_2(T)+c_4x_3(T)]\\ &\quad +\tfrac{1}{2}\{r_{11}[x_{11}(T)]^2+r_{12}[x_{12}(T)]^2\\ &\quad +r_2[x_2(T)-1]^2\}\end{aligned} \tag{81}$$

and the terminal control time, T, can be determined by the condition

$$\begin{aligned}\frac{dS''}{dT} &= 1+r_{11}x_{11}(T)\frac{dx_{11}(T)}{dT}+r_{12}x_{12}(T)\frac{dx_{12}(T)}{dT}\\ &\quad +r_2[x_2(T)-1]\frac{dx_2(T)}{dT} = 0\end{aligned} \tag{82}$$

Note that $c_1 = c_2 = c_3 = 0, c_4 = 1$, and

$$\frac{dx_3(T)}{dT} = 1$$

In other words, the terminal control time is chosen so that the penalty function, equation (81), is at a minimum with respect to this terminal time. It is possible, however, that the terminal time determined by equation (82) may not be the time which minimizes the penalty function. If there is any question concerning this assumption, we may examine the sign of the second derivative of S'' with respect to T when the first derivative of S'' with respect to T is zero, or we may carry out an exhaustive search or random search around this point to assure that it is indeed a minimum point.

Since the control policy is of the bang-bang type shown in equation (39) and the performance equations are linear, the number of switching points is one less than the dimensions of the system as mentioned previously[1,8]. Even though the time constant of the heat exchanger is not neglected in this example, its value is very small. Thus, the initial trial control pattern is assumed to be the optimal control solution given in Example 3 of the preceding part[1], that is

$$\begin{aligned}\theta &= 1 \qquad 0 \leq t \leq 0{\cdot}468\\ \theta &= -1 \quad 0{\cdot}468 < t \leq 1{\cdot}100\\ \theta &= 1 \qquad 1{\cdot}100 < t\end{aligned}$$

where the switching times, t_{s1} and t_{s2}, are 0·468 and 1·100 respectively.

With this initial trial control pattern the state variables x_{11}, x_{12} and x_2 can be obtained from equations (46), (47) and (48) for $0 \leq t \leq t_{s1}$, from equations (49), (50) and (51) for $t_{s1} \leq t \leq t_{s2}$, and from equations (52), (53) and (54) for $t_{s2} \leq t \leq T$, where the terminal control time, T, is unknown. This unknown terminal control time is then determined from equation (82).

The switching times, t_{s1} and t_{s2}, and the terminal control time, T, can be determined by simultaneously minimizing the penalty function, S'', given by equation (81) and satisfying the condition given by equation (82). This can be accomplished by employing a variety of techniques, for example as the sequential simplex pattern search[9] or the Hooke and Jeeves pattern search[10].

By use of the final time and value of $x(t)$, we can solve the adjoint equations, equations (33) through (35), backwards from T to 0 with the final conditions given by equations (76) through (78).

Let

$$t_b = T - t \tag{83}$$

Then

$$dt_b = -dt$$

Equations (33) through (35) become

$$\frac{dz_{11}}{dt_b} = a_{21}z_{12}-r_{11}z_{11} \tag{84}$$

$$\frac{dz_{12}}{dt_b} = a_{42}z_2-r_{12}z_{12} \tag{85}$$

$$\frac{dz_2}{dt_b} = a_{11}z_{11}-rz_2 \tag{86}$$

Eliminating z_{11} and z_{12} from these equations, we have

$$\begin{aligned}&\frac{d^3z_2}{dt_b^3}+(r+r_{11}+r_{12})\frac{d^2z_2}{dt_b^2}+(rr_{11}+r_{11}r_{12}\\ &\quad +rr_{12})\frac{dz_2}{dt_b}+(rr_{11}r_{12}-a_{11}a_{21}a_{42})z_2 = 0\end{aligned}$$

Solution of z_2 has the form

$$z_2 = D\exp(\lambda_1t_b)+E\exp(\lambda_2t_b)+F\exp(\lambda_3t_b) \tag{87}$$

where D, E and F are unknown constants. Inserting equation (87) to equations (84) through (86) and solving for z_{11} and z_{12}, we have

$$z_{11} = \frac{1}{a_{11}} [D(\lambda_1 + r)\exp(\lambda_1 t_b) + E(\lambda_2 + r)\exp(\lambda_2 t_b) + F(\lambda_3 + r)\exp(\lambda_3 t_b)] \tag{88}$$

and

$$z_{12} = \frac{1}{a_{11}a_{21}} \{D[\lambda_1^2 + (r + r_{12})\lambda_1 + rr_{11}]\exp(\lambda_1 t_b) + E[\lambda_2^2 + (r + r_{11})\lambda_2 + r_1 r_2 \exp(\lambda_2 t_b) + F[\lambda_3^2 + (r + r_{11})\lambda_3 + rr_{11}]\lambda \exp(\lambda_3 t_b)\} \tag{89}$$

Let

$$B_1 = \lambda_1 + r$$

$$B_2 = \lambda_2 + r$$

$$B_3 = \lambda_3 + r$$

$$B_4 = \lambda_1^2 + (r + r_{11})\lambda_1 + rr_{11}$$

$$B_5 = \lambda_2^2 + (r + r_{11})\lambda_2 + rr_{11}$$

$$B_6 = \lambda_3^2 + (r + r_{11})\lambda_3 + rr_1$$

Equations (87) through (89) become

$$z_{11}(t_b) = \frac{1}{a_{11}} [DB_1 \exp(\lambda_1 t_b) + EB_2 \exp(\lambda_2 t_b) + FB_3 \exp(\lambda_3 t_b)] \tag{90}$$

$$z_{12}(t_b) = \frac{1}{a_{11}a_{21}} [DB_4 \exp(\lambda_1 t_b) + EB_5 \exp(\lambda_2 t_b) + FB_6 \exp(\lambda_3 t_b)] \tag{91}$$

$$z_2(t_b) = D\exp(\lambda_1 t_b) + E\exp(\lambda_2 t_b) + F\exp(\lambda_3 t_b) \tag{92}$$

At $t = T$, $t_b = 0$, equations (76) through (78) become

$$z_{11}(0) = r_{11}x_{11}(0) \tag{93}$$

$$z_{12}(0) = r_{12}x_{12}(0) \tag{94}$$

$$z_2(0) = r_2[x_2(0) - 1] \tag{95}$$

Also at $t_b = 0$ equations (90) through (92) become

$$DB_1 + EB_2 + FB_3 = a_{11}z_{11}(0) \tag{96}$$

$$DB_4 + EB_5 + FB_6 = a_{11}a_{21}z_{12}(0) \tag{97}$$

$$D + E + F = z_2(0) \tag{98}$$

Solving for D, E and F from these equations, we have

$$D = \frac{B_{11}}{B_{10}}$$

$$E = \frac{B_{12}}{B_{10}}$$

$$F = \frac{B_{13}}{B_{10}}$$

where

$$B_{10} = B_1B_5 + B_2B_6 + B_3B_4 - B_1B_6 - B_2B_4 - B_3B_5$$

$$B_{11} = B_5B_7 + B_2B_6B_9 + B_3B_8 - B_6B_7 - B_2B_8 - B_3B_5B_9$$

$$B_{12} = B_1B_8 + B_6B_7 + B_3B_4B_9 - B_1B_9B_6 - B_4B_7 - B_3B_8$$

$$B_{13} = B_1B_5B_9 + B_2B_8 + B_4B_7 - B_1B_8 - B_2B_4B_9 - B_5B_7$$

$$B_7 = a_{11}r_{11}x_{12}(0)$$

$$B_8 = a_{11}a_{21}r_{12}x_{12}(0)$$

$$B_9 = r_2[x_2(0) - 1]$$

The condition $H = 0$ as given by equation (80) is verified by substituting the values of state variables obtained at the terminal control time, $x_{11}(T)$, $x_{12}(T)$, and $x_2(T)$, and the adjoint variables at the terminal control time, $z_{11}(T)$, $z_{12}(T)$, and $z_2(T)$, into the equation.

The optimal control pattern determined is shown in figure 1a. The optimal result is such that the first switching time t_{s1} is 0.487, the second switching time t_{s2} is 1.085, and terminal control time T is 1.096. The value of terminal control time is 0.018 longer than that of the case in which the response of the heat exchanger is negligibly small (Example 3 of Part 2[1]). In actual practice, the difference can be neglected. In general, the response of the heat exchanger is almost instantaneous, especially when the time constant of the heat exchanger is much smaller than that of the system proper.

The optimal response of x_{11} is also given in figure 1a and the corresponding responses of x_{12} and x_2 are given in figure 1b. Values of the system parameters employed in obtaining the numerical results correspond to those of Case 1 given in Part 2 of this series.

CONCLUSION

The reader should realize that the fixed right-end problem can also be solved by considering the problem as one with equality constraints on the final state variables and then employing the necessary conditions derived in this article.

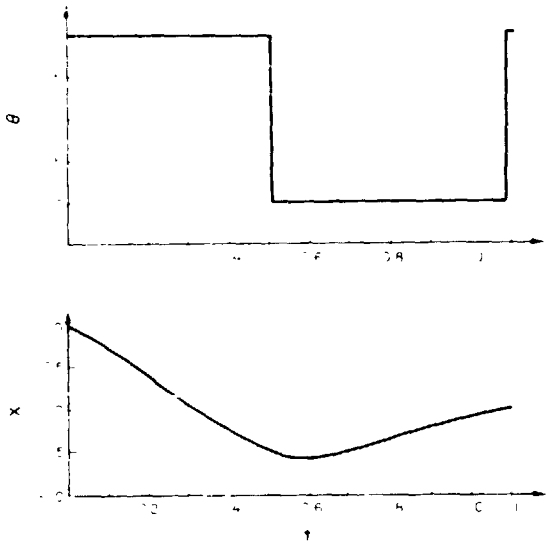

Fig. 1a. Optimal control policy and optimal response of x_{11} for Case 1 of the two CST's-in-series model with $\tau_2 \neq 0$, $r_{11} = 2$ and $r = 10$.

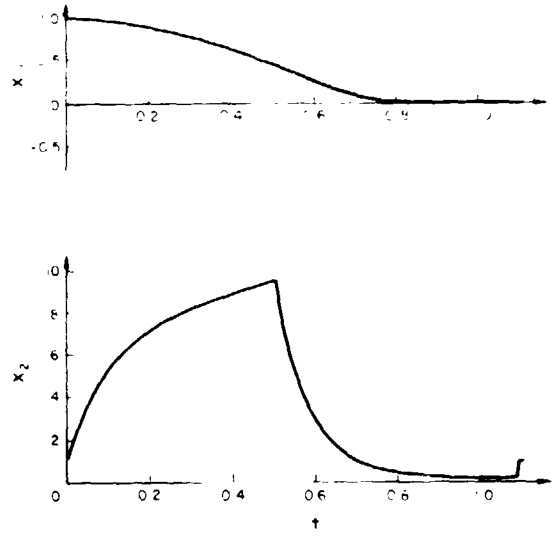

Fig. 1b. Optimal responses of x_{12} and x_2 for Case 1 of the two CST's-in-series model with $\tau_2 = 0$ and $r_{11} = 2$ and $r = 10$.

REFERENCES

1. L. T. Fan, Y. S. Hwang and C. L. Hwang, Applications of Modern Optimal Control Theory to Environmental Control of Confined Spaces and Life Support Systems, Part 2. *Basic Computational Algorithm of Pontryagin's Maximum Principle and its Application. Build. Sci.*, **5**, 81 (1970).
2. R. E. Kopp, *Pontryagin's Maximum Principle, in Optimization Techniques*, (edited by A. Leitmann), Academic Press. New York (1962).
3. L. T. Fan, *The Continuous Maximum Principle: A Study of Complex System Optimization*, Wiley. New York, (1966).
4. M. M. Denn, and R. Aris, An Elementary Derivation of the Maximum Principle, *A.I.Ch.E.J.*, **11**, 367 (1965).
5. A. P. Sage, *Optimal Systems Control*, Prentice Hall, New Jersey, (1968).
6. L. T. Fan, Y. S. Hwang and C. L. Hwang, Applications of Modern Optimal Control Theory to Environmental Control of Confined Spaces and Life Support Systems, Part 1 Modeling and Simulation. *Build. Sci.*, **5**, 57 (1970).
7. L. S. Pontryagin, V. G. Boltyanskii, R. V. Gamkrelidze, and E. F. Mishchenko, *The Mathematical Theory of Optimal Processes*, (English translation by K. N. Trirogoff), Interscience, New York, (1962).
8. R. Bellman, I. Glicksberg and O. Gross, On the Bang-bang Control Problem, *Quarterly Appl. Math.*, **14**, 11 (1956).
9. L. T. Fan, C. L. Hwang, and F. A. Tillman, A Sequential Simplex Pattern Search Solution to Production Planning Problems, *Trans. AIIE*, **1**, 267 (1969).
10. R. Hooke, and T. A. Jeeves, Direct Search Solution of Numerical and Statistical Problems, *J. Assoc. Comp. Mach.*, **8**, 212 (1961).

APPENDIX

Derivation of equation (14) *from equation* (12)

The objective function, S', is of the form given by equation (12), i.e.

$$S' = \sum_{i=1}^{s+1} c_i x_i(T) + \sum_{i=1}^{q} v_i g_i[x(T)] + \int_{t_0}^{T} \left\{ \mathscr{H}[x(t), \theta(t), z(t)] - \sum_{i=1}^{s+1} z_i(t) \frac{dx_i}{dt} \right\} dt \qquad (A.1)$$

Carrying out the Taylor series expansion of the above equation about $\bar{x}$, $\bar{\theta}$, $\bar{z}$ and $\bar{T}$, defining

$$x_i(t) = \bar{x}_i(t) + \delta x_i(t), \quad i = 1, 2, \ldots, s+1$$

$$\theta_i(t) = \bar{\theta}_i(t) + \delta\theta_i(t), \quad i = 1, 2, \ldots, r$$

$$T = \bar{T} + \delta T,$$

$$z_i(t) = \bar{z}_i(t) + \delta z_i(t), \quad i = 1, 2, \ldots, s+1,$$

discarding the terms higher than the first order, and dropping the bar notations, we have

$$\delta S' = \sum_{i=1}^{s+1} c_i \left[\delta x_i(T) + \frac{\partial x_i(T)}{\partial T} \delta T \right] + \sum_{j=1}^{q} v_j \left\{ \frac{\partial g_j[x(T)]}{\partial x_i(T)} \delta x_i(T) + \frac{\partial g_j[x(T)]}{\partial T} \delta T \right\}$$

$$+\int_{t_0}^{T}\Bigg\{\sum_{i=1}^{s+1}\frac{\partial\mathscr{H}}{\partial x_i}\,\delta x_i+\sum_{i=1}^{r}\frac{\partial\mathscr{H}}{\partial\theta_i}\,\delta\theta_i$$

$$+\sum_{i=1}^{s+1}\frac{\partial\mathscr{H}}{\partial z_i}\,\delta z_i+\frac{\partial\mathscr{H}}{\partial t}\,\delta t-\sum_{i=1}^{s+1}\Bigg[\delta z_i\,\frac{\mathrm{d}x_i}{\mathrm{d}t}$$

$$+z_i\delta\left(\frac{\mathrm{d}x_i}{\mathrm{d}t}\right)+\left(\frac{\mathrm{d}z_i}{\mathrm{d}t}\frac{\mathrm{d}x_i}{\mathrm{d}t}+z_i\frac{\mathrm{d}^2x_i}{\mathrm{d}t^2}\right)\delta t\Bigg]\mathrm{d}t \qquad \text{(A 2)}$$

Since

$$\int_{t_0}^{T}\frac{\partial\mathscr{H}}{\partial t}\,\delta t\mathrm{d}t=\int_{t_0}^{T}\frac{\partial\mathscr{H}}{\partial t}\,\mathrm{d}t\delta t=\mathscr{H}\Big|_T\delta T$$

$$\int_{t_0}^{T}\left(\frac{\mathrm{d}z_i}{\mathrm{d}t}\frac{\mathrm{d}x_i}{\mathrm{d}t}+z_i\frac{\mathrm{d}^2x_i}{\mathrm{d}t^2}\right)\delta t\mathrm{d}t=\int_{t_0}^{T}\frac{\mathrm{d}}{\mathrm{d}t}\left(z_i\frac{\mathrm{d}x_i}{\mathrm{d}t}\right)\delta t\mathrm{d}t$$

$$=\int_{t_0}^{T}\frac{\mathrm{d}}{\mathrm{d}t}\left(z_i\frac{\mathrm{d}x_i}{\mathrm{d}t}\right)\mathrm{d}t\delta t$$

$$=\left(z_i\frac{\mathrm{d}x_i}{\mathrm{d}t}\right)\Bigg|_T\delta T$$

and

$$\sum_{i=1}^{s+1}\int_{t_0}^{T}z_i\delta\left(\frac{\mathrm{d}x_i}{\mathrm{d}t}\right)\mathrm{d}t$$

$$=\sum_{i=1}^{s+1}\int_{t_0}^{T}z_i\frac{\mathrm{d}}{\mathrm{d}t}(\delta x_i)\mathrm{d}t$$

$$=\sum_{i=1}^{s+1}\left[(z_i\delta x_i)\Big|_T-\int_{t_0}^{T}\delta x_i\frac{\mathrm{d}z_i}{\mathrm{d}t}\,\delta t\right],$$

equation (A.2) becomes, after rearrangement,

$$\delta S'=\delta T\Bigg\{\mathscr{H}[x(T),\theta(T),z(T)]+\sum_{i=1}^{q}v_i\frac{\partial g_i}{\partial T}$$

$$+\sum_{i=1}^{s+1}c_i\frac{\partial x_i}{\partial T}-\sum_{i=1}^{s+1}z_i(T)\frac{\mathrm{d}x_i(T)}{\mathrm{d}T}\Bigg\}$$

$$+\sum_{i=1}^{s+1}\delta x_i\left\{\sum_{j=1}^{q}v_j\frac{\partial g_i}{\partial x_i}-z_i(T)+c_i\right\}$$

$$+\int_{t_0}^{T}\Bigg\{\sum_{i=1}^{s+1}\delta x_i\left[\frac{\partial\mathscr{H}}{\partial x_i}+\frac{\mathrm{d}z_i}{\mathrm{d}t}\right]+\sum_{i=1}^{r}\delta\theta_i\frac{\partial\mathscr{H}}{\partial\theta_i}$$

$$+\sum_{i=1}^{s+1}\delta z_i\left[\frac{\partial\mathscr{H}}{\partial z_i}-\frac{\mathrm{d}x_i}{\mathrm{d}t}\right]\Bigg\}\mathrm{d}t \qquad \text{(A.3)}$$

This is equation (14).

NOMENCLATURE

a_5 $= rK_2K_4$

a_6 $= rK_3K_4$

a_{11} $= r_1K_{11}r_{11}/K_4$

a_{12} $= r_1r_2K_{11}$

a_{21} $= r_{12}K_{12}/K_{11}$

a_{42} $= rK_4/K_{12}$

A = Integration constant

A_i = Constants in equations (45) through (66)

B = Integration constant

B_i = Constants in equations (90) through (92)

c_i = Constants defined in equation (9), $i = 1, 2, \ldots, s+1$

C = Integration constant

D = Integration constant in equation (87)

E = Integration constant in equation (87)

F = Integration constant in equation (87)

$g_i[x(T)]$ = a q-dimensional constraints defined in equation (4)

$\mathscr{H}[x(t), \theta(t), z(t)]$ = Hamiltonian function defined in equation (11)

$\mathscr{H}^*$ = The portion of $\mathscr{H}$ which depends on θ

K = A constant defined in equation (43)

K' = A constant defined in equation (51a)

K_1 $= \dfrac{T_2}{T_{c0}}$

K_2 $= \dfrac{1}{2T_2}(T_{r\,\max}-T_{r\,\min})$

K_3 $= \dfrac{1}{2T_2}(T_{r\,\max}+T_{r\,\min})$

K_4 $= \dfrac{T_2}{T_{i0}}$

K_{11} $= \dfrac{T_2}{T_{1c0}}$

K_{12} $= \dfrac{T_2}{T_{2c0}}$

Q = Q_1+Q_2, flow rate of air in the system proper in m^3/s

Q_1 = Air flow rate by circulation air in m^3/s

Q_2 = Flow rate of fresh air in m^3/s

Q_w = Flow rate of coolant in m^3/s

r $= \dfrac{\tau_1}{\tau_2}$, the ratio of time constant of system proper to that of heat exchanger

r_1 $= \dfrac{Q_1}{Q_1+Q_2}$, the fraction of circulation air

r_2 = $\frac{Q_2}{Q} = \frac{}{Q_2}$, the fraction of fresh air

r_{11} = $\frac{\tau_1}{\tau_{11}}$

r_{12} = $\frac{\tau_2}{\tau_{12}}$

S = Performance index defined in equation (9)

S' = A modified performance index defined in equation (10)

S'' = A modified performance index defined in equation (81)

t = $\frac{\alpha}{\tau_1}$, dimensionless time

t_a = Reference temperature in °C

t_b = $T-t$, dimensionless time used in equations (84) through (86)

t_c = Room temperature in °C

t_d = Disturbance temperature in °C

t_i = Temperature of incoming circulation air in °C

t_0 = Initial time

t_{si} = Switching times, $i = 1, 2$

t_{wc} = Inlet temperature of coolant in °C

t_{wh} = Outlet temperature of coolant in °C

t_2 = Outside air temperature in °C

T = Final time, dimensionless

T_c = $(t_c - t_a)$, room temperature in °C

T_{c0} = Room temperature at $\alpha = 0^+$ in °C

T_{c1} = Temperature of pool 1 in °C

T_{c10} = Temperature of pool 1 at $\alpha = 0^+$ in °C

T_{c2} = Temperature of pool 2 in °C

T_{c20} = Temperature of pool 2 at $\alpha = 0^+$

T_d = $(t_d - t_a)$, disturbance temperature in °C

T_i = $(t_i - t_a)$, temperature of the circulation air into the system, in °C

T_{i0} = Temperature of the circulation air into the system at $\alpha = 0^+$ in °C

T_r = $\frac{Q_w \rho_w c_{pw}(T_{wh} - T_{wc})}{Q_1 \rho c_p}$, hypothetical temperature

T_{rf} = Final steady state value of T_r

$T_{r\,max}$ = Upper bound of T_r in °C

$T_{r\,min}$ = Lower bound of T_r in °C

T_{r0} = Value of T_r at $\alpha = 0$ in °C

T_{wc} = $t_{wc} - t_a$ in °C

T_{wh} = $t_{wh} - t_a$ in °C

T_{11} = Temperature of pool 1 in °C

T_{12} = Temperature of pool 2 in °C

v_i = A Lagrange multiplier in equation (10)

V_1 = Volume of room in m^3

V_{11} = Volume of pool 1 of two completely stirred tanks in series model in m^3

V_2 = Volume of heat exchanger in m^3

V_{12} = Volume of pool 2 of two completely stirred tanks in series model in m^3

$x(t)$ = s-dimensional state vector defined in equation (1)

$x_i(t_0)$ = x_{i0}, $i = 1, 2, \ldots, s$, initial value of x at $t = t_0$

$x_1(t)$ = $\frac{T_c}{T_{c0}}$, dimensionless room temperature

$x_2(t)$ = $\frac{T_i}{T_{i0}}$, dimensionless temperature of the circulation air in equation (27)

x_{11} = $\frac{T_{c1}}{T_{c10}}$, dimensionless temperature of pool 1

x_{12} = $\frac{T_{c2}}{T_{c20}}$, dimensionless temperature of pool 2

$z_i(t)$ = adjoint variable defined in equations (10) and (17)

Greek letters

α = Time in s

α_f = Final time in s

$\delta(\alpha)$ = Impulse heat disturbance function, sec^{-1}

ρ = Air density in kg/m^3

ρ_w = Density of coolant in kg/m^3

σ = $\frac{T_d}{T_2}$, dimensionless disturbance temperature

τ_1 $= \dfrac{V_1}{Q_1+Q_2}$, time constant of the system proper in s

τ_{11} $= \dfrac{V_{11}}{Q_1+Q_2}$, time constant of pool 1 in s

τ_2 $= \dfrac{V_2}{Q_1}$, time constant of heat exchanger in s

τ_{12} $= \dfrac{V_{12}}{Q_1+Q_2}$, time constant of pool 2 in s

θ $= \dfrac{T_r - \frac{1}{2}(T_{r\,\max}+T_{r\,\min})}{T_{r\,\max} - \frac{1}{2}(T_{r\,\max}+T_{r\,\min})}$, control variable

$= \begin{cases} +1 & \text{at } T_r = T_{r\,\max} \\ -1 & \text{at } T_r = T_{r\,\min} \end{cases}$

$\bar{\theta}(t)$ = Optimum value of $\theta(t)$

λ_i = Roots of equation (42)

La forme fondamentale du principe du maximum de Pontryagin est élargie pour couvrir les problèmes optimaux avec contraintes d'égalité imposées sur les variables de l'état final. Les conditions nécessaires pour une police de contrôle optimum sont développées et appliquées à deux exemples concrets.

Le comportement dynamique du système de support de vie qui consiste en une cabine à air conditionné (le système lui-même) soumis à une perturbation de chaleur par impulsion et un échangeur de chaleur (l'élément de contrôle) est encore étudié. Le premier exemple considère la police de contrôle optimal pour un système ayant un échangeur de chaleur avec une constante de temps nègligeablement petite. La forme carrée de la condition finale de la variable d'état est considérée comme une contrainte d'égalité. Le second exemple considère la police optimale d'un système où le courant d'air dans la cabine est caractérisé par le modèle des deux vaisseaux en série (2 CST en série) complètement agités. La constante de temps de l'échangeur de chaleur n'est pas négligé, c'est-à-dire que la réponse de l'échangeur de chaleur n'est pas instantanée. Les carrés des conditions finales des variables sont encore considérés comme contraintes d'égalité.

Die grundlegende Form von Pontryagin's Maximum Prinzip wird erweitert, um Optimalprobleme mit Gleichheitsbeschränkungen zu umfassen, welche den Veränderlichen des Endzustandes auferlegt waren. Die notwendigen Bedingungen für Optimum Kontrollverfahren werden entwickelt und bei zwei konkreten Beispielen angewandt.

Das dynamische Verhalten des Lebensunterhaltungssystems wird untersucht, welches aus einer klimatisierten Kabine (dem eigentlichen System) in Abhängigkeit von einer Wärmeimpulsstörung und einem Wärmeaustauscher (dem Kontrollelement) besteht. Das erste Beispiel untersucht das Optimalkontrollverfahren für ein System, welches einen Wärmeaustauscher mit unbedeutend kleiner Zeitkonstante hat. Die Quadratform der Endbedingung der Zustandsveränderlichen wird als eine Gleichheitsbeschränkung angesehen. Das zweite Beispiel untersucht das Optimalverfahren eines Systems, in dem der Luftstrom in der Kabine durch zwei völlig durchgerührte Reihentanks (2 CST's-in-series) im Modell dargestellt wird. Die Zeitkonstante des Wärmeaustauschers wird nicht vernachlässigt, d.h. die Reaktion des Wärmeaustauschers ist nicht unverzüglich. Die Quadrate der Endbedingungen der Zustandsveränderlichen werden wieder als Gleichheitsbeschränkungen dargestellt.

(d) 4

Build. Sci. Vol. 5, pp. 137 147. Pergamon Press 1970. Printed in Great Britain

SfB	Ab8
UDC	697

Applications of Modern Optimal Control Theory to Environmental Control of Confined Spaces and Life Support Systems*

Part 4—Control of Systems with Inequality Constraints Imposed on State Variables

L. T. FAN†
Y. S. HWANG†
C. L. HWANG†

The necessary conditions for optimum of a dynamic system whose state variables are constrained by certain inequality conditions are derived by applying a variational technique. The conditions are employed to determine the optimal policy for the room or cabin temperature control of a life support system. The system consisting of an air-conditioned cabin subject to an inpulse heat disturbance and a heat exchanger acting as a control element is again studied. The flow of air in the cabin is characterized by the two completely stirred tanks-in-series (2 CST's-in-series) model. A constraint is imposed on the room temperature which has to be higher than a certain value for some physical or biological reasons.

INTRODUCTION

THE BASIC form of Pontryagin's maximum principle has been introduced in Part 2 of this series[1] and the optimal control of the systems in which inequality constraints are imposed on the state variables at the end of control action has been considered in Part 3[2]. In this part, we shall consider the necessary conditions for optimum for a dynamic system whose state variables are constrained by a certain inequality condition or conditions. Chang[3], Berkovitz[4] and Gamkrelidze [5] dealt with the fundamental aspects of the problem, and both the theoretical and computational aspects were treated in papers by Dreyfus[6], Denham[7] and Denham and Bryson[8]. Despite these and other efforts[9–12], the optimal control of a system with state variable constraints does not appear to be well understood. Here we shall first state the problem and the necessary conditions for optimum, and finally apply the conditions to the temperature control confined spaces and life support systems[13].

* This work was supported by the Air Force Office of Scientific Research, Office of Aerospace Research, United States Air Force, Under Contract F 44620-68-0020 (Themis Project), and NASA Grant Under Contract NGR-17-001-034.

† Institute for Systems Design and Optimization, Kansas State University, Manhattan, Kansas.

A DYNAMIC SYSTEM WITH STATE VARIABLE CONSTRAINT

Again let us consider a continuous process, the dynamic behavior of which can be represented by the following set of differential equations.

$$\frac{dx_i}{dt} = f_i[x_1(t), x_2(t), \ldots, x_s(t); \theta_1(t), \theta_2(t), \ldots, \theta_r(t)],\ i = 1, 2, \ldots, s \qquad (1)$$

or in vector form

$$\frac{dx}{dt} = f[x(t), \theta(t)] \qquad (1a)$$

where $x(t)$ is an s-dimensional state vector and $\theta(t)$ is an r-dimensional control vector. Now, we wish to find a piecewise continuous control vector $\theta(t)$ in the set Θ such that the function of the final state

$$S = \sum_{i=1}^{s} c_i x_i(T),\quad c_i = \text{constant} \qquad (2)$$

takes on its minimum (or maximum) value, subject to the condition that $x(t)$ stays within a specified region of the state space given by the inequalities

$$g_i[x(t), \theta(t)] \leq 0,\quad i = 1, 2, \ldots, q \qquad (3)$$

The duration of control, T, is specified. Functions f_i, S and g_i are assumed to possess continuous derivatives to at least the second order[3, 12]. In addition to these, the state vector must satisfy certain initial or final conditions or both.

NECESSARY CONDITION FOR OPTIMUM

The basic form of Pontryagin's maximum principle for systems without state variable constraint is given in Part 2 of this series[1]. It states that the Hamiltonian $\mathscr{H}$ and the adjoint variables are defined by

$$\mathscr{H} = \sum_{i=1}^{s} z_i(t) f_i[x(t), \theta(t)] \tag{4}$$

$$\frac{dz_i}{dt} = -\frac{\partial \mathscr{H}}{\partial x_i} = -\sum_{i=1}^{s} z_i(t)\frac{\partial f_i}{\partial x_i}, \quad i = 1, 2, \ldots, s \tag{5}$$

$$z_i(T) = c_i, \quad i = 1, 2, \ldots, s \tag{6}$$

and the necessary condition for the objective function S to be an extremum with respect to θ is

$$\frac{\partial \mathscr{H}}{\partial \theta_i} = 0, \quad i = 1, 2, \ldots, r \tag{7}$$

or

$\mathscr{H}$ = extremum on the boundary of the constraint (on decision variables) and the extremum value of the Hamiltonian is constant at every point of time under the optimal condition.

For systems with equality constraints $g_j[x(T)] = 0$, $j = 1, 2, \ldots, q$, imposed on the final state variables, the necessary condition for the objective function to be extremum remains the same except that equation (6) becomes

$$z_i(T) = \sum_{j=1}^{q} v_j \frac{\partial g_j}{\partial x_i(T)} + c_i, \quad i = 1, 2, \ldots, s \tag{8}$$

It also gives rise to the following additional condition at the control terminal time.

$$\mathscr{H}[x(T), \theta(T), z(T)] + \sum_{j=1}^{q} \frac{\partial g_j}{\partial T} v_j + \sum_{i=1}^{s} c_i \frac{\partial x_i}{\partial T} - \sum_{i=1}^{s} z_i(T)\frac{dx_i(T)}{dT} = 0 \tag{9}$$

Equations (8) and (9) were derived in the preceding part of this series[2].

For the system with one primary state variable and with one inequality constraint imposed on the state variable, the condition that the Hamiltonian is constant under the optimal condition remains the same. However, it has been explicitly indicated[14] that by employing the chain rule, the condition given by equation (5) must be rewritten as

$$\frac{dz_1}{dt} = -\frac{\partial \mathscr{H}}{\partial x_1} = -z_1\frac{df_1}{dt} - z_1\frac{df_1}{d\theta}\frac{d\theta}{dt} \tag{10}$$

because, the state variable and the control variable are related through the constraint on the constraint boundary. Here we wish to prove that the Hamiltonian is also constant along the constraint boundaries under the optimal condition for a system with two primary state variables represented by

$$\frac{dx_1}{dt} = f_1[x_1, x_2, \theta_1, \theta_2] \tag{11}$$

$$\frac{dx_2}{dt} = f_2[x_1, x_2, \theta_1, \theta_2], \tag{12}$$

and with the objective function of the form

$$S = \int_0^T F[x_1, x_2, \theta_1, \theta_2]dt \tag{13}$$

subject to the inequality constraints

$$g_1[x_1, x_2, \theta_1, \theta_2] \geq 0 \tag{14}$$

$$g_2[x_1, x_2, \theta_1, \theta_2] \geq 0 \tag{15}$$

$$|\theta| \leq 1 \tag{16}$$

Introducing an additional state variable, x_3, such that

$$x_3(t) = \int_0^t F[x_1, x_2, \theta_1, \theta_2]dt$$

it follows that

$$\frac{dx_3}{dt} = F[x_1, x_2, C_1, \theta_2] \tag{17}$$

$$x_3(0) = 0 \tag{18}$$

and

$$x_3(T) = S \tag{19}$$

or

$$\left.\begin{aligned} S &= \sum_{i=1}^{3} c_i x_i(T) \\ c_1 &= c_2 = 0, \quad c_3 = 1 \end{aligned}\right\} \tag{20}$$

Thus, the problem is transformed into that of minimizing $x_3(T)$.

According to equation (4), the Hamiltonian is

$$\mathscr{H} = z_1 f_1 + z_2 f_2 + z_3 f_3 \tag{21}$$

and the adjoint vector is defined by

$$\begin{aligned}\frac{dz_1}{dt} = -\frac{\partial \mathscr{H}}{\partial x_1} = &-z_1\left[\frac{\partial f_1}{\partial x_1} + \frac{\partial f_1}{\partial x_2}\frac{\partial x_2}{\partial x_1} + \frac{\partial f_1}{\partial \theta_1}\frac{\partial \theta_1}{\partial x_1} + \frac{\partial f_1}{\partial \theta_2}\frac{\partial \theta_2}{\partial x_1}\right] - z_2\left[\frac{\partial f_2}{\partial x_1} + \frac{\partial f_2}{\partial x_2}\frac{\partial x_2}{\partial x_1} + \frac{\partial f_2}{\partial \theta_1}\frac{\partial \theta_1}{\partial x_1} + \frac{\partial f_2}{\partial \theta_2}\frac{\partial \theta_2}{\partial x_1}\right] \\ &- z_3\left[\frac{\partial F}{\partial x_1} + \frac{\partial F}{\partial x_2}\frac{\partial x_2}{\partial x_1} + \frac{\partial F}{\partial \theta_1}\frac{\partial \theta_1}{\partial x_1} + \frac{\partial F}{\partial \theta_2}\frac{\partial \theta_2}{\partial x_1}\right]\end{aligned} \tag{22}$$

$$\frac{dz_2}{dt} = -\frac{\partial \mathscr{H}}{\partial x_2} = -z_1\left[\frac{\partial f_1}{\partial x_2}+\frac{\partial f_1}{\partial x_1}\frac{\partial x_1}{\partial x_2}+\frac{\partial f_1}{\partial \theta_1}\frac{\partial \theta_1}{\partial x_2}+\frac{\partial f_1}{\partial \theta_2}\frac{\partial \theta_2}{\partial x_2}\right]-z_2\left[\frac{\partial f_2}{\partial x_2}+\frac{\partial f_2}{\partial x_1}\frac{\partial x_1}{\partial x_2}+\frac{\partial f_2}{\partial \theta_1}\frac{\partial \theta_1}{\partial x_2}+\frac{\partial f_1}{\partial \theta_2}\frac{\partial \theta_2}{\partial x_2}\right]-z_3\left[\frac{\partial F}{\partial x_2}+\frac{\partial F}{\partial x_1}\frac{\partial x_1}{\partial x_2}+\frac{\partial F}{\partial \theta_1}\frac{\partial \theta_1}{\partial x_2}+\frac{\partial F}{\partial \theta_2}\frac{\partial \theta_2}{\partial x_2}\right] \tag{23}$$

$$\frac{dz_3}{dt} = -\frac{\partial \mathscr{H}}{\partial x_3} = 0, \quad z_3(T) = 1 \tag{24}$$

Note that equations (22) and (23) are different from that defined by equation (5), because the state variables and the control variables are related through the equality constraints, equations (14) or (15). For this reason, differentiation of the Hamiltonian with respect to x_i must be carried out by employing the chain rule of differentiation. Also note that equations (22) and (23) reduce to equation (5) when the state variable $x(t)$ is interior to the set of constraints, equations (15) and (16). The solution of equation (24) is

$$z_3(t) = 1, \quad 0 \leqq t \leqq T \tag{25}$$

Thus, equation (21) can be rewritten as

$$\mathscr{H} = z_1 f_1 + z_2 f_2 + F \tag{26}$$

The derivation of the above equation with respect to t is

$$\frac{d\mathscr{H}}{dt} = \frac{dF}{dt}+f_1\frac{dz_1}{dt}+f_2\frac{dz_2}{dt}+z_1\left[\frac{\partial f_1}{\partial \theta_1}\frac{\partial \theta_1}{\partial t}+\frac{\partial f_1}{\partial \theta_2}\frac{\partial \theta_2}{\partial t}+\frac{\partial f_1}{\partial x_1}f_1+\frac{\partial f_1}{\partial x_2}f_2\right]+z_2\left[\frac{\partial f_2}{\partial \theta_1}\frac{\partial \theta_1}{\partial t}+\frac{\partial f_2}{\partial \theta_2}\frac{\partial \theta_2}{\partial t}+\frac{\partial f_2}{\partial x_1}f_1+\frac{\partial f_2}{\partial x_2}f_2\right] \tag{27}$$

Inserting equations (22) and (23) into equation (27) gives

$$\begin{aligned}\frac{d\mathscr{H}}{dt} = {} & \frac{dF}{dt}+z_1\left[\frac{\partial f_1}{\partial \theta_1}\frac{\partial \theta_1}{\partial t}+\frac{\partial f_1}{\partial \theta_2}\frac{\partial \theta_2}{\partial t}+\frac{\partial f_1}{\partial x_1}f_1+\frac{\partial f_1}{\partial x_2}f_2\right]+z_2\left[\frac{\partial f_2}{\partial \theta_1}\frac{\partial \theta_1}{\partial t}+\frac{\partial f_2}{\partial \theta_2}\frac{\partial \theta_2}{\partial t}+\frac{\partial f_2}{\partial x_1}f_1+\frac{\partial f_2}{\partial x_2}f_2\right] \\ & +f_1\left[-z_1\left(\frac{\partial f_1}{\partial x_1}+\frac{\partial f_1}{\partial x_2}\frac{\partial x_2}{\partial x_1}+\frac{\partial f_1}{\partial \theta_1}\frac{\partial \theta_1}{\partial x_1}+\frac{\partial f_1}{\partial \theta_2}\frac{\partial \theta_2}{\partial x_1}\right)-z_2\left(\frac{\partial f_2}{\partial x_1}+\frac{\partial f_2}{\partial x_2}\frac{\partial x_2}{\partial x_1}+\frac{\partial f_2}{\partial \theta_1}\frac{\partial \theta_1}{\partial x_1}+\frac{\partial f_2}{\partial \theta_2}\frac{\partial \theta_2}{\partial x_1}\right)-\left(\frac{\partial F}{\partial x_1}+\frac{\partial F}{\partial x_2}\frac{\partial x_2}{\partial x_1}+\frac{\partial F}{\partial \theta_1}\frac{\partial \theta_1}{\partial x_1}+\frac{\partial F}{\partial \theta_2}\frac{\partial \theta_2}{\partial x_1}\right)\right] \\ & +f_2\left[-z_1\left(\frac{\partial f_1}{\partial x_2}+\frac{\partial f_1}{\partial x_1}\frac{\partial x_1}{\partial x_2}+\frac{\partial f_1}{\partial \theta_1}\frac{\partial \theta_1}{\partial x_2}+\frac{\partial f_1}{\partial \theta_2}\frac{\partial \theta_2}{\partial x_2}\right)-z_2\left(\frac{\partial f_1}{\partial x_2}+\frac{\partial f_2}{\partial x_1}\frac{\partial x_1}{\partial x_2}+\frac{\partial f_2}{\partial \theta_1}\frac{\partial \theta_1}{\partial x_2}+\frac{\partial f_2}{\partial \theta_2}\frac{\partial \theta_2}{\partial x_2}\right)-\left(\frac{\partial F}{\partial x_2}+\frac{\partial F}{\partial x_1}\frac{\partial x_1}{\partial x_2}+\frac{\partial F}{\partial \theta_1}\frac{\partial \theta_1}{\partial x_2}+\frac{\partial F}{\partial \theta_2}\frac{\partial \theta_2}{\partial x_2}\right)\right]\end{aligned} \tag{28}$$

Since x_1, x_2, θ_1 and θ_2 are functions of t only, we can write the following equation.

$$\frac{\partial x_2}{\partial x_1} = \frac{dx_2}{dx_1} = \frac{dx_2}{dt}\Big/\frac{dx_1}{dt} = f_2/f_1$$

$$\frac{\partial x_1}{\partial x_2} = \frac{dx_1}{dx_2} = \frac{dx_1}{dt}\Big/\frac{dx_2}{dt} = f_1/f_2$$

$$\frac{\partial \theta_1}{\partial t} = \frac{d\theta_1}{dt}$$

$$\frac{\partial \theta_2}{\partial t} = \frac{d\theta_2}{dt}$$

$$\frac{\partial \theta_1}{\partial x_1} = \frac{d\theta_1}{dx_1} = \frac{d\theta_1}{dt}\Big/\frac{dx_1}{dt} = \frac{d\theta_1}{dt}\Big/f_1$$

$$\frac{\partial \theta_1}{\partial x_2} = \frac{d\theta_1}{dx_2} = \frac{d\theta_1}{dt}\Big/\frac{dx_2}{dt} = \frac{d\theta_1}{dt}\Big/f_2$$

$$\frac{\partial \theta_2}{\partial x_1} = \frac{d\theta_2}{dx_1} = \frac{d\theta_2}{dt}\Big/\frac{dx_1}{dt} = \frac{d\theta_2}{dt}\Big/f_1$$

$$\frac{\partial \theta_2}{\partial x_2} = \frac{d\theta_2}{dx_2} = \frac{d\theta_2}{dt}\Big/\frac{dx_2}{dt} = \frac{d\theta_2}{dt}\Big/f_2$$

Inserting these equations into equation (28) gives

$$\begin{aligned}\frac{d\mathscr{H}}{dt} = {} & -f_1\frac{\partial F}{\partial x_1}-f_2\frac{\partial F}{\partial x_2}-\frac{\partial F}{\partial \theta_1}\frac{d\theta_1}{dt}-\frac{\partial F}{\partial \theta_2}\frac{d\theta_2}{dt} \\ & -f_2z_2\frac{\partial f_1}{\partial x_2}-z_2f_2\frac{\partial f_2}{\partial x_2}-f_1z_1\frac{\partial f_1}{\partial x_1} \\ & -f_1z_2\frac{\partial f_2}{\partial x_1}-z_1\frac{\partial f_1}{\partial \theta_1}\frac{d\theta_1}{dt}-z_1\frac{\partial \theta_1}{\partial \theta_2}\frac{d\theta_2}{dt} \\ & -z_2\frac{\partial f_2}{\partial \theta_1}\frac{\partial \theta_1}{dt}-z_2\frac{\partial f_2}{\partial \theta_2}\frac{d\theta_2}{dt}\end{aligned} \tag{29}$$

Note that we have used the relation

$$\frac{dF}{dt} = \frac{\partial F}{\partial x_1} f_1 + \frac{\partial F}{\partial x_2} f_2 + \frac{\partial F}{\partial \theta_1} \frac{d\theta_1}{dt} + \frac{\partial F}{\partial \theta_2} \frac{d\theta_2}{dt} \quad (30)$$

When the extremal solution is on the constraint boundary, $\theta(t)$ is determined in terms of the state variables and the independent variable t by the relation shown in equation (14). The corresponding neighboring solution must satisfy

$$dg_1 = \frac{\partial g_1}{\partial \theta_1} d\theta_1 + \frac{\partial g_1}{\partial \theta_2} d\theta_2 + \frac{\partial g_1}{\partial x_1} dx_1 + \frac{\partial g_1}{\partial x_2} dx_2 = 0$$

or solving for $\frac{d\theta_1}{dt}$

$$\frac{d\theta_1}{dt} = -\left(\frac{\partial g_1}{\partial \theta_2}\frac{d\theta_2}{dt} + \frac{\partial g_1}{\partial x_1} f_1 + \frac{\partial g_1}{\partial x_2} f_2\right)\left(\frac{\partial g_1}{\partial \theta_1}\right)^{-1} \quad (31)$$

Inserting equation (31) into equation (29) leads to

$$\frac{d\mathscr{H}}{dt} = 0 \quad (32)$$

or $\mathscr{H}$ is also constant along constraint $g_1 = 0$.* Similarly we can prove $\mathscr{H}$ is constant along constraint $g_2 = 0$.

This proof can probably be extended to the general cases. For a system whose dynamic behavior can be represented by equation (1), the necessary condition for the objective function, equation (2), to be extremum on the boundary subject to the constraints, equation (3), is that the Hamiltonian remains constant on the constraint boundary, or

$$\frac{d\mathscr{H}}{dt} = 0 \quad (33)$$

and the adjoint variables are of the form

$$\frac{dz_i}{dt} = -\frac{\partial \mathscr{H}}{\partial x_i} = -\sum_{j=1}^{s} z_j \left[\sum_{l=1}^{s} \frac{\partial f_j}{\partial x_l}\frac{\partial x_l}{\partial x_i} + \sum_{k=1}^{r} \frac{\partial f_j}{\partial \theta_k}\frac{\partial \theta_k}{\partial x_i}\right], \; i = 1, 2, \ldots, s \quad (34)$$

The condition $\mathscr{H}(T) = 0$ must hold when the control terminal time T is left free.

EXAMPLE

Example 3 in Part 2 of this series[1] is reconsidered here. In the example, the dimensionless room temperature assumes negative values during part of the control period. Very often, however, the room temperature has to be higher than a certain value for some physical or biological reasons. This requirement becomes the constraint of the problem. The performance equations are

$$\frac{dx_{11}}{dt} + r_{11}x_{11} = a_{11}a_{42}'x_{12} - a_{11}a_5'\theta - a_{11}a_6' + a_{12} \quad (35)$$

$$\frac{dx_{12}}{dt} + r_{12}x_{12} = a_{21}x_{11} \quad (36)$$

$$\left.\begin{aligned} x_{11}(0) &= 1 \quad \text{at} \quad t = 0 \\ x_{12}(0) &= 1 \quad \text{at} \quad t = 0 \end{aligned}\right\} \quad (37)$$

$$\begin{aligned} x_{11}(T) &= 0 \quad \text{at} \quad t = T \\ x_{12}(T) &= 0 \quad \text{at} \quad t = T \end{aligned} \quad (38)$$

where T is unspecified. The control variable and the state variable are constrained as

$$|\theta| \leqq 1 \quad (39a)$$

$$x_{11} \geqq m \quad (39b)$$

We wish to find a piecewise continuous control variable θ such that the system can be brought back from the initial deviated state, equation (37), to the final desired state, equation (38), in the minimum period of time. In other words, the objective function given by

$$S = \int_0^T dt \quad (40)$$

is minimized. Note that a constraint is not imposed on x_{12} because it is known from Example 3 of Part 2[1] that x_{12} does not cool down to the negative dimensionless temperature.

During a period in which the inequality constraint,

$$x_{11} > m,$$

is satisfied, the solution obtained in Example 3 of Part 2 is still applicable. Thus during such a period we have [see equations (75) through (78) in Ref. 1]:

$$x_{11} = \frac{1}{a_{21}}[(\lambda_{11}+r_{12})A\exp(\lambda_{11}t) + (\lambda_{12}+r_{12}) B\exp(\lambda_{12}t) + r_{12}K], \quad 0 \leqq t \leqq t_{sa} \quad (41)$$

$$x_{12} = A\exp(\lambda_{11}t) + B\exp(\lambda_{12}t) + K, \quad 0 \leqq t \leqq t_{sa} \quad (42)$$

$$x_{11} = \frac{1}{a_{21}}(\lambda_{11}+r_{12})D_1\exp(\lambda_{11}t) + (\lambda_{12}+r_{12}) D_2\exp(\lambda_{12}t) + r_{12}K'], \quad t_{sd} \leqq t \leqq T \quad (43)$$

$$x_{12} = D_1\exp(\lambda_{11}t) + D_2\exp(\lambda_{12}t) + K', \quad t_{sd} \leqq t \leqq T \quad (44)$$

where

* Proof of this statement is given in the Appendix.

$$K = \frac{a_{11}a_5'a_{21}+a_{11}a_{21}a_6'-a_{12}a_{21}}{a_{11}a_{42}'a_{21}-r_{11}r_{12}}$$

$$K' = \frac{a_{11}a_{21}a_6'+a_{11}a_5'a_{21}+a_{12}a_{21}}{a_{11}a_{42}'a_{21}-r_{11}r_{12}}$$

$$A = \frac{a_{21}-r_{12}-\lambda_{12}+\lambda_{12}K}{\lambda_{11}-\lambda_{12}}$$

$$B = \frac{r_{12}+\lambda_{11}-\lambda_{11}K-a_{21}}{\lambda_{11}-\lambda_{12}}$$

$$\lambda_{11} = \frac{-(r_{11}+r_{12}) + \sqrt{[(r_{11}+r_{12})^2+4(r_{11}r_{12}-a_{11}a_{21}a_{42}')]}}{2}$$

$$\lambda_{12} = \frac{-(r_{11}+r_{12}) - \sqrt{[(r_{11}+r_{12})^2-4(r_{11}r_{12}-a_{11}a_{21}a_{42}')]}}{2}$$

and where D_1 and D_2 are unknowns; whose values will be determined later. t_{sa} is the arrival time when the state variable x_{11} reaches the boundary where $x_{11} = m$. t_{sd} is the time when x_{11} departs from the boundary.

Since $x_{11} = m$ on the boundary, equations (35) and (36) become

$$mr_{11} = a_{11}a_{42}'x_{12}-a_{11}a_5'\theta-a_{11}a_6'+a_{12} \quad (45)$$

$$\frac{dx_{12}}{dt}+r_{12}x_{12} = ma_{21} \quad (46)$$

or solving for x_{12}, we have

$$x_{12} = \frac{ma_{21}}{r_{12}}+C\exp(-r_{12}t), \quad t_{sa} \leqq t \leqq t_{sd} \quad (47)$$

The corresponding θ and x_{11} are

$$\theta = \frac{1}{a_{11}a_5'}[a_{11}a_{42}'x_{12}-a_{11}a_6'+a_{12}-mr_{11}], \quad t_{sa} \leqq t \leqq t_{sd} \quad (48)$$

$$x_{11} = m, \quad t_{sa} \leqq t \leqq t_{sd} \quad (49)$$

where C is an unknown, the value of which can be determined by inserting $x_{11} = m$ into equation (41) and solving for t_{sa}. Then t_{sa} may be substituted into equation (42) to solve for C. Thus

$$x_{12} = A\exp(\lambda_{11}t_{sa})+B\exp(\lambda_{12}t_{sa})+K, \quad t = t_{sa}$$

from equation (47)

$$x_{12} = \frac{ma_{21}}{r_{12}}+C\exp(-r_{12}t_{sa}), \quad t = t_{sa}$$

Solving for C from these two equations, we obtain

$$C = \exp(r_{12}t_{sa})\left[A\exp(\lambda_{11}t_{sa})+B\exp(\lambda_{12}t_{sa}) - \frac{ma_{21}}{r_{12}}+K\right] \quad (50)$$

Because of the continuity of x_{11} and x_{12} with respect to t, we have at $t = t_{sd}$

$$x_{11}(t_{sd}) = m = \frac{1}{a_{21}}[(\lambda_{11}+r_{12})D_1\exp(\lambda_{11}t_{sd}) + (\lambda_{12}+r_{12})D_2\exp(\lambda_{12}t_{sd})+r_{12}K']$$

from equations (43) and (49), and

$$x_{12}(t_{sd}) = \frac{ma_{21}}{r_{12}}+C\exp(-r_{12}t_{sd}) = D_1\exp(\lambda_{11}t_{sd})+D_2\exp(\lambda_{12}t_{sd})+K$$

from equations (44) and (47). Solving for D_1 and D_2 from these equations leads to the following expressions.

$$D_1 = \frac{\begin{vmatrix} -K'+\dfrac{ma_{21}}{r_{12}}+C\exp(-r_{12}t_{sd}) & \exp(\lambda_{12}t_{sd}) \\ -r_{12}K'+ma_{21} & (\lambda_{12}+r_{12})\exp(\lambda_{11}t_{sd}) \end{vmatrix}}{\begin{vmatrix} \exp(\lambda_{11}t_{sd}) & \exp(\lambda_{12}t_{sd}) \\ (\lambda_{11}+r_{12})\exp(\lambda_{11}t_{sd}) & (\lambda_{12}+r_{12})\exp(\lambda_{12}t_{sd}) \end{vmatrix}}$$

$$= \frac{r_{12}K'-ma_{21}+(\lambda_{12}+r_{12})\left(-K'+\dfrac{ma_{21}}{r_{12}}+C\exp[-r_{12}t_{sd}]\right)}{(\lambda_{12}-\lambda_{11})\exp(\lambda_{11}t_{sd})} \quad (51)$$

and

$$D_2 = \frac{-r_{12}K'+ma_{21}+(\lambda_{11}+r_{12})\left(+K'-\dfrac{ma_{21}}{r_{12}}-C\exp[-r_{12}t_{sd}]\right)}{(\lambda_{12}-\lambda_{11})\exp(\lambda_{12}t_{sd})} \quad (52)$$

We now can see that D_1 and D_2 are functions of t_{sd}. Their values and that of T can be obtained by making use of the final conditions of equations (43) and (44) at $t = T$. Thus

$$\frac{1}{a_{21}}[(\lambda_{11}+r_{11})D_1\exp(\lambda_{11}T)+(\lambda_{12}+r_{12}) D_2\exp(\lambda_{12}T)+r_{12}K'] = 0 \quad (53)$$

$$D_1\exp(\lambda_{11}T)+D_2\exp(\lambda_{12}T)+K' = 0 \quad (54)$$

Solving for $D_1\exp(\lambda_{11}T)$ from equation (54) and then inserting it into equation (53) yields

$$D_2 = \frac{\lambda_{11}K'}{(\lambda_{12}-\lambda_{11})\exp(\lambda_{12}T)} \qquad (55)$$

Inserting equation (55) into equation (54) and solving D_1 gives

$$D_1 = \frac{\lambda_{12}K'}{(\lambda_{12}-\lambda_{11})\exp(\lambda_{11}T)} \qquad (56)$$

Equating equation (51) to equation (56), and equation (52) to equation (55), we obtain

$$D_1 = \frac{-r_{12}K'-ma_{21}+(\lambda_{12}+r_{12})\left(-K'+\frac{ma_{21}}{r_{12}}+C\exp[-r_{12}t_{sd}]\right)}{(\lambda_{12}-\lambda_{11})\exp(\lambda_{11}T)} = \frac{\lambda_{12}K'}{(\lambda_{12}-\lambda_{11})\exp(\lambda_{11}T)}$$

and

$$D_2 = \frac{-r_{12}K'+ma_{21}+(\lambda_{11}+r_{12})\left(K'-\frac{ma_{21}}{r_{12}}-C\exp[-r_{12}t_{sd}]\right)}{(\lambda_{12}-\lambda_{11})\exp(\lambda_{12}t_{sd})} = \frac{\lambda_{11}K'}{(\lambda_{12}-\lambda_{11})\exp(\lambda_{12}T)}$$

respectively. Eliminating the common factor $(\lambda_{12}-\lambda_{11})$ in these equations gives

$$\lambda_{12}K'\exp(\lambda_{11}t_{ds}) = \exp(\lambda_{11}T)\Big\{r_{12}K'-ma_{21}+\Big[\lambda_{12}+r_{12}\Big]\Big[-K'+\frac{ma_{21}}{r_{12}}+C\exp(-r_{12}t_{sd})\Big]\Big\} \qquad (57)$$

$$\lambda_{11}K'\exp(\lambda_{12}t_{sd}) = \exp(\lambda_{12}T)\Big[\Big(-r_{12}K'+ma_{21}+a_{11}+r_{12}\Big)\Big(K'-\frac{ma_{21}}{r_{12}}-C\exp(-r_{12}t_{sd})\Big)\Big] \qquad (58)$$

t_{sd} and T can be solved from equations (57) and (58) by a trial and error procedure. Then D_1 and D_2 can be obtained directly from equations (51) and (52) by substituting the value of t_{sd} into the equation.

The solutions of the problem are tabulated in Table 1 and are shown schematically in Figure 1. The optimal control policy is of the bang-bang type as shown in Example 3 of Part 2 of this series[1]. However, because of the existence of inequality constraint on the state variable x_{11}, the optimal control policy θ takes some intermediate value other than 1 or -1 during part of the operation.

Table 1. Minimum values of the objective function (duration of control) for Case 1 of the two CST's-in-series model with $\tau_2 = 0$ and various values m in the inequality constraint $x_{11} \geqq m$.

	$S = T$		
r_{11}	$m = -0{\cdot}2$	$m = -0{\cdot}4$	No constraint on x_{11}
1·2	0·992	0·992	0·992
1·5	1·051	1·047	1·047
2·0	1·233	1·103	1·078
5·0	2·483	1·998	1·007
10·0	3·457	2·862	0·956

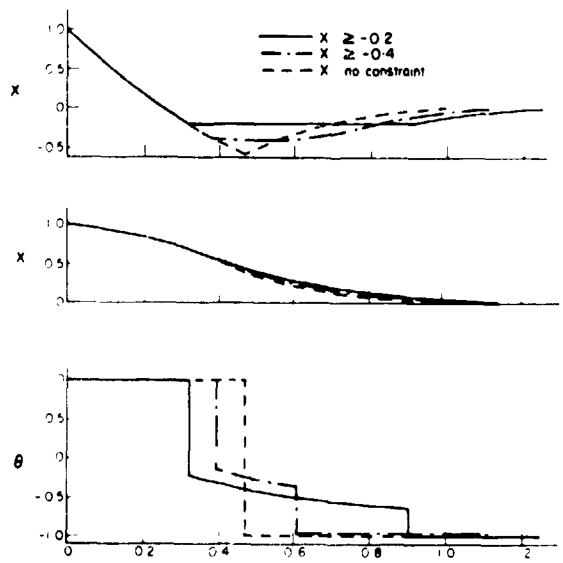

Fig. 1. Optimal control policies and system responses for Case 1 of the two CST's-in-series model with $\tau_2 = 0$ and $r_{11} = 2$ and with a constraint on the state variable.

Table 2. Simulation of Case 1 of the two CST's-in-series model with $\tau_2 = 0$, $r_{11} = 2$ and $x_{11} \geqq -0{\cdot}2$

Control Variable θ				
$t < t_{se}$	$t_{se} < t < t_s$	$t_s < t < t_{sd}$	$t_{sd} < t < T$	T
1·0	−1·0	1·0	−1·0	No solution
1·0	−1·0	0·8	−1·0	No solution
1·0	−1·0	0·6	−1·0	No solution
1·0	−0·8	1·0	−1·0	2·535
1·0	−0·8	0·8	−1·0	2·363
1·0	−0·8	0·6	−1·0	2·249
1·0	−0·6	1·0	−1·0	1·435
1·0	−0·6	0·8	−1·0	1·388
1·0	−0·6	0·6	−1·0	1·336

Simulation of this problem with $r_{11} = 2$ and $x_{11} = 0.2$ has been carried out extensively by the phase plane approach and results of the simulation are tabulated in Table 2 and are also shown graphically in Figure 2. These results confirm that the solutions in Table 1 are truly optimal.

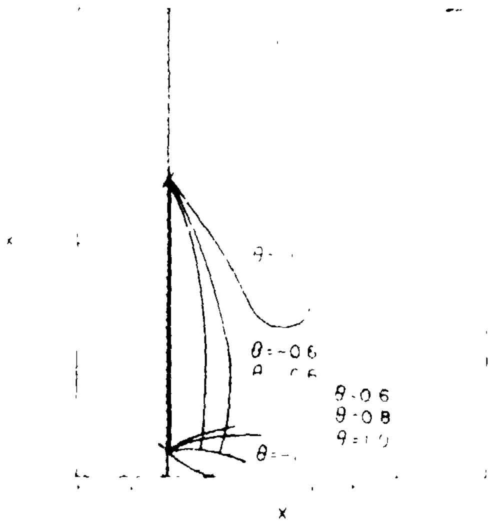

Fig. 2. Simulation of Case I of the two CSTR's-in-series model with $\tau_2 = 0$, $r_{11} = 2$, and $x_{11} = 0.2$

CONCLUSIONS

It should be evident that the necessary conditions for optimum for processes with inequality constraints imposed on the state variables remain the same as those for processes without state variable constraints. One exception, however, is that the adjoint variables possess the form shown in equation (34) instead of equation (5) on the constraint boundary.

Another fact which should also be pointed out is that Pontryagin's maximum principle which can handle constraints on state variables is probably a more useful form of the calculus of variations than the Bolza form which cannot treat constraints[14].

NOMENCLATURE

a_4'	K_2K_4
a_6'	K_3K_4
a_{11}	$r_1K_{11}r_{11}/K_4$
a_{12}	$r_1r_2K_{11}$
a_{21}	$r_{12}K_{12}/K_{11}$
a_{42}	rK_4/K_{12}
a_{42}'	K_4/K_{12}
A	Integration constant
B	Integration constant
c_i	Constants defined in equation (2), $i = 1, 2, \ldots, s$
c	Specific heat of air in kcal/kg °C
c_w	Specific heat of coolant in kcal/kg °C
D_1	Unknown constant in equation (43) and (44)
D	Unknown constant in equations (43) and (44)
g	The inequality constraints $i = 1, 2, \ldots$
$H[x(t), \theta(t), z(t)]$	Hamiltonian function defined in equation (4)
K	A constant in equations (41) through (44)
K	A constant in equations (41) through (44)
K	$\frac{1}{2T_2}(T_{c\,max} - T_{c\,min})$
K	$\frac{1}{2T_2}(T_{c\,max} + T_{c\,min})$
K_4	$\frac{T_2}{T_{10}}$
K_{11}	$\frac{T_2}{T_{1,0}}$
K_{12}	$\frac{T_2}{T_{2,0}}$
m	A lower bound dimensionless temperature of x_{11}
Q	$Q_1 + Q_2$, flow rate of air in the system proper in m³/s
Q_1	Air flow rate by circulation air in m³/s
Q_2	Flow rate of fresh air in m³/s
Q_w	Flow rate of coolant in m³/s
r_1	$\frac{Q_1}{Q_1+Q_2}$, the fraction of circulation air
r_2	$\frac{Q_2}{Q_1+Q_2}$, the fraction of fresh air
r_{11}	$\frac{\tau_1}{\tau_{11}}$
r_{12}	$\frac{\tau_2}{\tau_{12}}$
S	Performance index defined in equation (2)
t	$\frac{\alpha}{\tau_1}$, dimensionless time
t_{su}	Switching time when the state variable x_{11} reaches the boundary where $x_{11} = m$
t_{sd}	Switching time when x_{11} departs from the boundary
t_{wi}	Inlet temperature of coolant in °C
t_{wh}	Outlet temperature of coolant in °C
T	Final time, dimensionless
T_c	Room temperature in °C
T_{c0}	Room temperature at $\alpha = 0^+$ in °C
T_{c1}	Temperature of pool 1 in °C
T_{c10}	Temperature of pool 1 at $\alpha = 0^+$ in °C

T_{c2} Temperature of pool 2 in °C

T_{c20} Temperature of pool 2 at $\alpha = 0^+$

T_d Disturbance temperature in °C

T_i Temperature of the circulation air into the system in °C

T_{i0} Temperature of the circulation air into the system at $\alpha = 0^+$ in °C

T_r $\dfrac{Q_w \rho_w c_{pw} (T_{wh} - T_{wc})}{Q_1 \rho c_p}$, hypothetical temperature

$T_{r\,max}$ Upper bound of T_r in °C

$T_{r\,min}$ Lower bound of T_r in °C

T_{r0} Value of T_r at $\alpha = 0$ in °C

T_{wc} $t_{wc} - t_a$ in °C

T_{wh} $t_{wh} - t_a$ in °C

T_{11} Temperature of pool 1 in °C

T_{12} Temperature of pool 2 in °C

v_j A Lagrange multiplier in equations (8) and (9)

V_1 Volume of room in m^3

V_{11} Volume of pool 1 of two completely stirred tanks in series model in m^3

V_2 Volume of heat exchanger in m^3

V_{12} Volume of pool 2 of two completely stirred tanks in series model in m^3

$x(t)$ s-dimensional state vector defined in equation (1)

$x_i(t_0)$ x_{i0}, $i = 1, 2, \ldots, s$, initial value of x at $t = t_0$

x_{11} $\dfrac{T_{c1}}{T_{c10}}$, dimensionless temperature of pool 1

x_{12} $\dfrac{T_{c2}}{T_{c20}}$, dimensionless temperature of pool 2

$z_i(t)$ adjoint variable defined in equation (5)

Greek letters

ρ_w Density of coolant in kg/m^3

τ_1 $\dfrac{V_1}{Q_1 + Q_2}$, time constant of the system proper in s

τ_{11} $\dfrac{V_{11}}{Q_1 + Q_2}$, time constant of pool 1 in s

τ_2 $\dfrac{V_2}{Q_1}$, time constant of heat exchanger in s

τ_{12} $\dfrac{V_{12}}{Q_1 + Q_2}$, time constant of pool 2 in s

θ $\dfrac{T_r - \frac{1}{2}(T_{r\,max} + T_{r\,min})}{T_{r\,max} - \frac{1}{2}(T_{r\,max} + T_{r\,min})}$, control variable

$\begin{cases} +1 \text{ at } T_r = T_{r\,max} \\ -1 \text{ at } T_r = T_{r\,min} \end{cases}$

λ_{11} Constant in equation (41)

λ_{12} Constant in equation (42)

REFERENCES

1. L. T. Fan, Y. S. Hwang and C. L. Hwang, Applications of Modern Optimal Control Theory to Environmental Control of Confined Spaces and Life Support Systems, Part 2. The Basic Form of Pontryagin's Maximum Principle and Its Applications. *Build. Sci.* **5**, 81 (1970).
2. L. T. Fan, Y. S. Hwang and C. L. Hwang, Applications of Modern Optimal Control Theory to Environmental Control of Confined Spaces and Life Support Systems, Part 3. Optimal Control of Systems in which State Variables have Equality Constraints at the Final Process Time. *Build. Sci.* **5**, 125 (1970).
3. S. S. L. Chang, A Modified Maximum Principle for Optimum Control of a System with Bounded Phase Space Coordinates, *Automatica*, **1**, 55 (1962).
4. L. D. Berkovitz, On Control Problems with Bounded State Variables, *J. Math. Anal. Appl.*, **5**, 488 (1962).
5. L. S. Pontryagin, V. G. Boltyanskii, R. V. Gamkrelidze and E. F. Mishchenko, *The Mathematical Theory of Optimal Process*, (English translation by K. N. Trirogoff), Interscience, New York, (1962).
6. S. Dreyfus, Variational Problems with State Variable Inequality Constraints, Rand Corp., Santa Monica, California, (July 1962).
7. W. F. Denham, Steepest-ascent Solution of Optimal Programming Problems, Rept. Br-2939, Raytheon Co., Bedford, Massachusetts, (April 1963).
8. A. E. Bryson, and W. F. Denham, A Steepest Ascent Method for Solving Optimal Programming Problems, *J. Appl. Mech.*, **29**, 247 (1962).
9. L. T. Fan, *The Continuous Maximum Principle: A Study of Complex Systems Optimization*, Wiley, New York, (1966).
10. A. E. Bryson, Jr., W. F. Denham and S. E. Dreyfus, Optimal Programming Problems with Inequality Constraints I: Necessary Conditions for Extremal Solutions, *J. AIAA*, **1**, 2544 (1963).
11. J. M. Douglas, and M. M. Denn, Optimal Design and Control by Variational Methods, *I & EC Education*, **57**, 18 (1965).

12. J. McIntyre, On Optimal Control with Bounded State Variables. (edited by C. T. Leondes) Academic Press, New York (1967).

13. L. T. Fan, Y. S. Hwang, and C. L. Hwang, Applications of Modern Optimal Control Theory to Environmental Control of Confined Spaces and Life Support Systems, Part 1. Modeling and Simulation. *Build. Sci.* **5**, 57 (1970).

14. A. F. Ogunye, and W. H. Ray, Non-simple Control Policies for Reactors with Catalyst Decay, *Trans. Instn. Chem. Engrs.* **46**, T225 (1968).

APPENDIX

Derivation of equation (32) *from equation* (28)

Equation (28) has the form

$$
\begin{aligned}
\frac{\mathrm{d}\mathscr{H}}{\mathrm{d}t} = {} & \frac{\mathrm{d}F}{\mathrm{d}t}+z_1\Bigg[\frac{\partial f_1}{\partial\theta_1}\frac{\partial\theta_1}{\partial t}+\frac{\partial f_1}{\partial\theta_2}\frac{\partial\theta_2}{\partial t}+\underset{(1)}{\frac{\partial f_1}{\partial x_1}f_1}+\underset{(2)}{\frac{\partial f_1}{\partial x_2}f_2}\Bigg]+z_2\Bigg[\frac{\partial f_2}{\partial\theta_1}\frac{\partial\theta_1}{\partial t}+\frac{\partial f_2}{\partial\theta_2}\frac{\partial\theta_2}{\partial t}+\underset{(3)}{\frac{\partial f_2}{\partial x_1}f_1}+\underset{(4)}{\frac{\partial f_2}{\partial x_2}f_2}\Bigg]\\
& +f_1\Bigg[-z_1\left(\underset{(1)}{\frac{\partial f_1}{\partial x_1}}+\frac{\partial f_1}{\partial x_2}\frac{\partial x_2}{\partial x_1}+\frac{\partial f_1}{\partial\theta_1}\frac{\partial\theta_1}{\partial x_1}+\frac{\partial f_1}{\partial\theta_2}\frac{\partial\theta_2}{\partial x_1}\right)\\
& -z_2\left(\underset{(3)}{\frac{\partial f_2}{\partial x_1}}+\frac{\partial f_2}{\partial x_2}\frac{\partial x_2}{\partial x_1}+\frac{\partial f_2}{\partial\theta_1}\frac{\partial\theta_1}{\partial x_1}+\frac{\partial f_2}{\partial\theta_2}\frac{\partial\theta_2}{\partial x_1}\right)\\
& -\left(\frac{\partial F}{\partial x_1}+\frac{\partial F}{\partial x_2}\frac{\partial x_2}{\partial x_1}+\frac{\partial F}{\partial\theta_1}\frac{\partial\theta_1}{\partial x_1}+\frac{\partial F}{\partial\theta_2}\frac{\partial\theta_2}{\partial x_1}\right)\Bigg]\\
& +f_2\Bigg[-z_1\left(\underset{(2)}{\frac{\partial f_1}{\partial x_2}}+\frac{\partial f_1}{\partial x_1}\frac{\partial x_1}{\partial x_2}+\frac{\partial f_1}{\partial\theta_1}\frac{\partial\theta_1}{\partial x_2}+\frac{\partial f_1}{\partial\theta_2}\frac{\partial\theta_2}{\partial x_1}\right)-z_2\left(\underset{(4)}{\frac{\partial f_2}{\partial x_2}}+\frac{\partial f_2}{\partial x_1}\frac{\partial x_1}{\partial x_2}+\frac{\partial f_2}{\partial\theta_1}\frac{\partial\theta_1}{\partial x_2}\right.\\
& \left.+\frac{\partial f_2}{\partial\theta_2}\frac{\partial\theta_2}{\partial x_2}\right)-\left(\frac{\partial F}{\partial x_2}+\frac{\partial F}{\partial x_1}\frac{\partial x_1}{\partial x_2}+\frac{\partial F}{\partial\theta_1}\frac{\partial\theta_1}{\partial x_2}+\frac{\partial F}{\partial\theta_2}\frac{\partial\theta_2}{\partial x_2}\right)\Bigg]
\end{aligned}
\qquad (A.1)
$$

This equation can be simplified to

$$
\begin{aligned}
\frac{\mathrm{d}\mathscr{H}}{\mathrm{d}t} = {} & \frac{\mathrm{d}F}{\mathrm{d}t}+z_1\left[\frac{\partial f_1}{\partial\theta_1}\frac{\partial\theta_1}{\partial t}+\frac{\partial f_1}{\partial\theta_2}\frac{\partial\theta_2}{\partial t}\right]+z_2\left[\frac{\partial f_2}{\partial\theta_1}\frac{\partial\theta_1}{\partial t}+\frac{\partial f_2}{\partial\theta_2}\frac{\partial\theta_2}{\partial t}\right]\\
& +f_1\Bigg[-z_1\left(\frac{\partial f_1}{\partial x_2}\frac{\partial x_2}{\partial x_1}+\frac{\partial f_1}{\partial\theta_1}\frac{\partial\theta_1}{\partial x_1}+\frac{\partial f_1}{\partial\theta_2}\frac{\partial\theta_2}{\partial x_1}\right)-z_2\left(\frac{\partial f_2}{\partial x_2}\frac{\partial x_2}{\partial x_1}+\frac{\partial f_2}{\partial\theta_1}\frac{\partial\theta_1}{\partial x_1}+\frac{\partial f_2}{\partial\theta_2}\frac{\partial\theta_2}{\partial x_1}\right)\\
& -\left(\frac{\partial F}{\partial x_1}+\frac{\partial F}{\partial x_2}\frac{\partial x_2}{\partial x_1}+\frac{\partial F}{\partial\theta_1}\frac{\partial\theta_1}{\partial x_1}+\frac{\partial F}{\partial\theta_2}\frac{\partial\theta_2}{\partial x_1}\right)\Bigg]+f_2\Bigg[-z_1\left(\frac{\partial f_1}{\partial x_1}\frac{\partial x_1}{\partial x_2}+\frac{\partial f_1}{\partial\theta_1}\frac{\partial\theta_1}{\partial x_2}+\frac{\partial f_1}{\partial\theta_2}\frac{\partial\theta_2}{\partial x_2}\right)\\
& -z_2\left(\frac{\partial f_2}{\partial x_1}\frac{\partial x_1}{\partial x_2}+\frac{\partial f_2}{\partial\theta_1}\frac{\partial\theta_1}{\partial x_2}+\frac{\partial f_2}{\partial\theta_2}\frac{\partial\theta_2}{\partial x_2}\right)-\left(\frac{\partial F}{\partial x_2}+\frac{\partial F}{\partial x_1}\frac{\partial x_1}{\partial x_2}+\frac{\partial F}{\partial\theta_1}\frac{\partial\theta_1}{\partial x_2}+\frac{\partial F}{\partial\theta_2}\frac{\partial\theta_2}{\partial x_2}\right)\Bigg]
\end{aligned}
\qquad (A.2)
$$

Since x_1, x_2, θ_1 and θ_2 are functions only of t, we have

$$
\begin{aligned}
\frac{\partial x_2}{\partial x_1} &= \frac{\mathrm{d}x_2}{\mathrm{d}x_1} = \frac{\mathrm{d}x_2}{\mathrm{d}t}\Big/\frac{\mathrm{d}x_1}{\mathrm{d}t} = f_2/f_1\\
\frac{\partial x_1}{\partial x_2} &= \frac{\mathrm{d}x_1}{\mathrm{d}t} = \frac{\mathrm{d}x_1}{\mathrm{d}t}\Big/\frac{\mathrm{d}x_2}{\mathrm{d}t} = f_1/f_2\\
\frac{\partial\theta_1}{\partial t} &= \frac{\mathrm{d}\theta_1}{\mathrm{d}t}\\
\frac{\partial\theta_2}{\partial t} &= \frac{\mathrm{d}\theta_2}{\mathrm{d}t}\\
\frac{\partial\theta_1}{\partial x_1} &= \frac{\mathrm{d}\theta_1}{\mathrm{d}x_1} = \frac{\mathrm{d}\theta_1}{\mathrm{d}t}\Big/\frac{\mathrm{d}x_1}{\mathrm{d}t} = \frac{\mathrm{d}\theta_1}{\mathrm{d}t}\Big/f_1 \qquad (A.3)\\
\frac{\partial\theta_1}{\partial x_2} &= \frac{\mathrm{d}\theta_1}{\mathrm{d}x_2} = \frac{\mathrm{d}\theta_1}{\mathrm{d}t}\Big/\frac{\mathrm{d}x_2}{\mathrm{d}t} = \frac{\mathrm{d}\theta_1}{\mathrm{d}t}\Big/f_2\\
\frac{\partial\theta_2}{\partial x_1} &= \frac{\mathrm{d}\theta_2}{\mathrm{d}x_1} = \frac{\mathrm{d}\theta_2}{\mathrm{d}t}\Big/\frac{\mathrm{d}x_1}{\mathrm{d}t} = \frac{\mathrm{d}\theta_2}{\mathrm{d}t}\Big/f_1\\
\frac{\partial\theta_2}{\partial x_2} &= \frac{\mathrm{d}\theta_2}{\mathrm{d}x_2} = \frac{\mathrm{d}\theta_2}{\mathrm{d}t}\Big/\frac{\mathrm{d}x_2}{\mathrm{d}t} = \frac{\mathrm{d}\theta_2}{\mathrm{d}t}\Big/f_2
\end{aligned}
$$

Inserting these expressions into equation (A.2), we obtain

$$
\frac{\mathrm{d}\mathscr{H}}{\mathrm{d}t} = \frac{\mathrm{d}F}{\mathrm{d}t}+z_1\left[\underset{(5)}{\frac{\partial f_1}{\partial\theta_1}\frac{\mathrm{d}\theta_1}{\mathrm{d}t}}+\underset{(6)}{\frac{\partial f_1}{\partial\theta_2}\frac{\mathrm{d}\theta_2}{\mathrm{d}t}}\right]
$$

$$+z_2\left[\underset{(7)}{\frac{\partial f_2}{\partial\theta_1}\frac{d\theta_1}{dt}}+\underset{(8)}{\frac{\partial f_2}{\partial\theta_2}\frac{d\theta_2}{dt}}\right]$$

$$+f_1\left[-z_1\left(\frac{\partial f_1}{\partial x_2}f_2/f_1+\underset{(5)}{\frac{\partial f_1}{\partial\theta_1}\frac{d\theta_1}{dt}/f_1}\right.\right.$$

$$\left.+\underset{(6)}{\frac{\partial f_1}{\partial\theta_2}\frac{d\theta_2}{dt}/f_1}\right)-z_2\left(\frac{\partial f_2}{\partial x_2}f_2/f_1\right.$$

$$\left.+\underset{(7)}{\frac{\partial f_2}{\partial\theta_1}\frac{d\theta}{dt}/f_1}+\underset{(8)}{\frac{\partial f_2}{\partial\theta_2}\frac{d\theta_2}{dt}/f_1}\right)$$

$$-\left(\frac{\partial F}{\partial x_1}+\frac{\partial F}{\partial x_2}f_2/f_1+\frac{\partial F}{\partial\theta_1}\frac{d\theta_1}{dt}/f_1\right.$$

$$\left.\left.+\frac{\partial F}{\partial\theta_2}\frac{d\theta_2}{dt}/f_1\right)\right]+f_2\left[-z_1\left(\frac{\partial f_1}{\partial x_1}f_1/f_2\right.\right.$$

$$\left.+\frac{\partial f_1}{\partial\theta_1}\frac{d\theta_1}{dt}/f_2+\frac{\partial f_1}{\partial\theta_2}\frac{d\theta_2}{dt}/f_2\right)$$

$$-z_2\left(\frac{\partial f_2}{\partial x_1}f_1/f_2+\frac{\partial f_2}{\partial\theta_1}\frac{d\theta_1}{dt}/f_2\right.$$

$$\left.+\frac{\partial f_2}{\partial\theta_2}\frac{d\theta_2}{dt}/f_2\right)-\left(\frac{\partial F}{\partial x_2}+\frac{\partial F}{\partial x_1}f_1/f_2\right.$$

$$\left.\left.+\frac{\partial F}{\partial\theta_1}\frac{d\theta_1}{dt}/f_2+\frac{\partial F}{\partial\theta_2}\frac{d\theta_2}{dt}/f_2\right)\right]$$

or

$$\begin{aligned}\frac{d\mathscr{H}}{dt} = {} & \frac{dF}{dt}-f_2z_1\frac{\partial f_1}{\partial x_2}-z_2f_2\frac{\partial f_2}{\partial x_2}-f_1z_1\frac{\partial f_1}{\partial x_1}\\ & -f_1z_2\frac{\partial f_2}{\partial x_1}-f_1\frac{\partial F}{\partial x_1}-f_2\frac{\partial F}{\partial x_2}-\frac{\partial F}{\partial\theta_1}\frac{d\theta_1}{dt}\\ & -\frac{\partial F}{\partial\theta_2}\frac{d\theta_2}{dt}-z_1\frac{\partial f_1}{\partial\theta_1}\frac{d\theta_1}{dt}-z_1\frac{\partial f_1}{\partial\theta_2}\frac{d\theta_2}{dt}\\ & -z_2\frac{\partial f_2}{\partial\theta_1}\frac{d\theta_1}{dt}-z_2\frac{\partial f_2}{\partial\theta_2}\frac{d\theta_2}{dt}-f_2\frac{\partial F}{\partial x_2}\\ & -f_1\frac{\partial F}{\partial x_1}-\frac{\partial F}{\partial\theta_1}\frac{d\theta_1}{dt}-\frac{\partial F}{\partial\theta_2}\frac{d\theta_2}{dt}\end{aligned} \tag{A.4}$$

Since F is a function of x_1, x_2, θ_1 and θ_2,

$$\frac{dF}{dt}=\frac{\partial F}{\partial x_1}\frac{dx_1}{dt}+\frac{\partial F}{\partial x_2}\frac{dx_2}{dt}+\frac{\partial F}{\partial\theta_1}\frac{d\theta_1}{dt}+\frac{\partial F}{\partial\theta_2}\frac{d\theta_2}{dt} \tag{A.5}$$

Insertion of equation (A.5) into equation (A.4) gives

$$\frac{d\mathscr{H}}{dt}=\underset{(9)}{\frac{\partial F}{\partial x_1}\frac{dx_1}{dt}}+\underset{(10)}{\frac{\partial F}{\partial x_2}\frac{dx_2}{dt}}+\underset{(11)}{\frac{\partial F}{\partial\theta_1}\frac{d\theta_1}{dt}}+\underset{(12)}{\frac{\partial F}{\partial\theta_2}\frac{d\theta_2}{dt}}$$

$$-f_2z_1\frac{\partial f_1}{\partial x_2}-f_2z_2\frac{\partial f_2}{\partial x_2}-\underset{(11)}{f_1\frac{\partial F}{\partial x_1}}-\underset{(12)}{f_2\frac{\partial F}{\partial x_2}}$$

$$-\underset{(9)}{\frac{\partial F}{\partial\theta_1}\frac{d\theta_1}{dt}}-\underset{(10)}{\frac{\partial F}{\partial\theta_2}\frac{d\theta_2}{dt}}-f_1z_1\frac{\partial f}{\partial x_1}$$

$$-z_1\frac{\partial f_1}{\partial\theta_1}\frac{d\theta_1}{dt}-z_1\frac{\partial f_1}{\partial\theta_2}\frac{d\theta_2}{dt}-f_1z_2\frac{\partial f_2}{\partial x_1}$$

$$-z_2\frac{\partial f_2}{\partial\theta_2}\frac{d\theta_1}{dt}-z_2\frac{\partial f_2}{\partial\theta_2}\frac{d\theta_2}{dt}-f_2\frac{\partial F}{\partial x_2}$$

$$-f_1\frac{\partial F}{\partial x_1}-\frac{\partial F}{\partial\theta_1}\frac{d\theta_1}{dt}-\frac{\partial F}{\partial\theta_2}\frac{d\theta_2}{dt}$$

or

$$\begin{aligned}\frac{d\mathscr{H}}{dt} = {} & -f_2z_1\frac{\partial f_1}{\partial x_2}-f_2z_2\frac{\partial f_2}{\partial x_2}-f_1z_1\frac{\partial f_1}{\partial x_1}\\ & -z_1\frac{\partial f_1}{\partial\theta_1}\frac{d\theta_1}{dt}-z_1\frac{\partial f_1}{\partial\theta_2}\frac{d\theta_2}{dt}-f_1z_2\frac{\partial f_2}{\partial x_1}\\ & -z_2\frac{\partial f_2}{\partial\theta_1}\frac{d\theta_1}{dt}-z_2\frac{\partial f_2}{\partial\theta_2}\frac{d\theta_2}{dt}-f_2\frac{\partial F}{\partial x_2}\\ & -f_1\frac{\partial F}{\partial x_1}-\frac{\partial F}{\partial\theta_1}\frac{d\theta_1}{dt}-\frac{\partial F}{\partial\theta_2}\frac{d\theta_2}{dt}\end{aligned} \tag{A.6}$$

On the constraint boundary, we have

$$g_1(x_1, x_2, \theta_1, \theta_2) = 0$$

or

$$dg_1 = 0 = \frac{\partial g_1}{\partial\theta_1}d\theta_1+\frac{\partial g_1}{\partial\theta_2}d\theta_2+\frac{\partial g_1}{\partial x_1}dx_1+\frac{\partial g_1}{\partial x_2}dx_2$$

Solving this for $\frac{d\theta_1}{dt}$, we have

$$\frac{d\theta_1}{dt}=-\left(\frac{\partial g_1}{\partial\theta_1}\right)^{-1}\left(\frac{\partial g_1}{\partial\theta_2}\frac{d\theta_2}{dt}+\frac{\partial g_1}{\partial x_1}f_1+\frac{\partial g_1}{\partial x_2}f_2\right) \tag{A.7}$$

Inserting the above equation into equation (A.6) leads to

$$\begin{aligned}\frac{d\mathscr{H}}{dt} = {} & -f_2z_1\frac{\partial f_1}{\partial x_2}-f_2z_2\frac{\partial f_2}{\partial x_2}-f_1z_1\frac{\partial f_1}{\partial x_1}\\ & -f_1z_2\frac{\partial f_2}{\partial x_1}-z_1\frac{\partial f_1}{\partial\theta_2}\frac{d\theta_2}{dt}+z_1\frac{\partial f_1}{\partial\theta_1}\\ & \times\left(\frac{\partial g_1}{\partial\theta_1}\right)^{-1}\left(\frac{\partial g_1}{\partial\theta_2}\frac{d\theta_2}{dt}+\frac{\partial g_1}{\partial x_1}f_1+\frac{\partial g_1}{\partial x_2}f_2\right)\\ & +z_2\frac{\partial f_2}{\partial\theta_1}\left(\frac{\partial g_1}{\partial\theta_1}\right)^{-1}\left(\frac{\partial g_1}{\partial\theta_2}\frac{d\theta_2}{dt}+\frac{\partial g_1}{\partial x_1}f_1\right.\end{aligned}$$

$$+\frac{\partial g_1}{\partial x_2} f_2\Bigg) - z_2 \frac{\partial f_2}{\partial \theta_2}\frac{d\theta_2}{dt} - f_2 \frac{\partial F}{\partial x_2} - f_1 \frac{\partial F}{\partial x_1}$$

$$-\frac{\partial F}{\partial \theta_2}\frac{d\theta_2}{dt} + \frac{\partial F}{\partial \theta_1}\left(\frac{\partial g_1}{\partial \theta_1}\right)^{-1}\left(\frac{\partial g_1}{\partial \theta_2}\frac{d\theta_2}{dt}\right.$$

$$\left.+\frac{\partial g_1}{\partial x_1} f_1 + \frac{\partial g_1}{\partial x_2} f_2\right) \qquad \text{(A.8)}$$

Since functions, f_1, f_2, F and g_1, possess the continuous derivatives, at least, to the second order, equation (A.8) can be rewritten as

$$\frac{d\mathscr{H}}{dt} = \underset{(13)}{-f_2 z_1 \frac{\partial f_1}{\partial x_2}} \underset{(14)}{- f_2 z_2 \frac{\partial f_2}{\partial x_2}} \underset{(15)}{- f_1 z_1 \frac{\partial f_1}{\partial x_1}}$$

$$\underset{(16)}{-f_1 z_2 \frac{\partial f_2}{\partial x_1}} \underset{(17)}{- z_1 \frac{\partial f_1}{\partial \theta_2}\frac{d\theta_2}{dt}} \underset{(17)}{+ z_1 \frac{\partial f_1}{\partial \theta_2}\frac{d\theta_2}{dt}}$$

$$\underset{(15)}{+f_1 z_1 \frac{\partial f_1}{\partial x_1}} \underset{(16)}{+ z_1 f_2 \frac{\partial f_1}{\partial x_2}} \underset{(18)}{+ z_2 \frac{\partial f_2}{\partial \theta_2}\frac{d\theta_2}{dt}}$$

$$\underset{(13)}{+f_1 z_2 \frac{\partial f_2}{\partial x_1}} \underset{(14)}{+ f_2 z_2 \frac{\partial f_2}{\partial x_2}} \underset{(18)}{- z_2 \frac{\partial f_2}{\partial \theta_2}\frac{d\theta_2}{dt}}$$

$$\underset{(19)}{-f_2 \frac{\partial F}{\partial x_2}} \underset{(20)}{- f_1 \frac{\partial F}{\partial x_1}} \underset{(21)}{- \frac{\partial F}{\partial \theta_2}\frac{d\theta_2}{dt}} \underset{(21)}{+ \frac{\partial F}{\partial \theta_2}\frac{d\theta_2}{dt}}$$

$$\underset{(20)}{+\frac{\partial F}{\partial x_1} f_1} \underset{(19)}{+ \frac{\partial F}{\partial x_2} f_2}$$

or

$$\frac{d\mathscr{H}}{dt} = 0.$$

This is equation (32) in the text.

Les conditions nécessaires pour l'optimum d'un système dynamique dont les variables d'état sont contraintes par certaines conditions d'inégalité, sont obtenues par l'application d'une technique de variation. Les conditions sont utilisées pour déterminer la police optimale du contrôle de température de la pièce ou cabine d'un système de support de vie. On étudie encore le système consistant d'une cabine à air conditionné soumis à une perturbation de chaleur par impulsion et d'un échangeur de chaleu: agissant comme élément de contrôle. Le courant d'air dans la cabine est caractérisé par le modèle des deux vaisseaux en série (2 CST en série) complètement agités. Une contrainte est imposée sur la température environnante qui doit être plus d'une certaine valeur pour certaines raisons physiques ou biologiques.

Die notwendigen Bedingungen für Optimum eines dynamischen Systems, dessen Zustandsveränderliche durch bestimmte Ungleichheitsbedingungen begrenzt sind, werden unter Verwendung einer Variationstechnik abgeleitet. Es werden die Bedingungen verwandt, um das Optimalverfahren für die Raum- oder Kabinentemperaturkontrolle eines Lebensunterhaltungssystems festzulegen. Das System wird wieder untersucht, welches aus einer klimatisierten Kabine besteht, die einem Wärmestörungsimpuls und einem Wärmeaustauscher ausgesetzt wird, welcher als Kontrollelement dient. Der Luftstrom in der Kabine wird durch zwei völlig durchgerührte Reihentanks (2 CST's-in-series) im Modell dargestellt. Eine Einschränkung ist der Raumtemperatur auferlegt, die aus einigen physikalischen oder biologischen Gründen grösser als ein bestimmter Wert sein muss.

(d) 5

Build. Sci. Vol. 5, pp. 149 152. Pergamon Press 1970. Printed in Great Britain

SfB	Ab8
UDC	697

Applications of Modern Optimal Control Theory to Environmental Control of Confined Spaces and Life Support Systems*

Part—5 Optimality and Sensitivity Analysis

L. T. FAN†
Y. S. HWANG†
C. L. HWANG†

The sensitivities of a cabin with temperature control which has been considered in the first four parts of this series are examined. These include the sensitivities to (1) parameter variation, (2) change in dimensions of mathematical models and (3) change in constraints on state variables are examined.

The system is not sensitive to the variation of the parameter (the recycle ratio of air) when the magnitude of the variation is small. The effect, however, is noticeable when the variation is large. The effect of the change of the parameter (the ratio of the time constants of the system proper to that of the heat exchanger) is very small. The effect of variation of the parameter (the volume fraction of the first pool in the two CST's-in-series model) on the optimal conditions is substantial.

There is a small but not negligible effect of the dimensional change in the system equations, which is caused by neglecting the time constant of the heat exchanger. The complexity of the model describing the system component has a definite effect on the predicted performance of the system. The effect is apparent for the particular models considered here, which are the one CST model and the two CST's-in-series-model.

INTRODUCTION

THE PRECEDING parts of this series are concerned with the thermal modeling and simulation of confined spaces and ife support systems[1] and the optimal control of such systems[2–4]. Examination of the optimal results[2–4] naturally leads us to consider the deviation of a system from its nominal or optimal behavior. Such deviation of the system behavior is caused by deviation from their nominal performance characteristics of system components or other factors of the systems, which are often characterized by parameters of the system model. This is the essence of sensitivity analysis.

Tomovic[5] and Takamatsu[6] discussed the role of sensitivity analysis in engineering problems. They indicated that there are several areas of sensitivity analysis. While knowledge of the sensitivity of the performance of a system as predicted by its model to parameter variation is important, there are other aspects of sensitivity analysis which are important for a particular problem or system. These are (1) sensitivity to change in dimensions of the mathematical model representing the system, (2) sensitivity to transition from the continuous model to the discrete model in describing the system, (3) sensitivity to the influence of various functional blocks (system components) which comprise a system, and (4) sensitivity to change in constraints. Tomovic[7] discussed the contributions sensitivity analysis can make in analyzing the stability of a process. Demski[8] discussed the broad applications of sensitivity analysis in engineering and management sciences. Books by Pagurek[9] and Sage[10] are suggested references for sensitivity analysis of control systems.

Here we shall make use of the results presented in the first four parts of this series[1–4] to demonstrate the sensitivity to (1) parameter variation, (2) change in dimensions of mathematical models and (3) change in constraints.

* This work was supported by the Air Force Office of Scientific Research, Office of Aerospace Research, United States Air Force, Under Contract F 44620–68–0020 (Themis Project), and NASA Grant Under Contract NGR–17–001–134.

† Institute for systems design and optimization, Kansas State University, Manhattan, Kansas.

PRECEDING PAGE BLANK NOT FILMED

SENSITIVITIES TO PARAMETER VARIATION AND CHANGE IN DIMENSION OF MATHEMATICAL MODEL

In the literature pertaining to optimal control almost all the intensive studies in the field of sensitivity are related to the evaluation of the sensitivity of performance of a system, as characterized by its model, with respect to small parameter variations[5]. The specific values of the parameters used for design and control will differ to some extent from the actual values. Therefore, it is of practical importance to the process designer to know how sensitive the process designed by him is to these parameter uncertainties which may be due to, for example, the environmental and aging effects, the choice of a mathematical model both for the controlled system and the controller, and the measurements. Suppose that the value estimated for a parameter differs by 10 per cent from the true value. Does deviation of this magnitude significantly affect the optimal design of the process? The sensitivity analysis used to attempt to obtain quantitative answers to this question is thus an integral part for the complete optimal design of a process.

Table 1 and figures 5 and 6 in Part 1[1] show the effect of variation of the parameter r_1 (the recycle ratio of air) on the optimal conditions. It can be seen that the system is not sensitive to the variation of this parameter when the magnitude of the variation is small. The effect, however, is noticeable when the variation is large. Table 2 and figures 3 and 4 in Part 2[2] indicate the effect of the change of the parameter r (the ratio of the time constants of the system proper, cabin or room, to that of the heat exchanger). This effect is very small. Table 3 and figures 5 and 7 in Part 2[2] show the effect of variation of the parameter r_{11} (the volume fraction of the first pool) on the optimal conditions. This effect is substantial. To illustrate this aspect of the sensitivity analysis, the dimensionless room temperatures as a function of the dimensionless time under the optimal conditions presented in the previous articles of this series are summarized in figure 1. Curves 1 and 2 represent the change of the dimensionless room temperature as a function of time for the system with one CST room or cabin. Curve 1 is for the system with the heat exchanger having a negligibly small time constant ($\tau_2 \to 0$, $\tau_1 = 50$s). Curve 2 is for the system containing a heat exchanger with small but not negligible time constant ($\tau_2 = 5$s, $\tau_1 = 50$ s). Comparison of Curves 1 and 2 indicates that there is definitely a small but not negligible effect of the dimensional change of the system equation which is caused by neglecting the time constant of the heat exchanger. A similar conclusion can be obtained by comparing Curve 3 and Curve 4, which are for the systems represented by the two CST's-in-series model. Comparison of the group of curves, Curves 1 and 2, with the group, Curves 3 and 4, shows that the complexity of the model describing the system component (room or cabin) has a definite effect on the predicted performance of the system. It can be seen that such effect is substantial for the particular models considered here, which are the one CST model and the two CST's-in-series model.

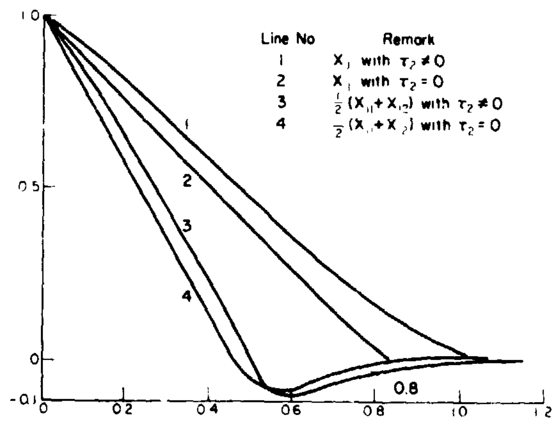

Fig. 1. The sensitivity to change in dimensions of the mathematical model.

THE SENSITIVITY TO CHANGE IN CONSTRAINTS

The system sensitivity to changes in constraints imposed on the system, more specially, imposed on the state variable (temperature) of the system is discussed here.

For this purpose, results presented in Part 4 of this series[4] are summarized in figure 2. Note that the systems considered are all represented by the two CST's-in-series model (with equal size tank).

Since the constraint is imposed on x_{11} (dimensionless temperature of the first compartment of the model), naturally the effect of the change of constraint on this state variable cannot be neglected. However, the effect on the dimensionless temperature of the second compartment, which is also the exit temperature of air from the room or cabin, is negligibly small. The effect of the change in the constraint on control policy is also very appreciable as indicated by the plot of θ vs. t in the same figure. These observations are valid for the particular model considered and for the particular values of the model parameters employed here.

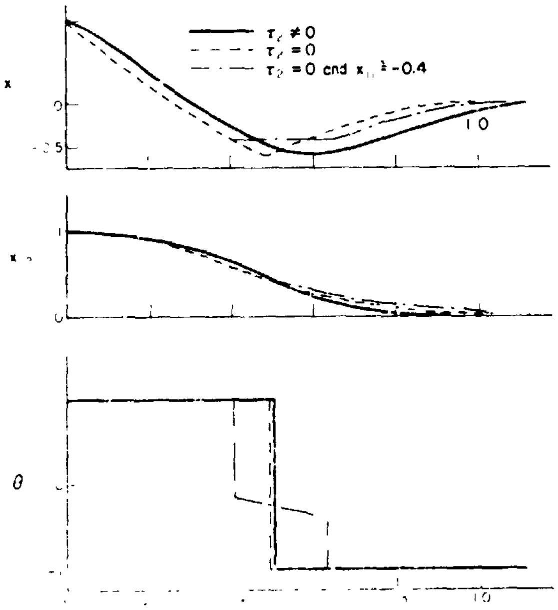

Fig. 2. The sensitivity to shift of the constraints of the mathematical model.

CONCLUSIONS

It should be evident that thorough consideration must be given to numerous aspects of the system in order to achieve a meaningful sensitivity analysis. The following must be considered in order to obtain the desired information.

1. Sensitivity to parameter variation.
2. Sensitivity to change in dimensions of the mathematical models.
3. Sensitivity to change in constraints.
4. Sensitivity to transition between continuous and discrete models.
5. Sensitivity to the influence of the functional blocks of a system. Items 1, 2 and 3 have been considered in this paper; items 4 and 5 will be briefly discussed below.

In certain cases, an alternative may exist in representing the model either by a continuous model or a discrete model. If the predicted behavior of the system is very sensitive to a particular type of the model, use of an appropriate model becomes important.

Complex systems generally consist of several functional blocks, stages or units. Complex chain reactions may follow alternative reaction paths and produce different intermediate reactants. The sensitivity of the entire system or process to variation in the types of functional blocks which are contained in the system and to the relative locations of the functional blocks is called the structural sensitivity[5].

In this sequence of five short articles, we have mainly resorted to Pontryagin's maximum principle and variational techniques to determine optimal temperature control policies of several fairly simple but typical life support systems. It is obvious that the maximum principle and variational techniques do not constitute the entirety of the modern control theory nor are the systems with temperature control the only type of life support systems. There are many facets to the modern control theory and there exists a wide variety of life support systems. For example, dynamic programming, originated by Bellman[11–13], has been and is being employed widely in solving optimal control problems. Its techniques and applications constitute a significant portion of the modern control theory. In life support systems humidity control and pressure control must often be provided besides temperature control and some life support systems are comprised of partially open spaces. It cannot be denied, however, that the maximum principle and variational techniques are major tools of the modern control theory[10,14,15] and that the temperature control system is the most vital component of practically every life support system. We believe that singling out particular but important techniques and applying them to fairly simple but significant examples facilitate presentation and understanding by readers of the basic aspects of the modern control theory and its applications to the control of life support systems.

It is well known that a majority of air conditioning systems and temperature controllers for life support systems works on the on-off or bang–bang principle. It appears, therefore, that the modern optimal control theory is very much suited for such systems. Admittedly, application of the modern control theory to the control of temperature in a small residential dwelling is the kind of luxury no one can afford or need in the forseeable future. There exist, however, many situations in which the duration of control and/or energy required for control must be critically adjusted. Such situations frequently can be found in applications of life support systems in space, underwater, and biomedical processes, and uses of the modern control theory in such applications deserve serious consideration.

REFERENCES

1. L. T. Fan, Y. S. Hwang, and C. L. Hwang, Applications of Modern Optimal Control Theory to Environmental Control of Confined Spaces and Life Support Systems, Part 1. Modeling and Simulation. *Build. Sci.*, **5**, 57 (1970).

2. L. T. FAN, Y. S. HWANG and C. L. HWANG, Applications of Modern Optimal Control Theory to Environmental Control of Confined Spaces and Life Support Systems. Part 2. The Basic Form of Pontryagin's Maximum Principle and Its Applications. *Build. Sci.*, **5**, 81 (1970).
3. L. T. FAN, Y. S. HWANG and C. L. HWANG, Applications of Modern Optimal Control Theory to Environmental Control of Confined Spaces and Life Support Systems, Part 3. Optimal Control of Systems in which State Variables have Equality Constraints at the Final Process Time. *Build. Sci.*, **5**, 125 (1970).
4. L. T. FAN, Y. S. HWANG and C. L. HWANG, Applications of Modern Optimal Control Theory to Environmental Control of Confined Spaces and Life Support Systems, Part 4. Control of Processes with Inequality Constraints Imposed on State Variables. *Build. Sci.*, **5**, 137 (1970).
5. R. TOMOVIC, Sensitivity Methods in Control Theory, (edited by L. RADNOVIC) Pergamon Press, London (1966).
6. T. TAKAMATSU, KAGAKU KOGAKU, *Chem. Eng. Japan*, **31**, 331 (1967).
7. R. TOMOVIC, *Sensitivity Analysis of Dynamic Systems*, McGraw-Hill, New York (1964).
8. J. S. DEMSKI, *J. Ind. Eng.*, **19**, 292 (1968).
9. B. PAGUREK, Ph.D. Thesis, University of Toronto, Toronto, Canada, (1965).
10. A. P. SAGE, *Optimum Systems Control*, Prentice-Hall, N.J., (1968).
11. L. E. STAMETS, Nonlinear Parameter Estimation and Sensitivity Analysis for Chemical Process Systems, Ph.D. dissertation, Kansas State University, Manhattan, Kansas.(1969).
12. R. BELLMAN, *Some Vistas of Modern Mathematics*, University of Kentucky Press, Lexington, (1968).
13. R. BELLMAN, *Dynamic Programming*, Princeton Univ. Press, N.J., (1959).
14. L. T. FAN, *The Continuous Maximum Principle: A Study of Complex Systems Optimization*. Wiley, New York (1966).
15. G. A. BLISS, *Lectures on the Calculus of Variations*, University of Chicago Press, Chicago, (1946).

On examine les sensibilités d'une cabine avec contrôle de température qui a été considérée dans les premières quatre parties de cette série. Elles comprennent les sensibilités (1) aux variations de paramètres (2) au changement de dimensions de modèles mathématiques et (3) au changement de contraintes sur les variables d'état.

Le système n'est pas sensible à la variation du paramètre (le rapport de recyclage d'air) lorsque la granduer de la variation est petite. L'effet est cependant important lorsque la variation est grande. L'effet du changement du paramètre (le rapport des constantes de temps du système lui-même à celui de l'échangeur de chaleur) est très petit. L'effet de la variation du paramètre (la fraction de volume du premier bassin dans le modèle des deux CST en série) sur les conditions optimales est sustantiel.

Il existe un effet petit mais non négligeable du changement dimensionnel dans les équations du système, qui est dû à la constante de temps de l'échangeur de chaleur étant négligée. La complexité du modèle décrivant le composant du système a un effet distinct sur la performance prévue du système. L'effet est apparent pour les modèles particuliers considérés ici qui sont le modèle à un CST et le modèle à deux CST en série.

Die Empfindlichkeit einer Kabine mit Temperaturkontrolle, welche in den ersten vier Teilen dieser Serie ins Auge gefasst wurde, wird untersucht. Man schliesst ein Empfindlichkeit gegen (1) Parameteränderung, (2) Änderung in Dimensionen mathematischer Modelle und (3) Änderung in Begrenzung der Zustandsveränderlichen.

Das System ist nicht gegen Änderung des Parameters (Luftkreislaufverhältnis) empfindlich, wenn der Grad der Änderung klein ist. Die Wirkung ist jedoch merkbar, wenn die Änderung gross ist. Die Wirkung der Änderung des Parameters, (das Verhältnis der Zeitkonstante des eigentlichen Systems zu der des Wärmeaustauschers) ist sehr klein. Die Wirkung der Parameteränderung (der Raumbruchteil des ersten Behälters in dem zwei CST's-in-series Modell) auf die Optimalbedingungen ist beträchtlich.

Es ergibt sich eine kleine, aber nicht unbedeutende Wirkung der Dimensionsänderung in den Systemgleichungen, die durch Vernachlässigung der Zeitkonstante des Wärmeaustauschers verursacht wird. Die Komplexität des Modells, das die Systemkomponente beschreibt, hat eine bestimmte Wirkung auf die vorausgesagte Leistung des Systems. Die Wirkung ist offensichtlich bei den hier dargestellten besonderen Modellen, welche das eine CST Modell und das zwei CST's-in-series Modell sind.

(d) 6

LOCKHEED

THERMODYNAMICS AND THERMOPHYSICS OF SPACE FLIGHT

PROCEEDINGS

March 23-25, 1970

Palo Alto, Calif.

APPLICATION OF MODERN OPTIMAL CONTROL THEORY TO ENVIRONMENTA'. CONTROL OF CONFINED SPACES AND LIFE SUPPORT SYSTEMS*

L. T. Fan, Y. S. Hwang, and C. L. Hwang
Institute for Systems Design and Optimization
Kansas State University, Manhattan, Kansas 66502

Abstract

Mathematical model of an environmental control system which consists of a confined space or cabin, a heat exchanger, and a feedback element such as a thermostat are presented. The performance equations of the system, which represent the dynamic characteristics of the air-conditioned cabin (the system proper) and the heat exchanger (the control element of the system), are derived. In the basic model the flow of air in the confined space is considered to be in the state of complete mixing and the disturbance is caused by an impulse heat input. The flow of air in the confined space or cabin characterized by the two completely stirred tanks-in-series (a CST's-in-series) model is also considered. Pontryagin's maximum principle, which is a keystone of the modern optimal control theory, is applied to the determination of optimal control policies of the temperature control of the life support systems.

1. INTRODUCTION

This paper contains results of the original investigation on the environmental control of confined spaces of life support systems or more specifically the temperature control of life support systems by means of the modern control theory. A life support system is a system for creating, maintaining, and controlling an environment so as to permit personnel to function efficiently. The control of temperature is probably the most important role of the life support system.

The need for providing an automatic control system to an air-conditioning system has long been recognized.[1, 2] It is also a well known fact that use of the automatic control is necessary for the life support system of a space cabin or submarine or underground shelter.[3, 4] It appears that analysis and synthesis of the control systems for the air-conditioning and life support systems have so far been carried out by the classical approach.[1, 2, 3, 4]

The classical approach to the analysis and synthesis of an automatic control system is essentially a trial-and-error procedure or a disturbance response (or input-output) approach. Extensive use is made of the transform methods such as the Laplace transform (s-domain), Fourier transform (ω-domain), and z transform (discrete time-domain). Even though mathematics is extensively used, the classical approach is essentially an empirical one.[5]

In recent years, an approach to the analysis and synthesis of a control system, which is distinctly

*This work was supported by the Air Force Office of Scientific Research, Office of Aerospace Research, United States Air Force, Under Contract F44620-68-0020 (Themis Project), and NASA Grant under Contract NGR-17-001-034.

different from the classical one, has been developed. This modern approach is generally called the modern (optimal) control theory.[5, 6, 7, 8, 9, 10, 11] It is based on the state-space characterization of a system. The state-space is the abstract space whose coordinates are the state properties of the system or the variables which define the characteristics of the system.[5] This approach involves mainly maximization or minimization of an objective function (functional) which is a function of state (plant) and control variables which are in turn functions of time and/or distance coordinate. The objective function is specified, constraints are imposed on the state and decision variables, and an optimal control policy is determined by extremizing the objective function by means of mathematical techniques such as the calculus of variations, maximum principle, and dynamic programming.[5, 6] This modern approach is entirely theoretical in the sense that no trial-and-error is involved in "adjusting the controller".

There are reasons to believe that the classical approach suffices in the analyses and syntheses of the control systems for a majority of air-conditioning and life support systems because usually the requirements are not extremely critical and specifications are not very tight. It is, therefore, justifiable that most of the control and dynamic investigations of air-conditioning and life support systems, which have appeared in the open literature, are based on the classical approach.[12 - 20] There is, however, a certain incentive in applying the modern approach to analysis and synthesis of automatic environmental control systems in space crafts, submarines, underground civil defense shelters and certain medical facilities. In these systems, very stringent requirements in the response time, control effort, and others are imposed. For example, the control system of a space craft must have an extremely small response time and furthermore, the amount of energy required for the control effort must be very small because of the weight limitation imposed on the space craft.

In the present work, the emphases are on the use of the maximum principle and related variational techniques.[5, 7, 8, 9, 10, 11] Their applications will be illustrated by means of concrete numerical examples.

The examples are concerned with the temperature control of a life support system consisting of an air-conditioned cabin subject to an impulse heat disturbance and of a heat exchanger. The optimal policies of the system where the flow of air in the cabin can be characterized by the one completely stirred tank model and by the two completely stirred tanks-in-series (2 CST's-in-series) model are studied.

2. PERFORMANCE EQUATIONS FOR ONE COMPARTMENT MODEL

A control system usually consists of three elements: the feedback element, the control element, and the system proper.[23] The feedback element in a life support control system or an environmental control system may be composed of a thermostat, humidistat and pressure regulator, or any combination of these, depending on the purpose of control. The control element may include a heat exchanger, humidifier, dehumidifier, blower, portable air-conditioner, or any combination of these, depending on the objective of control. For instance, both the thermostat and heat exchanger are often used to control the air temperature inside a building. The system proper may be a confined space, e.g., an underground shelter, a space vehicle, a space suit, a submarine or a building.

The system considered here is shown schematically in Fig. 1. The confined space may be a typical office located in a multi-story building or the cabin of a spaceship. Air or oxygen or a mixture of oxygen and nitrogen is circulated through the room or confined space via an air duct by mechanical means, e.g., a blower or fan. Control of air temperature in the system is accomplished with a duct system. The thermostat in the system adjusts the position of the control valve of the heat exchanger in order to provide the desired temperature.

The performance equations of the system, which represent the dynamic characteristics of the system and system components will be derived.

A. The System Proper

The following three main assumptions are made concerning the system proper:

(1) Room or cabin air is well mixed, or stated in another way, air temperature within the system is uniform throughout at any instant in time.

(2) The thermal capacitance of room walls, floor, ceiling, and window is neglected, as well as that of any furniture within the system.

(3) Heat loss through the walls and windows is negligible.

The performance equation of the system proper can be obtained by using the continuity law or heat balance. Assuming that the heat disturbance is an impulse form, the cabin performance equation becomes

$$\tau_1 \frac{dT_c}{d\alpha} + T_c = r_1 T_i + r_2 T_2 + \tau_1 T_d \, \delta(\alpha)$$

$$T_c = 0 \quad \text{at} \quad \alpha = 0 \tag{1}$$

where T_c is the room temperature, T_i, the temperature of the circulation air into the system proper, T_2, outside air temperature, T_d, disturbance temperature, τ_1, time constant of the system proper, r_1, the fraction of circulation air, r_2, the fraction of fresh air, α, the time, and $\delta(\alpha)$, impulse heat disturbance function.

In dimensionless form equation (1) becomes

$$\frac{dx_1}{dt} + x_1 = \frac{r_1 K_1 x_2}{K_4} + r_2 K_1 + K_1 \sigma \delta(t)$$

$$x_1 = 0 \quad \text{at} \quad t = 0 \tag{2}$$

B. The Control Element

The heat exchanger which is the control element of the system under consideration can perform its control function in various ways, for example, by changing the temperature or flow rate of the heat transfer medium, or changing both. The performance equation of the control element can be obtained again by employing the continuity law or heat balance, which can be expressed in equation form as follows:

$$\tau_2 \frac{dT_i}{d\alpha} + T_i = T_c - \frac{Q_w \rho_w C_{pw} (T_{wh} - T_{wc})}{Q_1 \rho C_p} \tag{3}$$

where τ_2 is the time constant of the heat exchanger. Note that $Q_w \rho_w C_{pw}(T_{wh} - T_{wc})$ is the amount of heat removed from or added to the system which can be controlled by adjusting either Q_w when ρ_w, C_{pw}, and $(T_{wh} - T_{wc})$ are constant, or $(T_{wh} - T_{wc})$ when Q_w, ρ_w, and C_{pw} are kept constant, or both Q_w and $(T_{wh} - T_{wc})$ when ρ_w and C_{pw} are constant. In order to have a mathematically neat form, a hypothetical temperature T_r is defined

$$T_r = Q_w \rho_w C_{pw} (T_{wh} - T_{wc}) / Q_1 \rho C_p \tag{4}$$

Inserting this definition into equation (3) yields

$$\tau_2 \frac{dT_i}{d\alpha} + T_i = T_c - T_r \tag{5}$$

or in dimensionless form

$$\frac{\tau_2}{\tau_1} \frac{dx_2}{dt} + x_2 = \frac{x_1 K_4}{K_1} - K_4 (K_2 \theta + K_3) \tag{6}$$

C. The Feedback Element - Thermostat

Here we simply assume that the sensing element measures the room temperature instantaneously and that there is no accumulation of heat in the element, or for simplicity, it will be assumed that the sensing element is the zero order element with its time constant, τ_3, equal to zero. Reference 23 gives a detailed explanation of the response of the thermostat.

3. PERFORMANCE EQUATIONS FOR TWO COMPARTMENTS MODEL

Next, let us consider the case in which air in the room or cabin is no longer in the state of complete mixing. Specifically, we shall consider the case in which flow of air in the room can be characterized by two completely stirred tanks (or pools or compartments) (2 CST's)-in-series model.

The following assumptions must be added to those already made for the system proper in the preceding section:

a) The room is divided into two well mixed compartments in series. Volume of each pool is denoted by V_{11} and V_{12}, and the temperature in each pool is denoted by T_{c1} and T_{c2}.

b) Backflow of air from the second compartment to the first compartment is negligible.

c) Disturbances are equally distributed over the system.

d) Fresh air comes into the first compartment at a constant flow rate, while exhaust air is released from the second compartment at a constant flow rate.

The schematic diagram of the system is shown in Fig. 2. The performance equation for each pool can be obtained by using the transient heat balance around each compartment. Thus, for pool 1, we have

$$\tau_{11} \frac{dT_{c1}}{d\alpha} + T_{c1} = r_1 T_i + r_2 T_2 + \frac{\tau_{11}}{\tau_1} \tau_{11} T_d \delta(\alpha) \quad (7)$$

$$T_{c1} = 0 \quad \text{at} \quad \alpha = 0$$

or

$$\tau_{11} \frac{dT_{c1}}{d\alpha} + T_{c1} = r_1 T_i + r_2 T_2$$

$$T_{c1} = T_{c10} \quad \text{at} \quad t = 0^+$$

Similarly, for pool 2 we have

$$\tau_{12} \frac{dT_{c2}}{d\alpha} + T_{c2} = T_{c1} + \frac{\tau_{12}}{\tau_1} \tau_{12} T_d \delta(\alpha) \quad (8)$$

$$T_{c2} = 0 \quad \text{at} \quad \alpha = 0$$

or

$$\tau_{12} \frac{dT_{c2}}{d\alpha} + T_{c2} = T_{c1}$$

$$T_{c2} = T_{c20} \quad \text{at} \quad \alpha = 0^+$$

or in dimensionless form

$$\frac{dx_{11}}{dt} + r_{11} x_{11} = a_{11} x_2 + a_{12} + a_{13} (t) \quad (9)$$

$$\frac{dx_{12}}{dt} + r_{12} x_{12} = a_{21} x_{11} + a_{2?} (t) \quad (10)$$

$$\frac{dx_2}{dt} + r x_2 = a_{42} x_{12} - a_5 - a_6 \quad (11)$$

4. OPTIMAL CONTROL OF ONE COMPARTMENT MODEL

Suppose that the dynamic behavior of a life support system consisting of an air-conditioned room or cabin subject to the impulse heat disturbance and a heat exchanger with negligibly small time constant ($\tau_2 \to 0$). Then the system performance equation in dimensionless form can be obtained by combining equations (2) and (6) and letting $\tau_2 \to 0$.

$$\frac{dx_1}{dt} + r_2 x_1 = r_2 K_1 - r_1 K_1 K_2 - r_1 K_1 K_3 \quad (12)$$

with

$$x_1(0) = 1 \quad \text{at} \quad t = 0^+$$

$$x_1(T) = 0 \quad \text{at} \quad t = T$$

where T is the unspecified final control time. We wish to determine θ so that the response of the system can return to its desired state in a minimum period of time, that is, to minimize

$$S = \int_0^T dt \quad (13)$$

If an additional state variable x_2 is introduced as

$$x_2(t) = \int_0^t dt,$$

it follows that

$$\frac{dx_2}{dt} = 1, \quad x_2(0) = 0 \quad (14)$$

The problem is thus transformed into that of minimizing $x_2(T)$.

According to Pontryagin's maximum principle,[7, 8] the Hamiltonian is

$H[z(t), x(t), \theta(t)]$

$$= z_1 \frac{dx_1}{dt} + z_2 \frac{dx_2}{dt}$$

$$= z_1[-r_2x_1 + r_2K_1 - r_1K_1K_2\theta - r_1K_1K_3] + z_2 \quad (15)$$

The components of the adjoint vector are defined by

$$\frac{dz_1}{dt} = -\frac{\partial H}{\partial x_1} = r_2z_1 \quad (16)$$

$$\frac{dz_2}{dt} = -\frac{\partial H}{\partial x_2} = 0, \quad z_2(T) = 1 \quad (17)$$

Solutions of equations (16) and (17) are

$$z_1(t) = Ae^{r_2t} \quad (18)$$

$$z_2(t) = 1, \quad 0 \le t \le T \quad (19)$$

where A is the integration constant to be determined later. Inserting equation (19) into equation (15) yields

$$H = -r_1K_1K_2z_1\theta - r_2z_1x_1 + r_2K_1z_1 - r_1K_1K_3z_1 + 1 \quad (20)$$

Therefore, the switching function, H^*, the portion of H which depends on θ, is

$$H^* = -r_1K_1K_2z_1\theta \quad (21)$$

Note that minimization of the Hamiltonian with respect to θ corresponds to that of the objective function. Equation (21), however, indicates that the minimization of the Hamiltonian with respect to θ is equivalent to that of the switching function. Thus, minimization of the switching function corresponds to that of the objective function. Equation (21) also indicates that for the switching function to assume the minimum value, θ must assume its minimum allowable or its maximum allowable value depending on the sign of the coefficient of θ.

$$\begin{aligned} \theta &= \theta_{max} = 1 \quad \text{if} \quad -r_1K_1K_2z_1 < 0 \\ \theta &= \theta_{min} = -1 \quad \text{if} \quad -r_1K_1K_3z_1 > 0 \end{aligned} \quad (22)$$

Time optimal control policy of this type is of bang-bang type.[3, 4, 6, 9]

In the case where the coefficient of θ in equation (21) vanishes, we have the possibility of singular control.[10] For singular control, the control variable takes on values which are intermediate to θ_{max} and θ_{min}; hence the name intermediate control is also used in place of the singular control.[10] Also inertialess control will be considered. An inertialess controller has the ability to shift from θ_{max} to θ_{min} instantaneously and vice versa.

The maximum principle now requires that the system equations, equations (12) and (14), be integrated simultaneously with the adjoint equation (16) so that the two-point boundary conditions

$$x_1(0) = 1, \qquad x_1(T) = 0$$

$$x_2(0) = 0, \qquad x_2(T) = \text{undetermined}$$

$$z_1(0) = \text{undetermined}, \quad z_1(T) = \text{undetermined}$$

are satisfied. For this minimum time problem extremum of the Hamiltonian must vanish at every point of its response.[7, 8]

In order to bring the initial deviated state $x_1(0^+) = 1$ to the final desired operating state $x_1(T) = 0$, we intuitively reject the control $\theta = \theta_{min} = -1$ (which corresponds to the minimum cooling action). Equation (12) can be integrated with the conditions

$$\theta = \theta_{max} = 1 \quad (23)$$

and

$$x_1(0) = 1 \quad \text{at} \quad t = 0^+ \quad (24)$$

as

$$x_1(t) = e^{-r_2t} + \frac{1}{r_2}(r_2K_1 - r_1K_1K_2 - r_1K_1K_3)(1 - e^{-r_2t})$$

$$= e^{-r_2t} + \frac{\eta}{r_2}(1 - e^{-r_2t}) \quad (25)$$

where

$$\eta = r_2K_1 - r_1K_1K_2 - r_1K_1K_3 \quad (26)$$

The integration constant A in equation (18) can be determined by using the condition that minimum

H is zero for all the process time in time optimal control. At $t = 0^+$, we have from equations (18), (20), (23) and (24)

$$A = z_1(0^+) = \frac{-1}{\eta - r_2}$$

and

$$z_1(t) = \frac{-1}{\eta - r_2} e^{r_2 t} \tag{27}$$

Equation (27) implies that $z(t)$ will not change sign since $z_1(t) \to 0$ only when t approaches negative infinity, or in other words, control will not shift from θ_{max} to θ_{min} (or from θ_{min} to θ_{max}). Therefore, this problem is a particular case of bang-bang control which has the bang part only. The optimal control policy starts with $T_{r\,max}$ and then keeps operating at the upper bound of T_r until the final desired state is reached. The final control time can be obtained from equations (20) and (33) together with the final condition

$$x_1(T) = 0 \quad \text{at} \quad t = T$$

as follows

$$H = z_1(T)[-r_2 x_1(T) + \eta] + 1 = 0$$

or solving for $z_1(T)$

$$z_1(T) = \frac{-1}{\eta} \tag{28}$$

Also we have, from equation (27), at $t = T$

$$z_1(T) = \frac{-1}{\eta - r_2} e^{r_2 T} \tag{29}$$

Solving for T from equations (28) and (29) gives

$$T = \frac{1}{r_2} \ln\left(\frac{\eta - r_2}{\eta}\right) \tag{30}$$

This solution may be verified by inserting it into equation (25) as

$$\begin{aligned} x_1(T) &= e^{-r_2 T} + \frac{\eta}{r_2}\{1 - e^{r_2 T}\} \\ &= \exp\left[-r_2 \frac{1}{r_2} \ln\left(\frac{\eta - r_2}{\eta}\right)\right] \\ &\quad + \frac{\eta}{r_2}\left(1 - \exp\left[-r_2 \frac{1}{r_2} \ln\left(\frac{\eta - r_2}{\eta}\right)\right]\right) \\ &= 0 \end{aligned}$$

This indicates that the hamiltonian is kept at zero at every point of its response in this minimum time problem. For

$$r_1 = 0.8 \qquad r_2 = 0.2$$

$$K_1 = 0.5 \qquad K_2 = 1.5$$

$$K_3 = 1.5 \qquad \eta = 2,$$

we have from equations (25), (27) and (30)

$$z_1(t) = \frac{1}{1.3} e^{0.2t} = 0.769 e^{0.2t} \tag{31}$$

$$x_1(t) = 6.5 e^{-0.2t} - 5.5 \tag{32}$$

$$T = 0.8353$$

and from equation (31)

$$z_1 = \frac{1}{1.3} = 0.769 \quad \text{at} \quad t = 0$$

$$z_1 = \frac{1}{1.1} = 0.909 \quad \text{at} \quad t = T$$

Equations (31) and (32) are graphically shown in Fig. 3. The state variable x_1 approaches asymptotically to the final state, the control variable remains at unity until the final state is reached, and the adjoint vector increases asymptotically. The optimal control can be verified by computing H at an arbitrary point, say 0.5, of the time coordinate as follows:

$$t = 0.5$$

$$z_1(t) = e^{-0.1}/1.3$$

$$x_1(t) = 6.5 e^{-0.1} - 5.5$$

and

$$\begin{aligned} H &= z_1(t)[-r_2 x_1 + r_2 K_1 - r_1 K_1 K_2 - r_1 K_1 K_3] + 1 \\ &= \frac{e^{0.1}}{1.3}[-0.2(6.5e^{-0.1} - 5.5) + 0.2 \times 0.5 - 1.2] + 1 \\ &= 0 \end{aligned}$$

This computation shows that the minimum value of H is zero at every point of this continuous process.

Four cases with different cooling capacities of the heat exchangers are considered here. $T_{r\,max}$ and $T_{r\,min}$ take the following values for these four cases:

Case 1: $T_{r\ max} = 30°C \quad T_{r\ min} = 0°C$

Case 2: $T_{r\ max} = 20°C \quad T_{r\ min} = 0°C$

Case 3: $T_{r\ max} = 10°C \quad T_{r\ min} = 0°C$

Case 4: $T_{r\ max} = 5°C \quad T_{r\ min} = 0°C$

The numerical solutions for these cases are obtained from equations (25), (27) and (30), and are tabulated in Table 1.

5. OPTIMAL CONTROL OF TWO COMPARTMENTS MODEL

Let us again consider a life support system consisting of an air-conditioned room and a heat exchanger as in the preceding example. However, suppose that the flow of air in the room can be characterized by the two CST's-in-series model. Again assuming that the heat exchanger has a negligibly small time constant ($\tau_2 \to 0$), the system performance equations, equations (9), (10), and (11), become

$$\frac{dx_{11}}{dt} + r_{11}x_{11} = a_{11}a_{42}'x_{12} - a_{11}a_5' \; - a_{11}a_6' + a_{12} \tag{33}$$

$$\frac{dx_{12}}{dt} + r_{12}x_{12} = a_{21}x_{11} \tag{34}$$

The initial and the final conditions are

$$\begin{aligned} x_{11}(0^+) &= x_{12}(0^+) = 1 \quad \text{at} \quad t = 0^+ \\ x_{11}(T) &= x_{12}(T) = 0 \quad \text{at} \quad t = T \end{aligned} \tag{35}$$

where T is unspecified. We are to minimize

$$S = \int_0^T dt \tag{36}$$

Introducing an additional state variable

$$x_3(t) = \int_0^t dt,$$

we have

$$\frac{dx_3}{dt} = 1, \quad x_3(0) = 0 \tag{37}$$

The problem is thus transformed into that of minimizing $x_3(T)$.

Then, the Hamiltonian is

$$\begin{aligned} H(z, x, \theta) &= z_{11}(-r_{11}x_{11} + a_{11}a_{42}'x_{12} - a_{11}a_5'\theta - a_{11}a_6' + a_{12}) \\ &\quad + z_{12}(-r_{12}x_{12} + a_{21}x_{11}) + z_3 \end{aligned} \tag{38}$$

According to the definition of the adjoint variables, we have

$$\frac{dz_{11}}{dt} = -\frac{\partial H}{\partial x_{11}} = r_{11}z_{11} - a_{21}z_{12} \tag{39}$$

$$\frac{dz_{12}}{dt} = -\frac{\partial H}{\partial x_{12}} = -a_{11}a_{42}'z_{11} + r_{12}z_{12} \tag{40}$$

$$\frac{dz_3}{dt} = -\frac{\partial H}{\partial x_3} = 0, \quad z_3(T) = 1 \tag{41}$$

The solution of z_3 can be obtained from equation (41) as

$$z_3(t) = 1, \quad 0 \le t \le T \tag{42}$$

Equation (38) can be rewritten as

$$\begin{aligned} H(z, x, \theta) &= z_{11}(-r_{11}x_{11} + a_{11}a_{42}'x_{12} - a_{11}a_5'\theta - a_{11}a_6' + a_{12}) \\ &\quad + z_{12}(-r_{12}x_{12} + a_{21}x_{11}) + 1 \end{aligned} \tag{43}$$

Therefore, the switching function H^* is

$$H^* = -a_{11}a_5'z_{11}\theta \tag{44}$$

Inspection of H^* shows that the optimal controller should be of a bang-bang type. The control action for this problem, however, is constrained in such a manner that

$$|\theta| \le 1 \tag{45}$$

The conditions for which the Hamiltonian is to be minimum are

$$\begin{aligned} \theta &= \theta_{max} = 1 \quad \text{if} \quad -a_{11}a_5'z_{11} < 0 \\ \theta &= \theta_{min} = -1 \quad \text{if} \quad -a_{11}a_5'z_{11} > 0 \end{aligned} \tag{46}$$

In order to bring the initial deviated state, $x_{11}(0^+) = x_{12}(0^+) = 1$ at $t = 0^+$, to the final desired operating state, $x_{11}(T) = x_{12}(T) = 0$, at $t = T$, we intuitively employ the control action of $\theta = \theta_{max} = 1$ (maximum cooling action). Substituting this value of θ into equations (33) and (34) and then eliminating x_{11}, we have

$$\frac{d^2x_{12}}{dt^2} + (r_{11} + r_{12}) \frac{dx_{12}}{dt} + (r_{11}r_{12} - a_{11}a_{42}'a_{21})x_{12}$$
$$+ a_{11}a_5'a_{21} + a_{11}a_{21}a_6' - a_{12}a_{21} = 0 \qquad (47)$$

Solution of x_{12} can be written in the form

$$x_{12} = Ae^{\lambda_{11}t} + Be^{\lambda_{12}t} + K, \quad 0 \le t \le t_s \qquad (48)$$

where λ_{11} and λ_{12} are roots of the characteristic equation

$$\lambda^2 + (r_{11} + r_{12})\lambda + (r_{11}r_{12} - a_{11}a_{21}a_{42}') = 0$$

and

$$K = \frac{a_{11}a_5'a_{21} + a_{11}a_{21}a_6' - a_{12}a_{21}}{a_{11}a_{42}'a_{21} - r_{11}r_{12}}$$

Inserting equation (48) and its derivative to equation (34) and solving for x_{11} yield

$$x_{11}$$
$$= \frac{1}{a_{21}}[(\lambda_{11} + r_{12})Ae^{\lambda_{11}t} + (\lambda_{12} + r_{12})Be^{\lambda_{12}t} + r_{12}K],$$
$$0 \le t \le t_s \qquad (49)$$

Constants A and B in equations (48) and (49) can be determined by employing the initial condition, equation (35) and Cramer's rule as follows:

$$A = \frac{\begin{vmatrix} a_{21} - r_{12}K & r_{12} + \lambda_{12} \\ 1 - K & 1 \end{vmatrix}}{\begin{vmatrix} r_{12} + \lambda_{11} & r_{12} + \lambda_{12} \\ 1 & 1 \end{vmatrix}}$$

$$= \frac{a_{21} - r_{12} - \lambda_{12} + \lambda_{12}K}{\lambda_{11} - \lambda_{12}}$$

and

$$B = \frac{\begin{vmatrix} r_{12} + \lambda_{11} & a_{21} - r_{12}K \\ 1 & 1 - K \end{vmatrix}}{\lambda_{11} - \lambda_{12}}$$

$$= \frac{r_{12} + \lambda_{11} - \lambda_{11}K - a_{21}}{\lambda_{11} - \lambda_{12}}$$

For $\theta = -1$, $x_{11}(t)$ and $x_{12}(t)$ are solved by using equations (33) and (34).

$$x_{11}(t) = \frac{1}{a_{21}} [(\lambda_{11} + r_{12})D_1e^{\lambda_{11}t}$$
$$+ (\lambda_{12} + r_{12})D_2 e^{\lambda_{12}t} + r_{12}K'], \qquad (50)$$
$$t_s \le t \le T$$

and

$$x_{12}(t) = D_1e^{\lambda_{11}t} + D_2e^{\lambda_{12}t} + K', \quad t_s \le t \le T \qquad (51)$$

where

$$K' = \frac{a_{11}a_{21}a_6' - a_{11}a_5'a_{21} - a_{12}a_{21}}{a_{11}a_{21}a_{42}' - r_{11}r_{12}}$$

Constants D_1 and D_2 can be specified by noting that x_{11} and x_{12} are continuous with respect to t. We obtain from equations (49) through (51) at $t = t_s$

$$x_{12}(t_s) = D_1e^{\lambda_{11}t_s} + D_2e^{\lambda_{12}t_s} + K'$$
$$= Ae^{\lambda_{11}t_s} + Be^{\lambda_{12}t_s} + K \qquad (52)$$

and

$$x_{11}(t_s)$$
$$= \frac{1}{a_{21}} [(\lambda_{11} + r_{12})D_1e^{\lambda_{11}t_s}$$
$$+ (\lambda_{12} + r_{12})D_2e^{\lambda_{12}t_s} + r_{12}K']$$
$$= \frac{1}{a_{21}} [(\lambda_{11} + r_{12})Ae^{\lambda_{11}t_s}$$
$$+ (\lambda_{12} + r_{12})Be^{\lambda_{12}t_s} + r_{12}K] \qquad (53)$$

Solving for D_1 and D_2 from these equations leads to

$$D_1 = A - E_1e^{-\lambda_{11}t_s} \qquad (54)$$

$$D_2 = B - E_2e^{-\lambda_{12}t_s} \qquad (55)$$

where

$$E_1 = \frac{\lambda_{12}(K' - K)}{\lambda_{12} - \lambda_{11}}$$

$$E_2 = \frac{\lambda_{11}(K' - K)}{\lambda_{11} - \lambda_{12}}$$

We see that D_1 and D_2 are functions of t_s. The value of t_s and that of T can be obtained by using the final conditions

$$x_{11}(T) = x_{12}(T) = 0 \quad \text{at} \quad t = T$$

Equations (50) and (51) thus become

$$D_1 e^{\lambda_{11}T} + D_2 e^{\lambda_{12}T} + K' = 0 \tag{56}$$

$$\frac{1}{a_{21}} [(\lambda_{11} + r_{12})D_1 e^{\lambda_{11}T} + (\lambda_{12} + r_{12})D_2 e^{\lambda_{12}T} + r_{12}K'] = 0 \tag{57}$$

Eliminating T from these equations and letting

$$E_3 = \frac{\lambda_{11}K'}{\lambda_{12} - \lambda_{11}}$$

$$E_4 = \frac{K'\lambda_{12}}{\lambda_{11} - \lambda_{12}},$$

we obtain

$$\left(\frac{E_4}{A - E_1 e^{-\lambda_{11}t_s}}\right)^{\lambda_{12}} = \left(\frac{E_3}{B - E_2 e^{-\lambda_{12}t_s}}\right)^{\lambda_{11}} \tag{58}$$

t_s can be solved from this equation by a trial and error procedure. Then D_1, D_2 and T can be calculated directly from equations (54) through (56).

The solutions of this problem are shown schematically in Figs. 4, 5 and 6 and are tabulated in Table 2. The solutions are very similar to those of the preceding example. However, one distinct difference between the response of the dimensionless room temperature in this problem and that in the preceding one is that the dimensionless room temperature can become negative in this problem while it can not be below zero in the preceding one.

6. CONCLUDING REMARKS

By now readers should be able to realize that the maximum principle has a certain advantage over other modern optimal control techniques. It is that it can be used to evaluate the number of switching points of the bang-bang control policy via the switching function and adjoint vectors. Two examples given in this article take advantage of this rule. Furthermore, the maximum principle can be applied not only to the system with linear performance equations but also to those with non-linear performance equations. Bellman[24] proved theoretically that the number of switching points is one less than the dimension of the problem for linear systems. However, this theory cannot be applied to non-linear systems.

It is worth noting that other forms of the objective functions can be considered. For example

$$S = \int_0^T [x_1]^2\, dt$$

$$S = \int_0^T [a + b_1(x_1)^2] dt$$

$$S = \int_0^T [\theta]^2\, dt$$

$$S = \int_0^T [a + c(\theta)^2] dt$$

$$S = \int_0^T [a + b_1(x_1)^2 + c(\theta)^2] dt$$

$$S = \int_0^T [b_1(x_1)^2 + c(\theta)^2] dt$$

$$S = \int_0^T |\theta| dt$$

The objective functions have different physical significance.[8, 9]

Table 1. Optimal solutions of the one CST model together with $\tau_2 = 0$

Case Number	Two Bounds of Control Variable	K_2	K_3	Final Time T
1	$T_{r\,max} = 30°C$ $T_{r\,min} = 0°C$	1.50	1.50	0.8353
2	$T_{r\,max} = 20°C$ $T_{r\,min} = 0°C$	1.00	1.00	1.2566
3	$T_{r\,max} = 10°C$ $T_{r\,min} = 0°C$	0.50	0.50	2.5541
4	$T_{r\,max} = 5°C$ $T_{r\,min} = 0°C$	0.25	0.25	5.493

Table 2. Optimal solutions of the two CST's-in-series model with $\tau_2 = 0$

Case	$T_{r\,max}$	$T_{r\,min}$	K_2	K_3	r_{11}	x_{11s}	x_{12s}	t_s	T
					1.2	-0.0760	0.7205	0.645	0.992
					1.5	-0.2298	0.4874	0.518	1.047
1	30	0	1.5	1.5	2.0	-0.6031	0.3862	0.471	1.078
					5.0	-3.8727	0.1852	0.598	1.007
					10.0	-9.4477	0.0896	0.715	0.956
					1.2	-0.0596	0.4538	0.975	1.275
					1.5	-0.1703	0.2984	0.775	1.225
2	20	0	1.0	1.0	2.0	-0.4526	0.2552	0.715	1.245
					5.0	-2.5520	0.1024	0.910	1.25
					10.0	-6.0425	0.05105	1.060	1.25
					1.2	-0.0343	0.1476	2.015	2.215
					1.5	-0.0998	0.1177	1.635	1.955
3	10	0	0.5	0.5	2.0	-0.2285	0.0882	1.500	1.860
					5.0	-1.1295	0.0353	1.875	2.115
					10.0	-2.6253	0.0171	2.180	2.310
					1.2	-0.0169	0.0192	4.520	4.625
					1.5	-0.0414	0.0223	3.780	3.940
4	5	0	0.25	0.25	2.0	-0.8831	0.0167	3.460	3.640
					5.0	-0.3865	0.0082	4.250	4.360
					10.0	-0.8734	0.0059	4.780	4.841

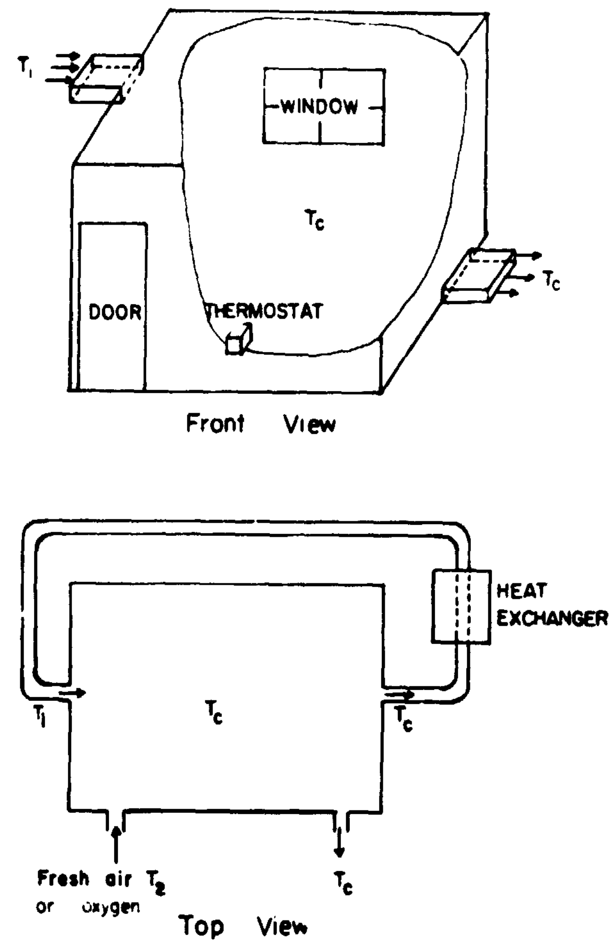

Fig. 1. Air-conditioned room.

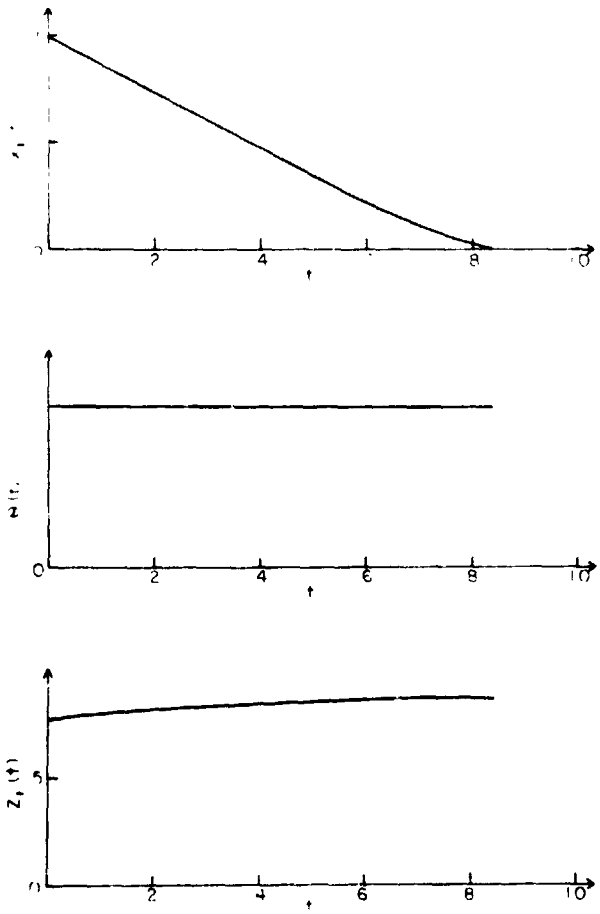

Fig. 3. Optimal control policy and system response of the one CST model with $T_2 = 0$

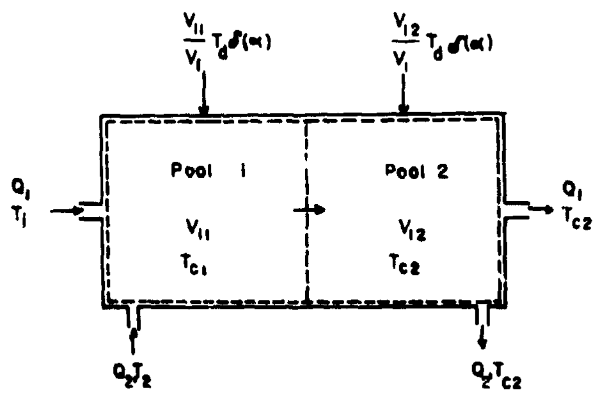

Fig. 2. Schematic expression of a room represented by the two CST's-in-series model.

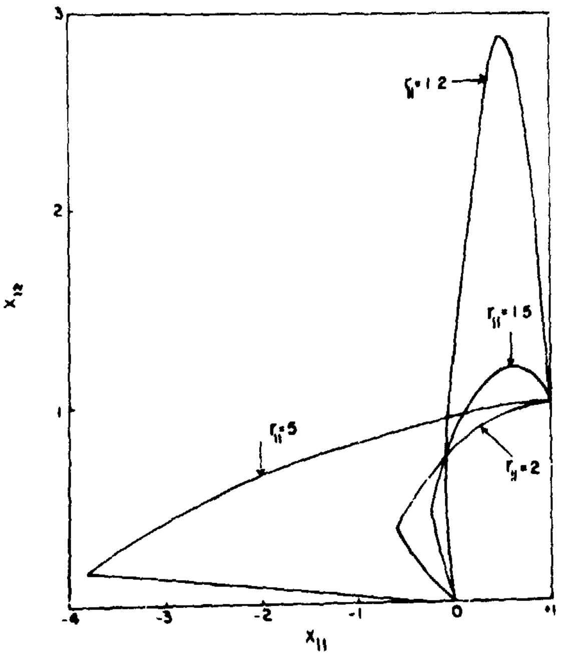

Fig 4 Phase plane plot for Case I of the two CST's – in – series model with $T_2 = 0$ and different values of r_{11}

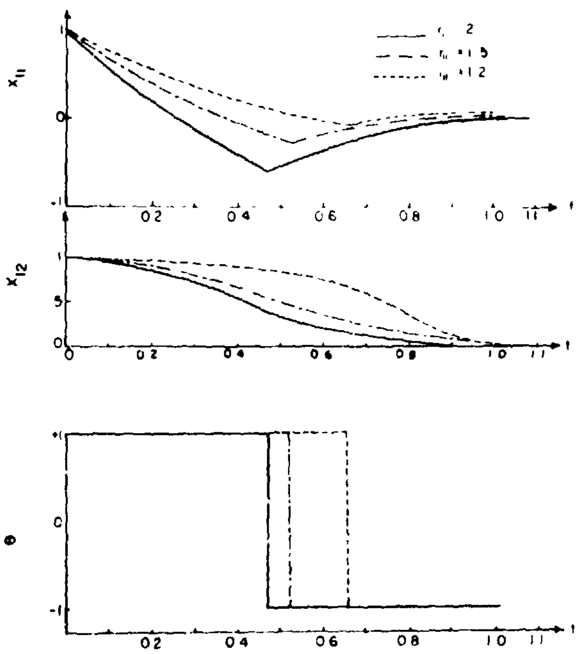

Fig 6 Optimal control policies and system responses of Case I of the two CST's-in-series model with $T_2 = 0$ and different values of r_{11}

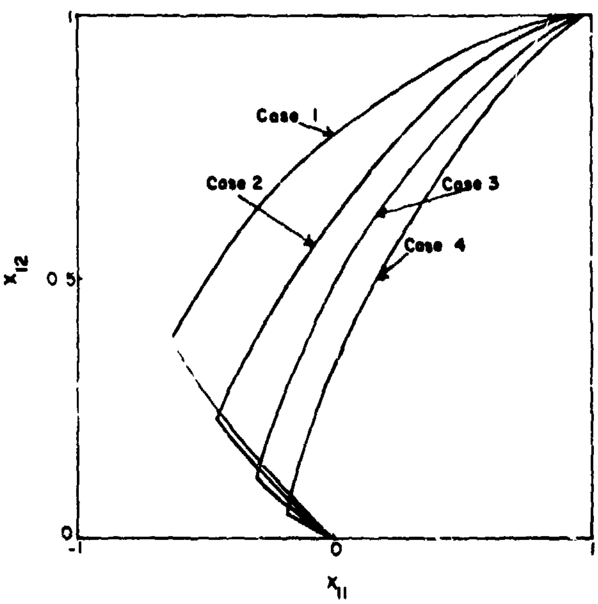

Fig. 5. Phase plane plot for different cases of the two CST's-in-series model with $T_2 = 0$ and $r_{11} = 2$.

NOMENCLATURE

a_1 = $r\,K_1/K_4$

a_2 = $r_2\,K_1$

a_3 = $K_1\sigma$

a_4 = $r\,K_4/K_1$

a_5 = $r\,K_2\,K_4$

a_6 = $r\,K_3\,K_4$

a_{11} = $r_1\,K_{11}\,r_{11}/K_4$

a_{12} = $r_1\,r_2\,K_{11}$

a_{13} = $T_d\,K_{11}/T_2\,r_{11}$

a_{21} = $r_{12}\,K_{12}/K_{11}$

a_{23} = $T_d\,K_{12}/T_2\,r_{12}$

a_{42} = $r\,K_4/K_{12}$

a'_{42} = K_4/K_{12}

A = Integration constant

A_1 = Integration constant

A_2 = Integration constant

B = Integration constant

c_p = Specific heat of air in Kcal/Kg °C

c_{pw} = Specific heat of coolant in Kcal/Kg °C

$H[x(t), \theta(t), z(t)]$ = Hamiltonian function

H^* = The portion of H which depends on θ

K = $\dfrac{ra_2 - a_1a_5 - a_1a_6}{r - a_1a_4}$

K' = $\dfrac{ra_2 + a_1a_5 - a_1a_6}{r - a_1a_4}$

K_1 = $\dfrac{T_2}{T_{c0}}$

K_2 = $\dfrac{1}{2T_2}(T_{r\,max} - T_{r\,min})$

K_3 = $\dfrac{1}{2T_2}(T_{r\,max} + T_{r\,min})$

K_4 = $\dfrac{T_2}{T_{10}}$

K_{11} = $\dfrac{T_2}{T_{1c0}}$

K_{12} = $\dfrac{T_2}{T_{2c0}}$

Q = $Q_1 + Q_2$, flow rate of air in the system proper in m^3/sec

Q_1 = Air flow rate by circulation air in m^3/sec

Q_2 = Flow rate of fresh air in m^3/sec

Q_w = Flow rate of coolant in m^3/sec

r = $\dfrac{\tau_1}{\tau_2}$, the ratio of time constant of system proper to that of heat exchanger

r_1 = $\dfrac{Q_1}{Q_1 + Q_2}$, the fraction of circulation air

r_2 = $\dfrac{Q_2}{Q_1 + Q_2}$, the fraction of fresh air

r_{11} = $\dfrac{\tau_1}{\tau_{11}}$

r_{12} = $\dfrac{\tau_2}{\tau_{12}}$

S = Performance index

t = $\dfrac{\alpha}{\tau_1}$, dimensionless time

t_a = Reference temperature in °C

t_c = Room temperature in °C

t_d = Disturbance temperature in °C

t_i = Temperature of incoming circulation air in °C

t_o = Initial time

t_s = Switching time

t_{wc} = Inlet temperature of coolant in °C

t_{wh} = Outlet temperature of coolant in °C

t_2 = Outside air temperature in °C

T = Final time, dimensionless

T_c = $(t_c - t_a)$, room temperature in °C

T_{c0} = Room temperature at $\alpha = 0^+$ in °C

T_{c1} = Temperature of pool 1 in °C

T_{c10} = Temperature of pool 1 at $\alpha = 0^+$ in °C

T_{c2} = Temperature of pool 2 in °C

T_{c20} = Temperature of pool 2 at $\alpha = 0^+$

T_d = $(t_d - t_a)$, disturbance temperature in °C

T_i = $(t_i - t_a)$, temperature of the circulation air into the system, in °C

T_{i0} = Temperature of the circulation air into the system at $\alpha = 0^+$ in °C

T_r = $\dfrac{Q_w \rho_w c_{pw}(T_{wh} - T_{wc})}{Q_1 \rho c_p}$, hypothetical temperature

T_{rf} = Final steady state value of T_r

$T_{r\,max}$ = Upper bound of T_r in °C

$T_{r\,min}$ = Lower bound of T_r in °C

T_{r0} = Value of T_r at $\alpha = 0$ in °C

T_{wc} = $t_{wc} - t_c$ in °C

T_{wh} = $t_{wh} - t_a$ in °C

T_2 = $(t_2 - t_a)$, outside air temperature

$U_0(t)$ = Step heat disturbance function

V_1 = Volume of room in m^3

V_{11} = Volume of pool 1 of two completely stirred tanks in series model in m^3

V_2 = Volume of heat exchanger in m^3

V_{12} = Volume of pool 2 of two completely stirred tanks in series model in m^3

$x_1(t)$ = $\dfrac{T_c}{T_{c0}}$, dimensionless room temperature

$x_2(t)$ = $\dfrac{T_i}{T_{i0}}$, dimensionless temperature of the circulation air

x_{11} = $\dfrac{T_{c1}}{T_{c10}}$, dimensionless temperature of pool 1

x_{12} = $\dfrac{T_{c2}}{T_{c20}}$, dimensionless temperature of pool 2

$z_i(t)$ = Adjoint variable

GREEK LETTERS

α = Time in sec.

α_f = Final time in sec.

$\phi(\alpha)$ = Impulse heat disturbance function, sec^{-1}

ρ = Air density in Kg/m^3

ρ_w = Density of coolant in Kg/m^3

σ = $\dfrac{T_d}{T_2}$, dimensionless disturbance temperature

τ_1 = $\dfrac{V_1}{Q_1 + Q_2}$, time constant of the system proper in sec.

τ_{11} = $\dfrac{V_{11}}{Q_1 + Q_2}$, time constant of pool 1 in sec.

τ_2 = $\dfrac{V_2}{Q_1}$, time constant of heat exchanger in sec.

τ_{12} = $\dfrac{V_{12}}{Q_1 + Q_2}$, time constant of pool 2 in sec.

θ = $\dfrac{T_r - \frac{1}{2}(T_{r\,max} + T_{r\,min})}{T_{r\,max} - \frac{1}{2}(T_{r\,max} + T_{r\,min})}$, control variable

$$= \begin{cases} +1 & \text{at} \quad T_r = T_{r\,max} \\ -1 & \text{at} \quad T_r = T_{r\,min} \end{cases}$$

$\tilde{\theta}(t)$ = Optimum value of $\theta(t)$

$\phi(\alpha)$ = Heat disturbance function

η = Defined in equation (26)

λ_{11} = Constant in equation (48)

λ_{12} = Constant in equation (48)

REFERENCES

1. Haines, J. E., "Automatic Control of Heating and Air Conditioning," pp. v-vi, McGraw-Hill, New York, 1953.

2. Uchida, H., et al., "Automatic Control of Air Conditioning (in Japanese)," pp. 7-44, Scientific Technology Center, Tokyo, 1963.

3. Webb, P., J. F. Annis, and S. J. Troutman, "Automatic Control of Water Cooling in Space Suits," NASA Report CR-1085, National Aero-

nautics and Space Administration, [illegible], D. C., 1968.

4. Vaughan, R. L., H. M. Stephenes, and R. S. Barker, "Generalized Environmental Control and Life Support System; Fortran Program - Vol. 1," Douglas Report SM-49403, Santa Monica, Calif., May 1966.

5. Tou, J. C., "Modern Control Theory," pp. 5-12, McGraw-Hill, New York, 1964.

6. Bellman, R., "Some Vistas of Modern Mathematics," pp. 1-49, U. of Kentucky Press, Lexington, 1968.

7. Pontryagin, L. S., V. G. Boltyanskii, R. V. Gamkrelidze, and E. F. Mishchenke, "The Mathematical Theory of Optimal Process," (English translation by K. N. Trirogoff), Interscience, New York, 1962.

8. Fan, L. T., "The Continuous Maximum Principle: A Study of Complex Systems Optimization," John Wiley and Sons, New York, 1966.

9. Sage, A. P., "Optimal System Control," Prentice Hall, Englewood Cliffs, New Jersey, 1968.

10. Lapidus, L. and R. Luus, "Optimal Control of Engineering Processes," Blaisdell, Waltham, Mass., 1967.

11. Leondes, C. T., "Modern Control Systems Theory," McGraw-Hill, New York, 1965.

12. Harrison, H. L., W. S. Hansen and R. E. Zelenski, "Development of a Room Transfer Function Model for Use in the Study of Short-term Transient Response," ASHRAE Trans. 74, Part 2, 198 (1968).

13. Zermuehlen, R. O. and H. L. Harrison, "Room Temperature Response to a Sudden Heat Disturbance Input," ASHRAE Trans., 71, Part 1, 206 (1965).

14. Gartner, J. R., H. L. Harrison, "Dynamic characteristics of water to air cross flow heat exchangers," ASHRAE (1965).

15. Allen, R., "Time modulations control increases comfort," Part I and II, American Artisan, July (1950).

16. Buchberg, H., "Cooling Load from Pretabulated Impedances," Heating, Piping and Air Conditioning, February 1958.

17. Buchberg, H., "Cooling Load from Thermal Network Solutions," Heating, Piping and Air Conditioning, October (1957).

18. Drake, W. B., "Transfer Admittance Functions," ASHRAE (1959).

19. Chapman, W. P., "Fundamentals of Linear Control Theory," ASHRAE J., 6 (4), 64-66 (1964).

20. Solvanson, K. R., "Some Control Problems and Their Solutions," ASHRAE J., 6, (5), 76-79 (1964).

21. Merriam III, C. W., "Optimization Theory and the Design of Feedback Control Systems," McGraw-Hill, New York, 1964.

22. [illegible], "The Optimization of Domestic Heating Systems," Ph.D. Dissertation, University of Michigan, 1967.

23. Coughanowr, D. R. and L. B. Koppel, "Process Systems Analysis and Control," McGraw-Hill, New York, 1965.

24. Bellman, R., I. Glicksberg and O. Gross, "On the Bang-bang Control Problems," Quarterly Appl. Math., 14, 11 (1955).

Liang-Tseng Fan

Liang-Tseng Fan received the B.S. degree in chemical engineering from the National Taiwan University in 1951, the M.S. degree in chemical engineering from Kansas State University, Manhattan, and the Ph.D. degree in chemical engineering from West Virginia University, Morgantown. In addition he received the M.S. degree in mathematics from West Virginia University, Morgantown in 1958.

He joined the faculty of Kansas State University in 1958 where he is a Professor and Head of Chemical Engineering, and Director of the Institute for Systems Design and Optimization. He has published two books on the maximum principle and more than 130 technical papers in optimization, fluidization, chemical process dynamics, and related fields.

Yuan-Sen Hwang

Yuan-Sen Hwang received the B.S. degree in chemical engineering from the National Taiwan University in 1966, and the M.S. degree from Kansas State University, Manhattan, in 1970. He is currently working as a project engineer at 3M Company, St. Paul, Minnesota.

Ching-Lai Hwang

Ching-Lai Hwang received the B.S. degree in mechanical engineering from the National Taiwan University in 1953, and the M.S. and Ph.D. degrees from Kansas State University, Manhattan, in 1960 and 1962 respectively.

He is currently an Associate Professor of Industrial Engineering at Kansas State University. His area of research interest includes optimization techniques, systems engineering and fluid dynamics.

(e)1

ELEVENTH JOINT AUTOMATIC CONTROL CONFERENCE OF THE AMERICAN AUTOMATIC CONTROL COUNCIL

COOPERATING SOCIETIES:

American Institute of Aeronautics and Astronautics

American Institute of Chemical Engineers

The American Society of Mechanical Engineers

Fluid Power Society

The Institute of Electrical and Electronics Engineers

Instrument Society of America

Simulation Councils, Inc.

Georgia Institute of Technology
Atlanta, Georgia
June 22-26, 1970

Paper No. 19-A

OPTIMAL STARTUP CONTROL OF A JACKETED TUBULAR REACTOR

D.R. Hahn, L.T. Fan, and C.L. Hwang

Institute for Systems Design and Optimization

Kansas State University, Manhattan, Kansas 66502

Published on behalf of the American Automatic Control Council

by

THE AMERICAN SOCIETY OF MECHANICAL ENGINEERS

United Engineering Center 345 East 47th Street, New York, N. Y. 10017

SESSION PAPER 19-A

OPTIMAL STARTUP CONTROL OF A JACKETED TUBULAR REACTOR+

D. R. Hahn,* L. T. Fan, and C. L. Hwang

Institute for Systems Design and Optimization

Kansas State University, Manhattan, Kansas 66502

ABSTRACT

The optimal startup policy of a jacketed tubular reactor, in which a first-order, reversible, exothermic reaction takes place, is presented. A distributed maximum principle is presented for determining weak necessary conditions for optimality of a diffusional distributed parameter system. A numerical technique is developed for practical implementation of the distributed maximum principle. This involves the sequential solution of the state and adjoint equations, in conjunction with a functional gradient technique for iteratively improving the control function.

INTRODUCTION

This paper presents an optimal policy for startup of a jacketed tubular reactor in which a first-order, reversible, exothermic reaction is taking place. The optimal control policy is determined by using a distributed maximum principle. The control or decision variable is the wall temperature of the reactor, which is manipulated to minimize a given performance index. Computational results are obtained for a case with and without a constraint on the maximum reaction temperature.

The mathematical model for the jacketed tubular reactor is a continuous distributed parameter flow system, which gives rise to a set of coupled nonlinear one-dimensional second-order parabolic partial differential equations. A distributed maximum principle used by the previous workers, for example Denn, et. al. [1], is extended to a general system of nonlinear diffusion equations, with two-point boundary conditions consisting of linear relationships between dependent variables and their axial gradients. A set of necessary conditions for optimality is obtained for a fairly general performance index.

In general, equations of the type treated cannot be solved by analytic methods and even numerical techniques for coupled, highly nonlinear axial diffusion equations are not generally available. Therefore, an iterative computational technique involving a gradient in functional space is presented, which enables the numerical implementation of the distributed maximum principle. It is shown that the technique is capable of accomodating inequality constraints on state variables by the addition of an appropriate penalty function to the performance index.

A DISTRIBUTED MAXIMUM PRINCIPLE

A distributed maximum principle is presented for determining weak necessary conditions for optimality for a class of distributed systems. Due to the complexity of partial differential equations, a completely general maximum principle, as exists for lumped parameter systems (2, 3) has not been found. However, sufficient generality has been retained that the results apply to a wide variety of systems of interest in process control.

System Description

Attention will be focused on systems which may be described by a general nonlinear vector partial differential equation of the form

$$\underline{u}_t(x, t) = \underline{f}(\underline{u}(x, t), \underline{u}_x(x, t), \underline{u}_{xx}(x, t), \underline{\theta}(x, t), x, t) \tag{1}$$

where $\underline{u}$ is an s-dimensional state vector defined on a normalized one-dimensional spatial domain x from $x = 0$ to $x = 1$ and over a fixed time interval $t = 0$ to $t = t_f$. The control vector $\underline{\theta}$ is considered to be distributed in space and time and is r-dimensional. An independent variable appearing as a subscript denotes partial differentiation with respect to that variable.

Equation (1) is augmented by the following set of initial and boundary conditions:

$$\xi_i(\underline{u}) = 0 \quad \text{at } t = 0,\ i = 1, \ldots, s \tag{2}$$

$$\phi_m(\underline{u}, \underline{u}_x) = 0 \quad \text{at } x = 0,\ m = 1, \ldots, p \tag{3}$$

$$\psi_n(\underline{u}, \underline{u}_x) = 0 \quad \text{at } x = 1,\ n = 1, \ldots, q = 2s-p \tag{4}$$

It is assumed that no boundary forcing is present (i.e., control action does not appear in the boundary conditions).

Variational Equations

Consider now small changes $\delta\underline{\theta}$ in the control vector $\underline{\theta}$. The resulting incremental responses δu_i in the state variables u_i must satisfy the following linear perturbation differential equations:

$$\delta u_{i_t} = f_{i_{\underline{u}}}^T \delta\underline{u} + f_{i_{\underline{u}_x}}^T \delta\underline{u}_x + f_{i_{\underline{u}_{xx}}}^T \delta\underline{u}_{xx} + f_{i_{\underline{\theta}}}^T \delta\underline{\theta} \tag{5}$$

$$i = 1, \ldots, s$$

where the above notation denotes the following:

$$f_{i_{\underline{u}}} = \begin{bmatrix} \frac{\partial f_i}{\partial u_1} \\ \vdots \\ \frac{\partial f_i}{\partial u_s} \end{bmatrix}, \quad f_{i_{\underline{u}_x}} = \begin{bmatrix} \frac{\partial f_i}{\partial u_{1_x}} \\ \vdots \\ \frac{\partial f_i}{\partial u_{s_x}} \end{bmatrix}, \quad f_{i_{\underline{u}_{xx}}} = \begin{bmatrix} \frac{\partial f_i}{\partial u_{1_{xx}}} \\ \vdots \\ \frac{\partial f_i}{\partial u_{s_{xx}}} \end{bmatrix},$$

+This study was supported in part by NASA Grant No. NGR-17-001-034, and by the Air Force Office of Scientific Research, Office of Aerospace Research, United States Air Force, Under Contract F44620-68-0020 (Themis Project).

*Present Address: The Bendix Corporation, Kansas City, Missouri.

PRECEDING PAGE BLANK NOT FILMED

$$f_{i_{\underline{\theta}}} = \begin{bmatrix} \frac{\partial f_i}{\partial \theta_1} \\ \vdots \\ \frac{\partial f_i}{\partial \theta_r} \end{bmatrix}$$

The variational initial and boundary conditions are

$$\xi_{i_{\underline{u}}} \; \delta \underline{u} = 0 \quad \text{at } t = 0,\; i = 1, \ldots, s \tag{6}$$

$$\phi^T_{m_{\underline{u}}} \; \delta \underline{u} + \phi^T_{m_{\underline{u}_x}} \; \delta \underline{u}_x = 0 \text{ at } x = 0,\; m = 1, \ldots, p \tag{7}$$

$$\psi^T_{n_{\underline{u}}} \; \delta \underline{u} + \psi^T_{n_{\underline{u}_x}} \; \delta \underline{u}_x = 0 \text{ at } x = 1,\; n = 1, \ldots, q = (2s - p) \tag{8}$$

All partial derivatives are evaluated on the nominal trajectory.

Equation (5) can be written in the form of a linearized vector partial differential equation

$$\delta \underline{u}_t = \underline{f}_{\underline{u}} \; \delta \underline{u} + \underline{f}_{\underline{u}_x} \; \delta \underline{u}_x + \underline{f}_{\underline{u}_{xx}} \; \delta \underline{u}_{xx} + \underline{f}_{\underline{\theta}} \; \delta \underline{\theta} \tag{9}$$

where

$$\underline{f}_{\underline{u}} = \begin{bmatrix} \frac{\partial f_1}{\partial u_1} & \cdots & \frac{\partial f_1}{\partial u_s} \\ \vdots & & \vdots \\ \frac{\partial f_s}{\partial u_1} & \cdots & \frac{\partial f_s}{\partial u_s} \end{bmatrix} \qquad \underline{f}_{\underline{u}_x} = \begin{bmatrix} \frac{\partial f_1}{\partial u_{1_x}} & \cdots & \frac{\partial f_1}{\partial u_{s_x}} \\ \vdots & & \vdots \\ \frac{\partial f_s}{\partial u_{1_x}} & \cdots & \frac{\partial f_s}{\partial u_{s_x}} \end{bmatrix}$$

$$\underline{f}_{\underline{u}_{xx}} = \begin{bmatrix} \frac{\partial f_1}{\partial u_{1_{xx}}} & \cdots & \frac{\partial f_1}{\partial u_{s_{xx}}} \\ \vdots & & \vdots \\ \frac{\partial f_s}{\partial u_{1_{xx}}} & \cdots & \frac{\partial f_s}{\partial u_{s_{xx}}} \end{bmatrix} \qquad \underline{f}_{\underline{\theta}} = \begin{bmatrix} \frac{\partial f_1}{\partial \theta_1} & \cdots & \frac{\partial f_1}{\partial \theta_r} \\ \vdots & & \vdots \\ \frac{\partial f_s}{\partial \theta_1} & \cdots & \frac{\partial f_s}{\partial \theta_r} \end{bmatrix}$$

Necessary Conditions For Optimality

It is desired to determine the control function $\underline{\theta}$ which yields a minimum for the following generalized objective functional:

$$S = \int_0^1 F(\underline{u}(x, t_f), x)dx + \int_0^{t_f} \int_0^1 G(\underline{u}(x, t), \underline{\theta}(x, t), x, t) \, dx \, dt \tag{10}$$

In order to obtain necessary conditions for optimality, it is required to find a relationship which expresses variations of the objective functional, δS, in terms of control perturbations, $\delta\underline{\theta}$. Taking first variations on the objective functional, Equation (10), gives

$$\delta S = \int_0^1 F_{\underline{u}}^T \delta \underline{u} \; dx \Big|_{t=t_f} + \int_0^{t_f} \int_0^1 [G_{\underline{u}}^T \delta \underline{u} + G_{\underline{\theta}}^T \delta \underline{\theta}] \; dx \; dt \tag{11}$$

where

$$F_{\underline{u}} = \begin{bmatrix} \frac{\partial F}{\partial u_1} \\ \vdots \\ \frac{\partial F}{\partial u_s} \end{bmatrix}, \; G_{\underline{u}} = \begin{bmatrix} \frac{\partial G}{\partial u_1} \\ \vdots \\ \frac{\partial G}{\partial u_s} \end{bmatrix}, \; G_{\underline{\theta}} = \begin{bmatrix} \frac{\partial G}{\partial \theta_1} \\ \vdots \\ \frac{\partial G}{\partial \theta_r} \end{bmatrix}$$

Consider now adjoining the variational system equation, Equation (9), as an equality constraint with the variational objective functional, Equation (11). This yields

$$\delta S = \int_0^1 F_{\underline{u}}^T \; \delta \underline{u} \; dx \Big|_{t=t_f} + \int_0^{t_f} \int_0^1 \{G_{\underline{u}}^T \; \delta \underline{u} + G_{\underline{\theta}}^T \delta \underline{\theta} - \underline{z}^T [\delta \underline{u}_t - \underline{f}_{\underline{u}} \; \delta \underline{u} - \underline{f}_{\underline{u}_x} \delta \underline{u}_x - \underline{f}_{\underline{u}_{xx}} \; \delta \underline{u}_{xx} - \underline{f}_{\underline{\theta}} \; \delta \underline{\theta}]\} dx \; dt \tag{12}$$

where $\underline{z}(x, t)$ is an s-dimensional adjoint vector.

The following identity is now introduced:

$$(\underline{z}^T \; \delta \underline{u})_t = \underline{z}_t^{\;T} \; \delta \underline{u} + \underline{z}^T \; \delta \underline{u}_t \tag{13}$$

Substitution of Equation (13) into Equation (12) yields

$$\delta S = \int_0^1 F_{\underline{u}}^T \; \delta \underline{u} \; dx \Big|_{t=t_f} + \int_0^{t_f} \int_0^1 \{G_{\underline{u}}^T \; \delta \underline{u} + G_{\theta}^T \; \delta \underline{\theta} - [(\underline{z}^T \; \delta \underline{u})_t - \underline{z}_t^T \; \delta \underline{u} - \underline{z}^T \; \underline{f}_{\underline{u}} \; \delta \underline{u} - \underline{z}^T \; \underline{f}_{\underline{u}_x} \; \delta \underline{u}_x - \underline{z}^T \; \underline{f}_{\underline{u}_{xx}} \; \delta \underline{u}_{xx} - \underline{z}^T \; \underline{f}_{\underline{\theta}} \; \delta \underline{\theta}]\} dx \; dt \tag{14}$$

A portion of the second integrand of Equation (14) is now integrated with respect to x from x = 0 to x = 1 by parts so that each term in the integrand involves either the variation $\delta \underline{u}$ or $\delta \underline{\theta}$. This gives

$$\int_0^1 \underline{z}^T \; \underline{f}_{\underline{u}_x} \; \delta \underline{u}_x \; dx = [\underline{z}^T \; \underline{f}_{\underline{u}_x} \; \delta \underline{u}]_{x=0}^1 - \int_0^1 (\underline{z}^T \; \underline{f}_{\underline{u}_x})_x \; \delta \underline{u} \; dx \tag{15}$$

$$\int_0^1 \underline{z}^T \; \underline{f}_{\underline{u}_{xx}} \; \delta \underline{u}_{xx} dx = [\underline{z}^T \; \underline{f}_{\underline{u}_{xx}} \; \delta \underline{u}_x - (\underline{z}^T \; \underline{f}_{\underline{u}_{xx}})_x \; \delta \underline{u}]_{x=0}^1 + \int_0^1 (\underline{z}^T \; \underline{f}_{\underline{u}_{xx}})_{xx} \; \delta \underline{u} \; dx \tag{16}$$

Another term in the second integral of Equation (14) is integrated with respect to t, yielding

$$\int_0^{t_f} (\underline{z}^T \; \delta \underline{u})_t \; dt = [\underline{z}^T \; \delta \underline{u}]_{t=0}^{t_f} \tag{17}$$

After some manipulation and noting that $\delta u(x, 0) = 0$, the following result is obtained:

$$\delta S = \int_0^1 [F_{\underline{u}}^T - \underline{z}^T] \; \delta \underline{u} \; dx \Big|_{t=t_f} + \int_0^{t_f} \int_0^1 \{[G_{\underline{\theta}}^T + \underline{z}^T \underline{f}_{\underline{\theta}}] \delta \underline{\theta} + [\underline{z}_t^T + \underline{z}^T \; \underline{f}_{\underline{u}} - (\underline{z}^T \; \underline{f}_{\underline{u}_x})_x + (\underline{z}^T \; \underline{f}_{\underline{u}_{xx}})_{xx} + G_{\underline{u}}^T] \delta \underline{u}\} dx \; dt + \int_0^{t_f} \Big[[\underline{z}^T \; \underline{f}_{\underline{u}_x} - (\underline{z}^T \; \underline{f}_{\underline{u}_{xx}})_x] \delta \underline{u} + \underline{z}^T \; \underline{f}_{\underline{u}_{xx}} \; \delta \underline{u}_x\Big]_{x=0}^1 dt \tag{18}$$

An equivalent result was obtained by Denn, et. al. (1) using a Green's function approach.

In order to eliminate terms not depending explicitly on $\delta\underline{\theta}$ from the second integrand of Equation (18), it is stipulated that each component of the adjoint vector $\underline{z}$ satisfy the following partial differential equation:

$$z_{i_t} = - \underline{z}^T \; \underline{f}_{u_i} + (\underline{z}^T \; \underline{f}_{u_{i_x}})_x - (\underline{z}^T \; \underline{f}_{u_{i_{xx}}})_{xx} - G_{u_i}, \quad i = 1, \ldots, s \tag{19}$$

where

$$\underline{f}_{u_i} = \begin{bmatrix} \frac{\partial f_1}{\partial u_i} \\ \vdots \\ \frac{\partial f_s}{\partial u_i} \end{bmatrix}, \quad \underline{f}_{u_{i_x}} = \begin{bmatrix} \frac{\partial f_1}{\partial u_{i_x}} \\ \vdots \\ \frac{\partial f_s}{\partial u_{i_x}} \end{bmatrix}, \quad \underline{f}_{u_{i_{xx}}} = \begin{bmatrix} \frac{\partial f_1}{\partial u_{i_{xx}}} \\ \vdots \\ \frac{\partial f_s}{\partial u_{i_{xx}}} \end{bmatrix}$$

The boundary conditions for Equation (19) are specified such that

$$\left[[\underline{z}^T \underline{f}_{\underline{u}_x} - (\underline{z}^T \underline{f}_{\underline{u}_{xx}})_x]\, \delta\underline{u} + \underline{z}^T \underline{f}_{\underline{u}_{xx}}\, \delta\underline{u}_x \right]_{x=0}^{1} = 0 \qquad (20)$$

This is accomplished by choosing the adjoint boundary conditions such that the coefficients of the unknown endpoint variation $\delta\underline{u}$ and $\delta\underline{u}_x$ vanish.

At this point, the system boundary conditions, Equations (3) and (4), are assumed to be linear and have the more explicit form

$$\phi_i(\underline{u}, \underline{u}_x) = 0 = u_{i_x} + a_i u_i + b_i \quad \text{at} \quad x = 0, \quad i = 1, \ldots, s \qquad (21)$$

$$\psi_i(\underline{u}, \underline{u}_x) = 0 = u_{i_x} + c_i u_i + d_i \quad \text{at} \quad x = 1, \quad i = 1, \ldots, s \qquad (22)$$

The corresponding boundary variational equations become

$$\delta u_{i_x} + a_i\, \delta u_i = 0 \quad \text{at} \quad x = 0, \quad i = 1, \ldots, s \qquad (23)$$

$$\delta u_{i_x} + c_i\, \delta u_i = 0 \quad \text{at} \quad x = 1, \quad i = 1, \ldots, s \qquad (24)$$

The unknown endpoint variations $\delta\underline{u}_x$ in Equation (18) can now be written in terms of the respective unknown variations $\delta\underline{u}$. To set the coefficients of the δu_i equal to zero, the adjoint variables z_i are required to satisfy the following 2s conditions at $x = 0$ and $x = 1$:

$$\underline{z}^T \underline{f}_{u_{i_x}} - (\underline{z}^T \underline{f}_{u_{i_{xx}}})_x - a_i\, \underline{z}^T \underline{f}_{u_{i_{xx}}} = 0 \quad \text{at} \quad x = 0, \quad i = 1, \ldots, s \qquad (25)$$

$$\underline{z}^T \underline{f}_{u_{i_x}} - (\underline{z}^T \underline{f}_{u_{i_{xx}}})_x - c_i\, \underline{z}^T \underline{f}_{u_{i_{xx}}} = 0 \quad \text{at} \quad x = 1, \quad i = 1, \ldots, s \qquad (26)$$

The specification of the adjoint vector is completed by stipulating the transversality conditions

$$z_i = F_{u_i} \quad \text{at} \quad t = t_f, \quad i = 1, \ldots, s \qquad (27)$$

This causes the first integral in Equation (8) to vanish and it follows that δS can now be expressed explicitly in terms of the control perturbation, $\delta\underline{\theta}$:

$$\delta S = \int_0^{t_f} \int_0^1 [\underline{G}_{\underline{\theta}}^T + \underline{z}^T \underline{f}_{\underline{\theta}}]\, \delta\underline{\theta}\, dx\, dt \qquad (28)$$

It is convenient to define a Hamiltonian function

$$H(\underline{u}, \underline{u}_x, \underline{u}_{xx}, \underline{\theta}, \underline{z}, x, t) = G(\underline{u}, \underline{\theta}, x, t) + \underline{z}(x, t)^T \underline{f}(\underline{u}, \underline{u}_x, \underline{u}_{xx}, \underline{\theta}, x, t) \qquad (29)$$

so that Equation (28) becomes

$$\delta S = \int_0^{t_f} \int_0^1 H_{\underline{\theta}}^T\, \delta\underline{\theta}\, dx\, dt \qquad (30)$$

where

$$H_{\underline{\theta}} = \begin{bmatrix} \frac{\partial H}{\partial \theta_1} \\ \vdots \\ \frac{\partial H}{\partial \theta_r} \end{bmatrix}$$

It follows by reasoning similar to that of Katz (4) who achieved a similar result for a more general and abstract class of problems, that the best choice of control action $\underline{\theta}$ which minimizes the objective functional S is that which makes

$$\int_0^1 H\, dx \qquad (31)$$

stationary over the interval $0 \le t \le t_f$ with respect to components of $\underline{\theta}$ lying interior to the admissible control region and a minimum for those lying on the boundary. For control components interior to the region, this means

$$\int_0^1 H_{\underline{\theta}}\, dx = 0 \qquad (32)$$

Essentially this is an infinite dimensional, or functional equivalent of Pontryagin's maximum principle (2, 3) for finite dimensional (lumped) systems.

Summary

The distributed maximum principle derived herein may now be summarized as follows. Given a system of partial differential equations

$$\underline{u}_t(x, t) = \underline{f}(\underline{u}(x, t), \underline{u}_x(x, t), \underline{u}_{xx}(x, t), \theta(x, t), x, t) \qquad (33)$$

subject to initial and boundary conditions

$$\xi_i(\underline{u}) = 0 \quad \text{at} \quad t = 0, \ i = 1, \ldots, s \qquad (34)$$

$$\phi_i(\underline{u}, \underline{u}_x) = 0 = u_{i_x} + a_i u_i + b_i \quad \text{at} \quad x = 0, \ i = 1, \ldots, s \qquad (35)$$

$$\psi_i(\underline{u}, \underline{u}_x) = 0 = u_{i_x} + c_i u_i + d_i \quad \text{at} \quad x = 1, \ i = 1, \ldots, s \qquad (36)$$

it is desired to obtain the control vector $\underline{\theta}(x, t)$ which minimizes the objective functional

$$S = \int_0^1 F(\underline{u}(x, t_f), x)\, dx + \int_0^{t_f} \int_0^1 G(\underline{u}(x, t), \underline{\theta}(x, t), x, t)\, dx\, dt \qquad (37)$$

for fixed t_f.

The solution to the optimization problem involves the simultaneous solution of Equation (33) with a set of adjoint partial differential equations

$$z_{i_t} = -\underline{z}^T \underline{f}_{u_i} + (\underline{z}^T \underline{f}_{\underline{u}_{i_x}})_x - (\underline{z}^T \underline{f}_{\underline{u}_{i_{xx}}})_{xx} - G_{u_i} \quad i = 1, \ldots, s \qquad (38)$$

which satisfy the boundary conditions

$$\underline{z}^T \underline{f}_{u_{i_x}} - (\underline{z}^T \underline{f}_{u_{i_{xx}}})_x - a_i \underline{z}^T \underline{f}_{u_{i_{xx}}} = 0 \quad \text{at} \quad x = 0, \quad i = 1, \ldots, s \tag{39}$$

$$\underline{z}^T \underline{f}_{u_{i_x}} - (\underline{z}^T \underline{f}_{u_{i_{xx}}})_x - c_i \underline{z}^T \underline{f}_{u_{i_{xx}}} = 0 \quad \text{at} \quad x = 1, \quad i = 1, \ldots, s \tag{40}$$

and the transversality conditions

$$z_i = F_{u_i} \quad \text{at} \quad t = t_f, \quad i = 1, \ldots, s \tag{41}$$

Equivalently, the problem can be formulated in terms of a Hamiltonian function defined as follows:

$$H = G + \underline{z}^T \underline{f} \tag{42}$$

The state and adjoint equations are equivalent, then, to the Hamiltonian canonical partial differential equations

$$u_{i_t} = H_{z_i} = f_i, \qquad i = 1, \ldots, s \tag{43}$$

$$z_{i_t} = - H_{u_i} + (H_{u_{i_x}})_x - (H_{u_{i_{xx}}})_{xx}, \quad i = 1, \ldots, s \tag{44}$$

The weak necessary conditions are that the spatial integral of the Hamiltonian is made stationary with respect to choices of components of $\underline{\theta}$ which lie interior to the admissible control region and a minimum with respect to components on the boundary.

The results can readily be extended to systems which include boundary forcing and free initial state (1). Extensions could also be made to accomodate multi-dimensional spatial coordinates and higher-order spatial derivatives

The solution of the two-point boundary value system of partial differential equations coupled with the satisfaction of the necessary conditions presents a formidible computational problem. However, an approximate numerical method involving a gradient in function space is introduced in the next section to greatly facilitate the obtaining of numerical results.

A COMPUTATIONAL APPROACH FOR DETERMINING OPTIMALITY

Developed in this section is a computational scheme for obtaining numerical results from the distributed maximum principle presented. The method is iterative in nature, involving repeated numerical integration of the performance and adjoint equations, combined with the use of a functional gradient technique to improve the control vector.

A Functional Gradient Technique

A relationship of the type of Equation (30) can be thought of in terms of a gradient in function space. In this case, $H_{\underline{\theta}}$ may be taken to be gradient $S_{\underline{\theta}}$ in the function space of $\underline{\theta}$. The maximum rate of decrease of the functional S in the space of $\underline{\theta}$ will be in the direction $H_{\underline{\theta}}$. This relationship provides the basis for a computational scheme by which the objective functional S can be minimized with respect to choices of $\underline{\theta}$.

Several papers have appeared recently (1, 5, 6), which have extended finite dimensional techniques to infinite dimensional systems in function space. The idea of a gradient in function space seems to have been originated by Courant and Hilbert (7).

It is desirable to insure that perturbations in the control vector, $\delta\underline{\theta}$, are small enough that linearization leading to Equation (9) is valid. To accomplish this, a technique originated by Bryson and Denham (8) and extended to the infinite dimensional case by Seinfeld (6) is utilized. Let

$$(\delta P)^2 = \int_0^{t_f} \int_0^1 \delta\underline{\theta}^T \underline{W}\, \delta\underline{\theta}\, dx\, dt \tag{45}$$

be a positive definite quadratic form with $\underline{W} = \underline{W}(x, t)$ a matrix of suitably chosen weighting functions and δP a scalar which is specified to limit the magnitude of the perturbations.

Equation (45) is introduced into Equation (30) in terms of an undetermined Lagrange multiplier λ as follows:

$$\delta S = \int_0^{t_f} \int_0^1 (H_{\underline{\theta}}^T - \lambda \delta\underline{\theta}^T \underline{W}) \delta\underline{\theta}\, dx\, dt + \lambda (\delta P)^2 \tag{46}$$

In order to attain the maximum rate of change of S with respect to $\underline{\theta}$, the integrand of Equation (46) is maximized by differentiating with respect to $\delta\underline{\theta}$ and equating the result to zero. This yields the following expression:

$$\delta\underline{\theta} = \frac{\underline{W}^{-1} H_{\underline{\theta}}}{2\lambda} \tag{47}$$

Substitution of Equation (47) into Equation (45) gives

$$2\lambda = \pm \left[\int_0^{t_f} \int_0^1 H_{\underline{\theta}}^T \underline{W}^{-1} H_{\underline{\theta}}\, dx\, dt \,/\, (\delta P)^2\right]^{1/2} \tag{48}$$

Using the above expression in Equation (47), the variation, $\delta\underline{\theta}$, can now be written

$$\delta\underline{\theta} = \pm \frac{\underline{W}^{-1} H_{\underline{\theta}}}{\left[\int_0^{t_f} \int_0^1 H_{\underline{\theta}}^T \underline{W}^{-1} H_{\underline{\theta}}\, dx\, dt/(\delta P)^2\right]^{1/2}} \tag{49}$$

where the minus sign is used for the case where the objective functional, S, is to be minimized.

For the case where $\underline{\theta} = \underline{\theta}(t)$ only, the weighted metric, δP, is defined as

$$(\delta P)^2 = \int_0^{t_f} \delta\underline{\theta}^T \underline{W}\, \delta\underline{\theta}\, dt \tag{50}$$

Introducing Equation (50) into Equation (30) by means of the undetermined Lagrange multiplier, λ, yields

$$\delta S = \int_0^{t_f} \left[\int_0^1 H_{\underline{\theta}}^T \delta\underline{\theta}\, dx - \lambda \delta\underline{\theta}^T \underline{W}\, \delta\underline{\theta}\right] dt + \lambda (\delta P)^2 \tag{51}$$

Differentiating of the integrand of Equation (51) with respect to $\delta\underline{\theta}$ and letting the result equal to zero so as to obtain the maximum rate of change of δS yields

$$\delta\underline{\theta} = \frac{\underline{W}^{-1} \int_0^1 H_{\underline{\theta}}\, dx}{2\lambda} \tag{52}$$

and substitution of the above expression into Equation (50) gives

$$2\lambda = \pm\left[\int_0^{t_f} \left[\int_0^1 H_{\underline{\theta}}^T\, dx\right] \underline{W}^{-1} \left[\int_0^1 H_{\underline{\theta}}\, dx\right] dt/(\delta P)^2\right]^{1/2} \tag{53}$$

Thus upon substituting the above equation into Equation (52), the variation, $\delta\underline{\theta}$, becomes

$$\delta\underline{\theta} = \pm \frac{\underline{W}^{-1} \int_0^1 H_{\underline{\theta}}\, dx}{\left[\int_0^{t_f} \left[\int_0^1 H_{\underline{\theta}}^T\, dx\right] \underline{W}^{-1} \left[\int_0^1 H_{\underline{\theta}}\, dx\right] dt/(\delta P)^2\right]^{1/2}} \tag{54}$$

The computational scheme for obtaining the optimal control policy via the necessary conditions of the distributed maximum principle and the functional gradient technique can now be summarized as follows:

1. An initial control policy $\theta(x, t)$ is assumed.
2. Using the assumed policy in the system equations these are solved forward in time from $t=0$ to $t=t_f$ and the transient solutions retained.
3. The performance functional S is evaluated using the values of the state variables computed in 2.
4. Using final values of the state variables to compute the final conditions on the adjoint variables and inserting computed values of the state variables where required in the adjoint equations, these are solved backwards in time from $t=t_f$ to $t=0$ and the transient solutions retained.
5. An improved control policy is calculated using the gradient technique with values of the adjoint variables computed in 4.
6. Steps 2 through 5 are repeated iteratively until the objective functional converges to within a specified tolerance.

A flow diagram for the method is shown in Figure 1.

Provision for State Variable Constraints

The development of the necessary conditions for optimality and the accompanying functional gradient technique thus far have not taken into account the presence of inequality constraints involving state variables. In cases where such constraints are imposed upon the system, it is required to modify the necessary conditions for an extremal solution so that constraint violations do not occur, or are at least reduced to an allowable tolerance.

Consider the following general inequality constraint

$$C(\underline{u}, \theta) \leq 0 \tag{55}$$

where C may or may not involve the control θ explicitly.

A convenient method for handling such constraints is the penalty function approach. This involves the addition of an extra term or terms to the performance functional to incorporate the constraint. These terms have zero value until a constraint is violated and impose a penalty when violations occur. By iteratively decreasing the magnitude of the penalty, the trajectories may be forced to converge to the constraint boundaries. This amounts to solving a sequence of unconstrained optimization problems with penalized performance functionals, each time decreasing the amount of penalty until constraint convergence is attained.

OPTIMAL STARTUP CONTROL OF A JACKETED TUBULAR REACTOR CONSTRAINT ON MAXIMUM REACTION TEMPERATURE

The computational scheme developed in the preceding section will be applied to control of a tubular, continuous flow chemical reactor in which an exothermic reaction is taking place. It is assumed that the reaction is first-order and reversible ($A \rightleftarrows B$). Since the reaction rate is temperature-dependent, it [illegible] that the yield can be controlled by varying the reaction temperature. In this example, the reaction temperature and thus yield are controlled by manipulation of the reactor wall temperature.

The mathematical model for the system is based upon the following assumptions:

1. System parameters are uniform and constant with respect to time.
2. Wall temperature is a function of time only.
3. Axial heat and mass dispersion and mixing are significant inside the reactor.
4. Concentration, temperature and velocity of the stream are constant with respect to radial distance.

A mass balance taken over a differential element along the reactor yields for component A:

$$\frac{\partial c_A}{\partial \tau} = D_m \frac{\partial^2 c_A}{\partial \ell^2} - v \frac{\partial c_A}{\partial \ell} + R_A \tag{56}$$

where, for the case of a first-order, reversible $A \rightleftarrows B$ reaction, the rate of production of A, R_A, is given by the Arrhenius expression

$$R_A = -[k_1 c_A - k_2 c_B]$$

$$= -[k_{10}\exp(-E_1/RT)c_A - k_{20}\exp(-E_2/RT)c_B]$$

A heat balance on the differential section of the reactor yields

$$\frac{\partial T}{\partial \tau} = \frac{k_{eff}}{C_p \rho}\frac{\partial^2 T}{\partial \ell^2} - v\frac{\partial T}{\partial \ell} + \frac{(-\Delta H)}{C_p \rho} R_A - \frac{2h}{C_p \rho r}(T - T_w) \tag{57}$$

It is assumed that the manner of mixing is such that the effective mass and thermal diffusivities are equal, i.e.,

$$D_m + \frac{k_{eff}}{C_p \rho} \equiv D$$

The boundary conditions for this problem are those first suggested by Danckwerts (9)

$$\frac{\partial c_A(0, \tau)}{\partial \ell} = \frac{v}{D}[c_A(0, \tau) - c_A^f] \quad \text{at} \quad \ell = 0 \tag{58}$$

$$\frac{\partial c_A(L, \tau)}{\partial \ell} = 0 \quad \text{at} \quad \ell = L \tag{59}$$

$$\frac{\partial T(0, \tau)}{\partial \ell} = \frac{v}{D}[T(0, \tau) - T^f] \quad \text{at} \quad \ell = 0 \tag{60}$$

$$\frac{\partial T(L, \tau)}{\partial \ell} = 0 \quad \text{at} \quad \ell = L \tag{61}$$

These boundary conditions are based on the consideration that mass and energy are neither created nor destroyed in the infinitesimal region $\ell = 0^-$ to $\ell = 0^+$.

Equations (56) and (57) are put in dimensionless form by defining the following quantities:

Mean residence time	: $\tau_r = L/v$ hr
Axial Peclet number	: $\beta = vL/D$
Dimensionless time	: $t = \tau/\tau_r$
Dimensionless axial distance	: $x = \ell/L$

Dimensionless concentration of A : $u_1 = c_A/(c_A + c_B)$

Dimensionless reaction temperature : $u_2 = T/T_r$

Dimensionless wall temperature : $\theta = T_w/T_r$

Other parameters :

$$Q = \frac{\Delta H(c_A + c_B)}{C_p \rho T_r}, \quad K = \frac{2h}{C_p \rho r}\ \mathrm{hr}^{-1}, \quad P_1 = E_1/RT_r, \quad P_2 = E_2/RT_r$$

Thus the system equations become

$$\frac{\partial u_1}{\partial t} = \frac{1}{\beta}\frac{\partial^2 u_1}{\partial x^2} - \frac{\partial u_1}{\partial x} - \tau_r \phi(u_1, u_2) \tag{62}$$

$$\frac{\partial u_2}{\partial t} = \frac{1}{\beta}\frac{\partial^2 u_2}{\partial x^2} - \frac{\partial u_2}{\partial x} - Q\tau_r \phi(u_1, u_2) - K\tau_r(u_2 - \theta) \tag{63}$$

where

$$\phi = k_{10}\exp(-P_1/u_2)u_1 - k_{20}\exp(-P_2/u_2)(1 - u_1)$$

The dimensionless boundary conditions are

$$\frac{\partial u_1(0, t)}{\partial t} = \beta[u_1(0, t) - u_1^f] \qquad \text{at} \quad x = 0 \tag{64}$$

$$\frac{\partial u_1(1, t)}{\partial t} = 0 \qquad \text{at} \quad x = 1 \tag{65}$$

$$\frac{\partial u_2(0, t)}{\partial t} = \beta[u_2(0, t) - u_1^f] \qquad \text{at} \quad x = 0 \tag{66}$$

$$\frac{\partial u_2(1, t)}{\partial t} = 0 \qquad \text{at} \quad x = 1 \tag{67}$$

The following numerical values are assumed:

$\beta = 5$, $\tau_r = .05$ hr, $Q = -200$, $K = 30\ \mathrm{hr}^{-1}$, $k_{10} = 2.51 \times 10^5\ \mathrm{hr}^{-1}$, $k_{20} = 1.995 \times 10^7\ \mathrm{hr}^{-1}$, $P_1 = 5.03$, $P_2 = 10.06$, $T_r = 1000\ ^\circ\mathrm{R}$, $u_1^f = .9$, $u_2^f = .6$

Initially the concentration and temperature profiles are assumed to be constant throughout the length of the reactor and at the values of the inlet conditions, i.e.,

$$u_1(x, 0) = u_1^f \qquad \text{at} \qquad t = 0 \tag{68}$$

$$u_2(x, 0) = u_2^f \qquad \text{at} \qquad t = 0 \tag{69}$$

It is presupposed that a steady state operating point has been determined which is optimal with respect to some performance criterion (e.g., maximum yield). The startup policy, in turn, is to be determined such that by controlling the addition or removal of heat, the process is driven from the initial state toward the final steady state in some optimal fashion. It is desired to minimize the spatial integral of the weighted sum of the squared concentration and temperature deviations from the desired steady state profiles, $u_{1_d}(x)$ and $u_{2_d}(x)$, integrated over a transient startup period of fixed length. The performance functional may thus be written

$$S = \int_0^{t_f}\int_0^1 \{\mu[u_1(x, t) - u_{1_d}(x)]^2 + \nu[u_2(x, t) - u_{2_d}(x)]^2\}\, dx\, dt \tag{70}$$

Here μ and ν are suitably chosen constant weighting coefficients. The manipulated variable is the dimensionless wall temperature, θ, which is considered to be a function of time only and lie within the range

$$\theta_{min} \le \theta(t) \le \theta_{max} \tag{71}$$

The Hamiltonian, as defined by Equation (42), is

$$H = \mu[u_1(x, t) - u_{1_d}(x)]^2 + \nu[u_2(x, t) - u_{2_d}(x)]^2 + z_1[\tfrac{1}{\beta} u_{1_{xx}} - u_{1_x} - \tau_r\phi(u_1, u_2)] + z_2[\tfrac{1}{\beta} u_{2_{xx}} - u_{2_x} - Q\tau_r\phi(u_1, u_2) - K\tau_r(u_2 - \theta)] \tag{72}$$

With reference to Equation (19), the adjoint partial differential equations corresponding to Equations (62) and (63) respectively are

$$z_{1_t} = -\frac{1}{\beta} z_{1_{xx}} - z_{1_x} + \tau_r\phi_{u_1}(u_1, u_2)z_1 + Q\tau_r\phi_{u_1}(u_1, u_2)z_2 - 2\mu[u_1(x, t) - u_{1_d}(x)] \tag{73}$$

$$z_{2_t} = -\frac{1}{\beta} z_{2_{xx}} - z_{2_x} + \tau_r\phi_{u_2}(u_1, u_2)z_1 + [Q\tau_r\phi_{u_2}(u_1, u_2) + K_r]z_2 - 2\nu[u_2(x, t) - u_{2_d}(x)] \tag{74}$$

where

$$\phi_{u_1} = \frac{\partial\phi}{\partial u_1} = k_{10}\exp(-P_1/u_2) + k_{20}\exp(-P_2/u_2) \tag{75}$$

$$\phi_{u_2} = \frac{\partial\phi}{\partial u_2} = \frac{1}{u_2^2}[P_1 k_{10}\exp(-P_1/u_2)u_1 - P_2 k_{20}\exp(-P_2/u_2)(1 - u_1)] \tag{76}$$

Since the boundary conditions given by Equations (64) through (67) correspond to the general forms, Equations (21) and (22), the adjoint boundary conditions correspond to Equations (25) and (26), respectively. Thus

$$z_{i_x}(0, t) = 0 \qquad \text{at} \quad x = 0,\ i = 1, 2 \tag{77}$$

$$z_{i_x}(1, t) + \beta_1 z_i(1, t) = 0 \quad \text{at} \quad x = 1,\ i = 1, 2 \tag{78}$$

The final conditions on the adjoint variables corresponding to Equation (27) are

$$z_i(x, t_f) = 0 \qquad \text{at} \qquad t = t_f,\ i = 1, 2 \tag{79}$$

The solution of Equations (62) and (63) forward in time from $t = 0$ to $t = t_f$ is accomplished by the use of quasilinearization (10, 11) together with an implicit difference scheme. The details of the computational method are presented in (12).

To apply the quasilinearization technique, the nonlinear terms $\phi(u_1, u_2)$ in equations (62) and (63) are first linearized by means of a first-order Taylor series expanded about the (k-1)-th iterative solution $u^{(k-1)}$ as follows:

$$\phi^{(k)} = \phi^{(k-1)} + \phi_{u_1}^{(k-1)}[u_1^{(k)} - u_1^{(k-1)}] + \phi_{u_2}^{(k-1)}[u_2^{(k)} - u_2^{(k-1)}] \tag{80}$$

Substitution of Equation (80) into Equations (62) and (63) yields the following linearized recurrence relationship:

$$u_{1_t}^{(k)} = \frac{1}{\beta} u_{1_{xx}}^{(k)} - u_{1_x}^{(k)} - \tau_r[\phi^{(k-1)} + \phi_{u_1}^{(k-1)}(u_1^{(k)} - u_1^{(k-1)}) + \phi_{u_2}^{(k-1)}(u_2^{(k)} - u_2^{(k-1)})] \tag{81}$$

$$u_{2_t}^{(k)} = \frac{1}{\beta} u_{2_{xx}}^{(k)} - u_{2_x}^{(k)} - Q\tau_r[\phi^{(k-1)} + \phi_{u_1}^{(k-1)}(u_1^{(k)} - u_1^{(k-1)}) + \phi_{u_2}^{(k-1)}(u_2^{(k)} - u_2^{(k-1)})] - K\tau_r[u_2^{(k)} - \theta] \tag{82}$$

The solution of Equations (81) and (82) is greatly simplified by "decoupling" the component equations. This is done in the i-th equation by setting

$$u_j^{(k)} - u_j^{(k-1)} = \begin{cases} u_i^{(k)} - u_i^{(k-1)}, & j = i \\ 0 & j \neq i \end{cases} \tag{83}$$

Then Equations (81) and (82) become

$$u_{1_t}^{(k)} = \frac{1}{\beta} u_{1_{xx}}^{(k)} - u_{1_x}^{(k)} - \tau_r[\phi^{(k-1)} + \phi_{u_1}^{(k-1)}(u_1^{(k)} - u_1^{(k-1)})] \tag{84}$$

$$u_{2_t}^{(k)} = \frac{1}{\beta} u_{2_{xx}}^{(k)} - u_{2_x}^{(k)} - Q\tau_r[\phi^{(k-1)} + \phi_{u_2}^{(k-1)}(u_2^{(k)} - u_2^{(k-1)})] - K\tau_r[u_2^{(k)} - \theta] \tag{85}$$

This is valid, for as convergence is attained, $u_i^{(k-1)}$ approaches $u_i^{(k)}$. The equations are still implicitly coupled as $\phi^{(k-1)}$ contains the solutions $u_1^{(k-1)}$ and $u_2^{(k-1)}$.

Equations (84) and (85) are most conveniently solved by finite difference methods. However, for parabolic equations care must be taken in applying explicit difference approximations that stability is ensured. In order to circumvent this stability problem, the implicit scheme due to Crank and Nicolson (13) is considered here. This method introduces more complexity into the difference model but guarantees stability for any increment of time, thus reducing the number of time increments required.

In applying the Crank-Nicolson method the spatial axis is discretized into M increments of equal length Δx so that $\Delta x = 1/M$. Time discretization is effected by solving the difference equations at equal time increments Δt. The solution $u(m,n)$ denotes the value of the dependent variable at the spatial location $(m-1)\Delta x$ and at time $(n-1)\Delta t$.

The partial time derivatives are approximated by taking forward differences between the (n-1)-th and n-th time steps, i.e.,

$$u_t \approx \frac{1}{\Delta t}[u(m, n) - u(m, n-1)] \tag{86}$$

For spatial discretization, implicit difference operators are constructed for the first and second spatial partial derivatives by taking central differences, averaged over the (n-1)-th and n-th time steps, i.e.,

$$u_{xx} \approx \frac{M^2}{2}[u(m+1, n) - 2u(m, n) + u(m-1, n) + u(m+1, n-1) - 2u(m, n-1) + u(m-1, n-1)] \tag{87}$$

$$u_x \approx \frac{M}{4}[u(m+1, n) - u(m-1, n) + u(m+1, n-1) - u(m-1, n-1)] \tag{88}$$

The above difference operators have a discretization error on the order of $(\Delta x)^2$. The dependent variable u is also averaged over the (n-1)-th and n-th time steps:

$$u \approx \frac{1}{2}[u(m, n) + u(m, n-1)] \tag{89}$$

The difference approximations for the first derivative terms occuring in the boundary conditions at $x = 0$ and $x = 1$ are taken to be three-point forward and backward differences respectively:

$$u_x\Big|_{x=0} \approx \frac{M}{2}[-u(3, n) + 4u(2, n) - 3u(1, n)] \tag{90}$$

$$u_x\Big|_{x=1} \approx \frac{M}{2}[3u(M+1, n) - 4u(M, n) + u(M-1, n)] \tag{91}$$

Substitution of the above difference operators into the recurrence relations, Equations (84) and (85), and the boundary conditions, give rise to the set of linearized difference equations for the k-th iteration

$$\left.\begin{aligned}
&[B_1^{(k-1)}(2, n) + \tfrac{4M}{2\beta + 3M} A_1]u_1^{(k)}(2, n) \\
&\quad + [C_1 - \tfrac{M}{2\beta + 3M} A_1]u_1^{(k)}(3, n) \\
&= -A_1u_1(1, n-1) - D_1^{(k-1)}(2, n)u_1(2, n-1) \\
&\quad - C_1u_1(3, n-1) - E_1^{(k-1)}(2, n) - \tfrac{2\beta u_1^f}{2\beta + 3M} A_1 \\
&A_1u_1^{(k)}(m-1, n) + B_1^{(k-1)}(m, n)u_1^{(k)}(m, n) \\
&\quad + C_1u_1^{(k)}(m+1, n) \\
&= -A_1u_1(m-1, n-1) - D_1^{(k-1)}(m, n)\, u_1(m, n-1) \\
&\quad - C_1u_1(m+1, n-1) - E_1^{(k-1)}(m, n) \\
&\qquad\qquad\qquad m = 3, \ldots, M-1 \\
&[A_1 - \tfrac{1}{3} C_1]u_1^{(k)}(M-1, n) \\
&\quad + [B_1^{(k-1)}(M, n) + \tfrac{4}{3} C_1]u_1^{(k)}(M, n) \\
&= -A_1u_1(M-1, n-1) - D_1^{(k-1)}(M, n)u_1(M, n-1) \\
&\quad - C_1u_1(M+1, n-1) - E_1^{(k-1)}(M, n)
\end{aligned}\right\} \tag{92}$$

$$\left.\begin{aligned}
&[B_2^{(k-1)}(2, n) + \tfrac{4M}{2\beta + 3M} A_2]u_2^{(k)}(2, n) \\
&\quad + [C_2 - \tfrac{M}{2\beta + 3M} A_2]u_2^{(k)}(3, n) \\
&= -A_2u_2(1, n-1) - D_2^{(k-1)}(2, n)u_2(2, n-1) \\
&\quad - C_2u_2(3, n-1) - E_2^{(k-1)}(2, n) - \tfrac{2\beta u_2^f}{2\beta + 3M} A_2 \\
&A_2u_2^{(k)}(m-1, n) + B_2^{(k-1)}(m, n)\, u_2^{(k)}(m, n) \\
&\quad + C_2u_2^{(k)}(m+1, n)
\end{aligned}\right\} \tag{93}$$

$$
\left.\begin{aligned}
&= -A_2u_2(m-1,\ n-1) - D_2^{(k-1)}(m,\ n)u_2(m,\ n-1) \\
&\quad -C_2u_2(m+1,\ n-1) - E_2^{(k-1)}(m,\ n) \\
&\qquad\qquad m = 3,\ \ldots,\ M-1 \\
&[A_2 - \tfrac{1}{3}C_2]\ u_2^{(k)}(M-1,\ n) \\
&\quad + [B_2^{(k-1)}(M,\ n) + \tfrac{4}{3}C_2]u_2^{(k)}(M,\ n) \\
&= -A_2u_2(M-1,\ n-1) - D_2^{(k-1)}(M,\ n)u_2(M,\ n-1) \\
&\quad -C_2u_2(M+1,\ n-1) - E_2^{(k-1)}(M,\ n)
\end{aligned}\right\}
$$

where

$$A_1 = A_2 = \frac{M^2}{2\beta} + \frac{M}{4}$$

$$B_1^{(k-1)}(m,\ n) = -\frac{1}{2}\tau_r\phi_{u_1}^{(k-1)}(m,\ n) - \frac{M^2}{\beta} - \frac{1}{\Delta t}$$

$$B_2^{(k-1)}(m,\ n) = -\frac{1}{2}Q\tau_r\phi_{u_2}^{(k-1)}(m,\ n) - \frac{1}{2}K\tau_r - \frac{M^2}{\beta} - \frac{1}{\Delta t}$$

$$C_1 = C_2 = \frac{M^2}{2\beta} - \frac{M}{4}$$

$$D_1^{(k-1)}(m,\ n) = -\frac{1}{2}\tau_r\phi_{u_1}^{(k-1)}(m,\ n) - \frac{M^2}{\beta} + \frac{1}{\Delta t}$$

$$D_2^{(k-1)}(m,\ n) = -\frac{1}{2}Q\tau_r\phi_{u_2}^{(k-1)}(m,\ n) - \frac{1}{2}K\tau_r - \frac{M^2}{\beta} + \frac{1}{\Delta t}$$

$$E_1^{(k-1)}(m,\ n) = -\tau_r[\phi^{(k-1)}(m,\ n) - u_1^{(k-1)}(m,\ n)\ \phi_{u_1}^{(k-1)}(m,\ n)]$$

$$E_2^{(k-1)}(m,\ n) = -Q\tau_r[\phi^{(k-1)}(m,\ n) - u_2^{(k-1)}(m,\ n)\phi_{u_2}^{(k-1)}(m,\ n)] + K\tau_r\theta$$

The endpoint values are determined from the following boundary equations

$$u_1^{(k)}(1,\ n) = -\frac{M}{2\beta + 3M}u_1^{(k)}(3,\ n) + \frac{M}{2\beta + 3M}u_1^{(k)}(2,\ n) + \frac{2\beta}{2\beta + 3M}u_1^{f} \tag{94}$$

$$u_1^{(k)}(M+1,\ n) = \frac{4}{3}u_1^{(k)}(M,\ n) - \frac{1}{3}u_1^{(k)}(M-1,\ n) \tag{95}$$

$$u_2^{(k)}(1,\ n) = -\frac{M}{2\beta + 3M}u_2^{(k)}(3,\ n) + \frac{4M}{2\beta + 3M}u_2^{(k)}(2,\ n) + \frac{2\beta}{2\beta + 3M}u_2^{f} \tag{96}$$

$$u_2^{(k)}(M+1,\ n) = \frac{4}{3}u_2^{(k)}(M,\ n) - \frac{1}{3}u_2^{(k)}(M-1,\ n) \tag{97}$$

Similarly the backwards solution of equations (73) and (74) from $t = t_f$ to $t = 0$ is accomplished by solving the following sets of implicit difference equations from $n = N$ to $n = 1$:

$$
\left.\begin{aligned}
&[B_3(2,\ n) + \tfrac{4}{3}A_3]z_1^{(k)}(2,\ n) \\
&\quad + [C_3 - \tfrac{1}{3}A_3]z_2^{(k)}(3,\ n) \\
&= -A_3z_1(1,\ n+1) - D_3(2,\ n+1)\ z_1(2,\ n+1) \\
&\quad -C_3z_1(3,\ n+1) + E_3^{(k-1)}(2,\ n) \\
&A_3z_1^{(k)}(m-1,\ n) + B_3(m,\ n)z_1^{(k)}(m,\ n) \\
&\quad + C_3z_1^{(k)}(m+1,\ n) \\
&= -A_3z_1(m-1,\ n+1) - D_3(m,\ n+1)\ z_1(m,\ n+1) \\
&\quad -C_3z_1(m+1,\ n+1) + E_3^{(k-1)}(m,\ n) \\
&\qquad\qquad m = 3,\ \ldots,\ M-1 \\
&[A_3 - \tfrac{M}{2\beta + 3M}C_3]z_1^{(k)}(M-1,\ n) \\
&\quad + [B_3(M,\ n) + \tfrac{4M}{2\beta + 3M}C_3]z_1^{(k)}(M,\ n) \\
&= -A_3z_1(M-1,\ n+1) - D_3(M,\ n+1)\ z_1(M,\ n+1) \\
&\quad -C_3z_1(M+1,\ n+1) + E_3^{(k-1)}(M,\ n)
\end{aligned}\right\} \tag{98}
$$

$$
\left.\begin{aligned}
&[B_4(2,\ n) + \tfrac{4}{3}A_4]z_2^{(k)}(2,\ n) \\
&\quad + [C_4 - \tfrac{1}{3}A_4]z_2^{(k)}(3,\ n) \\
&= -A_4z_2(1,\ n+1) - D_4(2,\ n)z_2(2,\ n+1) \\
&\quad -C_4z_2(3,\ n+1) + E_4^{(k-1)}(M,\ n) \\
&A_4z_2^{(k)}(m-1,\ n) + B_4(m,\ n)z_2^{(k)}(m,\ n) \\
&\quad + C_4z_2^{(k)}(m+1,\ n) \\
&= -A_4z_2(m-1,\ n) - D_4(m,\ n)z_2(m,\ n+1) \\
&\quad -C_4z_2(m+1,\ n+1) + E_4^{(k-1)}(m,\ n) \\
&\qquad\qquad m = 3,\ \ldots,\ M-1 \\
&[A_4 - \tfrac{M}{2\beta + 3M}C_4]z_2^{(k)}(M-1,\ n) \\
&\quad + [B_4(M,\ n) + \tfrac{M}{2\beta + 3M}C_4]z_2^{(k)}(M,\ n) \\
&= -A_4z_2(M-1,\ n+1) - D_4(M,\ n)z_2(M,\ n+1) \\
&\quad -C_4z_2(M+1,\ n+1) + E_4^{(k-1)}(N,\ n)
\end{aligned}\right\} \tag{99}
$$

where

$$A_3 = A_4 = \frac{M^2}{2\beta} - \frac{M}{4}$$

$$B_3(m,\ n) = -\frac{1}{2}\tau_r\phi_{u_1}(m,\ n) - \frac{M^2}{\beta} - \frac{1}{\Delta t}$$

$$B_4(m,\ n) = -\frac{1}{2}Q\tau_r\phi_{u_2}(m,\ n) - \frac{1}{2}K\tau_r - \frac{M^2}{\beta} - \frac{1}{\Delta t}$$

$$C_3 = C_4 = \frac{M^2}{2\beta} + \frac{M}{4}$$

$$D_3(m, n) = -\frac{1}{2} Q\tau_r \phi_{u_1}(m, n) - \frac{M^2}{\beta} + \frac{1}{\Delta t}$$

$$D_4(m, n) = -\frac{1}{2} Q\tau_r \phi_{u_2}(m, n) - \frac{1}{2} K\tau_r - \frac{M^2}{\beta} + \frac{1}{\Delta t}$$

$$E_3^{(k-1)}(m, n) = Q\tau_r \phi_{u_1}(m, n) z_2^{(k-1)}(m, n) - 2\mu[u_1(x, t) - u_{1_d}(x)]$$

$$E_4^{(k-1)}(m, n) = \tau_r \phi_{u_2}(m, n) z_1^{(k-1)}(m, n) - 2\nu[u_2(x, t) - u_{2_d}(x)]$$

The endpoint values for the adjoint variables are determined, using the following boundary equations:

$$z_1^{(k)}(1, n) = -\frac{1}{3} z_1^{(k)}(3, n) + \frac{4}{3} z_1^{(k)}(2, n) \tag{100}$$

$$z_1^{(k)}(M+1, n) = \frac{4M}{2\beta + 3M} z_1^{(k)}(M, n) - \frac{M}{2\beta + 3M} z_1^{(k)}(M-1, n) \tag{101}$$

$$z_2^{(k)}(1, n) = -\frac{1}{3} z_2^{(k)}(3, n) + \frac{4}{3} z_2^{(k)}(2, n) \tag{102}$$

$$z_2^{(k)}(M+1, n) = \frac{4M}{2\beta + 3M} z_2^{(k)}(M, n) - \frac{M}{2\beta + 3M} z_2^{(k)}(M-1, n) \tag{103}$$

Upon obtaining the adjoint solutions, an improved control function $\theta(t)$ may be obtained using Equation (54) and the Hamiltonian defined in Equation (72). The resulting change in control, $\delta\theta(t)$, is

$$\delta\theta(t) = -\alpha \frac{\int_0^1 K\tau_r z_2(x, t)dx}{\left[\int_0^{t_f} \left[\int_0^1 K\tau_r z_2(x, t)dx\right]^2 dt\right]^{1/2}} \tag{104}$$

where α can be considered as a perturbation coefficient representing step length. Using Simpson's integration scheme, values of $z_2(m, n)$, $m = 1, \ldots, M+1$, $n = 1, \ldots, N+1$, obtained by backwards solution of the adjoint equations, may be used in Equation (92) to compute $\delta\theta(n)$, $n = 1, \ldots, N$. The new control function $\theta(n)$, $n = 1, \ldots, N$ is then found from the relation

$$\theta(n)\big|_{new} = \theta(n)\big|_{old} + \delta\theta(n) \tag{105}$$

Computation was performed using a time increment of .02 residence time and a spatial increment of .05 dimensionless distance unit. The limits on the control were assumed to be $\theta_{max} = .670$ and $\theta_{min} = .530$ dimensionless temperature unit. The performance index S was evaluated using a terminal time of one residence time and the weighting coefficients μ and ν were each taken to be unity. The desired steady state profiles, $u_{1_d}(x)$ and $u_{2_d}(x)$, were chosen to correspond to a control value of $\theta = .6$ dimensionless temperature unit.

With regard to the selection of the initial approximation, it should be noted that the steady state value of the control must be known and used in the initial assumed trajectory at the terminal time t_f. This is because the algorithm is incapable of shifting the control at terminal time, as seen from Equation (104) and the transversality conditions, Equation (79). Thus for convenience, the initial control trajectory approximation was taken to be $\theta(t) = .6$ dimensionless temperature unit, the steady state value.

Figure 2 shows the optimal control trajectory obtained after 30 iterations, using a perturbation coefficient of $\alpha = .1$. This value, determined by trial and error, provided a reasonable rate of convergence of the performance index to a minimum without oscillations. The policy is seen to approach a bang-bang trajectory with maximum wall temperature applied to the system initially. At about .20 residence time a switch to minimum wall temperature occurs, followed by a singular approach to the steady state value starting at about .44 residence time.

The resulting transient concentration and temperature profiles, $u_1(x, t)$ and $u_2(x, t)$, obtained using the optimal startup policy are shown in Figures 3 and 4, respectively with time as a parameter. Shown in dashed lines for comparison are the transient profiles resulting from using steady state control. The value of the performance index obtained for the optimally controlled case was .046557 compared to .050435 with steady state control.

Since the optimal control policy so closely resembled bang-bang control, a purely bang-bang policy was considered. This consisted of starting with maximum effort, switching to minimum effort and finally switching to the steady state control level. These two switch points were approximated from the optimal trajectory to be .20 and .50 residence times respectively. The state equations were solved using the bang-bang policy and the performance index, Equation (70), was computed, yielding a value of .046555. Thus the performance index remained essentially unchanged using the bang-bang approximation and, because of its simplicity to implement, a bang-bang policy would probably be preferred for this application.

Constraint on Maximum Reaction Temperature

Suppose it is desired to determine the optimal startup control trajectory which minimizes the performance criterion, Equation (70), while at the same time holding the maximum reaction temperature at or below a specified upper limit. This inequality constraint can be written

$$u_2(x, t) - u_{2_{max}} \le 0 \tag{106}$$

The constraint is introduced into the performance index as a penalty by means of a weighting coefficient σ as follows:

$$S = \int_0^{t_f} \int_0^1 \{\mu[u_1(x, t) - u_{1_d}(x)]^2 + \nu[u_2(x, t) - u_{2_d}(x)]^2 + \sigma[u_2(x, t) - u_{2_{max}}]^2 \hat{h}[u_2(x, t) - u_{2_{max}}]\}dx\, dt \tag{107}$$

where $\hat{h}[u_2(x, t) - u_{2_{max}}]$ is the Heavyside unit step function. Thus a penalty is not invoked until a constraint is violated. The weighting coefficient σ is increased iteratively, stopping the iteration when the maximum temperature has converged to within a specified tolerance of the constraint boundary.

State variable constraints such as this require a corresponding modification of the adjoint equations since an additional term involving a state variable is introduced into the performance index. Thus the adjoint equations, Equations (73) and (74), become

$$z_{1_t} = -\frac{1}{\beta} z_{1_{xx}} - z_{1_x} + \tau_r \phi_{u_1}(u_1, u_2) z_1 + Q\tau_r \phi_{u_1}(u_1, u_2) z_2 - 2\nu[u_1(x, t) - u_{1_d}(x)] \quad (108)$$

$$z_{2_t} = -\frac{1}{\beta} z_{2_{xx}} - z_{2_x} + \tau_r \phi_{u_2}(u_1, u_2) z_1 + [Q\tau_r \phi_{u_2}(u_1, u_2) + K\tau_r] z_2 - 2\nu[u_2(x, t) - u_{2_d}(x)] - 2\sigma[u_2(x, t) - u_{2_{max}}]\,\hat{h}[u_2(x, t) - u_{2_{max}}] \quad (109)$$

Figure 5 shows the optimal control policy for the case of an upper constraint on maximum reaction temperature, $u_{2_{max}} = .700$ dimensionless temperature unit. The switch point from maximum to minimum wall temperature occurs earlier than for the case of an unconstrained state, thus reducing the amount of temperature overshoot. The following table lists the penalty weights σ and the corresponding maximum temperatures that resulted after each ascent:

σ	Maximum reaction temperature
(Unconstrained)	.7165
1	.7147
10	.7093
10^2	.7048
10^3	.7014
10^4	.7005

The iteration was stopped for $\sigma = 10^4$ as the resulting maximum temperature was considered in close enough proximity to the constraint boundary. Each time the value of σ was increased, it was found necessary to adjust the perturbation coefficient α downward in order to prevent oscillations and instability of the performance index.

Exit temperature trajectories for optimal control, with and without a state variable constraint, and for steady state control, are shown in Figure 6.

CONCLUSIONS

An optimal startup policy of a jacketed tubular reactor in which a first-order, reversible, exothermic reaction takes place is determined. A distributed maximum principle is presented for determining weak necessary conditions for optimality of diffusional distributed parameter systems.

Optimization of the two-point boundary value system of second order, non-linear, parabolic partial differential equations presents a formidable computational problem. An approximate numerical method which is iterative in nature, involving repeated numerical integration of the performance and adjoint equations, combined with the use of a functional gradient technique to improve the control vector is introduced to overcome computational difficulties. A convenient method for handling inequality constraints involving state variables is also presented.

REFERENCES

1. Denn, M. M., R. D. Gray, Jr., and J. R. Ferron, "Optimization in a Class of Distributed Parameter Systems," Ind. Eng. Chem. Fundamentals, 7, 286-295 (1968).
2. Pontryagin, L. S., V. G. Boltyanskii, R. V. Gamkrelidge, and E. F. Mishchenko, The Mathematical Theory of Optimal Processes, (English translation by K. N. Trirogoff), Interscience, New York, 1962.
3. Fan, L. T., The Continuous Maximum Principle, Wiley, New York, 1966.
4. Katz, S., "A General Maximum Principle for End-point Control Problems," J. Electronics and Control, 16, 189-222 (1964).
5. Jackson, R., "Optimum Temperature Gradients in Tubular Reactors with Decaying Catalyst," Proc. Int. Chem. Eng., 4, 32-38 (1965).
6. Seinfeld, J. H., "Optimal Control of Distributed Parameter Systems," Ph.D. Thesis, Princeton University, 1967.
7. Courant, R. and D. Hilbert, Methods of Mathematical Physics, Vol. 1, Interscience, New York, 1965.
8. Bryson, A. E. and W. F. Denham, "A Steepest-Ascent Method for Solving Optimum Programming Problems," J. of Applied Mechanics, Trans. ASME, 29, 247-257 (1962).
9. [illegible]kwerts, P. V., "Continuous Flow Systems," [illegible] Engr. Sci. 2, 1-13 (1953).
10. Bellman, R. E., and R. E. Kalaba, Quasilinearization and Nonlinear Boundary Value Problems, American Elsevier, New York, 1965.
11. Sage, A. P. and S. P. Chandhuri, "Gradient and Quasi-linearization Computational Techniques for Distributed Parameter Systems," Int. J. Contr., 6, 81-98 (1967).
12. Hahn, D. R., "Optimal Control of a Class of Distributed Parameter Processes," Ph.D. Thesis, Kansas State University, 1969.
13. Forsythe, G. E., and W. R. Wasow, Finite Difference Methods for Partial Differential Equations, Wiley, New York, 1965.

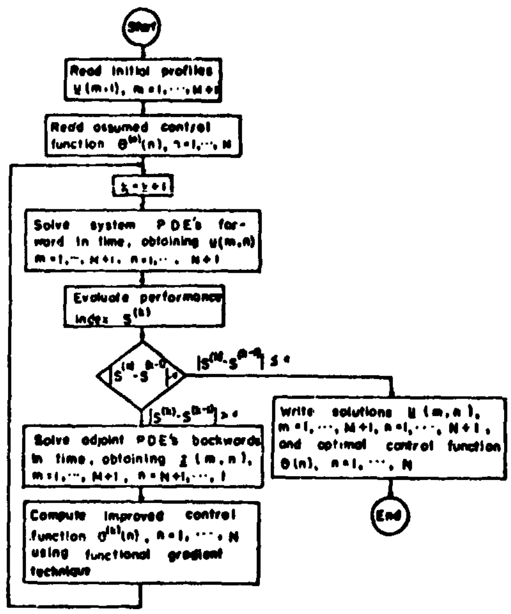

Fig. 1 Flow diagram for optimal control using the distributed maximum principle.

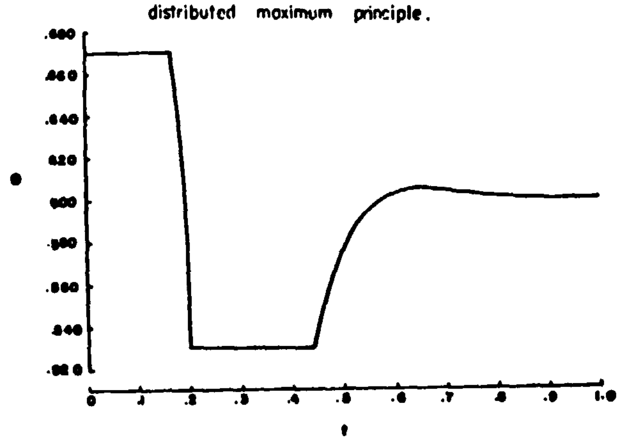

Fig. 2 Optimal startup control policy for tubular reactor using distributed maximum principle.

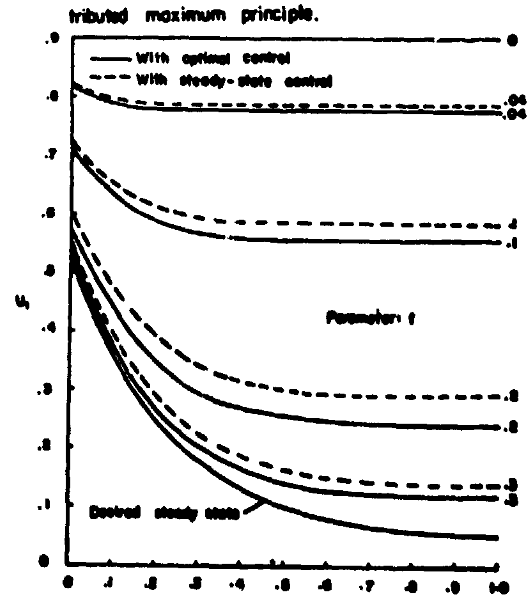

Fig. 3 Transient concentration profiles for tubular reactor startup.

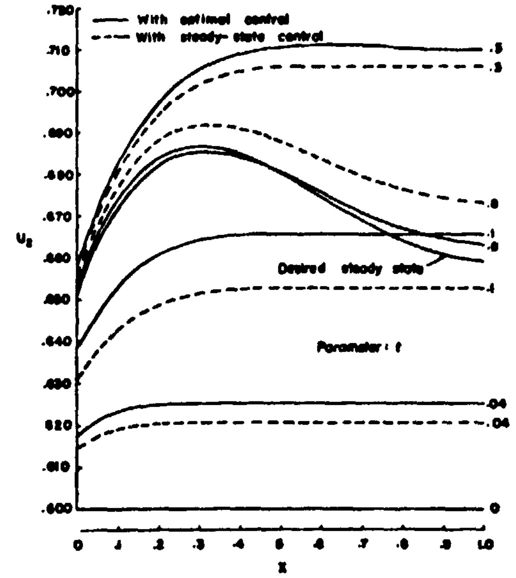

Fig. 4 Transient temperature profiles for tubular reactor startup.

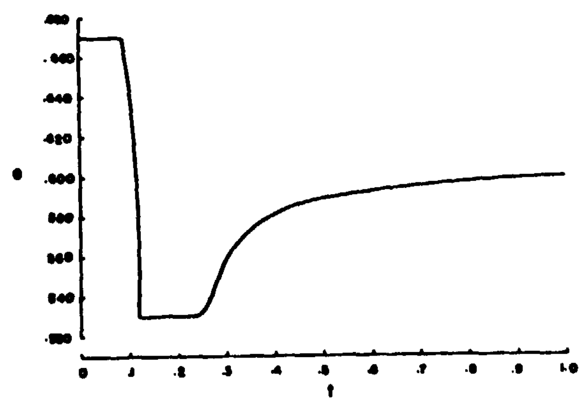

Fig. 5 Optimal startup control policy for tubular reactor using distributed maximum principle (with constraint on maximum reaction temperature, $u_{2_{max}} = .700$).

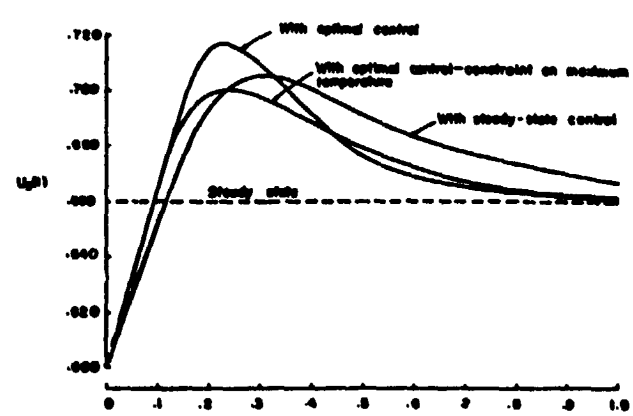

Fig. 6 Exit temperature trajectories for tubular reactor during startup

PREPRINTS OF PAPERS

FOR

IFAC

KYOTO SYMPOSIUM

ON

SYSTEMS ENGINEERING APPROACH TO COMPUTER CONTROL

organized by
IFAC Kyoto Symposium Committee

sponsored by
IFAC Technical Committee on Systems Engineering

co-sponsored by
IFAC Technical Committee on Applications

under the aegis of
Science Council of Japan

under the auspices of
The Society of Instrument and Control Engineers (Japan)
and
The Japan Association of Automatic Control Engineers

Kyoto International Conference Hall
Kyoto, Japan
August 11—14, 1970

11.1 CONTROL OF A CLASS OF NONLINEAR DISTRIBUTED PARAMETER SYSTEMS
VIA DIRECT SEARCH ON THE PERFORMANCE INDEX

D. R. Hahn, L. T. Fan, and C. L Hwang
Institute for Systems Design and Optimization
Kansas State University, Manhattan, Kansas U.S.A.

11.1 CONTROL OF A CLASS OF NONLINEAR DISTRIBUTED PARAMETER SYSTEMS VIA DIRECT SEARCH ON THE PERFORMANCE INDEX+

D. R. Hahn, Project Engineer
The Bendix Corporation, Kansas City, Missouri

L. T. Fan, Professor and Head of Chemical Engineering
Director of Institute for Systems Design and Optimization

C. L. Hwang, Associate Professor of Industrial Engineering
Kansas State University, Manhattan, Kansas 66502, U.S.A.

ABSTRACT

The synthesis of optimal controls is treated for a relatively wide class of mixed, continuous flow processes. This class is comprised of systems, the dynamics of which can be described by nonlinear, one-dimensional axial diffusion models with two-point boundary values. An overall direct search technique is considered which is applicable to nonlinear distributed systems with control saturation constraints. This method, iterative in nature, entails a scanning of an overall performance index for different trial control levels at increments of time, yielding a piecewise-constant control policy. State variable inequality constraints are handled by the penalty function method. The technique is applied to the tubular reactor startup problem and the resulting control policy is shown to closely approximate that obtained using a distributed maximum principle. A sub-optimal non-iterative direct search technique is also developed. This involves the evaluation of an instantaneous performance measure at the end of each time step for trial control values over the admissible range. This technique, applied to the tubular reactor startup problem, is shown to yield results similar to those of the other two approaches, namely, the distributed maximum principle and the overall direct search technique.

INTRODUCTION

In the field of industrial process control, increasing attention is being focused upon the study of systems from the distributed parameter point of view.

Perhaps the first work devoted to optimization of distributed parameter systems was undertaken by Butkovskii and Lerner.[1, 2] These papers considered mainly a class of first-order partial differential equations, which through a coordinate transformation, could be treated with Pontryagin's maximum principle.[3, 4] A thorough review of the literature on the optimization of distributed parameter systems is given in[5]. Most of the literature has dealt with linear distributed parameter systems. Relatively few papers have appeared thus far which report successful computational results for nonlinear distributed systems. However, with the advent of larger and more rapid computing systems coupled with more sophisticated numerical analysis techniques, strides are now being made in this area.[6, 7, 8, 9] Most of the workers in this field have employed variational techniques and have obtained various forms of maximum principles.

As an alternate method involving less computational complexity than the maximum principle, an overall direct search technique will be presented in this work. This approach is applicable to systems with saturation constraints on the control variable and entails a scanning of the performance index at increments of time for different trial control levels. The method is iterative and considers an assessment of performance based upon the entire period of operation. A simplified non-iterative direct search technique will also be considered in this work. This method involves the evaluation of an instantaneous performance measure at each time step for different control levels and thus yields a suboptimal policy. Provision for state variable inequality constraints will be considered for both direct search techniques.

The implementation of the direct search techniques is accomplished by utilizing quasi-

+This study was supported in part by NASA Grant No. NGR-17-001-034, and by the Air Force Office of Scientific Research, Office of Aerospace Research, United States Air Force, Under Contract F44620-68-0020 (Themis Project).

linearization, decoupling of the equations and the application of an implicit difference technique for obtaining the transient solutions to the system of nonlinear partial differential equations.

Optimal control of a startup of a jacketed tubular reactor in which a first-order, reversible, exothermic reaction is assumed to take place is considered. It is determined how the wall temperature should best be manipulated to minimize a given performance index. Computational results are obtained for cases with and without a constraint on maximum reaction temperature.

SYSTEM DESCRIPTION

Suppose that a system is described by a general nonlinear vector partial differential equation

$$\underline{u}_t(x,t) = \underline{f}[\underline{u}(x,t),\ \underline{u}_x(x,t),\ \underline{u}_{xx}(x,t),\ \theta(t)] \tag{1}$$

where $\underline{u}$ is an s-dimensional state vector defined on a normalized one-dimensional spatial domain x from x=0 to x=1 and over a fixed time interval t=0 to $t=t_f$. The control variable θ is considered to be distributed in time only and is one-dimensional, with maximum and minimum limits specified. An independent variable appearing as a subscript denotes partial differentiation with respect to that variable.

Initial and boundary conditions are

$$\xi_i(\underline{u}) = 0 \quad \text{at} \quad t=0, \quad i=1, \ldots, s \tag{2}$$

$$\phi_m(\underline{u},\underline{u}_x) = 0 \quad \text{at} \quad x=0, \quad m=1, \ldots, p \tag{3}$$

$$\psi_n(\underline{u},\underline{u}_x) = 0 \quad \text{at} \quad x=1, \quad n=1, \ldots, q=2s-p \tag{4}$$

It is assumed that no boundary forcing is present.

It is desired to determine the control function θ which yields a minimum for the following generalized objective functional:

$$S = \int_0^1 F[\underline{u}(x,t_f)]dx + \int_0^{t_f}\int_0^1 G[\underline{u}(x,t),\ \theta(t)]dx\, dt \tag{5}$$

OVERALL DIRECT SEARCH

The method of optimization based on the distributed maximum principle[5] is computationally complex and time consuming. The method to be discussed here stems from a similar direct search technique described by Lapidus and Luus[10] for nonlinear lumped parameter systems with saturation constraints on the control variables. A modified version has been employed by Seinfeld and Lapidus[8] to treat systems with distributed parameters, although somewhat different from the approach taken here.

Description of the Method

A number of control levels θ_j, j = 1, ..., J are selected, which are equally spaced over the range of admissibility and include the upper and lower limits. The time axis is discretizing from t = 0 to $t = t_f$ into N segments of length t_f/N and assuming a piece-wise-constant initial control policy $\theta^{(0)}(n)$, n = 1, ..., N.

Holding each $\theta^{(0)}(n)$, n = 2, ..., N fixed, the system state equations are solved from t = 0 to $t = t_f$, replacing $\theta^{(0)}(1)$, in turn, by each θ_j. After each solution of the state equations, the overall performance index S is computed. If either extreme control level, i.e., θ_1 or θ_J, minimizes S, that level replaces the original $\theta^{(0)}(1)$. If the performance index is minimized for a control level interior to the range of admissibility, interpolation is performed by fitting a three-point Lagrangian polynomial through the minimum point and each point immediately adjacent. The minimum value of the polynomial is then computed and the corresponding control level is taken to replace $\theta^{(0)}(1)$.

The procedure is repeated for each time increment n = 2, ..., N. whereupon each original assumed control has been improved. This ends the first overall iteration. Since at each time step, the assumed control level would be retained if no improvement could be realized with another level, the performance index must decrease monotonically.

The improved control policy then becomes $\theta^{(1)}(n)$, n = 1, ..., N and is used as the starting point for the second overall iteration. This iterative sequence is repeated until negligible further improvement is realized in the performance index.

A computer flow diagram for the overall direct search scheme is shown in Figure 1.

Provision for State Variable Constraints. The overall direct search method is very easily extended to account for inequality constraints on state variables. These constraints may appear in the form

$$C(\underline{u},\theta) \leq 0 \tag{6}$$

As in the maximum principle approach[5], a convenient means for handling constraints of this type is the penalty function method. This consists of adding additional terms to the integrand of the performance index which have zero value until a constraint is violated and imposing a penalty after a violation occurs. Thus the state trajectories can be forced to the constraint boundary by iteratively manipulating the amount of penalty to be imposed.

SIMPLIFIED DIRECT SEARCH

Both the maximum principle approach[5] and the overall direct search technique are relatively time consuming. This limits the usefulness of these procedures to off-line use in pre-calculating the open-loop system control policy and the resulting trajectory over the transient period of interest.

However, the response of a real process may differ significantly from that anticipated by the model because of model inaccuracies, changing parameters, load disturbances, etc., and it may become desirable to redetermine the control action periodically, using current information about the state of the system. It thus becomes essential to have a simpler optimization scheme which takes into account the current state and uses this information to compute on-line an appropriate updated control policy, perhaps in conjunction with an adaptive scheme in which the model itself is also updated.

An optimizing scheme called an "optimum predictor-controller" has been developed by Grethlein and Lapidus[11] for lumped nonlinear systems with bounded controls. The approach taken was to sample the state at discrete values of time, and using this data as the initial conditions, to calculate over one sampling period, the response for several levels of control within the allowable range. The optimal control was determined by evaluating the performance criterion for each control level and selecting that level which yielded the least value of the criterion.

A similar approach is taken in this work for the determination of the control policy for a distributed system whose dynamic behavior may be described by a system of nonlinear partial differential equations in which there is only one control variable, a function of time only.

The feasibility of the method for on-line computer control would be contingent upon the sampling, computation and actuation times being short in comparison to the dynamics of the process under control. However, many distributed processes are characterized by long time constants and exhibit sluggish behavior, possible making on-line computer control attractive.

Description of the Method. The proposed simplified direct search method, instead of assessing system performance over the whole period of operation, evaluates the effect of control action over a relatively small interval of time. Thus the technique must be considered suboptimal with respect to an overall performance index of the type of Equation (5). A measure of performance may take into consideration a time integral criterion involving the response of the state variables over the small interval, or simply an instantaneous measure involving the state profiles at the end of the interval. The latter approach is considered herein. Thus a performance index could be considered in the sense of the integrand of the time integral of Equation (5) evaluated at a discrete point in time.

Using the instantaneous state profiles as the initial conditions at each time $t = (n-1)\Delta t$, $n = 1, \ldots, N$, a numerical integration scheme is employed to predict the system response at $t = n\Delta t$ for a number of pre-selected control levels, each held constant for the duration of the time period. These control levels are equally spaced over the admissible region and include the upper and lower limits.

The performance index is evaluated at $t = n\Delta t$ for each value of the control and a direct search made to find the minimum value of the index. The determination of the optimal control level for the period is the same as described for the overall direct search. If the index is minimized for the upper or lower limit, that level is taken to be the optimal control level for the time period; otherwise an interior value is determined by interpolation. A computer flow diagram for this simplified procedure is shown in Figure 2.

Provision for State Variable Constraints. The simplified direct search technique can be extended to provide for state variable inequality constraints of the form of Equation (6). However, instead of a penalty function approach, a direct method will be considered.

Upon computing the optimal control $\theta(n)$ for the time period $t = (n-1)\Delta t$ to $t = n\Delta t$ and the corresponding state trajectories, a test is performed to detect violations of the inequality of Equation (6). If a violation appears eminent, another control level is selected which tends to force the state trajectory away from the constraint boundary.

The ability to prevent constraint violations depends on the capacity of the control system to avoid the constraint boundary once it is approached. It may be necessary to consider two time intervals; (1) the period over which the responses are computed, say, $(\Delta t)_1$, and (2) the interval over which the resulting control action is actually carried out, say, $(\Delta t)_2$, where $(\Delta t)_1 > (\Delta t)_2$. This would give the control system more advance warning of an impending constraint violation and thus prevent overshoot (or undershoot) of the constraint. This feature will be seen in the simplified direct search example.

OPTIMAL STARTUP CONTROL OF A JACKETED TUBULAR REACTOR

The Mathematical Model. Consider a tubular, continuous flow chemical reactor in which an exothermic reaction is taking place. The reaction considered is first-order and reversible ($A \rightleftarrows B$). In this example, the reaction temperature and thus yield are controlled by manipulation of the reactor wall temperature.

The mathematical model for the system is based on the assumptions that system parameters are uniform and constant with respect to time, wall temperature is a function of time only, axial heat and mass dispersion and mixing are significant inside the reactor, and concentration, temperature and velocity of the stream are constant with respect to radial distance.

A differential mass balance yields

$$\frac{\partial c_A}{\partial \tau} = D_m \frac{\partial^2 c_A}{\partial \ell^2} - v \frac{\partial c_A}{\partial \ell} + R_A \quad (7)$$

where, for the case of a first-order, reversible $A \rightleftarrows B$ reaction, the rate of production of A, R_A, is given by the Arrhenius expression

$$R_A = -[k_{10} \exp(-E_1/RT)c_A - k_{20} \exp(-E_2/RT)c_B]$$

A differential heat balance yields

$$\frac{\partial T}{\partial \tau} = \frac{k_{eff}}{C_p \rho} \frac{\partial^2 T}{\partial \ell^2} - v \frac{\partial T}{\partial \ell} + \frac{(-\Delta H)}{C_p \rho} R_A - \frac{2h}{C_p \rho r} (T - T_w) \quad (8)$$

It is assumed that the manner of mixing is such that the effective mass and thermal diffusivities are equal, i.e., $D_m = k_{eff}/C_p\rho = D$. The boundary conditions are[12]

$$\frac{\partial c_A(0,\tau)}{\partial \ell} = \frac{v}{D} [c_A(0,\tau) - c_A^f] \quad \text{at} \quad \ell = 0 \quad (9)$$

$$\frac{\partial c_A(L,\tau)}{\partial \ell} = 0 \quad \text{at} \quad \ell = L \quad (10)$$

$$\frac{\partial T(0,\tau)}{\partial \ell} = \frac{v}{D} [T(0,\tau) - T^f] \quad \text{at} \quad \ell = 0 \quad (11)$$

$$\frac{\partial T(L,\tau)}{\partial \ell} = 0 \quad \text{at} \quad \ell = L \quad (12)$$

In dimensionless form the system equations, equations (7) and (8) become

$$u_{1_t} = \frac{1}{\beta} u_{1_{xx}} - u_{1_x} - \tau_r \phi(u_1, u_2) \quad (13)$$

$$u_{2_t} = \frac{1}{\beta} u_{2_{xx}} - u_{2_x} - Q\tau_r \phi(u_1, u_2) - K\tau_r(u_2 - \theta) \quad (14)$$

where

$$\phi(u_1, u_2)$$

$$= k_{10} \exp(-P_1/u_2)u_1 - k_{20} \exp(-P_2/u_2)(1 - u_1) \quad (15)$$

where $\tau_r = L/v$ hr is mean residence time, $\beta = vL/D$, axial Peclet number, $t = \tau/\tau_r$, dimensionless time, $x = \ell/L$, dimensionless axial distance, $u_1 = c_A/(c_A + c_B)$, dimensionless concentration of A, $u_2 = T/T_r$, dimensionless reaction temperature, and $\theta = T_w/T_r$, dimensionless wall temperature. Other parameters are $Q = \Delta H(c_A + c_B)/C_p\rho T_r$, $K = 2h/C_p\rho r$ hr^{-1}, $P_1 = E_1/RT_r$, and $P_2 = E_2/RT_r$. The dimensionless boundary conditions are

$$u_{1_x}(0,t) = \beta[u_1(0,t) - u_1^f] \quad \text{at} \quad x=0 \quad (16)$$

$$u_{1_x}(1,t) = 0 \quad \text{at} \quad x=1 \quad (17)$$

$$u_{2_x}(0,t) = \beta[u_2(0,t) - u_2^f] \quad \text{at} \quad x=0 \quad (18)$$

$$u_{2_x}(1,t) = 0 \quad \text{at} \quad x=1 \quad (19)$$

The concentration and temperature profiles are assumed to be initially constant throughout the length of the reactor and at the values of the inlet conditions, i.e.,

$$u_1(x,0) = u_1^f \quad \text{at} \quad t=0, \quad (20)$$

$$u_2(x,0) = u_2^f \quad \text{at} \quad t=0 \quad (21)$$

It is presupposed that a steady-state operating point denoted by the subscript d has been determined which is optimal with respect to some performance criterion (e.g., maximum yield). The startup policy, in turn, is to be determined such that, by controlling the addition or removal of heat, the process is driven from the initial state toward the final steady state in some optimal fashion. In this example, the objective function to minimize is

$$S = \int_0^{t_f} \int_0^1 \{\mu[u_1(x,t) - u_{1_d}(x)]^2 + \nu[u_2(x,t) - u_{2_d}(x)]^2\} dx\, dt \quad (22)$$

where μ and ν are suitably chosen constant weighting coefficients. The manipulated variable is the dimensionless wall temperature, θ, which is considered to be a function of time only and lie within the range

$$\theta_{min} \le \theta(t) \le \theta_{max} \quad (23)$$

The following numerical values are assumed:

$\beta = 5$, $\tau_r = .05$ hr, $Q = -200$, $K = 30\ hr^{-1}$,

$k_{10} = 2.51 \times 10^5\ hr^{-1}$, $k_{20} = 1.995 \times 10^7\ hr^{-1}$,

$P_1 = 5.03$, $P_2 = 10.06$, $T_r = 1000°R$, $u_1^f = .9$,

$u_2^f = .6$.

The kinetic data for the reaction are due to Fan.[4]

The transient solution of Equations (13) and (14) forward in time from $t = 0$ to $t = t_f$ is accomplished by the use of quasilinearization(13) together with an implicit difference scheme. The details of the computational method are presented in ref. 5.

Optimal Control Using Overall Direct Search. The time axis was discretized into fifty increments of .02 residence time and the spatial increment was .05 dimensionless distance unit. The time increment over which a control level would be held constant was also taken to be .02 residence time. Initially, the assumed control policy was considered constant with respect to time and at the value corresponding to that required to maintain the desired steady state profiles; i.e., $u^{(0)}(n) = .600$, $n = 1, \ldots, 50$. Computation was performed for five levels of control equally spaced over the admissible range, i.e., .530, .565, .600, .635 and .670 dimensionless temperature units.

Figure 3 shows the resulting optimal control policy obtained after three overall iterations. Actually, after only two iterations, negligible improvement of the performance index was obtained. Also indicated on Figure 3 is the resulting optimal control policy obtained by the distributed maximum principle.(5) Comparison of these results shows marked similarity of the control policy to that obtained using the distributed maximum principle. The resulting value of the performance index was .046555, almost identical to the maximum principle result.

Constraint on Maximum Reaction Temperature. To demonstrate the technique for dealing with state variable inequality constraints, an upper constraint of $u_{2_{max}} = .700$ was placed on the dimensionless reaction temperature. The penalty weighting coefficient was taken to be $\sigma = 10^4$, which, as in the case of the distributed maximum principle was adequate to force convergence of the temperature trajectory to the constraint boundary.

The resulting control policy for the temperature-constrained case is shown in Figure 4. Again, comparison of this result with the result obtained by the distributed maximum principle(5) shows much similarity. For the constrained case, the overall direct search method was found to be quite sensitive to the initial assumed control policy. However, the initial assumption of a bang-bang policy approximating the maximum principle result yielded rapid convergence.

Suboptimal Startup Control Using Simplified Direct Search. The total time period $t = 0$ to $t = t_f$ is divided into N equal intervals of length Δt. Instead of evaluating the performance over the entire time period, the performance is appraised at the end of each interval, the control being held constant over the interval. The performance index for the n-th time increment, $n = 1, \ldots, N$, is taken to be the integrand of the time integral of Equation (22) evaluated at time $t = n\Delta t$.

$$S_n = \int_0^1 \{\mu[u_1(x,t_{n+1}) - u_{1_d}(x)]^2 + \nu[u_2(x,t_{n+1}) - u_{2_d}(x)]^2\}dx \qquad (24)$$

Again fifty time increments of $\Delta t = .02$ residence time were used. The distance increment was .05 dimensionless length unit. The performance index, Equation (24), was computed at the end of each time interval again for five control levels.

The resulting control policy is shown in Figure 5. Comparison with the results of the maximum principle and the overall direct search, illustrates great similarity. Although the performance was assessed over only one time interval at a time, without regard for the entire period of operation, the resulting transient concentration and temperature profiles were used to compute the overall performance index, Equation (22). The resulting value was .046555, essentially the same as those values obtained using the two previous approaches.

Constraint on Maximum Reaction Temperature. Again an upper constraint of $u_{2_{max}} = .700$ was placed on the dimensionless reaction temperature. After computing each optimal control value and the corresponding state trajectories, a test was made for constraint violations. When the test was made at the end of one time increment, corresponding to the intended time of application of the computed value, the control system had inadequate capacity to prevent overshoot of the constraint, even upon switching to the minimum level. A maximum dimensionless reaction temperature of .7096 was obtained, compared to .7175 without the constraint. Extending the check over two time increments, and switching to minimum control upon the detection of a violation, a maximum reaction temperature of .7007 resulted, which was considered within reasonable tolerance of the constraint boundary. The resulting control trajectory is shown in Figure 6. For more severe constraints, a check for violations might be required for several time intervals in advance, or perhaps a value lower than the actual constraint could be used in the test.

CONCLUSION

Two direct search techniques, each involving the scanning of a performance index for different trial control levels, were considered. These techniques have application to nonlinear distributed systems in which control saturation constraints are specified. The overall direct search technique considers an assessment of performance based on the entire period of operation and is iterative. The other method, a simplified non-iterative search procedure, yields a piecewise-constant suboptimal policy based on an instantaneous performance measure evaluated at the end of each time increment.

The tubular reactor startup problem was studied by using the overall direct search technique. The resulting optimal control policy closely ressembled that obtained using a distributed maximum principle and the value of the performance index was almost identical. The overall direct search technique was somewhat less complex to program than the maximum principle, however, it was actually more time consuming because many complete solutions of the state equations--one for each trial control level at each time step--were required for each overall iteration. The ability of the method to handle state variable constraints was demonstrated by imposing a maximum reaction temperature constraint.

The simplified direct search technique was employed to determine a suboptimal startup control policy for the tubular reactor, the objective being to minimize the integrand of the time integral of the overall objective functional at the end of each time interval. The resulting control policy closely approximated those obtained by a maximum principle approach and the overall direct search method and yielded an almost identical value for the performance index based on the whole period of operation. The method was also shown to be capable of dealing with state variable inequality constraints as demonstrated by treating the constraint on maximum reaction temperature.

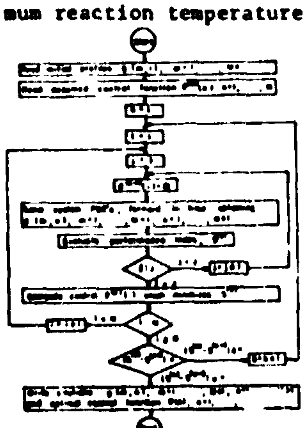

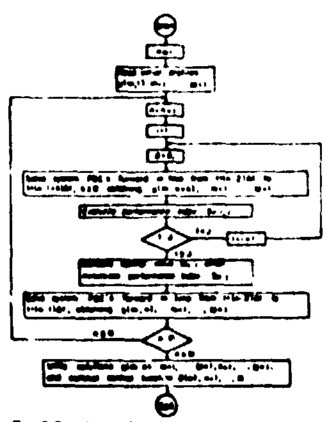

Because of the massiveness of the computation involved with a maximum principle and the overall direct search technique, it is limited to off-line use in computing optimal open-loop control and state trajectories based upon the anticipated transient behavior of the process over the time span of interest. Also both the distributed maximum principle and overall direct search technique can be used as a standard of comparison for evaluating less complicated suboptimal approaches such as the simplified direct search technique which has on-line control possibilities.

REFERENCES

1. Butkovskii, A. G. and A. Ya. Lerner, Soviet Physics Doklady (English trans.) 5, 936-939 (1961); 2. Butkovskii, A. G. and A. Ya. Lerner, Automation and Remote Control, 21, 472-477 (1960); 3. Pontryagin, L. S., V. G. Boltyanskii, R. V. Gamkrelidge, and E. F. Mishchenko, The Mathematical Theory of Optimal Processes, (English translation by K. N. Trirogoff), Interscience, New York, 1962; 4. Fan, L. T., The Continuous Maximum Principle, Wiley, New York, 1966; 5. Hahn, D. R., "Optimal Control of a Class of Distributed Parameter Processes," Ph.D. Thesis, Kansas State University, 1969; 6. Jackson, R., Proc. Int. Chem. Eng., 4, 32-38 (1965); 7. Denn, M. M., R. D. Gray, Jr., and J. R. Ferron, Ind. Eng. Chem. Fundamentals, 7, 286-295 (1968); 8. Seinfeld, J. H., and L. Lapidus, Chem. Eng. Sci. 23, 1461-1483 (1968); 9. Sage, A. P. and S. P. Chaudhuri, Int. J. Control, 6, 81-98 (1967); 10. Lapidus, L. and R. Luus, AIChE Journal 13, 101-108 (1967); 11. Grethlein, H. D. and L. Lapidus, AIChE Journal, 9, 230-239 (1963); 12. Dankwerts, P. V., Chem. Engr. Sci. 2, 1-13 (1953); 13. Bellman, R. E., and R. E. Kalaba, Quasilinearization and Nonlinear Boundary Value Problems, American Elsevier, N. Y., 1965; 14. Forsythe, G. E., and W. R. Wasow, Finite Difference Methods for Partial Differential Equations, Wiley, New York, 1965; 15. Lapidus, L., Digital Computation for Chemical Engineers, McGraw-Hill, N.Y., 1962.

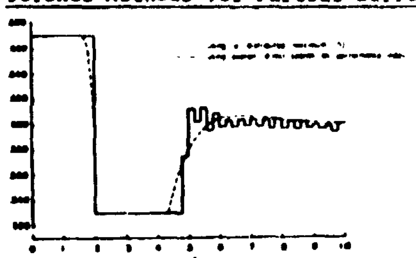

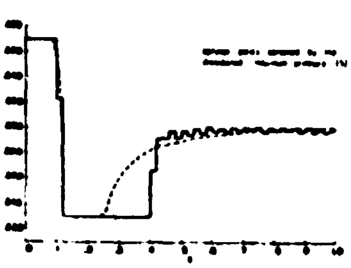

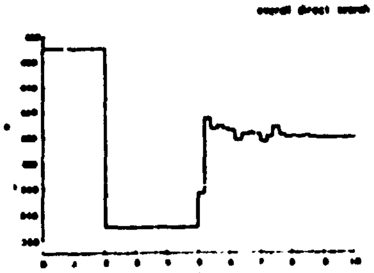

(e) 3

INT. J. CONTROL, 1971, VOL. 13, NO. 2, 363–382

Feedforward–feedback control of distributed parameter systems†

KA... EXP...

D. R. HAHN,‡ L. T. FAN and C. L. HWANG

Institute for Systems Design and Optimization, Kansas State University, Manhattan, Kansas 66502

[Received 10 February 1970]

Regulatory control of distributed systems subjected to load disturbances is considered by using feedforward and state measure control configurations. Dynamic compensation of the feedforward signal is accomplished with a lead-lag function, the time constants of which are determined by means of a numerical search technique. Compensation of the state measure signal is provided by the distributed nature of the process itself. Exit temperature regulation of a tubular heat exchanger acted upon by velocity and inlet temperature disturbances is considered as an application for feedforward control. Considerably better performance is obtained with the addition of dynamic compensation to the feedforward signal. State measure control is applied to the exchanger for a feed temperature upset and the effects of sensor location on outlet performance are investigated. An optimal sensor location is determined which minimizes the integral-square error at the outlet.

1. Introduction

Two types of control applicable to regulation of linear systems, or systems which can be linearized about an operating point, are to be examined in this work. One is feedforward control and the other is state measure control. Both approaches use system measurements to provide corrective control action to compensate for disturbance inputs. The former implies that disturbances are sensed at the inlet before they can affect the process and the latter involves the measurement of the disturbance response at some point within the system. A numerical search procedure will be applied to the synthesis of optimal compensation for the feedforward signal. For state measure control, the effect of sensor location on the dynamic system response will be investigated.

The methods are employed to obtain a desired control of a tubular heat exchanger by manipulating the steam temperature in a surrounding jacket. If the wall capacitance of the tubular heat exchanger is significant, it is necessary to perform an energy balance on the wall, resulting in an additional equation coupled with the energy equation for the process. Optimal control of a change in set-point will be considered for the tubular heat exchanger, using dynamically compensated feedforward control, the manipulated variable being the jacket steam temperature. Regulatory control will be evaluated with the exchanger acted upon by load disturbances, both for feedforward control with optimally

† Communicated by Professor L. T. Fan. This study was supported in part by NASA Grant No. NGR-17-001-034, and by the Air Force Office of Scientific Research, Office of Aerospace Research, United States Air Force, under Contract F44620-68-0020 (Themis Project).

‡ Present address: The Bendix Corporation, Kansas City, Missouri.

designed dynamic compensation and state measure control with the transducer optimally located.

Some attention has been given to the practical aspects of instrumentation and state feedforward feedback control of distributed processes. Watts (1965) used a frequency domain approach to find optimal feedforward thermocouple locations in a plug-flow heat exchanger with distributed heating. Parseval's theorem was employed to obtain the mean-square output error due to input forcing with known spectral density. Using proportional control only, he was able to find interior spatial locations which made the mean-square error stationary. Licht (1966) also considered a similar problem for a counter-current plug-flow heat exchanger and used a conjugate gradient minimization scheme to find sensor locations which minimized the output mean-square error. Given a number of probes at pre-specified locations, he was also able to find optimal weights to be given each probe.

McCann (1963) has considered a time domain approach for finding optimal probe locations and optimal weighting for multiple probes for a heat exchanger with axial diffusion. This involved a search on an analogue computer with the original system equation represented by a set of simultaneous ordinary differential equations.

2. Regulatory control of distributed systems

The techniques presented in this paper are applicable to compensation for load changes which upset the system response from its desired steady-state operating point. These disturbances may be initially localized and propagate through the system such as a feed temperature upset, or may occur simultaneously at all points as in the case of a flow velocity fluctuation.

In many distributed processes, although control must be extended over the entire spatial domain, the performance of the system is appraised at a single point, usually the exit. For example, the performance index of a tubular reactor may be a function of the exit concentration of one of the reactants—or it may be desired to regulate the outlet temperature of a tubular heat exchanger about a given set-point. The discussion herein pertains to such systems. It is also assumed that control action, although distributed in its effect, is initiated by a single, lumped input.

Conventional feedback control systems are sometimes inadequate for regulatory control of distributed processes. For example, consider a process in which it is desired to regulate the quality of the output stream. A localized load disturbance may enter the process at the inlet, but the feedback transducer will not sense the upset until the disturbance response propagates through the system and begins to occur at the exit. Then, as control action is applied to offset the disturbance, dead time and lag in control response create a poor transient exit response and make it difficult to regulate the exit stream effectively.

However, if it is possible to sense the disturbance at the inlet (or its response upstream from the exit), then this information may be utilized to initiate control action in advance of the arrival of the disturbance response at the exit. In this way, the control response can be made to match the disturbance response more closely, resulting in better control of the output quality.

3. Feedforward control

Consider the feedforward control schematic for a distributed process shown in fig. 1. A vector of disturbance inputs is sensed at the inlet to the process and fed forward to a control computer. The computer also has, as an input, the set-point signal.

Fig. 1

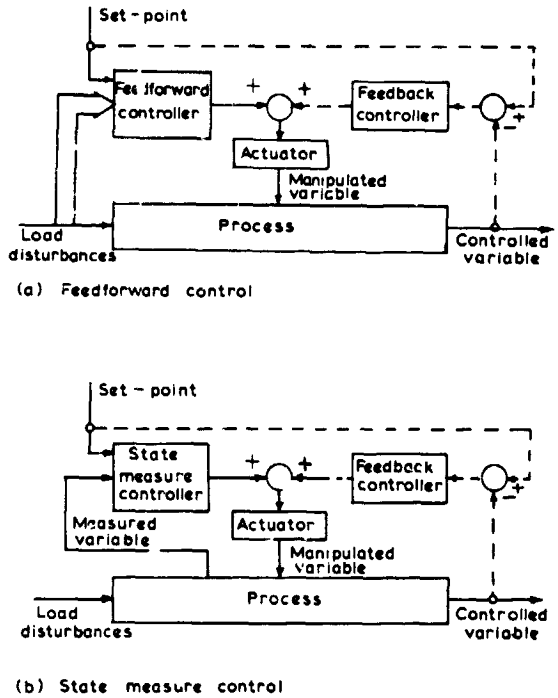

Feedforward and state measure control configurations for tubular heat exchanger.

In designing a feedforward control system, the usual approach is to consider the steady-state and transient aspects of the response separately (Shinskey 1968). Accordingly, the function of the feedforward computer is first to calculate the value of the manipulated variable necessary to produce zero steady-state error under the influence of the disturbance. Then, dynamic compensation of the control signal is effected so that the transient deviation dies out in some optimal manner. Dynamic compensation is necessary because of dynamic imbalances between disturbance and control responses.

One method for dynamic compensation of the control signal, where dead time in the disturbance response is not appreciable, is a simple lead–lag function (Shinskey 1968). The output, $\theta(t)$, is:

$$\theta(t) = \theta_s\left[1 + \frac{\tau_a -}{\tau_b}\exp(-t/\tau_b)\right], \tag{1}$$

where θ_s is the steady-state value of the manipulated variable and τ_a and τ_b are the lead and lag time constants, respectively.

In cases where dead time is a factor in the disturbance response, the lead–lag signal can be effectively combined with pure time delay. The control output, delayed by an amount t_d, can be written:

$$\theta(t-t_d) = \begin{cases} \theta_s\left\{1+\frac{\tau_a-\tau_b}{\tau_b}\exp\left[-(t-t_d)/\tau_b\right]\right\}, & (t-t_d) \geqslant 0, \\ 0, & (t-t_d) < 0. \end{cases} \tag{2}$$

Optimal design of the lead–lag compensation involves determining the lead and lag time constants such that the controlled system response is optimal with respect to some performance index. A procedure is developed here for performing a parameter search to determine the optimal time constants using the method of conjugate gradients due to Fletcher and Reeves (1964). A flow diagram for the overall search is shown in fig. 2.

Although gradients of the performance index with respect to the parameters to be searched are required, difference approximations can be used where analytic expressions are not available. For systems under consideration here, it is necessary to compute the full solutions to the system partial differential equations each time the performance index is evaluated or a gradient computed.

Constraints on the parameters or on the manipulated variable can be accommodated by the use of appropriate penalty functions in the performance index which penalize excessive excursions from the reference values.

4. State measure control

Instead of sensing the disturbance at the inlet as in feedforward control, consider now the measurement of the disturbance response within the system and using this information to provide corrective control. A complete appraisal of the disturbed state would entail measuring the entire profile. However, it has been shown (Licht 1966, McCann 1963), that good regulation can be provided by basing the state assessment on just a few points or even a single point along the spatial axis. Herein, state measure control is considered in terms of a single state measurement at some point within the system.

The state measure control scheme presented here is shown schematically in fig. 1. As noted by McCann (1963), state measure control is both feedforward and feedback. It is feedforward in that the disturbance response is measured ahead of the regulation point and this information used as an input to the controller. It is feedback in the sense that the effect of control action can be sensed at the measure point.

State measure control appears most useful in cases for which the exit response to a disturbance is slow in comparison to the response due to control action. By proper location of the probe, it is possible to utilize the distributed nature of the system for dynamic compensation so that the controller may consist of no more than a proportional mode.

As in the case of feedforward control, the steady-state portion of the response is considered separately from the transient. This consists of computing the steady-state proportional gain, which, multiplied by the steady-state value of the suppressed state deviation profile at the measure point, restores the exit state to zero steady-state error under the effect of the disturbance.

5. Provision for feedback

Both feedforward and state measure control are open-loop with respect to the controlled variable, i.e. the actual error at the exit regulation point is not used to provide corrective control action. For this reason the accuracies of the systems are susceptible to changing parameters, model inaccuracy, inaccuracy of load measurements, errors in computing components, etc. This indicates a need for a feedback signal to eliminate steady-state offset.

The feedback controller would include the integral mode to provide the long-term accuracy required but would not be expected to contribute significantly to the rapid initial correction. For this reason, in the examples presented, the feedback portion has been omitted from the transient computation.

6. Examples

6.1. *Outlet temperature regulation of a tubular heat exchanger using feedforward control*

To illustrate feedforward regulatory control theory, consider the problem of regulating the outlet temperature of a single-pass shell-and-tube heat exchanger. The control objective is to maintain the tube-side outlet temperature at a fixed set-point with the system subjected to load disturbances. These load disturbances are assumed to be fluctuations in the feed temperature and the mean flow velocity. The manipulated variable is taken to be the steam temperature in the shell, which is assumed to be a function of time only.

6.1.1. *The mathematical model*

The mathematical model of the tubular heat exchanger with axial diffusion is derived. A simple single-pass shell-and-tube heat exchanger is considered. A liquid stream enters the tube of the exchanger and is heated by convection from the inner wall. Heat is supplied to the tube by means of condensing steam in the jacket.

In deriving the mathematical model, the following assumptions are invoked:

(1) System parameters are uniform and constant with respect to time.

(2) Axial heat diffusion and mixing are significant for the tube-side stream.

(3) Steam temperature is a function of time only.

(4) Tube-side temperature and velocity are constant with respect to radial distance.

(5) Heat capacity of the tube is finite.

(6) Tube temperature is constant with respect to radial position.

(7) Axial heat conduction in the tube is negligible.

(8) Outer shell effects can be neglected.

An energy balance taken over a differential section dl of the tube-side of the exchanger yields:

$$\frac{\partial T_l}{\partial \tau} = D\frac{\partial^2 T_l}{\partial l^2} - v\frac{\partial T_l}{\partial l} + \frac{h_{wl} P_l}{C_{pl}\,\rho_l\,A_l}(T_w - T_l), \tag{3}$$

while taking an energy balance on a section of wall of length dl gives:

$$\frac{\partial T_w}{\partial \tau} = \frac{h_{ws} P_s}{C_{pw}\,\rho_w\,A_w}(T_s - T_w) + \frac{h_{wl} P_l}{C_{pw}\,\rho_w\,A_w}(T_l - T_w). \tag{4}$$

The system is subject to the following boundary conditions:

$$\frac{\partial T_l(0,\tau)}{\partial l} = \frac{v}{D}[T_l(0,t) - T_l^f] \quad \text{at} \quad l = 0, \tag{5}$$

$$\frac{\partial T_l(L,\tau)}{\partial l} = 0 \quad \text{at} \quad l = L. \tag{6}$$

Equations (3) and (4) are non-dimensionalized by introducing the following quantities:

Mean residence time: $\tau_r = L/v$ sec.

Axial Peclet number: $\beta = vL/D$.

Dimensionless time: $t = \tau/\tau_r$.

Dimensionless axial distance: $x = l/L$.

Dimensionless liquid temperature: $u_1 = T_l/T_r$.

Dimensionless wall temperature: $u_2 = T_w/T_r$.

Dimensionless steam temperature: $\theta = T_s/T_r$.

Other parameters: $\dfrac{1}{\tau_1} = \dfrac{h_{wl} P_l}{C_{pl}\rho_l A_l}$ sec^{-1},

$$\frac{1}{\tau_{21}} = \frac{h_{wl} P_l}{C_{pw}\rho_w A_w} \text{ sec}^{-1},$$

$$\frac{1}{\tau_{22}} = \frac{h_{ws} P_s}{C_{pw}\rho_w A_w} \text{ sec}^{-1}.$$

The system equations thus become:

$$\frac{\partial u_1}{\partial t} = \frac{1}{\beta}\frac{\partial^2 u_1}{\partial x^2} - \frac{\partial u_1}{\partial x} + \frac{\tau_r}{\tau_1}(u_2 - u_1), \tag{7}$$

$$\frac{\partial u_2}{\partial t} = \frac{\tau_r}{\tau_{22}}(\theta - u_2) + \frac{\tau_r}{\tau_{21}}(u_1 - u_2). \tag{8}$$

The dimensionless boundary conditions are:

$$\frac{\partial u_1(0,t)}{\partial x} = \beta[u_1(0,t) - u_1^f] \quad \text{at} \quad x = 0, \tag{9}$$

$$\frac{\partial u_1(1,t)}{\partial x} = 0 \quad \text{at} \quad x = 1. \tag{10}$$

The numerical values for the exchanger used in this study are assumed to be:

$$\beta = 10,$$
$$\tau_r = 3 \text{ sec},$$
$$\tau_1 = 3{\cdot}69 \text{ sec},$$
$$\tau_{21} = 2{\cdot}65 \text{ sec},$$
$$\tau_{22} = 1{\cdot}05 \text{ sec},$$
$$T_r = 1000\ ^\circ\text{R},$$
$$u_1^f = 0{\cdot}530,$$
$$\theta = 0{\cdot}795.$$

The time constants for the system were determined experimentally by Cohen and Johnson (1956).

6.1.2. *Perturbation equations*

Consider the following perturbation variables defined as deviations from a steady-state operating point:

$$
\begin{aligned}
\hat{u}_1(x,t) &= u_1(x,t) - u_{1_s}(x),\\
\hat{u}_2(x,t) &= u_2(x,t) - u_{2_s}(x),\\
\hat{\theta}(t) &= \theta(t) - \theta_s,\\
\hat{u}_1{}^f(t) &= u_1{}^f(t) - u_{1_s}{}^f,\\
\hat{v}(t) &= v(t) - v_s.
\end{aligned}
$$

If the following parameters are taken to be constant, i.e.

$$
\begin{aligned}
\tau_r &= L/v_s,\\
\beta &= v_s L/D,
\end{aligned}
$$

eqns. (7)–(10) can be written:

$$\frac{\partial u_1}{\partial t} = \frac{1}{\beta}\frac{\partial^2 u_1}{\partial x^2} - \frac{v}{v_s}\frac{\partial u_1}{\partial x} + \frac{\tau_r}{\tau_1}(u_2 - u_1), \tag{11}$$

$$\frac{\partial u_2}{\partial t} = \frac{\tau_r}{\tau_{22}}(\theta - u_2) + \frac{\tau_r}{\tau_{21}}(u_1 - u_2), \tag{12}$$

$$\frac{\partial u_1(0,t)}{\partial x} = \beta\frac{v}{v_s}[u_1(0,t) - u_1{}^f] \quad \text{at} \quad x = 0, \tag{13}$$

$$\frac{\partial u_1(1,t)}{\partial x} = 0 \quad \text{at} \quad x = 1. \tag{14}$$

The steady-state profiles $u_{1_s}(x)$ and $u_{2_s}(x)$ corresponding to the operating point must satisfy the following equations:

$$\frac{1}{\beta}\frac{d^2 u_{1_s}}{dx} - \frac{du_{1_s}}{dx} + \frac{\tau_r}{\tau_1}(u_{2_s} - u_{1_s}) = 0, \tag{15}$$

$$\frac{1}{\tau_{22}}(\theta_s - u_{2_s}) + \frac{1}{\tau_{21}}(u_{1_s} - u_{2_s}) = 0, \tag{16}$$

with the boundary conditions:

$$\frac{du_{1_s}(0)}{dx} = \beta[u_{1_s}(0) - u_{1_s}{}^f] \quad \text{at} \quad x = 0, \tag{17}$$

$$\frac{du_{1_s}(1)}{dx} = 0 \quad \text{at} \quad x = 1. \tag{18}$$

Subtracting eqn. (15) from eqn. (11) and eqn. (17) from eqn. (13) yields:

$$\frac{\partial \hat{u}_1}{\partial t} = \frac{1}{\beta}\frac{\partial^2 \hat{u}_1}{\partial x^2} - \left(\frac{v}{v_s}\frac{\partial u_1}{\partial x} - \frac{du_{1_s}}{dx}\right) + \frac{\tau_r}{\tau_1}(\hat{u}_2 - \hat{u}_1), \tag{19}$$

$$\frac{\partial \hat{u}_1(0,t)}{\partial x} = \beta\left[\frac{v}{v_s}u_1(0,t) - u_{1_s}(0) - \left(\frac{v}{v_s}u_1{}^f - u_{1_s}{}^f\right)\right]. \tag{20}$$

13

Thus with the introduction of a velocity perturbation, non-linearities are introduced. These non-linear terms may be linearized in a first-order Taylor series about the operating point, i.e.

$$\frac{v}{v_s}\frac{\partial u_1}{\partial x} \approx \frac{du_{1_s}}{dx} + \frac{\hat{v}}{v_s}\frac{du_{1_s}}{dx} + \frac{\partial \hat{u}_1}{\partial x}, \tag{21}$$

$$\frac{v}{v_s} u_1(0,t) \approx u_{1_s}(0) + \frac{\hat{v}}{v_s} u_{1_s}(0) + \hat{u}_1(0,t), \tag{22}$$

$$\frac{v}{v_s} u_1^f \approx u_{1_s}^f + \frac{\hat{v}}{v_s} u_{1_s}^f + \hat{u}_1^f. \tag{23}$$

Using the above approximations and subtracting eqn. (16) from eqn. (12) and eqn. (18) from eqn. (14), the following system of linearized dimensionless perturbation equations results:

$$\hat{u}_{1_t} = \frac{1}{\beta}\hat{u}_{1_{xx}} - \hat{u}_{1_x} + \frac{\tau_r}{\tau_1}(\hat{u}_2 - \hat{u}_1) - \frac{\hat{v}}{v_s}\frac{du_{1_s}}{dx}, \tag{24}$$

$$\hat{u}_{2_t} = \frac{\tau_r}{\tau_{22}}(\hat{\theta} - \hat{u}_2) + \frac{\tau_r}{\tau_{21}}(\hat{u}_1 - \hat{u}_2), \tag{25}$$

subject to the boundary conditions:

$$\hat{u}_{1_x}(0,t) = \beta[\hat{u}_1(0,t) - \hat{u}_1^f] + \beta\frac{\hat{v}}{v_s}[u_{1_s}(0) - u_{1_s}^f] \quad \text{at} \quad x = 0, \tag{26}$$

$$\hat{u}_{1_x}(1,t) = 0 \quad \text{at} \quad x = 1. \tag{27}$$

Here, the disturbance inputs are $\hat{u}_1^f(t)$ and $\hat{v}(\ )$, the feed temperature and velocity fluctuations, respectively.

The steady-state behaviour of the system is described by the following ordinary differential equation:

$$\frac{d^2\hat{u}_{1_s}}{dx^2} - \beta\frac{d\hat{u}_{1_s}}{dx} + \beta\psi(\hat{\theta} - \hat{u}_{1_s}) - \beta\frac{\hat{v}_s}{v_s}\frac{du_{1_s}}{dx} = 0, \tag{28}$$

subject to the boundary conditions:

$$\frac{d\hat{u}_{1_s}(0)}{dx} = \beta[\hat{u}_{1_s}(0) - \hat{u}_{1_s}^f] + \beta\frac{\hat{v}_s}{v_s}[u_{1_s}(0) - u_{1_s}^f] \quad \text{at} \quad x = 0, \tag{29}$$

$$\frac{du_{1_s}(1)}{dx} = 0 \quad \text{at} \quad x = 1, \tag{30}$$

where

$$\psi = \frac{\tau_r}{\tau_{21}}\frac{\tau_{21}}{\tau_{22} + \tau_{21}}.$$

Equation (28) is now reduced to state space form by letting:

$$\hat{u}_{1_s} = y_1, \quad \frac{d\hat{u}_{1_s}}{dx} = y_2.$$

To obtain the steady-state control variable $\hat{\theta}_s$ which provides zero steady-state exit error under the influence of the disturbances, a new state variable is introduced, i.e.

$$\hat{\theta}_s = y_3.$$

The complete system of equations is thus:

$$\frac{dy_1}{dx} = y_2, \tag{31}$$

$$\frac{dy_2}{dx} = \beta y_2 + \beta\psi y_1 - \beta\psi y_3 + \beta\frac{\hat{v}_s}{v_s}\frac{du_{1_s}}{dx}, \tag{32}$$

$$\frac{dy_3}{dx} = 0, \tag{33}$$

with the boundary conditions:

$$y_2(0) = \beta[y_1(0) - u_{1_s}{}'] + \beta\frac{\hat{v}_s}{v_s}[u_{1_s}(0) - u_{1_s}{}'] \quad \text{at} \quad x = 0, \tag{34}$$

$$y_2(1) = 0 \quad \text{at } x = 1, \tag{35}$$

$$y_1(1) = 0 \quad \text{at } x = 1. \tag{36}$$

Using computed values of $du_{1_s}(x)/dx$, eqns. (31)–(33) may be solved using Runge–Kutta integration and superposition as outlined in Hahn (1969), yielding the appropriate steady-state control value, $\hat{\theta}_s$, and the suppressed deviation profile $\hat{u}_1(x)$. Temperature deviation profiles are shown in fig. 3 for a feed temperature upset of $\hat{u}_1{}' = 1$ and a velocity change of $\hat{v}/v_s = 0{\cdot}1$.

Fig. 2

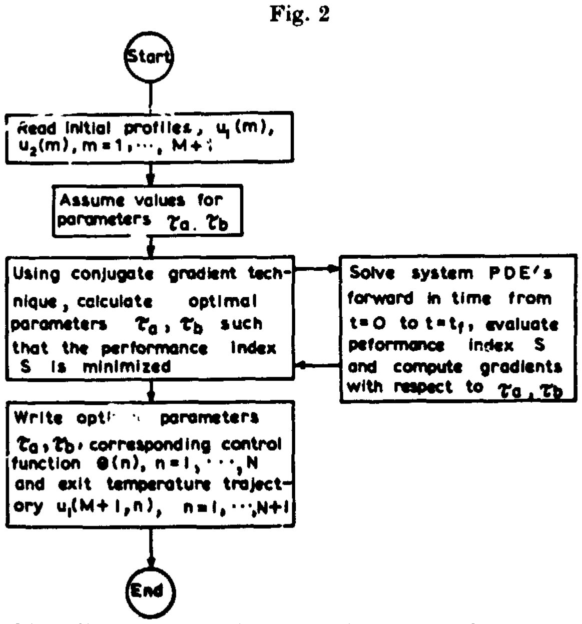

Flow diagram for conjugate gradient method of finding optimal lead–lag parameters.

The performance criterion to be minimized is taken to be the integral-square error of the fluid temperature deviations at the exit. This can be written:

$$S = \int_0^{t_f} [\hat{u}_1(1,t)]^2\,dt. \tag{37}$$

The solution of the transient perturbation equations given by eqns. (24) and (25) are solved forward in time $t = 0$ to $t = t_f$ by decoupling them and iteratively applying the implicit difference method.

Fig. 3

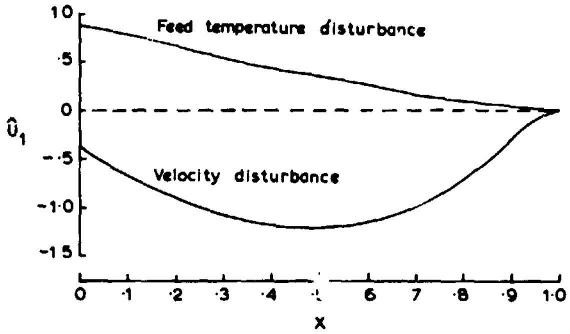

Steady-state deviation temperature profiles for feed temperature and velocity disturbances.

Equations (24) and (25) are most conveniently solved by finite-difference methods. However, for parabolic equations care must be taken in applying explicit difference approximations that stability is ensured. In order to circumvent this stability problem, the implicit scheme due to Crank and Nicolson (Forsythe and Wasow 1965) is considered here. This method introduces more complexity into the difference model but guarantees stability for any increment of time, thus reducing the number of time increments required.

In applying the Crank–Nicolson method the spatial axis is discretized into M increments of equal length Δx so that $\Delta x = 1/M$. Time discretization is effected by solving the difference equations at equal time increments Δt. The solution $u(m,n)$ denotes the value of the dependent variable at the spatial location $(m-1)\Delta x$ and at time $(n-1)\Delta t$.

The partial time derivatives are approximated by taking forward differences between the $(n-1)$th and nth time steps, i.e.

$$u_t \approx \frac{1}{\Delta t}[u(m,n) - u(m,n-1)]. \tag{38}$$

For spatial discretization, implicit difference operators are constructed for the first and second spatial partial derivatives by taking central differences, averaged over the $(n-1)$th and nth time steps, i.e.

$$\begin{aligned} u_{xx} \approx (M^2/2)\,[u(m+1,n) - 2u(m,n) + u(m-1,n) \\ + u(m+1,n-1) - 2u(m,n-1) + u(m-1,n-1)], \end{aligned} \tag{39}$$

$$u_x \approx (M/4)\,[u(m+1,n) - u(m-1,n) + u(m+1,n-1) - u(m-1,n-1)]. \tag{40}$$

The above difference operators have a discretization error on the order of $(\Delta x)^2$ (Forsythe and Wasow 1965). The solution of eqns. (24) and (25) is greatly simplified by 'decoupling' the component equations. This is done in the ith equation at the kth iterative solution by setting:

$$u_j^{(k)} - u_j^{(k-1)} = \begin{cases} u_i^{(k)} - u_i^{(k-1)}, & j = i, \\ 0, & j \neq i. \end{cases} \tag{41}$$

The dependent variable u is also averaged over the $(n-1)$th and nth time steps:

$$u \approx \tfrac{1}{2}[u(m,n)+u(m,n-1)]. \tag{42}$$

The difference approximations for the first derivative terms occurring in the boundary conditions at $x=0$ and $x=1$ are taken to be three-point forward and backward differences, respectively:

$$\hat{u}_x|_{x=0} \approx (M/2)[-\hat{u}(3,n)+4\hat{u}(2,n)-3\hat{u}(1,n)], \tag{43}$$

$$\hat{u}_x|_{x=1} \approx (M/2)[3\hat{u}(M+1,n)-4\hat{u}(M,n)+\hat{u}(M-1,n)]. \tag{44}$$

By substitution of the above difference operators given by eqns. (38)–(44) into eqns. (24)–(27), the following sets of difference equations for the kth iteration are obtained:

$$\left.\begin{aligned}
&\left[B_1+\frac{4M}{2\beta+3M}A_1\right]\hat{u}_1^{(k)}(2,n)+\left[C_1-\frac{M}{2\beta+3M}A_1\right]\hat{u}_1^{(k)}(3,n)\\
&= -A_1\hat{u}_1(1,n-1)-D_1\hat{u}_1(2,n-1)-C_1\hat{u}_1(3,n-1)-E_1^{(k-1)}(2,n)\\
&\qquad -\frac{2\beta}{2\beta+3M}\left[\hat{u}_1{}^{l}(n)-\frac{\hat{v}(n)}{v_s}(u_{1_s}(0)-u_{1_s}{}^{l})\right],\\
&A_1\hat{u}_1^{(k)}(m-1,n)-B_1\hat{u}_1(m,n)+C_1\hat{u}_1^{(k)}(m+1,n)\\
&= -A_1\hat{u}_1(m-1,n-1)-D_1\hat{u}_1(m,n-1)-C_1\hat{u}_1(m+1,n-1)\\
&\qquad -E_1^{(k-1)}(m,n)\quad m=3,\ldots,M-1,\\
&[A_1-\tfrac{1}{3}C_1]\hat{u}_1^{(k)}(M-1,n)+[B_1+\tfrac{4}{3}C_1]\hat{u}_1^{(k)}(M,n)\\
&= -A_1\hat{u}_1(M-1,n-1)-D_1\hat{u}_1(M,n-1)-C_1\hat{u}_1(M+1,n-1)\\
&\qquad -E_1^{(k-1)}(M,n),
\end{aligned}\right\} \tag{45}$$

$$\hat{u}_2^{(k)}(m,n)=\frac{1}{B_2}\left[-D_2\hat{u}_2(m,n-1)-\frac{\tau_r}{\tau_{21}}\hat{u}_1^{(k-1)}(m,n)-\frac{\tau_r}{\tau_{22}}\hat{\theta}(n-1)\right]$$

$$m=1,\ldots,M+1, \tag{46}$$

where

$$A_1=\frac{M^2}{2\beta}+\frac{M}{4},$$

$$B_1=-\frac{1}{2}\frac{\tau_r}{\tau_1}-\frac{M^2}{\beta}-\frac{1}{\Delta t},$$

$$B_2=-\frac{1}{2}\frac{\tau_r}{\tau_{22}}-\frac{1}{2}\frac{\tau_r}{\tau_{21}}-\frac{1}{\Delta t},$$

$$C_1=\frac{M^2}{2\beta}-\frac{M}{4},$$

$$D_1=-\frac{1}{2}\frac{\tau_r}{\tau_1}-\frac{M^2}{\beta}+\frac{1}{\Delta t},$$

$$D_2=-\frac{1}{2}\frac{\tau_r}{\tau_{22}}-\frac{1}{2}\frac{\tau_r}{\tau_{21}}+\frac{1}{\Delta t},$$

$$E_1^{(k-1)}(m,n)=\frac{\tau_r}{\tau_1}u_2^{(k-1)}(m,n)-\frac{\hat{v}(n)}{v_s}\frac{du_{1_s}(m)}{dx}.$$

The end-point values, $\hat{u}_1(1,n)$ and $\hat{u}_1(M+1,n)$, are determined respectively from the following boundary equations:

$$\hat{u}_1^{(k)}(1,n) = -\frac{M}{2\beta+3M}\hat{u}_1^{(k)}(3,n)+\frac{4M}{2\beta+3M}\hat{u}_1^{(k)}(2,n) + \frac{2\beta}{2\beta+3M}\left[\hat{u}_1^{f}(n)-\frac{\hat{v}(n)}{v_s}(u_{1_s}(0)-u_{1_s}^{f})\right], \quad (47)$$

$$\hat{u}_1^{(k)}(M+1,n) = \tfrac{4}{3}\hat{u}_1^{(k)}(M,n)-\tfrac{1}{3}\hat{u}_1^{(k)}(M-1,n). \quad (48)$$

In performing the computations, time and spatial increment sizes used were 0·05 residence time and 0·05 dimensionless distance unit respectively. Terminal time t_f was taken to be 3 residence times.

Fig. 4

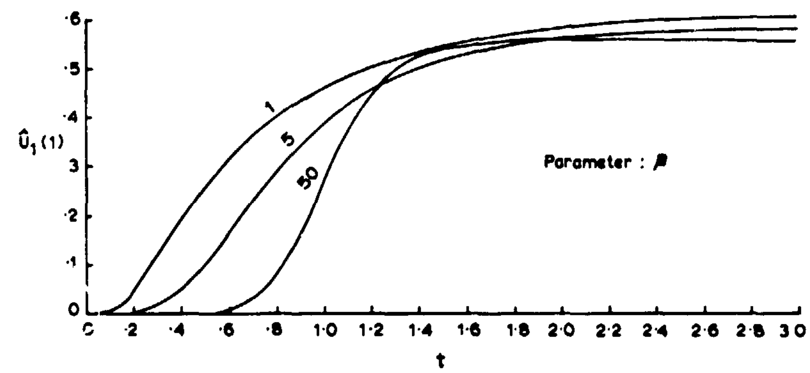

Outlet temperature responses to a step feed temperature upset for various effective axial diffusion coefficients.

Fig. 5

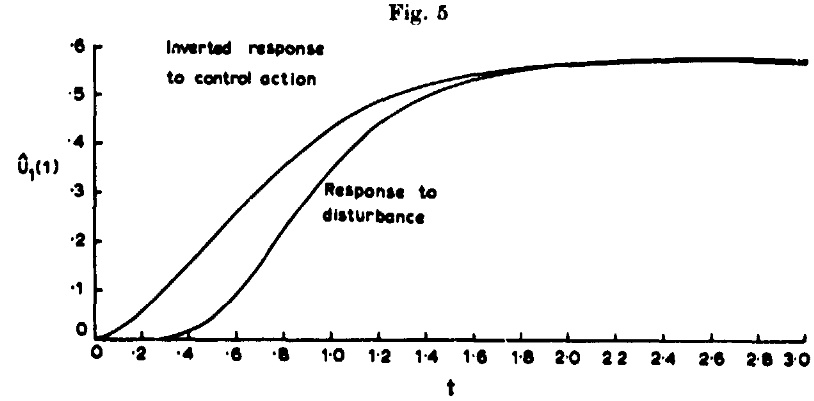

Comparison of open-loop disturbance and control outlet temperature responses for a step feed temperature disturbance.

6.1.3. *Feed temperature disturbance*

Consider a unit step upset in feed temperature, i.e. $\hat{u}_1^f = 1$. The uncontrolled disturbance responses at the exit are shown in fig. 4 for several effective diffusion coefficients. A comparison of the uncontrolled disturbance response with the corresponding step control response required for zero steady-state error is shown in fig. 5 for $\beta = 10$. As seen in fig. 6, with uncompensated feedforward control, an increase in feed temperature results in an initial decrease in exit temperature due to the relatively faster response to control action.

Thus compensation is i dicated which provides for less energy to be delivered to the system duri g the initial transient than that required for zero steady-state error under the effect of the upset.

Fig. 6

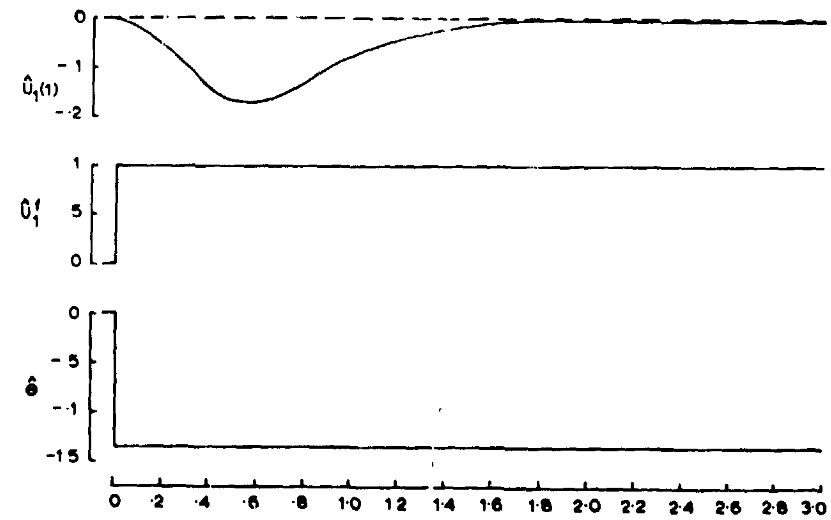

Uncompensated controlled outlet temperature response to a step feed temperature disturbance.

Due to the relatively slow exit response to the disturbance, it was necessary to incorporate a pure time delay in the control. The design procedure was to fix the delay at some increment of time, $j\Delta t, j = 0, 1, \ldots,$ and for this delay compute the optimal time constants, τ_a and τ_b, using the method of conjugate gradients. In difference form, the control is thus:

$$\hat{\theta}(n-j) = \begin{cases} \hat{\theta}_s\left\{1 + \dfrac{\tau_a - \tau_b}{\tau_b}\exp\left[-\dfrac{(n-1-j)\,\Delta t}{\tau_b}\right]\right\}, & (n-1-j) \geqslant 0, \\ 0, \quad (n-1-j) < 0, \end{cases} \tag{49}$$

where $\hat{\theta}_s$ represents the steady-state control necessary to completely cancel the disturbance at the exit.

The control yielding the lowest value of the performance index was determined, using a time delay of 0·15 residence time and lead and lag time constants of 0·0246 and 0·0937, respectively. The optimal control trajectory and corresponding exit response are shown in fig. 7. The ISE for the optimally compensated response was 0·00102 compared to 0·01552 for the uncompensated case.

6.1.4. *Velocity disturbance*

For a velocity disturbance, the situation is different Figure 8 shows the uncontrolled exit response to a step velocity disturbance, $\hat{v}/v_s = 0{\cdot}1$, and the corresponding step control response required to completely eliminate steady-state error. In this case the disturbance response leads the control response. The controlled but uncompensated exit response is shown in fig. 9.

Fig. 7

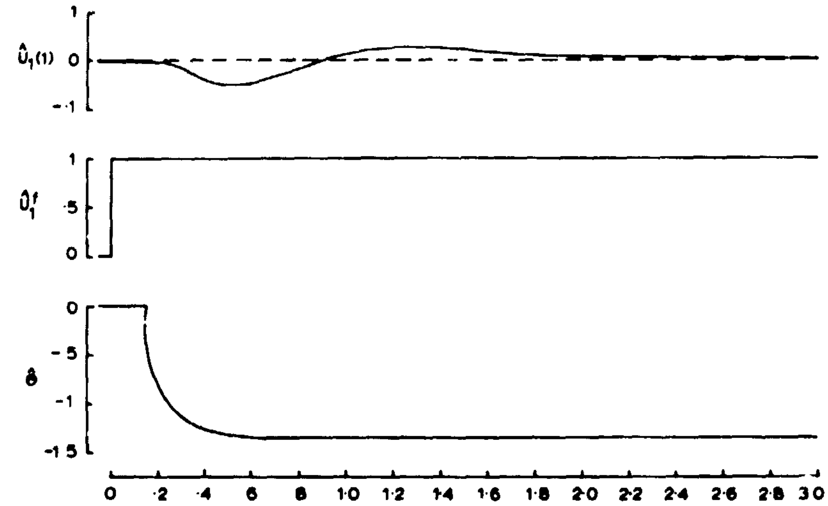

Outlet temperature response to a step feed temperature disturbance using optimal feedforward lead-lag control with delay.

Fig. 8

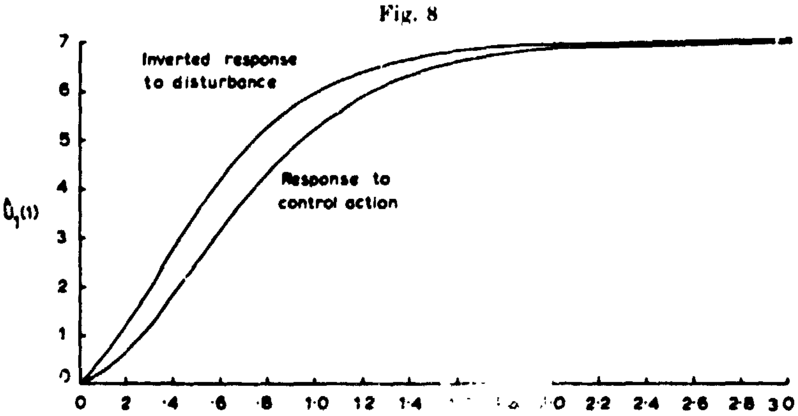

Comparison of open-loop dist[illegible] and control outlet [illegible]emperature responses for a [illegible] [illegible]locity disturbance.

It is thus desirable to provide dynamic compensation to the controller to enable the delivery of more energy to the system during the transient than required for zero steady-state output error under the influence of the disturbance.

To limit the magnitude of the control deviations, the performance index is modified to include a weighted penalty on excursions from the steady-state value, i.e.

$$S = \int_0^{t_f} \{[\hat{\theta}_1(1,t)]^2 + \gamma[\hat{\theta}(t) - \hat{\theta}_s]^2\}\, dt \qquad (50)$$

Fig. 9

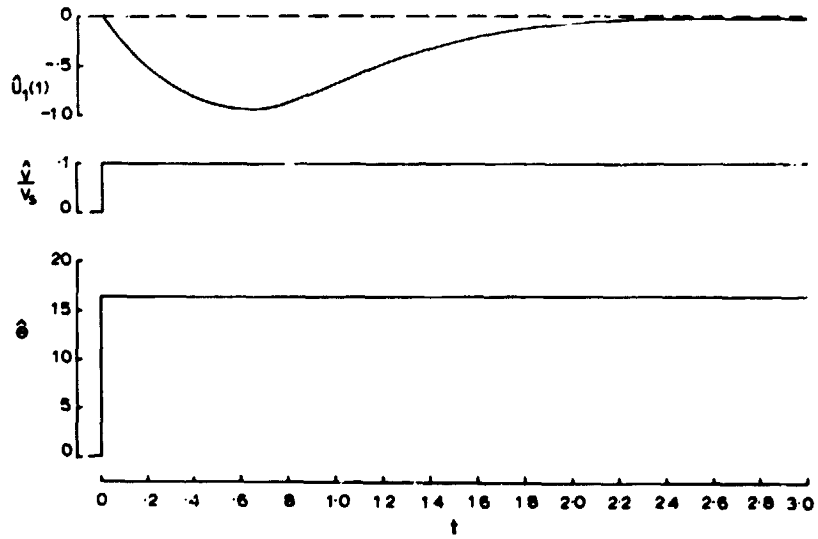

Uncompensated controlled outlet temperature response to a step velocity disturbance.

In this case, the difference representation of the lead–lag compensated feedforward signal is:

$$\hat{\theta}(n) = \hat{\theta}_s\left\{1 + \frac{\tau_a - \tau_b}{\tau_b}\exp\left[-\frac{(n-1)\,\Delta t}{\tau_b}\right]\right\}. \tag{51}$$

Using the conjugate gradient technique, optimal lead–lag time constants were computed for several amounts of control weighting. The results are as follows:

γ	S	τ_a	τ_b
Uncompensated	0·70219	1·0000	1·0000
0·1	0·46461	0·6686	0·6119
0·01	0·15216	0·3746	0·2571
0·001	0·03239	0·3357	0·1999

Figure 10 shows the optimal control trajectory and corresponding exit response for $\gamma = 0{\cdot}001$.

6.2. *Outlet temperature regulation of a tubular heat exchanger using state measure control*

Consider again the problem of outlet temperature regulation for the tubular heat exchanger, this time by means of state measure control. The load disturbance is assumed to be a unit step increase in feed temperature. It is proposed to offset the disturbance effect by placing a sensor at some axial position within the process and using only the proportional mode with the gain adjusted for zero steady-state offset at the outlet, under the influence of the disturbance.

The suppressed steady-state deviation profile $u_{1_s}(x)$ and the corresponding steady-state control $\hat{\theta}_s$ are determined by solving eqns. (31)–(35) with $\hat{\theta} = 0$ and $\hat{u}_1{}^f = 1$. Once these are known, the proportional gain G_m for any measure

Fig. 10

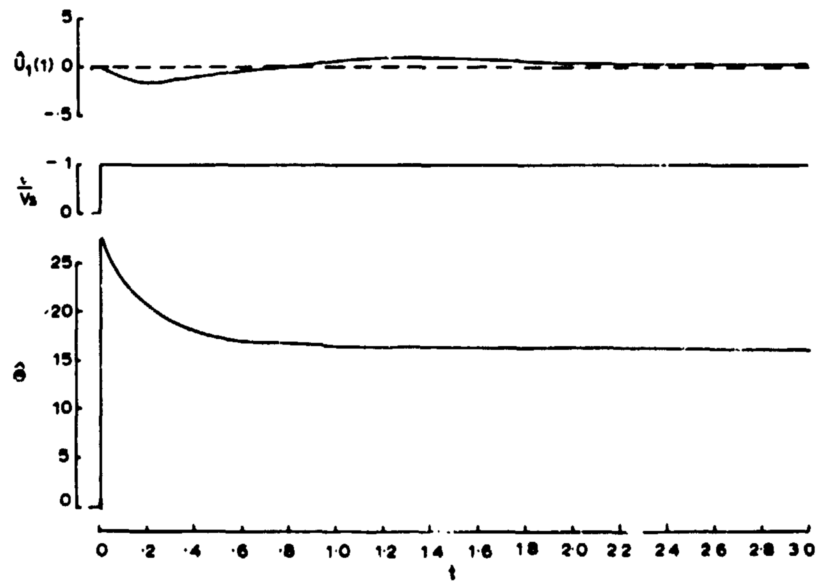

Outlet temperature response to a velocity disturbance using optimal feedforward lead lag control ($\gamma = 0{\cdot}001$).

point x_n can be computed from the relation:

$$G_m = \frac{\hat{\theta}_s}{\hat{u}_{1_s}(x_m)}. \tag{52}$$

A plot of the resultant gain as a function of sensor location is shown in fig. 11.

In order to appraise the dynamic performance of the exchanger under state measure control, a closed-loop digital simulation may be accomplished using the system difference representation, eqns. (45)–(48). Since the control is proportional to the instantaneous value of the state variable at the measure point, i.e.

$$\hat{\theta}(t) = G_m \hat{u}_1(x_m, t), \tag{53}$$

the difference form at the nth time step for the kth iteration may be written:

$$\hat{\theta}^{(k)}(n) = G_m \hat{u}_1^{(k-1)}(m', n), \tag{54}$$

where m' is the spatial node corresponding to the measure point x_m. The iteration is repeated at each time step until convergence is attained.

Computation was performed over 3 residence times using time and spatial increments of 0·05 residence time and 0·05 dimensionless distance unit, respectively. Upon computing the transient exit response at each spatial node, the exit integral-square error was computed using Simpson's integration. To penalize high gains obtained for larger x_m, a penalty term was added to the performance index, i.e.

$$S = \int_0^{t_f} \{[\hat{u}_1(1,t)]^2 + \gamma[\hat{\theta}(t) - \hat{\theta}_s]^2\}\, dt. \tag{55}$$

Figure 12 shows the resulting value of the performance index as a function of the sensor location, with and without the penalty.

Fig. 12

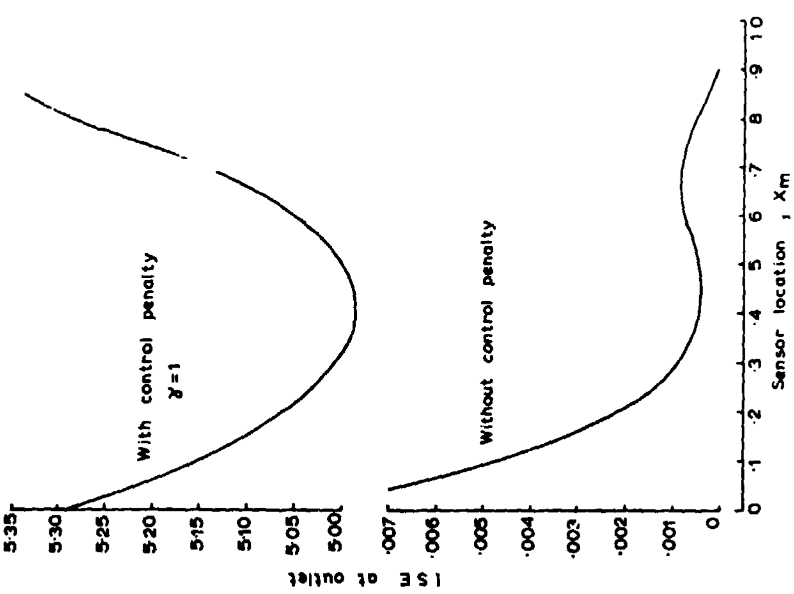

Integral-square outlet temperature error as a function of sensor location.

Fig. 11

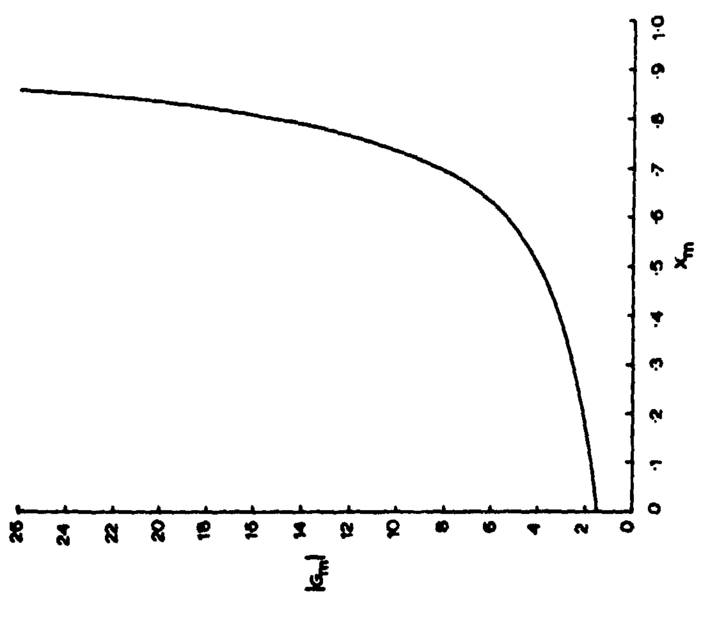

Proportional gain as a function of sensor location for a state measure control.

Figure 13 shows the control trajectories obtained from the simulation study for several sensor locations. The corresponding exit responses are shown in Figure 14.

In Figure 14 the top response indicates that the transducer is too close to the inlet. The control action is premature, causing an excessive undershoot of the set-point before the disturbance response starts to occur.

Fig. 13

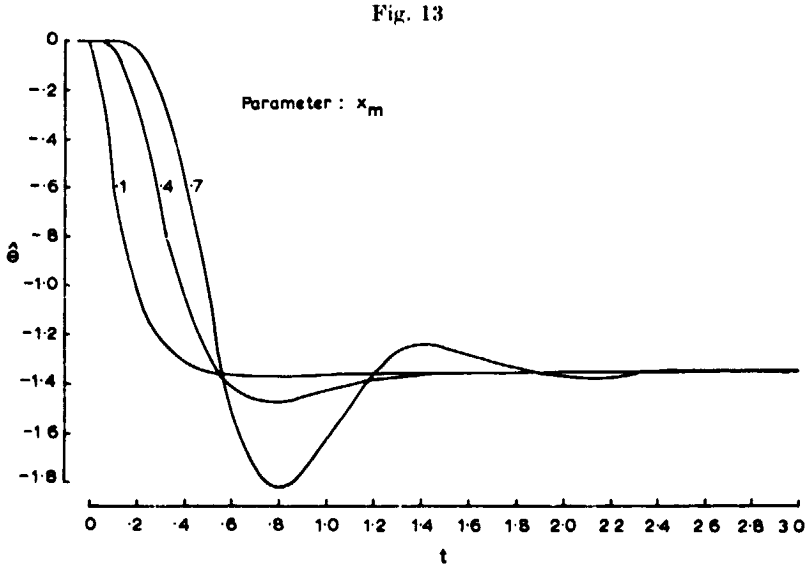

State measure control trajectories for a step feed temperature upset.

Fig. 14

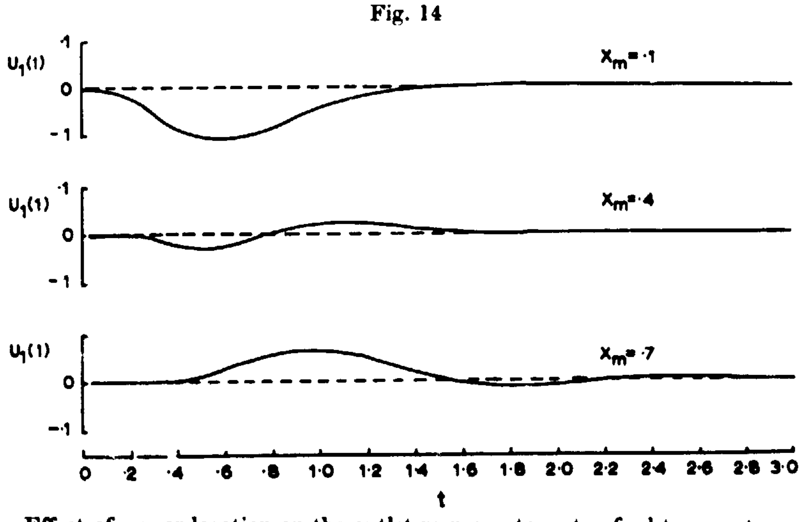

Effect of sensor location on the outlet response to a step feed temperature upset using state measure control.

The bottom response shows the effect of having the transducer too far down stream. The control response is too slow, resulting in excessive overshoot, due to the disturbance response. Also, with the transducer close to the exit, the proportional gain becomes high and cycling or instability may ensue.

The best response, in the sense of minimum integral-square error (with control penalty), is shown in the middle. The probe is located such that there is initially a small undershoot due to control action, followed by a small overshoot as the disturbance response arrives at the exit.

7. Conclusions

Two control schemes were investigated for regulating the exit state of a linear distributed system or one exhibiting linear behaviour about an operating profile. These were feedforward control in which a disturbance measurement was fed forward to a controller to indicate corrective action and state measure control in which the disturbance response was measured at a point within the system and used to generate a corrective signal. In practice, each would be used to provide rapid initial disturbance correction, but used in conjunction with a small amount of integral feedback from the regulation point to eliminate steady-state offset. Optimization for the feedforward scheme presented consisted of determining optimal values for lead and lag time constants whereas for state measure control, optimization involved the determination of an optimal measure point.

A computerized design procedure was demonstrated for determining optimal dynamic compensation for the feedforward signal. The method of conjugate gradients was used to compute optimal lead-and-lag-time time constants to minimize an index of performance. For the heat exchanger example presented compensation for a feed temperature disturbance required a time delay, in addition to the lead–lag compensation, to be inserted in the feedforward loop. For a velocity disturbance, it was necessary to impose a penalty on control effort in the performance index to constrain in the control to a physically realizable level.

A closed-loop (with respect to the measure point) digital simulation technique was devised for simulating the response of a tubular heat exchanger to a step increase in feed temperature, using state measure control. The scheme was an implicit one in which the transient state at a given spatial point was multiplied by a proportional gain to determine the value of the manipulated variable in the state equations. A one-dimensional search was performed to find the best measure point in the sense of minimizing the exit integral–square error. Using the resulting optimal measure point, state measure control provided somewhat better performance than compensated feedforward control for the same disturbance.

For distributed system regulation, state measure control has the advantage that the distributed nature of the process itself is utilized to provide dynamic compensation for the control signal and hence a simple proportional controller may suffice for this portion of the control. On the other hand, the specification of the proportional gain requires the knowledge of the nature of the disturbance. If multiple disturbances are likely to be present, it may be impossible to predict the exit error based on a single-point state measurement. In such situations it would seem advisable to use a feedforward configuration, thus isolating the disturbance inputs. Feedforward control would also be indicated in situations where the response to control action is slower than the disturbance response. Under these circumstances, the lag created by basing control action on the disturbance response would only degrade the performance.

References

Cohen, W. C., and Johnson, E. F., 1956, *Ind. Engng Chem.*, **48**, 1031.
Fletcher, R., and Reeves, C. M., 1964, *Computer J.*, **6**, 149.
Forsythe, G. E., and Wasow, W. R., *Finite Difference Methods for Partial Differential Equations* (New York: Wiley).
Hahn, D. R., 1969, Ph.D. Thesis, Kansas State University.
Licht, B. W., 1966, Case Institute of Technology Systems Research Center Report No. SRC84–C–66–34.
McCann, M. J., 1963, Ph.D. Thesis, London University.
Shinskey, F. G., 1968, *Process Control Systems* (New York: McGraw-Hill).
Watts, R. G., 1965, Ph.D. Thesis, Purdue University.

(e)4

OPTIMAL WALL TEMPERATURE CONTROL OF A HEAT EXCHANGER

Report No. 15

Harng-Sen Huang, L. T. Fan, C. L. Hwang

Institute for Systems Design and Optimization

KANSAS STATE UNIVERSITY MANHATTAN

OPTIMAL WALL TEMPERATURE CONTROL OF A HEAT EXCHANGER*

Harng-sen Huang, L. T. Fan, C. L. Hwang
Institute for Systems Design and Optimization
Kansas State University

ABSTRACT

An optimal wall temperature control of a single-duct heat exchanger is studied. The wall temperature which is the control variable is assumed to be uniform in space but a function of time. The system considered is a distributed parameter system where the fluid temperature is a function of time and a spatial coordinate. The control is to force optimally the temperature profile of the fluid from the initial state to a new desired steady temperature profile in a finite time. Two different performance indexes are considered. One is the integral of the absolute deviation of the system temperature profile at any moment from the new desired steady state profile and the other is the integral of the square of deviation of the system temperature profile at any moment from the new desired steady state profile. Both are to be minimized. Optimal solutions are obtained by two methods, namely, linear programming and a variational technique.

*This study was supported in part by NASA (Grant No. NGR-17-001-034) and AFOSR (Grant USAFOSR F44620-68-C-0020).

INTRODUCTION

A heat exchanger is often an important element in a variety of engineering systems including the life support system in space vehicles. It is used to absorb the heat generated by the adsorption bed for CO_2 removal, the metabolic heat of the human body, the heat generated in air conditioning units, and others.

In this study, optimal control of a single tube heat exchanger with a capability of controlling its wall temperature as a function of time is considered. However, temperature of the fluid in the heat exchanger is a function of both time and a spatial coordinate. In other words the heat exchanger considered in this work is a distributed parameter system which is usually described by a partial differential equation or a set of such equations with time and one or more spatial coordinates as independent variables. A dynamic lumped system, on the other hand, is usually modeled by a set of ordinary differential equations which involve time as the only independent variable. Basically, all physical systems possess the spatial distribution of dependent variables, but often the variables are uniform in space or they may be considered to be independent of space without excessive loss of information. Under such circumstances a system is said to be lumped. However, for many heat exchangers, a lumped approximation is inadequate and it is necessary to take into account spatial variations of the variables to provide sufficient detail regarding system behavior.

Specifically, the problem in this work is to find a certain pattern of the wall temperature variation with respect to time so that the fluid temperature will be changed from one steady state profile to the nearest possible vicinity of a new steady state profile in a finite time. Usually the wall temperature can not exceed a certain temperature constraint that is imposed on the control variable.

Yang [6] solved the transient response of fluid temperature in a single tube heat exchanger subject to wall temperature variation. Koppel et al. [2, 3] studied the optimal control of similar systems. The constraint that was imposed to the system is of the integral type instead of control saturation. They approached the problem based on the conjecture that the control variable is related to the system temperature by a certain relationship. Sakawa [4] was perhaps the first to use linear programming for obtaining the optimal control policy of the distributed parameter system. Huang and Yang [1] used this technique to solve a heat exchanger problem with internal wall heat generation as the control variable. Both wall and fluid transient temperature distributions depend on the internal heat generation.

In the present study both linear programming and a variational technique are employed. The variational technique employed here is similar to that used by Koppel [2, 3], but an analytical control function is obtained without Koppel's conjecture.

System Equations. The system considered in this work is shown in Fig. 1. It consists of a duct through which a coolant flows steadily. Its temperature distribution is changed from an initial state to a final desired state. The following assumptions are made [7].

a) The wall temperature may vary with time but uniform along the x-axis.

b) The fluid temperature and velocity are uniform along the radial direction.

c) Axial heat conduction is negligible in fluid. This is a reasonable assumption when the Peclet number exceeds 100.

d) The heat-transfer coefficient is constant along the x-axis and time. This assumption is experimentally verified to be reasonable [6].

e) The fluid is incompressible and all fluid properties are constant.

f) The flow channel has constant cross-sectional area.

g) The temperature of the fluid entering the duct is constant.

With these assumptions, the energy balance gives rise to the following differential equation for the fluid [2, 7].

$$\rho\ A\ \Delta x'\ C_p \frac{\partial \gamma}{\partial \tau} = u\ \rho\ A\ C_p\ \gamma\Big|_{x'+\Delta x'} - u\ \rho\ A\ C_p\ \gamma\Big|_{x'} + h\ P\ \Delta x'(\gamma_w - \gamma) \tag{1}$$

where γ and γ_w are the transient fluid temperature and wall temperature, respectively, ρ is the coolant density, C_p is the coolant specific heat, P is the wetted perimeter of the tube, A is the flow cross-sectional area, h is the heat transfer coefficient between the wall and the coolant, $\Delta x'$ is the differential distance along axial direction, and τ is time. The initial and boundary conditions are

$$\gamma(0,\ x') = \gamma_0 \tag{2}$$

$$\gamma(\tau,\ 0) = \gamma_0 \tag{3}$$

By introducing the new dimensionless variables

$$T = (\gamma - \gamma_0)/\gamma_0$$

$$\theta = (\gamma_w - \gamma_0)/\gamma_0$$

$$x = x'/L, \qquad 0 \leq x \leq 1$$

$$t = \tau\ u/L$$

$$K = \frac{h\,P\,L}{\rho\ A\ C_p\ u}$$

and letting

$$\Delta x \rightarrow 0,$$

the system equations, Equations (1) through (3), can be transformed to

$$\frac{\partial T}{\partial t} + \frac{\partial T}{\partial x} = K(\theta - T) \tag{4}$$

$$T(0, x) = 0 \tag{4a}$$

$$T(t, 0) = 0 \tag{4b}$$

The analytical solution of equation (4) subject to the boundary conditions was obtained by Yang [7].

Performing the Laplace transformation on equation (4) subject to the initial condition given by equation (4a), one obtains

$$s\bar{T} + \frac{d\bar{T}}{dx} = K(\bar{\theta} - \bar{T}) \tag{5}$$

Integrating this equation subject to the transformed boundary condition of equation (4b)

$$\bar{T}(s, 0) = 0$$

leads to

$$\bar{T}(s, x) = \frac{K}{s+K}(1 - e^{-Kx}\, e^{-sx})\bar{\theta} \tag{6}$$

The inverse Laplace transformation of equation (6) gives two solutions in two domains of real time

$$x \geq t, \quad T(t, x) = K \int_0^t e^{-K(t-\xi)}\, \theta(\xi)d\xi \tag{7}$$

$$\begin{aligned} x \leq t, \quad T(t, x) &= K \int_0^t e^{-K(t-\xi)}\theta(\xi)d\xi - Ke^{-Kx} \int_0^{t-x} e^{-K(t-x-\xi)}\theta(\xi)d\xi \\ &= K \int_0^t e^{-K(t-\xi)}\theta(\xi)d\xi - K \int_0^{t-x} e^{-K(t-\xi)}\theta(\xi)d\xi \\ &= K \int_{t-x}^t e^{-K(t-\xi)}\theta(\xi)d\xi \end{aligned} \tag{8}$$

Performance index. As stated previously the problem is to force the temperature profile from zero initial state, $T(0, x) = 0$, to a new desired steady temperature profile, $T_d(x)$, in a finite time t_f while minimizing a given performance index. The manipulated variable is taken to be the wall temperature, $\theta(t)$, which is a function of time only.

The desired new steady state fluid temperature profile, $T_d(x)$, can be obtained by solving the following steady state differential equation with the boundary condition [1, 2]

$$\frac{dT}{dx} = K(\theta - T)$$

$$T(t, 0) = 0$$

$$\theta(t) = \theta_d, \quad t > t_f$$

where θ_d is the desired final wall temperature. The solution of the above equation is

$$T_d(x) = \theta_d(1 - e^{-Kx}) \tag{9}$$

Two performance indices are to be minimized. One is the integral of the absolute deviation of the system temperature from the desired new steady temperature profile $T_d(x)$ at the final time, t_f, which is given by

$$S = \int_0^1 |T(t_f, x) - T_d(x)|\,dx \tag{10}$$

and the other is the integral of the square of deviation of the system temperature from $T_d(x)$ at the final time, which is given by

$$S = \int_0^1 [T(t_f, x) - T_d(x)]^2\,dx \tag{10a}$$

It is worth recalling that the flow through the system is of the slug flow or plug flow type. Therefore, if the final time is greater than the mean residence time, i.e., if $t_f \geq 1$, the control maintained at θ_d for $0 \leq t \leq t_f$, will lead to the final system temperature profile $T(t_f, x)$ which is exactly equal to $T_d(x)$ [compare equations (8) and (9)], and this in turn will always give rise to the minimum attainable performance index of zero. Therefore, the only case of practical interest is the case with t_f less than one residence time, i.e. $t_f < 1$.

While the two performance indexes given by equations (10) and (10a) are quantitatively different, qualitatively both represent the same entity, namely the integrated deviation of the systems temperature profile from the desired temperature profile.

APPROXIMATE SOLUTION BY LINEAR PROGRAMMING

Since the integrand of the objective function given by equation (10) is linear in the state variable, the well-developed linear programming approach can be used to obtain an approximate solution. In order to utilize the linear programming approach, equation (10) is linearized in a step-wise manner by means of Simpson's rule of integration as follows:

$$S = \int_0^1 |T(t_f, x) - T_d(x)| dx$$

$$\approx \sum_{i=0}^{m} c_i |T(t_f, x_i) - T_d(x_i)| \tag{11}$$

where

$$x_i = \frac{i}{m}, \qquad \text{for } i = 0, 1, 2, \ldots, m$$

$$c_0 = c_m = \frac{1}{3m},$$

$$c_1 = c_3 = \cdots = c_{m-1} = \frac{4}{3m}$$

and

$$c_2 = c_4 = \dots = c_{m-2} = \frac{2}{3m}$$

Equation (11) contains the summation of all linear terms and thus the linear programming approach can be utilized [1, 4]. Since the dimensionless inlet coolant temperature is always zero, the first term of the summation in equation (11) can be droped. In other words, the index of summation, i starts from one instead of zero.

Let

$$|T(t_f, x_i) - T_d(x_i)| = e_{si} + e_{pi}, \qquad i = 1, 2, \dots, m \qquad (12)$$

where e_{si}, e_{pi}, $i = 1, 2, \dots, m$ are non negative variables which satisfy the following relationship.

$$T(t_f, x_i) - T_d(x_i) = e_{pi} - e_{si}, \qquad i = 1, 2, \dots, m \qquad (13)$$

and

$$\left.\begin{array}{l} e_{pi} = 0 \text{ and } T(t_f, x_i) - T_d(x_i) = -e_{si} \text{ if } T(t_f, x_i) - T_d(x_i) < 0 \\ e_{si} = 0 \text{ and } T(t_f, x_i) - T_d(x_i) = e_{pi} \text{ if } T(t_f, x_i) - T_d(x_i) > 0 \\ e_{pi} = e_{si} = 0 \text{ if } T(t_f, x_i) - T_d(x_i) = 0 \end{array}\right\} \qquad (14)$$

$$i = 1, 2, \dots, m$$

By introducing these new variables, equation (11) can be expressed as

$$S = \sum_{i=1}^{m} c_i(e_{si} + e_{pi}) \qquad (15)$$

Equations (7) and (8) at the final time can be approximated by dividing the total transient time, t_f, into n segments and assuming that the θ is constant in each subinterval. Thus

$$T(t_f, x_i) = \sum_{j=1}^{n} A_{ij}\,\theta_j \qquad \text{for} \quad i = 1, 2, \dots, m \qquad (16)$$

where

$$\theta_j = \theta(t) \quad \text{for} \quad t_{j-1} \leq t \leq t_j,$$

$$t_j = j\, t_f/n \quad \text{for} \quad j = 0, 1, \ldots, n,$$

and A_{ij} are constants.

The linear programming model which will yield the optimal policy of the system can now be formulated.

Minimize

$$\sum_{i=1}^{m} c_i(e_{si} + e_{pi}) \tag{15}$$

subject to

$$T(t_f, x_i) - T_d(x_i) = e_{pi} - e_{si}, \qquad i = 1, 2, \ldots, m \tag{17}$$

$$\theta_j \leq \theta_{max} \qquad j = 1, 2, \ldots, n \tag{18}$$

$$e_{pi}, e_{si}, \quad \theta_j \geq 0 \qquad \begin{matrix} i = 1, 2, \ldots, m \\ j = 1, 2, \ldots, n \end{matrix} \tag{19}$$

where θ_{max} is the maximum allowable wall temperature.

From equations (7), (8), (9), and (16) through (19), it can be seen that the problem can be stated as follows:

Minimize

$$\sum_{i=1}^{m} c_i(e_{si} + e_{pi})$$

subject to

$$
\begin{array}{lr}
A_{11}\theta_1 + \ldots + A_{1n}\theta_n - e_{p1} + e_{s1} & = T_d(x_1) \\
A_{21}\theta_1 + \ldots + A_{2n}\theta_n \qquad - e_{p2} + e_{s2} & = T_d(x_2) \\
\vdots \qquad\qquad \vdots & \vdots \\
A_{m1}\theta_1 + \ldots + A_{mn}\theta_n \qquad\qquad -e_{pm} + e_{sm} & = T_d(x_m) \\
\theta_i & \leq \theta_{max} \\
\vdots & \vdots \\
\theta_n & \leq \theta_{max}
\end{array}
$$

$$e_{si},\ e_{pi},\ \theta_j \geq 0 \quad \text{for all } i,\ j.$$

This is a standard linear programming problem which can be solved by the linear programming simplex method [4]. An IBM subroutine in Mathematical Programming System/360 (360A-CO-14X), Linear and Separable Programming, is used for the computation.

SOLUTION BY A VARIATIONAL TECHNIQUE

Because the performance index given by equation (10a) is of the quadratic type, the linear programming approach can not be used for its minimization. While the quadratic programming can be employed to obtain an approximate solution, it appears that use of the variational technique is more appropriate because of the possibility of obtaining an exact or analytic solution.

The systems equations considered here are equations (4), (4a), (4b), and (10a).

Consider now a small change $\delta\theta$ in the control variable θ. The resulting incremental response δT in the state variable T of equation (4) must satisfy the following linear perturbation differential equation.

$$\delta \frac{\partial T}{\partial t} = - \delta \frac{\partial T}{\partial x} + K(\delta\theta - \delta T) \tag{20}$$

The variational initial and boundary conditions are

$$\delta T(0, x) = 0 \quad \text{at} \quad t = 0 \tag{21}$$

$$\delta T(t, 0) = 0 \quad \text{at} \quad x = 0 \tag{22}$$

Now the control function θ which gives rise to the minimum of the performance index given by equation (10a) must be determined. In order to obtain necessary conditions for optimality, a relationship must be found which expresses the variation of the performance index, δS, in terms of the control perturbation, $\delta\theta$.

The increment of the performance index, equation (10a), due to the system temperature variation is

$$\delta S = \int_0^1 2[(T(t, x) - T_d(x))\delta T]\Big|_{t=t_f} dx \tag{23}$$

By adjoining the variational system equation, equation (20), to the variational performance index, equation (23), one obtains

$$\delta S = \int_0^1 2[(T - T_d)\delta T]\Big|_{t=t_f} dx - \int_0^1 \int_0^{t_f} z[\delta \frac{\partial T}{\partial t} + \delta \frac{\partial T}{\partial x} - K\delta\theta + K\delta T]dt\, dx \tag{24}$$

where $z(t, x)$ is the adjoint variable.

Because of the identities of

$$\frac{\partial}{\partial t}(z\delta T) = \frac{\partial z}{\partial t}\delta T + z\,\delta \frac{\partial T}{\partial t} \tag{25}$$

$$\frac{\partial}{\partial x}(z\delta T) = \frac{\partial z}{\partial x}\delta T + z\,\delta \frac{\partial T}{\partial x}\,, \tag{26}$$

substitution of equations (25) and (26) into equation (24) yields

$$\delta S = \int_0^1 2[(T - T_d)\delta T]\Big|_{t=t_f} dx - \int_0^1 \int_0^{t_f} [\frac{\partial}{\partial t}(z\delta T) + \frac{\partial}{\partial x}(z\delta T)$$

$$- (\frac{\partial z}{\partial t} + \frac{\partial z}{\partial x} - Kz)\delta T - Kz\delta\theta]dt\, dx \tag{27}$$

The first term in the second integral of equation (27) is now integrated with respect to t from $t = 0$ to $t = t_f$, and the second term with respect to x from $x = 0$ to $x = 1$, so that each term in the integrand involves either the variation δT or $\delta\theta$. These give

$$\int_0^{t_f} \frac{\partial}{\partial t}(z\delta T)dt = [z\delta T]_{t=0}^{t_f} \tag{28}$$

$$\int_0^{1} \frac{\partial}{\partial x}(z\delta T)dx = [z\delta T]_{x=0}^{1} \tag{29}$$

After some manipulation and noting that $\delta T(0, x) = 0$ and $\delta T(t, 0) = 0$, the following result is obtained.

$$\delta S = \int_0^1 [(2T - 2T_d - z)\delta T]\Big|_{t=t_f} dx - \int_0^{t_f} [z\delta T]_{x=1}\, dt$$

$$+ \int_0^1 \int_0^{t_f} [(\frac{\partial z}{\partial t} + \frac{\partial z}{\partial x} - Kz)\delta T + Kz\delta\theta]dt\, dx \tag{30}$$

To eliminate terms not depending explicitly on $\delta\theta$ from the integrand of the third integral of equation (30), it is stipulated that the adjoint variable satisfies the differential equation,

$$\frac{\partial z}{\partial t} + \frac{\partial z}{\partial x} - Kz = 0 \tag{31}$$

This is accomplished by choosing the adjoint boundary conditions such that the coefficients of unknown endpoint variation δT vanish. For the coefficient of δT in the second integral of equation (30) to be zero, one has

$$z(t, 1) = 0 \tag{32}$$

For the coefficient of δT in the first integral of equation (30) to be zero, one has

$$z(t_f, x) = 2T(t_f, x) - 2T_d(x) \tag{33}$$

The resulting variational performance index, equation (27), can now be written as

$$\delta S = \int_0^1 \int_0^{t_f} Kz(t, x)\delta\theta \, dt \, dx \tag{34}$$

Assuming that for the adjoint variable z(t, x) is piece-wise continuous, equation (34) can be rearranged by interchanging the order of integration as follows:

$$\delta S = K \int_0^{t_f} [\int_0^1 z dx]\delta\theta \, dt \tag{35}$$

The analytical solution for the adjoint variable is obtained along the characteristic line along which the following general relation exists.

$$\frac{dz}{ds} = \frac{\partial z}{\partial t}\frac{dt}{ds} + \frac{\partial z}{\partial x}\frac{dx}{ds}$$

where s is the length along the characteristic line. Comparing equation (31) with this relation yields

$$\frac{dt}{ds} = -1,$$

$$\frac{dx}{ds} = -1,$$

$$\frac{dz}{ds} = -Kz$$

Integrating these equations, one obtains

$$\left.\begin{aligned} t &= t_0 - s, \\ x &= x_0 - s, \\ z &= e^{-Ks} z_0 \end{aligned}\right\} \tag{36}$$

where t_0, x_0, and z_0 are values of t, x, and z respectively at the starting point. The argument of the boundary condition given by equation (32) is represented by line segment $\overline{CD}$ in Fig. 2. The argument of equation (33) is split into two regions because $T(t_f, x)$ has two different expressions from equations (7) and (8). Line segment $\overline{AB}$ represents the argument of equations (33) and (8), i.e., for $x \le t_f$. Line segment $\overline{BC}$ represents the argument of equations (33) and (7), i.e., for $x \ge t_f$.

Now consider point Q in Fig. 2, which is inside the line segment $\overline{BC}$. At this point, $t_0 = t_f$. Let

$$t = t_f - s \tag{37}$$

$$x = x_0 - s \tag{38}$$

Then, eliminating s from these two equations, one obtains

$$x_0 = x + t_f - t \tag{39}$$

Rearranging equation (37) yields

$$s = t_f - t \tag{40}$$

The slope of the characteristic line $\overline{QP}$, $(t - t_f)/(x - x_0)$, can be obtained from equations (37) and (38), and is equal to 1. The same is true for the characteristic lines $\overline{BO}$ and $\overline{CJ}$, which divide the argument of adjoint variable into three regions, i.e., regions I, II, and III. Region I is determined from the boundary condition at $\overline{AB}$, region II is determined from the boundary condition at $\overline{BC}$, and region III is determined from the boundary condition at $\overline{CD}$. Substituting equations (7) and (9) into equation (33), the boundary condition at Q becomes

$$z_0(t_f, x_0) = 2K \int_0^{t_f} \theta(\rho) e^{K(\rho - t_f)} d\rho - 2\theta_d[1 - e^{-Kx_0}] \qquad (41)$$

Then along the characteristic line $\overline{QP}$, the solution for the adjoint variable can be obtained by substituting equation (39) into equation (41), and equations (40) and (41) into equation (36). This yields

$$z(t, x) = e^{K(t-t_f)} \{2K \int_0^{t_f} \theta(\rho) e^{K(\rho-t_f)} d\rho - 2\theta_d[1 - e^{-K(x+t_f-t)}]\}, \qquad (42)$$

for

$$1 + t - t_f \geq x \geq t$$

Since Q is an arbitrary point in the line segment $\overline{BC}$, equation (42) is the solution for the entire domain of region II. At any arbitrary time, region II is inside the line segment $\overline{FG}$ in Fig. 2, i.e., $t \leq x \leq 1 - t_f + t$. In the same manner, the solution for region I, i.e., $x \leq t$ of $\overline{EF}$, can be obtained by substituting equations (8) and (9) into equation (33), and by noting that x is changed to x_0 because it is on the boundary point where $t = t_f$, $x = x_0$. The resulting equation is then substituted into equation (36). Finally, replacing s in equation (36) by equation (40), one obtains

$$z(t, x) = e^{K(t-t_f)} \{2K \int_{t-x}^{t_f} \theta(\rho) e^{K(\rho-t_f)} d\rho - 2\theta_d[1 - e^{-K(x+t_f-t)}]\} \qquad (43)$$

for

$$0 \leq x \leq t.$$

Since the boundary condition for region III is zero, it can be seen from equation (36) that

$$z(t, x) = 0 \qquad (44)$$

for

$$1 \geq x > 1 + t - t_f.$$

<u>Numerical Procedure Based on the Gradient Technique in Function Space</u>. Because the control variable is constrained, and equation (1) is linear in the control variable, θ, it is impossible to let the gradient of

the Hamiltonian with respect to θ be zero. The control variable will be of the bang-bang type unless singular control occurs. However, the iterative procedure by the gradient technique can be employed to obtain the optimal control policy even in the singular control case. In fact, a part of the control policy obtained in this work is singular. For a lumped-parameter system, the perturbed performance index is obtained for continuous control processes by the gradient in function space method [5]. The resulting expression is

$$\delta S = \int_0^{t_f} \frac{\partial H}{\partial \theta} (\delta\theta) dt$$

where H is the Hamiltonian. If one wishes to minimize the performance index, the gradient $\partial H/\partial\theta$ is calculated and $\delta\theta$ is determined such that its direction is opposite to the gradient, i.e.,

$$\delta\partial = - \alpha \frac{\partial H}{\partial \theta}$$

where α is a positive constant. Analogous to this, the perturbed index given by equation (35) is

$$\delta S = K \int_0^{t_f} [\int_0^1 z dx] \delta\theta dt$$

and thus the control variation may be given by

$$\delta\theta = - \alpha [\int_0^1 z dx] \qquad (45)$$

Integration of the adjoint variable along x, which appears in this equation, can be accomplished by integrating equation (43) from $x = 0$ to $x = t$, integrating equation (42) from $x = t$ to $x = 1 + t - t_f$, and integrating equation (44) from $x = 1 + t - t_f$ to $x = 1$. This yields

$$\int_0^1 z dx = 2e^{K(t-t_f)}\{\int_0^t [\int_{t-x}^{t_f} K\theta(\rho)e^{K(\rho-t_f)} d\rho - \theta_d(1-e^{-K(x+t_f-t)})]dx$$

$$+ \int_t^{t-t_f+1} [K\int_0^{t_f} \theta(\rho)e^{K(\rho-t_f)} d\rho - \theta_d(1 - e^{-K(x+t_f-t)})]dx\} \quad (46)$$

Interchanging the order of integration and performing the integration with respect to x yield

$$\int_0^1 z(t, x)dx = 2e^{K(t-t_f)} \phi(t) \quad (47)$$

where

$$\phi(t) = (1 - t_f + t) \int_0^{t_f} \theta(\rho)e^{K(\rho-t_f)} d\rho - K \int_0^t \theta(\rho)e^{K(\rho-t_f)} (t-\rho)d\rho$$

$$- \theta_d\{1 - t_f + t + \frac{1}{K} [e^{-K} - e^{K(t-t_f)}]\} \quad (48)$$

In computing the optimal solution, the following iterative procedure has been employed:

(1) Assume a control pattern $\theta(t) = \theta_0(t)$.

(2) Compute the fluid temperature $T(t, x)$ from equations (7) and (8).

(3) Compute the adjoint variable $z(t, x)$ from equations (42), (43), and (44).

(4) Compute the integration of the adjoint variable $\int_0^1 z dx$ from equations (47) and (48).

(5) Let $\delta\theta = -\alpha\int_0^1 z dx$. Equation (35) will be $\delta S = -K\alpha\int_0^{t_f} (\delta\theta)^2 dt$ which is always decreasing.

(6) Change the control variable such that $\theta_{revised}(t) = \theta_{old}(t) + \delta\theta$, and repeat the whole procedure from step (2). If $\theta_{revised}(t)$ exceeds its upper bound θ_m somewhere between $t = a$ and $t = b$,

$$S = \int_0^1 [T(t_f, x) - T_d(x)]^2 dx$$
$$= \int_0^{t_f} [T_d(x) - T_d(x)]^2 dx + \int_{t_f}^1 [T_1(t_f) - T_d(x)]^2 dx \qquad (49)$$

Note that the first integral of the right-hand side is zero.

To find $T_1(t_f)$ which minimizes the performance index S, the gradient of S with respect to T_1 has to be zero.

$$\frac{dS}{dT_1} = 2 \int_{t_f}^1 (T_1 - T_d) dx = 0 \qquad (50)$$

Since T_1 is uniform for $t_f \leq x \leq 1$, this gives

$$T_1 = \frac{1}{1 - t_f} \int_{t_f}^1 T_d \, dx$$
$$= \frac{\theta_d}{1 - t_f} [1 - t_f + \frac{1}{K} (e^{-K} - e^{-Kt_f})] \qquad (51)$$

Substituting T_1 into equation (49), the minimum performance index will be

$$\min S = \int_{t_f}^1 [T_1 - \theta_d(1 - e^{-Kx})]^2 \, dx$$
$$= \int_{t_f}^1 [(T_1 - \theta_d)^2 + 2\theta_d(T_1 - \theta_d)e^{-Kx} + \theta_d^2 \, e^{-2Kx}] dx$$
$$= (T_1 - \theta_d)^2 \, (1 - t_f) - \frac{2\theta_d}{K} (T_1 - \theta_d)(e^{-K} - e^{-Kt_f})$$
$$- \frac{\theta_d^2}{2K} (e^{-2K} - e^{-2Kt_f}) \qquad (52)$$

While the case with the quadratic performance index as given by equation (10a) is the main concern of this section, the above argument is equally valid for the performance index given by equation (10). There always exists a point, $x = x_1$ in the region $t_f \leq x \leq 1$, where the fluid temperature, $T_1(t_f)$, will change from $T_1(t_f) > T_d(x)$ for $x < x_1$ to $T_1(t_f) < T_d(x)$ for $x > x_1$. Then the performance index becomes

$$S = \int_0^1 |T(t_f, x) - T_d| dx$$

$$= \int_0^{t_f} |T_d - T_d| dx + \int_{t_f}^{x_1} (T_1 - T_d) dx + \int_{x_1}^{1} (T_d - T_1) dx \qquad (53)$$

In order to minimize S, its partial derivative with respect to x_1 and T_1 must be zero. Taking partial derivative of S with respect to T_1 and letting it be zero yield

$$\frac{\partial S}{\partial T_1} = (x_1 - t_f) - (1 - x_1) = 0$$

This result implies that

$$x_1 = (1 + t_f)/2 \qquad (54)$$

Taking partial derivative of equation (53) with respect to x_1 and equating the resulting expression to zero yield

$$\frac{\partial S}{\partial x_1} = T_1 - T_d(x_1) - [T_d(x_1) - T_1] = 0$$

or

$$T_1 = T_d(x_1) = \theta_d(1 - e^{-Kx_1})$$

Substitution of equation (54) into this equation yields

$$T_1 = \theta_d[1 - e^{-K(1+t_f)/2}] \qquad (55)$$

Combination of equations (9) and (55) shows that

$$T_1 - T_d = \theta_d(e^{-Kx} - e^{-K(1+t_f)/2}) \qquad (56)$$

The minimum performance index of equation (53) becomes

$$S = \int_{t_f}^{(1+t_f)/2} \theta_d[e^{-Kx} - e^{-K(1+t_f)/2}]dx + \int_{(1+t_f)/2}^{1} \theta_d[e^{-K(1+t_f)/2} - e^{-Kx}]dx$$

$$= \theta_d[\frac{1}{K} e^{-Kt_f} - \frac{1}{K} e^{-K(1+t_f)/2}] - \theta_d[\frac{1+t_f}{2} - t_f]e^{-K(1+t_f)/2}$$

$$+ \theta_d[1 - \frac{1+t_f}{2}]e^{-K(1+t_f)/2} + \frac{\theta_d}{K} [e^{-K} - e^{-K(1+t_f)/2}]$$

$$= \frac{\theta_d}{K} [e^{-K} + e^{-Kt_f} - 2e^{-K(1+t_f)/2}] \qquad (57)$$

In the unconstrained case, the optimal control is infinite at $t = 0^+$ and this is immediately followed by the desired final steady state control, $\theta = \theta_d$. The optimal control with constraints on control may be analogous to this control for the unconstrained case. Therefore, it is assumed that the control is on the upper constraint boundary initially and then move to the inner part of the control domain. Provided this assumption is correct, one is required to locate the switching time, $t = t_1$, at which the control is moved from the upper bound to the inner part of the control domain, and find the control policy after this switching time, i.e. for $t > t_1$.

For the control to be optimal, the variation of the performance index, equation (35), must be identically zero. For the period $t < t_1$ when the optimal control is $\hat{\theta} = \theta_{max}$, two possibilities exist. One possibility is

$$\int_0^1 zdx = 0$$

so that the control variation $\delta\theta$, as given by equation (45), is zero. The other is

$$\int_0^1 z dx < 0$$

so that the control variation, $\delta\theta$, has to be positive. However, since the control is already at the upper boundary, and the control is constrained, $\delta\theta$ has to be zero. In this case, the variation of performance index, equation (35), is zero again.

For the portion of the optimal control not on the control boundary, only the first case can happen, i.e.,

$$\int_0^1 z dx = 0.$$

For the period $t > t_1$, therefore, $\delta\theta$ must be zero at the optimal control. From equations (45) and (47), one obtains

$$\phi(t) = 0 \quad \text{for} \quad t \geq t_1, \tag{58}$$

to satisfy

$$\int_0^1 z dx = 0.$$

The integral equation, equation (58), where $\phi(t)$ is expressed by equation (48), can be solved by twice differentiating it with respect to t. Note that the intervals of integrations in the right-hand side of equation (48) are from $\rho = 0$ to $\rho = t_f$ for the first term, and from $\rho = 0$ to $\rho = t$ for the second term. The interval of the first integration will be divided into two intervals ranging from $\rho = 0$ to $\rho = t_1$ and from $\rho = t_1$ to $\rho = t_f$. The interval of the second integration will also be divided into two intervals ranging from $\rho = 0$ to $\rho = t_1$ and $\rho = t_1$ to $\rho = t$.

For the period of $t < t_1$, the optimal control is $\hat{\theta}(t) = \theta_{max}$. Substituting this value into equation (58) and differentiating the resulting equation twice with respect to time, t, one obtains

$$\theta(t) = \theta_d, \quad \text{for} \quad t > t_1.$$

$\phi(t)$ is 0 at $t = t_1$ for the optimal control. Therefore, by substituting the optimal control policy [$\theta(t) = \theta_{max}$ for $t < t_1$, $\theta(t) = \theta_d$ for $t \geq t_1$] into equation (58), replacing t by t_1, and integrating the resulting equation, one obtains

$$\frac{\theta_{max} - \theta_d}{K} e^{K(t_1 - t_f)} (1 - \frac{1}{K} + t_1 - t_f) = \frac{\theta_d}{K^2} e^{-K} - \frac{\theta_{max}}{K} e^{-Kt_f} (t_f - 1 + \frac{1}{K}) \tag{59}$$

This equation can be solved for t_1 by iteration. For the unconstrained case, where $\theta_{max} \rightarrow \infty$, t_1 is zero.

A NUMERICAL EXAMPLE

Numerical values of the parameters of the system, the final dimensionless time $t_f = \tau_f u/L$, the dimensionless heat exchanger coefficient K, the desired wall temperature, θ_d, and the maximum allowable wall temperature, θ_{max}, are taken as follows:

$t_f = 0.5$

$K = 1.0$

$\theta_d = 0.5$

$\theta_{max} = 4.0$

The performance index given by equation (10a) will be denoted by S_1, i.e.,

$$S_1 = \int_0^1 [T(t_f, x) - T_d]^2 \, dx,$$

and the performance index given by equation (10) be denoted by S_2, i.e.,

$$S_2 = \int_0^1 |T(t_f, x) - T_d| \, dx.$$

Approximate Optimal Solution by Linear Programming. As stated previously, this approach is applicable to the case with the objective function S_2. Figure 3 shows the approximate optimal control pattern obtained by the linear programming method. This pattern is not strictly of the bang-bang type. Sakawa [4] and Huang and Yang [1] obtained similar results by using the linear programming method to solve a distributed parameter system. In this work, since the control is assumed to be a constant inside each time subinterval, the resulting pattern is discrete, which is in contrast to the continuous nature of the results obtained by Sakawa [4] and Huang and Yang [1].

Figure 4 shows the corresponding temperature distribution. This approximation was made by subdividing the tube into 20 segments. The time increment employed here is $\Delta t = 0.01$, i.e., 50 subinterval in time axis for $t_f = 0.5$. Since the integration in the performance index formula is approximated by Simpson's rule, the points in Fig. 4 of $x = .4, .45, .5$ are connected by a smooth curve. S_2 corresponding to this approximate optimal solution is 0.01576.

Variational Technique. As stated previously this technique is mainly applied to the case with S_1. However, for the corresponding unconstrained problems, both cases of S_1 and S_2 can be solved analytically with equal ease. The values of S_1 and S_2 are calculated from equations (57) and (52), respectively. The resulting final optimal system temperature profiles are given in Figures 5 and 6 . In these figures, the solid lines in the region of $x \leq 0.5$ and the dash lines in the region of $x \geq 0.5$ are the desired temperature distributions given by equation (9).

In Figure 5 for the case of minimizing S_1, the optimal temperature distribution is $T(t_f, x) = T_d(x)$ for $x < 0.5$ and $T(t_f, x) = T_2 = 0.26135$ for $x > 0.5$ which is obtained by equation (51). These are plotted by solid lines in Figure 5. The minimum S_1 as given by equation (52) has the value of 0.0005909. The value of S_2 corresponding to the temperature distribution given in Figure 5 is 0.0148641.

In Figure 6 for the case of minimizing S_2, the optimal temperature distribution is $T(t_f, x) = T_d(x)$ for $x < 0.5$ and $T(t_f, x) = T_1 = 0.2638$ for $x > 0.5$ which is obtained by equation (55). These are plotted by solid lines in Figure 6. The minimum S_2 as given by equation (57) has the value of 0.0148385. The value of S_2 obtained by the linear programming is 0.01576 as stated in the preceding sub-section. This result is anticipated because it is greater than the unconstrained optimal value. The temperature distribution in Figure 5 corresponds to the S_2 value of 0.0148641. This value is greater than the present S_2 value of 0.0148385 corresponding to the temperature profile of Figure 6. This result is anticipated because the temperature distribution in Figure 5 corresponds to the minimum S_1 which is 0.0005909. The S_1 value in Figure 6 is 0.0229 which is greater than this value.

Figure 7 shows the exact optimal control trajectory which minimizes S_1. The switching time of control, t_1, is obtained from equation (59) as $t_1 = 0.02914392$.

Figure 8 shows the temperature distribution at various transient time. Figure 9 shows the corresponding transient distribution of the adjoint variable. The dash line in Fig. 8 is the desired final temperature distribution, T_d, and is obtained from equation (9). The solid lines are the temperature distribution at various time along the optimal control trajectory. These lines are obtained by substituting the optimal control policy of Fig. 7 into equations (7) for $x \geq t$ and into equation (8) for $x \leq t$.

The lines in Fig. 9 are the distribution of the adjoint variable, $z(t, x)$, at various time along the optimal control trajectory. These lines are obtained by substituting the optimal control policy in Fig. 7 into equation (43) for $x \leq t$, into equation (42) for $t \leq x \leq 1 + t - t_f$, and into equation (44) for $1 \geq x > 1 + t - t_f$. Each equation represents a continuous line with continuous derivative. Equation (43) represents the curves with positive derivatives. Equation (42) represents the curves with negative derivatives and is continuously connected to the lines of equation (43) at $x = t$. Equation (44) represents the curves on the x axis and connected to the curves of equation (42) by dash lines. S_1 has the value of 0.000631104. While the same control pattern produces $S_2 = 0.0158354$, the S_2 value from the linear programming part is 0.01576.

Figure 10 shows the variation of $\int_0^1 z dx$ with respect to time, subject to the control obtained in Fig. 7. For $t < t_1$, it has a negative value, but the corresponding control lies on the upper limit; for $t \geq t_1$, it is zero. This result conforms with the previous analysis, i.e., $\int_0^1 z dx \leq 0$ for $t \leq t_1$, and $\int_0^1 z dx = 0$ for $t \geq t_1$.

Figure 11 shows the approximate optimal control policy obtained by the numerical iterative procedure based on the gradient technique. The reason it deviates from the exact optimal pattern as obtained by the analytical method is that the exact control pattern switches at $t = .029143$, which can not be realized by using time increment of $\Delta t = 0.01$ by the present numerical iteration method. The value of S_1 is 0.000658405. For the control pattern of $\theta = 4.0$, i.e., maximum allowable value, for $t < 0.03$ and $\theta = \theta_d = 0.5$, for $t > 0.03$, the corresponding S_1 has a value of 0.000660493, while the S_1 corresponding to the exact optimal control as obtained by the analytical method is 0.000631. The deviation of the temperature and the adjoint variable distribution between the analytical method and the numerical iterative method are negligibly small. These plots are neglected.

CONCLUDING REMARKS

In this work, practical aspects in computation and solution of the optimal control problem of a first order distributed parameter system, more specifically a heat exchanger, has been emphasized.

First it has been shown that linear programming can be advantageously employed to obtain an approximate optimal control policy for the case with an integral objective function, the integrand of which is linear in the state variable.

Both analytical and numerical procedures based on the variational technique have been successfully employed to determine the optimal solution for the case with an integral objective function, the integrand of which is quadratic in the state variable.

In connection with this variational approach, it has been shown that solution of the corresponding unconstrained problem which is less complicated than the original constrained problem, is indeed useful and beneficial in evaluating various approaches to be taken in solving the original constrained problem.

ACKNOWLEDGEMENT

The first author is indebted to Professor Wen-Jei Yang, University of Michigan, for suggestions and encouragement. Assistance given by Mr. F. T. Hsu is also acknowledged.

References:

[1] Huang, H. S., and Yang, W. J., "Minimum Time Control of Heat Exchangers Having Internal Heat Sources," Presented at IFAC Symposium on Multivariable Control Systems, Duesseldorf, Germany (1968).

[2] Koppel, L. B., Shih, Y. P., and Coughanowr, D. R., "Optimal feedback control of a class of distributed-parameter systems with space-independent controls," I&EC Fundamentals, Vol. 7, pp. 286-295 (1968).

[3] Koppel, L. B., and Shih, Y. P., "Optimal Control of a Class of Distributed-Parameter Systems with Distributed Controls," I&EC Fundamentals Vol. 7, pp. 414-422 (1968).

[4] Sakawa, Y., "Solution of an Optimal Control Problem in a Distributed-Parameter System," IEEE Trans. on Automatic Control, Vol. AC-9, pp. 420-426 (1964).

[5] Sage, A. P., Optimum Systems Control, Prentice Hall, Englewood Cliffs, N. J., 1968, pp. 395-397.

[6] Yang, W. J., "Dynamic response of heat exchangers with sinusoidal time dependent internal heat generation," Ph. D. Thesis, Dept. of Mechanical Engg., Univ. of Mich., April, 1960; Also J. of Heat Transfer, Tr. ASME, Series C, Vol. 83, pp. 321-328 (1961).

[7] Yang, W. J., "Dynamic Response of Heat Exchangers to the Disturbance of Wall Temperature," ASME Paper No. 62-WA-27 (1962).

NOMENCLATURE:

A = flow cross-sectional area, ft^2

A_{ij} = dimensionless constant

c_i = dimensionless constant

C_p = specific heat, $\frac{BTU}{lbm^\circ F}$

e_{si} = dimensionless variable defined by equation (14)

e_{pi} = dimensionless variable defined by equation (14)

H = Hamiltonian function

h = heat transfer coefficient between tube wall and the coolant, $\frac{BTU}{ft^2\ hr}$

i = dimensionless integer

K = dimensionless constant, $\frac{h\ P\ L}{\rho\ C_p\ A\ u}$

L = heat exchanger length, ft

m = dimensionless integer, total number of heat exchanger segments

n = dimensionless integer, total number of subintervals for t_f

P = wetted perimeter, ft

S, S_1, S_2 = performance indices, dimensionless

s = Laplace transformation variable, dimensionless; distance along the characteristic line, dimensionless

t = dimensionless time; t_1, switching time; t_f, final time

T = coolant dimensionless temperature; $\bar{T}$, Laplace transformed temperature; T_d, desired coolant temperature

u = coolant velocity, ft/hr

x = heat exchanger axial distance, dimensionless

z = adjoint variable, dimensionless

<u>Subscripts</u>

i = summation along x-axis

j = summation along time axis

m = total number of increment along x

n = total number of increment along t

Greek letters

α = dimensionless positive constant

γ = coolant temperature, °F

γ_0 = constant, °F

γ_w = wall temperature, °F

ρ = density, $\frac{lbm}{ft^3}$; integration variable

τ = time, hr

θ = dimensionless wall temperature; θ_d, desired wall temperature; $\bar{\theta}$, Laplace transformed wall temperature; θ_{max}, maximum wall temperature

$\phi(t)$ = dimensionless, defined by equation (48)

δ = variational operator, dimensionless

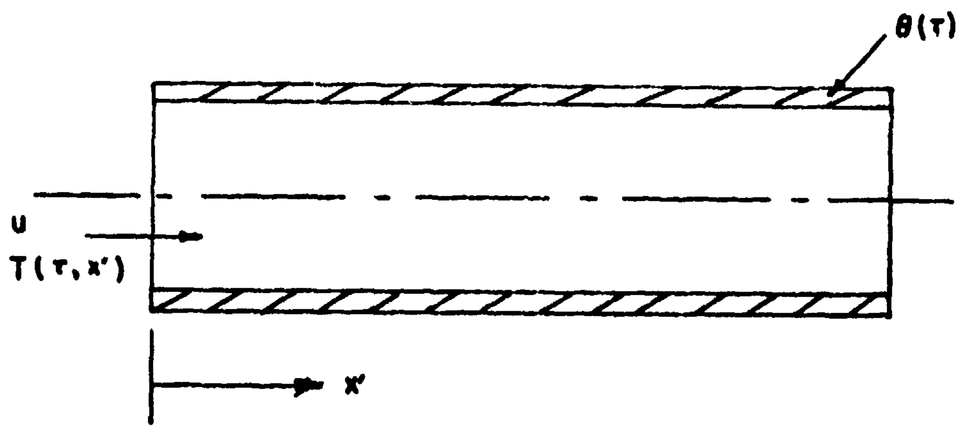

Fig. 1 A single tube heat exchanger.

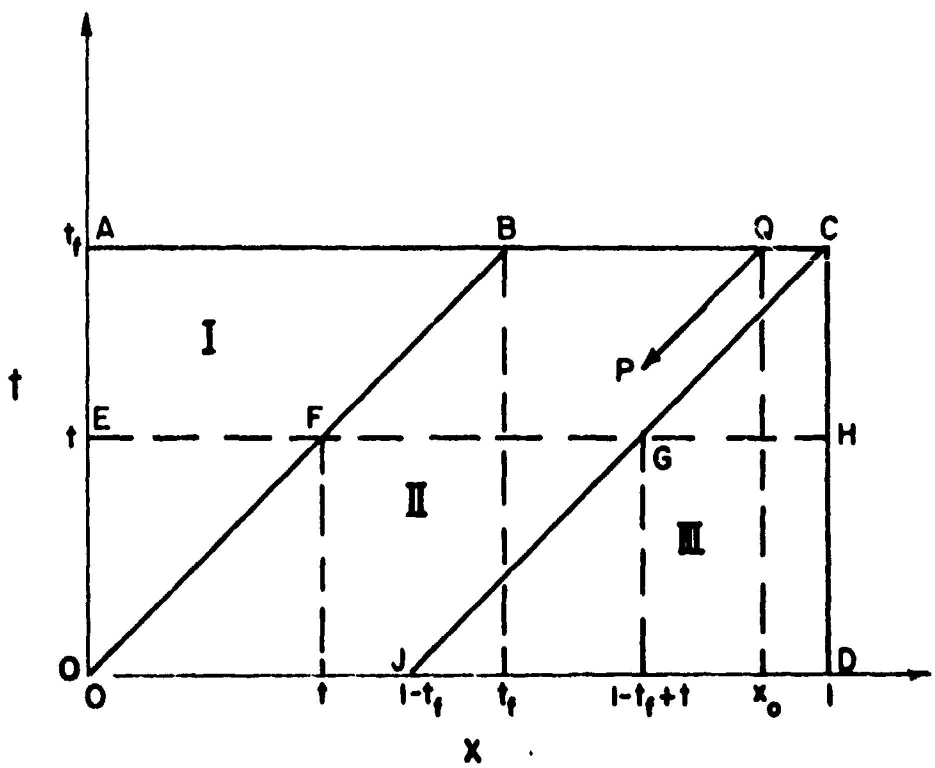

Fig. 2 Characteristic lines for the adjoint variable.

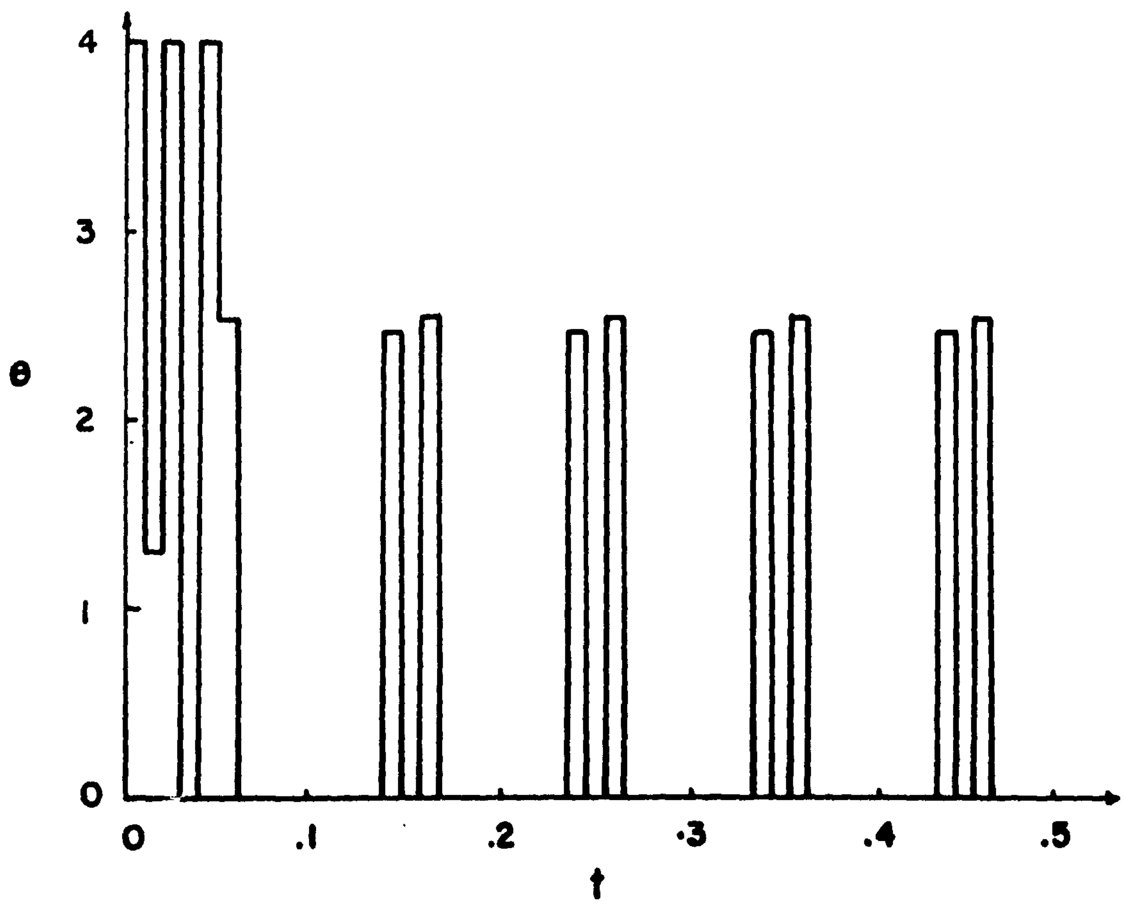

Fig. 3 Approximate optimal control policy obtained by the linear programming for the case of S_2.

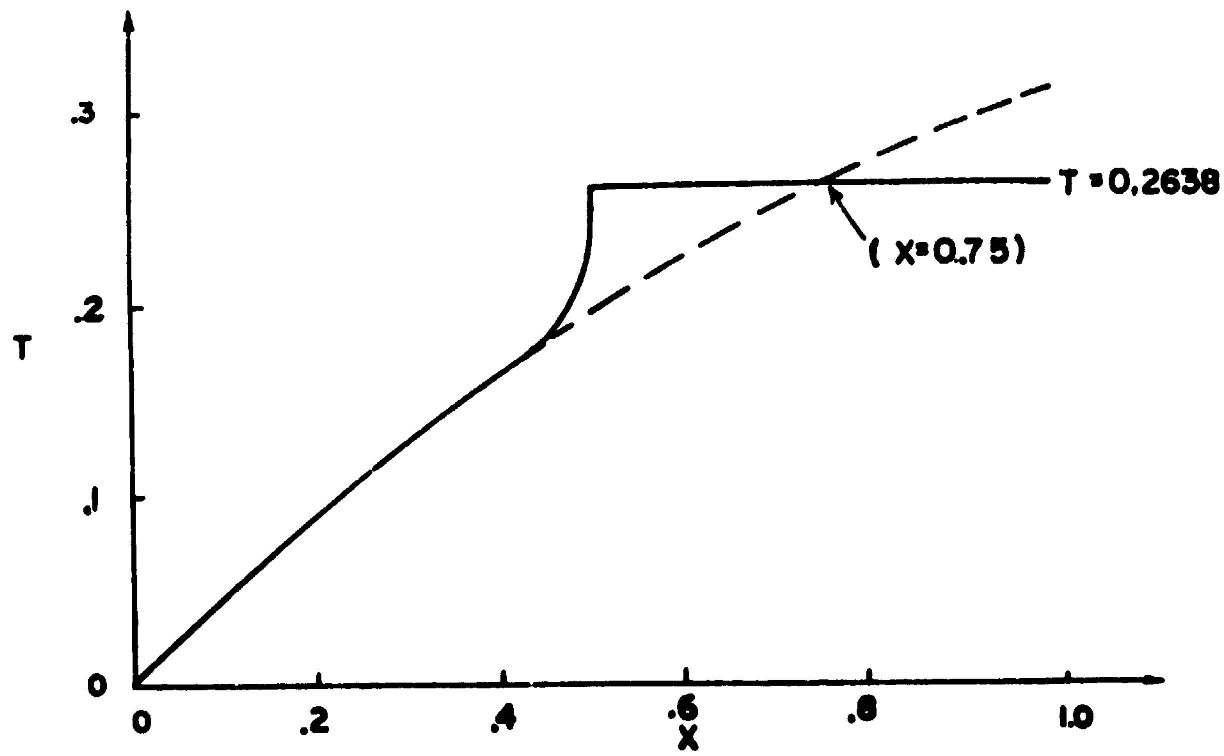

Fig. 4 Approximate final optimal temperature distribution obtained by linear programming approach for the case of S_2.

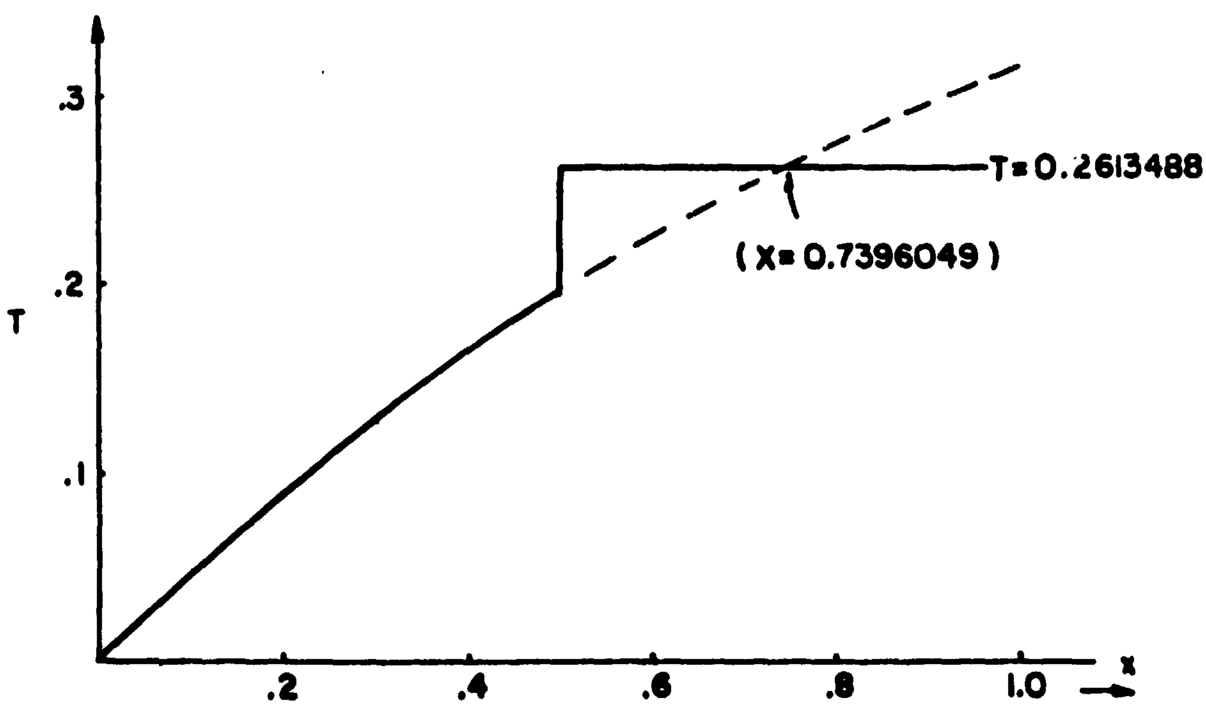

Fig. 5 Optimal final temperature distribution without control constraints for the case of S_1.

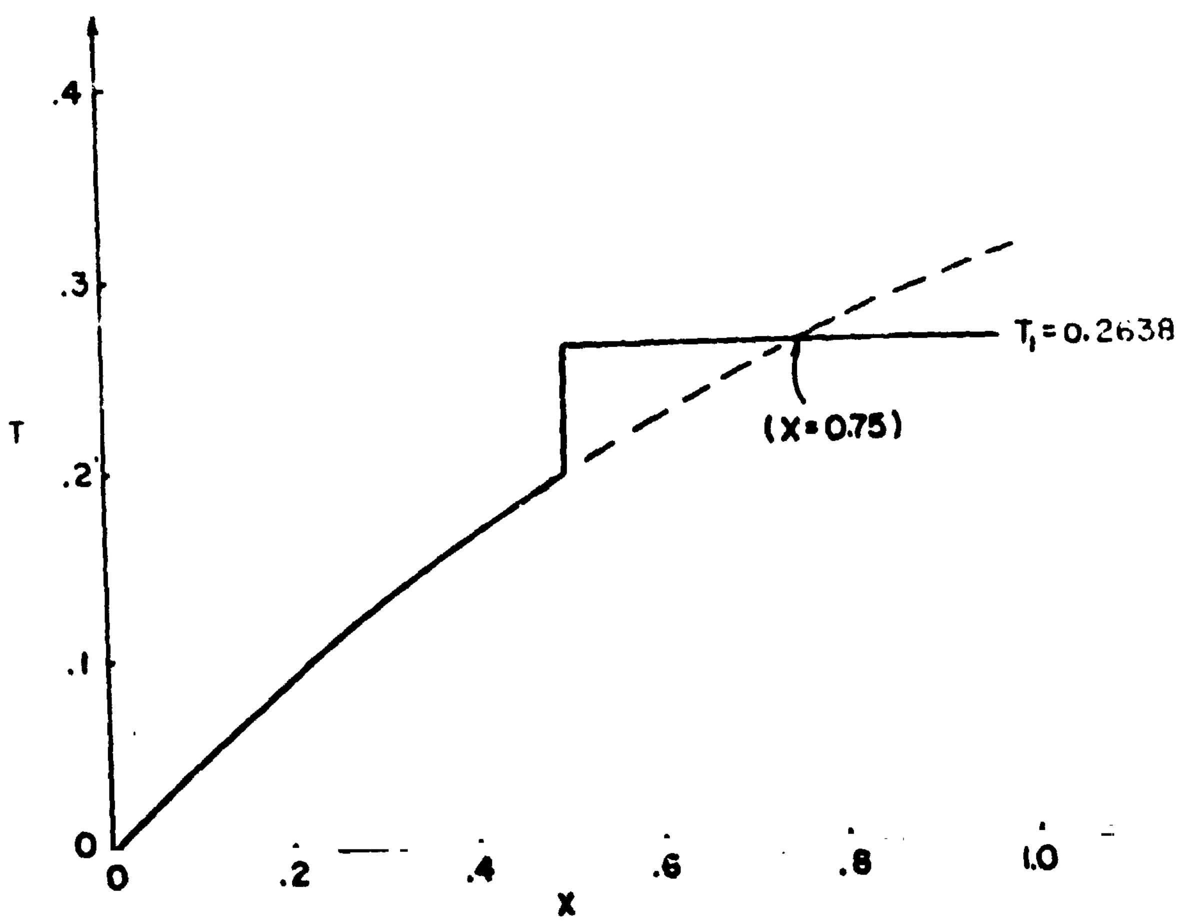

Fig. 6 Optimal final temperature distribution without control constraints for the case of S_2.

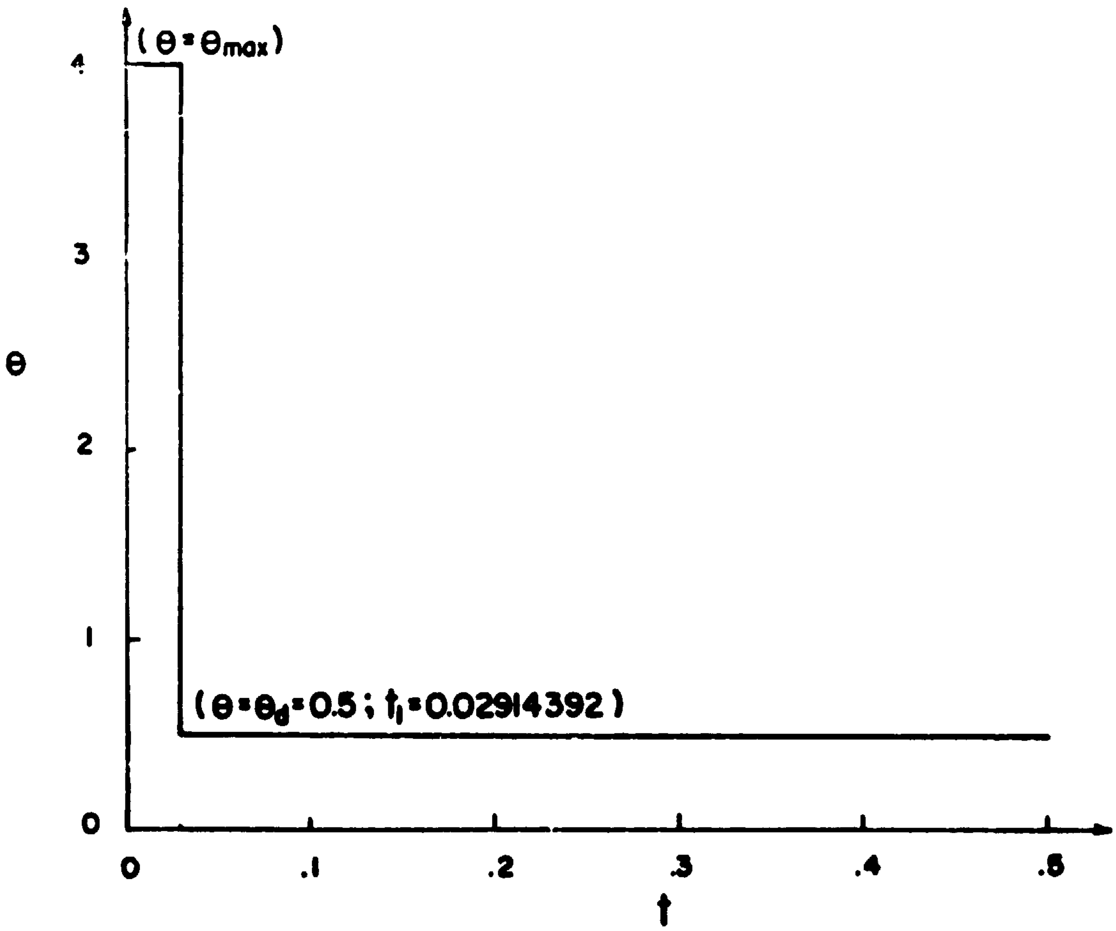

Fig. 7 Analytically determined exact optimal control policy for the case of S_1.

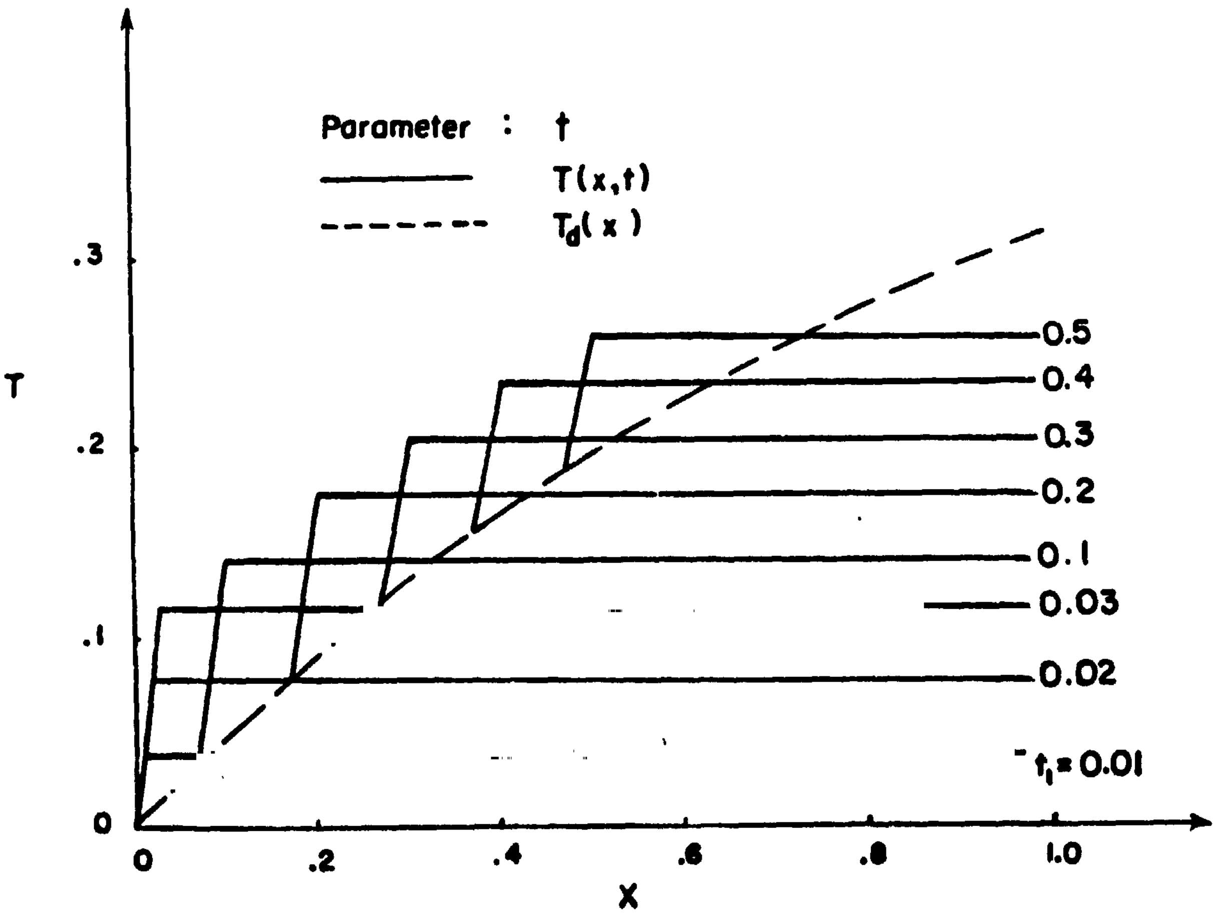

Fig. 8 Temperature distribution along the analytically determined optimal path for the case of S_1 .

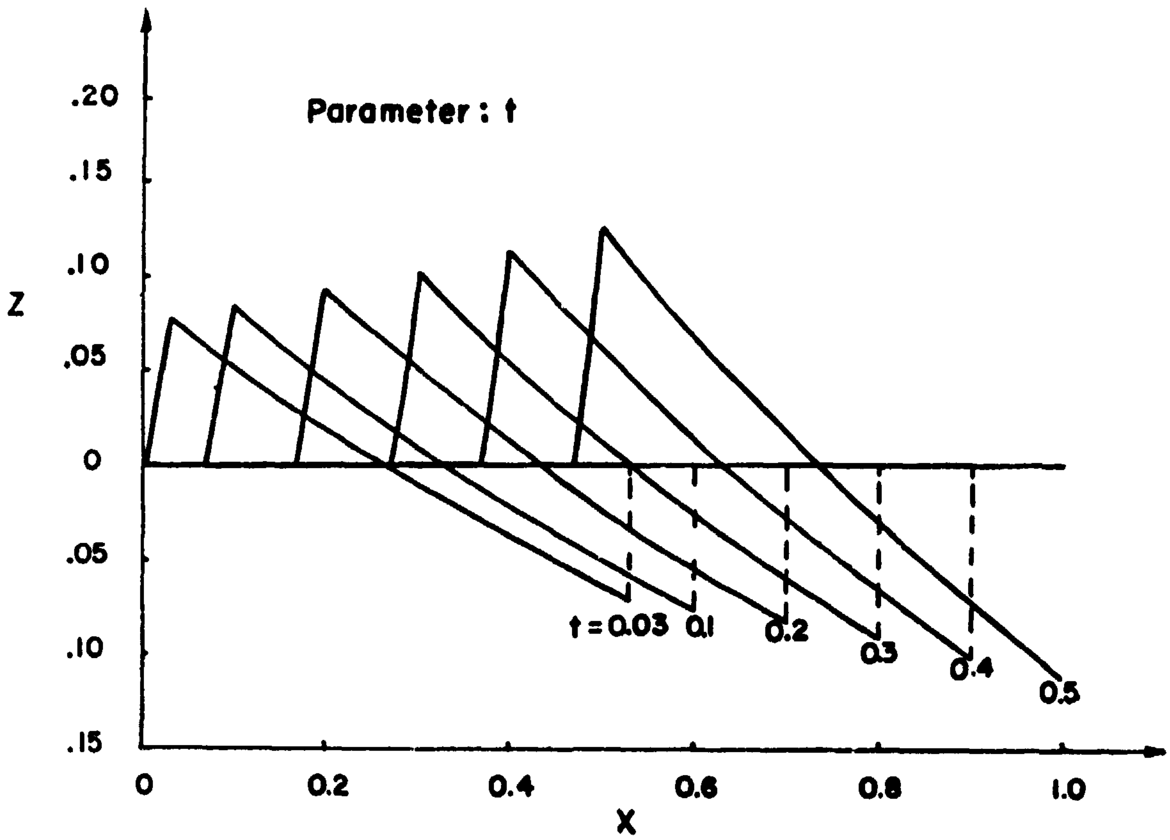

Fig. 9 Adjoint variable distribution along the analytically determined optimal path for the case of S_1.

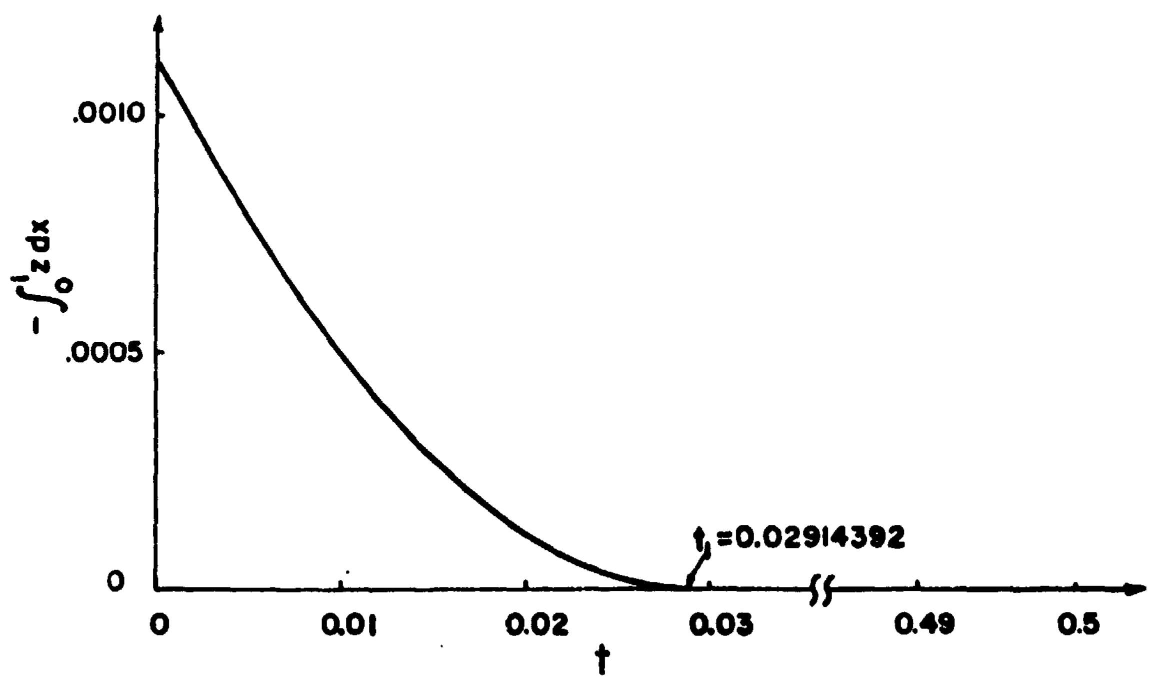

Fig. 10 Variation of $\int_0^1 z\,dx$ along the analytically determined optimal path for the case of S_1.

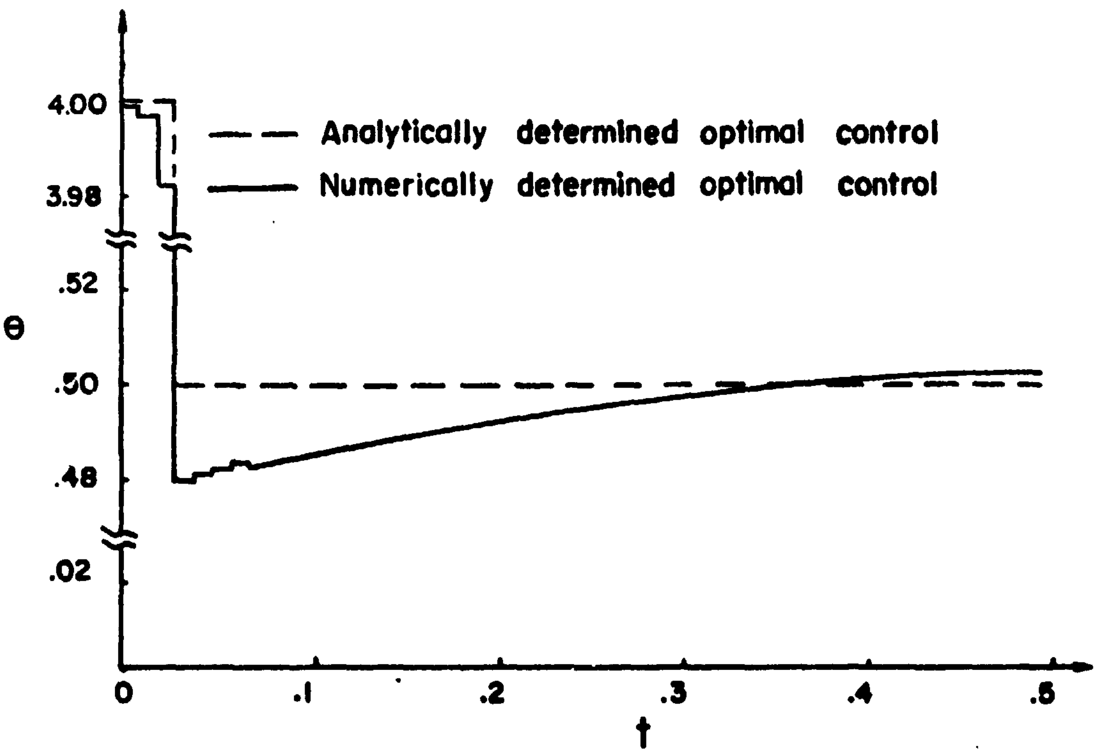

Fig. 11 Optimal control policy by the gradient technique based on the numerical iterative procedure for the case of S_1.

INSTITUTE FOR SYSTEMS DESIGN AND OPTIMIZATION REPORTS*

1. Estimation of Parameters in Differential Equations from Experimental Data, by E. S. Lee, January, 1968.

2. The Estimation of Variable Parameters in Differential Equations by Quasilinearization, by E. S. Lee, January, 1968.

3. Simulation and Feasibility Study of a Thermal Comfort Equation, by E. S. Lee, L. T. Fan, C. L. Hwang and M. A. Shaikh, January, 1968.

4. Optimization of Constrained System Reliability of the Stagewise System, by C. L. Hwang, F. A. Tillman, L. T. Fan, and S. A. Balbale, March, 1968.

5. Air Flow Models in a Confined Space - A Study in Age Distribution, by M. S. K. Chen, L. T. Fan, C. L. Hwang, and E. S. Lee, May, 1968.

6. Digital Computer Solution of Langhaar's Linearization Method on Entrance Region Flow of a Circular Tube, by C. L. Hwang, L. T. Fan, K. C. Li, and C. T. Lu, August, 1968.

7. Schiller's Momentum Integral Method for Entrance Region Flow of a Circular Tube, by C. L. Hwang, L. T. Fan, K. C. Li, and C. T. Lu, August, 1968.

8. Schlichting's Matching Method for Entrance Region Flow of a Parallel Plate Channel, by C. L. Hwang, L. T. Fan, K. C. Li, and C. T. Lu, September, 1968.

9. Invariant Imbedding, Iterative Linearization, and Multistage Counter-current Processes, by E. S. Lee, November, 1968.

10. Several Different Gas-Liquid Contactors Utilizing Centrifugal Force, by T. Takahashi and L. T. Fan, December, 1968.

11. Carbon Dioxide Reduction Contactors in Space Vehicles and Other Enclosed Structures, by T. Takahashi and L. T. Fan, January, 1969.

12. Removal of Sulfur Dioxide from Waste and Exhaust Gases, by T. Takahashi and L. T. Fan, January, 1969.

13. Analysis of a Reverse Osmosis Water Purification System and its Optimization Based on the Plug Flow Model for the Bulk Flow in the Membrane Unit, by L. T. Fan, L. E. Erickson, J. T. Tseng, C. L. Hwang and C. Y. Cheng, February, 1969.

14. Systems Analysis and Optimization of Reverse Osmosis Processes, by L. T. Fan, C. L. Hwang, L. E. Erickson, C. Y. Cheng and L. Y. S. Ho, March, 1969.

*Copies of these reports can be obtained by writing to:

Prof. L. T. Fan, Director
Systems Institute
c/o Department of Chemical Engineering
Kansas State University

(e)5

TERMINAL CONTROL OF LINEAR DISTRIBUTED PARAMETER SYSTEM BY LINEAR PROGRAMMING

Report No. 17

H. S. Huang, L. T. Fan, and C. L. Hwang

Institute for Systems Design and Optimization

KANSAS STATE UNIVERSITY MANHATTAN

TERMINAL CONTROL OF LINEAR DISTRIBUTED PARAMETER SYSTEM
BY LINEAR PROGRAMMING*

H. S. Huang, L. T. Fan, and C. L. Hwang

Institute for Systems Design and Optimization

Kansas State University

August 29, 1969

ABSTRACT

Literature on the optimal terminal control of linear distributed parameter systems by means of the linear programming technique is reviewed.

Some suggestions are made which may facilitate computational aspects of the problem. A brief account of the theory of linear programming is also given.

*This study was supported in part by NASA (Grant No. NGR-17-001-034) and AFOSR (Grant USAFOSR F44620-68-C-0020).

The main purpose of this report is to review critically and exhaustively literature on the use of linear programming for the optimal terminal control of the linear distributed parameter system. Because of the availability of well developed standard computer subroutines [for example, IBM subroutine, Mathematical Programming System/360 (360A-CO-14X), Linear and Separable Programming], linear programming can be a very powerful technique, if we can convert a problem to a standard linear programming problem. Zadeh and Whalen [1] appear to be the first to use the linear programming method for solving various lumped optimal control problems of the lumped system. Sakawa [2] is probably the first one to apply this approach to the linear distributed parameter system.

This paper is divided into three sections. In the first section linear programming is briefly explained. The second section shows how a problem of optimizing the linear distributed differential system with a linear performance index can be reduced to a standard linear programming problem. In this section a method for optimizing such a system is proposed, which is based on Lesser and Lapidus's [3] approach for solving the time-optimal control problem of a lumped system by linear programming. Their approach may be adopted for the more complex linear distributed parameter systems. Several practical examples of the linear optimally distributed parameters systems are reviewed in the third section.

THEORY OF LINEAR PROGRAMMING

Consider the general system described by the following linear equations.

$$
\begin{array}{l}
a_{11}x_1 + a_{12}x_2 + \dots + a_{1n}x_n = b_1 \\
\text{- - - - - - - - - - - - - - - - - -} \\
\text{- - - - - - - - - - - - - - - - - -} \\
\text{- - - - - - - - - - - - - - - - - -} \\
a_{m1}x_1 + a_{m2}x_2 + \dots + a_{mn}x_n = b_m
\end{array}
\qquad (1)
$$

where the x's are the unknowns, the a's and b's are the given constants and $n > m$. The problem of optimizing the system is to find the x's which satisfy the condition

$$x_j \geq 0, \qquad j = 1, 2, \dots, n, \qquad (2)$$

and minimize the objective function

$$z = c_1x_1 + c_2x_2 + \dots + c_nx_n, \qquad (3)$$

where the c's are constants. These x's are called the optimal solution of the system.

To obtain the solution by analytical means is very difficult if not impossible. However, the problem may be solved numerically by linear programming. One of the most commonly used techniques of linear programming is the so-called simplex method developed by Dantzig [4]. It is an iterative procedure for determining the optimal extreme point and may be explained in the following manner.

The Gauss-Jordon reduction method is applied to equations (1) and (3). The first step of this method is to divide the first expression of equation (1) by a_{11}. The next step is to eliminate terms containing x_1 from the remaining m-1 expressions. This is accomplished by subtracting each one of the other expression from the first expression after a simple manipulation. The second expression is then divided by the constant which normalizes the coefficient of x_2. Following the same procedure as that for the x_1 terms, terms containing x_2 are eliminated from all the other expressions. Repeating these procedures to all the m expressions and eliminating all the x_i, $i = 1, \ldots, m$, from equation (3), we obtain

$$
\begin{aligned}
x_1 + a'_{1,m+1}\, x_{m+1} + \ldots + a'_{1,n}\, x_n &= b'_1 \\
x_2 + a'_{2,m+1}\, x_{m+1} + \ldots + a'_{2,n}\, x_n &= b'_2 \\
- - - - - - - - - - - - - - - - - - & \qquad\qquad (4) \\
x_m + a'_{m,m+1}\, x_{m+1} + \ldots + a'_{m,n}\, x_n &= b'_m \\
c'_{m+1}\, x_{m+1} + \ldots + c'_n\, x_n &= z - z_0,
\end{aligned}
$$

where a'_{ij}, b'_i, and c'_j are the modified values of a_{ij}, b_i, and c_j, respectively and z_0 is a constant.

One of the many possible solutions of equation (4) may be expressed as

$$
\begin{aligned}
x_i &= b'_i, \quad \text{for} \quad i = 1, 2, \ldots, m, \\
&= 0, \quad \text{for} \quad i = m+1, \ldots, n.
\end{aligned} \qquad (5)
$$

where x_i, $i = 1, 2, \ldots, m$, are called the basic variables, and this set is called a basis. The value of the performance function is

$$z = z_0 \qquad (6)$$

A basis which satisfies equation (2) is said to be feasible. For the basis to be feasible, it is required that $b'_i \geq 0$, for $i = 1, 2, \ldots, m$. Now, from the sign of c'_j, $j = m+1, \ldots, n$, in equation (4), one can determine the basis for the adjacent extreme point for which the current value of the performance function tends to decrease, that is, the value of the performance function may be reduced by shifting one of the nonbasic variables with negative c_j' into the basis. Let this nonbasic variable be defined as c_s', where $m+1 \le s \le n$.

By shifting the x_s's column to the right hand side, equation (4) may now be rewritten as

$$
\begin{aligned}
x_1 \quad + a'_{1,m+1}\, x_{m+1} + \dots + 0 + \dots + a'_{1,n}\, x_n &= b'_1 - a'_{1,s}\, x_s \\
x_2 \quad + a'_{2,m+1}\, x_{m+1} + \dots + 0 + \dots + a'_{2,n}\, x_n &= b'_2 - a'_{2,s}\, x_s \\
- &- - - - - - \\
- &- - - - - - \\
x_m + a'_{m,m+1}\, x_{m+1} + \dots + 0 + \dots + a'_{m,n}\, x_n &= b'_m - a'_{m,s}\, x_s \\
c'_{m+1}\, x_{m+1} + \dots + 0 + \dots + \quad c'_n\, x_n &= z - z_0 - c'_s\, x_s
\end{aligned}
\tag{7}
$$

Since x_s is the only nonbasic variable allowed to deviate from zero, the basic variables and performance function are x_s-dependent,

$$x_i = b'_i - a'_{i,s}\, x_s, \qquad i = 1, 2, \dots, m, \tag{8}$$

$$z = z_0 + c'_s\, x_s. \tag{9}$$

Here, the $a'_{i,s}$ can be any finite value. From the condition $x_i \ge 0$, x_s must, in accordance with equation (8), satisfy the condition

$$b'_i - a'_{i,s}\, x_s \ge 0,$$

or

$$x_s \le \frac{b'_i}{a'_{i,s}}, \quad \text{if} \quad a'_{i,s} > 0. \tag{10}$$

By designating integer i, which yields the minimum value of $b'_i/a'_{i,s}$ for $a_{i,s} > 0$, as r we can write

$$\frac{b'_r}{a'_{r,s}} = \min_{a'_{i,s}>0} \frac{b'_i}{a'_{i,s}} = \max x_s \tag{11}$$

The ratio $b'_r/a'_{r,s}$ is the maximum x_s, which would reduce x_r to zero. This implies that the performance function may be reduced by replacing x_r by x_s as a new basic variable. As a result, the new basis effectively accomplishes a jump from the original extreme point to an adjacent one with a subsequent decrease in the value of z. In order to replace x_r by x_s in equation (4), the Gauss-Jordon reduction is applied to equation (4) to form another new cannonical form.

$$
\begin{array}{l}
x_1 \quad + a'^{*}_{1,r}\, x_r \qquad + a'^{*}_{1,m+1}\, x_{m+1} + \dots + 0 + \dots + a'^{*}_{1,n}\, x_n = b'^{*}_1 \\
\quad - \\
\quad a'^{*}_{r,r}\, x_r \qquad + a'^{*}_{r,m+1}\, x_{m+1} + \dots + 0 + \dots + a'^{*}_{r,n}\, x_n = b'^{*}_r \\
\quad - \\
\quad a'^{*}_{m,r}\, x_r + x_m \quad + a'^{*}_{m,m+1}\, x_{m+1} + \dots + 0 + \dots + a'^{*}_{m,n}\, x_n = b'^{*}_m \\
\quad c'^{*}_r\, x_r \qquad + c'^{*}_{m+1}\, x_{m+1} + \dots + 0 + \dots + c'^{*}_n\, x_n = z - z_0 - c'_s\, b'^{*}_r
\end{array}
\tag{12}
$$

This procedure is repeated until all coefficients of the performance function become positive. In the meantime, z cannot be reduced by the increase in the nonbasic variables. Therefore, the solution is the optimal basic solution.

The principal disadvantage of the simplex method is that, in the process of numerical reduction, many numbers have to be computed and recorded. These may not all be used in the succeeding computational steps or may be used only in an indirect way. However, the process is made necessary because it is not known a priori which numbers are needed and which are superfluous.
In order to eliminate this complexity, a revised simplex method has been developed [4]. Instead of computing all the coefficients $a'_{i,j}$, $i = 1, 2, \dots, m$, $j = m+1, \dots, n$, the revised simplex method needs to compute the $a'_{i,s}$,

$i = 1, 2, \ldots, m$ only. A linear programming subroutine based on the revised simplex method is available [for example, Mathematical Programming System/360 (360A-CO-14X), Linear and Separable Programming]. Since this revised method is basically identical in principle with the original simplex method, the detailed procedure of the revised simplex method is omitted.

OPTIMIZATION OF DISTRIBUTED PARAMETER PROBLEM

1. Integral Representation of State Equations.

Sakawa [2] is probably the first one to apply linear programming to the solution of linear distributed parameter problems. This section generally follows his approach.

The state equation of a linear distributed parameter system generally can be represented by the partial differential equation

$$\frac{\partial z}{\partial t} = f_0(x, t)\, z + f_1(x, t) \frac{\partial z}{\partial x} + \ldots + b(x, t)\, u(t) \qquad (13)$$

The state equation together with its boundary conditions may often be represented by the integral equation

$$z(x, t) = \int_0^t g[x, \lambda]\, u(\lambda) d\lambda + h(x, t) \qquad (14)$$

Suppose that a measure of the deviation from the desired state at the final time given by

$$S = \int_0^L |\, z(x, t_f) - z_d(x) | dx \qquad (15)$$

is defined as the performance criterion or index of the system. Optimization (minimization) of the system as represented by equations (13) through (15) can be accomplished by the linear programming approach.

Approximating the continuous control function u(t) by a number of discrete constants,

$$u_j = u(t) \qquad \text{for } t_{j-1} \leq t \leq t_j \tag{16a}$$

$$t_j = \frac{j\ t_f}{n} \qquad \text{for } j = 1, 2, \ldots, n, \tag{16b}$$

equation (14) at the final time can be rewritten as [5]

$$\begin{aligned} z(x, t_f) &= \int_0^{t_f} g(x, \lambda)\ u(\lambda) d\lambda + h(x, t_f) \\ &\doteq \sum_{j=1}^{n} \int_{t_{j-1}}^{t_j} g(x, \lambda)\ u_j\ d\lambda + h(x, t_f) \\ &= \sum_{j=1}^{n} u_j \int_{t_{j-1}}^{t_j} g(x, \lambda) d\lambda + h(x, t_f) \end{aligned} \tag{17}$$

Sakawa [2] originally used Simpson's rule to integrate approximately equation (14), i.e.,

$$z(x, t_f) \approx \sum_{j=0}^{n} g(x, t_j)\ u(t_j)\ d_j + h(x, t_f)$$

where

$$d_0 = d_n = \frac{t_f}{3n}$$

$$d_1 = d_3 = \ldots = d_{n-1} = \frac{4t_f}{3n}$$

$$d_2 = d_4 = \ldots = d_n = \frac{2t_f}{3n}$$

When the integrand in equation (14) is continuous, this approximation gives rise to a sufficiently accurate solution. However, in the case of a discontinuous integrand, the accuracy of this approximation will be very poor. Use of equation (17) does not give rise to such a difficulty even if u(t) is discontinuous [5].

The performance index given by equation (15) can now be approximated by Simpson's rule as

$$S = \int_0^L |z(x, t_f) - z_d(x)|dx$$

$$\approx \sum_{i=0}^{m} c_i |z(x_i, t_f) - z_d(x_i)| \tag{18}$$

where

$$x_i = \frac{Li}{m}, \qquad \text{for} \qquad i = 0, 1, 2, \ldots, m$$

$$c_0 = c_m = \frac{L}{3m},$$

$$c_1 = c_3 = \ldots = c_{m-1} = \frac{4L}{3m}$$

and

$$c_2 = c_4 = \ldots = c_{m-2} = \frac{2L}{3m}$$

$z(x_i, t_f)$ in equation (18) can be evaluated from equation (17).

$$z(x_i, t_f) = \sum_{j=1}^{n} u_j \int_{t_{j-1}}^{t_j} g(x_i, \lambda)d\lambda + h(x_i, t_f)$$

$$= \sum_{j=1}^{n} A_{ij} u_j + h(x_i, t_f),$$

$$i = 0, 1, 2, \ldots, n \tag{19}$$

Let

$$|z(x_i, t_f) - z_d(x_i)| = e_{si} + e_{pi}, \quad i = 0, 1, \ldots, m \tag{20}$$

where e_{si}, e_{pi}, $i = 0, 1, \ldots, m$, are non-negative variables which satisfy the following relationships.

$$z(x_i, t_f) - z_d(x_i) = e_{pi} - e_{si}, \quad i = 0, 1, \ldots, m, \tag{21}$$

and

$$\left.\begin{aligned} & e_{pi} = 0,\ z(x_i,\ t_f) - z_d(x_i) = -\ e_{si}, \\ & \text{if } [z(x_i,\ t_f) - z_d(x_i)] < 0 \\ & e_{si} = 0,\ z(x_i,\ t_f) - z_d(x_i) = e_{pi} \\ & \text{if } [z(x_i,\ t_f) - z_d(x_i)] > 0 \\ & \quad i = 0,\ 1,\ \ldots,\ m \end{aligned}\right\} \tag{22}$$

By introducing these new variables, equation (18) can be expressed as

$$S = \sum_{i=0}^{m} c_i(e_{si} + e_{pi}) \tag{23}$$

The linear programming model which will yield the optimal policy of the system can now be stated as follows:

Minimize

$$S = \sum_{i=0}^{m} c_i(e_{pi} + e_{si})$$

subject to

$$z(x_i,\ t_f) - z_d(x_i) = e_{pi} - e_{si}, \qquad i = 0,\ 1,\ \ldots,\ m$$

$$u_j \leq u_{max}$$

$$e_{pi},\ e_{si},\ u_j \geq 0, \qquad \begin{aligned} & i = 0,\ 1,\ \ldots,\ m \\ & j = 1,\ 2,\ \ldots,\ n \end{aligned}$$

where u_{max} is the maximal allowable control value. The inequality relation

$$u_j \leq u_{max}$$

can be removed by introducing a set of new variables e_{uj} such that

$$u_j + e_{uj} = u_{max}$$

$$e_{uj} \geq 0, \qquad j = 1, 2, \ldots, n$$

By substituting $z(x_i, t_f)$ from equation (19) into the above formulation, the problem can be restated as follows:

Minimize

$$S = \sum_{i=0}^{m} c_i(e_{pi} + e_{si})$$

subject to

$$\begin{array}{llll}
A_{01}u_1 + \ldots + A_{0n}u_n & - e_{p0} + e_{s0} & = & z_d(x_0) - h(x_0, t_f) \\
A_{11}u_1 + \ldots + A_{1n}u_n - & -e_{p1} + e_{s1} & = & z_d(x_1) - h(x_1, t_f) \\
A_{m1}u_1 + \ldots + A_{mn}u_n & -e_{pm} + e_{sm} & = & z_d(x_m) - h(x_m, t_f) \\
\vdots & & & \\
u_1 & +e_{u1} & = & u_{max} \\
\quad\quad \vdots & & & \vdots \\
\quad\quad u_n & + e_{un} & = & u_{max}
\end{array}$$

$$e_{si}, e_{pi}, e_{uj}, u_j \geq 0, \qquad \begin{array}{l} i = 0, 1, \ldots, m \\ j = 1, 2, \ldots, n \end{array}$$

This is a standard linear programming problem which can be solved by the simplex or the revised simplex method.

2. <u>Discrete Time Representation of State Equations</u>.

The integral representation of the differential system, equation (13), can be converted to the linear programming form without much difficulty. However, only a simple system with simple boundary conditions is amenable to the integral representation. It is, therefore, more advantageous to convert the partial differential equation of a complex system to a differential difference equation instead of an integral equation.

Very often a distributed diffusional process of the process industries can be represented by a model containing completely stirred tanks connected in sequence. For such processes, an equivalence can be established between a mathematical model given by the differential difference representation and a physical model of the stirred tanks in sequence.

By subdividing the system by m+1 segments, with the two half-sized segments at both ends, and lumping all the properties within each segment, the partial differential equation, equation (13), can be approximated by

$$\dot{z}_i(t) = \sum_{j=0}^{m} a_{ij}(t)\, z_j(t) + b_i(t)\, u(t), \qquad i = 0, 1, \ldots, m \tag{24}$$

where

$$z_i(t) = z(x_i, t)$$

Lesser and Lapidus [3] used the linear programming method to solve a time optimal problem of a lumped system represented by this set of differential equations. They converted a continuous control function involved in the system into a discrete-time function for approximation. We shall propose a scheme in which their approach is applied to the terminal control of the linear distributed parameter system. Approximating the continuous control function u(t) by a number of discrete constants, control functions, we have

$$u_j = u(t) \qquad t_{j-1} < t \leq t_j$$

$$t_j = \frac{j\, t_f}{n} \qquad j = 0, 1, \ldots, n$$

The coefficient matrix $[a_{ij}(t)]$ and $[b_i(t)]$ can be approximated by

$$\bar{A}^k = \frac{1}{2}\,[a_{ij}\ (t_k)] + \frac{1}{2}\,[a_{ij}(t_{k-1})]$$

$$b_i^k = \frac{1}{2}\,\{b_i(t_k) + b_i(t_{k-1})\}, \quad k = 1, 2, \ldots, n \tag{25}$$

Substituting the above relation into equation (24) yields

$$\dot{z}_i(t) \cong \bar{A}^k \cdot \bar{Z}(t) + b_i^k\ u_k, \qquad i = 0, 1, \ldots, m \tag{26}$$

$$t_{k-1} \leq t \leq t_k$$

This is a set of linear differential equations with constant coefficients, and the solution is

$$\bar{Z}(t_k) = \exp(\bar{A}^k\ \Delta t)\ \bar{Z}(t_{k-1}) + \int_0^{\Delta t} \exp(\bar{A}^k\ s)\ ds \cdot \bar{B}^k \cdot u_k \tag{27}$$

where $\bar{Z}$ and $\bar{B}^k$ are column vectors of $[z_0, z_1, \ldots, z_m]$ and $[b_0^k, b_1^k, \ldots, b_m^k]$, respectively.

Let

$$\left.\begin{aligned}
\bar{G}_i^k &= \prod_{j=i+1}^{k} \exp(\bar{A}^j\ \Delta t) = \exp[\Delta t \sum_{j=i+1}^{k} \bar{A}^j] \\
\bar{G}_k^k &= 1 \\
\bar{P}_k &= \int_0^{\Delta t} \exp(\bar{A}^k\ s)ds \cdot \bar{B}^k
\end{aligned}\right\}\ k = 1, 2, \ldots, n \tag{28}$$

By substituting these definitions into equation (27), the following set of equations is obtained

$$\bar{Z}(t_1) = \bar{G}_0^1 \cdot \bar{Z}(t_0) + \bar{P}_1 \cdot u_1$$

$$\bar{Z}(t_2) = \exp(\bar{A}^2\ \Delta t)\ [\bar{G}_0^1\ \bar{Z}(t_0) + \bar{P}_1\ u_1] + \bar{P}_2 u_2$$

$$= \bar{G}_0^2\ \bar{Z}(t_0) + \bar{G}_1^2 \cdot \bar{P}_1 u_1 + \bar{G}_2^2 \cdot \bar{P}_2 u_2$$

$$\bar{Z}(t_k) = \bar{G}_0^k \cdot \bar{Z}(t_0) + \sum_{j=1}^{k} \bar{G}_j^k \cdot \bar{P}_j \cdot u_j$$

$$\bar{Z}(t_f) = \bar{G}_0^n \cdot \bar{Z}(t_0) + \sum_{j=1}^{n} \bar{G}_j^n \cdot \bar{P}_j \cdot u_j \tag{29}$$

Replacing the matrix notation by its components yields

$$z_i(t_f) = \sum_{j=0}^{m} g_{i,j}^{n,0} z_j(t_0) + \sum_{j=1}^{n} [\sum_{k=0}^{m} g_{i,k}^{n,j} p_k^j]u_j$$

$$= h_i + \sum_{j=1}^{n} A_{i,j} u_j, \qquad i = 0, 1, \ldots, m \qquad (30)$$

where

$$\bar{G}_j^n = [g_{i,k}^{n,j}] \quad \text{and} \quad \bar{P}_j = [p_k^j]$$

The performance index, equation (15), is replaced by equation (18). This time discrete problem is then reduced to the same form as that given in the preceding subsection on the integral representation. Equation (30) is equivalent to equation (19). The rest of the procedure for applying linear programming is the same as in the preceding section.

EXAMPLES OF DISTRIBUTED PARAMETER SYSTEM

A. Heat Conduction System

Sakawa [2] applied the linear programming method to the solution of a practical example of optimization of the linear distributed parameter system. The process considered by him is a one-sided heating of a metal slab in a furnace and is described by the diffusion equation [see Fig. 1]

$$\frac{\partial^2 q(x,\ t)}{\partial x^2} = \frac{\partial q(x,\ t)}{\partial t} \tag{31}$$

where q(x, t) is the temperature distribution in the metal slab which depends on the space coordinate $x(0 \le x \le 1)$ and time $t(0 \le t \le T)$. The initial and boundary conditions are given by

$$q(x,\ 0) = 0 \tag{32}$$

$$\left.\frac{\partial q(x,\ t)}{\partial x}\right|_{x=0} = \alpha\{q(0,\ t) - v(t)\} \tag{33}$$

$$\left.\frac{\partial q(x,\ t)}{\partial x}\right|_{x=1} = 0 \tag{34}$$

where α is the heat transfer coefficient and v(t) is the furnace gas temperature. It is assumed that the gas temperature, v(t), has a first-order phase lag from the fuel flow, u(t), i.e.,

$$\gamma \frac{dv(t)}{dt} + v(t) = u(t) \tag{35}$$

where γ is the furnace time constant. The performance index is defined as the absolute deviation from the desired temperature profile at the final time T

$$S = \int_0^1 |q^*(x) - q(x,\ T)|\,dx \tag{36}$$

where $q^*(x)$ is the desired temperature profile.

This set of system equations is transformed into the integral representation by the Laplace transform. The resulting equation is

$$q(x,\ t) = \int_0^t g(x,\ t-\tau)\ u(\tau)d\tau$$

$$q(x,\ t)$$

$$= \frac{k^2 \cos k(1-x)}{\cos k - \frac{k}{\alpha} \sin k} e^{-k^2 t} + 2k^2 \sum_{i=1}^{\infty} \frac{\cos (1-x)\beta_i}{(k^2 - \beta_i^2)(\frac{1}{\alpha} + \frac{1+\alpha}{\beta_i^2}) \cos \beta_i} e^{-\beta_i^2 t} \tag{37}$$

where $k = 1/\sqrt{\gamma}$.

Equation (37) is equivalent to equation (14) and equation (36) is equivalent to equation (15). The procedure for solving this problem by linear programming has been given in the preceding section. A typical optimal control policy obtained by Sakawa [2] is shown in Fig. 2.

B. Single Heat Exchanger Without Wall Heat Capacity

Hwang, Fan and Hwang [5] determined the optimal control of a simple plug flow tubular heat exchanger by using the linear programming approach. A graphical representation of the system considered by them is similar to that shown in Fig. 3. The process is described by the equation

$$\frac{\partial T(x,\ t)}{\partial t} + \frac{\partial T(x,\ t)}{\partial x} = K[\theta(t) - T(x,\ t)] \tag{38}$$

where $T(x,\ t)$ is the fluid temperature distribution inside the heat exchanger and is dependent on the space coordinate $x(0 \le x \le 1)$ and time $t(0 \le t \le T)$, $\theta(t)$ is the tube wall temperature which is uniform along the space coordinate and is treated as a control variable, and K is a constant heat transfer coefficient.

The initial and boundary conditions are given by

$$T(x,\ 0) = 0 \tag{39}$$

$$T(0,\ t) = 0 \tag{40}$$

The performance index is defined as the absolute deviation from the desired temperature profile at the final time t_f.

$$S = \int_0^1 |\, T_d(x) - T(x,\ t_f)|\, dx \tag{41}$$

where $T_d(x)$ is the desired temperature profile.

This differential system is solved by the Laplace transform. The resulting integral representation is

$$\begin{aligned} T(x,\ t) &= K \int_0^t e^{-K(t-\xi)}\theta(\xi)d\xi, \quad x \geq t \\ T(x,\ t) &= K \int_{t-x}^t e^{-K(t-\xi)}\theta(\xi)d\xi, \quad x \leq t \end{aligned} \tag{42}$$

Equation (42) is equivalent to equation (14), and equation (41) is equivalent to equation (15). A typical result obtained by Huang et al. [5] is shown in Fig. 4.

C. <u>Tubular Heat Exchanger with Internal Heat Generation</u>

Huang and Yang [6, 7] solved an optimal control problem associated with a tubular heat exchanger with internal heat generation by the linear programming approach [see Fig. 3]. The system consists of a circular tube of length L through which a fluid flows steadily. Heat is generated in the tube wall. The process is described by the following equations.

$$\left.\begin{aligned} \frac{1}{K_w}\frac{\partial\theta}{\partial t} &= T - \theta + \frac{\phi(t)}{(\rho c_p)_w K_w} \\ \frac{1}{K}\left(\frac{\partial T}{\partial t} + u\frac{\partial T}{\partial x}\right) &= \theta - T \end{aligned}\right\} \tag{43}$$

where $\theta(x, t)$ and $T(x, t)$ are the wall and fluid temperature, respectively, $\phi(t)$ is the rate of heat generation in the unit volume of tube wall and is treated as the control variable, ρ is the density, c_p is the specific heat, K is the ratio of surface conductance to heat capacity, t is the time, u is the fluid velocity, and x is the axial distance measured from the inlet. The physical properties of the tube wall are distinguished from those of the fluid by the subscript w. The initial and boundary conditions are

$$\begin{aligned} &T(0, t, \phi) = 0 \\ &T(x, 0, \phi) = 0 \\ &\theta(x, 0, \phi) = 0 \end{aligned} \tag{44}$$

The performance index is defined as the absolute deviation from the desired temperature profile at the final time t_f, i.e.

$$S = \int_0^1 \{\left|1 - \frac{T(x, t_f, \phi)}{T^*(x)}\right| + \left|[1 - \frac{\theta(x, t_f, \phi)}{\theta^*(x)}] \frac{\theta^*(x)}{T^*(x)}\right|\} d(\frac{x}{L}) \tag{45}$$

where $T^*(x)$ and $\theta^*(x)$ are the desired fluid and wall temperature distribution, respectively.

The solution of the system equation, equation (43), which satisfies appropriate initial and boundary conditions may be obtained by using the Laplace transform. On applying the Laplace transform with respect to t, the partial differential equations are reduced to two ordinary differential equations of variable x. The general solutions of the ordinary differential equations are then fitted to the boundary conditions, and the final solutions are obtained by the application of the inverse transformation as follows:

$$\left.\begin{aligned}
&\frac{T(x,\ t,\ \phi)}{T^*(x)}\\
&= \frac{1}{(M+1)\ \frac{Kx}{u}}\ {}_0\int^{Kt} [1 - e^{-\frac{M+1}{M}K(t-\xi)}]\ \frac{\phi(\xi)}{\Phi}\ d(K\xi)\\
&\qquad - \frac{s}{M\ \frac{Kx}{u}}\ e^{-\frac{Kx}{u}}\ {}_0\int^{Kt^*} \pi(Kt^* - K\xi)\ \frac{\phi(\xi)}{\Phi}\ d(K\xi)\\
&\frac{\theta(x,\ t,\ \phi)}{\theta^*(x)}\\
&= \frac{1}{(1 + \frac{Kx}{u})}\ {}_0\int^{Kt} [\frac{1}{M+1} + \frac{1}{M(M+1)}\ e^{-\frac{M+1}{M}K(t-\xi)}]\ \frac{\phi(\xi)}{\Phi}\ d(K\xi)\\
&\qquad - \frac{s}{M(1 + \frac{Kx}{u})}\ e^{-\frac{Kx}{u}}\ {}_0\int^{Kt^*} \Lambda(Kt^* - K\xi)\ \frac{\phi(\xi)}{\Phi}\ d(K\xi)
\end{aligned}\right\} \qquad (46)$$

where

$$M = \frac{K}{K_w}$$

In equation (46), Φ is a constant rate of internal heat generation per unit volume; $s = 0$ when $1 + \frac{tu}{x} \geq 0$; $s = 1$ when $\frac{tu}{x} \geq 1$ and $t^* = t - \frac{x}{u}$. Furthermore π and Λ can be written as

$$\pi(\zeta) = \frac{M}{M+1}\ {}_0\int^{K\zeta} [\frac{1}{M} + e^{-(\frac{M+1}{M})(K\zeta - K\lambda)}]e^{-\frac{K\lambda}{M}}\ I_0[2\sqrt{\frac{Kx}{u}\frac{K\lambda}{M}}]\ d(K\lambda)$$

$$\Lambda(\zeta) = \frac{1}{M+1}\ {}_0\int^{K\zeta} [1 - e^{-(\frac{M+1}{M})(K\zeta - K\lambda)}]e^{-\frac{K\lambda}{M}}\ I_0[2\sqrt{\frac{Kx}{u}\frac{K\lambda}{M}}]d(K\lambda)$$

I_0 is the Bessel function of first-kind, zeroth-order, and $\zeta = t^* - \xi$.

Equation (46) is approximately the same as equation (14). The difference is that equation (46) consists of two integral equations while equation (14) contains only one. Equation (45) is approximately the same as equation (15). Two absolute value functions are inside the integration sign of equation (45). Each absolute function should be defined separately as in equation (20). Figure 5 shows a typical control policy obtained by Huang and Yang [6, 7].

SUMMARY

Although linear programming is a powerful technique for determining the optimal terminal control of the linear distributed parameter system, literature on this subject is fairly meager. Sakawa [2] appears to be the first one to apply the linear programming method to the terminal control of the linear distributed parameter system. He used Simpson's rule to transform the integral solution into a linear combination of control functions which were evaluated at equally spaced sample points. For the case of a highly discontinuous control function, e.g., bang-bang type, this approximation may give rise to a serious error. Use of an approximation which employs a piecewise constant control function may be able to circumvent this difficulty.

Lesser and Lapidus [3] solved a time optimal control problem of a high dimensional lumped parameter system by linear programming. It appears that this scheme can be modified for solving the optimal terminal control problem of complex linear distributed systems.

REFERENCES

1. L. A. Zadeh and B. H. Whalen, "On Optimal Control and Linear Programming," IRE Trans. on Automatic Control, Vol. AC-7, pp. 45-46 (1962).

2. Y. Sakawa, "Solution of an Optimal Control Problem in a Distributed-parameter System," IEEE Trans. on Automatic Control, Vol. AC-9, pp. 420-426 (1964).

3. H. A. Lesser and L. Lapidus, "The Time-Optimal Control of Discrete-Time Linear Systems with Bounded Controls," A.I.Ch.E. Journal, Vol. 12, pp. 143-152 (1966).

4. G. B. Dantzig , Linear Programming and Extensions, Princeton University Press, Princeton, New Jersey, 1963.

5. H. S. Huang, L. T. Fan and C. L. Hwang, "Optimal Wall Temperature Control of a Heat Exchanger," Institute for Systems Design and Optimization, Report No. 15, Kansas State University (1969).

6. H. S. Huang and W. T. Yang, "Optimal Control of Heat Exchangers with Internal Heat Generation," IFAC Symposium on Multivariable Control Systems, Duesseldorf, Germany (1968).

7. H. S. Huang, "Optimal Control of Heat Exchangers with Internal Heat Generation," Ph.D. Thesis, University of Michigan, Ann Arbor, Michigan, 1969.

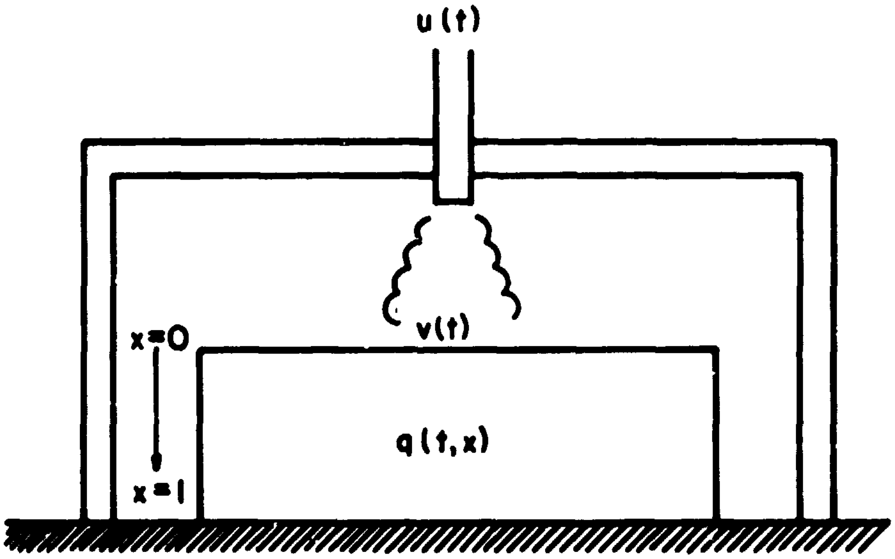

Fig.1. One-sided heating of metal in a furnace considered by Sakawa [2].

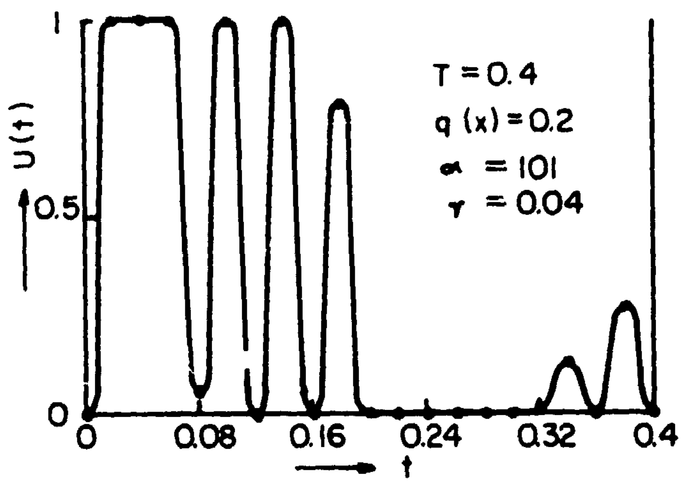

Fig. 2. A typical optimal control function obtained by Sakawa [2].

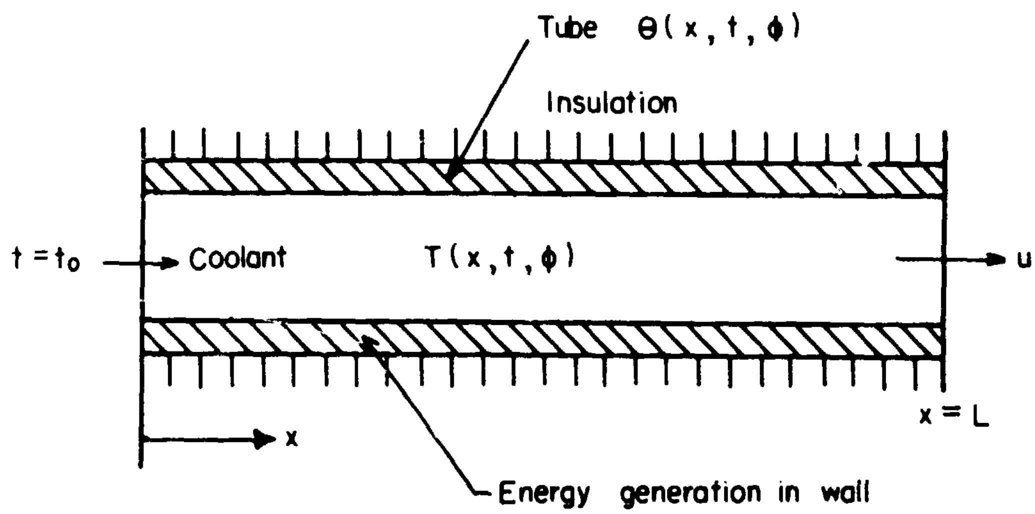

Fig. 3. Tubular heat exchanger considered by Huang and Yang [6,7].

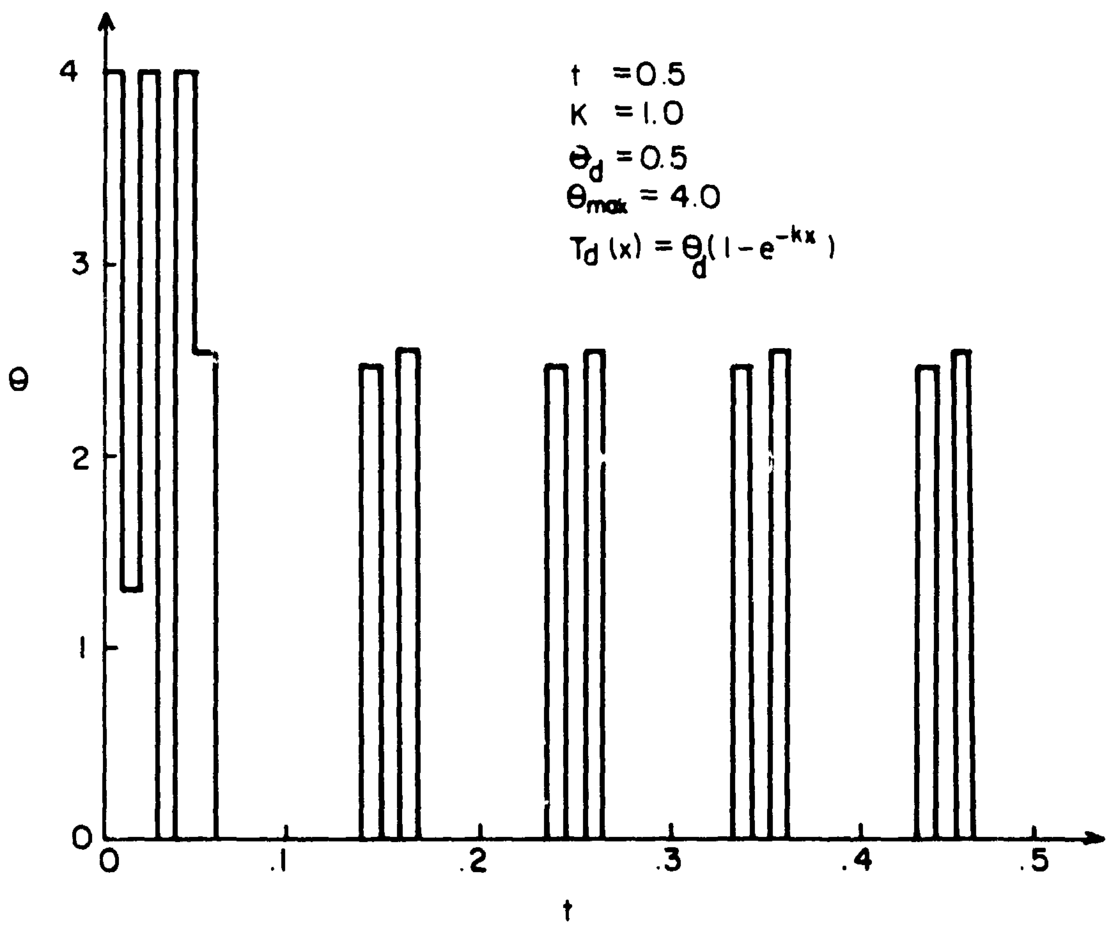

Fig. 4. A typical optimal control function obtained by Huang et al (5).

INSTITUTE FOR SYSTEMS DESIGN AND OPTIMIZATION REPORTS*

5. Air Flow Models in a Confined Space - A Study in Age Distribution, by M. S. K. Chen, L. T. Fan, C. L. Hwang, and E. S. Lee, May, 1968.

6. Digital Computer Solution of Langhaar's Linearization Method on Entrance Region Flow of a Circular Tube, by C. L. Hwang, L. T. Fan, K. C. Li, and C. T. Lu, August, 1968.

7. Schiller's Momentum Integral Method for Entrance Region Flow of a Circular Tube, by C. L. Hwang, L. T. Fan, K. C. Li, and C. T. Lu, August, 1968.

8. Schlichting's Matching Method for Entrance Region Flow of a Parallel Plate Channel, by C. L. Hwang, L. T. Fan, K. C. Li, and C. T. Lu, September, 1968.

9. Invariant Imbedding, Iterative Linearization, and Multistage Countercurrent Processes, by E. S. Lee, November, 1968.

10. Several Different Gas-Liquid Contactors Utilizing Centrifugal Force, by T. Takahashi and L. T. Fan, December, 1968.

11. Carbon Dioxide Reduction Contactors in Space Vehicles and Other Enclosed Structures, by T. Takahashi and L. T. Fan, January, 1969.

12. Removal of Sulfur Dioxide from Waste and Exhaust Gases, by T. Takahashi and L. T. Fan, January, 1969.

13. Analysis of a Reverse Osmosis Water Purification System and i: ^ntimization Based on the Plug Flow Model for the Bulk Flow in the ŀ rane Unit, by L. T. Fan, L. E. Erickson, J. T. Tseng, C. L. Hwang, and C. Y. Cheng, February, 1969.

14. Systems Analysis and Optimization of Reverse Osmosis Processes, by L. T. Fan, C. L. Hwang, L. E. Erickson, C. Y. Cheng and L. Y. S. Ho, March, 1969.

15. Optimal Wall Temperature Control of a Heat Exchanger, by H. S. Huang, L. T. Fan and C. L. Hwang, April, 1969.

16. Systems Analysis and Optimization of Dual-Purpose Nuclear Power and Desalting Plants, by L. T. Fan, C. L. Hwang, N. C. Pereira, L. E. Erickson, and C. Y. Cheng, April, 1969.

*Copies of these reports can be obtained by writing to:

Prof. L. T. Fan, Director
Systems Institute
c/o Department of Chemical Engineering
Kansas State University
Manhattan, Kansas 66502

[35] discretizes the temperature profile of the element and considers the variation of physical parameters, but the regional variations are not included in the model.

Although the physiological thermal regulation has been recognized for some time as an important factor in the human thermal system, the mathematical description of this phenomenon is still not satisfactory. The model developed by Crosbie *et al.* [11] uses the geometry of an infinite slab rather than a series of concentric cylinders, and builds in the function of physiological thermal regulation by allowing the effective thermal conductivity, metabolic rate, and rate of vaporization to vary as a function of the weighted mean temperature of the body. The model, however, does not include the effect of regional variations in heat generation rates and blood flow rates.

A physiological thermal regulator has been developed by Stolwijk and Hardy [27]. The model, however, does not consider the countercurrent heat exchange between large arteries and veins. A mathematical model of physiological thermoregulation developed recently by Stolwijk and Cunningham [26] can consider high metabolic rates. Future human thermal models probably should include both regional variations of the physiological parameters and physiological thermoregulation of each element.

The slab geometry was also utilized by Buchberg and Harrah [6] in establishing the relationship between the temperature of coolant in tubes and the mean skin temperature. Their model, however, does not consider the heat transfer by the blood circulation, regional variations in heat generation rates, and blood flow rates.

To utilize physiological information available in open literature [1]–[5], [10], [12], [13], [16], [19], [24] and to combine Wissler's model [31] with Stolwijk and Hardy's [27] model of the physiological thermoregulation, it is very desirable to provide an improved model for the human thermal system. Such a model should consider the effects of regional variation of physiological parameters and the physiological thermoregulation of each element. This new model would adopt Buchberg and Harrah's [6] conduction cooling to investigate the responses of the human thermal system to an external control device such as the space suit. The primary purpose of the external thermal regulation device is to keep the human body in thermal comfort [21], [22] by satisfying the requirement of thermoneutrality.

NOMENCLATURE

- A Body surface area.
- A' Effective area of the exchanger.
- A_c Effective area of the body creating convection losses.
- A_e Effective area of the body creating evaporation losses.
- A_r Effective radiation area.
- a, b Factors which weigh the contributions to the rate of change of body heat content by the increment of the rectal temperature and by the increment of the skin temperature respectively [in (10)].
- a_i Radius of the ith element.
- C Rate of heat exchange with the environment by convection.
- C_{EC} Thermal capacitance of the core of the extremities.
- C_{ES} Thermal capacitance of the skin of the extremities.
- C_{HC} Thermal capacitance of the core of the head.
- C_{HS} Thermal capacitance of the skin of the head.
- C_p Specific heat.
- C_{TC} Thermal capacitance of the core of the torso.
- C_{TM} Thermal capacitance of the muscles of the torso.
- C_{TS} Thermal capacitance of the skin of the torso.
- D Rate of change of body heat content.
- D_1 Diameter of the cylinder.
- E Rate of heat exchange with the environment by evaporation.
- E_v Evaporative heat loss.
- E_{vTC} Respiratory water vapor loss of the core of the torso.
- E_{vR} Respiratory heat loss assigned to the core of the head.
- EX Exercise (kcal/m²/h).
- F_i Wetted fraction of the surface.
- f_a Effective contact area factor, dimensionless.
- H Effective heat loss assigned to the core of the head.
- H_{av} Heat transfer coefficient for direct transfer between the large arteries and veins.
- H_i Effective heat transfer coefficient at the surface of the ith element.
- H_c Heat transfer coefficient for convection.
- H_e Heat transfer coefficient for evaporation.
- H_r Heat transfer coefficient for radiation.
- h Heat transfer coefficient (skin to air) also known as surface conductance.
- h_{ai} Proportionality constant of heat transfer between the arteries and tissue per unit volume.
- h_b Rate of heat transfer from blood to tissue.
- h_m Rate of tissue heat generation by metabolic reactions.
- h_{vi} Proportionality constant of heat transfer between the veins and tissue per unit volume.
- K Thermal conductivity.
- K_1 Universal radiation constant $\approx 4.92 \times 10^{-8}$ cal/m²/h.
- K_c Coefficient, heat exchange by convection.

K_{D_i} Mass transfer coefficient for passive diffusion of water through the epidermis.

K_{ECES} Thermal conductance between the core of the extremities and the skin of the extremities.

K_e Coefficient of heat exchange by evaporation.

K_e' Evaporation conductance in (20).

K_f Thermal conductivity of the fluid.

K_{fp} Thermal conductivity in functional periphery zone (Btu/h·ft °F).

K_{HCHS} Thermal conductance between the core and skin of the head.

K_c' Mass transfer coefficient for convection.

K_0 1.1×10^{-3} cal/(cm·s°C) = 0.4 kcal/m/h/°C.

K_r Coefficient of heat exchange by radiation.

K_r' Approximate radiation conductance constant.

K_T Thermal conductivity of the tube.

K_{TCTM} Thermal conductance between the muscle and the core of the torso.

K_{TMTS} Thermal conductance between the muscle and the skin of the torso.

L_i Length of the ith element.

L' Length of tube, ft.

M Metabolic rate.

M' Metabolic rate per unit volume.

M_0 Basal metabolism.

M_{ai}' Mass of the blood contained in the arterial pool of the ith element.

M_{0ES} Basal metabolism in the skin of the extremities.

M_{0TC} Basal metabolism assigned to the core of the torso.

M_{0TM} Basal metabolism of the muscle of the torso.

M_{0HC} Basal metabolism heat production assigned to the core of the head.

M_{0HS} Basal metabolic rate of the skin of the head.

M_{vi}' Mass of the blood contained in the venous pool of the ith element.

$\dot{m}$ Mass flow rate (lb/h).

N Sweat loss (kg/m).

n Slope of the curve which represents the relationship between T_{st} and T_r.

$(dp/dT)_i$ Rate of change of partial pressure of water with temperature T_i.

Q Volumetric blood flow rate (m^3/h).

Q_{ai} Product of the mass flow rate and the specific heat for blood entering the arterial pool of the ith element from the adjacent mth element.

Q_{fp} Internal heat generation per unit volume in functional periphery zone (Btu/h·ft^3).

Q_r The rate of heat loss through the respiratory system.

Q_{vi} Product of the mass flow rate and the specific heat for venous blood flowing into the venous pool of the ith element from the adjacent nth element.

q Heat flux (Btu/h).

q_c Heat loss by convection.

q_c' Product of the mass flow rate and specific heat of blood entering the capillary beds per unit volume.

q_{ca} Product of the mass flow rate and specific heat for arterial blood flowing into the capillaries.

q_{cv} Product of the mass flow rate and specific heat for venous blood flowing into the pulmonary capillaries.

q_e Heat loss by evaporation.

q_r Heat loss by radiation.

q_{rv} Rate at which heat is transferred from venous blood in the thorax to air in the respiartory system.

q_s Total heat loss from the body (kcal/h).

R Rate of heat exchange with environment by radiation.

R' Heat loss due to radiation and convection effect per unit volume.

R_h Relative humidity of the ambient air

r Radial distance from axis of cylinder

r' Latent heat for evaporation (kcal/kg).

S Conduction shape factor, dimensionless

T Tissue temperature.

T_1 Temperature of middle layer.

T_2 Temperature of core layer.

T_a Temperature of blood in artery.

T_a' Temperature of the arterial blood entering the capillary bed.

T_{am} Temperature of the blood entering the arterial pool from the mth element.

T_{ax} Temperature at the axis.

T_B Average body temperature.

T_{CB} Temperature of the central blood compartment.

T_e Effective environmental temperature.

T_{EC} Temperature of the core of the extremities.

T_{eq} New equilibrium skin temperature defined in (12).

T_{ES} Temperature of the skin of the extremities.

T_{ha} Arterial blood temperature at the heart.

T_{HC} Temperature of the core of the head.

T_{HS} Temperature of the head skin.

T_{hvi} Venous blood temperature flowing into heart from ith element.

T_{in} Inlet coolant temperature.

T_0 Initial skin temperature.

T_r Internal temperature (core temperature).

ΔT_r Increment of the rectal temperature.

T_s Mean skin temperature.

ΔT_s Increment of the skin temperature.

$\bar{T}_s$ Mean radiation absolute temperature of the body surface in (13).

$\bar{T}_{s1}$ Mean contact surface temperature °F.

T_{st} Skin temperature at time t.

T_v Temperature of blood in vein.

T_{vn} Venous blood temperature in the nth element.

T_w Mean radiant temperature of surroundings.

T_w Mean radiant absolute temperature of the surrounding wall.

U Overall heat transfer coefficient.

V Rate of heat exchange by respiration.

V_1 Volumetric blood flow rate in the capillary bed

V_2 Velocity of the fluid which approaches the cylinder (cm/s).

V_e Heat loss due to evaporation per unit area, $V_{e0} = 7$ kcal/m^2/h.

V_e' Heat loss due to evaporation per unit volume.

VP_a Partial pressure of moisture in the air (=percent RH $\times$ VP at T_a).

VP_s Partial pressure of water at temperature T_s.

v Velocity of surrounding air (cm/s).

v_1 Velocity of surrounding air (ft/min).

W Body weight.

X Distance from the surface of skin.

X_1 Distance from the center of the tube to the end of the contact surface of the tube.

ΔX_1 Thickness of core layer.

ΔX_s Thickness of surface layer.

ΔX_{s1} $\frac{1}{2}(\Delta X_s + \Delta X_1)$.

ΔX_{12} $\frac{1}{2}(\Delta X_1 + \Delta X_2)$.

y_2 Sum of the thickness of the skin zone and the functional periphery zone.

α_{EC} Countercurrent factor of the core of the extremities.

α_{HC} Dimensionless fraction accounting for the effect of countercurrent heat exchange of the core of the head.

α_{HS} Factor for countercurrent heat exchange of the skin of the head.

α_{k+} Thermal conductivity coefficient of proportional control for $(\Delta T_B > 0) = 0.147/°C$ in (30).

α_{k-} Thermal conductivity coefficient of proportional control for $(\Delta T_B < 0) = 0.066/°C$ in (31).

α_m Metabolic rate coefficient of proportional control; $\Delta T_B < 0$.

α_{TC} Countercurrent factor of the core of the torso (63).

α_{TM} Countercurrent factor of the muscles of the torso (64).

α_{TS} Countercurrent factor of the skin of the torso (65).

α_v Evaporation coefficient of proportional control $= 11$ kcal/m^3/h/°C; $\Delta T_B > 0$.

λ_i Latent heat of water at T_i.

λ_v Evaporation coefficient of fourth power proportional control 53 kcal/m^3/h/°C; $\Delta T_B > 0$.

ρ Density of blood.

γ Density (kg/m^3).

γ_k Thermal conductivity coefficient of rate control (s/°C $\simeq 3.5$ s/°C).

δ_{EX} Increase in evaporation coefficient due to violent exercise.

μ Viscosity of the fluid.

REFERENCES

[1] M. J. Allwood and H. S. Burry, "The effect of local temperature on blood flow in the human foot," *J. Physiol.* (London), vol. 124, 1954, p. 345.

[2] A. R. Behnke and T. L. Willmon, "Cutaneous diffusion of helium in relation to peripheral blood flow and absorption of atmospheric nitrogen through the skin," *J. Physiol.*, vol. 131, 1941, p. 627.

[3] T. H. Benzinger, "On physical heat regulation and the sense of temperature in man," *Proc. Nat. Acad. Sci. U. S.*, vol. 45, 1959, p. 645.

[4] T. H. Benzinger and C. Kitzinger, "The human thermostat," in *Temperature—Its Measurement and Control in Science and Industry*, vol. 3, part 3. New York: Reinhold, 1963, ch. 56, p. 637.

[5] D. F. Brehner, D. McK. Kerslake, and F. L. Waddell, "The relation between the coefficients for heat exchange by convection and by evaporation in man," *J. Physiol.*, vol. 141, 1958, pp. 164–168.

[6] H. Buchberg and C. B. Harrah, "Conduction cooling of the human body—A biothermal analysis," in *Thermal Problems in Biotechnology.* American Society of Mechanical Engineers, 1968.

[7] A. C. Burton, "The application of the theory of heat flow to the study of energy metabolism," *J. Nutr.*, vol. 7, 1934, p. 497.

[8] ——, "The operating characteristics of the human thermoregulatory system," in *Temperature—Its Measurement and Control in Science and Industry.* Am. Inst. Phys. New York: Reinhold, 1941.

[9] J. Clifford, D. McK. Kerslake, and J. L. Waddell, *J. Physiol.* (London), vol. 147, 1959, p. 235.

[10] K. E. Cooper, O. G. Edholm, and R. F. Mottram, "The blood flow in skin and muscle of the human forearm," *J. Physiol.* (London), vol. 128, 1955, p. 258.

[11] R. J. Crosbie, J. D. Hardy, and E. Fessenden, in *Temperature—Its Measurement and Control in Science and Industry*," J. D. Hardy, Ed., vol. 3, pt. 3. New York: Reinhold, 1963, pp. 627–635.

[12] O. G. Edholm, R. H. Fox, and R. K. MacPherson, "The effect of body heating on the circulation in skin and muscle," *J. Physiol.* (London), vol. 134, 1956, p. 612.

[13] L. W. Eichna, W. F. Ashe, W. B. Bean, and W. B. Shelly, "The upper limits of environmental heat and humidity tolerated by acclimatized men working in hot environment," *J. Ind. Hyg. Toxicol.*, vol. 27, 1945, p. 59.

[14] J. D. Hardy and H. T. Hammel, "Control system in physiological temperature regulation," in *Temperature—Its Measurement and Control in Science and Industry*, J. D. Hardy, Ed., pt. 3. New York: Rienhold, 1963, ch. 54, p. 613.

[15] J. D. Hardy and G. F. Soderstrom, "Heat loss from the nude body and peripheral blood flow at temperature of 22°C to 35°C," *J. Nutr.*, vol. 16, 1938, p. 493.

[16] A. B. Hertzman and W. C. Randall, "Regional differences in the basal and maximal rates of blood flow in the skin," *J. Appl. Physiol.*, vol. 1, 1948, p. 234.

[17] D. McK. Kerslake and J. L. Waddell, "The heat exchanges of wet skin," *J. Physiol.*, vol. 141, 1958, pp. 156–163.

[18] W. Machle and T. F. Hatch, "Heat: man's exchanges and physiological responses, *Physiol. Rev.*, vol. 27, 1947, pp. 200–227.

[19] D. K. C. MacDonald and C. H. Wyndham, "Heat transfer in man," *J. Appl. Physiol.*, vol. 3, 1950, pp 3[illegible]–360.

[20] W. H. McAdams, *Heat Transmission*, 2nd ed. New York: McGraw-Hill, 1942.

[21] P. E. McNall, J. Jaax, F. H. Rohles, R. H. Nevins, and W. Springer, "Thermal comfort (thermally neutral) conditions for three levels of activity," *ASHRAE Trans.*, vol. 73, 1967, pt. I, sec. 3.

[22] R. G. Nevins, F. H. Rohles, W. E. Springer, and A. M. Feyerherm, "A temperature-humidity chart for thermal comfort of seated persons," *ASHRAE Trans.*, vol. 72, 1966, pt. I, p. 283.

[23] H. H. Pennes, "Analysis of tissue and arterial blood temperatures in the resting human forearm," *J. Appl. Physiol.*, vol. 1, 1948, 93–122.

[24] S. Robinson, F. R. Meyer, J. L. Newton, C. H. Ts'ao, and L. O. Holgersen, "Relations between sweating, cutaneous blood flow, and body temperature in work," *J. Appl. Physiol.*, vol. 20, 1965, p. 575.

[25] P. E. Smith and E. W. James, II, "Human response to heat stress," *Arch. Environ. Health*, vol. 9, 1954, pp. 323–342.
[26] J. A. J. Stolwijk and D. J. Cunningham, "Expansion of a mathematical model of thermoregulation to include high metabolic rates," Nat. Acad. Sci., NAS-9-7140, 1969.
[27] J. A. J. Stolwijk and J. D. Hardy, "Temperature regulation in man—A theoretical study," *Pfluegers Archiv.*, vol. 291, 1966, pp. 129–162.
[28] C. E. A. Winslow, L. P. Herrington, and A. P. Gagge, "Physiological reactions of the human body to varying environmental temperatures," *Amer. J. Physiol.*, vol. 120, 1937, p. 1.
[29] E. H. Wissler, "Steady-state temperature distribution in man," *J. Appl. Physiol.*, vol. 16, 1961, pp. 734–740.
[30] ——, in *Temperature—Its Measurement and Control in Science and Industry*, J. D. Hardy, Ed., vol. 3, pt. 3. New York: Reinhold, 1963, pp. 603–612.
[31] ——, "A mathematical model of the human thermal system," *Bull. Math. Biophys.*, vol. 26, 1964, pp. 147–166.
[32] ——, "A mathematical model of the human thermal system," *Chem. Eng. Progr. Symp. Ser.*, vol. 62, 1966.
[33] C. H. Wyndham and A. R. Atkins, "An approach to the solution of the human biothermal problem with the aid of an analog computer," in *Proc. 3rd Internat. Conf. Med. Electron.*, London, 1960
[34] C. H. Wydham, W. R. D. M. Bouwer, M. G. Device, H. E. Paterson, and D. K. C. MacDonald, "Examination of use of heat-exchange equation for determining changes in body temperature," *J. Appl. Physiol.*, vol. 5, 1952, p. 299.
[35] H. Yamamoto, M. Masubuchi, and Y. Kawashima, "Human thermal regulation," unpublished res. rep., Yokohama Univ., Yokohama, Japan, 1968.
[36] H. Yamamoto, T. Suzuki, Y. Kawashima, and K. Ishikawa, "An analog model of body temperature," unpublished res. rep., Inst. of Public Health, Tokyo, Japan, 1969.

Liang-Tseng Fan was born in Formosa, on August 7, 1929. He received the B.S. degree in chemical engineering from the National Taiwan University, Taipei, in 1951, the M.S. degree in chemical engineering from Kansas State University, Manhattan, in 1954, and the Ph.D. degree in chemical engineering from West Virginia University, Morgantown, in 1957. He also received the M.S. degree in mathematics from West Virginia University, in 1958.

In 1958 he joined the faculty of Kansas State University where he is now a Professor and Head of Chemical Engineering, and Director of the Institute for Systems Design and Optimization. He has published two books on the maximum principle and more than 130 technical papers in optimization, fluidization, chemical process dynamics, and related fields.

Fu-Tong Hsu was born in Taipei, Formosa, on May 7, 1936. He received the B.S.C.E. degree from the National Taiwan University, Taipei, in 1959, the M.S.C.E. degree from the University of Oklahoma, Norman, in 1962, the M.S.O.R. degree from Case Institute of Technology, Cleveland, Ohio, in 1968, and the Ph.D. degree from Kansas State University, Manhattan, in 1971.

From 1962 to 1963 he worked as an Assistant Engineer for the New Jersey Highway Department. From 1963 to 1966 he was employed as a Structural Engineer by Ammann and Whitney, Consulting Engineers, New York, N. Y. He is currently an Assistant Professor of Industrial Engineering and Operations Research at Wayne State University, Detroit, Mich.

Ching-Lai Hwang was born in Formosa, on January 22, 1929. He received the B.S. degree in mechanical engineering from the National Taiwan University, Taipei, in 1953, and the M.S. and Ph.D. degrees from Kansas State University, Manhattan, in 1960 and 1962, respectively.

He is currently an Associate Professor of Industrial Engineering at Kansas State University, and has collaborated on the book, *The Continuous Maximum Principle*. His research interests include optimization techniques, systems engineering, and fluid dynamics.

Steady-State Simulation of the Human Thermal System

6.24

LIANG-TSENG FAN, FU-TONG HSU and CHING-LAI HWANG
Institute for Systems Design and Optimization
Kansas State University
Manhattan, Kansas 66502

Biomechanics
P.M., Monday
16 November

Steady-state simulations of the human thermal system with and without an external thermal regulation device are carried out. The mathematical model of the human thermal system without the external thermal regulation device is essentially the model by Wissler. The model with the regulation device is obtained by modifying Wissler's model. The thermal regulation device is controlled in such a way that the requirements of the thermoneutrality of the human body under the specific environmental condition and specific body activity are satisfied. The effects of localized control of the external thermal regulation device on the totality of the human thermal system are examined. The results indicate that the thermoneutrality of the human body can be attained through the partial cooling or warming of the body.

The geometry on which the human thermal system is based consists of a number of cylindrical elements representing the head, torso, arms, and legs. In each element, the large arteries and veins are approximated by an arterial pool and a venous pool. The heat transfer from the tissue to the surface of the skin and the heat transfer by bulk flow of blood between adjacent elements are taken into account. Axial thermal gradient in every element is neglected. A model based on this description of the human thermal system is simulated on a digital computer under a variety of external conditions.

The external thermal regulation device consisting of a network of tubes which are held in contact with the surface of the skin is for removing metabolic heat generated in the body. The operating or control variables of the external thermal regulation device are the inlet coolant temperature and its flow rate. A model of the integrated system is formulated by incorporating the mathematical model of the external thermal regulation device into the mathematical model of the human thermal system.

Steady-state computer simulations of the integrated system are carried out and the temperature distributions of the human body are determined for a variety of the inlet coolant temperatures and coolant flow rate combinations. The effects of localized cooling or warming of head as well as head and torso for various body metabolic rates are also examined. The variations of physiological parameters, such as the local blood flow rate and local metabolic rate, in the muscle layer and skin layer are considered. In addition, the regional variations in the blood flow rate, metabolic rate, and rate of vaporization are considered.

In carrying out the simulations on a digital computer, the finite difference techniques are used to approximate the models which consist of partial differential equations. Two typical simulation results of the model with the regulation device are shown in Figures 1 and 2. Figure 1 shows the temperature profiles in various elements of a human body under the specific condition in which the head is being cooled by a hood with specified coolant temperature of 40.0°F and flow rate of 250 lbs/hr while the other elements are exposed to the effective environmental temperature of 107.6°F (42.0°C). The results indicate that proper cooling of the head will adequately control the temperature at other parts of the body. Figure 2 shows the effect of the liquid coolant temperature on cooling of the human body which wears a cooling hood and jacket while arms and legs are insulated from their hostile environment. The results indicate that a comfortable brain temperature of 98.0°F (36.7°C) can be achieved by a number of combinations between the liquid coolant temperature and its flow rate.

Acknowledgement. This work has been supported in part by NASA (Grant No. NGR-17-001-034) and AFOSR (Grant USAFOSR F44620-68-C-0020).

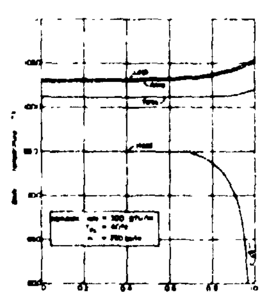

Fig. 1. Steady-state temperature profiles of the human body with cooling hood

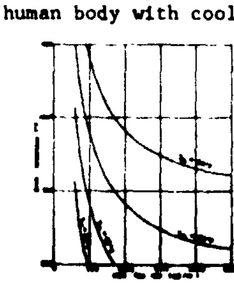

Fig. 2. The effect of coolant temperature on the cooling of human body with hood and jacket. (Metabolic rate = 3000 BTU/HR)

PRECEDING PAGE BLANK NOT FILMED

6.25

Unsteady-State Simulation of the Human Thermal System

Biomechanics
P.M., Monday
16 November

FU-TONG HSU, LIANG-TSENG FAN and CHING-LAI HWANG

Institute for Systems Design and Optimization
Kansas State University
Manhattan, Kansas 66502

Unsteady-state simulations of the human thermal system with and without an external thermal regulation device are carried out. The mathematical model of the human thermal system without the external thermal regulation device is essentially the model by Wissler. The model with the regulation device is obtained by modifying Wissler's model. The thermal regulation device is controlled in such a way that the requirements of the thermoneutrality of the human body at any moment during the transient period are satisfied. The effects of localized control of the external thermal regulation device on the totality of the human thermal system are examined. The results indicate that the thermoneutrality of the human body can be attained through the partial cooling or warming of the body.

The geometry on which the human thermal system is based consists of a number of cylindrical elements representing the head, torso, arms, and legs. In each element, the large arteries and veins are approximated by an arterial pool and a venous pool. The heat transfer from the tissue to the surface of the skin and the heat transfer by bulk flow of blood between adjacent elements are taken into account. Axial thermal gradient in every element is neglected. An unsteady-state model based on this description of the human thermal system is simulated on a digital computer under a variety of external conditions.

The external thermal regulation device consisting of a network of tubes which are held in contact with the surface of the skin is for removing metabolic heat generated in the body. The operating or control variables of the external thermal regulation device are the inlet coolant temperature and its flow rate. An unsteady-state model of the integrated system is formulated by incorporating the mathematical model of the external thermal regulation device into the mathematical model of the human thermal system.

Unsteady-state computer simulations of the integrated system are carried out and the temperature distributions of the human body at any given time are determined for a variety of the inlet coolant temperatures and coolant flow rate combinations. The effects of localized cooling or warming of head as well as head and torso for various body metabolic rates are also examined. The variations of physiological parameters, such as the local blood flow rate and local metabolic rate, in the muscle layer and skin layer are considered. In addition, the regional variations in the blood flow rate, metabolic rate, and rate of vaporization are considered.

In carrying out the simulations on a digital computer, the finite difference techniques are used to approximate the models which consist of partial differential equations. Two typical simulation results of the model with the regulation device are shown in Figures 1 and 2. Figure 1 shows the change of core temperatures of various elements during two hours simulation time. A human subject in this simulation is exposed to an effective environmental temperature of 107.6°F. (42.0°C) except head which is being cooled by a hood with coolant temperature of 60.0°F. and flow rate of 250 lbs/Hr. The results indicate that the human subject will reach its uncomfortable state within one and a half hours because the core temperature (rectal temperature) of torso will increase more than 2.0°F. These results are compared favorably with the experimental data. Figure 2 shows the temperature profiles of torso at various simulation time. A human subject in this simulation wears a cooling hood and jacket while arms and legs are insulated from their hostile environment. The results indicate that if the constant thermal comfort is to be maintained, the operating variables have to be controlled properly.

Acknowledgement. This work has been supported in part by NASA (Grant No. NGR-17-001-034) and AFOSR (Grant USAFOSR F44620-68-C-0020).

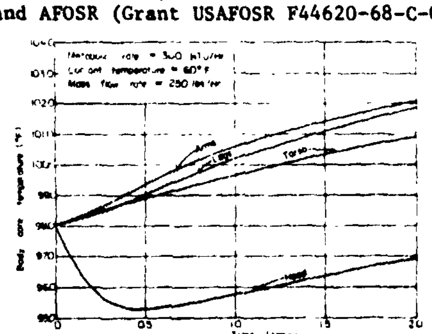

Fig 1 Unsteady-state core temperatures of the body with cooling hood on head

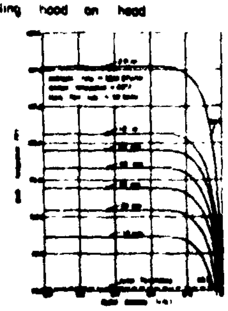

Fig 2 [illegible]

(g) 4

STEADY-STATE SIMULATIONS OF THE HUMAN THERMAL SYSTEM

Report No. 23

F. T. Hsu, L. T. Fan, and C. L. Hwang

Institute for Systems Design and Optimization

KANSAS STATE UNIVERSITY MANHATTAN

STEADY-STATE SIMULATIONS OF

THE HUMAN THERMAL SYSTEM*

F.T. Hsu†, L.T. Fan#, and C.L. Hwang†
Institute for Systems Design and Optimization
Kansas State University, Manhattan, Kansas 66502

July 14, 1970

* This study was supported by NASA Grant No. NGR-17-001-034, and by the Air Force Office of Scientific Research, Office of Aerospace Research, U.S. Air Force, Under Contract F44620-68-0020 (Themis Project).

† Department of Industrial Engineering

Department of Chemical Engineering

STEADY-STATE SIMULATIONS OF THE HUMAN THERMAL SYSTEM

TABLE OF CONTENTS

ABSTRACT

A mathematical model of the human thermal system under steady state conditions is formulated by using six cylindrical elements representing longitudinal segments of the head, torso, arms, and legs to approximate the human body. The model allows the use of different physiological parameters such as local rate of metabolic heat generation and local blood flow rate in various locations of an element. The regional variations of the physiological parameters are also taken into consideration.

A set of ordinary differential equations representing the thermal behavior of all elements are approximated by a set of algebraic equations which resulted from the application of the explicit forward finite difference method. Specifically twenty-eight linear algebraic simultaneous equations are obtained by using five grid points in the spacial coordinate of each element. The model [illegible] imulated for a number of steady state environmental conditions.

1. INTRODUCTION

Due to the difficulties of predicting the human thermal responses of persons who are often exposed to the hostile environment of industrial and mining plants such as chemical, atomic and metal plants and coal mines, and of persons who are involved in underwater or space exploration, a need exists for a mathematical model which will provide a method for predicting the human thermal responses under a variety of environmental conditions. A need also exists for a mathematical model which will provide a method for estimating the physiological parameters such as the local blood flow rate and the local rate of heat generation by metabolic reactions which are often difficult to obtain by direct experimental measurement Although many early models were developed for the purpose of describing the physiological phenomenon, the quantitative description of the intracorporeal transport of heat by circulating blood, which has been recognized for sometime as an important factor in thermal physiology, is still unsatisfactory [9,16].

The purpose of this report is to present a mathematical model of the human thermal system and results of simulation of its thermal responses to a specific environmental condition under steady state conditions. The model describes quantitatively the physiological phenomenon of heat transfer inside the human body and heat transfer between the human body and its environment. The model is capable of predicting the temperature distribution in the various elements of the body. The simulation of the mathematical model can be advantageous employed to verify the goodness of the model. It also enables one to replicate the experiments, to study control scheme, and to investigate the system sensitivity and stability. [15,19]

Pennes [12] (1948) has demonstrated the utility of a mathematical model by comparing measured and computed temperature profiles in the human forearm. Although the discrepancies of the temperature profiles in the vicinity of large arteries and veins are sizable, his model has been considered as a more satisfactory description of the human body than the "core and shell" concept which has often been used by early researchers. The models developed by Eichna, Ashe, Bean, and Shelly [3] (1945) and by Machle and Hatch [11] (1947) are based on the concept of "core and shell" in which the rectal temperature and mean skin temperature are used as measures of the core and shell temperatures, respectively. These models fail in many cases because the amount of build-in information is relatively small and the effects of peripheral circulation is not considered explicitly.

Wyndham and Atkins' model [20] (1960) approximates the structure of the human body by a series of concentric cylinders. The effects of peripheral circulation are considered implicitly by allowing the effective thermal conductivity to vary as a function of temperature but the regional variations of physiological parameters are not considered. The model by Crosbie, Hardy, and Fessenden [2] (1961) uses the concept of infinite slab rather than a cylinder. Many important physiological responses to thermal stress are considered in their model by allowing the effective thermal conductivity, metabolic rate and rate of vaporization to vary as the mean temperature of the body varies. However, the effect of regional variations in heat generation rates and blood flow rates are excluded.

The earliest model developed by Wissler [17] (1961) is an extension of Pennes' work [12] (1948). The steady-state temperature distribution in the human body can be obtained [17] when the environmental conditions, the distribution of metabolic heat generation, the distribution of blood flow, and the size of the body are specified. One of Wissler's models [18] (1963), which is a modification of Wyndham and Atkins' model, can be used to obtain the transient-state temperature distribution of the human body. A review of the mathematical models of the human thermal systems has been presented [4] (1970).

The mathematical model presented in this report is based on one of Wissler's models [19] (1964). The present model considers the local variations of the effective thermal conductivity, metabolic rate, and rate of vaporization. The regional variations of physiological parameters are also taken into account.

The formulation of the mathematical model and the finite difference approximation of the system equations of the model are presented in considerable detail in this report. The results of steady state simulation of an experiment in which a hypothetical human subject is exposed to a specified environmental condition are also included. The environmental condition specified is that a nude human body is exposed to an effective environmental temperature of 107.6°F (42.0°C.) except the head which is exposed to a lower effective environmental temperature of 77.0°F. (25.0°C).

FORMULATION OF THE MATHEMATICAL MODEL

A mathematical model which represents the steady-state condition of the human thermal system is formulated in this section. The model is based on one of Wissler's models [19] (1964) which is for the unsteady-state conditions. The present model differs slightly from that of Wissler's in the expression of thermal energy balance equations of the torso. The present model assumes the existence of an arterial pool and a venous pool in the torso and considers the heat exchange of the torso with adjacent elements only through the pools. Wissler's model considers the heat exchange of the torso with adjacent elements through pulmonary capillaries.

2.1 Description and Mathematical Expression

The mathematical model of the human thermal system formulated in this report considers the following important factors: (1) local generation of heat by metabolic reactions, (2) conduction of heat due to thermal gradients, (3) convection of heat by circulating blood, (4) the geometry of the human body, (5) the existence of an insulating layer of fat and skin, (6) countercurrent heat exchange between adjacent large arteries and veins, (7) sweating, and (8) the condition of the environment, including its temperature, wind velocity, and relative humidity.

The geometry of the human body on which the system equations are based is shown in Fig. 1. It consists of a number of cylindrical elements representing arms, legs, torso, and head. Each element, consisting of tissue, fat and skin, has a vascular system which can be divided into three subsystems representing the arteries, the veins, and the capillaries.

The h... which is generated in an element by metabolic reactions is sto... ement, carried away by circulating blood to other elements ... r ... to the surface where it is generally transfered to the environment. If the environmental temperature is higher than the skin temperature, the direction of heat flow is reversed. Based on the first law of thermodynamics the phenomenon can be expressed mathematically as the differential heat balance equation for the ith element as follows:

$$\frac{1}{r}\frac{d}{dr}\left(K_i\, r\,\frac{dT_i}{dr}\right) + h_{mi} + q_{ci}\,(T_{ai} - T_i)$$

$$+ h_{ai}\,(T_{ai} - T_i) + h_{vi}\,(T_{vi} - T_i) \qquad (1)$$

$$= 0$$

where

$T_i(r)$ = temperature of the tissue, bone, fat, or skin at a distance r from the axis of the ith element,

$K_i(r)$ = thermal conductivity of tissue, bone, fat, or skin,

h_{mi} = metabolic heat generation per unit volume,

q_{ci} = product of the mass flow rate and specific heat of blood entering the capillary beds per unit volume,

h_{ai} = proportionality constant of heat transfer between the arteries and tissue per unit volume,

h_{vi} = proportionality constant of heat transfer between the veins and tissue per unit volume,

T_{ai} = temperature of the arterial blood,

T_{vi} = temperature of the venous blood

The terms on the left-hand side of equation (1) represent the net rate of heat conduction into the unit volume, the rate of heat generation by metabolic reactions in the unit volume, the net rate at which heat is carried into the unit volume by the bulk flow of blood, the rate at which heat is transfered into the unit volume from arterial blood, and the rate at which heat is transfered into the unit volume from venous blood.

The longitudinal effect of heat conduction is neglected in equation (1). Pennes [12] (1948) has shown that the longitudinal heat conduction is negligible in arms. This is probably also true in legs because their shape is similar to that of the arms, but it might not be true in the head and torso. Hence the future human thermal model probably should include the effect of longitudinal heat conduction in the head and torso.

An assumption that the temperature of blood leaving the capillary beds is equal to the temperature of the neighboring tissue is also made. This assumption is acceptable because the capillary has very small diameter which ranges from 10μ to 20μ [17]. Such a condition does not prevail in the large arteries and veins. Therefore, it is necessary to assume that the rate of heat transfer from the blood in the larger vessels to the neighboring tissue is proportional to the temperature difference between the blood and tissue. The proportionality constant is expressed by h_{ai} for the arteries and h_{vi} for the veins in the ith element.

It is known that the human blood temperature in the various locations of the body are different [6, 8, 10]. Therefore, two additional equations which represent the overall thermal energy balances in arteries and veins are required. In deriving such equations it is assumed that the blood in the large arteries and veins of the ith element has uniform temperatures T_{ai} and T_{vi} respectively as shown in Fig. 2. The resulting equations are

$$Q_{ai} \left(T_{am} - T_{ai}\right) + 2\pi L_i \int_0^{a_i} h_{ai} \left(T_i - T_{ai}\right) r \, dr$$

$$+ H_{avi} \left(T_{vi} - T_{ai}\right) \tag{2}$$

$$= 0$$

$$Q_{vi} \left(T \quad - T_{vi}\right) + 2\pi L_i \int_0^{a_i} \left(q_{ci} + h_{vi}\right) \left(T_i - T_{vi}\right) r \, dr$$

$$+ H_{avi} \left(T_{ai} - T_{vi}\right) \tag{3}$$

$$= 0$$

where

Q_{ai} = product of the mass flow rate and specific heat for blood entering the large arteries of the ith element from the mth element,

$T_{am}(t)$ = temperature of the blood entering the large arteries of the ith element from the mth element,

L_i = length of the ith element,

a_i = radius of the ith element

H_{avi} = proportionality constant of direct heat transfer between large arteries and veins,

Q_{vi} = product of the mass flow rate and specific heat for venous blood entering the large veins of the ith element from the nth element,

$T_{vn}(t)$ = temperature of the blood entering the large veins of the ith element from the nth element.

The terms on the left-hand side of equation (2) represent, in order the rate at which heat is carried into the large arteries in the ith element by the bulk flow of blood from the adjacent element, the rate at which heat is transferred into the blood in the large arteries of the element from neighboring tissue, and the rate at which heat is transferred directly from the large veins to the large arteries.

Equation (3) which is for the venous blood contains the corresponding terms. The only difference between equations (2) and (3) appears in the second term. This difference appears as an additional expression

$$2\pi L_i \int_0^{a_i} q_{ci} \, (T_i - T_{vi}) \, r \, dr$$

in the second term of equation (3). This expression corresponds to the rate at which heat is carried into the large veins in the ith element from the capillary bed by flowing blood. The integral appears in equations (2) and (3) because the tissue temperature, $T_i(r)$, is a function of r. The rate of blood flowing into an element is assumed to be equal to the rate of blood flowing out of the element.

2.2 Boundary Conditions

The boundary condition which represents the heat transfer from the surface of the skin to its environment takes the following form.

$$-\left[K_i \frac{dT_i}{dr}\right]_{r=a_i} = H_i\left[T_i(a_i) - T_{ei}\right] \tag{4}$$

where

H_i = heat transfer coefficient at the surface of the ith element (see Appendix A)

T_{ei} = effective environmental temperature at the surface of the ith element

Equation (4) states that at the surface of the skin the local rate of heat conduction to the surface through the tissue is equal to the rate of heat transfer from the surface to the environment.

Due to the axial symmetry of each element the following condition also exists

$$\left(\frac{dT_i}{dr}\right)_{r=0} = 0 \tag{5}$$

3. FINITE DIFFERENCE APPROXIMATION OF THE MODEL

The finite-difference technique which is employed in this section enables one to consider the variation of physiological properties at various positions of the body. According to this technique the independent variables are discretized. More specifically, each of the cylindrical elements is divided into a series of concentric cylinders and appropriate values are assigned to the physiological parameters of each element. One of the advantages of the finite difference technique is that one can use a smaller segment of the radial distance near the surface of the element where the temperature profile has steeper gradient and a larger segment can be used in an inner core where the temperature profile is nearly flat.

3.1 Finite Difference Scheme

The explicit forward finite difference technique is employed to approximate equation (1). [1, 5] The general expression of the forward finite difference technique can be written as

$$\frac{dT(x)}{dx} = \frac{T(x+\Delta x) - T(x)}{\Delta x}$$

Each term in equation (1) can be integrated from $r = r_j - (\Delta\ell_-/2)$ to $r = r_j + (\Delta\ell_+/2)$ where $\Delta\ell_-$ represents the space increment to the left of r_j and $\Delta\ell_+$ represents the space increment to the right of r_j.

$$\int_{r_j - \frac{\Delta\ell_-}{2}}^{r_j + \frac{\Delta\ell_+}{2}} d\left(K_i\, r \frac{dT_i}{dr}\right) + \int_{r_j - \frac{\Delta\ell_-}{2}}^{r_j} h_{mi-}\, r dr$$

$$+ \int_{r_j}^{r_j + \frac{\Delta\ell_+}{2}} h_{mi+}\, r dr + \int_{r_j - \frac{\Delta\ell_-}{2}}^{r_j} [(q_{ci-} + h_{ai-})(T_{ai} - T_i) + h_{vi-}(T_{vi} - T_i)]\, r dr$$

$$+ \int_{r_j}^{r_j + \frac{\Delta \ell_+}{2}} [(q_{ci+} + h_{ai+})(T_{ai} - T_i) + h_{vi+} (T_{vi} - T_i)] rdr$$

$= 0$

The finite difference approximation of the equation becomes

$$K_{i+} (r_j + \frac{\Delta \ell_+}{2}) \frac{T_{i(j+1)} - T_{ij}}{\Delta \ell_+} - K_{i-} (r_j - \frac{\Delta \ell_-}{2}) \frac{T_{ij} - T_{i(j-1)}}{\Delta \ell_-}$$

$$+ \{ \frac{\Delta \ell_-}{2} (r_j - \frac{\Delta \ell_-}{4}) h_{mi-} + \frac{\Delta \ell_+}{2} (r_j + \frac{\Delta \ell_+}{4}) h_{mi+} \}$$

$$+ \{ \frac{\Delta \ell_-}{2} (r_j - \frac{\Delta \ell_-}{4}) [(q_{ci-} + h_{ai-})(T_{ai} - T_{ij}) + h_{vi-} (T_{vi} - T_{ij})]$$

$$+ \frac{\Delta \ell_+}{2} (r_j + \frac{\Delta \ell_+}{4}) [(q_{ci+} + h_{ai+})(T_{ai} - T_{ij}) + h_{vi+} (T_{vi} - T_{ij})]\}$$

$$= 0 \tag{6}$$

where T_{ij} represents the tissue temperature of the ith element at the jth radial point. The quantity with the negative subscript (-) represents the physiological parameters at the left of r_j whereas the positive subscript (+) represents the same properties at the right of r_j.

Let

$$A1 = \frac{\Delta \ell_-}{2} (r_j - \frac{\Delta \ell_-}{4})$$

$$A2 = \frac{\Delta \ell_+}{2} (r_j + \frac{\Delta \ell_+}{4})$$

$$A3 = K_{i+} \; (r_j + \frac{\Delta \ell_+}{2})$$

$$A4 = K_{i-} \; (r_j - \frac{\Delta \ell_-}{2})$$

$$A5 = q_{ci-} + h_{ai-}$$

$$A6 = q_{ci+} + h_{ai+}$$

Then equation (6) can be written by

$$A3 \times \frac{T_{i(j+1)} - T_{ij}}{\Delta \ell_+} - A4 \times \frac{T_{ij} - T_{i(j-1)}}{\Delta \ell_-}$$

$$+ \{A1 \times h_{mi-} + A2 \times h_{mi+}\} + \{A1[A5(T_{ai} - T_{ij}) + h_{vi-}(T_{vi} - T_{ij})]$$

$$+ A2[A6(T_{ai} - T_{ij}) + h_{vi+}(T_{vi} - T_{ij})]\}$$

$$= 0 \tag{7}$$

Equation (7) can be rearranged as

$$T_{i(j-1)} [\frac{A4}{\Delta \ell_-}] + T_{ij}[- \frac{A3}{\Delta \ell_+} - \frac{A4}{\Delta \ell_-} - A1 \times A5 \times h_{vi-} - A2 \times A6$$

$$-A2 \times h_{vi+}] + T_{i(j+1)} [\frac{A3}{\Delta \ell_+}] + T_{ai}[A2 \times A6 + A1 \times A5]$$

$$+ T_{vi} [A1 \times h_{vi-} + A2 \times h_{vi+}]$$

$$= -[A1 \times h_{mi-} + A2 \times h_{mi+}] \tag{8}$$

which can be further simplified to

$$X_{ij}\ T_{i(j-1)} + Y_{ij}\ T_{ij} + Z_{ij}\ T_{i(j+1)} + A_{ij}\ T_{ai} + V_{ij}\ T_{vi} = C_{ij} \tag{9}$$

where

$$X_{ij} = \frac{A4}{\Delta\ell_-}$$

$$Y_{ij} = -\frac{A3}{\Delta\ell_+} - \frac{A4}{\Delta\ell_-} - A1 \times A5 - A1 \times h_{vi-} - A2 \times A6 - A2 \times h_{vi+}$$

$$Z_{ij} = \frac{A3}{\Delta\ell_+}$$

$$A_{ij} = A1 \times A5 + A2 \times A6$$

$$V_{ij} = A1 \times h_{vi-} + A2 \times h_{vi+}$$

$$C_{ij} = -A1 \times h_{mi-} - A2 \times h_{mi+}$$

It is worth mentioning that X_{ij}, Y_{ij}, Z_{ij}, A_{ij}, V_{ij}, and C_{ij} are all functions of the physiological parameters and mesh size. The metabolic heat generations, h_{mi-} and h_{mi+}, are considered only at certain layers of the body. Assumptions have been made that heat generation by metabolic reactions in the layer of fat and skin is zero and that basal metabolism occurs only at the core layer. Any additional heat generated by metabolic reactions due to body exercise is considered to occur in the muscle layers.

At the boundary where $r = r_J$, the integration of equation (1) from $r = r_j - (\Delta\ell_- /2)$ to $r = r_J$ can be approximated by

$$K_{i+}(r_J)\left[\frac{dT}{dr}\right]_{r=r_J} - K_{i-}\left(r_J - \frac{\Delta\ell_-}{2}\right)\frac{T_{iJ} - T_{i(J-1)}}{\Delta\ell_-}$$

$$+ \frac{\Delta\ell_-}{2}\left(r_J - \frac{\Delta\ell_-}{4}\right)[(q_{ci-} + h_{ai-})(T_{ai} - T_{iJ}) + h_{vi-}(T_{vi} - T_{iJ})]$$

$$= 0 \tag{10}$$

The boundary condition given in equation (4) is employed to evaluate the value of $[K_{i+}(\frac{dT}{dr})]$ at $r = r_J$ in equation (10). This yields

$$-(r_J)\, H_i[T_{iJ} - T_{ei}] - K_{i-}\left(r_J - \frac{\Delta\ell_-}{2}\right)\frac{T_{iJ} - T_{i(J-1)}}{\Delta\ell_-}$$

$$+ \frac{\Delta\ell_-}{2}\left(r_J - \frac{\Delta\ell_-}{4}\right)[(q_{ci-} + h_{ai-})(T_{ai} - T_{iJ}) + h_{vi-}(T_{vi} - T_{iJ})]$$

$$= 0$$

or

$$-(r_J)\, H_i[T_{iJ} - T_{ei}] - B1 \times \frac{T_{iJ} - T_{i(J-1)}}{\Delta\ell_-} + B2[B3(T_{ai} - T_{iJ})$$

$$+ h_{vi-}(T_{vi} - T_{iJ})]$$

$$= 0 \tag{11}$$

where

$$B1 = K_{i-}\left(r_J - \frac{\Delta\ell_-}{2}\right)$$

$$B2 = \frac{\Delta\ell_-}{2}\left(r_J - \frac{\Delta\ell_-}{4}\right)$$

$$B3 = q_{ci-} + h_{ai-}$$

Equation (11) can be rearranged as

$$T_{i(J-1)} \left[\frac{B1}{\Delta \ell_-}\right] + T_{iJ}\left[-r_J\, H_i - \frac{B1}{\Delta \ell_-} - B2 \times B3 - B2 \times h_{vi-}\right]$$

$$+T_{ai}[B2 \times B3] + T_{vi}[B2 \times h_{vi-}]$$

$$= -r_J\, H_i\, T_{ei} \tag{12}$$

It should be noted that the value of metabolic heat generation, h_{mi}, is assumed to be zero in equations (10) through (12). This is due to the assumption that the layers of fat and skin do not generate heat by metabolic reactions.

Equation (12) can be simplified as

$$X_{iJ}\, T_{i(J-1)} + Y_{iJ} T_{iJ} + A_{iJ} T_{ai} + V_{iJ} T_{vi} = C_{iJ} \tag{13}$$

where

$$X_{iJ} = \frac{B1}{\Delta \ell_-}$$

$$Y_{iJ} = -r_J\, H_i - \frac{B1}{\Delta \ell_-} - B2 \times B3 - B2 \times h_{vi-}$$

$$A_{iJ} = B2 \times B3$$

$$V_{iJ} = B2 \times h_{vi-}$$

$$C_{iJ} = -r_J\, H_i\, T_{ei}$$

Similarly, the finite difference approximation for equation (1) at the center of each cylindrical element can be obtained by integrating equation (1) from $r = 0$ to $r = \frac{\Delta\ell_+}{2}$.

$$K_{i+} \left(\frac{\Delta\ell_+}{2}\right) \frac{T_{i2} - T_{i1}}{\Delta\ell_+} + \left\{\frac{\Delta\ell_+}{2}\left(\frac{\Delta\ell_+}{4}\right) h_{mi+}\right\} + \frac{\Delta\ell_+}{2}\left(\frac{\Delta\ell_+}{4}\right) [(q_{ci+} + h_{ai+})$$

$$(T_{ai} - T_{i1}) + h_{vi+} (T_{vi} - T_{i1})]$$

$$= 0$$

or

$$C1 \times \frac{T_{i2} - T_{i1}}{\Delta\ell_+} + C2 \times h_{mi+} + C2[C3(T_{ai} - T_{i1}) + h_{vi+}(T_{vi} - T_{i1})]$$

$$= 0 \tag{14}$$

where

$$C1 = K_{i+}\left(\frac{\Delta\ell_+}{2}\right)$$

$$C2 = \frac{\Delta\ell_+}{2}\left(\frac{\Delta\ell_+}{4}\right)$$

$$C3 = q_{ci+} + h_{ai+}$$

Equation (14) can be rearranged as follows:

$$T_{i1}\left[-\frac{C1}{\Delta\ell_+} - C2 \times C3 - C2 \times h_{vi+}\right] + T_{i2}\left[\frac{C1}{\Delta\ell_+}\right]$$

$$+ T_{ai}[C2 \times C3] + T_{vi}[C2 \times h_{vi+}]$$

$$= - C2 \times h_{mi+} \tag{15}$$

Further simplification of equation (15) yields

$$Y_{i1}T_{i1} + Z_{i1}T_{i2} + A_{i1}T_{ai} + V_{i1}T_{vi} = C_{i1} \tag{16}$$

where

$$Y_{i1} = -\frac{C1}{\Delta\ell_+} - C2 \times C3 - C2 \times h_{vi+}$$

$$Z_{i1} = \frac{C1}{\Delta\ell_+}$$

$$A_{i1} = C2 \times C3$$

$$V_{i1} = C2 \times h_{vi+}$$

$$C_{i1} = -C2 \times h_{mi+}$$

The coefficients X_{iJ}, Y_{iJ}, A_{iJ}, V_{iJ}, and C_{iJ} in equation (13) and the coefficients Y_{i1}, Z_{i1}, A_{i1}, V_{i1} and C_{i1} in equation (16) are also functions of the physiological parameters and mesh size.

By using Simpson's rule [14] to carry out the integration, equation (2) becomes

$$Q_{ai}(T_{am} - T_{ai}) - 2\pi L_i h_{ai} T_{ai} \cdot \frac{(a_i)^2}{2} + 2\pi L_i h_{ai} \sum_{j=1}^{J} C'_{ij} T_{ij} r_j$$

$$+ H_{avi}(T_{vi} - T_{ai})$$

$$= 0$$

or

$$Q_{ai}(T_{am} - T_{ai}) - \pi L_i h_{ai} T_{ai} (a_i)^2 + 2\pi L_i h_{ai} \sum_{j=1}^{J} C'_{ij} T_{ij} r_j$$

$$+ H_{avi}(T_{vi} - T_{ai}) \tag{17}$$

$$= 0$$

where

$$C'_{i1} = C'_{iJ} = \frac{r_{iJ}}{3(J-1)}$$

$$C'_{i2} = C'_{i4} = \ldots = C'_{i(J-1)} = \frac{4\ r_{iJ}}{3(J-1)} \tag{18}$$

$$C'_{i3} = C'_{i5} = \ldots = C'_{i(J-2)} = \frac{2\ r_{iJ}}{3(J-1)}$$

In order to use a smaller mesh size for the special coordinate around the outer layers where the gradient of the temperature is steeper than that in the inner part of the cylinder, equation (18) is modified slightly and the following values of C'_{ij} are used in the computer program.

The radius of the cylinder is divided into three equally spaced intervals. The outer third is then divided into two halves. The grid points are designated as r_1, r_2, r_3, r_4, and r_5.

The values of C'_{ij} can be given as follows:

$$C'_{i1} = \frac{1}{3}\left(\frac{a_i}{3}\right)$$

$$C'_{i2} = \frac{4}{3}\left(\frac{a_i}{3}\right)$$

$$C'_{i3} = \frac{1}{3}\left(\frac{a_i}{3}\right) + \frac{1}{3}\left(\frac{a_i}{6}\right)$$

$$C'_{i4} = \frac{4}{3}\left(\frac{a_i}{6}\right)$$

$$C'_{i5} = \frac{1}{3}\left(\frac{a_i}{6}\right)$$

Substituting the values of C'_{ij} into equation (17), one obtains

$$Q_{ai}(T_{am}-T_{ai}) - \pi L_i h_{ai} T_{ai} \; (a_i)^2 + 2\pi L_i h_{ai} \; \{[\frac{1}{3}\;(\frac{a_i}{3})] \;\; T_{i1}r_1$$

$$+ [\frac{4}{3}\;(\frac{a_i}{3})] \; T_{i2}r_2 + [\frac{1}{3}\;(\frac{a_i}{3}) + \frac{1}{3}\;(\frac{a_i}{6})] \; T_{i3}r_3$$

$$+[\frac{4}{3}\;(\frac{a_i}{6})] \; T_{i4}r_4 + [\frac{1}{3}\;(\frac{a_i}{6})] \; T_{i5}r_5\} + H_{avi} \; (T_{vi}-T_{ai})$$

$$= 0$$

or

$$2\pi L_i h_{ai} \; \{[\frac{1}{3}\;(\frac{a_i}{3})] \; r_1T_{i1} + [\frac{4}{3}\;(\frac{a_i}{3})] \; r_2T_{i2}$$

$$+ [\frac{1}{3}\;(\frac{a_i}{3}) + \frac{1}{3}\;(\frac{a_i}{6})] \; r_3T_{i3} + [\frac{4}{3}\;(\frac{a_i}{6})] \; r_4T_{i4}$$

$$+ [\frac{1}{3}\;(\frac{a_i}{6})] \; r_5T_{i5}\} + [-Q_{ai}-\pi L_i h_{ai} \; (a_i)^2-H_{avi}] \; T_{ai}$$

$$+ H_{avi}T_{vi} + Q_{ai}T_{am}$$

$$= 0$$

This equation can be simplified as

$$P_{i1}T_{i1} + P_{i2}T_{i2} + P_{i3}T_{i3} + P_{i4}T_{i4} + P_{i5}T_{i5} + A_{i6}T_{ai}$$

$$+ V_{i6}T_{vi} + E_{i6}T_{am}$$

$$= 0 \tag{19}$$

where

$$P_{i1} = 2\pi L_i h_{ai}[\tfrac{1}{3}\ (\tfrac{a_i}{3})]r_1$$

$$P_{i2} = 2\pi L_i h_{ai}[\tfrac{4}{3}\ (\tfrac{a_i}{3})]r_2$$

$$P_{i3} = 2\pi L_i h_{ai}[\tfrac{1}{3}\ (\tfrac{a_i}{3}) + \tfrac{1}{3}\ (\tfrac{a_i}{6})]r_3$$

$$P_{i4} = 2\pi L_i h_{ai}[\tfrac{4}{3}\ (\tfrac{a_i}{6})]r_4$$

$$P_{i5} = 2\pi L_i h_{ai}[\tfrac{1}{3}\ (\tfrac{a_i}{6})]r_5$$

$$A_{i6} = -Q_{ai} - \pi L_i h_{ai}(a_i)^2 - H_{avi}$$

$$V_{i6} = H_{avi}$$

$$E_{i6} = Q_{ai}$$

Equation (3) can be similarly approximated as

$$Q_{vi}(T_{vn} - T_{vi}) - 2\pi L_i(q_{ci} + h_{vi})\ \frac{(a_i)^2}{2}\ T_{vi}$$

$$+ 2\pi L_i(q_{ci} + h_{vi})\ \sum_{j=1}^{J} C''_{ij}\ T_{ij}\ r_j + H_{avi}(T_{ai} - T_{vi})$$

$$= 0 \tag{20}$$

The values of C''_{ij} can be given as

$$C''_{i1} = \frac{1}{3}\,(\frac{a_i}{3})$$

$$C''_{i2} = \frac{4}{3}\,(\frac{a_i}{3})$$

$$C''_{i3} = \frac{1}{3}\,(\frac{a_i}{3}) + \frac{1}{3}\,(\frac{a_i}{6})$$

$$C''_{i4} = \frac{4}{3}\,(\frac{a_i}{6})$$

$$C''_{i5} = \frac{1}{3}\,(\frac{a_i}{6})$$

Substituting the values of C''_{ij} into equation (20) and rearranging the terms, one obtains

$$\begin{aligned} 2\pi L_i(q_{ci}+h_{vi})\ \{&[\frac{1}{3}\,(\frac{a_i}{3})]\ r_1T_{i1} + [\frac{4}{3}\,(\frac{a_i}{3})]\ r_2T_{i2} \\ &+ [\frac{1}{3}\,(\frac{a_i}{3}) + \frac{1}{3}\,(\frac{a_i}{6})]\ r_3T_{i3} + [\frac{4}{3}\,(\frac{a_i}{6})]\ r_4T_{i4} \\ &+ [\frac{1}{3}\,(\frac{a_i}{6})]\ r_5T_{i5}\} + H_{avi}T_{ai} \\ &+ [-Q_{vi}-\pi L_i(q_{ci}+h_{vi})(a_i)^2 - H_{avi}]\ T_{vi} + Q_{vi}T_{vn} \\ &= 0 \end{aligned}$$

This equation can be simplified as

$$Q_{i1}T_{i1} + Q_{i2}T_{i2} + Q_{i3}T_{i3} + Q_{i4}T_{i4} + Q_{i5}T_{i5} + A_{i7}T_{ai}$$

$$+ V_{i7}T_{vi} + E_{i7}T_{vn}$$

$$= 0 \tag{21}$$

where

$$Q_{i1} = 2\pi L_i(q_{ci}+h_{vi})[\frac{1}{3}(\frac{a_i}{3})]r_1$$

$$Q_{i2} = 2\pi L_i(q_{ci}+h_{vi})[\frac{4}{3}(\frac{a_i}{3})]r_2$$

$$Q_{i3} = 2\pi L_i(q_{ci}+h_{vi})[\frac{1}{3}(\frac{a_i}{3}) + \frac{1}{3}(\frac{a_i}{6})]r_3$$

$$Q_{i4} = 2\pi L_i(q_{ci}+h_{vi})[\frac{4}{3}(\frac{a_i}{6})]r_4$$

$$Q_{i5} = 2\pi L_i(q_{ci}+h_{vi})[\frac{1}{3}(\frac{a_i}{6})]r_5$$

$$A_{i7} = H_{avi}$$

$$V_{i7} = -Q_{vi} - \pi L_i(q_{ci}+h_{vi})(a_i)^2 - H_{avi}$$

$$E_{i7} = Q_{vi}$$

The system equations, equations (1), (2), and (3), for the ith element can now be replaced by a set of linear algebraic simultaneous equations represented by equations (9), (13), (16), (19), and (21). In summary,

$$\left.\begin{aligned}
Y_{i1}T_{i1} + Z_{i1}T_{i2} \phantom{+ Z_{i4}T_{i5}} & + A_{i1}T_{ai} + V_{i1}T_{vi} = C_{i1} \\
X_{i2}T_{i1} + Y_{i2}T_{i2} + Z_{i2}T_{i3} & + A_{i2}T_{ai} + V_{i2}T_{vi} = C_{i2} \\
X_{i3}T_{i2} + Y_{i3}T_{i3} + Z_{i3}T_{i4} & + A_{i3}T_{ai} + V_{i3}T_{vi} = C_{i3} \\
X_{i4}T_{i3} + Y_{i4}T_{i4} + Z_{i4}T_{i5} & + A_{i4}T_{ai} + V_{i4}T_{vi} = C_{i4} \\
X_{i5}T_{i4} + Y_{i5}T_{i5} & + A_{i5}T_{ai} + V_{i5}T_{vi} = C_{i5} \\
P_{i1}T_{i1} + P_{i2}T_{i2} + P_{i3}T_{i3} + P_{i4}T_{i4} + P_{i5}T_{i5} & + A_{i6}T_{ai} + V_{i6}T_{vi} = -E_{i6}T_{am} \\
Q_{i1}T_{i1} + Q_{i2}T_{i2} + Q_{i3}T_{i3} + Q_{i4}T_{i4} + Q_{i5}T_{i5} & + A_{i7}T_{ai} + V_{i7}T_{vi} = -E_{i7}T_{vn}
\end{aligned}\right\} \quad (22)$$

3.2 Linear Algebraic Simultaneous Equations

The number of difference equations obtained from the technique employed in this work depends on the number of grid point used to discretize the independent variable. A set of simultaneous linear algebraic equations included in equation (22) are obtained by using five grid points to discretize the radial distance of the ith element. With seven simultaneous linear algebraic equations representing the thermal characteristics of each element, the total of twenty-eight simultaneous linear algebraic equations are required to represent the human thermal system. The synthesized system equations for the entire system are illustrated in Table 1.

The first set of linear algebraic equations in the upper left hand corner represents the thermal characteristics of the head. The second, third, and fourth sets of linear algebraic equations from the upper left hand corner represent the thermal characteristics of the torso, arm, and leg, respectively. The interdependence between elements is represented by the terms scattered around the blocks of terms. The coefficient of these interconnecting terms are the function of blood flow rate between the adjacent elements.

Since the coefficients of all the terms appearing in Table 1 are functions of the physiological parameters and mesh size, the local and regional variations of the physiological parameters can be conveniently examined. The temperature distribution in each element for a given environmental condition can also be determined by solving these twenty-eight simultaneous linear algebraic equations.

The method of solving these equations is by elimination using the largest pivotal divisor [7]. Each stage of elimination consists of interchanging rows when necessary to avoid division by zero or small elements. The computer program for this method is conveniently provided by the IBM System/360 Scientific Subroutine Package under the subrouting name SIMQ.

4. SIMULATION OF THE MATHEMATICAL MODEL

To test the validity of the mathematical model of the human thermal system, a number of simulations have been carried out and the results are described in this section. An experiment with a human subject is carried out in an environment in which the torso, arms, and legs are exposed to an effective environmental temperature of 107.6°F (42.0°C) whereas the head is exposed to a cooler temperature of 77.0°F (25.0°C). This particular environment is selected in order to lay the ground work for future studies on the effects of localized cooling (or warming) on the entire human thermal system. The following types of simulations have been carried out and they are listed in the increasing order of complexity.

(1) The blood flow rate between the adjacent elements and the local heat generation by metabolic reactions are assumed to be zero in the system. The assumption implies that a human body is disjointed into six independent elements, namely, the head, torso, two arms, and two legs.

(2) The disjointed independent elements are connected by blood circulation between adjacent elements. The local rates of heat generation by metabolic reactions are, however, neglected.

(3) The elements are all connected by blood circulation between adjacent elements. Each element is generating heat by metabolic reactions. These particular types of simulations are selected because one can obtain results which can be verified fairly easily.

The purpose of the subsection is to present the results of simulations and employ them to test the validity of the model. Table 2 summerizes the numerical values of physical dimension of the human body and its physiological parameters.

Figure 3 presents the results of the first type of simulation stated previously. It shows the temperature profiles of various elements under steady-state condition. The metabolic rates in various elements and blood flow rates between adjacent elements are assumed to be zero. The results indicate that the temperature profile of the arms, legs, and torso are nearly straight around 107.6°F (42.0°C) which is assumed to be the effective environmental temperature of these elements. The temperature profile for the head is also nearly straight around its effective environmental temperature which is assumed to be 77.0°F (25.0°C). The slight deviation of temperature profile from its effective environmental temperature is caused by the errors due to the finite difference approximation and Simpson's rule of integration. The results also show that the model works properly when the metabolic rates of all the elements and the blood flow rates between adjacent elements are assumed to be zero.

The purpose of the second type of simulation in which the blood circulation between the adjacent elements is considered while the metabolic heat generation in all the elements is neglected is to investigate the interdependence among the elements. The cooler effective environmental temperature of the head is expected to affect the temperature profile of other elements where the effective environmental temperatures are higher than that of the head. The temperature profiles are also expected to fall within the two bounds: the upper limit of 107.6°F (42.0°C) and the lower limit of 77.0°F (25.0°C). Figure 4 presents the results of this second simulation. It shows the temperature profiles of all elements. Because of the direct connection by blood circulation between the torso and head, arms, and legs, the temperature profiles among them show only a slight difference of about 1°F in temperature at the inner core. This slight difference is caused by the assumption that both the arterial blood pool and venous blood pool have a uniform temperature throughout a given element. A difference of about 7°F can be seen, however, between the temperature at the surface of the head and those of the other elements.

The main reason that the temperature profiles are lower than 107.6°F (42.0°C) which is the effective environmental temperature of the torso, arms, and legs is that the effective environmental temperature of the head is 77.0°F (25.0°C). This lower effective environmental temperature is intended to cool the blood temperature inside the head. The venous blood flowing out of the head, in turn, cools off the blood temperature of the torso, arms, and legs. Because the amount of blood distributed to each element is assumed to be approximately 20% in the head, 60% in the torso, 8% in the arms and 12% in the legs, the steady-state temperatures obtained which are around 105.8°F (41.0°C) can be reasonably expected.

Some of the most significant temperature profiles of all the elements are shown in Figure 5. It presents the results of the third type of simulation. Blood circulation between the adjacent elements and metabolic heat generation in each element are permitted. The results indicate that the effect of the lower effective environmental temperature on the head is overcomed by its high rate of heat generation by metabolic reactions. The same reasoning can account for the higher temperature profile of the head than that of the arms. The temperature profile of the arms is slightly lower than that of the legs even though the same metabolic rate is assigned. This is due to the fact that the arm has a smaller volume than the leg and is easily affected by the effective environmental temperature. The results also indicate that the simulated environment is not adequate for a person to stay indefinitely because the steady state core temperatures of the elements of the body are around 112.0°F.

Figure 6 presents the results of a parametric study of the temperature at various locations of the body. The core and skin temperatures of the head and torso are presented. The results indicate that the temperatures increase almost linearly as the metabolism increases.

5. DISCUSSION AND CONCLUDING REMARKS

As mentioned in the previous section, the model presented in this report is a modified steady-state version of Wissler's unsteady-state model [19] (1964). The main difference between these two models is in the expressions of heat conduction of the torso and energy balance equations of the arterial blood and venous blood in the torso. Wissler [19] (1964) used Crank-Nicholson's implicit finite difference technique to approximate the unsteady-state system equations and employed the Gausian elimination method to solve a set of interrelated linear algebraic equations for each element. The model discussed in this report uses the explicit forward finite difference technique to approximate the steady-state system equations and employs the elimination method by using the largest pivotal division to solve the simultaneous linear algebraic equation for the entire system which considers the interdependence of all the elements.

The technique illustrated in this report also gives rise to great flexibility in using different values of local physiological parameters. But because of limited information concerning the different rates of heat generation by metabolic reaction in various locations of an element, a uniform rate is assumed to each element. The variation of local blood flow rates, however, has implicitly been taken into consideration by assigning different values of thermal conductivities in different layers of the element.

One of the important results of this simulation is that one can visualize the effects of localized cooling (or warming) on the thermal system of the human body. The investigation of these effects will provide valuable information as to the feasibility of creating a local microenvironment for those persons who are often exposed to the hostile environment. This study will also be useful for devicing ways to protect persons involved in space exploration or underwater activities and to prolong the working period of workers in hostile environments such as steel mills or mines.

References

1. Carslaw, H. S. and J. C. Jaeger, The Conduction of Heat in Solids, Oxford University Press, 1959.

2. Crosbie, R. J., J. D. Hardy and E. Fessenden, in "Temperature - Its Measurement and Control in Science and Industry," J. D. Hardy, ed., Vol. 3, Pt. 3, pp. 627-635, Reinhold, New York, 1963.

3. Eichna, L. W., W. F. Ashe, W. B. Bean and W. B. Shelly, "The Upper Limits of Environmental Heat and Humidity Tolerated by Acclimatized Men Working in Hot Environment," Jour. Ind. Hyg. Toxical. 27, 59 (1945).

4. Fan, L. T., F. T. Hsu and C. L. Hwang, "A Review of Mathematical Models on the Human Thermal Systems," Report No. 20, Institute for Systems Design and Optimization, Kansas State University, 1970.

5. Forsythe, G. E. and W. R. Wasow, Finite Difference Methods for Partial Differential Equations, John Wiley and Sons, N. Y., 1960.

6. Guyton, A. C., Text Book of Medical Physiology, 3rd Edition, Saunders, Philadelphia, 1966.

7. IBM System/360 Scientific Subroutine Package (360A-CM-03X), Version III, Programmer's Manual.

8. King, B. G. and M. J. Showers, Human Anatomy and Physiology, 6th Edition, Saunders, Philadelphia, 1969.

9. Konz, S., Private Communications (1969).

10. Licht, S., Medical Climatology, The eight volume of Physical Medicine Library, Waverly Press, Baltimore, 1964.

11. Machle, W. and T. F. Hatch, "Heat: Man's Exchanges and Physiological Responses," Physio. Rev., 27, 200-227 (1947).

12. Pennes, H. H., "Analysis of Tissue and Arterial Blood Temperatures in the Resting Human Forearm," Jour. Appl. Physiol., 1, 93-112 (1948)

13. Perry, R. H., C. H. Chilton and S. D. Kirkpatrick, Chemical Engineer's Handbook, 4th Edition, McGraw-Hill, N. Y., 1963.

14. Salvadori, M. G. and M. L. Baron, Numerical Methods in Engineering, 2nd Edition, Prentice Hall, N. J., 1961.

15. Stolwijk, J. A. J. and D. J. Cunningham, "Expansion of a Mathematical Model of Thermoregulation to Include High Metabolic Rates," NAS-9-7140, John B. Pierce Foundation, 1969.

16. Stolwijk, J. A. J. and J. D. Hardy, "Temperature Regulation in Man-A Theoretical Study," Pflugers Archiv, 291, 129-162 (1966).

17. Wissler, E. H., "Steady-state Temperature Distribution in Man," Journal of Applied Physiology, Vol. 16, No. 4, 1961.

18. Wissler, E. H., "An Analysis of Factors Affecting Temperature Levels in the Nude Man," in Temperature - Its Measurement and Control in Science and Industry, Vol. 3, Pt. 3, Reinhold, N. Y., 1963.

19. Wissler, E. H., "A Mathematical Model of the Human Thermal System," Bulletin of Mathematical Biophysics, Vol. 26, 1964.

20. Wyndham, C. H. and A. R. Atkins, "An Approach to the Solution of the Human Biothermal Problem with the Aid of an Analog Computer," Proceedings of the Third International Conference on Medical Electronics, London, 1960.

Table 1. Linear Algebraic Equations for the Human Thermal System.

$$Y_{21}T_{21} + Z_{21}T_{22} + A_{21}T_{a2} + V_{21}T_{v2} = C_{21}$$
$$X_{22}T_{21} + Y_{22}T_{22} + Z_{22}T_{23} + A_{22}T_{a2} + V_{22}T_{v2} = C_{22}$$
$$X_{23}T_{22} + Y_{23}T_{23} + Z_{23}T_{24} + A_{23}T_{a2} + V_{23}T_{v2} = C_{23}$$
$$X_{24}T_{23} + Y_{24}T_{24} + Z_{24}T_{25} + A_{24}T_{a2} + V_{24}T_{v2} = C_{24}$$
$$X_{25}T_{24} + Y_{25}T_{25} + A_{25}T_{a2} + V_{25}T_{v2} = C_{25}$$
$$P_{21}T_{21} + P_{22}T_{22} + P_{23}T_{23} + P_{24}T_{24} + P_{25}T_{25} + A_{26}T_{a2} + V_{26}T_{v2} \boxed{+ E_{26}T_{a1}} = C_{26}$$
$$Q_{21}T_{21} + Q_{22}T_{2} + Q_{23}T_{23} + Q_{24}T_{24} + Q_{25}T_{25} + A_{27}T_{a2} + V_{27}T_{v2} = C_{27}$$

$$A_{11}T_{a1} + V_{11}T_{v1} + Y_{11}T_{11} + Z_{11}T_{12} = C_{11}$$
$$A_{12}T_{a1} + V_{12}T_{v1} + X_{12}T_{11} + Y_{12}T_{12} + Z_{12}T_{13} = C_{12}$$
$$A_{13}T_{a1} + V_{13}T_{v1} + X_{13}T_{12} + Y_{13}T_{13} + Z_{13}T_{14} = C_{13}$$
$$A_{14}T_{a1} + V_{14}T_{v1} + X_{14}T_{13} + Y_{14}T_{14} + Z_{14}T_{15} = C_{14}$$
$$A_{15}T_{a1} + V_{15}T_{v1} + X_{15}T_{14} + Y_{15}T_{15} = C_{15}$$
$$A_{16}T_{a1} + V_{16}T_{v1} + P_{11}T_{11} + P_{12}T_{12} + P_{13}T_{13} + P_{14}T_{14} + P_{15}T_{15} = C_{16}$$
$$\boxed{E_{17}T_{v2} +} A_{17}T_{a1} + V_{17}T_{v1} + Q_{11}T_{11} + Q_{12}T_{12} + Q_{13}T_{13} + Q_{14}T_{14} + Q_{15}T_{15} + \boxed{E_{17}T_{v3}^{*2}} + \boxed{E_{17}T_{v4}^{*2}}. = C_{17}$$

$$V_{31}T_{v3} + Y_{31}T_{31} + Z_{31}T_{32} + A_{31}T_{a3} = C_{31}$$
$$V_{32}T_{v3} + X_{32}T_{31} + Y_{32}T_{32} + Z_{32}T_{33} + A_{32}T_{a3} = C_{32}$$
$$V_{33}T_{v3} + X_{33}T_{32} + Y_{33}T_{33} + Z_{33}T_{34} + A_{33}T_{a3} = C_{33}$$
$$V_{34}T_{v3} + X_{34}T_{33} + Y_{34}T_{34} + Z_{34}T_{35} + A_{34}T_{a3} = C_{34}$$
$$V_{35}T_{v3} + X_{35}T_{34} + Y_{35}T_{35} + A_{35}T_{a3} = C_{35}$$
$$\boxed{E_{36}T_{a1}} + V_{36}T_{v3} + P_{31}T_{31} + P_{32}T_{32} + P_{33}T_{33} + P_{34}T_{34} + P_{35}T_{35} + A_{36}T_{a3} = C_{36}$$
$$V_{37}T_{v3} + Q_{31}T_{31} + Q_{32}T_{32} + Q_{33}T_{33} + Q_{34}T_{34} + Q_{35}T_{35} + A_{37}T_{a3} = C_{37}$$

$$V_{41}T_{v4} + Y_{41}T_{41} + Z_{41}T_{42} + A_{41}T_{a4} = C_{41}$$
$$V_{42}T_{v4} + X_{42}T_{41} + Y_{42}T_{42} + Z_{42}T_{43} + A_{42}T_{a4} = C_{42}$$
$$V_{43}T_{v4} + X_{43}T_{42} + Y_{43}T_{43} + Z_{43}T_{44} + A_{43}T_{a4} = C_{43}$$
$$V_{44}T_{v4} + X_{44}T_{43} + Y_{44}T_{44} + Z_{44}T_{45} + A_{44}T_{a4} = C_{44}$$
$$V_{45}T_{v4} + X_{45}T_{44} + Y_{45}T_{45} + A_{45}T_{a4} = C_{45}$$
$$\boxed{E_{46}T_{a1}} + V_{46}T_{v4} + P_{41}T_{41} + P_{42}T_{42} + P_{43}T_{43} + P_{44}T_{44} + P_{45}T_{45} + A_{46}T_{a4} = C_{46}$$
$$V_{47}T_{v4} + Q_{41}T_{41} + Q_{42}T_{42} + Q_{43}T_{43} + Q_{44}T_{44} + Q_{45}T_{45} + A_{47}T_{a4} = C_{47}$$

Table 2. Numerical Data for Basal Man [6,9,13,17]

Cylindrical Element	Radius A_i (cm)	Length L_i (cm)	q_{ci}, h_{ai}, h_{vi} $\left(\frac{cal}{cm^3 \times sec \times °C}\right)$	h_{mi} $\left(\frac{cal}{cm^3 \times sec}\right)$	Q_{ai} $\left(\frac{cal}{sec \times °C}\right)$	H_{avi} $\left(\frac{cal}{sec \times °C}\right)$	Q_{vi} $\left(\frac{cal}{sec \times °C}\right)$	Remarks
1 (torso)	14.0	74	0.00118	0.000319	0	0.00118	23.25	$(\rho C_p)_i = 0.9$ cal/cm^3 x °C, i = 1, 2, 3, 4
2 (head)	8.9	23	0.00118	0.000727	11.25	0.00118	0	$K_{tissue} = 0.001$ cal/cm x sec x °C
3 (arm)	4.5	60	0.0003	0.000133	2.4	0.0003	0	$K_{skin \ \& \ fat} = 0.0005$ cal/cm x sec x °C
4 (leg)	7.0	77	0.0002	0.000133	3.6	0.0002	0	

where

q_{ci} = product of the mass flow rate and specific heat of blood entering the capillary beds per unit volume of the ith element,

h_{ai} = proportionality constant of heat transfer between the arteries and tissue per unit volume of the ith element,

h_{vi} = proportionality constant of heat transfer between the veins and tissue per unit volume of the ith element,

h_{mi} = metabolic heat generation per unit volume,

Q_{ai} = product of the mass flow rate and specific heat for blood entering the large arteries of the ith element from the mth element,

Q_{vi} = product of the mass flow rate and specific heat for venous blood entering the large veins of the ith element from the nth element,

H_{avi} = proportionality constant of direct heat transfer between large arteries and veins,

K = thermal conductivity,

ρ = density of blood in tissue,

C_p = specific heat of blood in tissue.

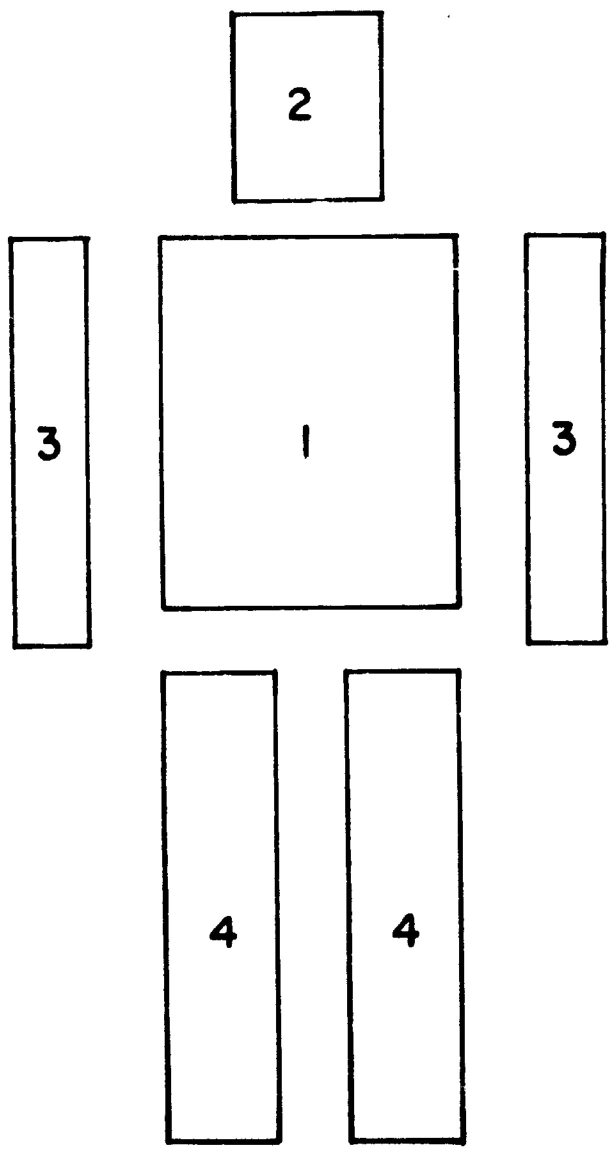

Fig. 1. A schematic diagram of human body.

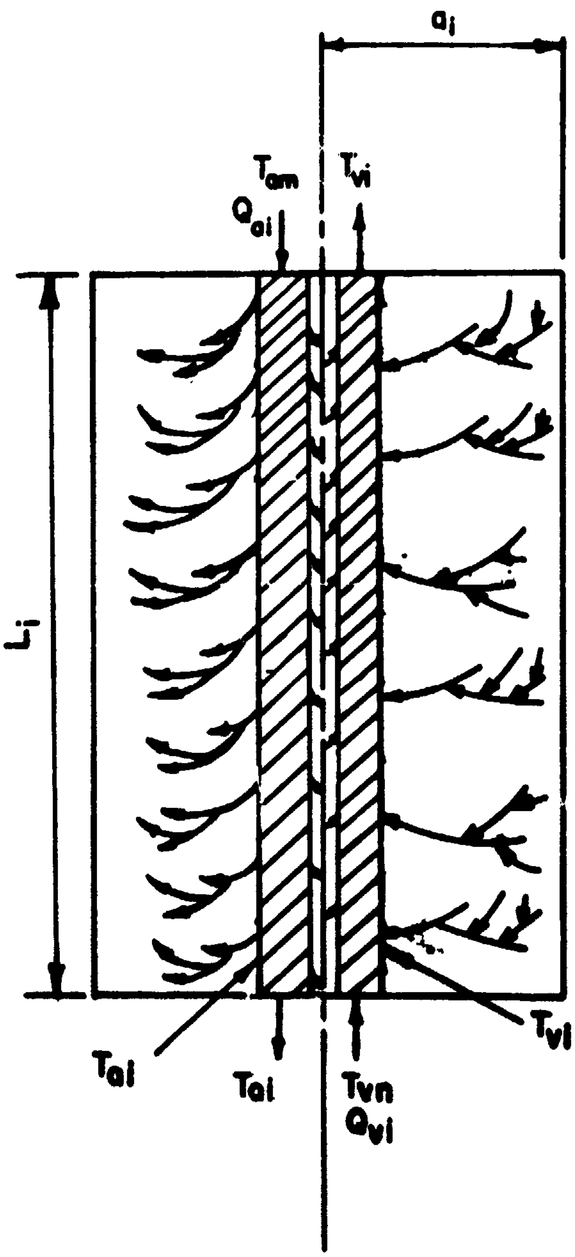

Fig. 2. Vascular system of ith element.

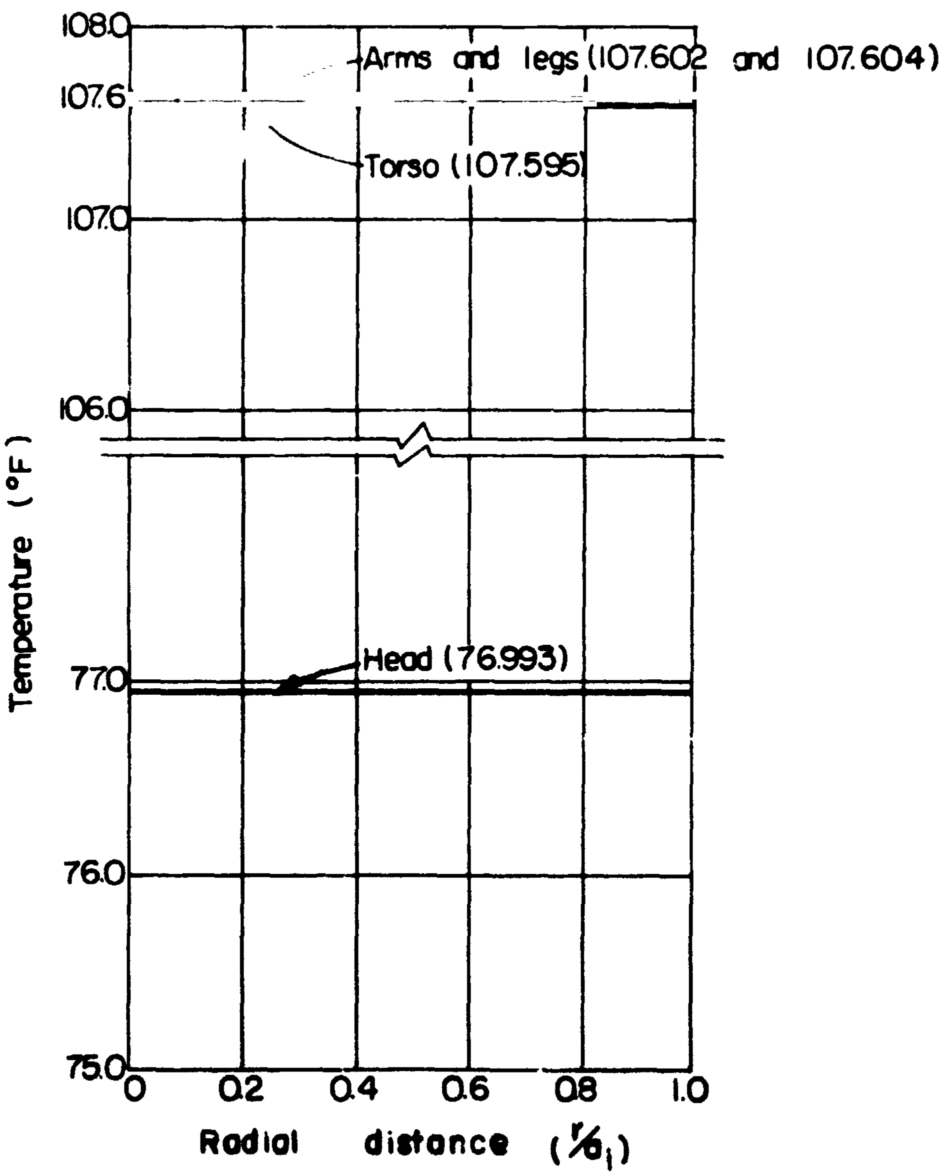

Fig. 3. Temperature profile of steady state case along radial distance. (Blood flow and metabolic rates are both zero).

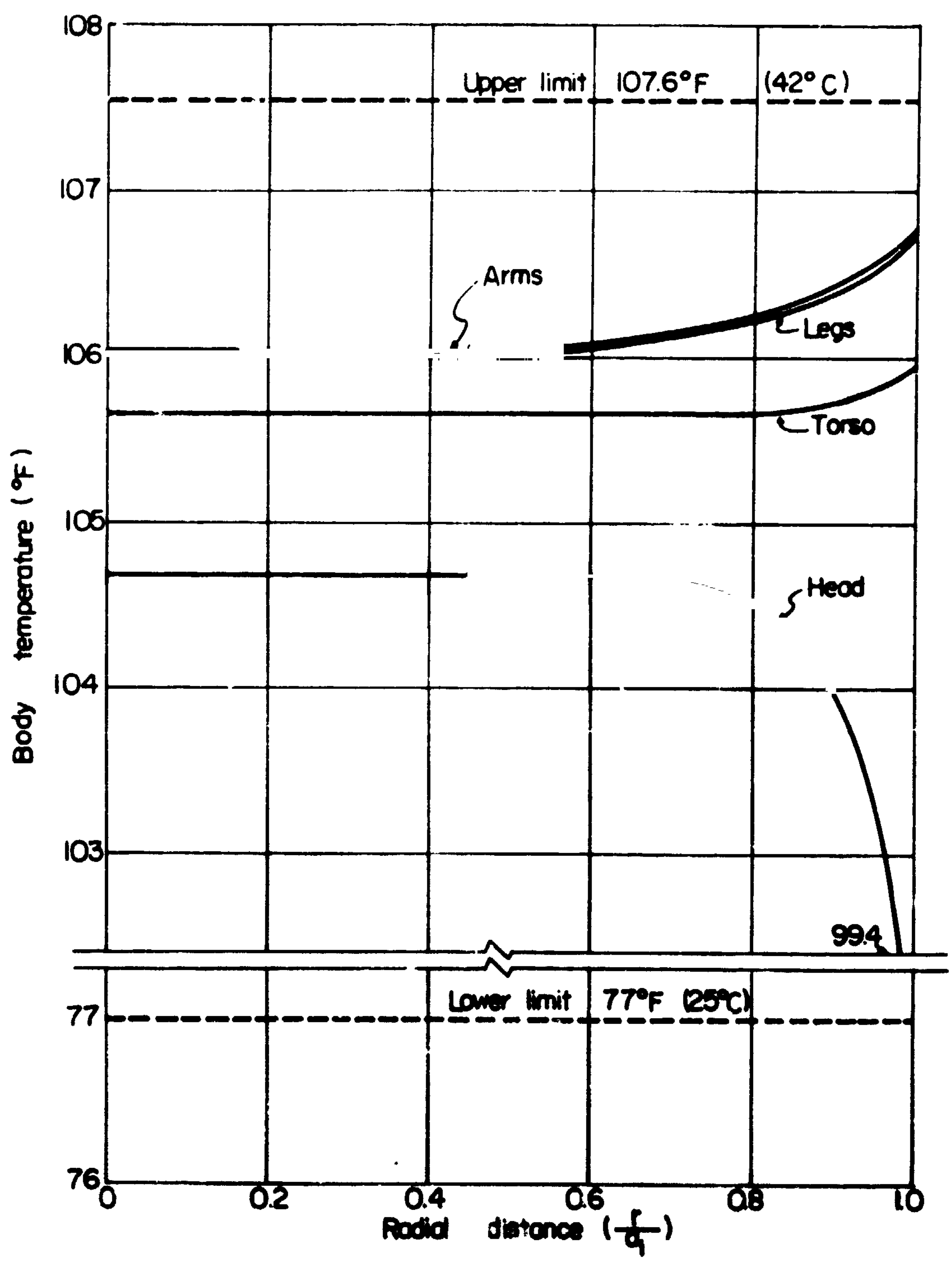

Fig. 4. Temperature profiles of steady-state case with blood flowing between elements. (Metabolic rate = 0).

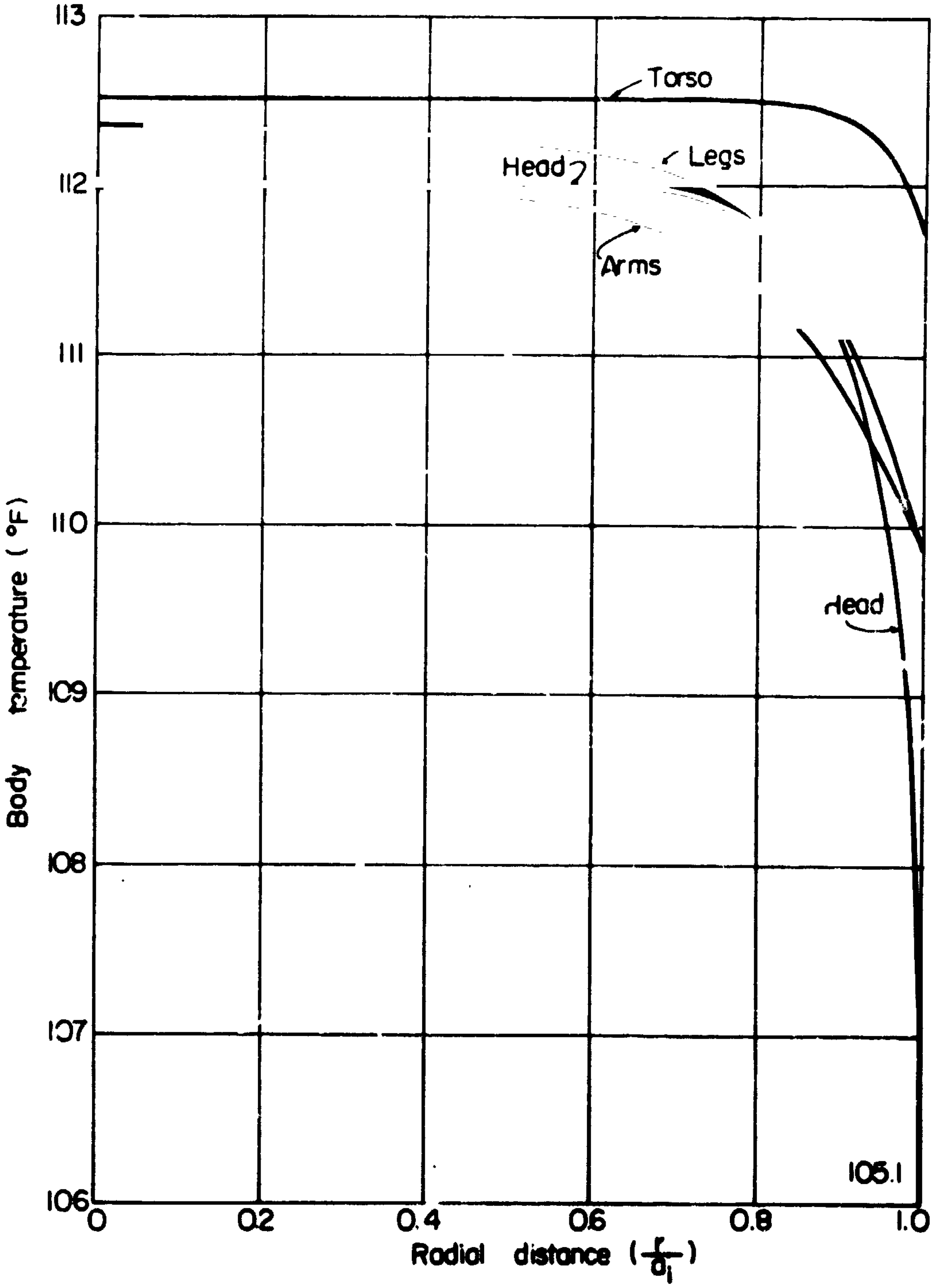

Fig. 5. Temperature profile of various elements at steady—state condition. (Metabolic rate = 300 BTU/hr)

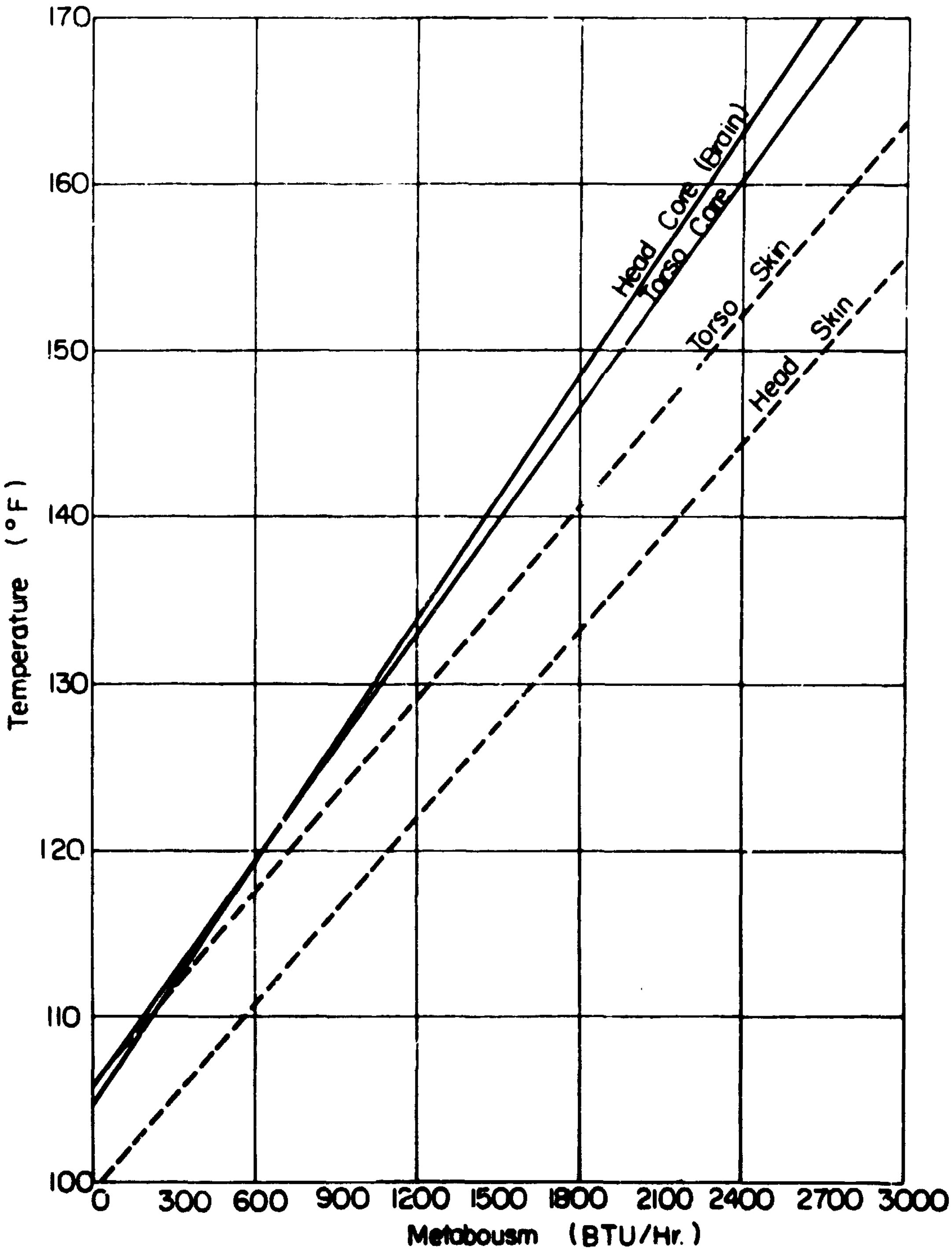

Fig.6. Steady—state core and skin temperatures of head and torso at various levels of activity.

APPENDIX A

Heat transfer coefficient from the human skin to its environment is contributed by four factors; namely, conduction, convection, radiation, and evaporation. The magnitude of the effective heat transfer coefficient depends very much on the physical properties of the surrounding medium, the motion of the medium, the relative humidity of the medium, and the wetness of the surface of the skin. Hence, the effective heat transfer coefficient , H, can be expressed by

$$H = H_c + H_r + H_e \tag{A-1}$$

where

H_c = heat transfer coefficient for convection

H_r = heat transfer coefficient for radiation

H_e = heat transfer coefficient for evaporation

The heat transfer coefficient for conduction is neglected because of its small magnitude. The heat transfer coefficient for convection can be predicted using the following equation

$$\frac{H_c D}{K_f} = 0.26\left(\frac{DV\rho}{\mu_f}\right)^{0.6} \left(\frac{C_p \mu_f}{K_f}\right)^{0.3} \tag{A-2}$$

where

D = diameter of the cylinder

K_f = thermal conductivity of the medium

V = velocity with which the fluid approaches the cylinder

ρ = fluid density

μ_f = viscosity of the fluid

C_p = specific heat of the fluid

Equation (A-2) is applicable only if the fluid approaches to a single cylinder in the direction which is perpendicular to the axis of the cylinder. The heat transfer coefficient is proportional to the 0.6 power of the velocity and inversely proportional to the 0.4 power of the diameter. For a cylinder that is 8 cm in diameter

$$H_c = 1.8 \times 10^{-4}\ V^{0.6}\ \frac{\text{cal}}{\text{cm}^2 \times \text{sec} \times {}^\circ\text{C}} \tag{A-3}$$

where V is measured in centimeters per second. For a cylinder that is 26 cm in diameter the corresponding equation is

$$H_c = 0.95 \times 10^{-5}\ V^{0.6}\ \frac{\text{cal}}{\text{cm}^2 \times \text{sec} \times {}^\circ\text{C}} \tag{A-4}$$

Equations (A-3) and (A-4) are used to approximate the values of H_c for the arms, lege, torso, and head.

The value of H_r increases from 0.000145 cal/cm^2 x sec x °C to 0.0001663 cal/cm^2 x sec x °C as the temperature changes from 10°C to 40°C. It is nearly constant. Hence, the complex geometry of the human body and the wide variety of the area for radiant transfer as the posture of the individual varies will not effect the value of H_r significantly.

The heat transfer coefficient for evaporation in the absence of sweating is approximated as follows

$$H_e = 0.16 \times 10^{-4}\ \frac{\text{cal}}{\text{cm}^2 \times \text{sec} \times {}^\circ\text{C}}$$

This approximation is used in this report because in the future study of human subject under control the sweating will be minimized.

INSTITUTE FOR SYSTEMS DESIGN AND OPTIMIZATION REPORTS*

11. Carbon Dioxide Reduction Contactors in Space Vehicles and Other Enclosed Structures, by T. Takahashi and L. T. Fan, January, 1969.

12. Removal of Sulfur Dioxide from Waste and Exhaust Gases, by T. Takahashi and L. T. Fan, January, 1969.

13. Analysis of a Reverse Osmosis Water Purification System and its Optimization Based on the Plug Flow Model for the Bulk Flow in the Membrane Unit, by L. T. Fan, L. E. Erickson, J. T. Tseng, C. L. Hwang and C. Y. Cheng, February, 1969.

14. Systems Analysis and Optimization of Reverse Osmosis Processes, by L. T. Fan, C. L. Hwang, L. E. Erickson, C. Y. Cheng and L. Y. S. Ho, March, 1969.

15. Optimal Wall Temperature Control of a Heat Exchanger, by H. S. Huang, L. T. Fan, and C. L. Hwang, April, 1969.

16. Systems Analysis and Optimization of Dual-Purpose Nuclear Power and Desalting Plants, by L. T. Fan, C. L. Hwang, N. C. Pereira, L. E. Erickson, and C. Y. Cheng, April, 1969.

17. Terminal Control of Linear Distributed Parameter System, by H. S. Huang, L. T. Fan, and C. L. Hwang, August, 1969.

18. Hooke and Jeeves Pattern Search Solution to Optimal Production Planning Problems, by C. L. Hwang, L. T. Fan, and S. Kumar, September, 1969.

19. Collection and Analysis of Water Quality Data, by J. S. Shastry, L. T. Fan, and L. E. Erickson, February, 1970.

20. Simulation of Biological Processes by Analog and Digital Computers, by L. T. Fan, P. S. Shah, and L. E. Erickson, July, 1970.

21. Systems Analysis and Optimization of an Electrodialysis Desalination Process, by K. Osakada, N. C. Pereira, L. T. Fan, C. L. Hwang and L. E. Erickson, July, 1970.

22. A Review on Mathematical Models of the Human Thermal System, by L. T. Fan, F. T. Hsu and C. L. Hwang, July, 1970.

*Copies of these reports can be obtained be writing to:

Prof. L. T. Fan, Director
Systems Institute
c/o Department of Chemical Engineering
Kansas State University
Manhattan, Kansas 66502